

**The Synthesis of 6,12-Guaianolide Analogs and Related Chemical Tools for Probing their
Mechanism of NF- κ B Inhibition**

by

Sarah M. Wells

B.S. Chemistry, Grove City College, 2011

Submitted to the Graduate Faculty of the
Kenneth P. Dietrich School of Arts and Sciences in partial fulfillment
of the requirements for the degree of
Doctor of Philosophy

University of Pittsburgh

2016

UNIVERSITY OF PITTSBURGH

Kenneth P. Dietrich School of Arts and Sciences

This dissertation was presented

by

Sarah M. Wells

It was defended on

July 22, 2016

and approved by

Paul Floreancig, Professor, Department of Chemistry

Joseph Grabowski, Associate Professor, Department of Chemistry

Daniel A. Harki, Associate Professor, Department of Medicinal Chemistry, University of
Minnesota

Dissertation Advisor: Kay M. Brummond, Professor, Department of Chemistry

Copyright © by Sarah M. Wells

2016

The Synthesis of 6,12-Guaianolide Analogs and Related Chemical Tools for Probing their Mechanism of NF- κ B Inhibition

Sarah M. Wells, PhD

University of Pittsburgh, 2016

Guaianolides, the largest class of sesquiterpene lactones, possess a wide range of biological activities, particularly in the areas of anti-inflammation and anticancer. The allenic Pauson-Khand reaction (APKR) is a rhodium (I) catalyzed [2 + 2 + 1] cyclocarbonylation reaction of allene-ynes and has been established as a viable methodology for accessing the guaianolide 5,7,5-tricyclic framework. However, allene-yne precursors with methyl substituted allenes and alkynes have been poorly tolerated. Optimization of high dilution APKR conditions is described for these methyl substituted allene-ynes, which give direct access to C4 and C10 methyl substituted bicyclo[5.3.0]decadienones, consistent with the guaianolide framework.

This APKR approach was also applied to continuing the synthesis of highly oxygenated guaianolide analogs, capable of inhibiting NF- κ B. The α -methylene- γ -butyrolactone moiety is incorporated into allene-yne tether prior to the APKR. Given the potent NF- κ B inhibitory properties demonstrated by our analogs, derivatives were synthesized in effort to examine the biological mechanism of inhibition. Installation of alkyne ligation handles onto the base-sensitive guaianolide analogs, for use in biomechanistic studies, was achieved using the acid mediated Nicholas reaction. This method was also established for the general installation of alkyne ligation handles onto hydroxyl, sulfhydryl, amino, and carboxyl groups. Synthesis and biological evaluation of an α -methyl- γ -butyrolactone guaianolide analog established the importance of the α -methylene- γ -butyrolactone moiety for potent NF- κ B inhibition.

TABLE OF CONTENTS

LIST OF TABLES	IX
LIST OF FIGURES	XI
LIST OF SCHEMES	XIV
LIST OF ABBREVIATIONS	XX
ACKNOWLEDGEMENTS	XXII
1.0 AN ALLENIC PAUSON-KHAND APPROACH TOWARDS 6,12-GUAIANOLIDES	1
1.1 INTRODUCTION	1
1.1.1 Previous approaches toward the 6,12-guaianolide framework	6
1.1.2 Development and applications of the allenic Pauson-Khand reaction...	13
1.1.3 An allenic Pauson-Khand approach toward guaianolides.....	18
1.1.4 Low yielding APKR examples with methyl substituted allene-yne	20
1.2 OPTIMIZATION OF THE APKR FOR METHYL SUBSTITUTED ALLENE-YNE TETHERS	22
1.2.1 Model system substrate design	22
1.2.2 Synthesis of allene-yne 1.91	23
1.2.3 Optimization of APKR with 1.91.....	23

1.2.4	Application of high dilution conditions to synthesis of bicyclo[5.3.0]decadienones	29
1.2.5	Efforts towards a large-scale allene-yne synthesis and APKR reaction for <i>Organic Syntheses</i>	33
1.2.6	Synthesis of Bicyclo[6.3.0]dienones	35
1.3	CONCLUSION	38
1.4	EXPERIMENTALS	39
1.4.1	General Methods.....	39
1.4.2	Experimental procedures detailed in published papers.....	40
1.4.3	General Procedures	41
1.4.4	Experimental procedures with compound characterization data	43
2.0	GUAIANOLIDE ANALOG SYNTHESIS VIA AN ALLYLBORATION/LACTONIZATION SEQUENCE AND THE APKR REACTION ..	48
2.1	INTRODUCTION	48
2.2	RESULTS AND DISCUSSION.....	51
2.2.1	Synthesis of allenyl-ynoate 2.1a	51
2.2.2	Optimization of allylboronate formation.....	53
2.2.3	Completing the synthesis of guaianolide analog 1.83.	62
2.2.4	Distinguishing stereochemistry of <i>trans</i> -and <i>cis</i> - α -methylene lactones..	65
2.2.5	Assignment of 1.83 diastereomers using NMR calculations	68
2.3	CONCLUSIONS	71
2.4	EXPERIMENTALS	73
2.4.1	General Methods.....	73

2.4.2	Synthesis of ynoate 2.1a.....	74
2.4.3	Optimization of Allylboronate formation (Experiments for Table 5)..	80
2.4.4	Completing the synthesis of <i>trans</i> -guaianolide 1.83.....	87
2.4.5	Computational Methods.....	93
3.0	INSTALLATION OF ALKYNE LIGATION HANDLES VIA THE NICHOLAS REACTION.....	95
3.1	INTRODUCTION	95
3.1.1	Activity Based Protein Profiling for Protein Target Identification.....	96
3.1.2	Probe design for target identification of bioactive small molecules.....	97
3.1.3	Bioorthogonal reactions and the value of alkyne ligation handles.....	98
3.1.4	Traditional methods for installation of alkyne handles.....	100
3.1.5	The Nicholas reaction: an acid mediated propargylation reaction	104
3.2	RESULTS AND DISCUSSION.....	106
3.2.1	Preparation of alcohol 3.40 as a model system.....	106
3.2.2	Optimization of the Nicholas reaction conditions	107
3.2.3	Testing the scope and limitations of the Nicholas reaction conditions on amino acid derived nucleophiles	110
3.2.4	The synthesis of sesquiterpene lactone alkyne probes.....	124
3.3	CONCLUSIONS	126
3.4	EXPERIMENTALS	127
3.4.1	General Methods.....	127
3.4.2	General Procedures	129
3.4.3	Experimental procedures with compound characterization data	133

4.0	STUDIES ON THE GUAIANOLIDE NF-κB MECHANISM OF INHIBITION	
		167
4.1	INTRODUCTION	167
4.2	EFFECT OF C8 STEREOCHEMISTRY ON NF-κB INHIBITION	173
4.3	THE IMPORTANCE OF THE α-METHYLENE-γ-BUTYROLACTONE	
	FOR NF-κB INHIBITION.....	175
4.3.1	Synthesis of reduced methylene guaianolide analog 4.10.....	177
4.3.2	Assignment of relative C11 stereochemistry for α-methyl lactones 4.15	
	and 4.10.	183
4.3.3	NF-κB inhibition of α-methyl-γ-butyrolactone analog 4.10a.....	185
4.4	REACTIVITY OF GUAIANOLIDE ANALOG 1.83 WITH CYSTEINE.	186
4.5	ABPP TARGET IDENTIFICATION STUDIES.....	187
4.5.1	Synthesis of active and non-active guaianolide alkyne probes	188
4.5.2	NF-κB inhibition of guaianolide alkyne probe 3.79.....	189
4.6	CONCLUSIONS	191
4.7	EXPERIMENTALS	192
4.7.1	General Methods.....	192
4.7.2	General Procedures	193
4.7.3	General Calculations Procedure for 4.10 isomers.	194
4.7.4	Experimental procedures with compound characterization data	194
APPENDIX A	206
APPENDIX B	213
BIBLIOGRAPHY	331

LIST OF TABLES

Table 1. Optimization of the APKR for methyl substituted allene-yne 1.91.....	24
Table 2. Result from large scale conversion of 2-butyne-1-ol (1.92) to allenyl ester 1.93.	34
Table 3. Antiproliferative data of guaianolide analogs, <i>trans</i> -1.83 and <i>cis</i> -1.84, compared to parthenolide (PTL).....	50
Table 4. Previously reported results for conversion of ynoate 2.1a to allylboronate 2.2a. ⁴³	57
Table 5. Reaction optimization for conversion of alkynoates 2.1 to allylboronates 2.2.....	59
Table 6. Experimental ¹ H NMR spectral data of 8βH-1.83a and 8αH-1.83b compared to calculated chemical shifts (corrected).....	70
Table 7. Calculated chemical shifts for 8βH-1.83a and 8αH-1.83b.	94
Table 8. Optimization of the Nicholas reaction with alcohol 3.40.	109
Table 9. Propargylation of <i>N</i> -protected serine methyl esters 3.45a,b.	112
Table 10. Propargylation of cysteine derivatives 3.49.....	114
Table 11. Propargylation of <i>N</i> -protected tyrosine methyl esters 3.55a,b.....	116
Table 12. Propargylation of L-proline methyl ester 3.67.	121
Table 13. Synthesis of MeIB cobalt complexed alkyne probe 3.80.....	125
Table 14. Relative NF-κB activity of cells treated with 8βH-1.83a and 8αH-1.83b.	175
Table 15. Initial attempts to reduce methylene of <i>trans</i> -1.83: Solvent effects.	178
Table 16. Optimization of Stryker's reagent equiv using model system 4.16.....	180

Table 17. ^1H NMR calculations compared to experimental data for 4.15a and 4.10a.....	185
Table 18. ^1H NMR calculations compared to experimental data for 4.15b.	185
Table 19. Relative NF- κ B activity of cells treated with 11 β H,8 β H-4.10a.	186
Table 20. Relative NF- κ B activity averages for cells treated with alkyne probe 3.79.	189
Table 21. ^1H and ^{13}C NMR data for 1.83a and 1.83b.	207
Table 22. ^1H and ^{13}C NMR data for 3.78 and 3.79.	208
Table 23. ^1H and ^{13}C NMR data for 4.15a and 4.15b.	209
Table 24. ^1H and ^{13}C NMR data for 4.10a and 4.10b.	210
Table 25. ^1H and ^{13}C NMR data for cysteine adduct 4.23.	211
Table 26. ^1H NMR data for 4.25 and 4.24.	212

LIST OF FIGURES

Figure 1. Medicinally relevant sesquiterpene lactones.	2
Figure 2. Selected SLs representing families that inhibit NF- κ B, and the 6,12-guaianolide analog 1.10 proposed as a lead inhibitor by Merfort.	4
Figure 3. Frameworks of the guaianolide and pseudoguaianolide SL families.	5
Figure 4. Euclidean distances between the drug formestane (1.12) and NPs 1.11 and 1.13 in chemical space.	6
Figure 5. Semisynthetic approaches to the 6,12-guaianolide framework.	7
Figure 6. Previously published compounds for which synthetic procedures and characterization data can be found in <i>Tetrahedron Lett.</i> 2015, 56, 3546-3549.	41
Figure 7. NF- κ B inhibition of 1.83 and 1.84 benchmarked with parthenolide (PTL, 1.3). A) Compounds tested. B) NF- κ B luciferase reporter assay in A549 cells induced with TNF- α (15 ng/mL) 30 min after molecular treatment. 1.83 and 1.84 were dosed at 20, 10, and 1 μ M. PTL (1.3) was dosed at 10, 1 μ M. NI = noninduced, I = Induced.	49
Figure 8. The <i>Z</i> - and <i>E</i> -isomers of allylboronate 2.2d.	60
Figure 9. Comparison of coupling constants for 2.24, 1.83, and 2.25 with previously reported guaianolide analogs.	66
Figure 10. Coupling constants for mono-cyclic <i>trans</i> - and <i>cis</i> -methylene lactones.	66

Figure 11. 3D-representations of <i>trans</i> -2.28a and <i>trans</i> -1.83 (Chem3D) with highlighted H _a , H _b dihedral angle.....	67
Figure 12. Structure of 8 β H-1.83a and 8 α H-1.83b.....	68
Figure 13. ¹ H NMR spectra for 1.83a,b from 6.7-3.7 ppm.....	69
Figure 14. Overview of activity-based protein profiling (ABPP). Reprinted from MDPI Open Access: Martell, J.; Weerapana, E. <i>Molecules</i> , 2014, <i>19</i> , 1378-1393. ⁷⁶	97
Figure 15. Popular reporter groups for ABPP.	98
Figure 16. Advantages of a two-step ABP with an alkyne ligation handle. A) Bulky reporter groups interfere with warhead-protein binding. B) Alkyne ligation handle can be modified for analytical interpretation after covalent binding of reactive group with target protein. Reprinted by permission from John Wiley & Sons, Inc.: Lehmann, J.; Wright, M. H.; Sieber, S. A. <i>Chem. Eur. J.</i> 2016, <i>22</i> , 4666-4678. © 2016 WILEY-VCH Verlag GmbH & Co. KGaA, Weinheim.	98
Figure 17. Orlistat 3.27 and Orlistat probe 3.28, synthesized using early-alkyne incorporation.	103
Figure 18. Base-sensitive sesquiterpene-lactone analogs.	104
Figure 19. Comparison of coupling constants of 3.38 with previously synthesized 2.28.	107
Figure 20. Homodimerization of 3.30a results in byproduct 3.43.....	110
Figure 21. ¹ H NMR analysis of electrophilic aromatic substitution byproduct 3.57.....	116
Figure 22. ¹ H NMR analysis of Nicholas reaction products 3.63 and 3.64.....	119
Figure 23. Compounds synthesized and characterized by collaborator John Widen.	129
Figure 24. Examples of SL reactivity with biological thiols; A) Helenalin (1.7) adducts with cysteine and glutathione, B) Costunolide (4.3) adduct with cysteamine (4.4).	169

Figure 25. The NF- κ B pathway leading to gene transcription. ¹¹ Reprinted by permission from Macmillan Publishers Ltd: <i>Nature Reviews Drug Discovery</i> , 2008, 7, 1031-1040, copyright 2008.....	170
Figure 26. Structures of parthenolide derivatives used by Kwok to investigate the SL mechanism of inhibition.....	171
Figure 27. Sesquiterpene lactones evaluated in NF- κ B mutant (Cys \rightarrow Ser) experiments.	172
Figure 28. Structures of the two <i>trans</i> -1.83 diastereomers.....	174
Figure 29. Pictorial representation of relative NF- κ B activity for cells treated with 8 β H-1.83a and 8 α H-1.83b.	175
Figure 30. Isolated diastereomers of 4.15 and 4.10 for which experimental ¹ H NMR spectra were obtained.....	183
Figure 31. Diastereomers of 4.10 evaluated computationally.	184
Figure 32. Pictorial representation of relative NF- κ B activity for cells treated with 4.10a. Induced cells were treated with TNF- α (15 ng/mL).....	186
Figure 33. Proposed structures for an active and inactive activity based probe related to guaianolide analog 1.83.	188
Figure 34. Pictorial representation of relative NF- κ B activity for cells treated with alkyne probe 3.79. Data obtained for cells treated with both diastereomers of <i>trans</i> -1.83 are also included for comparison. Cells were induced with TNF- α (15ng/mL).....	190

LIST OF SCHEMES

Scheme 1. Mechanism for a Michael-type addition of a sulfhydryl group to an α -methylene- γ -butyrolactone (1.4).....	2
Scheme 2. Three step synthesis of arglabin (1.15) from parthenolide (1.3).....	7
Scheme 3. Access to the guaianolide framework from (-)- α -santonin (1.16) and representative natural products synthesized via this method.	8
Scheme 4. Photochemical rearrangement of 1.21 toward 7,11-dihydroxyguaianolide analog 1.23.	8
Scheme 5. Access to highly functionalized 5-membered ring (-)-1.26 via the Favorskii rearrangement and a radical cascade approach toward (+)-cladanthiolide (1.29).	9
Scheme 6. RCM approach for 7-membered ring formation in the total synthesis of thapsigargin (1.1).....	10
Scheme 7. RCM approach to arglabin (1.15).	10
Scheme 8. Synthesis of (\pm)-estafiatin (1.19) via an oxidative ring expansion.	10
Scheme 9. Total synthesis of (\pm)-geigerin 1.40 from tropylium ion 1.36.	11
Scheme 10. Application of novel 7-membered ring syntheses to guaianolide analogs.....	12
Scheme 11. General intramolecular Pauson-Khand reaction and allenic Pauson-Khand reaction.	13
Scheme 12. Diverging reactivity of 1.54 when using $[\text{Rh}(\text{CO})_2\text{Cl}]_2$ and $\text{Mo}(\text{CO})_6$	14

Scheme 13. Diverging mechanisms of the APKR with rhodium and molybdenum lead to regioselectivity.....	15
Scheme 14. Synthesis of bicyclo[5.3.0]decadienones via a Rh(I)-catalyzed allenic Pauson-Khand reaction.....	16
Scheme 15. Selected examples of the APKR towards linearly and angularly fused 6,7,5-tricyclic frameworks.	17
Scheme 16. An APKR approach toward the total synthesis of (+)-ingenol (1.74) and (+)-phorbol (1.75).....	18
Scheme 17. Retrosynthetic analysis of 6,12-guaianolide framework 1.76.....	18
Scheme 18. An APKR approach to the 5,7,5-fused ring system 1.81.	19
Scheme 19. Synthesis of highly-functionalized guaianolide analogs 1.83 and 1.84 via the APKR.	20
Scheme 20. An APKR approach to 8,12 guaianolide (+)-achalensolide (1.87).	20
Scheme 21. Scope expansion for guaianolide analogs 1.81 reveals sensitivity to methyl substitutions.	21
Scheme 22. Synthesis of 5,7,6-ring systems 1.89a-d.....	21
Scheme 23. Retrosynthetic analysis of dienone 1.90.....	22
Scheme 24. Synthesis of allene-yne tether 1.91.	23
Scheme 25. Allene dimerization as a competing process for the [5 +2] cycloaddition of terminal allenes with VCPs.	25
Scheme 26. Comparison of various Rh(I) catalysts for the formation of dienone 1.86.	28
Scheme 27. Synthesis of diester allene-yne tether 1.101 with a terminal alkyne.	29

Scheme 28. Transformation of diester allene-yne 1.91 and 1.101 to acetonide containing allene-yne 1.103a,b.	30
Scheme 29. Synthesis of heteroatom containing allene-yne tethers 1.104 and 1.105.	30
Scheme 30. Result of high dilution conditions on a variety of allene-yne. Conditions A high dilutions conditions where the allene-yne was added by a syringe pump over 1.5 h. Conditions B added the allene-yne all at once.	31
Scheme 31. Reaction of 1,3-diubstituted allene 1.111 in the APKR with dilute, dropwise conditions.	32
Scheme 32. Original <i>Organic Syntheses</i> procedures for the APKR synthesis of bicyclo[5.3.0]decadienones.	33
Scheme 33. Retrosynthetic analysis for dienone 1.113.	34
Scheme 34. Previous syntheses of bicyclo[6.3.0]undecadienones via the APKR.	36
Scheme 35. Synthesis of bicyclo[6.3.0]dienone 1.120 from bis(sulfonylallene) 1.119.	36
Scheme 36. Attempted synthesis of bicyclo[6.3.0]undecadienone 1.123b.	36
Scheme 37. Synthesis of extended allene-yne diester tether 1.125.	38
Scheme 38. Synthesis of bicyclo[6.3.0]undecadienone 1.128 via the APKR.	38
Scheme 39. Previous synthesis of oxygenated guaianolide analogs 1.83 and 1.84.	49
Scheme 40. Synthesis of allenyl-ynoate 2.1a from 2-butyne-1,4-diol (2.3) in 7 steps.	52
Scheme 41. Conjugate reduction of ynoate 2.1 to afford the <i>Z</i> and <i>E</i> isomers of 2.2.	54
Scheme 42. Proposed reaction pathway for the formation of allylboronate 2.2 using catalytic CuMe.	55
Scheme 43. Previous syntheses of trisubstituted pinacol allylboronates from alkynoates.	56

Scheme 44. Synthesis of tetrasubstituted allylboronate 2.20, with high selectivity for the <i>Z</i> isomer.....	57
Scheme 45. Repeated synthesis of allylboronate 2.2a.	61
Scheme 46. Previously reported synthesis of <i>trans</i> - and <i>cis</i> -lactone 1.82a,b via allylboration followed by lactonization.....	62
Scheme 47. Formation of <i>trans</i> - and <i>cis</i> -lactones 1.82a and 1.82a from allylboronate 2.2a.....	63
Scheme 48. Zimmerman-Traxler transition states for the reaction between allylboronate 2.2a and aldehyde 2.22.	64
Scheme 49. Completing the synthesis of <i>trans</i> -guaianolide analog 1.83.	64
Scheme 50. Isolation of cyclocarbonylation adducts <i>trans</i> -2.24 and <i>cis</i> -2.25.....	65
Scheme 51. Selected bioorthogonal reactions.	99
Scheme 52. Synthesis of Src-directed alkyne probe 3.16 via base mediated propargylation.....	101
Scheme 53. Propargylation of Fmk 3.17.	101
Scheme 54. Synthesis of alkyne probes 3.20, 3.22, and 3.24 using amide coupling reactions. .	102
Scheme 55. Synthesis of EuPAYne 3.26 via Rh(I) catalyzed C-H amination.	103
Scheme 56. Synthesis of propargyl derivatives via Nicholas reaction followed by oxidative decomplexation.	105
Scheme 57. Synthesis of unsymmetrical ether 3.36 via the Nicholas reaction.....	105
Scheme 58. Synthesis of molecularly complex model system 3.40.	107
Scheme 59. Cobalt complexation of propargyl alcohol to afford 3.30a.	108
Scheme 60. Decomplexation of 3.42 to afford propargyl ether 3.44.....	110
Scheme 61. Oxidative decomplexation to afford alkynyl serine derivatives 3.47a,b.....	112
Scheme 62. Synthesis of <i>N</i> -protected cysteine ethyl esters 3.49a,b.	113

Scheme 63. Oxidative decomplexation for the formation of alkynyl cysteine derivatives 3.51a,b.	114
Scheme 64. Previous example of a phenolic nucleophile in the Nicholas reaction.....	115
Scheme 65. Oxidative decomplexation of tyrosine derivatives 3.56a,b.	117
Scheme 66. Use of a carboxylic acid in the Nicholas reaction for formation of propargylic ester 3.61.....	118
Scheme 67. Result of employing N-Cbz-L-serine 3.62 in the Nicholas Reaction.	119
Scheme 68. Desired result compared to actual result for Entry 3 of Table 12.	121
Scheme 69. Synthesis of propargylium cation tetrafluoroborate salt 3.30d.	122
Scheme 70. Decomplexation of proline derivative 3.68.....	123
Scheme 71. Reaction of L-phenylalanine methyl ester (3.70) with 3.30d followed by decomplexation.	123
Scheme 72. Synthesis of 3.74 and its application to the formation of 3.75 and 3.77.....	124
Scheme 73. Synthesis of guaianolide analog alkyne probe 3.79.	125
Scheme 74. Oxidative decomplexation of 3.80 to afford propargylated Mel B 3.81.	126
Scheme 75. Retrosynthetic analysis of 4.10.	176
Scheme 76. Synthesis of α -methyl lactone 4.14 and eremantholide 4.13 from furanoheliangolide 4.11.....	177
Scheme 77. Reduction of 2.24 with [CuH(PPh ₃) ₆] gave impure 4.15.	179
Scheme 78. Reactions of Merrifield's resin/ NaI scavenging system with Ph ₃ P 4.18 and Ph ₃ PO 4.21.....	180
Scheme 79. Reduction of 4.16 to afford 4.17 after triphenylphosphine scavenging.	181
Scheme 80. Synthesis and purification of <i>trans</i> -4.15, 4.10 and <i>cis</i> -4.22.....	182

Scheme 81. Guaianolide analog 4.10 is not compatible with iodine-modified Merrifield's resin.	182
Scheme 82. Reaction of <i>trans</i> -1.83 with L-cysteine to afford adduct 4.23.	187
Scheme 83. Synthesis of active alkyne probe 3.79 and inactive probe 4.24.	189

LIST OF ABBREVIATIONS

^1H NMR	proton nuclear magnetic resonance
^{13}C NMR	carbon nuclear magnetic resonance
ABPP	activity based protein profiling
ABPs	activity based probes
Ac	acetyl
AcOH	acetic acid
AIBN	azobisisobutyronitrile
APKR	allenic Pauson-Khand Reaction
atm	atmosphere
B3LYP	Becke, 3-parameter, Lee-Yang-Parr
Boc	<i>tert</i> -butyloxycarbonyl
Bz	benzoyl
CAN	cerium ammonium nitrate
Cbz	carboxybenzyl
CDCl_3	deuterated chloroform
ClCH_2BPin	pinacol chloromethylboronate
CO	carbon monoxide
COMU	(1-cyano-2-ethoxy-2-oxoethylideneaminoxy)dimethylamino-morpholino-carbenium hexafluorophosphate
COSY	correlation spectroscopy
CSA	camphorsulfonic acid
DBU	1,8-diazabicyclo[5.4.0]undec-7-ene
DCE	1,2-dichloroethane
DCM	dichloromethane
DIAD	diisopropyl azodicarboxylate
DIBAL-H	diisobutylaluminium hydride
DIC	diisopropylcarbodiimide
DIPEA, DIEA	<i>N,N</i> -diisopropylethylamine
DMF	<i>N,N</i> -dimethylformamide
DMP	2,2-dimethoxypropane
DMSO	dimethylsulfoxide
DNA	deoxyribonucleic acid
EDC	1-ethyl-3-(3-dimethylaminopropyl)carbodiimide
EDs	euclidean distances
EMSA	electrophoretic mobility shift assay
ESI	electrospray ionization

Et ₂ O	diethyl ether
EtOAc	ethyl acetate
EtOH	ethanol
EuPA	eupalmerin acetate
Fmoc	fluorenylmethyloxycarbonyl
FTMS	fourier transform mass spectrometer
HMPA	hexamethylphosphoramide
HPLC	high performance liquid chromatography
HOBT	hydroxybenzotriazole
HRMS	high-resolution mass spectroscopy
HSQC	heteronuclear single quantum coherence
IPNBSH	<i>N</i> -isopropylidene- <i>N'</i> -2-nitrobenzenesulfonyl hydrazine
IR	infrared spectroscopy
LA	Lewis acid
LAH	lithium aluminum hydride
<i>m</i> -CPBA	<i>meta</i> -chloroperoxybenzoic acid
MelB	melampomagnolide B
MMFF	merck molecular force field
MP	melting point
MS	mass spectrometry
NF-KB	nuclear factor kappa B
NMO	<i>N</i> -methylmorpholine <i>N</i> -oxide
NPs	natural products
<i>p</i> -TSA	<i>p</i> -toluenesulfonic Acid
Ph ₃ P	triphenylphosphine
Ph ₃ PO	triphenylphosphine oxide
PKR	Pauson-Khand reaction
PPTS	pyridinium <i>p</i> -toluenesulfonate
PTL	parthenolide
pyr	pyridine
QSAR	quantitative structure activity relationship
RCM	ring closing metathesis
rt	room temperature
SLs	sesquiterpene lactones
TBAF	tetra- <i>n</i> -butylammonium fluoride
TBDPS	tert-butyl-diphenylsilyl
TFA	trifluoroacetic acid
THF	tetrahydrofuran
TLC	thin layer chromatography
TNF – α	tumor necrosis factor
TOF	time-of-flight
UV	ultraviolet

ACKNOWLEDGEMENTS

While this document is a reflection of the work I have completed throughout my time in graduate school, this would never have been possible without the widespread support that I have received. First, I want to thank my advisor Professor Kay Brummond who has provided me with an amazing example of the skills, work ethic, and critical thinking that are necessary to be a successful chemist. I will be forever grateful to Kay for the opportunity to work on fruitful projects, for her frequent guidance and support, and insightful feedback on my work.

I must also recognize my other faculty mentors. Professor Dan Harki has provided invaluable collaboration and support, particularly evidenced by his willingness to travel from Minnesota to serve on my PhD committee. My other committee members, Professor Joe Grabowski and Professor Paul Floreancig, have always been open and eager to assist me when necessary. I also want to thank Professor Dennis Curran for his willingness to chair my Original Proposal Project and for the support he provided throughout that process. Finally, I need to thank Dr. Ericka Huston for her constant support, encouragement, and friendship. She saw my love for teaching and chemical education at an early time in my graduate career, and has gone out of her way to foster that passion of mine ever since. I would also like to thank the NMR and MS facility staff including Sage Bowser, Viswanathan Elumalai, Bhaskar Gadugu, and Damodaran Krishan for their technical support and advice.

I want to specifically thank John Widen and Joe Hexum, as well as Dr. Harki, at the University of Minnesota, for their collaboration on this work. Working as part of a collaboration has elevated the success of this research and I am grateful for their contributions and input. I am also grateful for the efforts of former Brummond Group members Bo Wen and Francois Grillet whose work provided the foundations for my chemistry.

Finally, I must recognize other former and current Brummond Group members whose moral and technical support were vital to my success and sanity. Specifically, I would like to thank Dr. Laura Kocsis, for her wisdom and mentorship even after leaving Pittsburgh, Lauren Parrette for her friendship, proofreading, and willingness to work next to me every day (even the bad days!), Ashley Bober for weekly baked goods and a listening ear, as well as Paul Jackson, Joe Burchick, Humair Omer, and Justin Proto for their everyday support and collaboration.

My graduate school experience also would not have been possible without the love and support of my family and friends outside of the University of Pittsburgh. First, I want to thank my parents for their willingness to selflessly celebrate my successes and comfort me in harder times. Their never-ending encouragement and faith in me has always been the foundation for me to push forward. Next, I want to thank my church community of South Side Anglican Church and its pastors Sean and Kate Norris. Even when work limited my free time, their constant friendship, prayers, and reminders of God's grace sustained me through my darkest days.

Finally, I must thank my husband, Dan Wells. I am truly struggling to come up with the words to express how grateful I am to have him as my teammate! I have no doubt that I could not have accomplished my degree without his love, encouragement, patience, and comic relief through both the best and worst days. I cannot wait to see what is next!

1.0 AN ALLENIC PAUSON-KHAND APPROACH TOWARDS 6,12-GUAIANOLIDES

This chapter is partially based upon results published in: Wells, S. M.; Brummond, K. M. Conditions for a Rh(I)-catalyzed [2+2+1] cycloaddition reaction with methyl substituted allenes and alkynes. *Tetrahedron Letters*, **2015**, 56, 3546-3549. Memorial Symposium-in-Print for Harry Wasserman.

1.1 INTRODUCTION

For decades, natural products (NPs) have been a rich source of inspiration for the development of new drugs, as their structural frameworks are considered to be privileged for biological activity.¹ One class of NPs, sesquiterpene lactones (SLs), are a large group of metabolites with 15-carbon frameworks, consisting of 3 isoprene units (5 carbons), and a lactone ring. SLs exemplify high structural diversity and a wide range of biological properties, with potent anti-inflammatory and anticancer effects being of particular interest.² Currently a few SLs are undergoing clinical trials for cancer therapies (Figure 1). Thapsigargin (**1.1**) is a potent sarco/endoplasmic reticulum Ca^{2+} -ATPase (SERCA) inhibitor which leads to apoptosis. A prodrug derivative of **1.1**, under the name of Mipsagargin, has been developed to target the blood vessels of cancer cells and is undergoing phase II clinical trials.³ Artemisinin (**1.2**) is an

antimalarial compound, originally extracted for this use in the 1970's by Youyou Tu, who was awarded a share of the 2015 Nobel Prize in Physiology or Medicine for this effort.⁴ Artemisinin has also shown anticancer activity, and is undergoing clinical trials for breast and colorectal cancers.² Finally, a dimethylamino analog of parthenolide (**1.3**) is being tested for targeting human leukemia stem cells.⁵

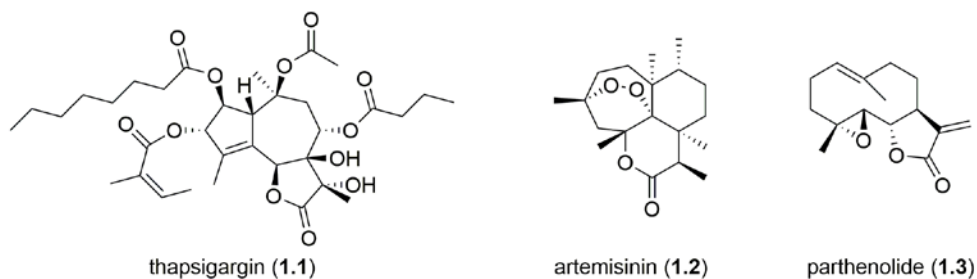
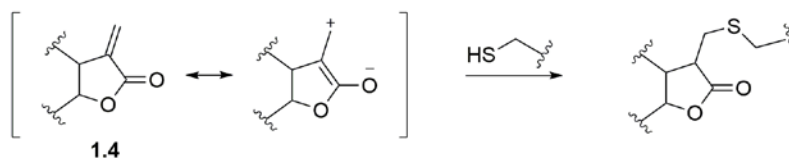


Figure 1. Medicinally relevant sesquiterpene lactones.

Even with these successful examples and prevalent biological activities of other SLs, realization and development for the class of molecules as potential pharmaceuticals has been slow overall. One major contribution to this slow progression is the presence of reactive α -methylene- γ -butyrolactones (**1.4**) in a vast majority of the SLs, and as seen in parthenolide (**1.3**). This moiety is present in 3% of all NPs.⁶ Despite this evolutionary prevalidation, the α -methylene- γ -butyrolactone (**1.4**) has been classified as a covalent modifier, due to its ability to undergo hetero-Michael addition reactions with biological nucleophiles (Scheme 1). While thiol alkylating events are often responsible for the biological activities of α -methylene- γ -butyrolactone containing SLs, these events also contribute to the toxicity of the compounds.⁷



Scheme 1. Mechanism for a Michael-type addition of a sulfhydryl group to an α -methylene- γ -butyrolactone (**1.4**).

Conventional non-covalent drugs inhibit their target protein through reversible, non-covalent binding interactions. Covalent inhibitors undergo these non-covalent interactions, but also undergo a bond-forming reaction with the protein to form a stable linkage that is irreversible within the protein's half-life.⁸ This mode of inhibition has traditionally been avoided due to the safety concern that poor selectivity of the electrophilic groups inherently leads to toxicity. However, many successful drugs operate by a covalent mechanism, including aspirin and penicillin. In fact, at this time, there are at least 42 approved drugs that operate by a covalent mechanism.^{8c} The mechanisms of action for many of these drugs were discovered after their clinical abilities had been established. Covalent inhibitors are only recently becoming the focus of drug development programs due to their potential for increased biochemical efficiency compared to non-covalent drugs; covalent binding may lower the development of drug resistance, allow for lower dosages, overcome competing endogenous non-covalent interactions, and could address targets with shallow binding sites.^{8c} To overcome the inherent toxicity risks, development teams are focusing on selectivity for specific binding sites and tuning the reactivity of the covalent modifiers for specific covalent binding events.^{8b} For all potential covalent inhibitors, the mechanism of action and possible non-specific, or off-target activity must be thoroughly examined.

One event that led to increased interest in SLs as potential drug targets, despite their covalent modifier classification, was the discovery that helenalin (**1.7**) (Figure 2), along with other SLs, inhibits the central transcription factor NF- κ B, which plays a major role in immune response, cell proliferation, cell death, and inflammation.⁹ Inhibition of NF- κ B has emerged as a potential strategy for cancer therapy, as overstimulation of NF- κ B has been shown to affect all 6 hallmarks of cancer; self-sufficiency in proliferative growth signals, insensitivity to growth

inhibition, evasion of apoptosis, limitless replicative potential, induction of angiogenesis and finally, induction of invasion and metastasis.¹⁰ Parthenolide (**1.3**) was also shown to inhibit NF- κ B and activate p53, a DNA-binding transcription factor that leads to tumor suppression, simultaneously, thereby increasing its therapeutic potential.¹¹ The NF- κ B inhibition potential of SLs lead to a series of studies to determine their mechanism of inhibition (See Section 4.1).

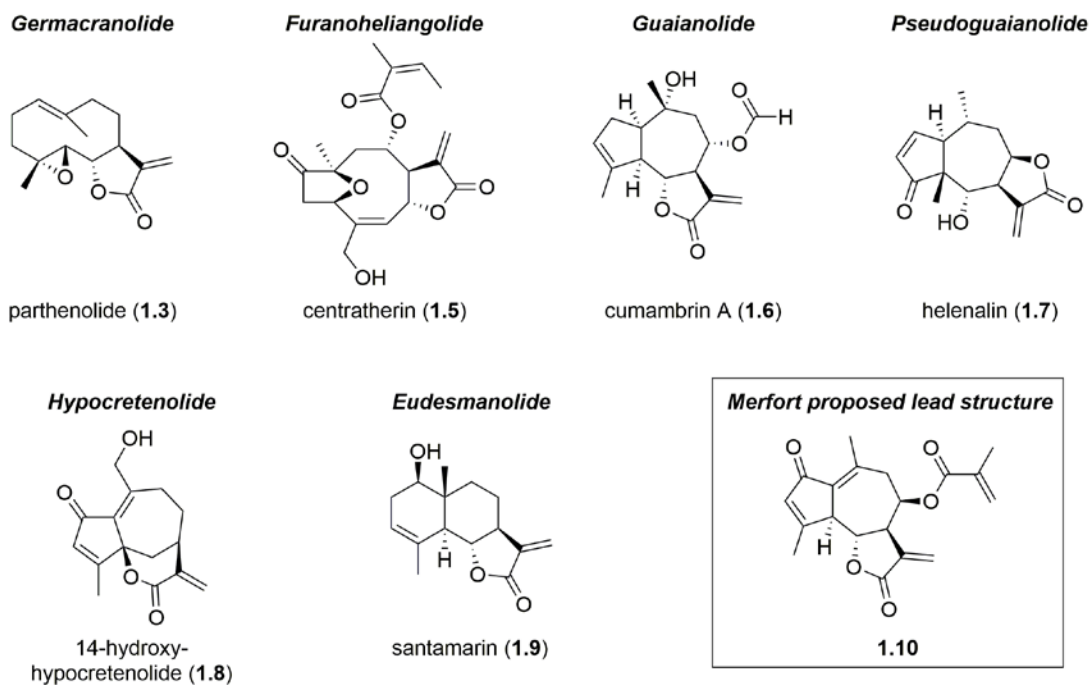


Figure 2. Selected SLs representing families that inhibit NF- κ B, and the 6,12-guaianolide analog **1.10** proposed as a lead inhibitor by Merfort.

SL subclasses are divided by carbocyclic frameworks. Compounds in the germacranolide, furanoheliangolide, guaianolide, pseudoguaianolide, hypocretenolide, and eudesmanolide families have all been shown to inhibit NF- κ B (Figure 2). A quantitative structure activity relationship (QSAR) study performed by Irmgard Merfort evaluated the structural and chemical features of 103 SLs in these families and their ability to inhibit NF- κ B. For all the SL families, inhibition ability greatly correlated with the presence of alkylating centers such as the α -methylene- γ -butyrolactone. While the QSAR study resulted in limited correlations for many of

the SL families, guaianolides were identified as having good correlation coefficients for other structural coding parameters, such as lipophilicity. Merfort later proposed a potential lead SL analog **1.10** for potent NF- κ B inhibition consistent with the guaianolide framework.⁷

Guaianolides represent the largest natural product class of SLs. This family is made up of a 5,7,5-fused ring system with methyl or methylene groups at the C4, C10, and C11 positions. Guaianolides can be categorized further into 6,12- and 8,12-guaianolides, based upon the position of the lactone ring (Figure 3).¹² The only difference between guaianolides and pseudoguaianolides is the placement of one of the methyl substituents, which is found on C5 for pseudoguaianolides rather than C4. The 6,12-guaianolides have become the focus of our synthetic efforts, consistent with the proposed lead structure **1.10**.

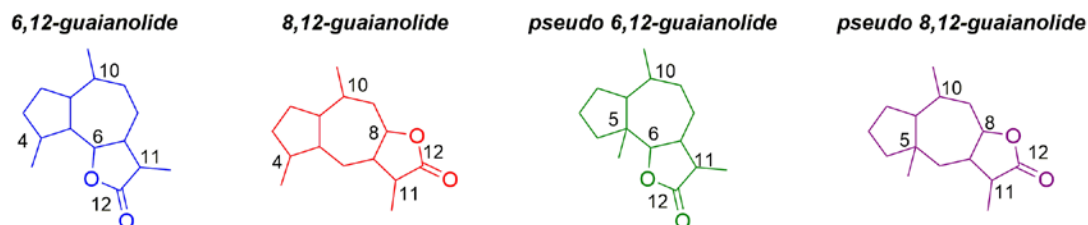


Figure 3. Frameworks of the guaianolide and pseudoguaianolide SL families.

Our focus on the 6,12-guaianolide framework was also validated by a chemical space analysis performed by Oprea and coworkers that identified a 6,12-guaianolide as a lead NP in underrepresented chemical space with medicinal potential.¹³ The biologically relevant chemical space was analyzed by comparing the physicochemical properties (size, shape, polarizability, lipophilicity, polarity, flexibility, rigidity, and hydrogen bonding capacity) of NPs, with bioactive medicinal compounds from the database WOMBAT. This allowed for identification of regions occupied by NPs, with favorable physiological properties, but were lacking occupancy by medicinally relevant molecules. A 6,12-guaianolide was identified as a lead in one of these underrepresented regions. In addition, Euclidean distances (EDs) were calculated between NPs

guaianolide framework being achieved from either the germacranolide or eudesmanolide SL frameworks (Figure 5).

Parthenolide (**1.3**), a germacranolide with potent biological activity, can be extracted from the root bark of *Magnolia delavayi* in bulk quantities (3.1-8.0%), and is also commercially available, making it a common starting material for biomimetic semisynthesis.¹⁵ Parthenolide (**1.3**) was utilized as the starting material in a 3-step synthesis of arglabin (**1.15**), which has a low bioavailability from its natural source of *Artemisia glabella* (0.27% yield).^{15b} The transformation from the germacranolide framework of **1.3** to the 6,12-guaianolide framework of micheliolide (**1.14**) is achieved under the acidic medium of *p*-TSA in DCM. Epoxidation of **1.14**, followed by dehydration afforded arglabin (**1.15**) in an overall 45% yield (Scheme 2).

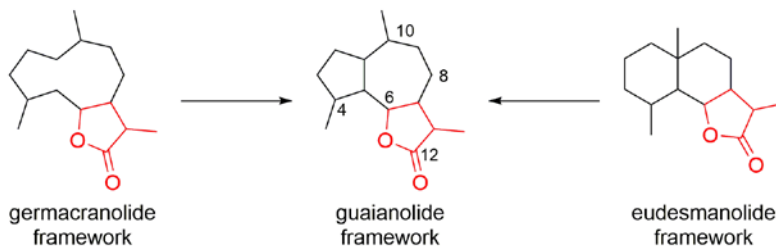
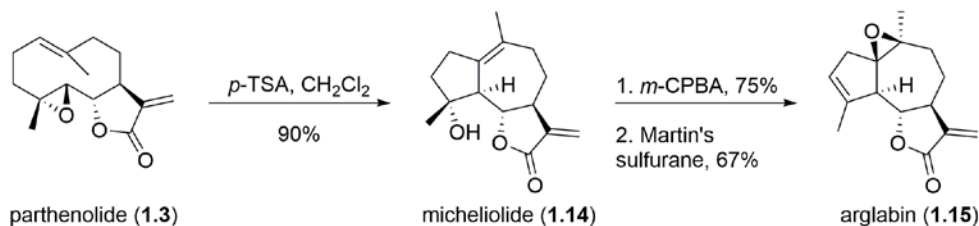


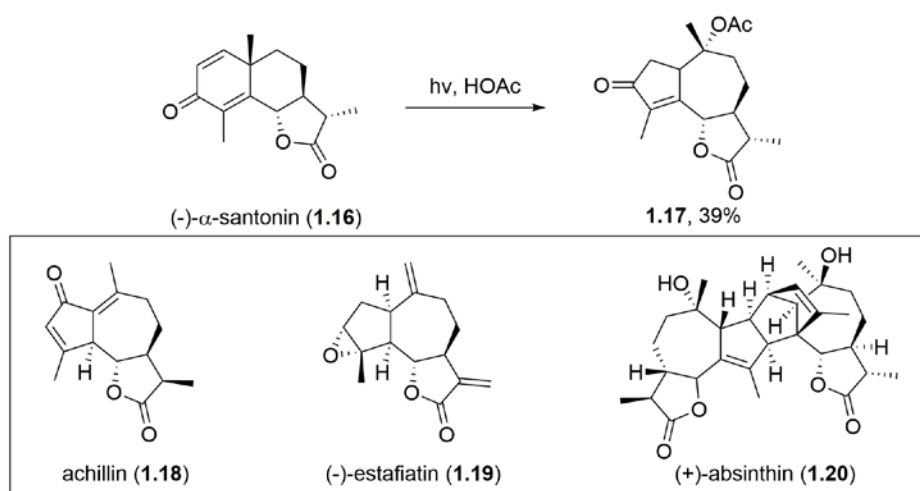
Figure 5. Semisynthetic approaches to the 6,12-guaianolide framework.



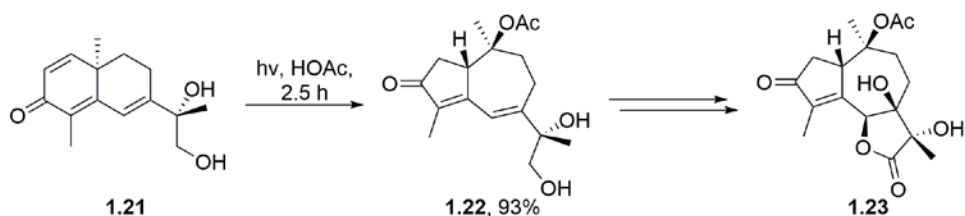
Scheme 2. Three step synthesis of arglabin (**1.15**) from parthenolide (**1.3**).

(-)- α -Santonin (**1.16**), is an abundant and commercially available eudesmanolide and represents the most widely used method for accessing guaianolides. Photochemical rearrangement of **1.16** in the presence of a protic solvent, such as acetic acid, affords guaianolide analog **1.17** (Scheme 3).¹⁶ This transformation has been applied to numerous guaianolide natural

product syntheses, including achillin (**1.18**), (-)-estafiatin (**1.19**), and dimerized guaianolide (+)-absinthin (**1.20**).¹⁷ Structural variations of santonin (**1.16**) have also undergone photochemical rearrangements. For example, in efforts towards the synthesis of thapsigargin analogs, photoirradiation of **1.21** in the presence of acetic acid gave **1.22** in 93% yield. Hydroazulene **1.22** was taken on to give 7,11-dihydroxyguaianolide analog **1.23** (Scheme 4).¹⁸ This strategy of constructing 5,7-hydroazulene core, followed by installation of the lactone ring near the end of the synthesis is a common approach toward 6,12-guaianolides.



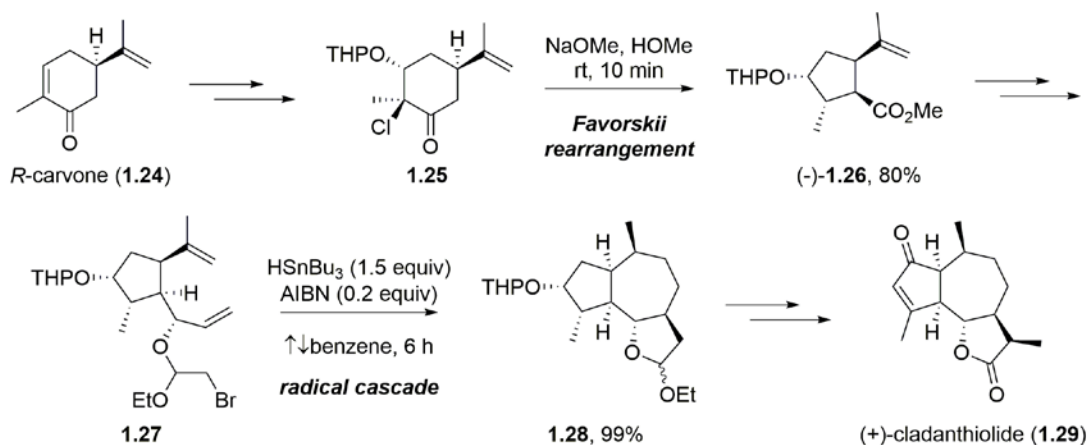
Scheme 3. Access to the guaianolide framework from (-)- α -santonin (**1.16**) and representative natural products synthesized via this method.



Scheme 4. Photochemical rearrangement of **1.21** toward 7,11-dihydroxyguaianolide analog **1.23**.

In addition to semisynthesis, development of total synthetic methods for the construction of guaianolides from commercially available building blocks is an important area of research. Multiple routes to building the 5,7,5-fused ring system have been employed. The Favorskii

rearrangement is a common strategy for the stereoselective synthesis of functionalized 5-membered rings, and has been applied in the early stages of multiple guaianolide total syntheses. In the synthesis of (+)-cladanthiolide (**1.29**),¹⁹ functionalization of *R*-carvone (**1.24**) affords **1.25**, which under basic conditions rearranges to afford 5-membered ring (-)-**1.26** in 80% yield.²⁰ This synthesis also features a unique construction of the 7-membered ring of **1.28**, which is obtained from **1.27** in 99% yield via a radical cascade.

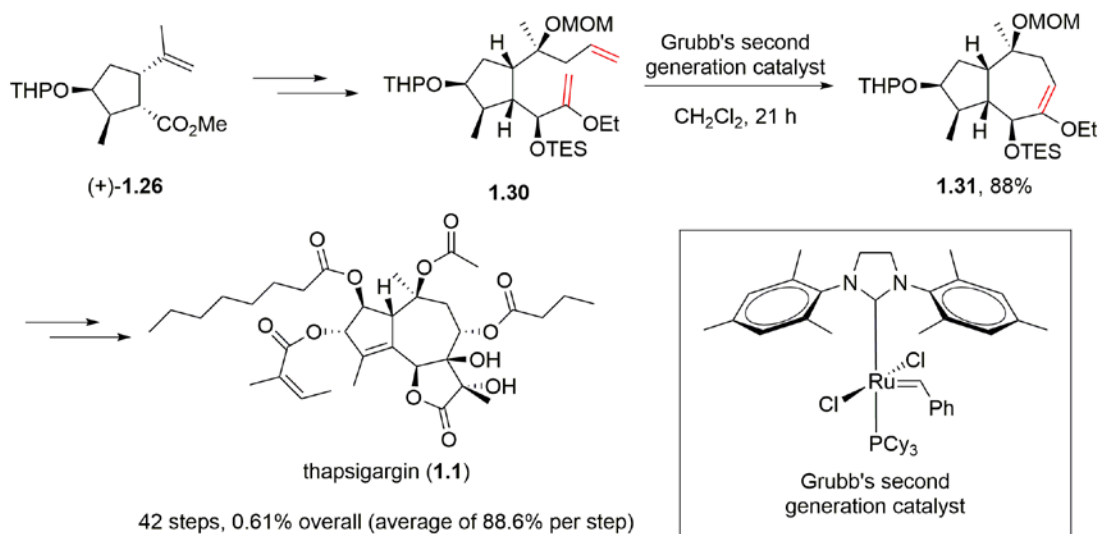


Scheme 5. Access to highly functionalized 5-membered ring (-)-**1.26** via the Favorskii rearrangement and a radical cascade approach toward (+)-cladanthiolide (**1.29**).

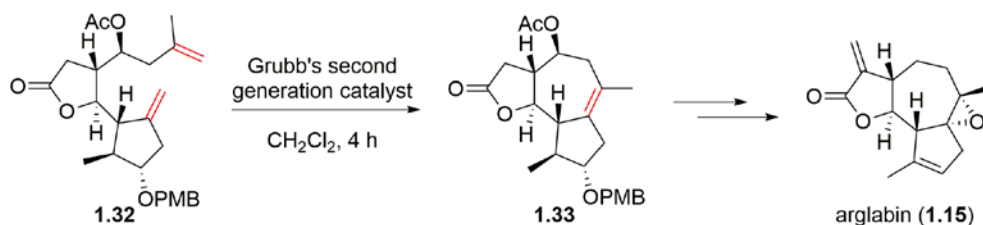
The 2007 total synthesis of thapsigargin (**1.1**), accomplished by Ley and coworkers, also begins with the Favorskii rearrangement; (+)-**1.26** was prepared from *S*-carvone. However, the 7-membered ring was constructed using a ring closing metathesis (RCM). RCM precursor **1.30** was reacted with Grubb's second generation catalyst in DCM for 21 h to afford the 5,7-fused ring system **1.31**, which was taken on to complete the synthesis of thapsigargin (**1.1**) in 42 steps overall (Scheme 6).²¹

RCM has become a popular method for 7-membered ring construction within guaianolides and is not unique to the described thapsigargin synthesis. The total synthesis of

arglabin (**1.15**) also showcases this approach; RCM precursor **1.32** containing both 5-membered rings undergoes RCM to form the 7-membered ring of **1.33** (Scheme 7).²²

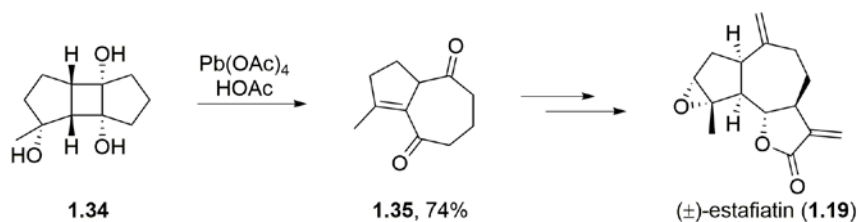


Scheme 6. RCM approach for 7-membered ring formation in the total synthesis of thapsigargin (**1.1**).



Scheme 7. RCM approach to arglabin (**1.15**).

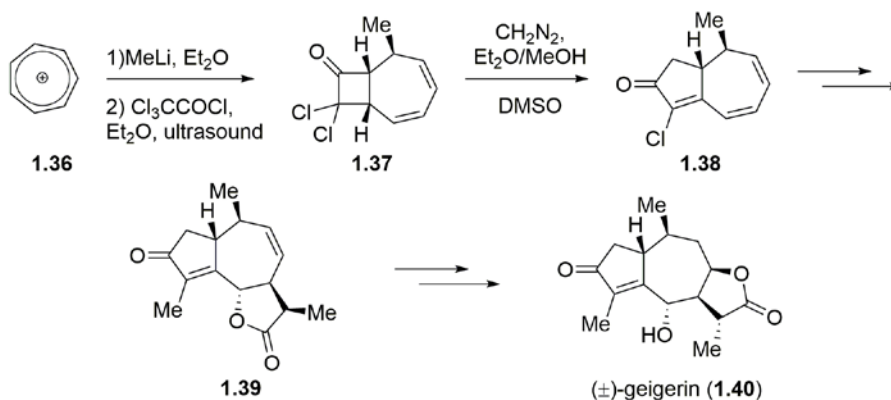
The 5,7-hydroazulene core of guaianolides has also been accessed by ring expansion of a 5,4,5-fused ring system. α -Diol oxidative cleavage of **1.34** using $\text{Pb}(\text{OAc})_4$ affords **1.35**, which was used to access (-)-estafiatin (**1.19**) (Scheme 8).²³



Scheme 8. Synthesis of (\pm)-estafiatin (**1.19**) via an oxidative ring expansion.

Another strategy to synthesize guaianolides involves forming the 5,7-hydroazulene core from a commercially available 7-membered ring, followed by installation of the lactone ring. One example of this method is the transformation of tropylium cation **1.36** to hydroazulene **1.38** via a [2 + 2] cycloaddition, ring expansion, and elimination sequence. **1.38** was taken on towards geigerin (**1.40**). Interestingly, this synthesis also features a 6,12-guaianolide framework **1.39** as an intermediate in route to the 8,12-guaianolide **1.40** (Scheme 9).²⁴

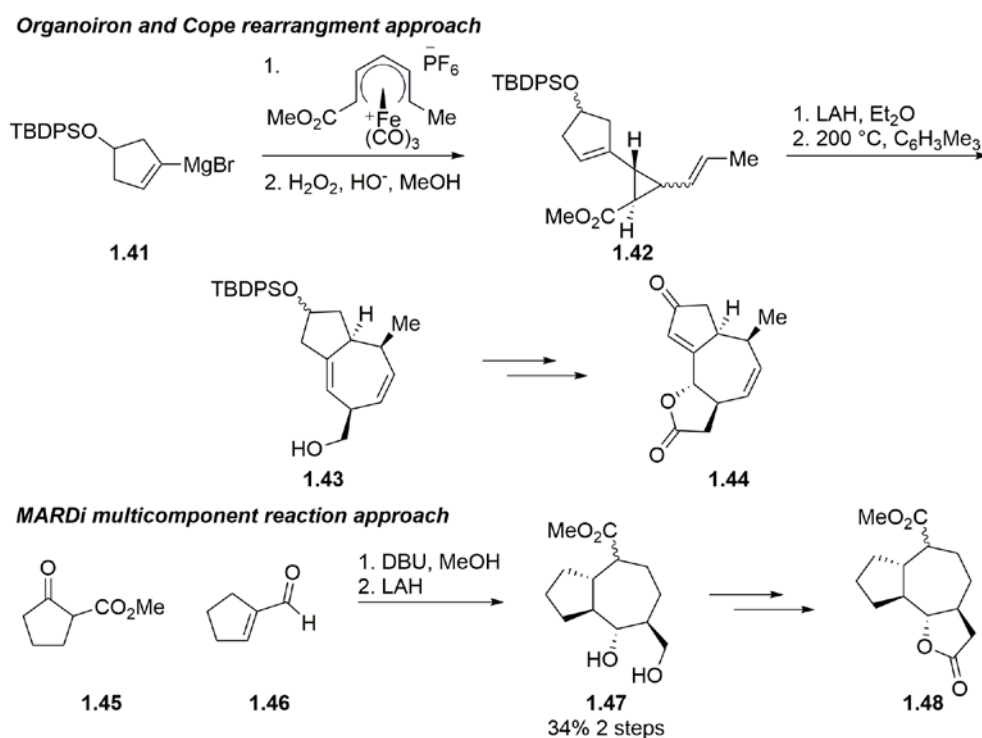
More recently, perhaps due to a resurgence in the interest in the guaianolides for pharmaceutical applications, researchers have been developing diversity oriented approaches towards the guaianolide framework, rather than attempting to synthesize specific targets.²⁵ This has especially been observed for synthetic efforts towards the 5,7-hydroazulene core of the guaianolide framework, as the lactone is typically the most accessible ring.



Scheme 9. Total synthesis of (±)-geigerin **1.40** from tropylium ion **1.36**.

Novel approaches for the synthesis of 7-membered rings are being applied to cyclopentane containing systems in order to demonstrate their feasibility for synthetic efforts toward the hydroazulene portion of guaianolides. For example, addition of stabilized alkenyl nucleophiles, such as Grignard reagents, to (1-methoxycarbonylpentadienyl)iron(1+) cation, followed by oxidative decomplexation, affords divinylcyclopropanes, which then undergo a Cope rearrangement to give functionally dense 7-membered rings.²⁶ This methodology was

applied to the formation of 5,7-fused ring system **1.43** by employing cyclopentenyl nucleophile **1.41** (Scheme 10).²⁷ Alternatively, the Michael-aldol-retro-Dieckmann (MARDi) cascade multicomponent reaction is an anionic 2-carbon ring expansion of the Dieckmann ester **1.45**, for the synthesis of stereodefined cycloheptanols.²⁸ Reaction of ester **1.45** and cyclopentene carbaldehyde **1.46** with DBU, followed by selective reduction of one ester moiety affords **1.47**, taken on to give the guaianolide framework **1.48** (Scheme 10).²⁹ Both of these methodologies were described as showing feasibility for synthesis of more biologically relevant guaianolide analogs.

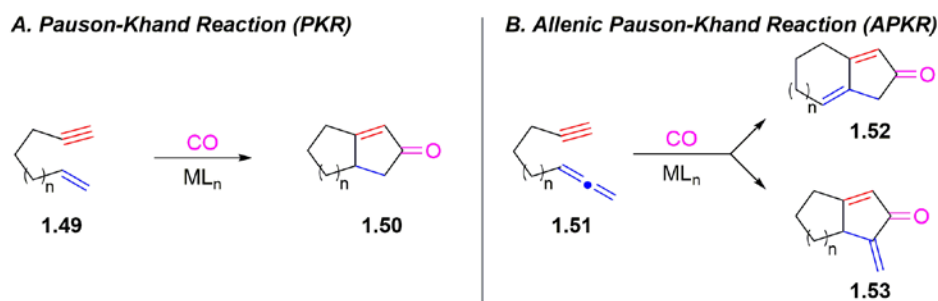


Scheme 10. Application of novel 7-membered ring syntheses to guaianolide analogs.

1.1.2 Development and applications of the allenic Pauson-Khand reaction

The Pauson-Khand reaction (PKR) is a formal [2 + 2 + 1] cyclocarbonylation reaction between an alkyne, an alkene, and a carbon monoxide molecule (Scheme 11, A). The first example, reported in the early 1970's, was an intermolecular cyclocarbonylation between a dicobalt hexacarbonyl complexed alkyne and norbornene to generate a fused cyclopentenone.³⁰ The discovery of an intramolecular version of the reaction significantly increased the synthetic utility by rendering the reaction regioselective and expanding the scope beyond strained alkenes. Many researches have embraced the challenge of increasing the efficiency and scope of the PKR, which is now one of the most popular methods for cyclopentenone formation. These advances include development of catalytic conditions, alternative metal mediators (including but not limited to Rh, Mo, Ru, Ti, Fe, Ir, and Zr), asymmetric conditions, effective intermolecular reactions, and solid supported protocols.³¹

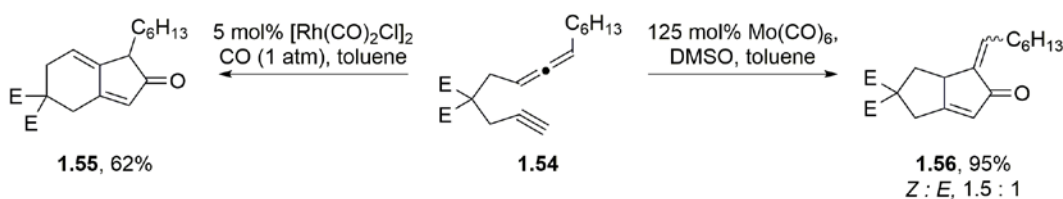
A variation of the PKR where the alkene is replaced with an allene emerged in the late 1990's. The allenyl moiety contains two pi bonds, both of which could undergo the cyclocarbonylation reaction. Reaction with the distal double bond leads to the formation of 4-alkylidene cyclopentenone **1.52**, where reaction with the proximal double bond results in α -alkylidene cyclopentenone **1.53** (Scheme 11, B).



Scheme 11. General intramolecular Pauson-Khand reaction and allenic Pauson-Khand reaction.

At first, regioselectivity between the distal and proximal double bond of the allene was substrate dependent. A cobalt carbonyl mediated allenic Pauson-Khand reaction (APKR) of allene-ynes, promoted by NMO, gave mixtures of the corresponding 4-alkylidene and α -alkylidene cyclopentenones, except for trisubstituted allenes, which gave the α -alkylidene system.³² When mono-, 1,3-di-, and 1,1,3-trisubstituted allenyl alkynes were reacted with stoichiometric amounts of molybdenum carbonyl, selective reaction with the proximal double bond afforded α -alkylidene cyclopentenones, while 1,1-disubstituted allenyl alkynes reacted selectively with the distal double bond to afford 4-alkylidene cyclopentenones.³³

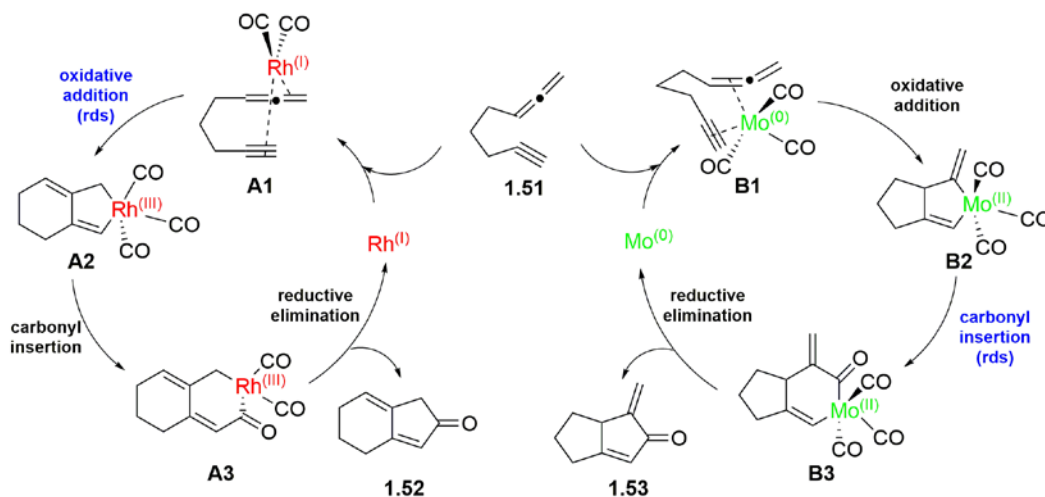
However, in an effort to identify reaction conditions that would allow for double bond selectivity independent of the substrate, it was discovered that catalytic rhodium biscarbonyl chloride dimer ($[\text{Rh}(\text{CO})_2\text{Cl}]_2$) reacted selectively with the distal double bond whereas molybdenum carbonyl reacted selectively with the proximal double bond.³⁴ For example, when diester allene-yne **1.54** is reacted with $[\text{Rh}(\text{CO})_2\text{Cl}]_2$ (5 mol%), dienone **1.55** is formed selectively, and when **1.54** is reacted with $\text{Mo}(\text{CO})_6$ (125 mol%), exocyclic methylene **1.56** is afforded (Scheme 12).^{34b}



Scheme 12. Diverging reactivity of **1.54** when using $[\text{Rh}(\text{CO})_2\text{Cl}]_2$ and $\text{Mo}(\text{CO})_6$.

This observation was later explained through density functional theory computational modeling of potential energy pathways with both metal mediators. For both metals, the generally accepted mechanism of 1) coordination of the metal to the alkene and alkyne, 2) oxidative addition, 3) carbonyl insertion, and 4) reductive elimination was used (Scheme 13). For the

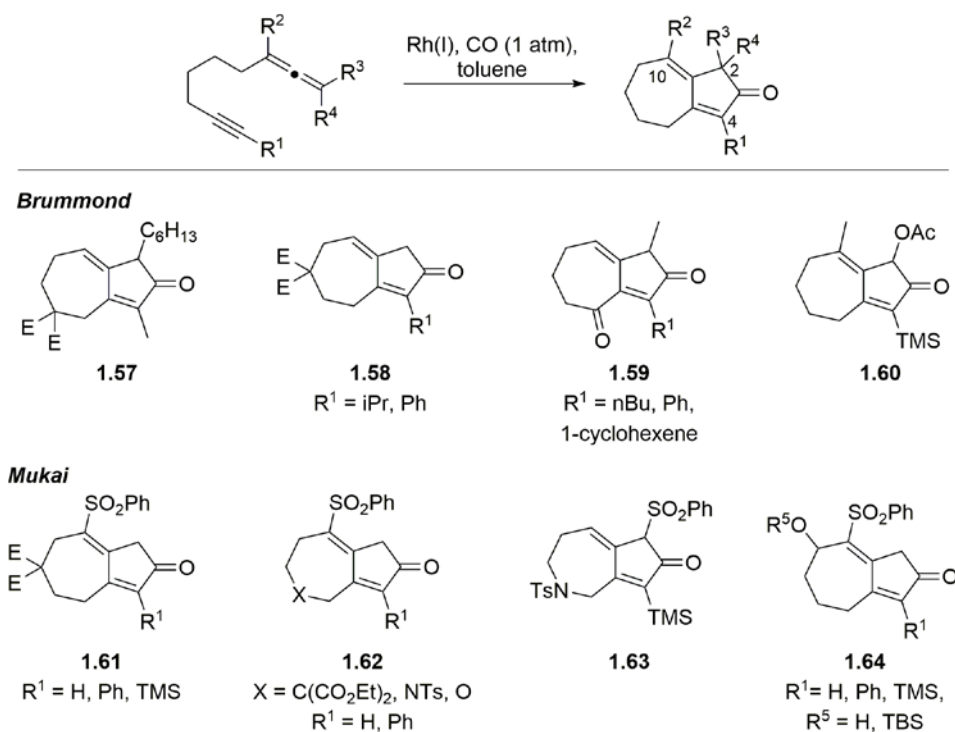
rhodium catalyzed pathway, it was determined that oxidative addition of the allene-yne to the Rh(I) to give Rh(III) complex **A2** had the highest energy barrier of the entire pathway (16.8 kcal/mol), and was therefore the rate determining step. As a result, the product is determined at an early stage in the reaction where the rhodium has a square planar geometry as seen in **A1**. Coordination to the distal double bond is favored by 5.5 kcal/mol over the proximal double bond, eventually leading to formation of the 4-alkylidene **1.52**. In contrast, calculations for the molybdenum pathway showed that CO insertion from **B2** to **B3** is the rate determining step. For oxidative addition, molybdenum has a trigonal bipyramidal geometry (**B1**), and therefore, reaction with the proximal double bond of the allene is energetically preferred by 4.8 kcal/mol over the distal double bond. Even the highest energy in this pathway, for the CO insertion step, is 2.5 kcal/mol more favorable than the oxidative addition with the distal double bond. This leads to the experimentally observed selective formation of α -alkylidene cyclopentenones (**1.53**).³⁵



Scheme 13. Diverging mechanisms of the APKR with rhodium and molybdenum lead to regioselectivity.

The observed regioselectivity displayed for rhodium catalyzed Pauson-Khand reactions of allene-ynes motivated the application to fused 5,7-bicyclic ring systems from an extended carbon tether. Synthesis of these bicyclo[5.3.0]decadienones had only been previously achieved

as a mixture of products or with a narrow substrate scope. Brummond^{34b, 36} and Mukai³⁷ independently exploited the selectivity of Rh(I) catalysts for the distal double bond to demonstrate the generality of this method for the synthesis of 5,7-fused systems (see Scheme 14 for selected examples). A variety of allene and alkyne substitutions were tolerated including mono-, di-, and tri-substituted allenes, as well as both terminal and substituted alkynes. Mukai focused on allenes substituted with phenylsulfonyl groups due to their ease of preparation (**1.61**-**1.64**). Various functionalities in the tethers were also well-tolerated, including diesters (**1.57**, **1.58**, **1.61**), carbonyls (**1.59**), heteroatoms (**1.62**), and oxygen substituents (**1.64**).

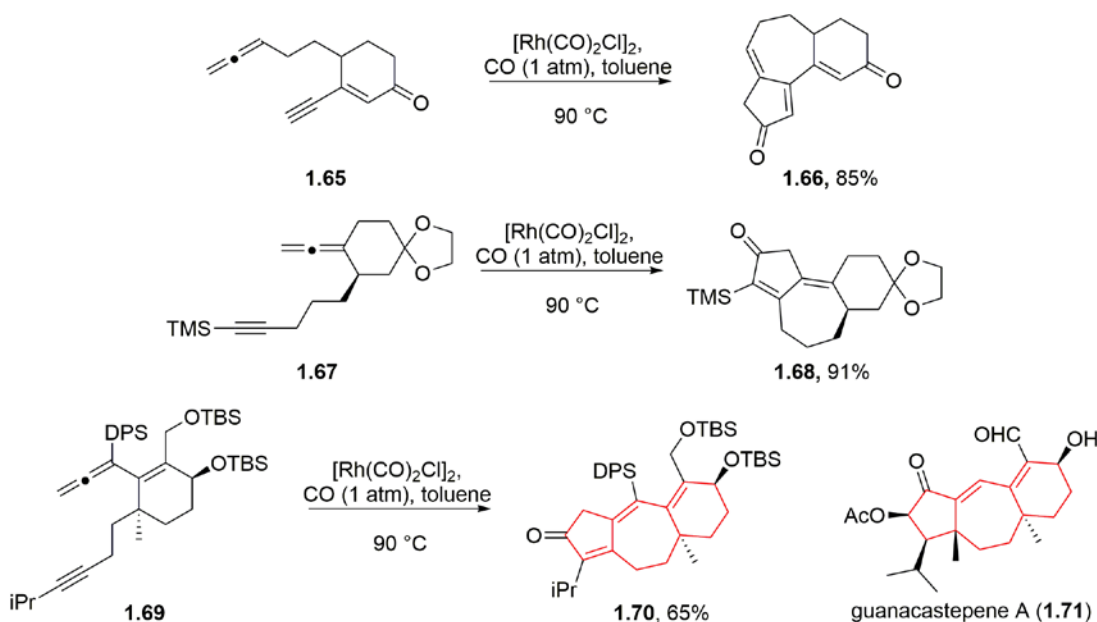


Scheme 14. Synthesis of bicyclo[5.3.0]decadienones via a Rh(I)-catalyzed allenic Pauson-Khand reaction.

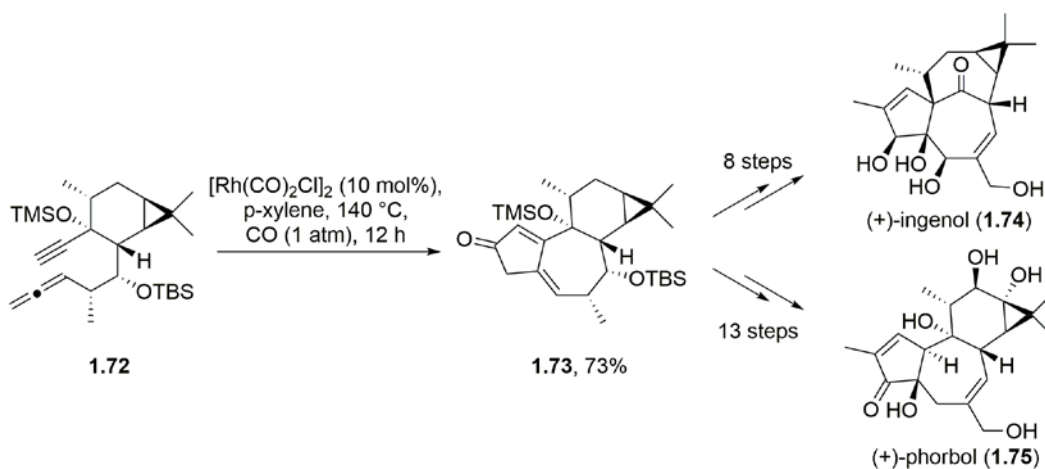
By incorporating cyclohexane rings into the allene-yne tethers, Brummond also demonstrated the capability of the APKR to access linearly and angularly fused 6,7,5-tricyclic frameworks (Scheme 15).^{36a, 38} Some of these examples are among the highest yielding APKR results, as seen for the synthesis of **1.66** and **1.68**, formed in 85% and 91% yield respectively.³⁸

The potential of the APKR for application to biologically relevant carbocyclic frameworks was demonstrated by the cyclocarbonylation of allene-yne **1.69** to afford **1.70**; this example was performed in an effort towards the synthesis of NP guanacastepene A (**1.71**).³⁹

The dienone moiety generated by the APKR is also optimally positioned for further functionalization of the 5,7-ring system towards biologically relevant systems. This has been demonstrated by functionalization of the dienone C1-C10 π -bond via hydrogenation, dihydroxylation, and epoxidations, as well as by addition to the carbonyl.³⁸⁻⁴⁰ In addition, the potential of the APKR and functionalization of dienone moiety towards natural products was demonstrated in the total syntheses of (+)-ingenol (**1.74**) and (+)-phorbol (**1.75**), performed by Baran and coworkers (Scheme 16).⁴¹ APKR precursor **1.72** was constructed from (+)-carene in 5 steps. The APKR reaction was successfully performed on gram scale using $[\text{Rh}(\text{CO})_2\text{Cl}]_2$ (10 mol%) with $\text{CO}(\text{g})$ in xylenes to afford dienone **1.73** in 73% yield. This cycloadduct was functionalized to efficiently afford (+)-ingenol (**1.74**) in 8 steps (14 steps overall), as well as (+)-phorbol (**1.75**) in 13 steps (19 steps overall).



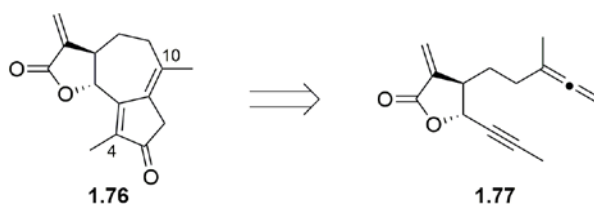
Scheme 15. Selected examples of the APKR towards linearly and angularly fused 6,7,5-tricyclic frameworks.



Scheme 16. An APKR approach toward the total synthesis of (+)-ingenol (**1.74**) and (+)-phorbol (**1.75**).

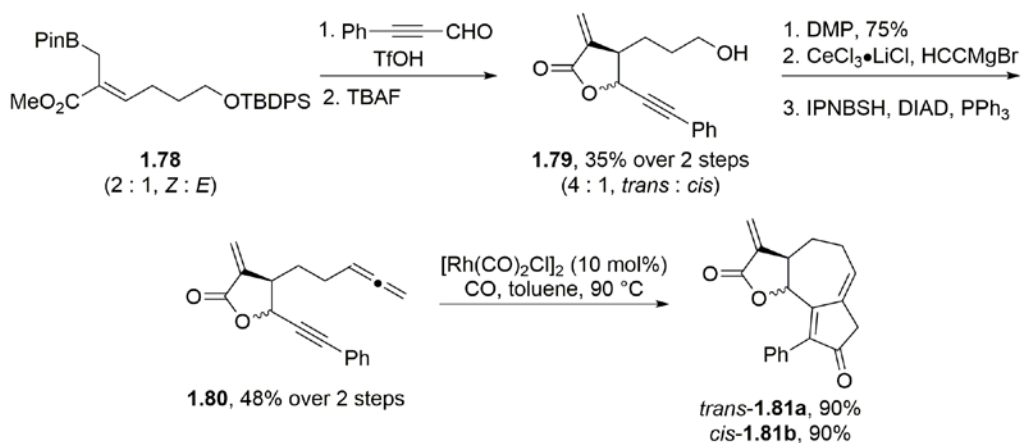
1.1.3 An allenic Pauson-Khand approach toward guaianolides.

As mentioned, the synthesis of tricyclic fused ring systems are among the highest yielding APKR examples. In turn, the Brummond group proposed that the 5,7,5-fused ring system of 6,12-guaianolides, represented by **1.76**, could be accessed in a similar fashion from a lactone containing allene-yne tether **1.77** (Scheme 17). Some hesitation with respect to the reactivity of α -methylene- γ -butyrolactones, and their stability in the APKR was acknowledged during the design of this approach.⁴² Motivation toward this approach was also encouraged by the influential work of Dennis Hall, who developed an allylboration/ lactonization sequence for the synthesis of substituted α -methylene- γ -butyrolactones.



Scheme 17. Retrosynthetic analysis of 6,12-guaianolide framework **1.76**.

To establish the feasibility of the proposed route to the 6,12-guaianolide framework, allene-yne **1.80** was made (Scheme 18). The lactone ring was formed via an allylboration/lactonization reaction between allylboronate **1.78** and phenylpropynal as a mixture of the *trans*- and *cis*-lactone rings (4:1 ratio). The TBDPS group was removed by treatment with TBAF to afford alcohol **1.79**. The allene moiety of **1.80** was installed in 3 steps from **1.79**. The *trans*- and *cis*- lactones can either be separated as **1.79** or as the allene-yne **1.80**. The isomers of **1.80** were subjected separately to the APKR to afford *trans*-**1.81a** and *cis*-**1.81b**, both in 90% yield. The α -methylene- γ -butyrolactone was unaffected throughout the sequence of reactions from **1.79** to **1.81**, including the high yielding APKR.

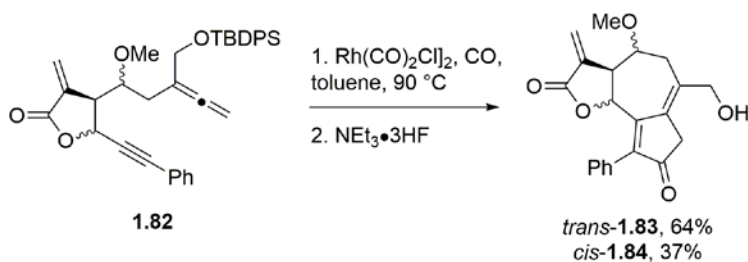


Scheme 18. An APKR approach to the 5,7,5-fused ring system **1.81**.

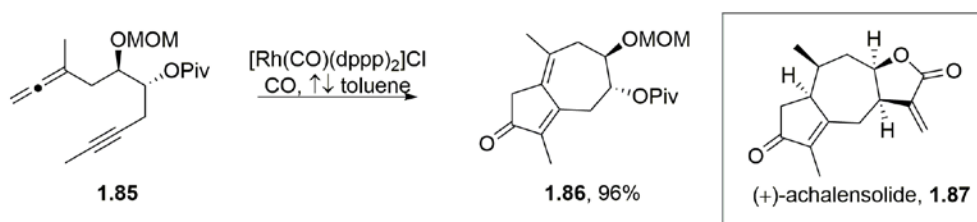
The APKR approach was also successfully applied to guaianolide analogs **1.83** and **1.84**,⁴³ with increased oxygen functionality and therefore, molecular complexity (Scheme 19).⁴⁴ This redox economical synthesis expands the scope of both the allylboration/lactonization as well as the APKR chemistries. For more information on this synthesis, see Section 2.1.

It should be noted that Mukai and coworkers have also utilized the APKR in the synthesis of an 8,12-guaianolide natural product, (+)-achalensolide (**1.87**) (Scheme 20).⁴⁰ However, the APKR was performed on allene **1.85** using a phosphine ligated Rh(I) catalyst,

[Rh(CO)(dppp)₂]Cl to form the hydroazulene core **1.86**. The lactone was installed at a later stage in the synthesis, typical of previous approaches toward guaianolides (Section 1.1.1).



Scheme 19. Synthesis of highly-functionalized guaianolide analogs **1.83** and **1.84** via the APKR.



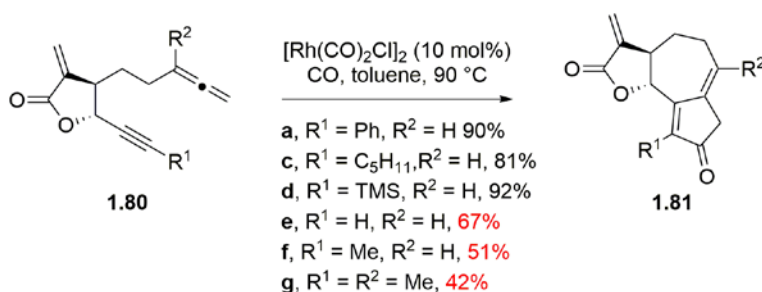
Scheme 20. An APKR approach to 8,12 guaianolide (+)-achalensolide (**1.87**).

1.1.4 Low yielding APKR examples with methyl substituted allene-ynes

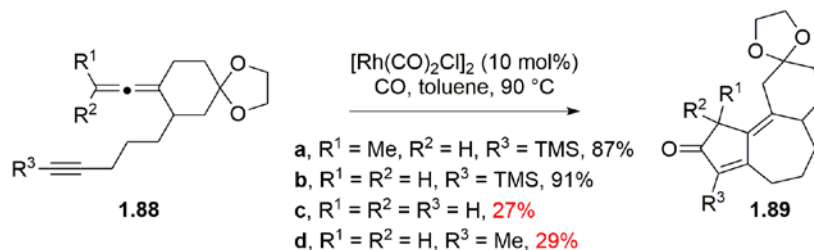
As mentioned, the conversion of α -methylene- γ -butyrolactone containing allene-yne tether **1.80a**, with a phenyl substituted alkyne, to the guaianolide analog **1.81a** is among the highest yielding APKR examples to date. The success of this example, as well as the synthesis of highly functionalized guaianolide analogs **1.83** and **1.84**, establishes the feasibility of this approach toward the guaianolide framework. To show the generality of the approach, the scope of the APKR precursor **1.80** was expanded to include alternative alkynyl and allenyl substitutions (Scheme 21). Pentyl and trimethylsilyl substituted alkynes (**1.80c** and **1.80d**) also gave excellent yields; **1.81c** and **1.81d** were formed in 81% and 92% yields respectively. However, the efficiency of the APKR for a terminal alkyne and a methyl substituted alkyne was

significantly decreased; **1.81e** was afforded in a moderate 67% yield while **1.81f** was produced in 51% yield. The intolerance of methyl substitutions was further magnified when allene-yne tether **1.80g** encompassing a methyl substituted alkyne as well as a methyl substitution on the proximal allene carbon gave the corresponding dienone product **1.81g** in only 42% yield.⁴²

The low efficiency of methyl substituted and terminal alkynes has also been observed in previously reported APKR examples. For the synthesis of 5,7,6-linearly fused ring systems, trimethylsilyl groups on the alkyne afforded the cycloadducts **1.89a** and **1.89b** in excellent yields (87% and 91%), however terminal and methyl substituted alkynes gave significantly lower yields of 27% and 29% for **1.89c** and **1.89d** respectively (Scheme 22).³⁸



Scheme 21. Scope expansion for guaianolide analogs **1.81** reveals sensitivity to methyl substitutions.



Scheme 22. Synthesis of 5,7,6-ring systems **1.89a-d**.

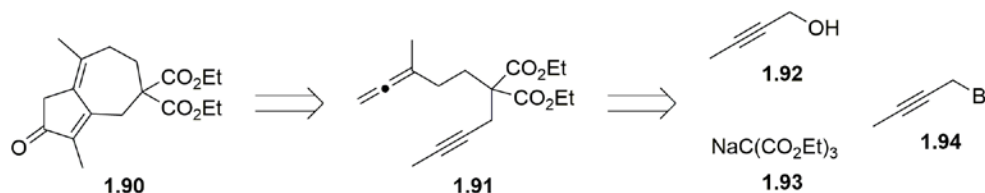
The 6,12-guaianolide framework includes methyl substitutions at the C4 and C10 positions. For our allenic Pauson-Khand approach to this framework, the C4 and C10 methyl substitutions of **1.76** correlate directly to the substituents on the proximal carbon of the allene and the terminus of the alkyne of the allene-yne precursor **1.77** (Scheme 17). Therefore, for this

approach to be optimized for the synthesis of guaianolide analogs, an efficient reaction for methyl substituted substrates is required. Reported herein are our investigations for optimizing the APKR for these methyl substituted allenes and alkynes, as well as terminal alkynes.

1.2 OPTIMIZATION OF THE APKR FOR METHYL SUBSTITUTED ALLENE-YNE TETHERS

1.2.1 Model system substrate design

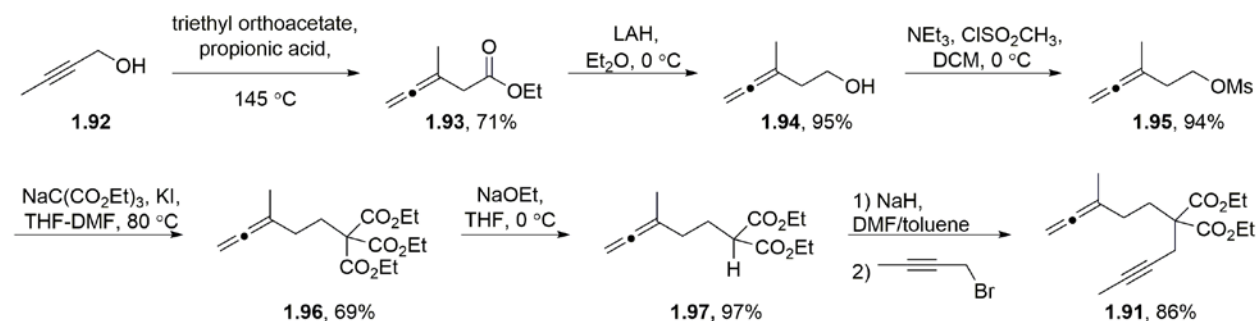
To optimize the allenic Pauson-Khand reaction for allene-yne with methyl substitutions on the proximal carbon of the allene and on the alkyne terminus, we designed a simple dienone system **1.90** as a model for this transformation. Due to the nature of the guaianolide framework, we desired an all-carbon 5,7-ring system, with methyl substituents at the C4 and C10 positions. We envisioned that dienone **1.90** would be accessed from allene-yne **1.91** via the APKR (Scheme 23). The design of the diester tether found in allene-yne **1.91** was inspired by previous work in our group using diester containing allene-yne tethers,^{34b, 36c} and from the work of Rapoport for malonic ester synthesis using tricarboxylates.⁴⁵ The allene-yne **1.91** could be accessed from the three building blocks of 2-butyn-1-ol (**1.92**), which is a precursor for the allene moiety, sodium methanetricarboxylate **1.93**, and propargyl bromide **1.94**.



Scheme 23. Retrosynthetic analysis of dienone **1.90**.

1.2.2 Synthesis of allene-yne 1.91

Conversion of 2-butyn-1-ol **1.92** to allene-yne **1.91** was executed in 6 steps in an overall 36% yield (Scheme 24). A Johnson-Claisen rearrangement of **1.92** in the presence of triethyl orthoacetate and propionic acid provided allenyl ester **1.93** in 71% yield.⁴⁶ Reduction of ester **1.93** with lithium aluminum hydride in diethyl ether at 0 °C gave alcohol **1.94** in 95% yield which was then converted to mesylate **1.95** in 94% yield using triethyl amine and methanesulfonyl chloride. Next, the mesylate group was replaced by the methane tricarboxylate anion to afford **1.96** in 69% yield. Conversion of tricarboxylate **1.96** to the malonate species **1.97** was accomplished in 97% yield using sodium ethoxide in THF. Finally, deprotonation of **1.97** with sodium hydride, followed by the addition of propargyl bromide produced the allene-yne tether **1.91** in 86% yield.



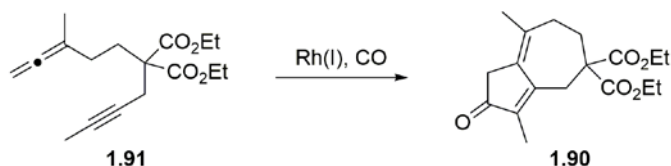
Scheme 24. Synthesis of allene-yne tether **1.91**.

1.2.3 Optimization of APKR with 1.91

With allene-yne **1.91** in hand, the APKR was optimized for this substrate. These efforts are described within and organized by the various reaction parameters examined (Table 1).

Result of previously developed APKR conditions. Initially, the APKR reaction conditions previously developed in our group were employed. Allene-yne **1.91** was heated at 90 °C in 0.1 M toluene with 15 mol% [Rh(CO)₂(Cl)]₂, under a CO atmosphere for 1.5 h, which afforded dienone **1.90** in 27% yield (Entry 1). A significant byproduct was also produced and isolated from the reaction mixture (R_f = 0.38, 20% EtOAc in hexanes). Analysis of the byproduct by ¹H NMR spectroscopy did not allow for structure determination but did reveal signals similar to those present in the ¹H NMR spectrum for dienone **1.90**. Large signals were observed at 4.21 and 1.23 ppm corresponding to the –OCH₂CH₃ groups of the ethyl esters. It was clear that the allene moiety had reacted due to the disappearance of the signal representing the allene hydrogens seen at 4.63 ppm for **1.91**. However, small signals were observed in the aromatic region ranging from 8.22-7.07 ppm. These observations led to a hypothesis that an intermolecular reaction was occurring.

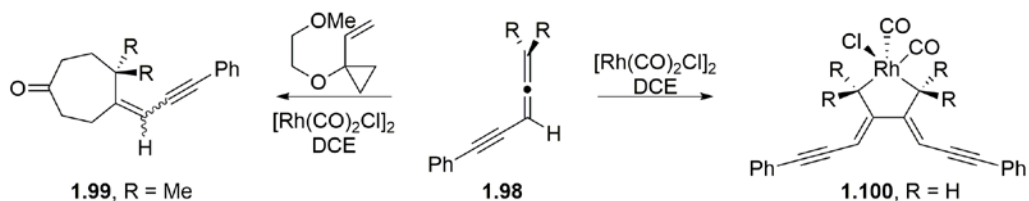
Table 1. Optimization of the APKR for methyl substituted allene-yne **1.91**.



Entry	Rh(I)	Rh(I) mol%	Temp. (°C)	Solvent	Conc. (M)	Time	Yield (%)
1	[Rh(CO) ₂ Cl] ₂	15	90	Toluene	0.1	1.5 h	27
2	[Rh(CO) ₂ Cl] ₂	15	90	Toluene	0.1	1.5h	32 ^a
3	[Rh(CO) ₂ Cl] ₂	15	90	Toluene	0.01	1.5 h	53
4	[Rh(CO) ₂ Cl] ₂	15	110	Toluene	0.01	25 min	57
5	[Rh(CO) ₂ Cl] ₂	15	75	DCE	0.01	30 min	40
6	[Rh(CO) ₂ Cl] ₂	10	110	Toluene	0.01	b	81
7	[Rh(CO)₂Cl]₂	5	110	Toluene	0.01	b	80
8	[Rh(CO) ₂ Cl] ₂	2	110	Toluene	0.01	b	62
9	[Rh(CO) ₂ Cl] ₂	1	110	Toluene	0.01	b	63
10	[Rh(CO) ₂ Cl] ₂	0.1	110	Toluene	0.01	b	23
11	[Rh(CO)(dppp) ₂ Cl]	10	110	Toluene	0.1	21 h	27
12	[Rh(CO)(dppp) ₂ Cl]	10	110	Toluene	0.01	21 h	46
13	[Rh(CO)Cl(dppp) ₂]	10	110	Toluene	0.01	6 h	29

^aTriphenylphosphine polymer bound was used as a Rh(I) scavenger prior to evaporation of reaction solvent. ^b**1.91** was added dropwise over 1.5 h and reaction was complete 15 min after addition period.

Wender has reported that terminal allenes, such as those found in allene-yne **1.91**, were ineffective in Rh(I) catalyzed [5+2] intermolecular cycloadditions between allenes and vinyl cyclopropanes (VCPs).⁴⁷ Computational analysis lead to the proposal that this limitation was a result of two terminal allenes undergoing an intermolecular dimerization, with Rh(I), to form rhodacycle **1.100** (Scheme 25). This process was shown to be irreversible and therefore poisons the Rh catalyst.⁴⁸ Allenes with terminal methyl substitutions, however, readily underwent the desired [5 + 2] cycloaddition for the formation of 7-membered ring **1.99**. This is reasoned that the steric nature of the methyl substitution increases the energy barrier for the competing allene dimerization. This report, as well as other synthetic reports of intermolecular reactions between allenes and alkynes provide precedent for the proposed intermolecular competing pathway, resulting in disappearance of the allene functional group.⁴⁹



Scheme 25. Allene dimerization as a competing process for the [5 + 2] cycloaddition of terminal allenes with VCPs.

Analysis of the byproduct by ESI mass spectroscopy revealed a base peak with an exact mass of 581.3099 ([M+H]) when run in the positive ion mode. The same mass spectroscopy analysis of allene-yne **1.91** and dienone **1.90** revealed [M+H] molecular ion peaks with exact masses of 293.1751 and 321.1687 respectively. Homodimerization of allene-yne **1.91** would result in a substrate with an exact mass of 584.3350 (C₃₄H₄₈O₈), while the mass of a rhodacycle consistent with **1.100** proposed by Wender and Houk would have a theoretical exact mass of 778.1992 (C₃₆H₄₈O₁₀ClRh). The mass data obtained for the byproduct does not assist with

determining a structure, but it supports the speculation a competing intermolecular process, evidenced by the near doubling of the mass compared to allene-yne **1.91** and cycloadduct **1.90**.

Scavenger for Rh(I) catalyst. Upon completion of the reaction, the traditional protocol for reaction work up involves filtration of the toluene reaction solution through a celite plug, rinsing with diethyl ether, followed by solvent evaporation. The celite filtration is not sufficient for removal of the rhodium catalyst, evidenced by the presence of baseline impurities, consistent with the coloration and TLC observations of the $[\text{Rh}(\text{CO})_2\text{Cl}]_2$. We hypothesized that concentration of the cyclocarbonylation adduct in the presence of rhodium could lead to problematic substrate/catalyst interactions, thereby lowering the overall yield of dienone **1.90**. To efficiently remove the rhodium prior to concentration, polymer bound triphenylphosphine was tested as a rhodium catalyst scavenger. After completion of the cyclocarbonylation reaction, the reaction solvent was cooled to rt, followed by addition of polymer bound triphenylphosphine. Stirring at room temperature for 14 h completely scavenged the rhodium, as evidenced by disappearance of the baseline TLC spot. The polymer was removed via vacuum filtration prior to evaporation of the reaction solvent. While this procedure only marginally increased the yield of **1.90** to 32% yield (Entry 2), polymer bound triphenylphosphine was utilized as a scavenger in the work up of subsequent experiments.

Concentration, Solvent, and Carbon Monoxide. Next, a screening of reaction concentrations were performed on small scale reactions (5 mg of **1.91**, 0.017 mmol). We predicted that lower concentrations would reduce formation of the byproduct based upon our hypothesis that it is a result of an intermolecular process. Reaction monitoring was performed by TLC analysis; relative amounts of **1.90** and the undesired byproduct were compared. First, toluene was employed at various concentrations including the standard 0.1 M, 0.02 M, and 0.01

M. TLC observations revealed that as the reaction concentration was diluted, the amount of dienone **1.90** formed increased, while the formation of the unknown byproduct decreased. These qualitative observations were confirmed quantitatively when the APKR reaction of allene-yne **1.91** was performed at 0.01 M in toluene on a larger scale (45 mg of **1.91**, 0.15 mmol) at 90 °C with 15 mol% $[\text{Rh}(\text{CO})_2\text{Cl}]_2$ and a CO atmosphere. The yield of dienone **1.90** increased to 53% (Entry 3). Increasing the temperature to 110 °C shortened the reaction time from 1.5 h to 25 min, and slightly increased the yield of **1.90** to 57% (Entry 4).

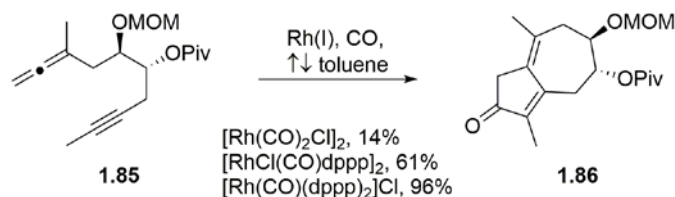
TLC screening was also performed for different solvents including toluene, THF, and DCE while maintaining a 0.01 M concentration. Use of THF resulted in increased formation of the byproduct, and decreased formation of **1.90**. DCE was comparable to toluene based upon TLC observations, however, when utilized for a larger scale, this solvent resulted in a lower, 40% yield, of **1.90** (Entry 5). Toluene was determined to be the optimal solvent.

A comparison between the use of 100% CO gas and 10% CO in argon gas was made. TLC observations revealed that the partial carbon monoxide atmosphere decreased formation of **1.90**. Therefore, use of 100% CO gas was maintained for subsequent experiments.

Due to the increased yield observed lowering the reaction concentration, the reaction was further diluted by employing a drop-wise, syringe-pump addition procedure. This strategy minimizes the concentration of allene-yne **1.91**, while avoiding the use of uneconomical amounts of solvent.⁵⁰ To this end, allene-yne **1.91**, dissolved in toluene, was added dropwise over 1.5 h, using a syringe pump, to a refluxing solution of $[\text{Rh}(\text{CO})_2\text{Cl}]_2$ (10 mol%) in toluene (0.01 M overall with respect to **1.91**), under a CO atmosphere. The reaction was complete 15 min after the addition period; **1.90** was obtained in 81% yield with no byproduct observed (Entry 6).

Catalyst Loading. Next, the catalyst loading was examined while using the dropwise addition of allene-yne **1.91** to the Rh(I) catalyst in toluene. Lowering the loading to 5 mol% maintained a high, 80% yield of **1.90** (Entry 7). However, lower catalyst loadings resulted in decreased yields; catalyst loadings of 2 mol %, 1 mol %, and 0.1 mol % gave **1.90** in 62%, 63%, and 23% respectively (Entries 8-10). Therefore, 5 mol% was determined to be the optimal amount of $[\text{Rh}(\text{CO})_2\text{Cl}]_2$ needed for this type of transformation.

Alternative Rh(I) catalysts. Mukai and coworkers have reported the use of alternative Rh(I) catalysts $[\text{RhCl}(\text{CO})\text{dppp}]_2$ and $[\text{Rh}(\text{CO})\text{dppp}]_2\text{Cl}$ for overcoming low-yielding APKR results.⁵¹ In particular, their synthesis of (+)-achalensolide (**1.87**) utilizes the APKR for conversion of methyl substituted allene-yne **1.85** to dienone **1.86** (Scheme 26). Use of $[\text{Rh}(\text{CO})_2\text{Cl}]_2$ afforded **1.86** in only 14% yield. Alternatively, use of $[\text{RhCl}(\text{CO})\text{dppp}]_2$ increased the yield of **1.86** to 61%, while $[\text{Rh}(\text{CO})\text{dppp}]_2\text{Cl}$ gave the best yield of 96%.⁴⁰



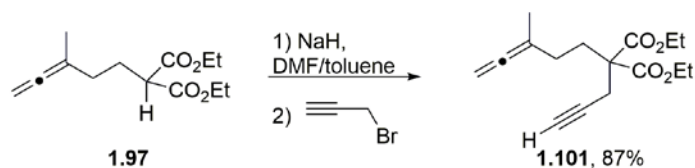
Scheme 26. Comparison of various Rh(I) catalysts for the formation of dienone **1.86**.

Comparisons were made between $[\text{Rh}(\text{CO})_2\text{Cl}]_2$ and these alternative Rh(I) catalysts for the APKR of methyl substituted allene-yne **1.91**. Allene-yne **1.91** was reacted with $[\text{Rh}(\text{CO})(\text{dppp})_2]\text{Cl}$, a rhodium monomer catalyst generated from 10 mol% rhodium (1,5-cyclooctadiene) chloride dimer ($[\text{Rh}(\text{cod})\text{Cl}]_2$) and 50 mol% 1,3-bis(diphenylphosphino)propane (dppp), under a CO atmosphere in toluene (0.1 M);⁵² these conditions afforded dienone **1.90** in 27% yield after stirring for 21 h (Entry 11). Lowering the concentration of the reaction to 0.01 M, using the same catalyst, afforded **1.90** in 46% yield (Entry 12). Both of these results are

comparable to the yields of **1.90** obtained while using $[\text{Rh}(\text{CO})_2\text{Cl}]_2$ at the same concentrations (Entries 2 and 3). However, the longer reaction times and the more tedious procedure required when using $[\text{Rh}(\text{CO})(\text{dppp})_2]\text{Cl}$ favor use of $[\text{Rh}(\text{CO})_2\text{Cl}]_2$. Rhodium dimer catalyst $[\text{RhCl}(\text{CO})\text{dppp}]_2$, generated from 10 mol% $[\text{Rh}(\text{cod})\text{Cl}]_2$ and 20 mol% dppp,⁵² was also employed; at 0.01 M concentration, **1.90** was afforded in only 29% yield (Entry 13).

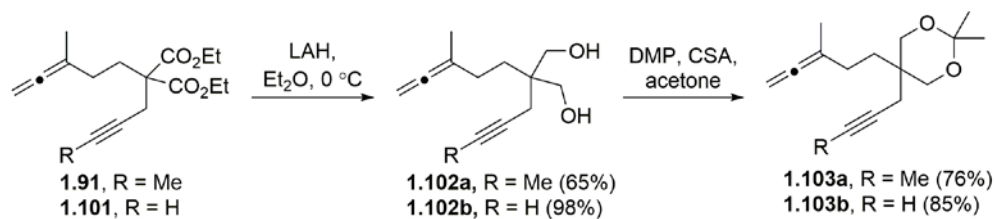
1.2.4 Application of high dilution conditions to synthesis of bicyclo[5.3.0]decadienones

Next, we examined the generality of the syringe-pump, “high dilution” conditions on a series of allene-yne with methyl substituents on the proximal allene carbon and either methyl substituted or terminal alkynes. This allene-yne series was prepared with a variety of functionalities present in the allene-yne tethers. Diester-containing allene-yne **1.101**, with a terminal alkyne, was prepared in a manner analogous to allene-yne **1.91**; malonate **1.97** was reacted with sodium hydride, followed by propargyl bromide to afford **1.101** in 87% yield (Scheme 27).



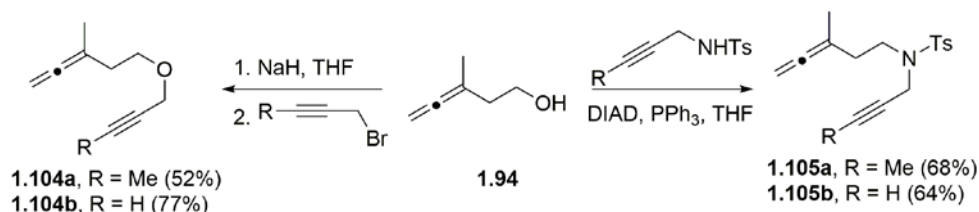
Scheme 27. Synthesis of diester allene-yne tether **1.101** with a terminal alkyne.

The diester tethers **1.91** and **1.101** were manipulated to afford additional allene-yne substrates (Scheme 28). The esters were reduced using lithium aluminum hydride to afford diols **1.102a** and **b** in 65% and 98% respectively. The diols were protected using camphor sulfonic acid and dimethoxypropane in acetone to afford acetonide containing tethers **1.103a** and **b** in 76% and 85% yields respectively.



Scheme 28. Transformation of diester allene-ynes **1.91** and **1.101** to acetonide containing allene-ynes **1.103a,b**.

Heteroatom-containing tethers were prepared from allenyl-alcohol **1.94** (Scheme 29).^{36c} To prepare oxygen containing tethers, the Williamson ether synthesis was employed. Deprotonation of alcohol **1.94** with sodium hydride followed by reaction with 1-bromo-2-butyne resulted in formation of allene-yne **1.104a** in 52% yield. Alternatively the corresponding alkoxide of **1.94** was reacted with propargyl bromide to afford terminal alkyne-containing tether **1.104b** in 77% yield. Nitrogen containing tethers **1.105a** and **b** were prepared in 68% and 64% respectively, using Mitsunobu reaction conditions with alcohol **1.94**, DIAD, triphenylphosphine, and the corresponding tosylated propargyl amine.

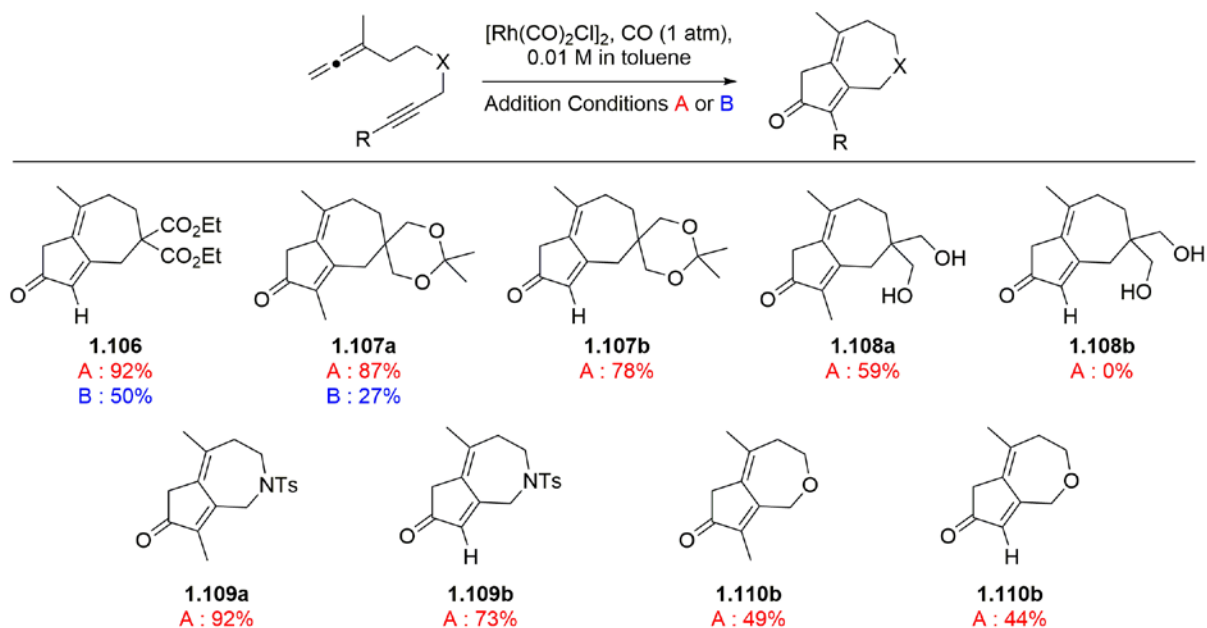


Scheme 29. Synthesis of heteroatom containing allene-yne tethers **1.104** and **1.105**.

The prepared allene-yne tethers were subjected to the optimized high dilution APKR conditions (Scheme 30). When diester tether **1.101**, with a terminal alkynyl group, was added dropwise over 1.5 h to a solution of $[\text{Rh}(\text{CO})_2\text{Cl}]_2$ (5 mol%) in toluene (0.01 M), under a CO atmosphere at 110 °C (Conditions A), dienone **1.106** was afforded in 92% yield. For comparison, a 0.01 M solution of **1.101** in toluene was heated with 5 mol% $[\text{Rh}(\text{CO})_2\text{Cl}]_2$, under a CO atmosphere, without the dropwise addition (Conditions B) which afforded **1.106** in only 50% yield. Therefore, the dropwise addition of the allene-yne to the reaction medium resulted in 42%

yield increase for **1.106**. A comparison of Conditions A and B were also made for the reaction of acetonide tether **1.103a**, with a methyl substituted alkynyl group. The dropwise Conditions A afforded dienone **1.107a** in 87% yield, a 60% increase compared to the 27% yield of **1.107a** obtained when adding the allene-yne all at once (Conditions B). Acetonide **1.103b** with a terminal alkynyl group also successfully afforded dienone **1.107b** in 78% yield using the dropwise conditions.

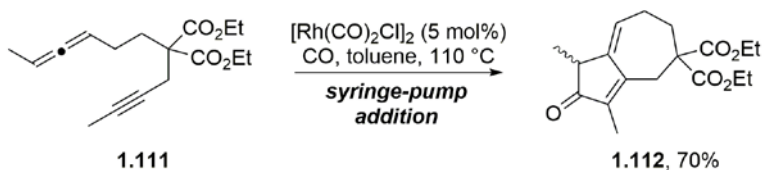
When diol **1.102a** was reacted under the optimized conditions dienone **1.108a** was afforded in a moderate 59% yield. Unfortunately, when diol **1.102b** with a terminal alkyne was reacted, the corresponding dienone **1.108b** was not obtained. Other examples involving the presence of hydroxyl groups in Pauson-Khand precursors have resulted in significantly reduced yield.⁵¹ We presume that the hydroxyl groups may be reacting with the rhodium catalyst, rendering it useless for the cyclocarbonylation pathway.



Scheme 30. Result of high dilution conditions on a variety of allene-ynes. **Conditions A** high dilutions conditions where the allene-yne was added by a syringe pump over 1.5 h. **Conditions B** added the allene-yne all at once.

Tethers containing either a nitrogen or oxygen atom were examined next. Tosyl amine tethers **1.105a,b** were well tolerated in the APKR reaction and afforded dienones **1.109a** and **b** in 92% and 73% respectively. However, allene-yne ethers **1.104a,b** only afforded the corresponding dienones **1.110a** and **b** in moderate yields (49% and 44% respectively). Other reports have also observed diminished yield for the synthesis of oxabicyclic compounds using the APKR reaction compared to the corresponding azabicyclic compounds.^{36c, 53}

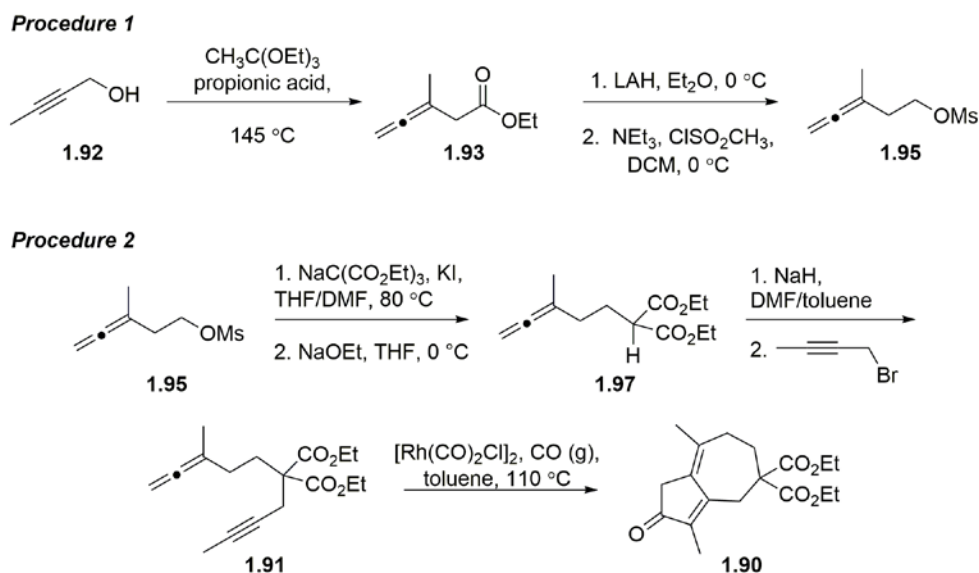
Finally, 1,3-disubstituted allene containing tether **1.111**, previously prepared in our group, was reacted under the high dilution conditions (Scheme 31).^{36c} While 1,3-disubstituted allenes have been tolerated previously in the APKR, we wanted to determine if the yield of dienone **1.112** could be improved using the dropwise conditions. Allene-yne **1.111** was added dropwise over 1.5 h to a solution of $[\text{Rh}(\text{CO})_2\text{Cl}]_2$ (5 mol%) in toluene (0.01 M) at 110 °C. After the addition period, an additional 3 h of stirring was required to afford dienone **1.112** in 70% yield (Scheme 31). Dienone **1.112** was previously reported to be prepared in 71% yield from **1.111** under more concentrated conditions (10 mol% $[\text{Rh}(\text{CO})_2\text{Cl}]$, 0.1 M toluene, 90 °C). Therefore, the dilute, dropwise conditions did not alter the effectiveness of the reaction. The longer required reaction time may have minimized the positive dilution effects of the dropwise conditions.



Scheme 31. Reaction of 1,3-disubstituted allene **1.111** in the APKR with dilute, dropwise conditions.

1.2.5 Efforts towards a large-scale allene-yne synthesis and APKR reaction for *Organic Syntheses*.

Based upon the success of this drop-wise addition modification and the APKR in general for the synthesis of bicyclo[5.3.0]decadienones, we sought to perform the synthesis of dienone **1.90** on a large scale, suitable for publication in *Organic Syntheses*. Two separate procedures, seen in Scheme 32, were invited for submission to the journal. The first procedure was to synthesize 10g of allenyl-mesylate **1.95** (59 mmol) from 2-butyn-1-ol (**1.92**) via the Johnson-Claisen rearrangement, reduction, and mesylation reactions, showcasing the allene functional group as a robust building block for subsequent transformations. The second procedure involved the synthesis of allene-yne **1.91** and subsequent APKR for the formation of 5 g of dienone **1.90**.

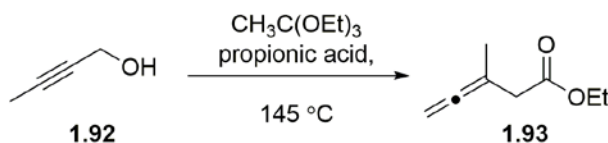


Scheme 32. Original *Organic Syntheses* procedures for the **APKR** synthesis of bicyclo[5.3.0]decadienones.

For procedure 1, scale-up of the Johnson-Claisen reaction toward allenyl ester **1.93** was required. This reaction was performed successfully at 28.5 and 45.0 mmol scales, affording **1.93** in 61% and 71% respectively (Table 2, Entries 1 and 2). However, issues arose when the reaction

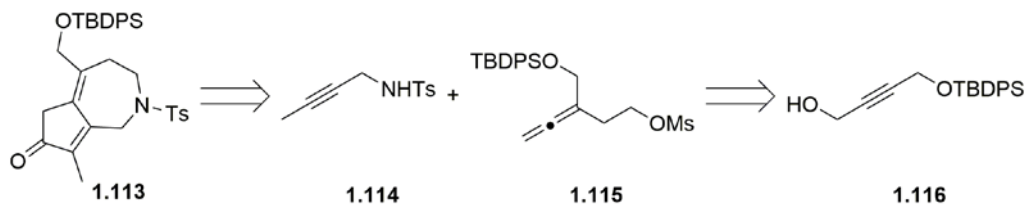
was attempted at a larger, 117 mmol scale, required to meet the synthesis goal. This procedure only gave allenyl ester **1.93** in 33% yield (Entry 3).

Table 2. Result from large scale conversion of 2-butyn-1-ol (**1.92**) to allenyl ester **1.93**.



Entry	mmol of 2-butyn-1-ol (1.92)	Time	Yield 1.93 (g)	Yield 1.93 (%)
1	28.5	5 h	2.44 g	61%
2	45.0	6.5 h	4.52 g	71%
3	117.0	6.5 h	5.41 g	33%

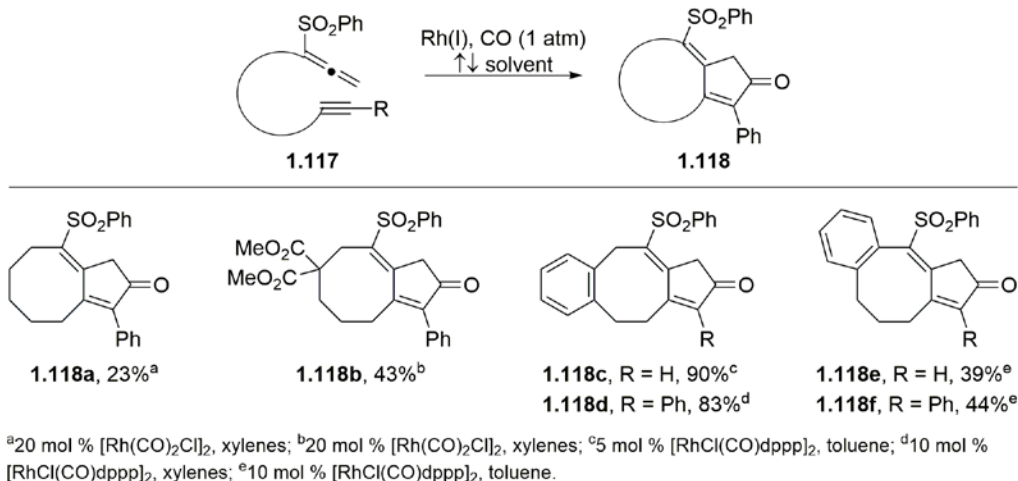
The poor yield at the larger scale for the formation of **1.93**, as well as the volatility of the corresponding allenyl alcohol, formed after reduction of **1.93**, ultimately led us to redesign the *Organic Syntheses* proposal using a more robust substrate. Our group has shown that the Johnson-Claisen rearrangement of propargyl alcohol **1.116** (Scheme 33) affords the corresponding allenyl ester in high yields.⁴³ Due to this fact, and the high yielding APKR examples observed for tosylamide containing allene-yne tethers **1.105a,b**, we planned to synthesize azabicyclic dienone **1.113**, according to the retrosynthetic analysis seen in Scheme 33. The remainder of this effort was successfully carried out by Joe Burchick, another member of the Brummond group.



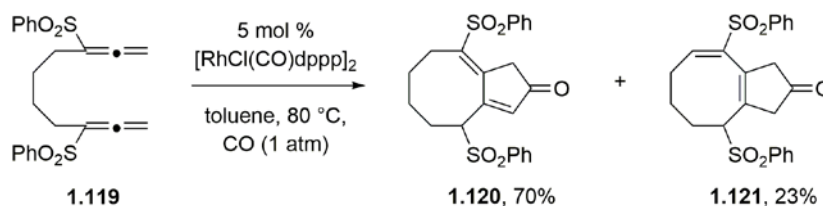
Scheme 33. Retrosynthetic analysis for dienone **1.113**.

1.2.6 Synthesis of Bicyclo[6.3.0]dienones

The optimized “high dilution” conditions were also applied to the synthesis of bicyclo[6.3.0]dienones by extending the allene-yne tether of the APKR precursor by one carbon. Synthesis of bicyclo[6.3.0]dienones via the APKR has been limited. A report published by Mukai in 2005 is limited to phenylsulfonyl-substituted allene-yne tethers **1.117** to afford the fused 5,8-bicyclic systems **1.118** (Scheme 34).⁵⁴ The phenylsulfonyl-substituted allenes are popular for the APKR because they are readily available. For all systems, optimized conditions were determined and used either $[\text{Rh}(\text{CO})_2\text{Cl}]_2$ or $[\text{RhCl}(\text{CO})\text{dppp}]_2$, in refluxing solvent (xylenes or toluene). An unsubstituted, all-carbon, tether afforded **1.118a** in 23% yield. Efficiency of the reaction was improved by incorporating a diester into the allene-yne tether, which afforded **1.118b** in 43% yield. The presence of a phenyl ring in the tether further improved the efficiency of the reaction; **1.118c** and **1.118d** were afforded in 90% and 83% respectively. However, the location of the phenyl group within the tether was an important factor. Bicyclo[6.3.0]undecadienones have more readily been synthesized by a Rh(I) catalyzed cyclocarbonylation reaction of a bis(sulfonylallene). For example, dienone **1.120** was prepared from bis(allene) **1.119** in 70% yield along with **1.121** as a byproduct (Scheme 35).⁵⁵

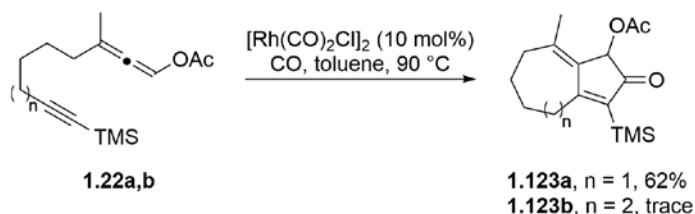


Scheme 34. Previous syntheses of bicyclo[6.3.0]undecadienones via the APKR.



Scheme 35. Synthesis of bicyclo[6.3.0]dienone **1.120** from bis(sulfonylallene) **1.119**.

Our group has also attempted the synthesis of bicyclo[6.3.0]undecadienones via the APKR, but has had little success. For example, allenyl acetate **1.122b**, with a five-carbon tether between the allene and the alkyne, was subjected to APKR conditions and afforded the cyclocarbonylation product **1.123b** in only trace amounts, as determined by ¹H NMR spectroscopy (Scheme 36).^{36b} For comparison, the corresponding bicyclo[5.3.0]decadienone **1.123a** was afforded in 62% yield under the same conditions.

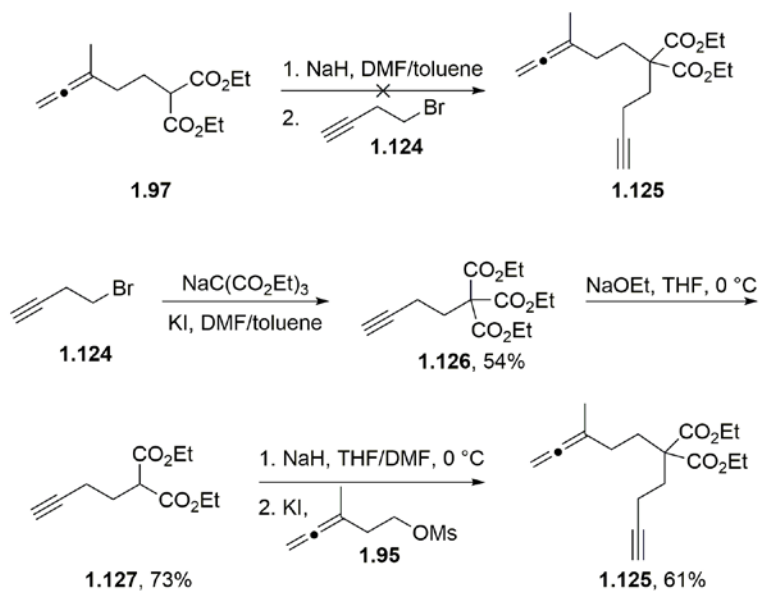


Scheme 36. Attempted synthesis of bicyclo[6.3.0]undecadienone **1.123b**.

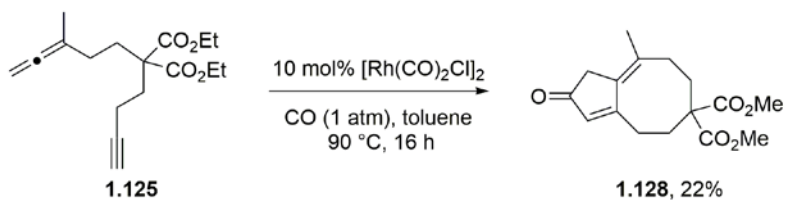
To test the high dilution conditions for the synthesis of bicyclo[6.3.0]undecadienones, we synthesized allene-yne **1.125**, where the allene and alkyne were connected by a five-carbon, diester-containing tether. Initial attempts to react allenyl malonate **1.97** with sodium hydride followed by 1-bromobut-3-yne (**1.124**) were unsuccessful, resulting in recovery of malonate **1.97** (Scheme 37). Potassium iodide was also employed in attempt to increase the reactivity between **1.97** and the alkyl halide, but this effort was also unsuccessful. Alternatively, 1-bromobut-3-yne **1.124** was reacted with sodium methantricarboxylate and potassium iodide in a mixture of DMF and toluene to afford tricarboxylate **1.126** in 54% yield. In turn, decarboxylation of **1.126** with sodium ethoxide gave malonate **1.127** in 73% yield. Finally, deprotonation of malonate followed by reaction with allenyl mesylate **1.95** afforded allene-yne **1.125** in 61% yield.

With allene-yne **1.125** in hand, we began exploring the APKR for the formation of 5,8-fused bicyclic dienones. First, the optimal conditions determined for the synthesis of the 5,7-bicyclic dienones were employed. Allene-yne **1.125** was added drop-wise (over 1.5 h) to a solution of $[\text{Rh}(\text{CO})_2\text{Cl}]_2$ in toluene (110°C, 1 atm CO). After the addition period, an additional 6 h of stirring was required to consume **1.125**. Dienone **1.128** was isolated in 14% yield. By decreasing the temperature to 90 °C, yield of **1.128** was improved to 22% but a significantly longer reaction time (16 h) was required (Scheme 38). The column was flushed with 100% ethyl acetate to collect baseline material. Analysis of this baseline material by ^1H NMR spectroscopy revealed decomposition, however, broad signals were observed at 4.19 and 1.24 ppm, consistent with the ethyl ester functional groups. Changing the solvent to THF resulted in complete decomposition while changing the CO atmosphere to 10% CO in argon resulted in a decreased yield of **1.128** (determined by TLC). While the yield of **1.128** was low in these reactions, this

represents the first synthesis of a bicyclo[6.3.0]dienone without a phenylsulfonyl substitution via the APKR.



Scheme 37. Synthesis of extended allene-yne diester tether **1.125**.



Scheme 38. Synthesis of bicyclo[6.3.0]undecadienone **1.128** via the APKR.

1.3 CONCLUSION

In summary, optimized conditions were developed for the synthesis of bicyclo[5.3.0]decadienones with methyl substitutions at the C4 and C10 positions via the APKR reaction. A model allene-yne, **1.91**, with methyl substitutions on the proximal carbon of the allene, a methyl substituted alkyne, and an all carbon tether was synthesized and used for this

optimization process. Traditional APKR conditions developed previously in the group resulted in low yields of dienone **1.90** and the formation of an unidentified byproduct, hypothesized to be a result of a competing intermolecular process. High yields of **1.90** were obtained after implementing a syringe-pump, “high dilution” protocol. These conditions also eliminated the formation of the byproduct, supporting the hypothesis of a competing intermolecular reaction.

The optimized APKR conditions were applied to a series of allene-ynes. Improved yields for allene-ynes containing a terminal alkyne were also observed using the dilute conditions compared to more concentrated reactions. Diester, acetonide, and tosyl amide containing tethers resulted in high yields of the corresponding dienones. Oxygen and diol containing tethers gave moderate yields, with the exception of diol tether **1.102b**, which did not successfully afford the corresponding dienone. These conditions for the high yielding synthesis of bicyclo[5.3.0]decadienones with methyl substitutions at C4 and C10 via an APKR further establishes this approach as a viable synthetic method for generation of guaianolide analogs.

1.4 EXPERIMENTALS

1.4.1 General Methods

All commercially available compounds were used as received unless otherwise noted. Dichloromethane (DCM), diethyl ether (Et₂O), and tetrahydrofuran (THF) were purified by passing through alumina using the Solv-Tek ST-002 solvent purification system. Toluene was freshly distilled from calcium hydride prior to use. *N,N*-dimethylformamide (DMF) was distilled prior to use and stored over 4 Å molecular sieves. Deuterated chloroform (CDCl₃) was stored

over 4 Å molecular sieves. Carbon monoxide (CO) was purchased from Matheson Tri Gas and the purity level was Matheson Purity (99.99%). Triphenylphosphine polymer bound was purchased from Aldrich as a copolymer of styrene and divinyl benzene. Purification of the compounds by flash column chromatography was performed using silica gel (40-63 µm particle size, 60 Å pore size) purchased from Sorbent Technologies. TLC analyses were performed on Silicycle SiliaPlate G silica gel glass plates (250 µm thickness). ¹H NMR and ¹³C NMR spectra were recorded on Bruker Avance 300 MHz, 400 MHz, or 500 MHz. Spectra were referenced to residual chloroform (7.26 ppm, ¹H, 77.16 ppm, ¹³C). Chemical shifts are reported in ppm, multiplicities are indicated by s (singlet), bs (broad singlet), d (doublet), t (triplet), q (quartet), p (pentet), and m (multiplet). Coupling constants, *J*, are reported in hertz (Hz). All NMR spectra were obtained at rt. IR spectra were obtained using a Nicolet Avatar E.S.P. 360 FT-IR. ES mass spectroscopy was performed on a Waters Q-TOF Ultima API, Micromass UK Limited or a Thermo Scientific Q Exactive high resolution mass spectrometer.

1.4.2 Experimental procedures detailed in published papers

Characterization data, including ¹H and ¹³C NMR spectra, and details of the preparation for the compounds shown in Figure 6 were previously published and can be found in the Supporting Information of Wells, S. M.; Brummond, K. M. Conditions for a Rh(I)-catalyzed [2+2+1] cycloaddition reaction with methyl substituted allenes and alkynes. *Tetrahedron Letters*, **2015**, 56, 3546-3549.

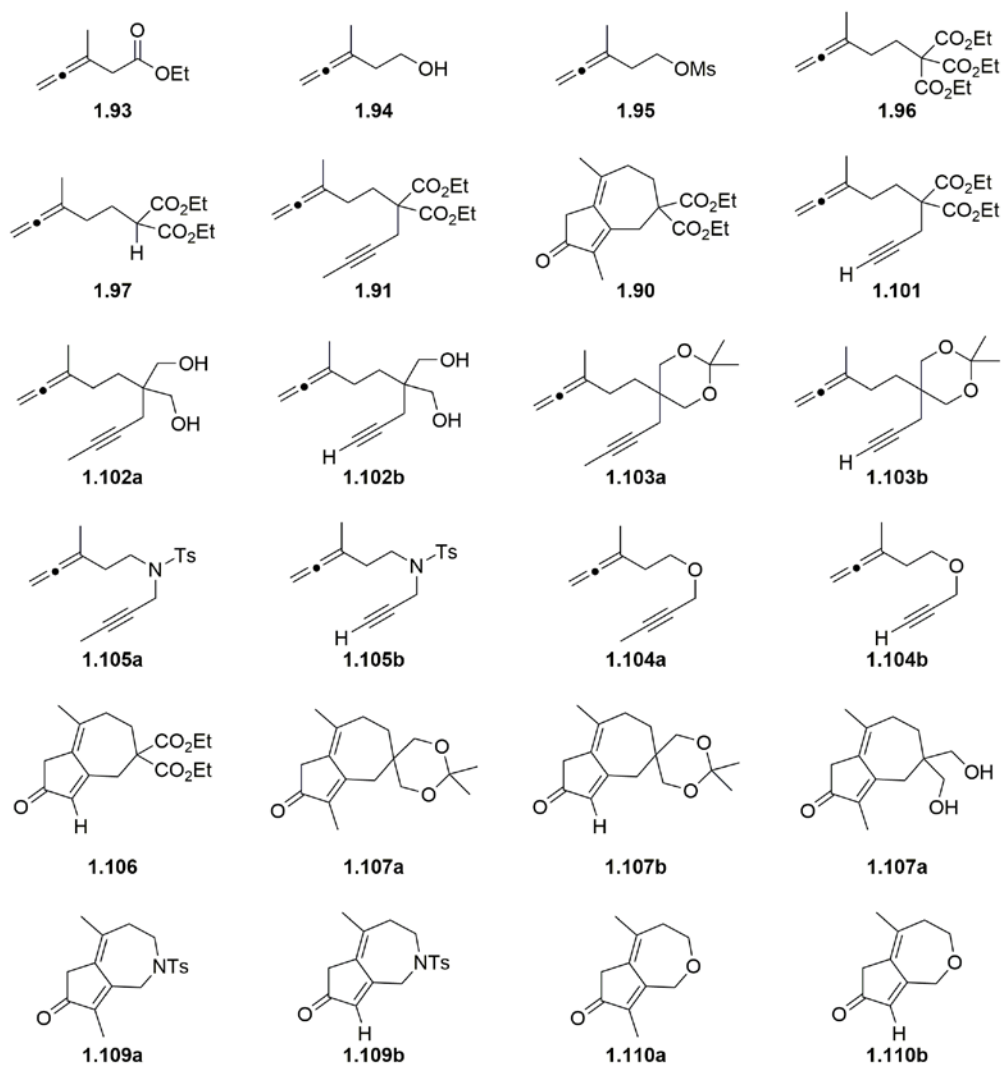


Figure 6. Previously published compounds for which synthetic procedures and characterization data can be found in *Tetrahedron Lett.* **2015**, *56*, 3546-3549.

1.4.3 General Procedures

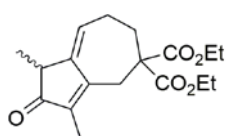
General Procedure 1A: A High Dilution Allenic Pauson-Khand Reaction (APKR). A flame-dried, 2-necked, round-bottomed flask equipped with a stir bar, a condenser topped with a septum pierced with a nitrogen inlet needle, and a septum in the side arm was charged with $[\text{Rh}(\text{CO})_2\text{Cl}]_2$ (0.05 equiv) and toluene (0.0013 M with respect to the Rh(I) catalyst). The

apparatus was evacuated through a needle connected to the vacuum gas manifold and then filled with CO with a balloon (3 x). The flask was placed in a pre-heated oil bath (110 °C). In a separate flask, allene-yne (1 equiv) was dissolved in toluene (0.04 M with respect to the allene-yne). The allene-yne solution was drawn into a syringe and added to the Rh(I) solution dropwise over 1.5 h using a syringe pump. After the addition was complete, heating and stirring were maintained until the reaction was complete, as evidenced by TLC. The oil bath was removed and the reaction was allowed to cool to rt. Triphenylphosphine polymer bound (~3.0 mmol/g, 1 equiv) was added and the reaction was stirred for 14 h. The polymer was removed by vacuum filtration and rinsed with diethyl ether (10 mL). The filtrate was concentrated under reduced pressure rotary evaporation, and the residue was purified by silica gel flash column chromatography to yield the bicyclo[5.3.0]decadienone.

General Procedure 1B: APKR Conditions B (Scheme 30). A flame-dried, 2-necked, round-bottomed flask equipped with a stir bar, a condenser topped with a septum pierced with a nitrogen inlet needle, and a septum in the side arm was charged with the allene-yne (1 equiv), dissolved in toluene (0.01 M). The apparatus was evacuated through a needle connected to the vacuum gas manifold and then filled with CO gas with a balloon (3 x). $[\text{Rh}(\text{CO})_2\text{Cl}]_2$ (0.05 equiv) was added by temporarily removing the septum in the side arm. The apparatus was again evacuated and filled with CO gas (3 x). The flask was placed in a pre-heated oil bath (110 °C) and stirred until the reaction was complete, as evidenced by TLC. The oil bath was removed and the reaction was allowed to cool to rt. Triphenylphosphine polymer bound (~3.0 mmol/g, 1 equiv) was added and the reaction was stirred for 14 h. The polymer was removed by vacuum filtration and rinsed with diethyl ether. The filtrate was concentrated under reduced pressure

rotary evaporation, and the residue was purified by silica gel flash column chromatography to yield the bicyclo[5.3.0]decadienone.

1.4.4 Experimental procedures with compound characterization data



Diethyl 1,3-dimethyl-2-oxo-2,4,6,7-tetrahydroazulene-5,5(1H)-

dicarboxylate (1.112). Follows general procedure 1A: Toluene (6.0 mL),

[Rh(CO)₂Cl]₂ (2 mg, 0.0043 mmol, 0.05 equiv), allene-yne **1.111** (25 mg, 0.086 mmol, 1 equiv) in toluene (2.5 mL). Reaction stirred for 3 h after addition period. Polymer bound triphenyl phosphine (25 mg) was added and stirred overnight. The crude residue was purified by silica gel flash column chromatography (18% EtOAc in hexanes) to afford the title compound (19 mg, 70%) as a clear oil. Characterization matches that previously reported for **1.112**.^{36c}

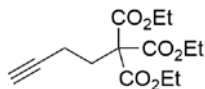
Data for 1.112.

¹H NMR (400 MHz, CDCl₃)

5.81 (t, *J* = 5.7 Hz, 1H), 4.23-4.15 (m, 4H), 3.21 (s, 2H), 2.77-2.68 (m, 1H), 2.53-2.46 (m, 2H), 2.39-2.32 (m, 2H), 1.84 (s, 3H), 1.28-1.22 (m, 6H), 1.26 (d, *J* = 7.5 Hz, 3H) ppm;

TLC R_f = 0.31 (20% EtOAc in hexanes)

Silica gel, UV visible, KMnO₄



Triethyl pent-4-yne-1,1,1-tricarboxylate (1.126). A flame-dried, 2-necked,

round-bottomed flask equipped with a stir bar, a condenser topped with a nitrogen inlet adaptor, and a septum in the side arm was charged 1:1 mixture of DMF and toluene (6 mL) and sodium methanetricarboxylate (380 mg, 1.49 mmol, 1 equiv). 1-Bromobut-3-yne (0.14 mL, 1.49 mmol, 1 equiv), dissolved in a 1:1 mixture of DMF and toluene (1 mL) was

added to the reaction flask all at once via syringe, followed by the addition of potassium iodide (272 mg, 1.64 mmol, 1.1 equiv) The reaction flask was lowered into a pre-heated oil bath (80 °C) and stirred for 14 h. The oil bath was removed and the reaction contents were cooled to rt. Saturated NH₄Cl (8 mL) was added and the mixture was transferred to a separatory funnel. The organic layer was separated and the aqueous layer was extracted with diethyl ether (3 x 8 mL). The combined organic extracts were dried with MgSO₄, filtered, and concentrated under reduced pressure rotary evaporation. The crude residue was purified by silica gel flash column chromatography (10% EtOAc in hexanes) to yield the title compound as a clear oil (229 mg, 54%). Characterization data matched that previously reported for **1.126**.⁵⁶

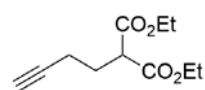
Data for **1.126**.

¹H NMR (400 MHz, CDCl₃)

4.26 (q, *J* = 7.2 Hz, 6H), 2.51-2.44 (m, 2H), 2.43-2.37 (m, 2H), 1.97 (t, *J* = 2.4 Hz, 1H), 1.29 (t, *J* = 7.2 Hz, 9H) ppm;

TLC R_f = 0.26 (20% Et₂O in hexanes)

Silica gel, KMnO₄



Diethyl 2-(but-3-yn-1-yl)malonate (1.127). To a single-necked, round-bottomed flask equipped with a stir bar and septum pierced with a nitrogen inlet adapter was added ethanol (5 mL). Freshly cut sodium (77.3 mg, 3.38 mmol, 1.2 equiv) was added piecewise to the ethanol. The solution was stirred until all sodium had dissolved. The stir bar and septum were removed and the excess ethanol was removed using reduced pressure rotary evaporation followed by drying on a high vacuum for 1 h. The stir bar and septum with nitrogen inlet needle were replaced and the flask was charged with THF (14 mL) and cooled to 0 °C on an ice/water bath. Tricarboxylate **1.126** (800 mg, 2.81 mmol, 1 equiv), dissolved in THF (2.5 mL),

was added to the reaction dropwise over 5 min. The reaction stirred for 2.5 h and was quenched by the addition of 1 M HCl (15 mL). The mixture was transferred to a separatory funnel. The organic layer was separated and the aqueous layer was extracted with DCM (3 x 12 mL). The combined organic layers were dried over magnesium sulfate, filtered and concentrated using reduced pressure rotary evaporation. The crude residue was purified by silica gel flash column chromatography (8% ethyl acetate in hexanes) to yield the title compound as a clear oil (437 mg, 73%). Characterization data matched that previously reported for **1.127**.⁵⁷

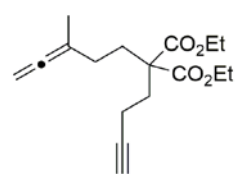
Data for 1.127.

¹H NMR (300 MHz, CDCl₃)

4.27-4.12 (m, 4H), 3.57 (t, *J* = 7.2 Hz, 1H), 2.30 (td, *J* = 7.2, 2.6 Hz, 2H), 2.12 (q, *J* = 7.2 Hz, 2H), 1.99 (t, *J* = 2.6 Hz, 1H), 1.27 (t, *J* = 7.2 Hz, 6H) ppm;

TLC *R*_f = 0.34 (10% EtOAc in hexanes)

Silica gel, KMnO₄



Diethyl 2-(but-3-yn-1-yl)-2-(3-methylpenta-3,4-dien-1-yl)malonate

(1.125). To a flame-dried, 2-necked, 100 mL, round-bottomed flask with a stir bar, condenser topped with N₂ inlet adaptor, and a septum in the side arm,

was added THF (22 mL), DMF (22 mL), and sodium hydride (98 mg of a 60% dispersion in mineral oil, 2.45 mmol, 1.3 equiv). The suspension was cooled to 0 °C on an ice/water bath. Malonate **1.127** (400 mg, 1.88 mmol, 1 equiv) was dissolved in DMF (1 mL), added dropwise to the suspension, and stirred for 1 h. The ice bath was removed. Allenyl mesylate **1.195** (398 mg, 2.26 mmol, 1.2 equiv) was added followed by potassium iodide (375 mg, 2.26 mmol, 1.2 equiv). The reaction flask was lowered into a pre-heated oil bath (80 °C) and stirred overnight. The reaction was cooled to rt and quenched by the addition of saturated NH₄Cl (30 mL). The mixture

was diluted with 15 mL of diethyl ether and transferred to a separatory funnel. The organic layer was separated and the aqueous layer was extracted with diethyl ether (2 x 10 mL). The combined organic layers were dried over MgSO₄, filtered, and concentrated using reduced pressure rotary evaporation. The crude residue was purified by silica gel flash column chromatography (5% EtOAc in hexanes) to afford the title compound (333 mg, 61%) as a clear oil.

Data for 1.125.

¹H NMR (400 MHz, CDCl₃)

4.63 (sextet, *J* = 3.2 Hz, 2H), 4.22-4.16 (m, 4H), 2.19-2.15 (m, 4H), 2.04-2.00 (m, 2H), 1.97-1.94 (m, 1H), 1.85-1.79 (m, 2H), 1.68 (t, *J* = 3.2 Hz, 3H), 1.25 (t, *J* = 7.2 Hz, 6H) ppm;

¹³C NMR (100 MHz, CDCl₃)

206.0, 171.2, 97.8, 83.5, 75.2, 68.8, 61.5, 56.9, 31.8, 30.6, 28.1, 19.0, 14.2, 14.1 ppm;

HRMS (TOF MS AP+)

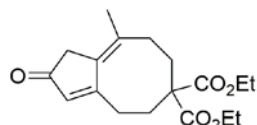
[M + H]⁺ calcd for C₁₇H₂₅O₄, 293.1753; found, 293.1783;

IR (thin film)

3292, 2979, 1959, 1728, 1447, 1255, 1187, 1095, 1027 cm⁻¹;

TLC R_f = 0.42 (20% Et₂O in hexanes)

Silica gel, KMnO₄



Diethyl (Z)-9-methyl-2-oxo-1,2,4,5,7,8-hexahydro-6H-cyclopenta[8]annulene-6,6-dicarboxylate (1.128). Follows general

procedure 1A: Toluene (15.0 mL), [Rh(CO)₂Cl]₂ (8 mg, 0.0021 mmol, 0.1 equiv), allene-yne **1.125** (20 mg, 0.021 mmol, 1 equiv) in toluene (5.0 mL). The solution heated at 90 °C and stirred

for 13 h after addition period. Polymer bound triphenylphosphine (75 mg) was added and stirred for 8 h. The crude residue was purified by silica gel flash column chromatography (gradient of 20-30% EtOAc in hexanes) to afford the title compound (14 mg, 22%) as a sticky residue.

Data for 1.128.

¹H NMR (400 MHz, CDCl₃)

5.97 (s, 1 H), 4.18-4.10 (m, 4 H), 2.95-2.88 (m, 4 H), 2.59-2.53 (m, 2 H), 2.39-2.33 (m, 2 H), 2.31-2.26 (m, 2 H), 1.87 (s, 3 H), 1.23 (t, *J* = 7.2 Hz, 6 H) ppm;

Impurities visible at 4.20, 1.29, 0.87 ppm.

¹³C NMR (150 MHz, CDCl₃)

204.9, 173.5, 171.7, 138.0, 133.0, 132.0, 61.7, 57.2, 41.7, 31.5, 31.4, 29.7, 28.1, 24.6, 14.2 ppm;

HRMS (FTMS + p ESI)

[*M* + *H*]⁺ calcd for C₁₈H₂₅O₅, 321.1697; found, 321.1702;

IR (thin film)

2980, 2930, 1729, 1687, 1566, 1446, 1247, 1188, 1082, 1031cm⁻¹;

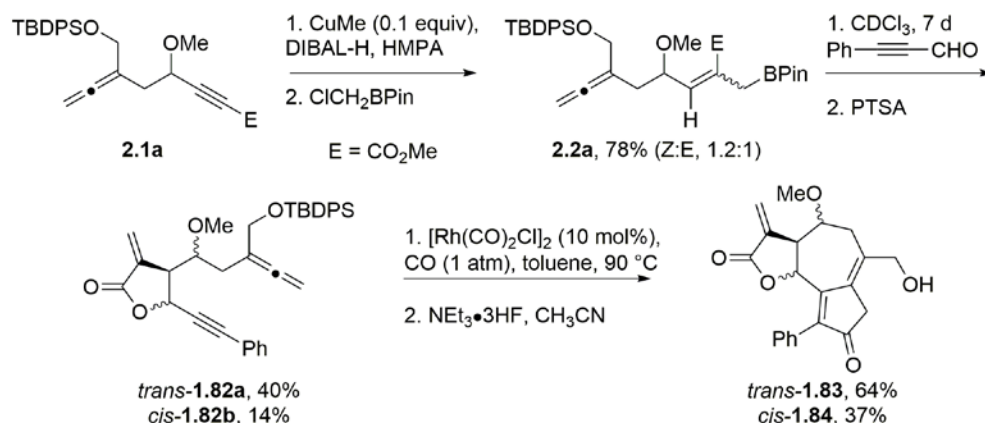
TLC R_f = 0.13 (20% EtOAc in hexanes)

Silica gel, UV visible, KMnO₄

2.0 GUAIANOLIDE ANALOG SYNTHESIS VIA AN ALLYLBORATION/LACTONIZATION SEQUENCE AND THE APKR REACTION

2.1 INTRODUCTION

The Brummond group has successfully applied the allenic Pauson-Khand reaction (APKR) to the synthesis of oxygenated 6,12-guaianolide analogs *trans*-**1.83** and *cis*-**1.84**.⁴³ Access to the guaianolide framework was achieved via an allylboration/lactonization sequence to afford lactones **1.82a** and **b**, inspired by the work of Dennis Hall,⁵⁸ followed by an APKR to access the 5,7,5-fused ring system (Scheme 39). Overall, this synthesis extended the scope of the APKR to the preparation of highly oxygenated substrates. Typically for the synthesis of guaianolides, the α -methylene- γ -butyrolactone is installed at the end of the synthesis due to its potential reactivity, however this moiety was well tolerated in the APKR and the subsequent silyl deprotection toward **1.83** and **1.84**. This synthesis afforded racemic mixtures of the *trans*-lactone **1.83** as a mixture of diastereomers with respect to the methoxy group at C8, and the *cis*-lactone **1.84**, as a single diastereomer. Through collaboration with the Harki lab at the University of Minnesota, these guaianolide analogs (*trans*-**1.83** and *cis*-**1.84**) were tested for relative nuclear factor kappa B (NF- κ B) inhibition and antiproliferative activity to cancerous cell lines.



Scheme 39. Previous synthesis of oxygenated guaianolide analogs **1.83** and **1.84**.

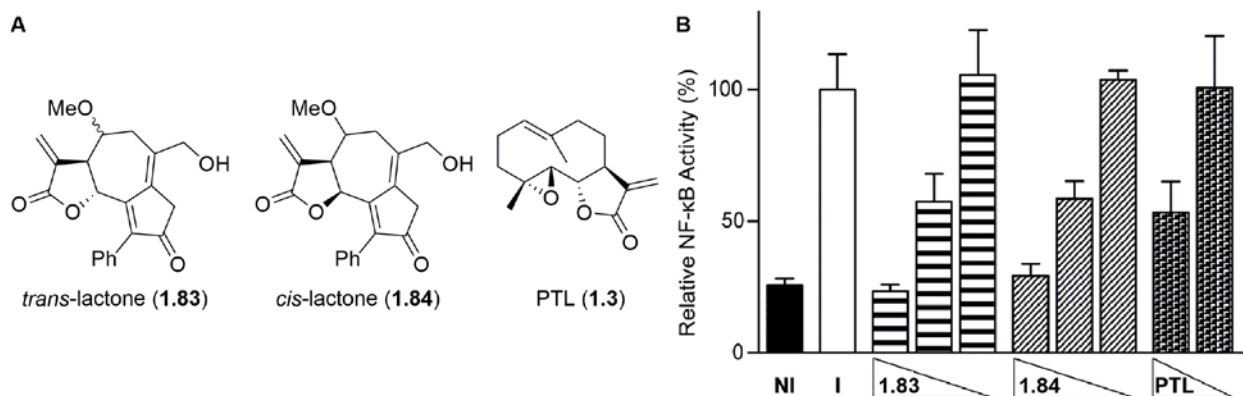


Figure 7. NF- κ B inhibition of **1.83** and **1.84** benchmarked with parthenolide (PTL, **1.3**). A) Compounds tested. B) NF- κ B luciferase reporter assay in A549 cells induced with TNF- α (15 ng/mL) 30 min after molecular treatment. **1.83** and **1.84** were dosed at 20, 10, and 1 μM . PTL (**1.3**) was dosed at 10, 1 μM . NI = noninduced, I = Induced.

NF- κ B is a transcription factor that regulates the gene expression of many physiological processes including acute phase inflammatory response.⁵⁹ For more information on the NF- κ B activity pathway, see Section 4.1. To evaluate the *trans*-**1.83** and *cis*-**1.84** for inhibition of induced NF- κ B activity, the compounds were dosed at varying concentrations on A549 cells that had been activated by TNF- α (Figure 7). Activation of NF- κ B signaling results in an increase of reporter luminescence; the presence of an NF- κ B inhibitor will then diminish the reporter luminescence. *Trans*-**1.83** and *cis*-**1.84** were benchmarked against a known SL NF- κ B inhibitor, parthenolide (PTL, **1.3**). *Trans*-**1.83** and *cis*-**1.84** were shown to be equal inhibitors in the assay,

as both diminished induced NF- κ B activity to non-induced levels at 20 μ M treatment. The NF- κ B levels were also significantly diminished when **1.83** and **1.84** were dosed to cells at a concentration of 10 μ M; with residual activity at 57 and 59%, respectively. PTL (**1.3**) was slightly more active at this concentration, inhibiting NF- κ B to a 53% residual activity level.

Inhibition of NF- κ B pathway has also been described as a viable strategy for treating cancer, as upregulated NF- κ B signaling has been shown to result in transcriptional activation of genes associated with all 6 hallmarks of cancer.¹⁰ In addition, other sesquiterpene lactones have been shown to display antiproliferative properties; these factors motivated the antiproliferative evaluation of these guaianolide analogs. *Trans*-**1.83** and *cis*-**1.84** were evaluated for growth inhibitory activity for an array of cancerous cell lines as well as one non-cancerous cell line (Vero). PTL was again used as a benchmark (Table 3). Against DU-145 (human prostate cancer) cells, *trans*-**1.83** and *cis*-**1.84** showed similar antiproliferative activity compared to each other, but were less potent than PTL. However, against HeLa (cervical cancer) and HL-60 (leukemia) cell lines, *trans*-**1.83** was almost two times more active than *cis*-**1.84** and PTL. Against U-87 MG (glioblastoma), *trans*-**1.83** was less potent compared to both *cis*-**1.84** and PTL. *Cis*-**1.84** was shown to be the most potent of these three compounds toward NCI/ADR-RES cell lines, which model ovarian cancer as a result of over-expression of p-glycoprotein (p-gp) efflux pump. Toxicity towards healthy cells (Vero) of *trans*-**1.83** and *cis*-**1.84** was slightly lower than PTL, with all three compounds causing moderate levels of cell death.

Table 3. Antiproliferative data of guaianolide analogs, *trans*-**1.83** and *cis*-**1.84**, compared to parthenolide (PTL).

Compound	DU-145	HeLa	HL-60	U-87 MG	NCI/EDR-RES	Vero
<i>trans</i> - 1.83	29.1 \pm 4.7	20.3 \pm 6.0	5.5 \pm 0.4	27.1 \pm 4.8	80.9 \pm 24.0	32.2 \pm 7.0
<i>cis</i> - 1.84	21.6 \pm 1.9	39.7 \pm 16.4	7.8 \pm 2.3	9.8 \pm 1.4	24.4 \pm 1.0	30.1 \pm 5.5
PTL	8.9 \pm 4.6	45.1 \pm 3.7	9.3 \pm 3.8	8.8 \pm 2.1	57.6 \pm 8.9	22.4 \pm 1.5

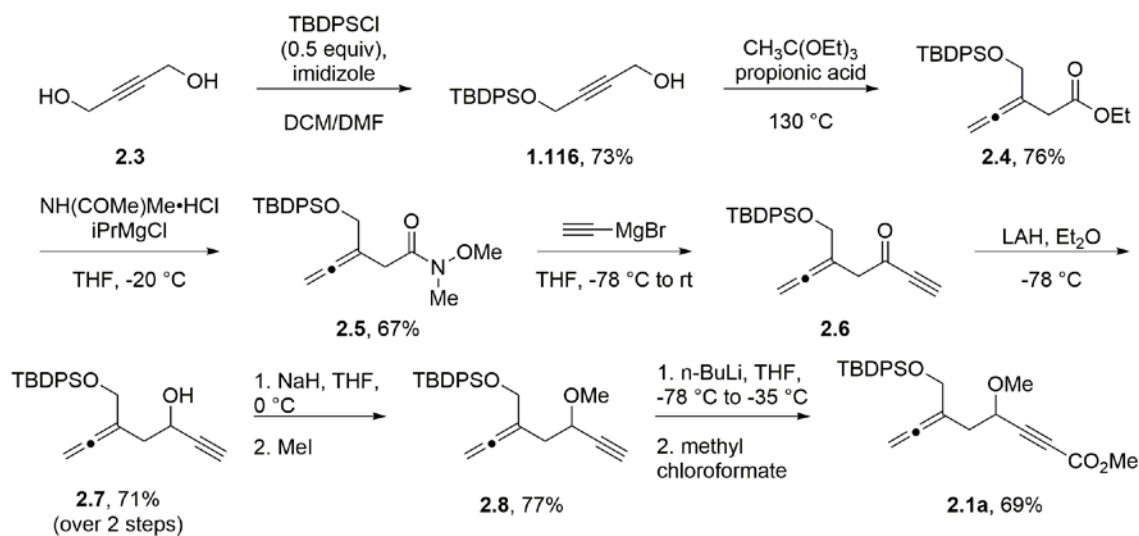
^aCompounds were dosed to cells and incubated for 48 h. Cell viability was measured by Alamar Blue staining. Mean IC₅₀ values \pm SD (μ M) are shown.

Given the potent NF- κ B inhibition and antiproliferative properties of **1.83** and **1.84**, we were motivated to investigate the NF- κ B mechanism of inhibition further. Having a greater understanding of how these molecules behave *in vivo* to inhibit NF- κ B would help guide future synthetic endeavors toward additional guaianolide analogs with high therapeutic potential. However, in order to continue these biochemical investigations, the synthesis of **1.83** had to be repeated. Reproducibility for the formation of allylboronate **2.2a** and the subsequent allylboration/ lactonization step has been challenging. Herein, I report my efforts to reproduce and optimize the synthesis of *trans*-guaianolide analog **1.83**. We also set out to separate and characterize the two diastereomers of *trans*-**1.83** in order to evaluate their corresponding biochemical properties.

2.2 RESULTS AND DISCUSSION

2.2.1 Synthesis of allenyl-ynoate 2.1a

The first phase of the synthesis involves preparation of ynoate **2.1a** in 7 synthetic steps from commercially available butyn-1,4-diol **2.3** (Scheme 40). Mono-protection of diol **2.3** with *tert*-butyldiphenylsilane has been previously achieved by reacting excess butyn-1,4-diol with imidazole and *tert*-butyl(chloro)diphenylsilane (TBDPSCl) in DCM (0.5 M with respect to TBDPSCl).⁶⁰ When this procedure was attempted, the diol was not fully soluble in DCM, causing formation of the corresponding disilylated alkyne as the major product rather than **1.116**. To overcome this issue, DMF was used as a co-solvent to completely solubilize diol **2.3** prior to addition of imidazole and TBDPSCl, which afforded **1.116** in 73% yield (Scheme 40).



Scheme 40. Synthesis of allenyl-ynoate **2.1a** from 2-butyne-1,4-diol (**2.3**) in 7 steps.

The allenyl ester **2.4** was furnished from **1.116** via a Johnson-Claisen rearrangement reaction. The apparatus for this step included a 2-necked, round-bottomed flask equipped with a Dean-Stark trap, condenser, nitrogen inlet adapter and a septa in the side arm. The size of the Dean-Stark trap made a significant difference in the progression of the reaction. When a smaller trap was used (14/20 fittings, 2.0 mL collection volume) **2.4** was afforded in 76% yield, however when a larger trap was used (19/22 fittings, 10.0 mL collection volume), **2.4** was afforded in 36% yield, and 63% of the starting material was recovered (97% yield based on recovered starting material). We presume that the larger Dean-Stark trap hindered efficient removal of ethanol, slowing the reaction progression.

Next, ester **2.4** was transformed to Weinreb amide **2.5**. Use of previously reported conditions (1.3 equiv *N,O*-dimethylhydroxylamine hydrochloride and 2.5 equiv of *iso*-propyl magnesium chloride) resulted in significant recovery of **2.4**. Optimal yields were achieved when the ester **2.4** was reacted initially with 1.5 equiv *N,O*-dimethylhydroxylamine hydrochloride and 2.5 equiv of *iso*-propyl magnesium chloride (2.0 M), with extra equivalents of these reagents

being added after 2 h (additional 0.7 equiv *N,O*-dimethylhydroxylamine hydrochloride and 1.2 equiv *iso*-propyl magnesium chloride) which gave **2.5** in 67% yield.

Ethynylmagnesium bromide was added to amide **2.5** to form ketone **2.6**. The reaction temperature was important for the success of this reaction. While the reaction was previously reported to occur cleanly at 0 °C, repetition of these conditions afforded **2.6** in only 35% yield along with a significant byproduct. Structural assignment of the byproduct was not obtained but ¹H NMR resonances were observed in the alkene region (~ 5.2 ppm). Lowering the temperature to -10 °C improved the yield of **2.6** to 49% but the byproduct was still observed. By adding ethynylmagnesium bromide to a stirring solution of **2.5** at -78 °C and then allowing the reaction to warm slowly to rt and stirred for 2 h, **2.6** was afforded in 69% yield and the byproduct was not observed.⁶¹ It was later determined that **2.6** may be unstable to silica gel column chromatography, and the crude mixture should be taken on directly to the reduction step. Reduction of crude ketone **2.6** using lithium aluminum hydride (LAH) at -78 °C afforded alcohol **2.7** in 71% yield over two steps from Weinreb amide **2.5**. When the reduction was performed at a warmer temperature (0 °C), undesired desilylation of the protected alcohol was observed.

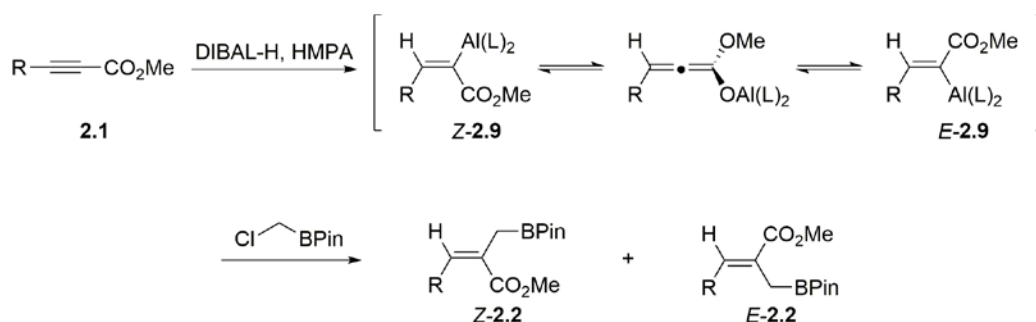
In turn, deprotonation of alcohol **2.7** with sodium hydride followed by reaction with iodomethane at 0 °C readily gave **2.8** in 77% yield. Finally, formation of ynoate **2.1a** was accomplished in 69% yield by reacting the lithium acetylide of **2.8** with methyl chloroformate.

2.2.2 Optimization of allylboronate formation

The conversion of ynoate **2.1a** to allylboronate **2.2a** is accomplished by an aluminum hydride 1,4-conjugate addition to the ynoate using DIBAL-H and HMPA, followed by trapping

of the aluminium intermediate with pinacol chloromethylboronate (ClCH₂BPin). This process can be done either with or without the use of catalytic copper iodide and methyl lithium.

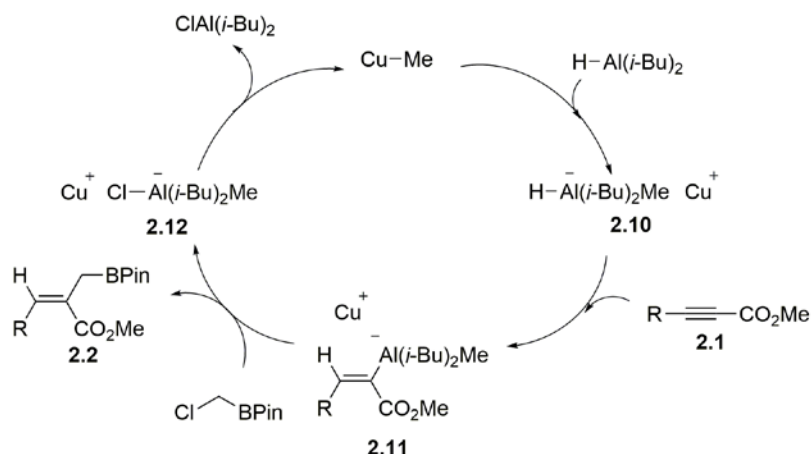
Mechanistically, when the CuI/MeLi catalyst is not used, the reaction of an ynoate **2.1** with DIBAL-H and HMPA, affords an aluminum intermediate **2.9**, which can undergo isomerization via an allenyl intermediate. HMPA acts as a ligand on the aluminate species to assist with the selective 1,4-addition.⁶² Trapping of the aluminum intermediates **2.9**, with ClCH₂BPin affords the *E/Z* mixture of the allylboronate **2.2** (Scheme 41).



Scheme 41. Conjugate reduction of ynoate **2.1** to afford the *Z* and *E* isomers of **2.2**.

While the mechanism for transformation of alkynoates to allylboronates catalyzed by CuI/MeLi has not been reported explicitly, the literature lends itself to suggest the following proposed mechanism for the transformation (Scheme 42). Equimolar amounts of CuI and MeLi combine to form the catalyst, methyl copper (CuMe), in solution.⁶³ In contrast, when 2 equiv of MeLi are reacted with CuI, lithium dimethyl cuprate is generated, which is a source of a methyl anion. Formation of this cuprate should be avoided for the formation of the desired allylboronates.⁶⁴ Reaction of CuMe with the DIBAL-H affords the aluminate species **2.10** which can undergo *cis*-1,4-addition to ynoate **2.1** to generate alkene aluminate **2.11** (which can also undergo isomerization as shown in Scheme 41). This reactive species is trapped by ClCH₂BPin, to afford allylboronate **2.2** as well as a chlorine substituted aluminate species **2.12**. Formation of chlorobis(*iso*-butyl) aluminum as a byproduct regenerates the CuMe catalyst. The CuMe catalyst

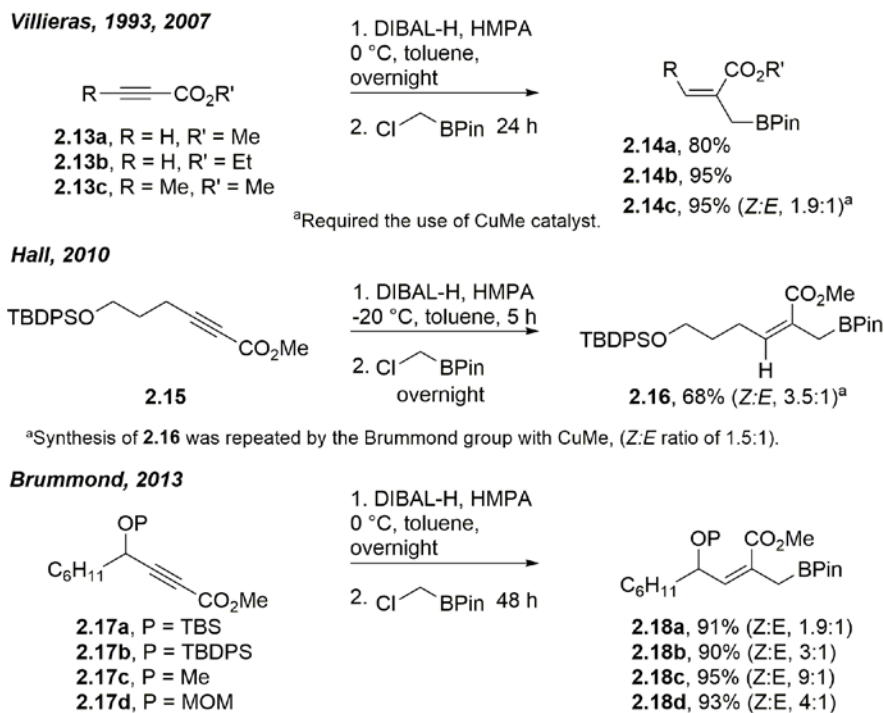
accelerates the overall process of this transformation due to the increased nucleophilicity of aluminate species **2.11** compared to the corresponding aluminum species **2.9**, generated in the reaction without CuMe.



Scheme 42. Proposed reaction pathway for the formation of allylboronate **2.2** using catalytic CuMe.

The need for CuMe catalyst and the resulting alkene *E/Z* geometry ratios both seem to be substrate dependent for this transformation. In 1993, Villieras reported the preparation of (2-methoxycarbonyl)allylboronate **2.14a** from ynoate **2.13a** using DIBAL-H and HMPA (Scheme 43).⁶⁵ Later in 2007, the same group extended this transformation to ethyl ester **2.14b**, for which they got a 95% yield. However, for the methyl propynoate **2.13c**, with a methyl substituted alkyne, the CuI/MeLi catalyst was required to afford **2.14c** (the reaction is slower without the catalyst), in a *Z:E* ratio of 1.9:1 (Scheme 43).⁶⁶

During the synthesis of 6,12-guaianolide, chinensiolide, Hall and coworkers used DIBAL-H and HMPA to form allylboronate **2.16** in 68% yield as 3.5:1 mixture of *Z:E* isomers (Scheme 43).^{58b} Our group also synthesized **2.16** in our first report of the APKR to the 6,12-guaianolide framework, however, the CuI/MeLi catalyst was required and a lower *Z:E* selectivity of 1.5:1 was observed (no yield was reported).⁴²

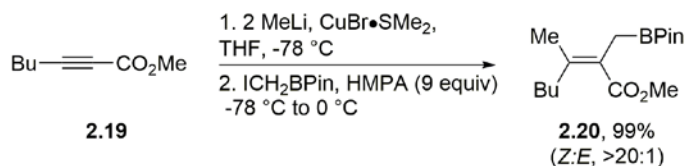


Scheme 43. Previous syntheses of trisubstituted pinacol allylboronates from alkynoates.

Previous members of the Brummond group tested the allylboronate synthesis on a series of model substrates with substitutions at the propargyl position because of instability of the protecting group (P) in the lactonization reaction. Alkynoates **2.17a-d** formed the corresponding allylboronates **2.18a-d** in high yields (95-90% yield) using DIBAL-H and HMPA; however, long reaction times were required. The ratio of Z/E alkene isomers varied based upon the substrate, but the Z isomer was always favored (Scheme 43).⁴³

The Hall group has also published reports on the synthesis of tetrasubstituted allylboronates from ynoates using organocopper reagents, optimized for selective *cis*-addition across the alkyne. For example, when 2-heptynoic acid methyl ester **2.19** was reacted with 2 equiv of methyl lithium and copper bromide (to form Me₂CuLi *in situ*), followed by HMPA (9 equiv) and pinacol iodomethylboronate, **2.20** was afforded in 99% yield, with high selectivity for the Z isomer (Scheme 44). This degree of selectivity for the *cis*-addition has not yet been

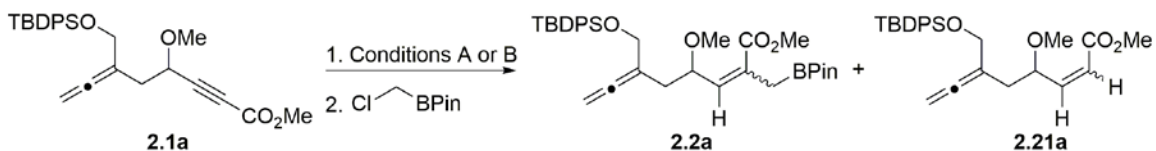
observed for this formation of the trisubstituted allylboronates seen in Scheme 43.⁶⁷ These tetrasubstituted allylboronates have been reacted with aldehydes for the synthesis of methylene lactones with a quaternary center.



Scheme 44. Synthesis of tetrasubstituted allylboronate **2.20**, with high selectivity for the *Z* isomer.

Within our report for the synthesis of guaianolide analog **1.83**, allene-containing allylboronate **2.2a** was obtained using two protocols, either with or without the CuI/MeLi catalyst system (Table 4).⁶⁸ When a pre-stirred mixture of HMPA (3 equiv) and DIBAL-H (1.6 equiv) was reacted with ynoate **2.1a** overnight, followed by stirring with pinacol chloromethylboronate for 48 h, **2.2a** was obtained in 80% yield as a 2.2:1 mixture of *Z* and *E* isomers. However, this alkene byproduct **2.21a** was also obtained in 20% yield, resulting from protonation of the aluminum intermediate (Entry 1). Employing the CuI/MeLi catalyst system significantly improved the reaction rate and lowered alkene byproduct formation. However, the stereoselectivity of the reaction was lower (*Z*:*E*, 1.2:1, Entry 2).

Table 4. Previously reported results for conversion of ynoate **2.1a** to allylboronate **2.2a**.⁴³



Entry	Conditions (Step 1)	Time (Step 2)	Yield 2.2a , (Z:E)	Yield 2.21a (Z:E)
1	A: DIBAL-H (1.6 equiv), HMPA (3 equiv), 0 °C, toluene, overnight	48 h	80%, (2.2:1)	20%, (3:1)
2	B: CuI (0.1 equiv), MeLi (0.1 equiv), DIBAL-H (1.5 equiv), HMPA (2 equiv), -30 °C, toluene/THF, 5 h	Overnight	89% ^a (1.2:1)	11%, (2:1)

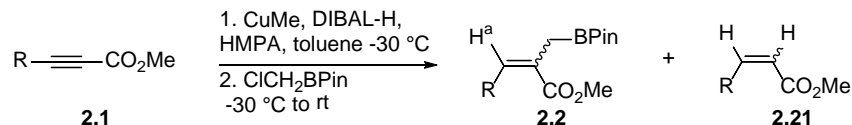
^aYield reported is the crude yield determined by NMR. **2.2a** was purified and isolated in 78%.

Difficulties reproducing the preparation of allylboronate **2.2a** have included recovery of **2.1a**, or large amounts of the unwanted alkene byproduct **2.21a**. To determine which reaction component may be hindering the formation of **2.2a**, we attempted simplified transformations (Table 5). First, conjugate reduction of allene-containing alkynoate **2.1a** was achieved using excess HMPA and DIBAL-H without CuI and MeLi and without the addition of ClCH₂BPin. Stirring of allenyl-ynoate **2.1a** with HMPA (6 equiv) and DIBAL-H (3 equiv) for 5 h at 0 °C, successfully gave unsaturated ester **2.21a** with a small amount of starting material remaining (10 : 1 ratio of alkene **2.21a** : ynoate **2.1a**) (Entry 1). Next, ClCH₂BPin was re-incorporated in attempts to form allylboronate **2.2a**. Reacting ynoate **2.1a** with HMPA (4 equiv) and DIBAL-H (2 equiv) for 3 h completely consumed allenyl-ynoate **2.1a**; ClCH₂BPin (1.5 equiv) was then added to trap the aluminum intermediate. After stirring overnight (16 h), allylboronate **2.2a** and alkene **2.21a** were afforded in a 1 : 7.8 ratio (Entry 2). Increasing the amount of ClCH₂BPin to 2.6 equiv showed an improved 1: 1.7 ratio of allylboronate **2.2a** to alkene **2.21a** after stirring for 10 h. This reaction was allowed to continue stirring to see if the reaction was still progressing. However, after 41 hours, the ratio of allylboronate **2.2a**: alkene **2.21a** had lowered to 1: 2.6, suggesting allylboronate **2.2a** was not stable to the reaction conditions over time (Entry 3). It was evident that the aluminum intermediate was not nucleophilic enough to react with ClCH₂BPin efficiently.

Due to the sensitive nature of the reaction, attempts to incorporate the CuI/MeLi catalyst were performed on propargyl-substituted model system **2.1b**. Unfortunately, using the previously reported procedure and reagent equivalents resulted in complete recovery of alkynoate **2.1b** (Entry 4). The reaction was again simplified by eliminating the addition of ClCH₂BPin to isolate the conjugate reduction product **2.21b**. Model ynoate **2.1b** was reacted with CuI and MeLi (0.1

equiv each), distilled HMPA (2 equiv), and DIBAL-H (1.5 equiv), but no alkene **2.21b** was obtained (Entry 5).

Table 5. Reaction optimization for conversion of alkynoates **2.1** to allylboronates **2.2**.



Entry	Alkynoate (2.1)	CuMe (Equiv)	HMPA (Equiv)	DIBAL (Equiv)	Time A	ClCH ₂ BPin (equiv)	Time B	Product ratio (2.2 : 2.21 : 2.1)
1	 2.1a	0	6	3 ^a	5 h	0	---	N/A : 10 : 1
2	2.1a	0	4	2 ^a	3 h	1.5	16 h	1 : 7.8 : 0
3	2.1a	0	4	2 ^a	2 h	2.6	10 h 41 h	1 : 1.7 : 0 1 : 2.6 : 0
4	 2.1b	0.1	2	1.5 ^a	5 h	1.2	16 h	0 : 0 : 1
5	2.1b	0.1	2	1.5 ^a	5 h	0	---	N/A : 0 : 1
6	 2.1c	0.1	2	1.5 ^b	5 h	0	---	N/A : 1 : 4
7	 2.1a	0.1	2	1.5 ^b	5 h	0	---	Messy
8	 2.1d	0.1 ^c	3	2 ^b	5 h	2	16 h	1 : 1 : 0
9	2.1d	0.1	3	2 ^b	4 h	2 ^c	16 h	1 : 0 : 0

Reactions w/o CuI, MeLi were performed on a 0.034-0.041 mmol scale. Reactions w/ CuI and MeLi performed on a 0.23-0.32 mmol scale. **Time A**: time after addition of ynoate, prior to addition of ClCH₂BPin. **Time B**: time after addition of ClCH₂BPin. Product ratios were determined by crude ¹H NMR spectroscopy. ^aDIBAL-H in hexanes. ^bDIBAL-H in toluene, ^cNew bottle of halogen free MeLi. ^dFreshly distilled ClCH₂BPin.

Next, an alkynoate lacking substitution at the propargyl position, methyl 2-nonynoate (**2.1c**), was subjected to these conditions. Also, DIBAL-H as a solution in toluene, rather than hexanes, was employed. As a result, the corresponding α,β -unsaturated ester **2.21c** was obtained in small amounts; (1:4 ratio of alkene **2.21c** : ynoate **2.1c**) (Entry 6). Reaction of allene-containing ynoate **2.1a** under these conditions resulted in a complicated mixture, evidenced by TLC analysis (Entry 7).

Next, in an effort to avoid inaccurate measuring of reagents for small-scale reactions, excess equivalents of CuI and MeLi were pre-stirred in THF and then the appropriate 0.1 equiv was transferred to the reaction flask. Also, the equivalents of HMPA (3 equiv) and DIBAL-H (2 equiv) were increased. Using this method, methyl 2-octynoate (**2.1d**) was reacted with CuI/MeLi, HMPA, and DIBAL-H, followed by ClCH₂BPIn to afford allylboronate **2.2d** (*Z*:*E*, 3.6:1) and alkene **2.21d** in a 1 : 1 mixture (Entry 8). The improved result of this experiment may also be attributed to the use of a new bottle of MeLi (1.0 M in THF). Next, employing freshly distilled ClCH₂BPIn in the reaction significantly improved reactivity, giving the allylboronate **2.2d** as the only product (Entry 9).

Identification of the *Z* and *E* isomers of **2.2d** were determined by comparing the chemical shift of the corresponding alkene signals (H_a). The signal representing H_a is seen at 5.93 ppm and 6.74 ppm for the *Z* and *E* isomers respectively (Figure 8). H_a for the *E* isomer is further downfield because of closer proximity to the ester group.

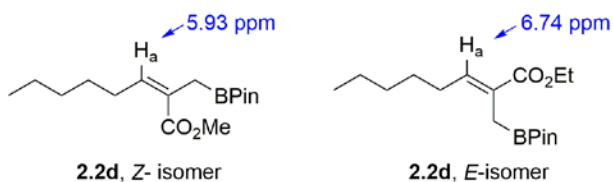
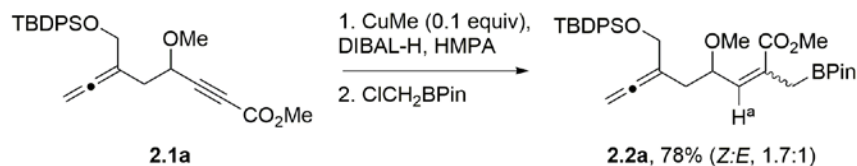


Figure 8. The *Z*- and *E*-isomers of allylboronate **2.2d**.

With the successful formation of model allylboronate **2.2d**, we applied the optimized reaction conditions to the formation of **2.2a** (Scheme 45). Careful observation of the appearance of the reaction was recorded for each step. CuI and MeLi (0.1 equiv each) were stirred at -30 °C, and the solution changed from pale white to dark yellow to brown over 30 min. HMPA (3 equiv) and DIBAL-H (2 equiv) were added resulting in a dark black solution. Ynoate **2.1a** was added and stirred at -20 °C for 5 h, and the black color was maintained. After overnight stirring with freshly distilled pinacol chloromethylboronate (2 equiv) at rt, the solution had turned to a pale,

translucent green. Analysis of the crude residue by ^1H NMR revealed allylboronate **2.2a** as the only product. Purification of the crude material through a short silica plug afforded allylboronate **2.2a** in 78% yield as a 1.7:1 ratio of the *Z* and *E* isomers. Allylboronate **2.2a** may be unstable towards silica gel because when purified by standard silica gel flash column chromatography, **2.2a** was obtained in only 22% yield.



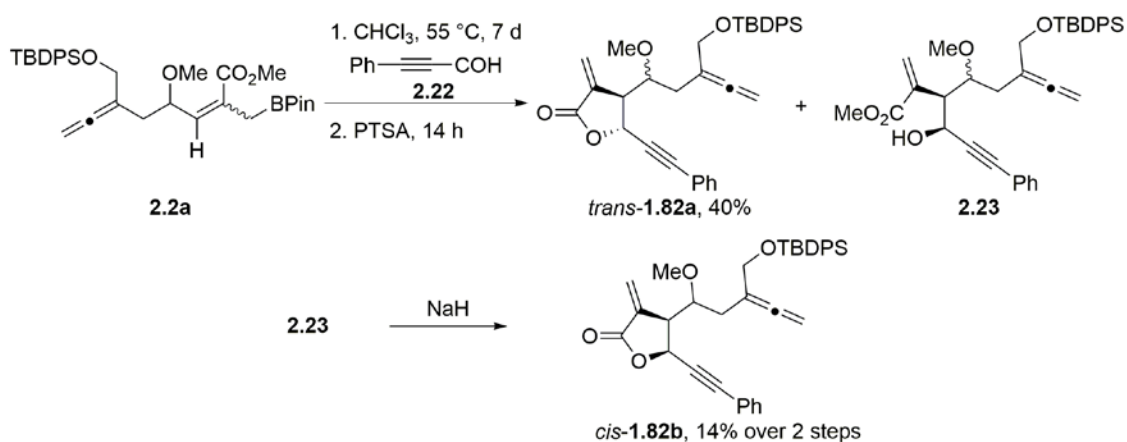
Scheme 45. Repeated synthesis of allylboronate **2.2a**.

In summary, many factors were critical to the successful formation of allylboronate **2.2a**. The quality of reagents is of utmost importance; use of impure reagents can render the entire reaction unsuccessful. Therefore, for best practice, relatively new DIBAL-H and MeLi solutions should be employed. No-D NMR titration techniques can be used to ascertain the quality and accurate concentrations of these reagents prior to use.⁶⁹ The HMPA should be distilled and stored over molecular sieves. The toluene solvent as well as the ClCH₂BPin need to be freshly distilled. For a small scale reaction, a solution of CuI/MeLi can be prepared on a larger scale than required for the reaction, with the appropriate amount being transferred as a solution to the reaction flask.

If a reaction does not go as expected, trouble shooting can be performed by methodically simplifying the reaction. Conjugate reduction of the ynoate, by quenching an aliquot of the reaction prior to addition of ClCH₂BPin, confirms formation of aluminum intermediates. Also, performing the reaction both with and without the CuI/MeLi catalyst can help determine what reagent may be leading to poor results.

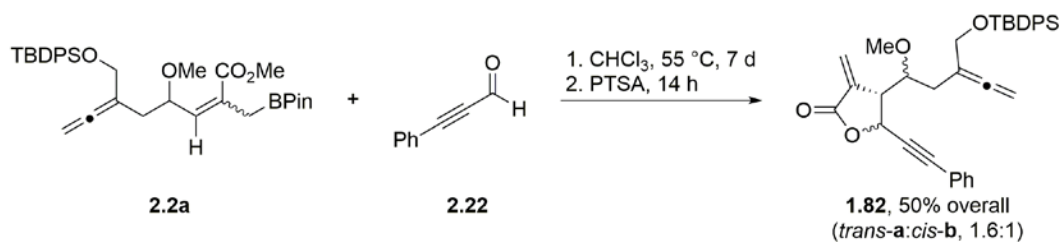
2.2.3 Completing the synthesis of guaianolide analog 1.83.

The final synthetic steps to complete the synthesis of *trans*-guaianolide analog **1.83** include the allylboration/lactonization, cyclocarbonylation, and deprotection of the silyl group. For the allylboration/lactonization step, Hall and coworkers have employed various acids to assist the allylic addition to aldehydes including boron trifluoride diethyl etherate, scandium triflate, and triflic acid.^{58a} In previous efforts toward the synthesis of guaianolide **1.83**, use of acidic reagents to accelerate the allylboration of phenylpropynal (**2.22**) resulted in decomposition of allylboronate **2.2a**. Thermal heating in toluene at 50 °C was not sufficient for the reaction to proceed and increasing the temperature to 90 °C resulted in decomposition of **2.2a**.⁶⁵ Interestingly, heating of allylboronate **2.2a** and aldehyde **2.22** in chloroform for 7 days at 50 °C followed by stirring with PTSA overnight at rt gave *trans*-lactone **1.82a** in 40% yield as a mixture of two diastereomers. The *cis*-hydroxy ester **2.23** was also obtained and required stirring with sodium hydride to afford the *cis*-lactone **1.82b** in 14% yield as a single diastereomer (Scheme 46).⁴³



Scheme 46. Previously reported synthesis of *trans*- and *cis*-lactone **1.82a,b** via allylboration followed by lactonization.

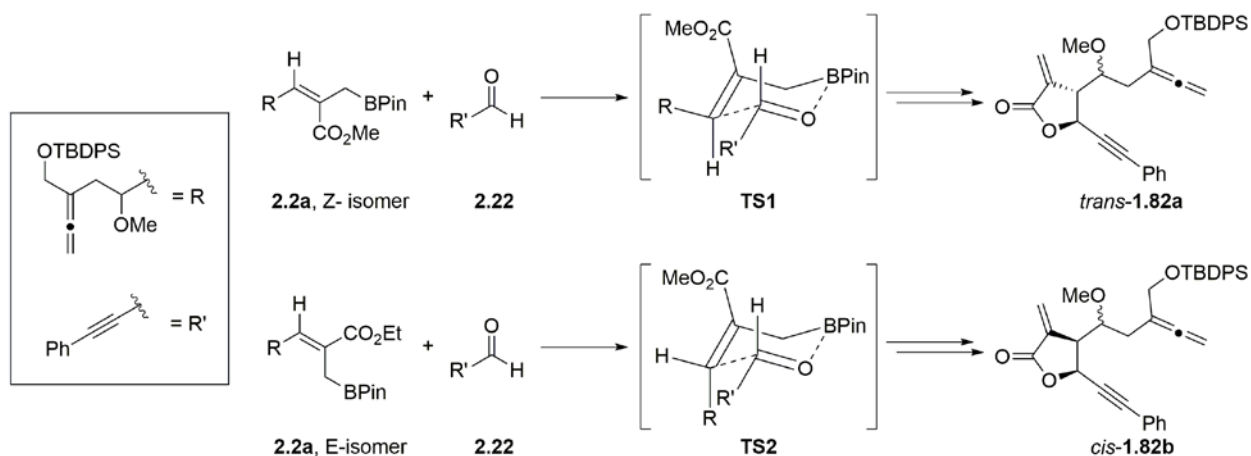
Our efforts to repeat this synthetic step gave similar results. The *Z* and *E* isomers of allylboronate **2.2a** were inseparable and taken on to the lactonization step as a mixture. Stirring **2.2a** with phenylpropynal **2.22** in chloroform for 7 days followed by the addition of PTSA, which stirred for 14 h at room temperature, resulted in 3 major product spots as observed by TLC. The *trans*-lactone **1.82a** ($R_f = 0.33$, 10% EtOAc in hexanes) was obtained as a 1.7:1 mixture of diastereomers (pertaining to the methoxy group stereochemistry). The other two product spots pertained to the two *cis*-lactone **1.82b** diastereomers, which were separable by TLC and column chromatography (Diastereomer 1: $R_f = 0.25$, Diastereomer 2: $R_f = 0.19$, 10% EtOAc in hexanes). However, Diastereomer 1 of *cis*-**1.82b** was contaminated with unreacted allylboronate **2.2a** (*E* isomer). No evidence of the hydroxyl ester intermediate **2.23** was observed. *Trans*-**1.82a** and *cis*-**1.82b** were obtained in an overall 50% yield (*trans*:*cis*, 1.6:1) (Scheme 47).



Scheme 47. Formation of *trans*- and *cis*-lactones **1.82a** and **1.82b** from allylboronate **2.2a**.

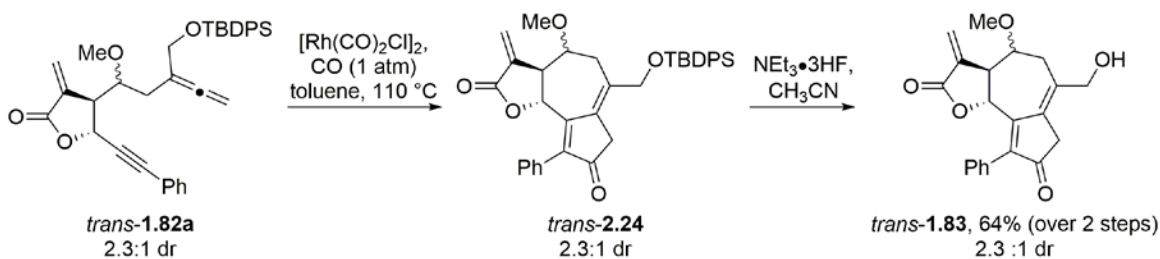
Formation of the *trans*-**1.82a** and *cis*-**1.82b** and the corresponding product ratio can be understood using Zimmerman-Traxler transition states for the reaction between the allylboronate **2.2a** and phenylpropynal **2.22**. Reaction of the *Z* isomer of **2.2a** with **2.22** results in a *trans*-hydroxyl ester via **TS1**, which is then cyclized to afford *trans*-lactone **1.82a**. In a similar fashion, the *E* isomer of **2.2a** eventually affords the *cis*-lactone **1.82b** via **TS2** (Scheme 48). This also explains why *trans*-**1.82a** is the major product; the *Z* isomer is the major allylboronate isomer. In addition, when the reaction between **2.2a** and **2.22** is monitored by ^1H NMR

spectroscopy, the *Z* isomer reacts faster than the *E* isomer, which is often recovered in small amounts.



Scheme 48. Zimmerman-Traxler transition states for the reaction between allylboronate **2.2a** and aldehyde **2.22**.

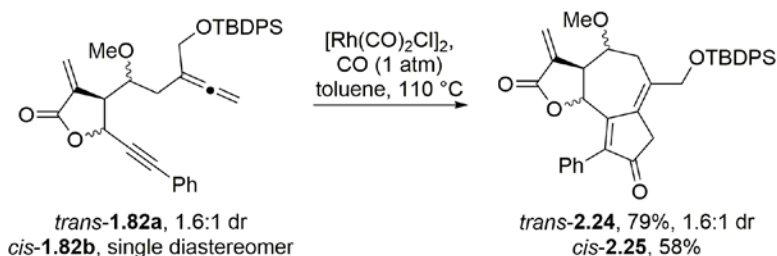
Next, *trans*-allene-yne **1.82a** was successfully subjected to the APKR, using the optimized high dilution conditions described in Section 1.2.3, to afford *trans*-guaianolide analog **2.24**. Due to previous reports that **2.24** was unstable towards silica, the crude material was carried on without purification; subsequent deprotection using trimethylamine trihydrofluoride afforded guaianolide **1.83** in 64% yield over the two steps (Scheme 49). Because our previous report also obtained *trans*-**1.83** in 64% over two steps, we can conclude that the high dilution conditions did not make a significant impact on the yield.



Scheme 49. Completing the synthesis of *trans*-guaianolide analog **1.83**.

It was later determined that the silyl-protected guaianolide analog **2.24** could in fact be purified by chromatography without any evidence of decomposition. By employing the high

dilution APKR conditions, guaianolide analog **2.24** was obtained in 79% yield. It should be noted that if *trans*-lactone **1.82a** is obtained from the previous lactonization reaction as a mixture with unreacted allylboronate **2.2a**, the mixture can be taken on to the APKR to afford **2.24a**, which is more easily separable from impurities. One diastereomer of the *cis*-**1.82b** was also subjected to the high dilution conditions, which afforded *cis*-**2.25** in 58% yield (Scheme 50).



Scheme 50. Isolation of cyclocarbonylation adducts *trans*-**2.24** and *cis*-**2.25**.

2.2.4 Distinguishing stereochemistry of *trans*- and *cis*- α -methylene lactones

The stereochemical identity of the guaianolide analogs *trans*-**2.24**, *cis*-**2.25**, and *trans*-**1.83** were confirmed using the coupling constant of H_a and comparing this to the X-ray crystal structure of **2.26a** (Figure 9). *Trans*-guaianolide analog **2.26a** was part of a series of guaianolide analogs synthesized in our group. All of the *trans*-analogs **2.26** had coupling constants for H_a ranging from 9.0 to 10.0 Hz. The *cis*-analogs **2.27** had coupling constants of 7.0-7.5 Hz. Similarly, the highly oxygenated *trans*-guaianolide analogs **2.24** and **1.83** (2 diastereomers of each) have H_a coupling constants from 9.2-10.5 Hz, while *cis*-**2.25** has a coupling constant of 7.5 Hz (Figure 9).

Interestingly, for the allene-yne APKR precursors *trans*-**1.82a** and *cis*-**1.82b**, the coupling constant of H_a with H_b, is larger for the *cis* isomer than the *trans* isomer, which is opposite of the trend seen for the guaianolide analogs in Figure 9. The major and minor diastereomers of *trans*-

1.82a had J_{ab} values of 4.4 Hz and 3.2 Hz respectively, while the major and minor diastereomers of *cis*-**1.82b** had J_{ab} values of 8.0 Hz and 7.0 Hz (Figure 10). This trend was also previously reported for α -methylene lactones *trans*- and *cis*-**2.28**, a synthetic precursor to the corresponding guaianolide analog **2.26**. *Trans*-**2.28a** has a H_a coupling constant of 6.0 Hz, while the *cis*-isomer **2.28b** coupling constant for H_a is 8.4 Hz (Figure 10).⁴²

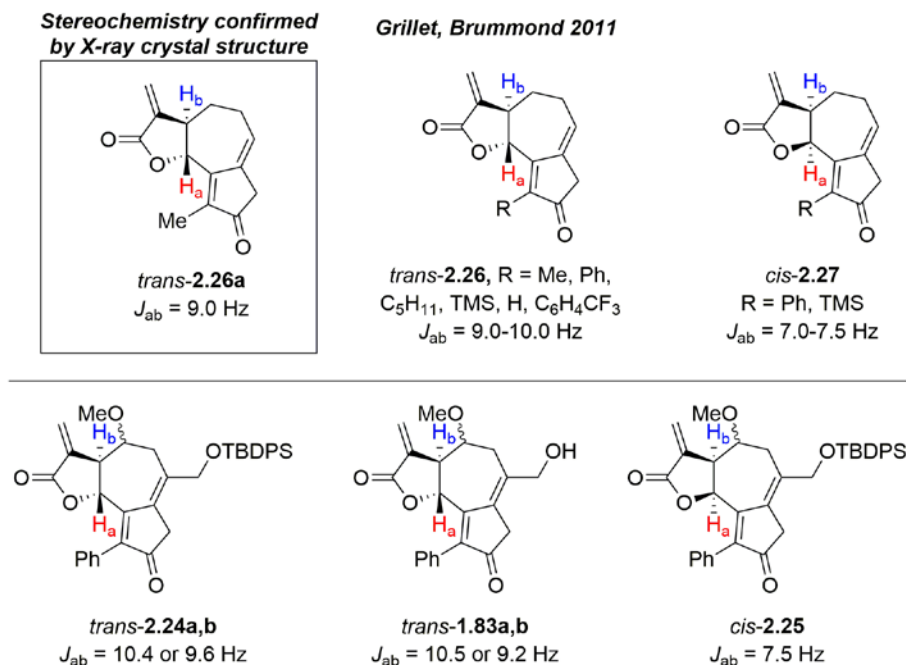


Figure 9. Comparison of coupling constants for **2.24**, **1.83**, and **2.25** with previously reported guaianolide analogs.

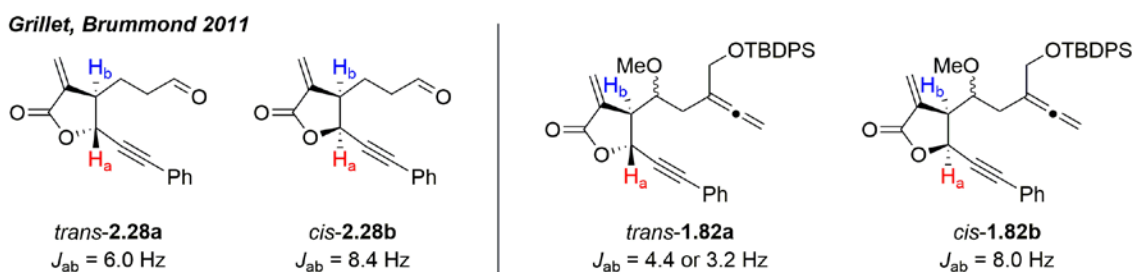


Figure 10. Coupling constants for mono-cyclic *trans*- and *cis*-methylene lactones.

The change in the coupling constant between H_a and H_b when comparing the mono-cyclic *trans*- α -methylene lactones (Figure 10) and the *trans*- α -methylene lactone of the fused 5,7,5-tricyclic frameworks (Figure 9) can be understood by comparing the orientations of H_a and H_b

(Figure 11). *Trans*-**1.82a** and *trans*-**1.83** were drawn in Chem3D 15.0 and MM2 minimization calculations were performed to show a low energy conformer of the structures. For these conformers, the H_a, H_b dihedral angle was observed. Mono-cyclic lactone **1.82a** had a dihedral angle of 114.8 ° for H_a and H_b. However, the fused ring system **1.83** requires the alkyl substituents of the lactone ring to be in a more planar configuration, resulting in a larger dihedral angle for H_a and H_b, estimated to be 147.7°. This larger dihedral angle is responsible the larger coupling constant observed for the fused *trans*-methylene lactones. *Trans*-**2.28a** also had a dihedral angle for H_a and H_b of 114.4 ° and was shown in Figure 11 rather than allene-yne **1.82a** for ease of visualization.

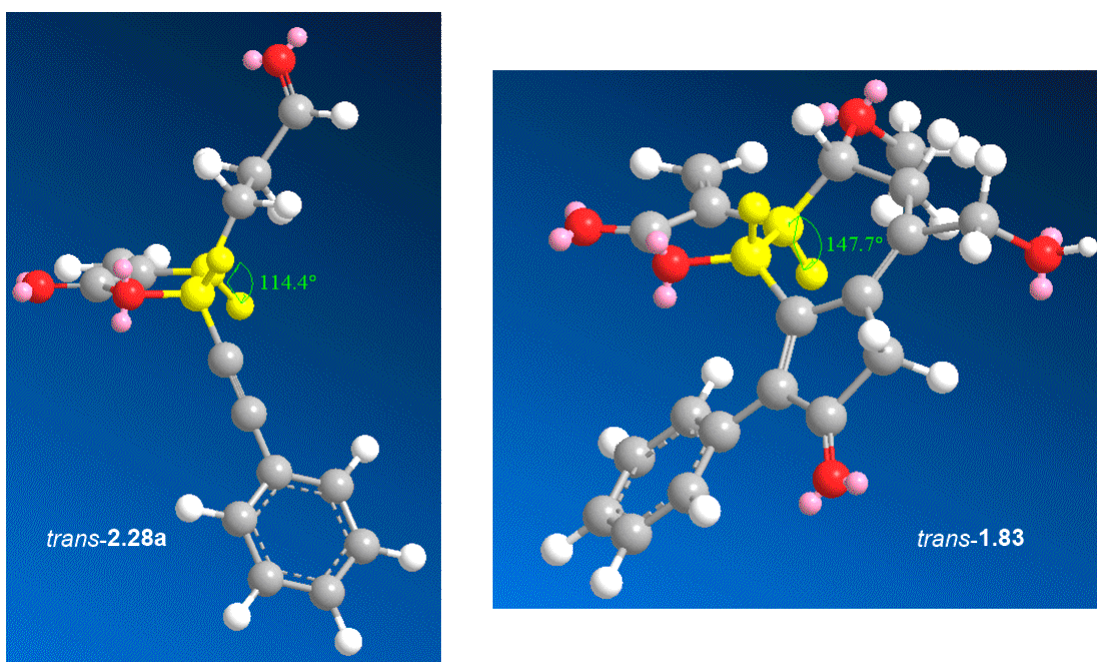


Figure 11. 3D-representations of *trans*-**2.28a** and *trans*-**1.83** (Chem3D) with highlighted H_a, H_b dihedral angle.

2.2.5 Assignment of **1.83** diastereomers using NMR calculations

The described synthesis provides *trans*-guaianolide analog **1.83** as a mixture of diastereomers with respect to the methoxy group at C8 of the guaianolide framework. Biological evaluations previously described for *trans*-**1.83** (NF- κ B inhibition and antiproliferative activity) are representative of this diastereomeric mixture. However, we were interested to know if the diastereomers had equal or differing biological properties. Slight separation of the **1.83** diastereomers is observed by TLC. We assigned the faster moving ($R_f = 0.41$, 100% EtOAc), major spot as Diastereomer A, and the slower moving ($R_f = 0.34$, 100% EtOAc), minor spot as Diastereomer B. Column chromatography was insufficient for complete separation. However, HPLC purification afforded the separated isomers. The following method was used: 100% EtOAc for 20 min followed by a gradient increase to 5% EtOH in EtOAc over 5 min, which was then maintained until completion. Diastereomer A eluted at 14.004 min while Diastereomer B eluted at 17.009 min. The major diastereomer (Diastereomer A) was determined to be 8β H-**1.83a** isomer while the minor diastereomer (Diastereomer B) was the 8α H-**1.83b** isomer by comparing computational and experimental 1 H NMR data for the two isomers (Figure 12).

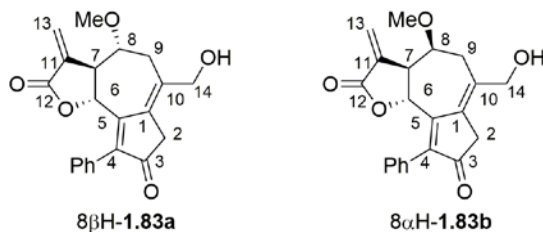


Figure 12. Structure of 8β H-**1.83a** and 8α H-**1.83b**.

The two diastereomers have distinct 1 H NMR spectra, particularly for the α -methylene protons H₁₃ and H_{13'}, and the proton α to the oxygen of the lactone ring (H₆). These signals all appear between 6.5 and 5.0 ppm (Figure 13). Computational methods have been utilized to

assign closely related chemical structures by comparing predicted chemical shifts with experiment.⁷⁰

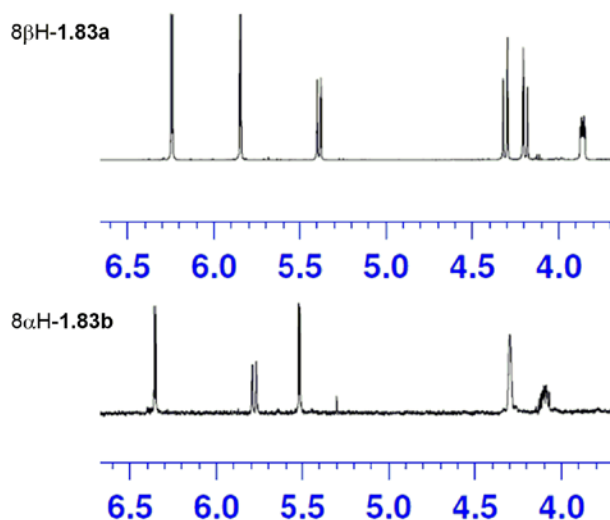


Figure 13. ¹H NMR spectra for **1.83a,b** from 6.7-3.7 ppm.

The two possible isomers were drawn in Spartan. **8βH-1.83a** has a *trans* relationship for H₆ and H₇ of the lactone ring, as well as a *trans* relationship between H₇ and H₈. **8αH-1.83b** also has a *trans*-lactone, but H₇ and H₈ have a *cis*-relationship. The lowest energy conformations of each were determined using molecular mechanics (MMFF) calculations. Then, ¹H NMR chemical shifts were predicted using EDF2/6-31 methods. Spartan assigned the predicted chemical shifts to the corresponding hydrogen atoms.

Next, COSY and HSQC NMR spectra were obtained for each diastereomer, which assisted the assignment of the ¹H NMR signals to the corresponding protons for each structure. For complete signal assignments, see Figure 12 and Table 6. Due to complicated splitting patterns of each diastereomer, the COSY and HSQC spectra were key in determining the identity of a few protons. The signals of protons H₂ and H_{2'} were confirmed because the only COSY correlations were with each other, and the HSQC confirmed that these two signals were on the

same carbon. This was also the case for protons H₁₄ and H_{14'}, however, these protons were shifted further down field (~4.2 ppm) indicating their proximity to the hydroxyl group. COSY correlations were particularly useful for the assignment of H₇, H₉, and H_{9'}. Even though H₉ and H_{9'} have significantly different chemical shifts (~3.2 and 2.5 ppm for both diastereomers), COSY correlations with only H₈ and each other lead to their assignment. HSQC also confirmed that H₉ and H_{9'} were on the same carbon. H₇ has a similar chemical shift to H₉ (~3.1 ppm), however H₇ has COSY correlations with H₈, H₆, H₁₃, and H_{13'} for both diastereomers.

Table 6. Experimental ¹H NMR spectral data of 8βH-**1.83a** and 8αH-**1.83b** compared to calculated chemical shifts (corrected).

Diastereomer A (8βH- 1.83a)			Diastereomer B (8αH- 1.83b)		
H	Exp δ (ppm)	Calc δ (ppm)	H	Exp δ (ppm)	Calc δ (ppm)
Ph	7.40-7.32 (m, 3 H), 7.27-7.24 (m, 2 H)	7.73, 7.69, 7.26, 7.26, 7.25	Ph	7.45-7.32 (m, 3 H), 7.30-7.26 (m, 2 H)	7.66, 7.32, 7.28, 7.28, 7.26
13	6.25 (d, <i>J</i> = 3.5 Hz, 1 H)	6.23	13	6.36 (d, <i>J</i> = 3.6 Hz, 1 H)	6.35
13'	5.85 (d, <i>J</i> = 3.0 Hz, 1 H)	5.78	13'	5.52 (d, <i>J</i> = 3.2 Hz, 1 H)	5.36
6	5.39 (d, <i>J</i> = 10.5 Hz, 1 H)	5.37	6	5.78 (d, <i>J</i> = 9.2 Hz, 1 H)	5.83
14, 14'	4.31 (d, <i>J</i> = 12.5 Hz, 1H), 4.19 (d, <i>J</i> = 12.5 Hz, 1 H)	4.28, 4.12	14, 14'	4.34-4.26 (m, 2 H)	4.39, 4.31
8	3.86 (ddd, <i>J</i> = 8.0, 4.0, 2.5 Hz, 1 H)	3.59	8	4.14-4.07 (m, 1 H)	4.09
OMe	3.54 (s, 3 H)	3.54	OMe	3.45 (s, 3 H)	3.39
2, 2'	3.29 (d, <i>J</i> = 21.0 Hz, 1 H), 3.17 (d, <i>J</i> = 21.0 Hz, 1 H)	2.92, 2.54	2, 2'	3.28-3.15 (m, 2 H)	2.89, 2.51
7	3.18-3.13 (m, 1 H)	3.04	7	3.37-3.31 (m, 1H)	3.22
9,9'	3.16-3.12 (m, 1 H) 2.56 (dd, <i>J</i> = 15.8, 2.5 Hz, 1H)	3.12, 2.28	9, 9'	3.27 (dd, <i>J</i> = 15.2, 6.8 Hz, 1H) 2.53 (dd, <i>J</i> = 15.2, 8.4 Hz, 1H)	3.28, 2.24
OH	1.73 (bs, 1 H)	0.27	OH	1.26 (t, <i>J</i> = 7.2 Hz, 1 H)	0.27

Using proton assignments determined by analyzing the ¹H, COSY, HSQC NMR spectra, experimental chemical shifts were compared to the chemical shifts that Spartan had generated for

each corresponding hydrogen (Table 6, entries are listed in order of decreasing experimental chemical shift for both diastereomers). Comparison of the experimental and calculated chemical shifts of protons H₁₃, H_{13'}, and H₆ were instrumental in making this conclusion. In 8 α H-**1.83b**, H₆ is shifted further down field than H_{13'} at 5.83 ppm; whereas H₆ appears at 5.37 ppm for 8 β H-**1.83a**. The predicted chemical shifts were also quite accurate, with errors of less than 0.1 ppm for protons H₁₃, H_{13'}, and H₆.

2.3 CONCLUSIONS

In conclusion, the synthesis of racemic *trans*-guaianolide analog **1.83** was successfully reproduced. The synthesis was performed in three phases; 1) synthesis of ynoate **2.1a** from 2-butyn-1,4-diol in 7 steps, 2) generation of the allylboronate **2.2a**, and 3) allylboronation/lactonization followed by the APKR to generate the 5,7,5-fused ring system.

The synthesis of ynoate **2.1a** was achieved with minimal modifications to the previously published protocols. Some minor changes were required related to reaction temperatures, especially for conversion of the Weinreb amide **2.5** to ketone **2.6**. This segment of the guaianolide synthesis showcases the robust nature of the allene functional group. In synthetic endeavors, allenes are generally made directly prior to being utilized for unique functionalization. However, in this sequence, the allene was formed during an early synthetic step, and carried through many reaction steps, showing compatibility with a variety of reagents.

Conversion of ynoate **2.1a** to allylboronate **2.2a** was the most difficult step to reproduce. The experimental conditions used to successfully achieve formation of allylboronate **2.2a** were similar to that previously reported. The equivalents of DIBAL-H and HMPA were increased to 2

and 3 equiv respectively (previously 1.5 and 2 equiv). Also, for small scale reactions, the CuI/MeLi catalyst was made in excess as a solution, and then the required amount was transferred to the reaction flask. However, we found that the quality and nature of many reagents affected the success of the reaction. Use of model systems, quenching of aluminate intermediates, and performing a non-CuMe catalyzed variant of the reaction all contributed to the trouble shooting, and eventual success of the reaction.

Finally, the ring-forming lactonization and APKR reactions were readily reproduced. The allylboration/lactonization reaction between allylboronate **2.2a** and phenylpropynal **2.22** successfully afforded both *trans*-allene-yne **1.82a** and *cis*-allene-yne **1.82b**. While the yield of *trans*-**1.82a** was comparable to the previous report, improvements were observed for the formation of *cis*-**1.82b**. The hydroxyester intermediate **2.23** was not observed, and lactonization of both *cis*-diastereomers were achieved directly from the reaction. Both *cis*- and *trans*- lactones are found in guaianolide natural products, so having a synthesis that can afford both, with ease of separation, is advantageous. Use of the dropwise addition conditions for the APKR did not significantly improve the yield of *trans*-guaianolide **1.83**. Silyl protected guaianolides *trans*-**2.24** and *cis*-**2.25** were found to be stable to column chromatography despite previous reports of instability.

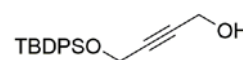
One major improvement made to this synthesis was the separation and relative stereochemical assignments of the two *trans*-**1.83** diastereomers, 8 β H-**1.83a** and 8 α H-**1.83b**. Separation was achieved by HPLC. NMR methods were used alongside computational predictions, obtained using Spartan software, to assign the corresponding structures. We plan to evaluate the separated diastereomers for relative NF- κ B inhibition and compare to the previous data obtained using a mixture of the compounds (See Section 4.2).

2.4 EXPERIMENTALS

2.4.1 General Methods

All commercially available compounds were used as received unless otherwise noted. Dichloromethane (DCM), diethyl ether (Et₂O), and tetrahydrofuran (THF) were purified by passing through alumina using a solvent purification system. Deuterated chloroform (CDCl₃) was stored over 4 Å molecular sieves. Toluene was freshly distilled from CaH₂. Acetonitrile was distilled and stored over 4 Å molecular sieves. HMPA was distilled from CaH₂ under vacuum pressure. Pinacol chloromethylboronate (ClCH₂BPin) was distilled at 14 mmHg. Carbon monoxide gas was purchased from Matheson gas (Grade: Matheson 99.99%). Purification of the compounds via manual flash column chromatography was performed using silica gel (40-63 μm particle size, 60 Å pore size) purchased from Sorbent Technologies. TLC analyses were performed on Silicycle SiliaPlate G silica gel glass plates (250 μm thickness) and visualized by UV irradiation (at 254 nm) and KMnO₄ stain. ¹H NMR and ¹³C NMR spectra were recorded on Bruker Avance 300 MHz, 400 MHz, 500 MHz, or 600 MHz. Spectra were referenced to residual chloroform (7.26 ppm, ¹H; 77.16 ppm, ¹³C). Chemical shifts are reported in ppm, multiplicities are indicated by s (singlet), bs (broad singlet), d (doublet), t (triplet), q (quartet), p (pentet), and m (multiplet). Coupling constants, *J*, are reported in hertz (Hz). All NMR spectra were obtained at room temperature. IR spectra were obtained using a Nicolet Avatar E.S.P. 360 (NaCl plate) FT-IR. ESI mass spectrometry was performed on a Waters Q-TOF Ultima API, Micromass UK Limited. Separation of 8βH-**1.83a** and 8αH-**1.83b** was performed on a Varian Prostar HPLC chromatograph using a Varian Dynamax Microsorb 100-5 Si column.

2.4.2 Synthesis of ynoate 2.1a.

 **4-((*tert*-Butyldiphenylsilyloxy)but-2-yn-1-ol (1.116).** A 15 mL, round-bottomed flask, equipped with a stir bar, septum, and nitrogen inlet needle was charged with DCM (5 mL), 2-butyn-1,4-diol **2.3** (0.132 g, 1.54 mmol, 2 equiv), and DMF (1 mL). Imidazole (0.063 g, 0.920 mmol, 1.2 equiv) was added followed by *tert*-butyl(chloro)diphenylsilane (0.211 g, 0.770 mmol, 1 equiv) and the reaction stirred for 3 h at rt. The reaction was diluted with water (3 mL) and DCM (3 mL). The contents were transferred to a separatory funnel. The organic layer was separated and the aqueous layer was extracted with DCM (2 x 6 mL). The combined organic layers were dried over MgSO₄, filtered, and concentrated via reduced pressure rotary evaporation. The crude residue was purified by silica gel flash column chromatography (gradient of 10-20% EtOAc in hexanes) to afford 250 mg of **1.116** in 73% yield as an oil. The characterization data obtained matches previously reported data.⁶⁰

- Performing the reaction on 40.6 mmol scale afforded 8.76 g of **1.116** (66% yield).

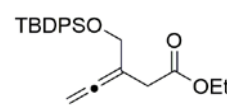
Data for 1.116.

¹H NMR (300 MHz, CDCl₃)

7.73-7.68 (m, 4H), 7.48-7.37 (m, 6H), 4.37 (t, *J* = 1.8 Hz, 2H), 4.20 (dt, *J* = 6.3, 1.8 Hz, 2H), 1.29 (t, *J* = 6.3 Hz, 1H), 1.06 (s, 9H) ppm;

TLC R_f = 0.38 (20% EtOAc in hexanes)

Silica gel, UV visible

 **Ethyl 3-(((*tert*-butyldiphenylsilyloxy)methyl)penta-3,4-dienoate (2.4).** A 100 mL, 2-necked, round-bottomed flask, equipped with a stir bar, a Dean-Stark trap topped with a condenser and nitrogen inlet adapter, and a septum in the side arm was charged with **1.116** (7.31 g, 22.5 mmol, 1 equiv) and triethyl orthoacetate (12.7 mL, 69.1 mmol,

3 equiv). The flask was placed in a pre-heated oil bath (130 °C) and propionic acid (0.3 mL, 4.0 mmol, 0.18 equiv) was added. Additional propionic acid was added after 1.5 h and after 3.5 h (0.2 mL each time, 2.7 mmol, 0.12 equiv). After 5 h, an additional 0.1 mL of propionic acid (1.3 mmol, 0.06 equiv) was added. The reaction stirred for a total of 6 h. The oil bath was removed and the reaction cooled to rt. The reaction was diluted with diethyl ether (20 mL). 1M HCl (40 mL) was added and contents were transferred to a separatory funnel. The aqueous layer was separated and extracted with diethyl ether (3 x 15 mL). The combined organics were washed with saturated NaHCO₃ (40 mL) and brine (40 mL), dried over MgSO₄, filtered, and concentrated using reduced pressure rotary evaporation. The crude residue was purified by silica gel flash column chromatography (gradient of 10-20% EtOAc in hexanes) to afford **2.4** (6.74g, 76%) as a pale yellow oil. The characterization data obtained matches previously reported data.⁴³

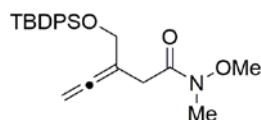
Data for **2.4**.

¹H NMR (300 MHz, CDCl₃)

7.69-7.65 (m, 4H), 7.45-7.33 (m, 6H), 4.75 (quintet, $J = 2.4$ Hz, 2H), 4.27 (t, $J = 2.4$ Hz, 2H), 4.12 (q, $J = 7.2$ Hz, 2H), 3.12 (t, $J = 2.4$ Hz, 2H), 1.23 (t, $J = 7.2$ Hz, 3H), 1.05 (s, 9H) ppm;

TLC $R_f = 0.47$ (10% EtOAc in hexanes)

Silica gel, UV visible, KMnO₄ stain



3-(((*tert*-Butyldiphenylsilyloxy)methyl)-*N*-methoxy-*N*-methylpenta-

3,4-dienamide (2.5). A 200 mL, single-necked, round-bottomed flask,

equipped with a stir bar, septum, and nitrogen inlet needle was charged with THF (68 mL), ester **2.4** (3.12 g, 7.91 mmol, 1 equiv), and *N,O*-dimethylhydroxylamine hydrochloride (1.16 g, 11.9 mmol, 1.5 equiv). The resulting slurry was cooled to -20 °C on a cryo-cool and ethanol bath.

Isopropylmagnesium chloride (9.89 mL of a 2.0 M solution in THF, 19.8 mmol, 2.5 equiv) was added over 5 min via syringe. The reaction stirred for 1 h at -20 °C and 2 h at -10 °C. A significant amount of **2.4** remained, as evidenced by TLC, so additional *N,O*-dimethylhydroxylamine hydrochloride (600 mg, 6.15 mmol) and isopropylmagnesium chloride (5.0 mL, 10.0 mmol) were added. The reaction stirred for 2.5 h at -10 °C, until the reaction was complete. The reaction was quenched with saturated NH₄Cl solution (75 mL) and the contents were transferred to a separatory funnel. The aqueous layer was extracted with diethyl ether (3 x 50 mL). The combined organics were dried over MgSO₄, filtered, and concentrated under reduced pressure rotary evaporation. The crude residue was purified by silica gel flash column chromatography (gradient of 10-30% EtOAc in hexanes) to afford 2.17 g of **2.5** in 67% yield as a pale yellow oil. The characterization data obtained matches previously reported data.⁴³

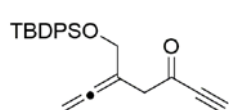
Data for **2.5**.

¹H NMR (300 MHz, CDCl₃)

7.70-7.64 (m, 4H), 7.42-7.33 (m, 6H), 4.75 (quintet, *J* = 2.6 Hz, 2H), 4.29 (t, *J* = 2.4 Hz, 2H), 3.67 (s, 3H), 3.26 (b s, 2H), 3.18 (s, 3H), 1.05 (s, 9H) ppm;

TLC R_f = 0.32 (20% EtOAc in hexanes)

Silica gel, UV visible



5-(((*tert*-Butyldiphenylsilyl)oxy)methyl)hepta-5,6-dien-1-yn-3-one **2.6.** A

flame-dried, 250 mL, round-bottomed flask, equipped with a stir bar and septum was charged with amide **2.5** (3.17 g, 7.7 mmol, 1 equiv), dissolved in THF (77 mL). The flask was cooled to -78 °C in a dry ice and acetone bath. Ethynylmagnesium bromide (46.4 mL of a 0.5 M solution in THF, 23.2 mmol, 3 equiv) was added over 5 min via syringe. The reaction stirred for 30 min. The dry ice bath was removed and the solution was allowed to warm slowly to

rt. After 1 h of stirring, the reaction was complete as evidenced by TLC. The reaction was quenched with saturated NH_4Cl (100 mL), and the flask contents were transferred to a separatory funnel. The organic layer was separated and the aqueous layer was extracted with diethyl ether (3 x 60 mL). The combined organics were dried over MgSO_4 , filtered, and concentrated to afford 2.92 g of crude **2.6** (quantitative). The NMR showed contamination with THF, but the crude material was taken onto the next step without further purification. The characterization data obtained matches previously reported data.⁴³

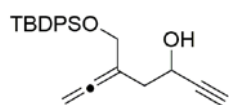
Data for 2.6.

^1H NMR (300 MHz, CDCl_3)

7.70-7.64 (m, 4H), 7.46-7.32 (m, 6H), 4.79 (t, $J = 2.4$ Hz, 2H), 4.23 (t, $J = 2.4$ Hz, 2H), 3.35 (t, $J = 2.4$ Hz, 2H), 3.19 (s, 1H), 1.05 (s, 9H) ppm;

TLC $R_f = 0.34$ (10% Et_2O in hexanes)

Silica gel, UV visible



5-(((*tert*-Butyldiphenylsilyl)oxy)methyl)hepta-5,6-dien-1-yn-3-ol 2.7. A

flame-dried, 250 mL, round-bottomed flask equipped with a stir bar and septum, pierced with a nitrogen inlet needle was charged with Et_2O (31 mL) and LAH (8.47 mL of a 1.0 M solution in Et_2O , 8.47 mmol, 1.1 equiv). The flask was cooled to -78 °C on a dry ice and acetone bath. Ketone **2.6** was dissolved in Et_2O (20 mL) and was added over 5 minutes via syringe. The reaction stirred for 25 min until complete, as evidenced by TLC. The dry ice bath was removed and the reaction was quenched slowly with water as the solution warmed to rt. The solution was diluted with Et_2O (60 mL) and water (60 mL). The flask contents were transferred to a separatory funnel. The organic layer was separated and the aqueous layer was extracted with Et_2O (3 x 40 mL). The combined organics were dried over MgSO_4 , filtered, and concentrated.

The crude material was purified by silica gel flash column chromatography (gradient of 20-30% Et₂O in hexanes) to afford 2.04 g of **2.7** in 71% yield (over 2 steps from **2.5**). The characterization data obtained matches previously reported data.⁴³

Data for **2.7**.

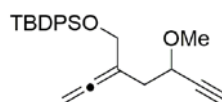
¹H NMR (300 MHz, CDCl₃)

7.73-7.67 (m, 4H), 7.48-7.36 (m, 6H), 4.74 (quintet, *J* = 2.1 Hz, 2H), 4.60-4.53 (m, 1H), 4.25-4.14 (m, 2H), 3.14 (d, *J* = 5.7 Hz, 1H), 2.62-2.45 (m, 2H), 2.44 (d, *J* = 2.1 Hz, 1H), 1.06 (s, 9H) ppm;

Impurities observed at 1.55, 1.27, 0.96, 0.88 ppm.

TLC R_f = 0.38 (20% EtOAc in hexanes)

Silica gel, UV visible

 **tert-Butyl((4-methoxy-2-vinylidenehex-5-yn-1-yl)oxy)diphenylsilane **2.8**.**

A flame-dried, 25 mL, round-bottomed flask equipped with a stir bar, septum, and nitrogen inlet needle was charged with THF (9 mL) and sodium hydride (53.5 mg of a 60% dispersion in mineral oil, 1.34 mmol, 1.2 equiv). The suspension was cooled to 0 °C on an ice bath. Alcohol **2.7** (375 mg, 0.996 mmol, 1 equiv) was dissolved in THF (2 mL) and added to the reaction. The solution stirred for 15 min prior to addition of iodomethane (0.14 mL, 2.23 mmol, 2 equiv). The reaction was allowed to warm to rt and stirred for 3.5 h until complete, as evidenced by TLC. The solution was quenched with saturated NH₄Cl (20 mL) and transferred to a separatory funnel. The organic layer was separated and the aqueous layer was extracted with Et₂O (3 x 20 mL). The combined organics were dried over MgSO₄, filtered, and concentrated. The crude material was purified by silica gel flash column chromatography (gradient of 2-10%

EtOAc in hexanes) to afford 300 mg of **2.8** in 77% yield. The characterization data obtained matches previously reported data.⁴³

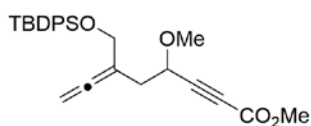
Data for **2.8**.

¹H NMR (300 MHz, CDCl₃)

7.71-7.64 (m, 4H), 7.45-7.34 (m, 6H), 4.78-4.69 (m, 2H), 4.21 (app s, 2 H), 4.08 (dt, *J* = 6.8, 1.6 Hz, 1H), 3.38 (s, 3H), 2.57-2.41 (m, 2H), 2.41 (d, *J* = 1.6 Hz, 1H), 1.05 (s, 9H) ppm;

TLC R_f = 0.46 (10% Et₂O in hexanes)

Silica gel, UV visible



Methyl 6-(((*tert*-butyldiphenylsilyl)oxy)methyl)-4-methoxyocta-6,7-dien-2-ynoate **2.1a.**

A flame-dried, 25 mL, round-bottomed flask equipped with a stir bar, septum, and nitrogen inlet needle was charged with alkyne **2.8** (315 mg, 0.806 mmol, 1 equiv) dissolved in THF (4 mL). The reaction was cooled to -78 °C on a dry ice and acetone bath. *n*-Butyl lithium (0.61 mL of a 1.6 M soln in hexanes, 0.967 mmol, 1.2 equiv) was added dropwise via syringe. The reaction stirred for 1 h while the ice bath was warmed slowly to -35 °C by the addition of acetone to the dry ice bath. Methyl chloroformate (0.12 mL, 1.61 mmol, 2 equiv), dissolved in THF (2 mL), was added and solution stirred for 15 min. The reaction was quenched with saturated NH₄Cl and diluted with Et₂O. The flask contents were transferred to a separatory funnel and the organic layer was separated. The aqueous layer was extracted with Et₂O (3 x 10 mL). The combined organics were dried over MgSO₄, filtered, and concentrated. The crude residue was purified by silica gel flash column chromatography (gradient of 5-10% EtOAc in hexanes) to afford 244 mg of **2.1a** in 69% yield as a pale yellow oil. The characterization data obtained matches previously reported data.⁴³

Data for **2.1a**.

¹H NMR (300 MHz, CDCl₃)

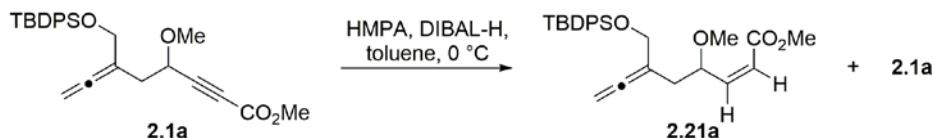
7.71-7.64 (m, 4H), 7.44-7.32 (m, 6H), 4.78 (quintet, *J* = 2.7 Hz, 2H), 4.21 (t, *J* = 7.2 Hz, 1H), 4.20 (t, *J* = 2.7 Hz, 1H), 3.78 (s, 3H), 3.39 (s, 3H), 2.56-2.49 (m, 2H), 1.05 (s, 9H) ppm;

TLC R_f = 0.27 (10% Et₂O in hexanes)

(Silica gel, UV visible)

2.4.3 Optimization of Allylboronate formation (Experiments for Table 5)

Reaction of **2.1a** with HMPA and DIBAL-H (Entry 1)



A flame-dried, 5 mL, round-bottomed flask, equipped with a stir bar and septum pierced with a nitrogen inlet needle was charged with toluene (0.3 mL) and cooled to 0 °C on an ice and water bath. HMPA (36 μ L, 0.21 mmol, 6 equiv) and DIBAL-H (0.10 mL of a 1.0 M solution in toluene, 0.10 mmol, 3 equiv) were added sequentially and stirred for 30 min. Alkynoate **2.1a** (15 mg, 0.034 mmol, 1 equiv), dissolved in toluene (0.2 mL), was added to the reaction in one portion via syringe and stirred for 5 h. A small aliquot was removed from the reaction, diluted with diethyl ether (2 mL) and washed with 1 M HCl, saturated NaHCO₃, and brine (2 mL each), dried over MgSO₄, filtered and concentrated. Crude ¹H NMR revealed a 10:1 mixture of alkene **2.21a** and ynoate **2.1a**. Alkene **2.21a**, although previously reported, was not previously

characterized.⁴³ Characterization was obtained from a sample obtained by a previous group member; the sample had a 6.1: 1, *Z:E* isomeric ratio.

Data for 2.21a.

¹H NMR (400 MHz, CDCl₃)

7.71-7.65 (m, 4 H), 7.44-7.34 (m, 6 H), 6.82 (dd, *J* = 15.6, 6.4 Hz, 1 H)*, 6.08 (dd, *J* = 11.6, 8.6 Hz, 1 H), 5.98 (dd, *J* = 15.6, 1.2 Hz, 1 H)*, 5.90 (dd, *J* = 11.6, 1.2 Hz, 1 H), 4.99-4.92 (m, 1 H), 4.73-4.69 (m, 2 H), 4.20 (t, *J* = 2.8, 2 H), 3.75 (s, 3 H)*, 3.69 (s, 3 H), 3.27 (s, 3 H), 2.37 (ddt, *J* = 14.8, 7.2, 2.8 Hz, 1 H), 2.27 (ddt, *J* = 14.8, 5.2, 2.8 Hz, 1 H), 1.05 (s, 9H)*, 1.04 (s, 9 H) ppm;

*discernable signal for *E*-2.21a

¹³C NMR (100 MHz, CDCl₃)

206.7, 166.3, 150.4, 135.8, 129.7, 127.8, 127.7, 121.6, 99.7, 75.4, 64.9, 57.1, 51.5, 34.4, 27.0, 19.5 ppm;

IR (thin film)

2931, 2858, 1961, 1725, 1429, 1196, 1109, 824, 703 cm⁻¹;

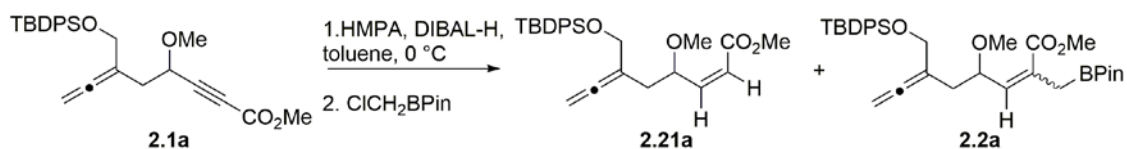
HRMS (FTMS + p ESI Full ms)

[*M* + *H*]⁺ calcd for C₂₇H₃₅O₄Si, 451.2299; found, 451.2280;

TLC R_f = 0.65 (20% EtOAc in hexanes)

Silica gel, UV visible

Reaction of 2.1a with HMPA, DIBAL-H, ClCH₂BPin (Entries 2, 3).

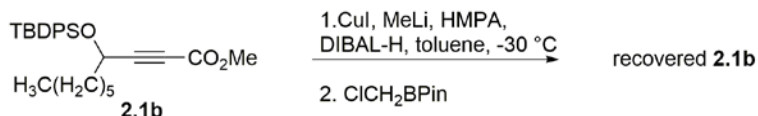


Entry 2: A flame-dried, 10 mL, round-bottomed flask, equipped with a stir bar and septum pierced with a nitrogen inlet needle was charged with toluene (0.4 mL) and cooled to 0 °C on an ice and water bath. HMPA (29 μ L, 0.17 mmol, 4 equiv) and DIBAL-H (0.14 mL of a 0.6 M solution in toluene, 0.082 mmol, 2 equiv) were added sequentially and stirred for 1 h. Alkynoate **2.1a** (18 mg, 0.041 mmol, 1 equiv), dissolved in toluene (0.3 mL), was added to the reaction in one portion via syringe and stirred for 3 h. ClCH₂BPin (11 mg, 0.062 mmol, 1.5 equiv), dissolved in toluene (0.2 mL), was added and stirred overnight at rt. The reaction was quenched with addition of 1 M HCl (3 mL) and diluted with Et₂O. The organics were washed with 1 M HCl, saturated NaHCO₃, and brine (3 mL each), dried over MgSO₄, filtered and concentrated. The crude residue was purified by silica gel flash column chromatography (10% EtOAc in hexanes) to afford 6 mg of alkene **2.21a** (33% yield) and 1 mg allylboronate **2.2a** (4% yield) (a 7.8 : 1 molar ratio).

- When 2.6 equiv of ClCH₂BPin were used, a crude ¹H NMR taken 10 h after the boronate addition revealed a 1.7:1 ratio of alkene **2.21a**: boronate **2.2a**. Stirring was continued; at 41 h, crude ¹H NMR showed a 2.6:1 ratio of alkene **2.21a**: boronate **2.2a** (Entry 3).

Data for **2.2a**, see below.

Attempted reaction of ynoate **2.1b** (Table 5, Entries 4, 5).

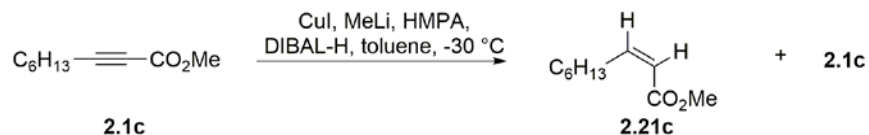


Entry 4: A flame-dried, 15 mL, round-bottomed flask equipped with a stir bar and septum was charged with THF (0.7 mL), and copper iodide (4 mg, 0.023 mmol, 0.1 equiv). The flask was cooled to -30 °C (dry ice and acetonitrile bath). Methyl lithium (14 μ L of a 1.6 M solution in diethyl ether, 0.023 mmol, 0.1 equiv) was added and the solution stirred for 30 min. Toluene (1.6

mL) was added followed by sequential addition of HMPA (80 μ L, 0.46 mmol, 2 equiv) and DIBAL-H (0.34 mL of a 1.0 M solution in hexanes, 0.34 mmol, 1.5 equiv). The reaction was stirred for 2 h. Alkynoate **2.1b** (100 mg, 0.23 mmol, 1 equiv) was dissolved in toluene (1.1 mL) and added to the reaction in a single portion via syringe. The reaction stirred for 5 h. ClCH₂BPIn (48 mg, 0.27 mmol, 1.2 equiv) was added and the reaction stirred overnight at rt. No change in the reaction was observed by TLC. The reaction was diluted with Et₂O (5 mL), quenched with 1 M HCl (5 mL). The organic layer was separated and washed with 1 M HCl (2 x 5 mL), saturated NaHCO₃ (5 mL), and brine (5 mL), dried over Na₂SO₄, filtered, and concentrated. The crude ¹H NMR showed ynoate **2.1b** with signals consistent with literature values.⁶⁸

Entry 5: Follows same procedure as described for entry 4 with THF (0.35 mL), copper iodide (2 mg, 0.012 mmol, 0.1 equiv), methyl lithium (8 μ L of a 1.6 M solution in diethyl ether, 0.012 mmol, 0.1 equiv), toluene (0.8 mL), distilled HMPA (40 μ L, 0.23 mmol, 2 equiv), DIBAL-H (0.17 mL of a 1.0 M solution in toluene, 0.17 mmol, 1.5 equiv), ynoate **2.1b** (50 mg, 0.12 mmol, 1 equiv) dissolved in toluene (0.5 mL). After addition of ynoate **2.1b**, no reaction had occurred after 5 h of stirring. ClCH₂BPIn was not added to this experiment. ¹H NMR of the crude residue showed ynoate **2.1b**⁶⁸ and no alkene **2.21b**.

Attempted 1,4-reduction of ynoate 2.1c (Table 5, Entry 6).

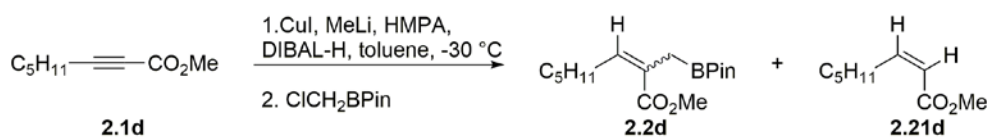


A flame-dried, 15 mL, round-bottomed flask equipped with a stir bar and septum was charged with THF (0.9 mL), and copper iodide (6 mg, 0.030 mmol, 0.1 equiv). The flask was cooled to -30 $^\circ$ C (cryocool and ethanol bath). Methyl lithium (19 μ L of a 1.6 M solution in Et₂O, 0.030 mmol, 0.1 equiv) was added and the solution stirred for 30 min. Toluene (2.0 mL) was

added followed by sequential addition of HMPA (0.10 mL, 0.59 mmol, 2 equiv) and DIBAL-H (0.34 mL of a 1.0 M solution in hexanes, 0.45 mmol, 1.5 equiv). The reaction was stirred for 2 h. Alkynoate **2.1c** (50 mg, 0.30 mmol, 1 equiv) was dissolved in toluene (1.4 mL) and added to the reaction in a single portion via syringe. The reaction stirred at -20 °C for 5 h. An aliquot was taken from the reaction and concentrated. Crude NMR of this residue showed a 4:1 mixture of ynoate **2.1c**: alkene **2.21c**. Presence of alkene **2.21c** was determined by ¹H NMR signals at 6.3 and 5.8 ppm, which is consistent with literature values of this compound.⁷¹

- Allenyl-ynoate **2.1a** was subjected to the same procedure which resulted in a complicated mixture as determined by TLC analysis (Entry 7).

Reaction of methyl 2-octynoate **2.1d** (Table 5, Entries 8, 9).



A flame-dried, 10 mL, round-bottomed flask, equipped with a stir bar and septum was charged with THF (3.6 mL), and copper iodide (24 mg, 0.13 mmol, 0.4 equiv). The flask was cooled to -30 °C (cryocool and ethanol bath). Methyl lithium (80 μL of a 1.6 M solution in diethyl ether, 0.013 mmol, 0.4 equiv) was added and the solution stirred for 30 min. In a separate, 10 mL flask, toluene (1.3 mL) was cooled to -30 °C. 0.9 mL of the stirring CuMe solution (0.032 mmol, 0.1 equiv) was added followed by sequential addition of HMPA (0.17 mL, 0.97 mmol, 3 equiv) and DIBAL-H (1.28 mL of a 0.6 M solution in toluene, 0.64 mmol, 2 equiv). The reaction was stirred for 1 h. Alkynoate **2.1d** (50 mg, 0.32 mmol, 1 equiv) was dissolved in toluene (0.4 mL) and added to the reaction in a single portion via syringe. The reaction stirred at -20 °C for 5 h until the ynoate was consumed, as evidenced by crude ¹H NMR spectroscopy. ClCH₂BPin (113 mg, 0.64 mmol, 2 equiv), dissolved in toluene (0.2 mL), was

added and stirred overnight. The reaction was quenched by 1 M HCl and diluted with diethyl ether. The organic layer was washed with 1 M HCl, saturated NaHCO₃, and brine, dried over MgSO₄, filtered, and concentrated. Analysis by crude ¹H NMR revealed a 1 : 1 mixture of alkene **2.21d** (signals observed matched literature values)⁷² and allylboronate **2.2d** (3.6:1, *Z*:*E* isomeric ratio). The crude mixture was purified by silica gel flash column chromatography (gradient of 10-20% diethyl ether in hexanes) to afford 7 mg of the *Z*-**2.2d** and 9 mg of the *Z*- and *E*-isomers of allylboronate **2.2d** (1.4: 1 isomeric ratio) (35% yield overall).

- With freshly distilled ClCH₂BPin, the crude ¹H NMR showed **2.2d** as the only product; no alkene **2.21d** was observed.

Data for **2.2d**.

¹H NMR *Z*-isomer only: (600 MHz, CDCl₃) 5.93 (t, *J* = 7.2 Hz, 1H), 3.70 (s, 3H), 2.48 (q, *J* = 7.2 Hz, 2H), 1.83 (s, 2H), 1.44-1.37 (m, 2H), 1.34-1.24 (m, 4H), 1.23 (s, 12H), 0.88 (t, *J* = 7.2 Hz, 3H) ppm;

Z- and *E*-isomer: (400 MHz, CDCl₃) 6.74 (t, *J* = 7.4 Hz, 1H)*, 5.93 (t, *J* = 7.4 Hz, 1H)**, 3.71 (s, 3H)*, 3.70 (s, 3H)**, 2.48 (q, *J* = 7.4 Hz, 2H)**, 2.14 (q, *J* = 7.4 Hz, 2H)*, 1.85 (s, 2H)*, 1.83 (s, 2H)**, 1.44-1.37 (m, 2H), 1.34-1.25 (m, 4H), 1.232 (s, 12H)**, 1.228 (s, 12H)*, 0.88 (m, 3 H) ppm;

E* isomer, *Z* isomer

Impurities observed at 7.03, 3.65, 1.58 ppm.

¹³C NMR *Z*-isomer (150 MHz, CDCl₃)
168.5, 143.9, 127.8, 83.4, 51.2, 31.7, 29.8, 29.3, 27.4, 24.9, 22.7, 14.2 ppm;

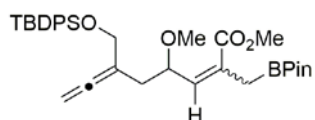
HRMS (FTMS + p ESI Full ms)
[M + H]⁺ calcd for C₁₆H₃₀O₄B, 297.2232; found, 297.2235;

IR (thin film)

2927, 2858, 1723, 1435, 1354, 1324, 1201, 1147 cm^{-1} ;

TLC $R_f = 0.45$ (20% diethyl ether in hexanes)

Silica gel, UV visible, KMnO_4



Allylboronate 2.2a. To a flame-dried, single-necked, round-bottomed flask, equipped with a stir bar and septum pierced with a nitrogen inlet

needle, was added THF (1.2 mL) and copper iodide (8 mg, 0.040 mmol, 0.1 equiv) to form an off-white slurry. The flask was cooled to $-30\text{ }^\circ\text{C}$ using a cryocool/ethanol bath. Methyl lithium (0.025 mL of a 1.6 M solution in Et_2O , 0.040 mmol, 0.1 equiv) was added and the solution turned dark brown. The solution was stirred for 40 min. Toluene (1.7 mL) was added followed successively by HMPA (0.21 mL, 1.19 mmol, 3 equiv) and DIBAL-H (0.80 mL of a 1.0 M solution in toluene) and the black solution stirred for 2 h. Alkynoate **2.1a** (174 mg, 0.40 mmol, 1 equiv) was dissolved in toluene (0.5 mL) and added to the reaction all at once via syringe. The temperature was warmed to $-20\text{ }^\circ\text{C}$ stirred for 3 h until all of the ynoate **2.1a** had been consumed, determined by crude ^1H NMR spectroscopy (shows formation of alkene **2.21a**). Freshly distilled ClCH_2BPin (141 mg, 0.80 mmol, 2 equiv), dissolved in toluene (0.4 mL), was added and stirred overnight at rt. Over this time, the reaction solution went from black to translucent pale green. The reaction was quenched by the addition of 1 M HCl (10 mL). The mixture was transferred to a separatory funnel and diluted with Et_2O (10 mL). The organic layer was separated and the aqueous layer was extracted with Et_2O (2 x 10 mL). The combined organics were washed with 1 M HCl (12 mL), saturated NaHCO_3 (12 mL), and brine (12 mL), dried over MgSO_4 , filtered, and concentrated using reduced pressure rotary evaporation. The crude material was purified by elution through a small silica column using 20% diethyl ether in hexanes to afford the title

compound **2.2** (183 mg, 78%) as a 1.6:1, *Z:E* isomeric ratio and as a colorless oil. The isomers were inseparable and taken on to the next step as a mixture. The characterization for the mixture is reported and the data matches previously reported data.⁴³

Data for **2.2a**.

¹H NMR (400 MHz, CDCl₃)

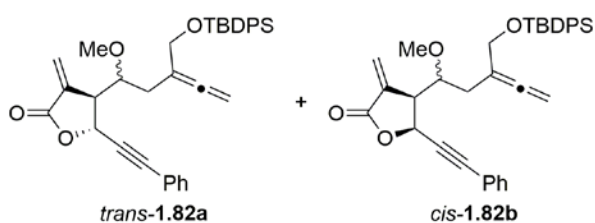
7.71-7.66 (m, 4H), 7.43-7.32 (m, 6H), 6.53 (d, *J* = 9.2 Hz, 1H)*, 5.74 (d, *J* = 8.8 Hz, 1H)**, 4.74-4.69 (m, 2H), 4.72-4.63 (m, 1H)**, 4.23-4.17 (m, 2H), 4.16-4.05 (m, 1H)*, 3.73 (s, 3H)*, 3.66 (s, 3H)**, 3.25 (s, 3H)**, 3.23 (s, 3H)*, 2.40-2.20 (m, 2H), 1.92-1.82 (m, 2H), 1.21 (s, 12H)**, 1.20 (s, 12H)*, 1.04 (s, 9H) ppm;

*E isomer, **Z isomer

TLC R_f = 0.48 (20% EtOAc in hexanes)

Silica gel, UV visible

2.4.4 Completing the synthesis of *trans*-guaianolide **1.83**.



Trans-lactone 1.82a and cis-lactone 1.82b. A 2-5 mL Biotage microwave irradiation vial, equipped with a stir bar, was charged with chloroform (3.7 mL), allylboronate **2.2a** (222 mg

of a 1.7:1 mixture of *Z:E* isomers, 0.376 mmol, 1 equiv), and phenylpropynal (108 mg, 0.827 mmol, 2.2 equiv). The vial was sealed with a septum, pierced with a N₂ inlet needle, and flushed with N₂. The vial was lowered into an oil bath (50 °C) and stirred for 7 d. Disappearance of allylboronate **2.2a** was monitored by ¹H NMR spectroscopy. *p*-Toluene sulfonic acid monohydrate (7 mg, 0.038 mmol, 0.1 equiv) was added and the reaction stirred for 16 h at rt. The

reaction was quenched by the addition of saturated NaHCO₃ (8 mL) and diluted with DCM (6 mL). The organic layer was separated and the aqueous layer was extracted with DCM (2 x 10 mL). The combined organics were dried over MgSO₄, filtered, and concentrated. The crude residue was purified by silica gel flash column chromatography (10% Et₂O in hexanes) to provide 61 mg of *trans*-lactone **1.82a** as a 1.5:1 ratio of diastereomers, 13 mg of *cis*-lactone **1.82b** (Diastereomer 1) contaminated with recovered allylboronate **2.2a** (*E* isomer), and 35 mg *cis*-lactone **1.82b** (Diastereomer 2) in an overall 50% yield. The characterization data obtained for *trans*-**1.82a** and *cis*-**1.82b** (Diastereomer 2) matches previously reported data.⁴³

Data for *trans*-**1.82a**

¹H NMR (400 MHz, CDCl₃)

7.69-7.62 (m, 5H), 7.46-7.28 (m, 10H), 6.38 (d, *J* = 2.4 Hz, 1H)*, 6.35 (d, *J* = 2.4 Hz, 1H)**, 5.73 (d, *J* = 2.0 Hz, 1H)*, 5.66 (d, *J* = 2.0 Hz, 1H)**, 5.38 (d, *J* = 4.4 Hz, 1H)**, 5.20 (d, *J* = 3.2 Hz, 1H)*, 4.79-4.75 (m, 2H), 4.23-4.19 (m, 2H), 3.62-3.56 (m, 1H), 3.49-3.46 (m, 1H)*, 3.42-3.38 (m, 1H)**, 3.36 (s, 3H)*, 3.33 (s, 3H)**, 2.51-2.43 (m, 1H)**, 2.42-2.32 (m, 1H)*, 2.31-2.21 (m, 1H), 1.06 (s, 9H)*, 1.05 (s, 9H)** ppm;

* Major diastereomer, ** minor diastereomer.

Impurities observed at 1.54, 1.43, 1.25, and 1.20 ppm.

TLC R_f = 0.33 (10% EtOAc in hexanes)

Silica gel, UV visible

Data for *cis*-**1.82b**, Diastereomer 1

¹H NMR (500 MHz, CDCl₃)

7.70-7.62 (m, 5H), 7.43-7.30 (m, 10H), 6.34 (d, $J = 1.5$ Hz, 1H), 5.73 (d, $J = 1.5$ Hz, 1H), 5.39 (d, $J = 7.0$ Hz, 1H), 4.79-4.72 (m, 2H), 4.22-4.16 (m, 2H), 4.01 (dt, $J = 9.5, 4.0$ Hz, 1H), 3.37 (s, 3H), 3.26-3.22 (m, 1H), 2.53-2.47 (m, 1H), 2.40-2.31 (m, 1H), 1.04 (s, 9H) ppm;

Signals for *E*-**2.2a** observed at 6.53, 4.62, 3.73, 3.23 ppm.

^{13}C NMR (125 MHz, CDCl_3)
206.8, 186.7, 141.6, 135.7, 134.8, 133.4, 131.9, 129.9, 129.3, 128.6, 127.9, 127.8, 124.2, 99.5, 83.6, 83.1, 79.3, 70.5, 64.9, 57.0, 45.9, 28.1, 27.0, 19.4 ppm;

IR (thin film)
3070, 2932, 2858, 1962, 1774, 1721, 1428, 1360, 1265, 1110, 703 cm^{-1} ;

HRMS (FTMS + p ESI Full ms)
[M + H]⁺ calculated for $\text{C}_{36}\text{H}_{39}\text{O}_4\text{Si}$, 563.2612; found, 563.2589;

TLC $R_f = 0.25$ (10% EtOAc in hexanes)
Silica gel, UV visible

Data for *cis*-**1.82b**, Diastereomer 2

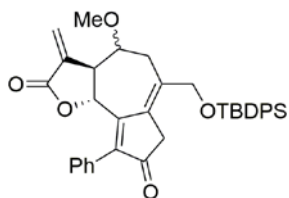
^1H NMR (600 MHz, CDCl_3)
7.68-7.61 (m, 5H), 7.43-7.28 (m, 10H), 6.37 (d, $J = 2.1$ Hz, 1H), 5.78 (d, $J = 2.1$ Hz, 1H), 5.48 (d, $J = 8.4$ Hz, 1H), 4.77-4.72 (m, 1H), 4.69-4.63 (m, 1H), 4.22-4.11 (m, 2H), 3.93-3.87 (m, 1H), 3.54-3.48 (m, 1H), 3.38 (s, 3H), 2.61-2.55 (m, 1H), 2.16-2.08 (m, 1H), 1.02 (s, 9H) ppm;

^{13}C NMR (150 MHz, CDCl_3)

206.1, 169.4, 135.8, 135.7, 133.7, 132.1, 129.82, 129.77, 129.30, 128.5, 127.8, 125.2, 121.7, 100.8, 90.1, 82.4, 80.0, 77.7, 69.5, 65.0, 57.3, 44.4, 30.5, 26.9, 19.4 ppm;

TLC $R_f = 0.19$ (10% EtOAc in hexanes)

Silica gel, UV visible



Trans-guaianolide analog 2.24. Followed general procedure 1A (Section 1.4.3), using $[\text{Rh}(\text{CO})_2\text{Cl}]_2$ (2 mg, 0.0057 mmol, 0.05 equiv) in toluene (8.5 mL), *trans*-lactone allene-yne **1.82a** (64 mg, 0.114 mmol, 1 equiv) dissolved in toluene (2.9 mL), and triphenylphosphine polymer bound (65 mg). The residue was purified by silica gel flash column chromatography (gradient of 30-40% EtOAc in hexanes) to yield the title compound (53 mg, 79%) as a colorless oil. The characterization data obtained matches previously reported data.⁴³

Data for 2.24.

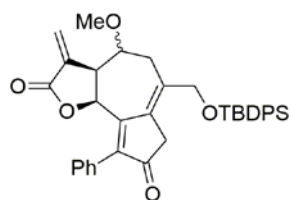
^1H NMR (400 MHz, CDCl_3)

7.73-7.64 (m, 4H), 7.48-7.32 (m, 9H), 7.27-7.21 (m, 2H), 6.35 (d, $J = 3.6$ Hz, 1H)**, 6.23 (d, $J = 3.6$ Hz, 1H)*, 5.85 (d, $J = 2.8$ Hz, 1H)*, 5.71 (d, $J = 9.6$ Hz, 1H)**, 5.48 (d, $J = 3.2$ Hz, 1H)**, 5.32 (d, $J = 10.4$ Hz, 1H)*, 4.33 (d, $J = 13.2$ Hz, 1H)*, 4.31 (d, $J = 12.4$ Hz, 1H)**, 4.27 (d, $J = 12.8$ Hz, 1H)**, 4.23 (d, $J = 13.2$ Hz, 1H)*, 4.01-3.94 (m, 1H)**, 3.86-3.82 (m, 1H)*, 3.424 (s, 3H)*, 3.418 (s, 3H)**, 3.39-3.31 (m, 1H), 3.17-3.07 (m, 1H), 2.86 (d, $J = 20.8$ Hz, 1H)*, 2.83 (d, $J = 20.8$ Hz, 1H)**, 2.76 (d, $J = 20.4$ Hz, 1H)**, 2.73 (d, $J = 21.2$ Hz, 1H)*, 2.45-2.37 (m, 1H), 1.11 (s, 9H)**, 1.10 (s, 9H)* ppm;

*Major diastereomer, ** Minor diastereomer

TLC $R_f = 0.18$ (20% EtOAc in hexanes)

Silica gel, UV visible.



Cis-guaianolide analog 2.25. Followed general procedure 1A (Section 1.4.3), using $[\text{Rh}(\text{CO})_2\text{Cl}]_2$ (3 mg, 0.0083 mmol, 0.05 equiv) in toluene (12.0 mL), *cis*-lactone allene-yne **1.82b** (93 mg, 0.11 mmol, 1 equiv) dissolved in toluene (4.5 mL). Cooled reaction solution was filtered through a celite plug, rinsed with Et_2O and concentrated using reduced pressure rotary evaporation. The residue was purified by silica gel flash column chromatography (gradient of 20-40 % EtOAc in hexanes) to yield the title compound (56 mg, 58%) as a colorless oil. The characterization data obtained matches previously reported data.⁴³

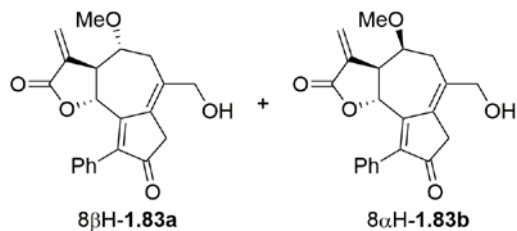
Data for 2.25.

^1H NMR (300 MHz, CDCl_3)

7.70-7.63 (m, 4H), 7.49-7.38 (m, 9H), 7.29-7.22 (m, 2H), 6.51 (bs, 1H), 5.93 (bs, 1H), 5.58 (d, $J = 7.5$ Hz, 1H), 4.28 (d, $J = 12.6$ Hz, 1H), 4.18 (d, $J = 12.0$ Hz, 1H), 3.77-3.70 (m, 1H), 3.59 (dd, $J = 9.8, 5.0$ Hz, 1H), 3.44 (s, 3H), 2.96 (d, $J = 18.3$ Hz, 1H), 2.91 (d, $J = 20.4$ Hz, 1H), 2.80 (d, $J = 20.4$ Hz, 1H), 2.41-2.29 (m, 1H), 1.07 (s, 9H) ppm;

TLC $R_f = 0.39$ (30% EtOAc in hexanes)

Silica gel, UV visible.



Trans-guaianolide analog 1.83. A flame-dried, 10 mL, round-bottomed flask, equipped with a stir bar and septum pierced with a nitrogen inlet needle, was charged with acetonitrile (1.0 mL) and crude silyl

protected *trans*-guaianolide **2.24** (0.076 mmol of 2.3:1 mixture of diastereomers, 1 equiv). Triethylamine trihydrofluoride was added and the flask was lowered into a pre-heated oil bath (60 °C) and stirred overnight. The oil bath was removed and the solution cooled to rt. The solution was diluted with Et₂O and water (5 mL each). The organic layer was separated and the aqueous was extracted with Et₂O (2 x 10 mL). The combined organics were washed with saturated NaHCO₃ (2 x 6 mL), dried over MgSO₄, filtered, and concentrated. The crude material was purified by silica gel flash column chromatography (100% EtOAc) to afford 17 mg of the title compounds as 2.3:1 mixture of diastereomers (64% over two steps). The ¹H NMR spectra obtained of the diastereomer mixture was consistent with that previously reported.⁴³ The diastereomers were separated for by HPLC utilizing the following eluent method with a flow rate of 4 mL/min: 100% EtOAc for 20 min, gradient increase from 100% EtOAc to 5% methanol in EtOAc for 5 min, followed by constant 5% methanol in EtOAc for 5 min. 8βH-**1.83a** had a retention time of 14.0 min and 8αH-**1.83b** had a retention time of 17.0 min. Each diastereomer was analyzed by ¹H, ¹³C, COSY, and HSQC NMR spectroscopy.

Data for Diastereomer A: 8βH-**1.83a**

HPLC 14.004 min retention time

¹H NMR (500 MHz, CDCl₃)

7.40-7.32 (m, 3H), 7.27-7.24 (m, 2H), 6.25 (d, *J* = 3.5 Hz, 1H), 5.85 (d, *J* = 3.0 Hz, 1H), 5.39 (d, *J* = 10.5 Hz, 1H), 4.31 (d, *J* = 12.5 Hz, 1H), 4.19 (d, *J* = 12.5 Hz, 1H), 3.86 (ddd, *J* = 8.0, 4.0, 2.5 Hz, 1H), 3.54 (s, 3H), 3.29 (d, *J* = 21.0 Hz, 1H), 3.17 (d, *J* = 21.0 Hz, 1H), 3.18-3.13 (m, 1H), 3.16-3.12 (m, 1H), 2.56 (dd, *J* = 15.8, 2.5 Hz, 1H), 1.73 (bs, 1H) ppm;

¹³C NMR (125 MHz, CDCl₃)

201.4, 167.8, 161.6, 143.3, 137.2, 133.9, 133.0, 130.7, 130.0, 128.8, 127.8, 122.1, 81.7, 75.8, 65.3, 56.9, 50.0, 39.5, 30.6 ppm;

TLC $R_f = 0.41$ (100% ethyl acetate)

Silica gel, UV visible.

Data for Diastereomer B: 8 α H-1.83b.

HPLC 17.006 min retention time

^1H NMR (400 MHz, CDCl_3)

7.45-7.32 (m, 3H), 7.30-7.26 (m, 2H), 6.36 (d, $J = 3.6$ Hz, 1H), 5.78 (d, $J = 9.2$ Hz, 1H), 5.52 (d, $J = 3.2$ Hz, 1H), 4.34-4.26 (m, 2H), 4.14-4.07 (m, 1H), 3.45 (s, 3H), 3.37-3.31 (m, 1H), 3.27 (dd, $J = 15.2, 6.8$ Hz, 1H), 3.28-3.15 (m, 2H), 2.53 (dd, $J = 15.2, 8.4$ Hz, 1H), 1.26 (t, $J = 7.2$ Hz, 1H) ppm;

^{13}C NMR (150 MHz, CDCl_3)

201.3, 168.4, 162.2, 144.1, 134.2, 133.7, 132.2, 130.8, 130.0, 128.9, 127.9, 123.0, 74.9, 74.0, 65.6, 57.5, 49.8, 39.9, 33.9 ppm;

TLC $R_f = 0.34$ (100% ethyl acetate)

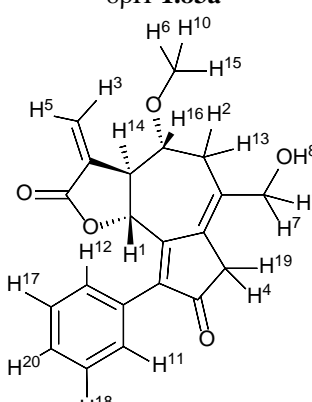
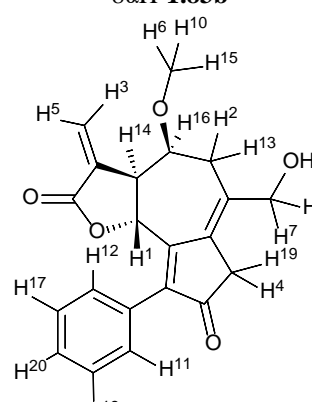
Silica gel, UV visible.

2.4.5 Computational Methods

Predicted ^1H NMR chemical shift calculations were performed using Spartan 10 software for windows.^{70c} The structure was drawn in the drawing window, and lowest energy conformers were determined by performing conformer distribution calculations using molecular mechanics and MMFF. For 8 β H-1.83a, this generated 37 possible conformers and the lowest energy conformer was ~79 kcal/mol. For 8 α H-1.83b, 43 possible conformers were generated and the

lowest energy conformer was ~81 kcal/mol. Using the lowest energy conformers, ¹H NMR chemical shift calculations were performed using EDF2/6-31G* (subset of equilibrium geometry and density functional theory) functionals in a vacuum. Corrected chemical shifts were displaced as atom labels (shown by clicking Model>Configure>Chem Shift), these values were recorded.

Table 7. Calculated chemical shifts for **8βH-1.83a** and **8αH-1.83b**.

8βH-1.83a		8αH-1.83b	
			
Calculated ppm	Spartan Assignment	Calculated ppm	Spartan Assignment
7.728	20	7.662	11
7.69	11	7.315	12
7.263	17	7.279	17
7.263	18	7.276	20
7.249	12	7.259	18
6.226	5	6.354	5
5.784	3	5.831	1
5.369	1	5.355	3
4.275	7	4.389	7
4.117	9	4.312	9
3.588	16	4.089	16
3.544	6, 10, 15	3.393	6, 10, 15
3.119	2	3.284	2
3.038	14	3.220	14
2.915	4	2.890	4
2.543	19	2.505	19
2.278	13	2.237	13
0.272	8	0.272	8

3.0 INSTALLATION OF ALKYNE LIGATION HANDLES VIA THE NICHOLAS REACTION

This chapter is based upon results described in “Alkyne Ligation Handles: Propargylation of Hydroxyl, Sulfhydryl, Amino, and Carboxyl Groups via the Nicholas Reaction,” by Sarah M. Wells, John C. Widen, Daniel A. Harki, and Kay M. Brummond, submitted for publication 7/16/2016.

3.1 INTRODUCTION

One factor contributing to the slow realization of guaianolides as therapeutics is the presence of covalent modifiers and limited understanding of their biological mechanism of action. Despite prevalent bioactivity, covalent modifiers have been criticized for their irreversible interactions with protein targets and poor selectivity. For progress to be made for this class of molecules, their protein targets and mechanism of action must be understood. Towards this end, we sought to synthesize activity based protein profiling (ABPP) probes for the guaianolide NF- κ B inhibitors synthesized in our group to determine their protein targets.

3.1.1 Activity Based Protein Profiling for Protein Target Identification

Natural products (NPs) are distinguished classes of organic molecules and provide inspiration for a large portion of pharmaceuticals.¹ For NPs and derivatives there-of to be approved for therapeutic use, a complete understanding of their molecular targets and mechanism of action should be understood.⁷³ This is particularly true for covalent modifiers, often criticized for irreversibly and indiscriminately modifying proteins.

ABPP has been established as a fundamental technique for characterizing specific protein activity within a complex proteome, popular for its ability to examine proteins *in vivo* without disturbing natural function.⁷⁴ The method depends on the development of activity based probes (ABPs) capable of selective covalent interaction with active enzymes and analytical detection *ex post facto*. These probes contain three essential parts; 1) a binding group that enables protein selectivity presumably through non-covalent binding interactions, 2) the reactive group (or warhead) that covalently binds to active proteins, and 3) a reporter group, or detectable agent that is used for analytical characterization. While ABPP has been a powerful tool for understanding the functional characteristics of individual proteins in native proteomes, the method has also been applied to identifying specific protein targets and mechanism of action for NPs and other drug candidates.^{73b, 75}

ABPs for target identification studies are derivatives of the active small molecules, which are modified to contain an analytical tag, or reporter group. ABPP exploits the reactive groups of the covalent modifiers, which serve as the war head and form covalent linkages with nucleophilic amino acids near the protein binding pocket. Once the interaction between the bioactive molecule and the proteome have been established, analytical methods, such as gel

electrophoresis, fluorescence detection, and mass spectrometry are employed to characterize the interactions (Figure 14).

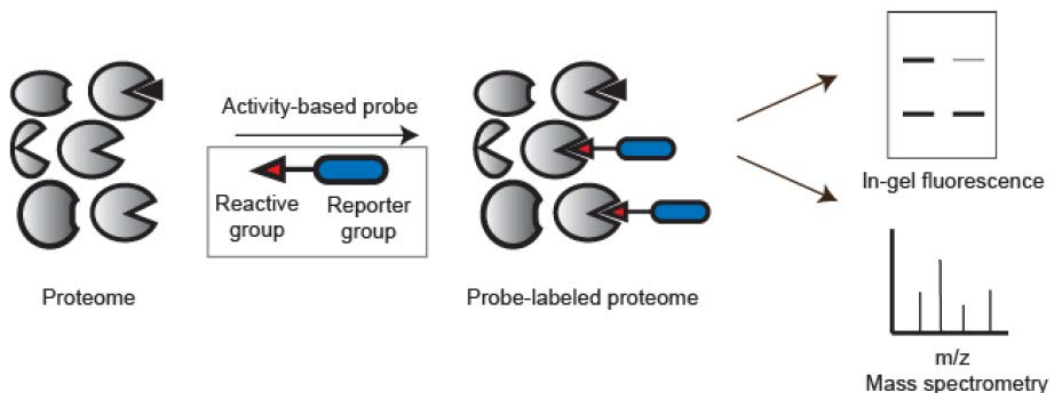


Figure 14. Overview of activity-based protein profiling (ABPP). [Reprinted from MDPI Open Access: Martell, J.; Weerapana, E. *Molecules*, 2014, 19, 1378-1393.](#)⁷⁶

3.1.2 Probe design for target identification of bioactive small molecules.

Probe design for target identification experiments involves the installation of the reporter group onto the bioactive molecule. Two main considerations for tag installation are the size and position of the tag; minimizing perturbation of the parent molecule's natural biological activity is a major concern.⁷⁷ Some of the most common tags include biotin **3.1**, which is commonly detected by western blot analysis and avidin enrichment prior to mass spectroscopy, and rhodamine **3.2**, a fluorophore detectable by in-gel fluorescence (Figure 15). These analytical tags allow for direct evaluation of the protein target(s), but their size has led to major disadvantages such as perturbation of protein-probe interactions, decreased cell permeability, and destruction of native biological conditions (Figure 16A).

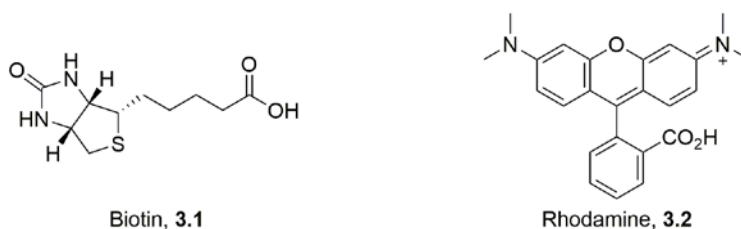


Figure 15. Popular reporter groups for ABPP.

The advances and popularity of bioorthogonal chemistry, or “Click chemistry,” have allowed for an alternative, two-step probe, where bioactives are modified to contain smaller, less obstructive ligation handles, or “pre-tags”.⁷⁷ After forming their respective covalent linkages with active proteins in the cell, these ligation handles can be elaborated with a fluorophore or enrichment tag containing the complementary bioorthogonal functionality (Figure 16B). The “pre-tag” probe also allows for the utilization of numerous reporter groups and characterization methods while employing a single synthetic probe.^{74b}

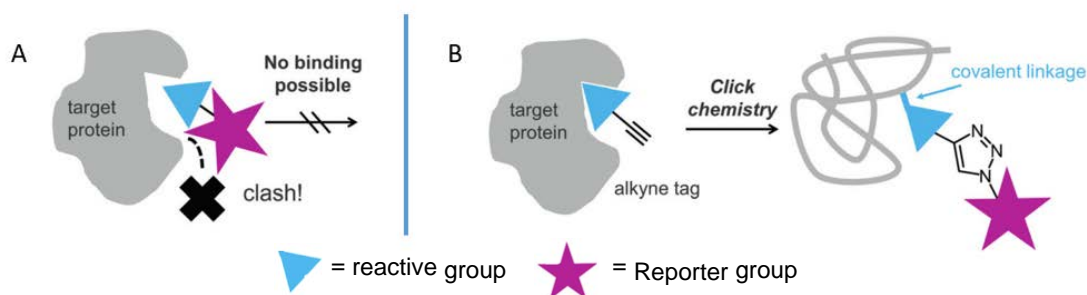
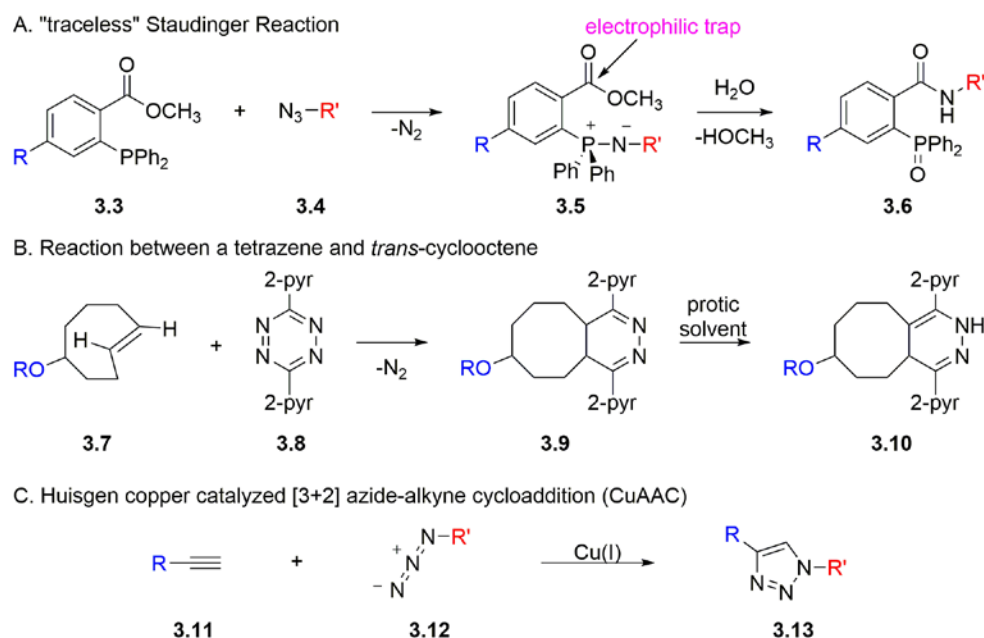


Figure 16. Advantages of a two-step ABP with an alkyne ligation handle. A) Bulky reporter groups interfere with warhead-protein binding. B) Alkyne ligation handle can be modified for analytical interpretation after covalent binding of reactive group with target protein. [Reprinted by permission from John Wiley & Sons, Inc.](#); Lehmann, J.; Wright, M. H.; Sieber, S. A. *Chem. Eur. J.* **2016**, *22*, 4666-4678. © 2016 WILEY-VCH Verlag GmbH & Co. KGaA, Weinheim.

3.1.3 Bioorthogonal reactions and the value of alkyne ligation handles

An ideal bioorthogonal reaction involves rapid coupling of two precursors without the formation of byproducts, and can be done under physiological conditions.⁷⁸ The coupling

precursors must also be biologically inert. The development of new bioorthogonal reactions has become a prevalent research area; some of the most popular reactions used for ABPP are shown in Scheme 51. First, Bertozzi and coworkers developed a “traceless” Staudinger reaction. The classical Staudinger reaction occurs between a trialkyl phosphine and an azide to form an aza-ylide, which in the presence of water, readily undergoes hydrolysis affording the corresponding amine and phosphine oxide.⁷⁹ Bertozzi’s modified reaction utilizes an electrophilic trap, incorporated into the phosphine component (**3.3**), which allows rearrangement of the aza-ylide **3.5** to form a stable amide linkage **3.6**. (Scheme 51A).⁸⁰ Many methodologies utilize Diels-Alder chemistry for the coupling of two substrates; one example is the reaction between a tetrazene (**3.8**) and either a *trans*-cyclooctene (**3.7**) or cyclopropene (Scheme 51B).⁸¹ The Huisgen copper catalyzed [3+2] cycloaddition of an alkyne (**3.11**) and azide (**3.12**) to form 1,2,3-triazoles (**3.13**), also called the click reaction, was revisited by Sharpless in 2002 (Scheme 51C).⁸²



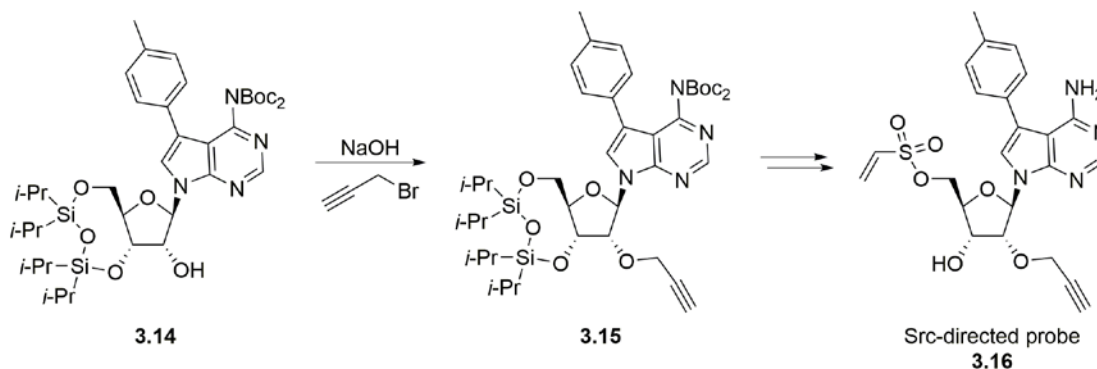
Scheme 51. Selected bioorthogonal reactions.

The copper-catalyzed [3+2] click reaction has arguably become the most prominently used bioorthogonal reaction with over 5848 papers including 927 reviews citing the 2002 report by Sharpless.⁸² Many advancements have allowed the Huisgen cycloaddition, often criticized for corresponding cell toxicity of the copper/ascorbate catalyst, to be applied to numerous biological applications. Water-soluble, accelerating tris(triazolylmethyl)amine ligands have been shown to intercept harmful oxygenative species generated by the catalyst system. This protocol allows an accelerated reaction which minimizes both the concentration of the catalyst and time required to perform the click-based labeling, resulting in increased cell viability.⁸³ Also, a variation that exploits the reactivity of strained cyclooctynes does not require a copper catalyst.⁸⁴ Utility of the click reaction for biochemical applications also stems from the nature of the click reaction precursors, the azide and alkyne. These functional groups are rarely found in biological systems, minimizing potential side reactions, and they are small in size, which minimizes their effect on the activity or physical characteristics of the parent molecule. For ABPP specifically, it has become most common to incorporate the alkyne moiety on the small molecule probe, while the azide is installed on the analytical tag.^{77, 85} As a result, synthetic methodology for incorporation of an alkynyl group in small molecules is valuable.

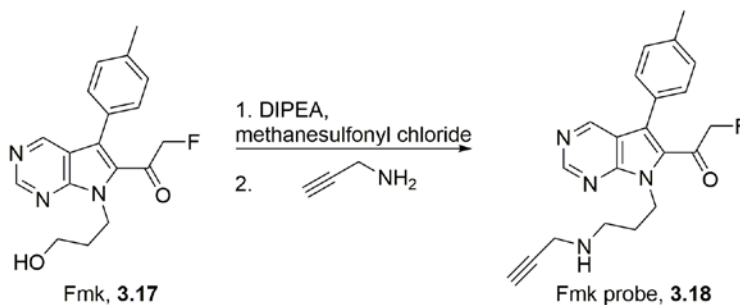
3.1.4 Traditional methods for installation of alkyne handles

Typically, late-stage incorporation of an alkyne handle has been achieved by either alkylation or acylation of an existing amino, hydroxyl, or carboxyl group where the installed alkyl or acyl group contained an alkyne. Alkylation is most commonly achieved by propargylation of an alcohol via the base-mediated Williamson ether synthesis with propargyl bromide. For example, the synthesis of Src-directed probe **3.16** included the propargylation of

3.14 using sodium hydroxide and propargyl bromide (Scheme 52).⁸⁶ A series of hydroxyl and amino protecting groups were required to avoid over-propargylation. Alternatively, a hydroxyl group can be converted to a propargyl amine by conversion to a mesylate followed by reaction with propargyl amine; this method was used for the synthesis of Fmk probe **3.18** (Scheme 53).



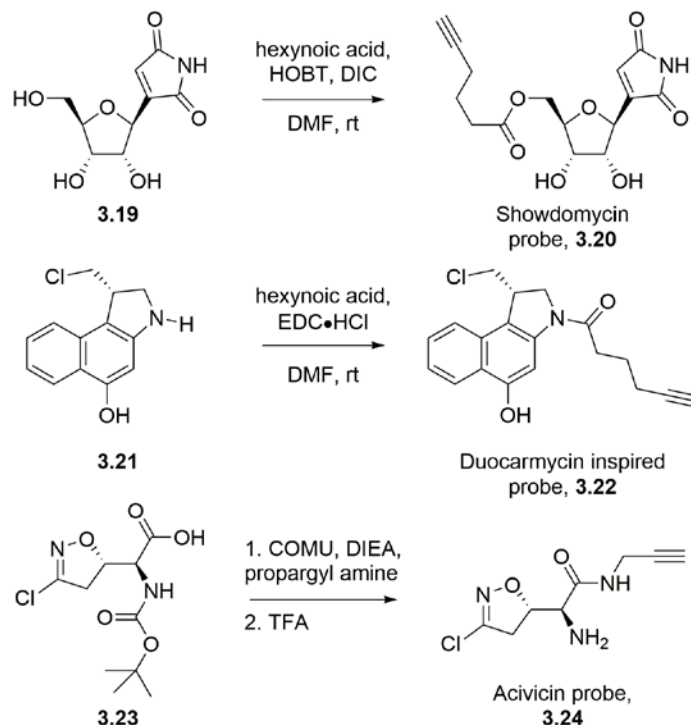
Scheme 52. Synthesis of Src-directed alkyne probe **3.16** via base mediated propargylation.



Scheme 53. Propargylation of Fmk **3.17**.

Acylation is commonly performed by incorporating a hexynoic carbonyl onto an amino or hydroxyl group. This transformation can also be accomplished under basic conditions, where a hydroxyl group reacts with hexynoyl chloride.⁸⁷ Carbodiimide coupling reactions offer neutral alternatives for acylation; an activated carbodiimide facilitates coupling between hexynoic acid and either an alcohol or amine (Scheme 54). Showdomycin **3.19** was modified using diisopropylcarbodiimide (DIC) and 1-hydroxybenzotriazole (HOBT) with hexynoic acid to selectively acylate the primary alcohol, affording showdomycin probe **3.20**.⁸⁸ Mitsunobu reaction conditions are typically employed for the acylation of secondary alcohols.⁷⁷

Modification of the secondary amino group of **3.21** gave the duocarmycin probe **3.22** under 1-ethyl-3-(3-dimethylaminopropyl)carbodiimide (EDC) coupling conditions.⁸⁹ Alternatively, propargyl amine can be coupled with an available carboxylic acid for the formation of amide linkages. This strategy is used in the synthesis of **3.24**, which was made as part of a series of acivicin probes.⁹⁰



Scheme 54. Synthesis of alkyne probes **3.20**, **3.22**, and **3.24** using amide coupling reactions.

In 2013, the Romo and Cravatt groups applied C-H amination of allylic and benzylic hydrogens, previously developed by DuBois,⁹¹ to the incorporation of alkyne ligation handles onto natural products for biochemical studies.⁹² Amination using sulfonamide derivatives is achieved using $\text{Rh}_2(\text{esp})_2$ and oxidant $(\text{PhI}(\text{O}_2\text{C}^t\text{Bu})_2)$ reagent system. One example described therein was the amination of Eupalmerin acetate (EuPA, **3.25**) to afford **3.26** in 28% yield (Scheme 55). An advantage of this method is that it functionalizes the natural product at a previously “unfunctionalized” position to avoid rendering the probe inactive. However, low

probe for NP melampomagnolide B (MelB, **3.29**, Figure 18). MelB is base-sensitive and could not be propargylated under classical conditions. Also, attempted oxidations of the allylic alcohol were unsuccessful. A biotinylated derivative of MelB has been achieved via an ester linkage, however the stability of esters *in vivo* is still a concern. Consequently, non-basic conditions for propargylation of these functionally dense molecules were needed.

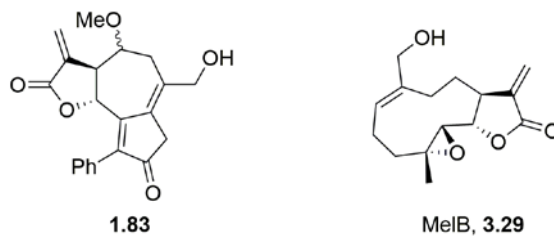


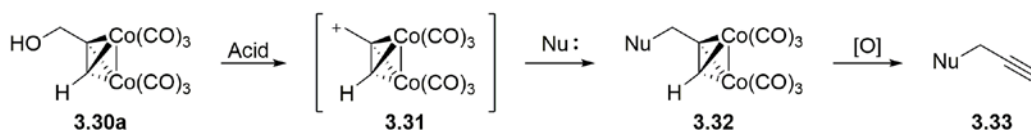
Figure 18. Base-sensitive sesquiterpene-lactone analogs.

3.1.5 The Nicholas reaction: an acid mediated propargylation reaction

The Nicholas reaction provides propargyl synthons via an acid mediated reaction. Dicobalt hexacarbonyl complexed propargyl alcohol **3.30a** ($\text{Co}_2(\text{CO})_6$ -propargyl alcohol) derivatives react in the presence of either a Lewis or protic acid to yield a cobalt stabilized propargylic carbocation **3.31**. Trapping of this intermediate with a nucleophile affords the corresponding cobalt-complexed alkyne **3.32** species (Scheme 56).⁹³ Even primary propargyl alcohols, which result in *pseudo*-primary carbocations, can be employed in the Nicholas reaction due to the stabilization that the adjacent cobalt provides.⁹⁴ Oxidative decomplexation of the cobalt complex **3.32** affords the corresponding alkyne **3.33**. To our knowledge, the Nicholas reaction has not been applied to the synthesis of biochemical probes.^{93c}

The click reaction works most efficiently when the alkynyl group has no substituents other than the connecting methylene unit ($\text{R-CH}_2\text{-CCH}$). Therefore, the Nicholas reaction offers

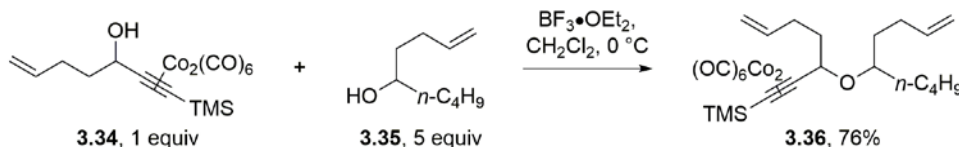
advantages over other acid mediated methods for preparing propargyl ethers. For example, metal triflates, such as $\text{Al}(\text{OTf})_3$, are effective Lewis acid catalysts for preparing propargyl ethers from 2° and 3° propargyl alcohols. However, primary alcohols are not tolerated due to cationic instability.⁹⁵



Scheme 56. Synthesis of propargyl derivatives via Nicholas reaction followed by oxidative decomplexation.

A variety of nucleophiles have been used in the Nicholas reaction. Nucleophiles for the formation of a carbon-carbon bond include enol derivatives, allyl metals, electron-rich alkenes, aryl groups.^{93b} Nucleophilic heteroatoms have also been employed; predominantly hydroxyl groups, used for the formation of both cyclic and acyclic propargyl ethers.

Typically, the standard protocol for preparing ethers via an intermolecular Nicholas reaction requires use of the nucleophilic hydroxyl group in excess compared to the $\text{Co}_2(\text{CO})_6$ -alkyne. For example, unsymmetrical ether **3.36**, a precursor for a ring-closing metathesis reaction, was made in 76% yield by reacting 1 equiv of cobalt complex **3.34** with 5 equiv of alcohol **3.35** and $\text{BF}_3 \cdot \text{OEt}_2$ (Scheme 57);⁹⁶ a molar equivalencies ratio that limits a competing homodimerization of the $\text{Co}_2(\text{CO})_6$ -propargyl alcohol.⁹⁷



Scheme 57. Synthesis of unsymmetrical ether **3.36** via the Nicholas reaction.

We expected that the Nicholas reaction could be applied to the synthesis of biologically relevant alkyne probes. However, employing the nucleophilic bioactive molecule in excess

would be uneconomical. Therefore, we set out to determine reaction conditions where the high-value, nucleophilic species (bioactive compound) could be employed as the limiting reagent.

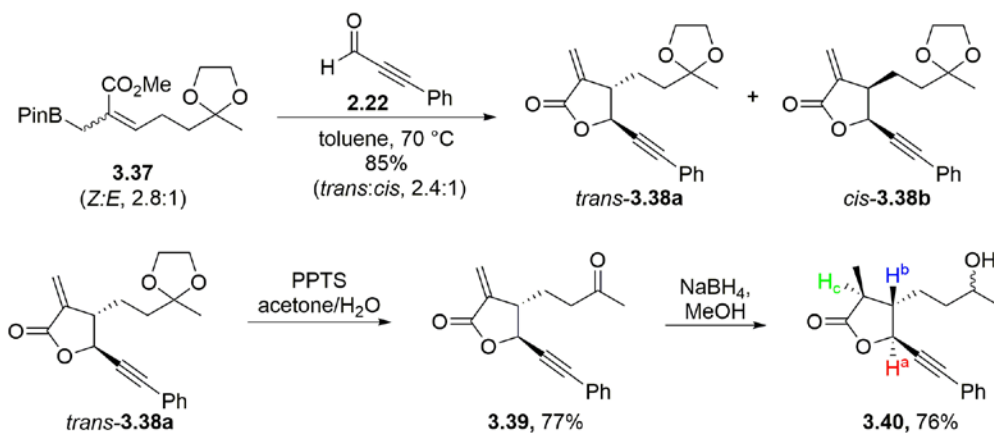
3.2 RESULTS AND DISCUSSION

3.2.1 Preparation of alcohol **3.40** as a model system.

In order to optimize Nicholas reaction conditions for use of high-value, nucleophilic species as the limiting reagent, molecularly complex alcohol model **3.40** was prepared in 3 steps from allylboronate **3.37**, previously synthesized in our group (Scheme 58).⁹⁸ Addition of allylboronate **3.37** (2.8:1 mixture of *Z*:*E* alkene isomers) to phenylpropynal **2.22** followed by lactonization gave a 2.4:1 ratio of the *trans*- and *cis*-lactone **3.38** in 85% yield. The stereochemical identification of the *trans*- and *cis*-**3.38** isomers was confirmed using the coupling of proton H_a with comparison to an X-ray crystal structure of α -methylene- γ -butyrolactone **2.26a**, as discussed in Section 2.2.4.⁴² *Trans*-**3.38a** has a J_{ab} of 5.2 Hz, while *cis*-**3.38b** has a coupling constant of 8.0 Hz. These J_{ab} values compare favorably to the *trans*- and *cis*- isomers of **2.28** published previously, which have coupling constants for H_a of 6.0 Hz and 8.4 Hz respectively (Figure 19).⁴²

Trans-**3.38a** was taken on; the acetal protecting group was removed to afford ketone **3.39** in 77% yield. Reaction of **3.39** with sodium borohydride reduced both the ketone and methylene group, producing **3.40** in 76% yield (Scheme 58). Alcohol **3.40** was obtained as a 1: 1 ratio of two diastereomers; the methylene group was reduced diastereoselectively while reduction of the ketone resulted in two stereoisomers.⁹⁹ The relative geometry of the lactone ring

was determined by examining the ^1H NMR spectra; H_c appears at 2.34 ppm as a doublet of quartets with the corresponding coupling constants of 10.8 and 6.6 Hz. The 10.8 Hz coupling constant between H_c and H_b , as well as the 9.0 Hz coupling between H_b and H_a indicates a *trans,trans*-relationship for the tri-substituted butyrolactone ring, which prefers an envelope conformation with the alkyl groups in the equatorial positions and hydrogens in the axial positions.¹⁰⁰



Scheme 58. Synthesis of molecularly complex model system **3.40**.

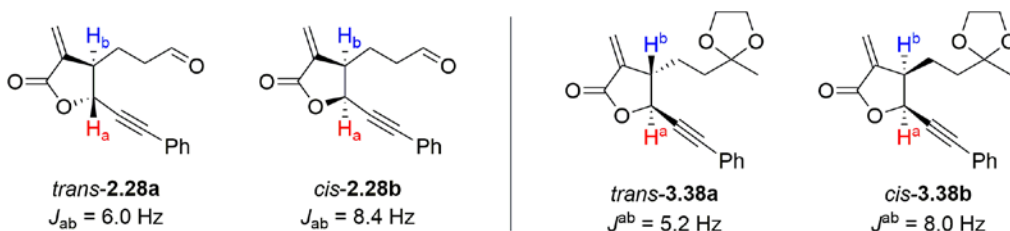
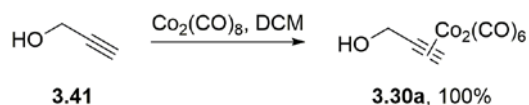


Figure 19. Comparison of coupling constants of **3.38** with previously synthesized **2.28**.

3.2.2 Optimization of the Nicholas reaction conditions

The Nicholas reaction requires a dicobalt hexacarbonyl complexed alkyne with an adjacent oxygen leaving group. $\text{Co}_2(\text{CO})_6$ -propargyl alcohol **3.30a** was prepared by stirring propargyl alcohol with $\text{Co}_2(\text{CO})_8$ in DCM until bubbles (presumed to be evolution of CO gas)

were no longer observed. This procedure afforded complex **3.30a** in quantitative yield. **3.30a** is stable to air and moisture and was purified by silica gel chromatography (Scheme 59).



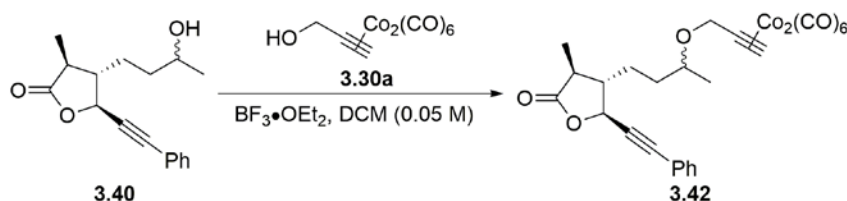
Scheme 59. Cobalt complexation of propargyl alcohol to afford **3.30a**.

With alcohol **3.40** and complex **3.30a** in hand, optimization for propargylation of molecularly complex compounds via the Nicholas reaction began. Alcohol **3.40** was used as the limiting reagent in all experiments. Initially, we examined the effects of various equivalencies of complex **3.30a** and the Lewis acid, $\text{BF}_3 \cdot \text{OEt}_2$, while the order of reagent addition remained constant. Due to the multiple Lewis base coordination sites of alcohol **3.40** that could potentially compete for the Lewis acid, we predicted that the addition of the $\text{Co}_2(\text{CO})_6$ -propargyl alcohol **3.30a** to a stirring solution of $\text{BF}_3 \cdot \text{OEt}_2$, prior to the addition of **3.40**, would allow efficient formation of the propargylic cation. In turn, complex **3.30a** (2 equiv) and alcohol **3.40** (1 equiv) were added sequentially to a stirring solution of $\text{BF}_3 \cdot \text{OEt}_2$ (2.5 equiv) at 0 °C in DCM which afforded $\text{Co}_2(\text{CO})_6$ -propargyl ether **3.42** in 47% yield (Table 8, Entry 1). Increasing the equivalents of the $\text{BF}_3 \cdot \text{OEt}_2$ and complex **3.30a** decreased the yield of **3.42** to 36% (Entry 2). Adding alcohol **3.40** dropwise also resulted in decreased yields of **3.42** (28%, Entry 3).

These low yields led to examination of the reagent addition order. Inverting the addition of $\text{Co}_2(\text{CO})_6$ -propargyl alcohol **3.30a** and alcohol **3.40** to the $\text{BF}_3 \cdot \text{OEt}_2$ solution did not have a significant effect on the yield of **3.42** (44%, Entry 4 compared to 47%, Entry 1). Next, alcohol **3.40** and $\text{BF}_3 \cdot \text{OEt}_2$ were added sequentially to a solution of $\text{Co}_2(\text{CO})_6$ -propargyl alcohol **3.30a** in DCM, an addition order more commonly seen in previous Nicholas reaction reports. Reacting **3.40**, **3.30a** and $\text{BF}_3 \cdot \text{OEt}_2$ in molar equivalencies of 1:2:2.5 afforded $\text{Co}_2(\text{CO})_6$ -propargyl ether **3.42** in 55% yield (Entry 5). Again, increasing equivalencies of alcohol **3.40** and the Lewis acid

decreased yield of **3.42** (22%, Entry 6). Despite the stability of **3.30a** to air and moisture, it was reasoned that generation of the cobalt complex *in situ* from propargyl alcohol and dicobalt octacarbonyl may be advantageous. Stirring of propargyl alcohol (2 equiv) and $\text{Co}_2(\text{CO})_8$ (2 equiv) in DCM, followed by addition of alcohol **3.40** and $\text{BF}_3 \cdot \text{OEt}_2$ gave the highest yield of **3.42** (60%, Entry 7). This protocol was used in subsequent experiments.

Table 8. Optimization of the Nicholas reaction with alcohol **3.40**.



Entry	Equiv (3.40 : 3.30a : $\text{BF}_3 \cdot \text{OEt}_2$)	Order of Addition	Temp (°C)	Time (h)	Yield
1	1:2:2.5	LA, 3.30 , 3.40	0	4.5	47%
2	1:3:5	LA, 3.30 , 3.40	0	4	36%
3	1:2:2.5	LA, 3.30 , 3.40 ^a	0	4	28%
4	1:2:2.5	LA, 3.40 , 3.30	0	4.5	44%
5	1:2:2.5	3.30 , 3.40 , LA	0	4	55%
6	1:3:5	3.30 , 3.40 , LA	0	5	22%
7	1:2:2.5	3.30 , 3.40 , LA ^b	0	3.5	60%
8	1:2:2.5	3.30 , 3.40 , LA	-40	3.5	23%
9	1:2:2.5	3.30 , 3.40 , LA	-10	3.5	38%

LA: Lewis Acid, ^aAlcohol **3.40** was added dropwise over 5 min. ^b**3.30a** was generated *in situ* from propargyl alcohol and dicobalt octacarbonyl.

Efforts were made to increase mass balance and decrease material on the baseline of the TLC by lowering the reaction temperature. The reaction was performed at -40 °C and -10 °C, which afforded **3.42** in 23% and 38% yield, respectively (Entries 8, 9). Both of these experiments were quenched after 3.5 h because degradation of the product was observed over time by TLC. Further experiments showed that extended reaction times resulted in lower yields suggesting that **3.42** may not be stable in the reaction media.

All experiments also afforded byproduct **3.43** resulting from homodimerization of excess **3.30a** (Figure 20).¹⁰¹ Formation of this byproduct is the reason the nucleophilic species has

traditionally been used in high excess compared to the cobalt complex. However, byproduct **3.43** is non-polar and easily separable from **3.42** using column chromatography.

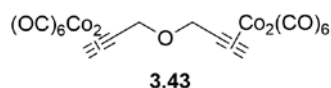
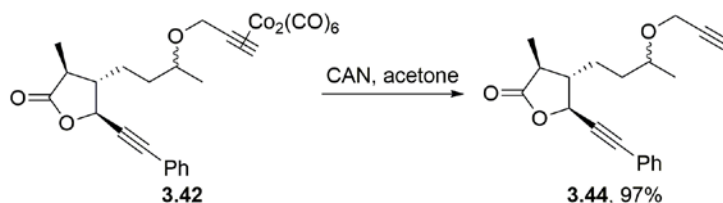


Figure 20. Homodimerization of **3.30a** results in byproduct **3.43**.

Decomplexation of $\text{Co}_2(\text{CO})_6$ -alkynes can be accomplished using an oxidant such as CAN. Stirring **3.42** with CAN for 10 minutes afforded **3.44** in 97% yield without the need for purification (Scheme 60). NMO was also employed as an oxidant but resulted in decomposition of **3.42**.¹⁰² Evidence of cobalt decomplexation can be easily observed by comparison of the ^1H and ^{13}C NMR spectra for the cobalt complex and resulting alkyne. For the cobalt-complexed alkyne **3.42**, the hydrogen on the terminus of the alkyne is observed at 6.01 ppm. The corresponding proton of **3.44** is shifted up-field to 2.39 ppm when the alkyne is decomplexed. Also, the carbonyl ligands bound to cobalt can be observed at 199.8 ppm in the ^{13}C NMR spectrum for the complexed alkyne **3.42**; this signal disappears upon decomplexation.



Scheme 60. Decomplexation of **3.42** to afford propargyl ether **3.44**.

3.2.3 Testing the scope and limitations of the Nicholas reaction conditions on amino acid derived nucleophiles

Next, we sought to establish the generality of these efficient Nicholas reaction conditions for the propargylation of a range of heteroatomic nucleophiles. Amino acids residues were

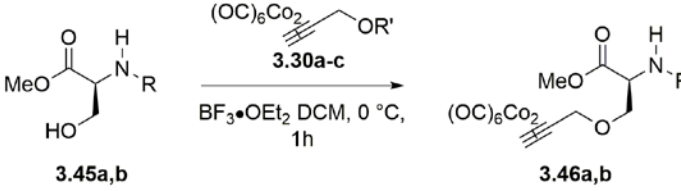
chosen for these experiments due to the wide variety of functionality available in a single compound class. In addition, alkyne-containing amino acid residues have been used in many click-chemistry applications.^{78b} Alkynyl groups are most commonly installed onto amino acid residues by alkylating a heteroatom containing side chain using basic conditions, or by transforming the C-terminus carboxylic acid into an alkyne via Corey-Fuchs or Seyferth-Gilbert protocols.¹⁰³ Therefore, the Nicholas reaction would provide a viable alternative for the synthesis of these unnatural alkynylated residues.

N,O-protected amino acid derivatives were employed to examine reactions with the heteroatomic side chains. Continuing our investigation of aliphatic alcohols, *N*-Boc and *N*-Fmoc serine methyl esters **3.45a,b** were subjected to the Nicholas reaction by our collaborator, John Widen (Table 9). Stirring of *N*-Boc-L-serine methyl ester (**3.45a**) with Co₂(CO)₆-propargyl alcohol (generated *in situ*) and BF₃•OEt₂ resulted in only a 20% yield of Co₂(CO)₆-propargyl ether **3.46a** (Entry 1). Further analysis revealed that the majority of Co₂(CO)₆-propargyl alcohol had been consumed, presumably due to the competing homodimerization, and 76% of serine **3.45a** was recovered. Subjecting *N*-Fmoc-L-serine ethyl ester (**3.45b**) gave a similar result, where Co₂(CO)₆-propargyl ether **3.46b** was obtained in 29% yield and 63% of **3.46b** was recovered (Entry 4). It was clear that the cobalt complexed propargylium ion was reacting faster with excess Co₂(CO)₆-propargyl alcohol **3.30a** than with the hydroxyl group of serine.

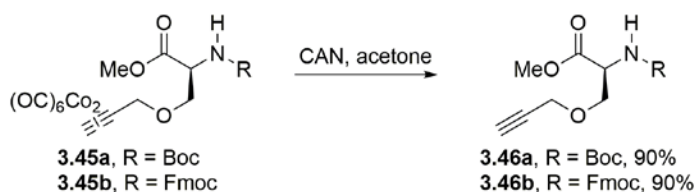
Through our weekly collaboration discussions, we decided to try alternative sources of the propargylium ion that would not undergo homodimerization. Many substituted oxygens have been employed in the Nicholas reaction as leaving groups, including but not limited to esters (Ac, Bz, Piv, MS, and Tf) as well as cyclic and non-cyclic ethers (Me, Bn, and TBS).^{93b} We chose to test the dicobalt hexacarbonyl complexes of propargyl acetate (**3.30b**) and methyl

propargyl ether (**3.30c**) in the reactions with the serine derivatives **3.45a,b**. Both reactions of $\text{Co}_2(\text{CO})_6$ -propargyl acetate **3.30b** with **3.45a** and **3.45b** in the presence of $\text{BF}_3 \cdot \text{OEt}_2$ successfully afforded the $\text{Co}_2(\text{CO})_6$ -propargyl ethers **3.46a** and **3.46b** in 29% and 23% yield respectively, similar to the results obtained when $\text{Co}_2(\text{CO})_6$ -propargyl alcohol **3.30a** was employed (Entries 2 and 5). However, using $\text{Co}_2(\text{CO})_6$ -methyl propargyl ether **3.30c** as the precursor for the propargylium cation resulted in significant improvements; **3.46a** was afforded in 97% yield, a 5-fold increase compared to the use of propargyl alcohol (Entry 3), while **3.46b** was afforded in 54% yield, representing a 2-fold increase in yield (Entry 6). By eliminating the possible homodimerization reaction of the propargylium ion, the hydroxyl group of the serine derivatives became the prominent nucleophilic species. Oxidative decomplexation of **3.46a,b** with CAN readily gave propargyl ethers **3.47a** and **3.47b**, both in 90% yield (Scheme 61).

Table 9. Propargylation of *N*-protected serine methyl esters **3.45a,b**.

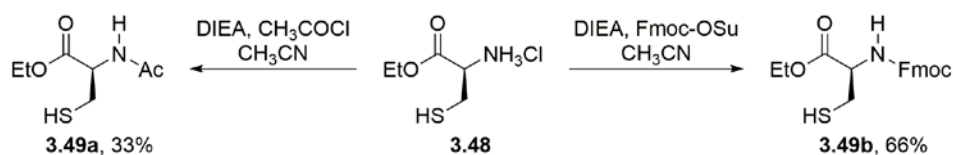


Entry	R	R'	Yield 3.46 (%)
1	Boc (3.45a)	H (3.30a)	20
2	Boc	Ac (3.30b)	29
3	Boc	Me (3.30c)	97
4	Fmoc (3.45b)	H	29
5	Fmoc	Ac	23
6	Fmoc	Me	54



Scheme 61. Oxidative decomplexation to afford alkynyl serine derivatives **3.47a,b**.

Next, the Nicholas reaction conditions were applied to the propargylation of cysteine residues. While thiols have been used previously in the Nicholas reaction, examples have been limited, with most reports pertaining to the synthesis of sulfur containing macrocycles.¹⁰⁴ Cysteine residues have never been employed in the Nicholas reaction. Towards this end, *N*-protected cysteine ethyl esters **3.49a,b** were prepared (Scheme 62). *N*-Acetyl-L-cysteine ethyl ester **3.49a** was obtained in 33% yield, from L-cysteine ethyl ester hydrochloride **3.48** using *N,N*-diisopropylethylamine (DIEA) and acetyl chloride. This procedure has been previously used for the synthesis of *N*-acetyl-L-cysteine methyl ester.¹⁰⁵ *N*-Fmoc-L-cysteine ethyl ester **3.49b** was also prepared from **3.48** in 66% yield using DIEA and Fmoc-OSu.



Scheme 62. Synthesis of *N*-protected cysteine ethyl esters **3.49a,b**.

These cysteine derivatives were first subjected to the Nicholas reaction with $\text{Co}_2(\text{CO})_6$ -propargyl alcohol **3.30a**. In the presence of **3.30a** (generated *in situ*) and $\text{BF}_3 \cdot \text{OEt}_2$, *N*-acetyl-L-cysteine ethyl ester **3.49a** readily afforded $\text{Co}_2(\text{CO})_6$ -propargyl thioether **3.50a** in 86% yield (Table 10, Entry 1). *N*-Fmoc-L-cysteine ethyl ester **3.49b** afforded cysteine derivative **3.50b** in 71% yield (Entry 2). A comparison was made between the use of propargyl alcohol complex **3.30a** and methyl propargyl ether complex **3.30c** for the synthesis of the Fmoc-cysteine example **3.50b**. Reacting **3.49b** with complex **3.30c**, formed *in situ*, gave a moderate yield of 58% for formation of **3.50b** (Entry 3). Alternatively, when $\text{Co}_2(\text{CO})_6$ -methyl propargyl ether complex **3.30c** was prepared prior to the reaction, **3.50b** was afforded in 67% yield (Entry 4). Overall, we concluded that for the cysteine examples, methyl propargyl ether complex **3.30c** gives comparable results to the use of propargyl alcohol complex **3.30a**. The increased nucleophilicity

of the sulfhydryl group compared to the hydroxyl groups likely minimizes the competing homodimerization of **3.30a**.

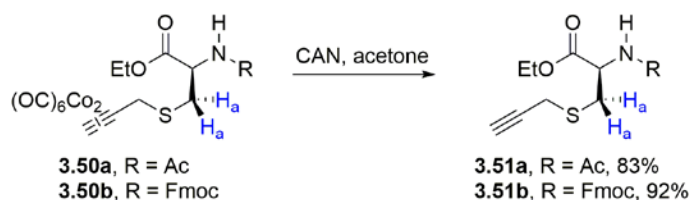
Table 10. Propargylation of cysteine derivatives **3.49**.



Entry	R	R'	Time	Yield 3.50 (%)
1	Ac (3.49a)	H	2 h	86
2	Fmoc (3.49b)	H	45 min	71
3	Fmoc	Me	2 h	58
4	Fmoc	Me ^a	2 h	67

^aCo₂(CO)₆-methyl propargyl ether was prepared prior to the reaction.

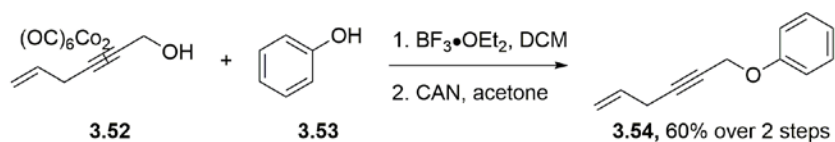
Both Co₂(CO)₆-alkynes **3.50a** and **3.50b** underwent oxidative decomplexation with CAN which gave propargyl thioethers **3.51a** and **3.51b** in 83% and 92% respectively (Scheme 63). The reactions were clean, with no evidence of byproducts. We were concerned that the sulfur atoms may undergo oxidation in the presence of CAN to afford sulfoxides, however, this was not observed. The chemical shift for the α -hydrogens to the sulfur atom (H_a) were at about 3.1 ppm for all four compounds **3.50a,b** and **3.51a,b**. We would have expected the chemical shift of H_a to move downfield if the sulfur had been oxidized. Mass spec data obtained for **3.51a** and **3.51b** also confirmed the structures.



Scheme 63. Oxidative decomplexation for the formation of alkynyl cysteine derivatives **3.51a,b**.

Phenolic nucleophiles were then examined by employing tyrosine amino acid derivatives. Only one example exists where a phenol was used as a nucleophile in a Nicholas reaction; during

the synthesis of unsymmetrical ethers, $\text{Co}_2(\text{CO})_6$ -hex-5-en-2-yn-1-ol (**3.52**) was reacted with $\text{BF}_3 \cdot \text{OEt}_2$ in the presence of phenol (**3.53**), followed by a cobalt decomplexation with CAN to afford the ether **3.54** in 60% yield.⁹⁷



Scheme 64. Previous example of a phenolic nucleophile in the Nicholas reaction.

To evaluate the phenolic side chains of tyrosine in the Nicholas reaction, *N*-Boc- and *N*-Fmoc-L-tyrosine methyl esters **3.55a,b** were employed. When our collaborator, John Widen, subjected *N*-Boc-L-tyrosine methyl ester **3.55a** to the Nicholas reaction conditions using $\text{Co}_2(\text{CO})_6$ -propargyl alcohol **3.30a**, the desired product **3.56a** was obtained consistently in 45% yield (Table 11, Entry 1). **3.55a** was recovered in 22% while complex **3.30a** was fully consumed, due to homodimerization. A byproduct was also been observed during the reaction, but was not isolated. When I repeated this reaction, I also observed two major products by TLC. The desired product **3.56a** was obtained in 32% yield but the byproduct appeared to be unstable and was only obtained in trace amounts. After careful NMR analysis, we determined this byproduct to be **3.57** (Figure 21), presumably resulting from an electrophilic aromatic substitution process.

A key ^1H NMR signal that led to the structure assignment was a new aromatic singlet at 6.95 ppm (H_a). Also, the integration of the aromatic protons totaled three. In addition, the signals at 6.07 and 4.10 ppm correspond to the presence of the $\text{Co}_2(\text{CO})_6$ -alkyne (H_d , H_h). The remaining proton assignments were made by comparison to literature values for **3.55a**.¹⁰⁶ Based on these assignments, the signal at 4.75 ppm represents phenolic proton (H_f); the presence of this signal also supports the proposed structure of **3.57**. The regiochemistry of the propargyl substitution on the aryl ring was confirmed by comparing the aromatic region in the ^1H NMR

spectrum of **3.57** to the ^1H NMR spectra of 3,4-xylenol and 2,4-xylenol. For these trisubstituted aromatic rings, aromatic protons ortho to the hydroxyl group are observed at about 6.6 ppm while meta protons are observed at about 6.9 ppm. Both byproduct **3.57** and 2,4-xylenol had two aromatic signals at ~ 6.9 ppm and one aromatic signal at ~ 6.6 ppm. Also, substitution of **3.55a** at the ortho position in relation to the hydroxyl group is expected when considering electrophilic aromatic substitution cationic intermediates.

Table 11. Propargylation of *N*-protected tyrosine methyl esters **3.55a,b**



Entry	R	R'	Yield 3.56 (%)	Time	Observations
1	Boc (3.55a)	H	45	1 h	3.55a recovered in 22% Unstable byproduct 3.57 observed by TLC (Figure 21)
2	Boc	Me	23	3 h	Partial decomposition
3	Fmoc (3.55b)	H	6	1 h	3.55b recovered in 89%
4	Fmoc	Me	73	1 h	---

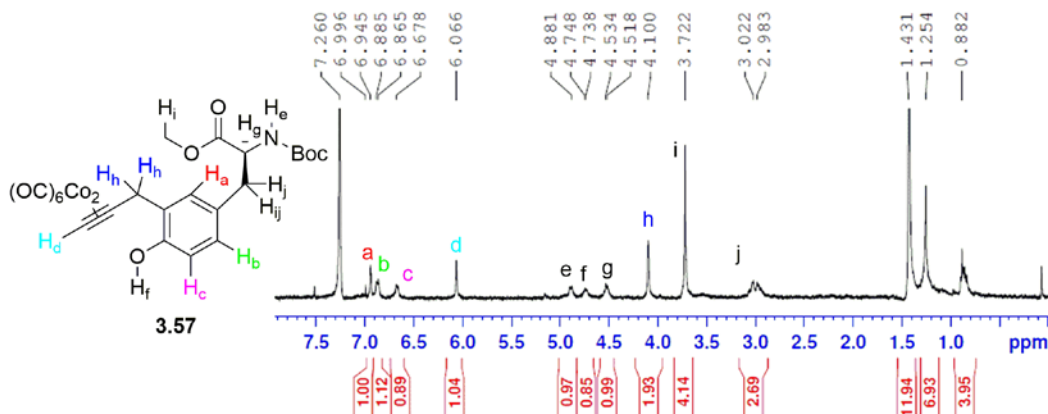
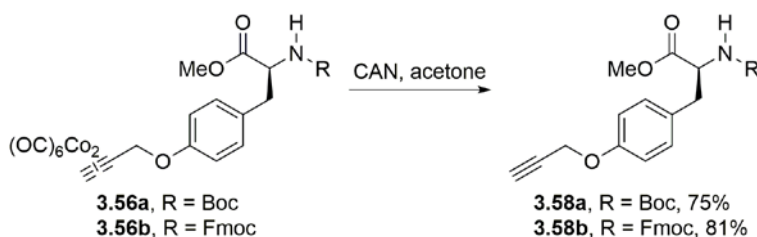


Figure 21. ^1H NMR analysis of electrophilic aromatic substitution byproduct **3.57**.

To avoid homodimerization of $\text{Co}_2(\text{CO})_6$ -propargyl alcohol **3.30a**, $\text{Co}_2(\text{CO})_6$ -methyl propargyl ether **3.30c** was employed. However, this did not result in an improved yield for the formation of $\text{Co}_2(\text{CO})_6$ -propargyl *N*-Boc-tyrosine **3.56a**, which was isolated in 23% yield (Table 11, Entry 2). We believe that the Boc protecting group was unstable under the extended reaction time required; a significant amount of baseline material was observed after the reaction. $\text{BF}_3 \cdot \text{OEt}_2$ has been reported as a viable deprotecting agent for Boc groups.¹⁰⁷

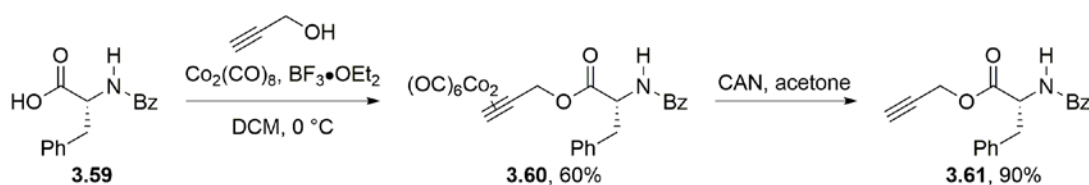
However, for the conversion of *N*-Fmoc-L-tyrosine methyl ester **3.55b** to the corresponding $\text{Co}_2(\text{CO})_6$ -propargyl phenyl ether **3.56b**, the precursor for the propargylium ion made a significant difference. When propargyl alcohol complex **3.30a** was used, **3.56b** was isolated in 6% yield and 89% of **3.55b** was recovered (Entry 3). Alternatively, the reaction with methyl propargyl ether complex **3.30c** afforded **3.56b** in 73% yield (Entry 4). Evidence of a byproduct, presumably formed via electrophilic aromatic substitution, was also observed by TLC during these reactions with **3.55b**, but was not isolated. The decomplexed propargyl phenyl ether derivative of tyrosine **3.58a** and **3.58b** were successfully obtained from the corresponding cobalt complexes in 75% and 81% respectively (Scheme 65).



Scheme 65. Oxidative decomplexation of tyrosine derivatives **3.56a,b**.

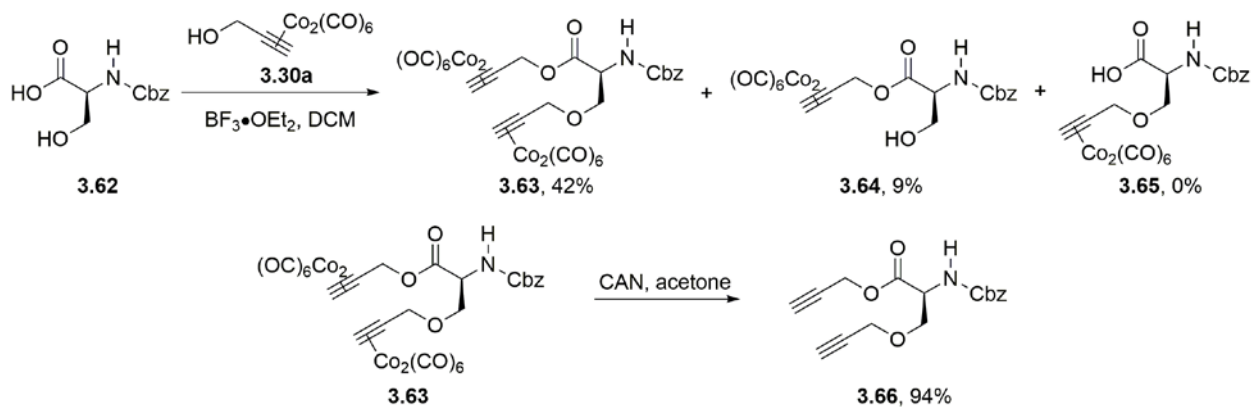
In addition to the side chain hydroxyl and sulfhydryl groups, we examined the reactivity unprotected carboxyl and amino functionality of amino acids with the cobalt complexed propargylium ions. *N*-benzoyl-D-phenylalanine (**3.59**) was used to establish the reactivity of the carboxyl group as a nucleophile in the Nicholas reaction. To date, only two reports of using a

carboxylic acid in a Nicholas reaction have been reported. In the process of studying the use of chiral auxiliaries in the Nicholas reaction, Martin and coworkers transformed propargyl alcohols to propargyl acetates by employing acetic acid as the nucleophilic species.¹⁰⁸ The Shea group has exploited this reactivity of carboxylic acids for the synthesis of macrocyclic diolides.¹⁰⁹ Amino acids have never been used in the Nicholas reaction for the synthesis of propargylic esters. *N*-benzoyl-D-phenylalanine **3.59** was reacted with complex **3.30a** (generated *in situ*) and $\text{BF}_3 \cdot \text{OEt}_2$ to afford the $\text{Co}_2(\text{CO})_6$ -propargylic ester **3.60** in 60% yield. Decomplexation of **3.60** with ceric ammonium nitrate generated propargyl ester **3.61** in 90% yield (Scheme 66).



Scheme 66. Use of a carboxylic acid in the Nicholas reaction for formation of propargylic ester **3.61**.

Next, a serine derivative, *N*-benzyloxycarbonyl-L-serine (**3.62**), containing an unprotected carboxylic acid was examined to determine if the cobalt-complexed propargylic cation reacted more readily with the aliphatic alcohol or the carboxylic acid. Bis-propargylated serine **3.63** was obtained as the major product in 42% yield, resulting from alkylation of both the hydroxyl and the carboxyl groups. $\text{Co}_2(\text{CO})_6$ -complexed propargyl ester **3.64** was also isolated in 9% yield, suggesting that the carboxylic acid is more reactive than the aliphatic alcohol. When $\text{Co}_2(\text{CO})_6$ -diyne **3.63** was reacted with excess CAN, diyne **3.66** was obtained in 94% yield (Scheme 67).



Scheme 67. Result of employing N-Cbz-L-serine **3.62** in the Nicholas Reaction.

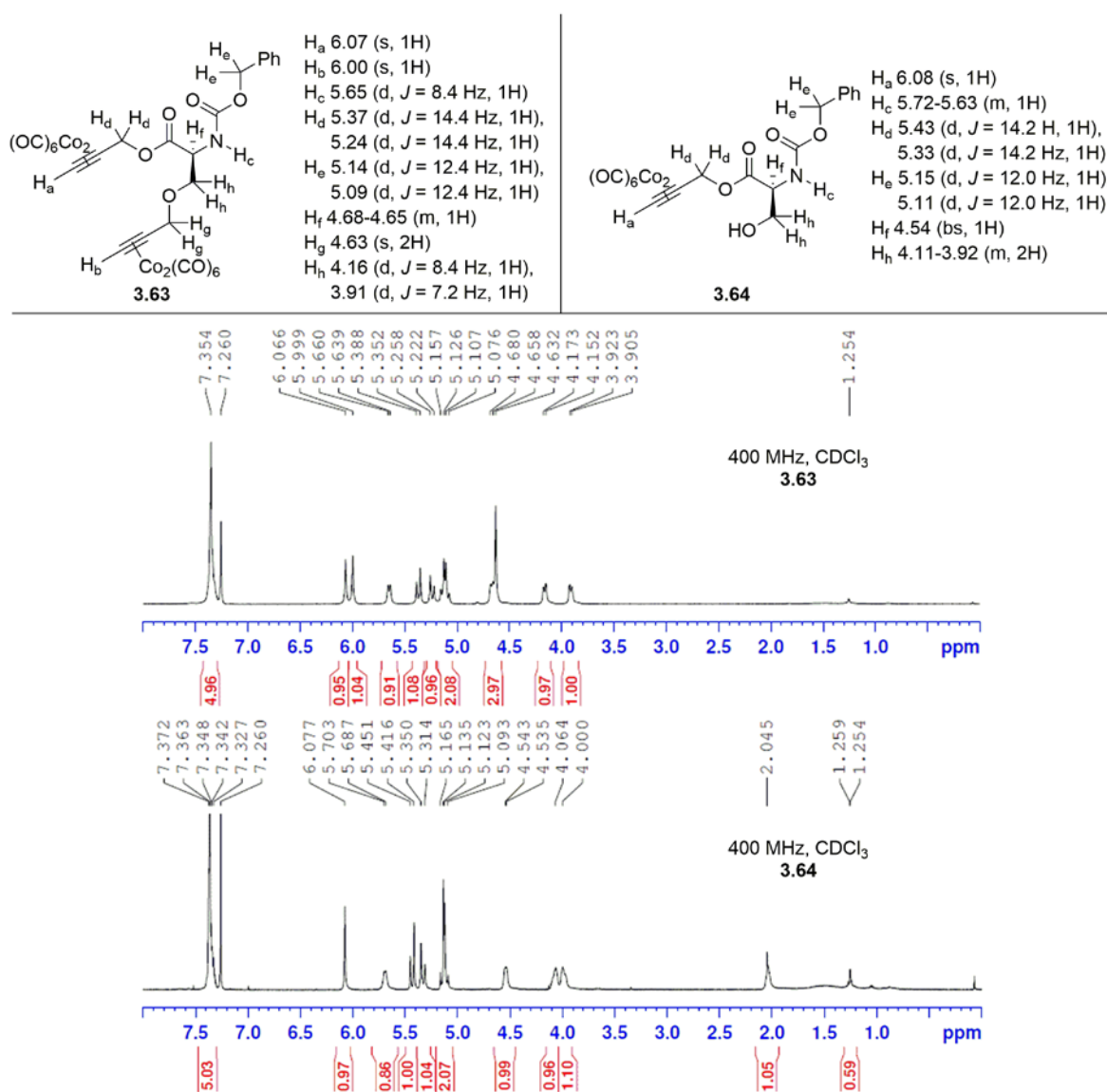


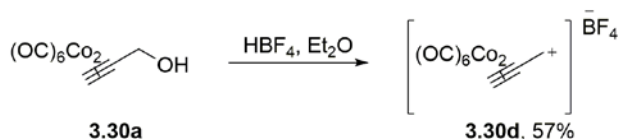
Figure 22. ¹H NMR analysis of Nicholas reaction products **3.63** and **3.64**.

Structural assignment of byproduct **3.64** was determined by comparison of its ^1H NMR spectrum with that of $\text{Co}_2(\text{CO})_6$ -diyne **3.63** (Figure 22). For both **3.63** and **3.64**, the AB doublets at ~ 5.1 ppm were assigned to belong to H_e of the Cbz group by comparison to the *N*-Cbz-*L*-serine **3.62**. For diyne **3.63**, the singlet at 6.07 (H_a) and doublets at 5.37 and 5.24 ppm (H_d) represent the propargyl ester group, shifted downfield compared to the propargyl ether signals H_b and H_g (singlet at 6.00 ppm and signal at 4.63 ppm respectively). Analysis of the byproduct **3.64** spectrum revealed propargyl signals represented by a singlet at 6.08 ppm (H_a) and doublets at 5.43 and 5.33 ppm (H_d) consistent with the propargyl ester signals of **3.63**.

Next, amino groups were subjected to the Nicholas reaction conditions. When *L*-proline methyl ester (**3.67**) was reacted with $\text{Co}_2(\text{CO})_6$ -propargyl alcohol **3.30a** and $\text{BF}_3 \cdot \text{OEt}_2$, $\text{Co}_2(\text{CO})_6$ -propargyl amine **3.68** was not obtained. TLC analysis showed that upon addition of the Lewis acid, *L*-proline methyl ester **3.67** was no longer present, but no product were observed (Table 12, Entry 1). We concluded that $\text{BF}_3 \cdot \text{OEt}_2$ immediately coordinates with the amine, preventing formation of **3.68**. Next, $\text{Co}_2(\text{CO})_6$ -methyl propargyl ether **3.30c** was employed and stirred with $\text{BF}_3 \cdot \text{OEt}_2$ for 30 minutes, prior to addition of proline derivative **3.67**, however this experiment also resulted in no formation of **3.68** (Entry 2).

For some previous Nicholas reaction reports where an amino group was used as the nucleophile in the Nicholas reaction, formation and isolation of the propargylium ion as a salt was achieved prior to the reaction by reacting the corresponding propargyl alcohol derivative with a protic acid, such as tetrafluoroboric acid (HBF_4).¹¹⁰ We predicted that if $\text{Co}_2(\text{CO})_6$ -methyl propargyl ether **3.30c** was reacted with HBF_4 , tetrafluoroborate salt **3.30d** could be formed *in situ* without homodimerization, thereby allowing an efficient reaction with proline **3.67** to afford the desired product **3.68** (Scheme 68, desired result). To test this hypothesis, **3.30c** was stirred

not afford salt **3.30d**; precipitation was never observed. As a result we decided to use diethyl ether as the solvent for this transformation because **3.30a** is soluble in ether, while the salt **3.30d** is not. $\text{Co}_2(\text{CO})_6$ -propargyl alcohol **3.30a** was reacted with HBF_4 in diethyl ether at $-10\text{ }^\circ\text{C}$. Precipitation of **3.30d** was observed and removal from the ethereal solution was obtained using a Schlenk filtration apparatus. **3.30d** is sensitive to air and water and therefore was both isolated (57% yield) and stored in a nitrogen filled glove box (Scheme 69).

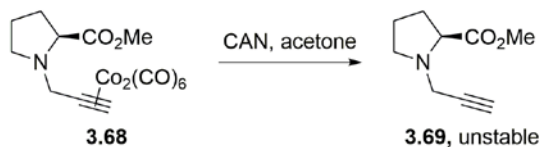


Scheme 69. Synthesis of propargylium cation tetrafluoroborate salt **3.30d**.

L-Proline methyl ester **3.67** was reacted with 1.5 equiv of **3.30d** in DCM at 0°C to successfully afford $\text{Co}_2(\text{CO})_6$ -propargyl amine **3.68** in 31% yield after 1.5 h (Table 12, Entry 4). Reducing the amount of **3.30d** to 1.3 equiv increased the yield of **3.68** to 46% (Entry 5). For both of these reactions, salt **3.30d** was used within 14 h of isolation. Over time, the salt changes from a deep red color to a darker maroon/brown color. When salt **3.30d** was reacted with proline **3.67** after being stored in the glove box for 2 weeks, the yield of **3.68** suffered (19%, Entry 6). This revealed that **3.30d** is unstable, even when stored under nitrogen.

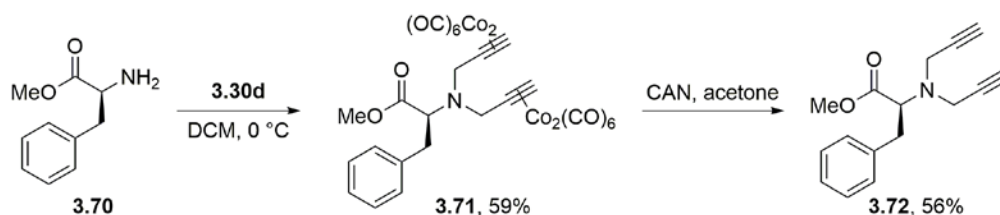
With **3.68** in hand, decomplexation to obtain the proline derived propargyl amine **3.69** was attempted. Unfortunately, **3.69** was determined to be unstable (Scheme 70). When **3.38** was reacted with 4 equiv of CAN, **3.68** and **3.69** were obtained as a mixture. Increasing the amount of CAN to 5 equivalents resulted in complete decomposition. By reacting **3.68** with 4 equiv of CAN for 1 h, and then an additional 0.5 equiv of CAN for 20 min, **3.69** was obtained in 68% yield and was characterized by NMR spectroscopy, HRMS, and TLC analysis before undergoing non-specific decomposition. Attempts to repeat this result were unsuccessful. Additional

oxidizing agents were examined. Stirring of **3.68** in the presence of trimethylamine oxide¹¹² resulted in decomposition while iron(III) nitrate nonahydrate was unreactive, resulting in recovery of **3.68**.¹¹³



Scheme 70. Decomplexation of proline derivative **3.68**.

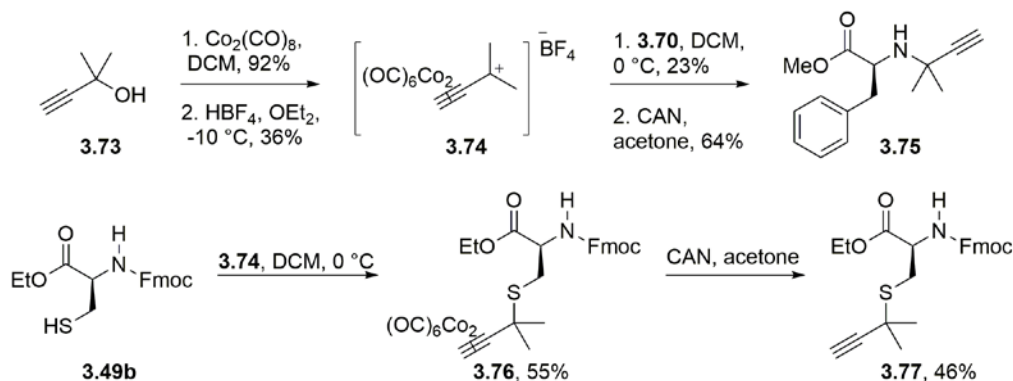
Next, *L*-phenylalanine methyl ester (**3.70**) was subjected to the Nicholas reaction, allowing us to ascertain the reactivity of primary amino groups as nucleophiles. Reaction of **3.70** with tetrafluoroborate salt **3.30d** in DCM at 0 °C for 1.5 h afforded **3.71** in 59% yield, resulting from dipropargylation of the primary amino group. Decomplexation in the presence of CAN (8 equiv) gave the dipropargyl amine **3.72** in 56% yield (Scheme 71).



Scheme 71. Reaction of *L*-phenylalanine methyl ester (**3.70**) with **3.30d** followed by decomplexation.

To effect mono-propargylation of primary amines, we increased the steric bulk of the tetrafluoroborate propargylium cation. The $\text{Co}_2(\text{CO})_6$ -2-methyl-3-butyn-2-ol was prepared in 92% yield from **3.73**. In turn, $\text{Co}_2(\text{CO})_6$ -2-methyl-3-butyn-2-ol was stirred with HBF_4 in diethyl ether to afford tetrafluoroborate salt **3.74** in 36% yield (Scheme 72). Addition of *L*-phenylalanine methyl ester **3.70** to **3.74** afforded the corresponding $\text{Co}_2(\text{CO})_6$ -alkyne in 23% yield. No evidence of the dipropargylation product was observed. Decomplexation afforded alkyne **3.75** in 64% yield. Next, one of the most effective nucleophiles tested, *N*-Fmoc-*L*-cysteine ethyl ester

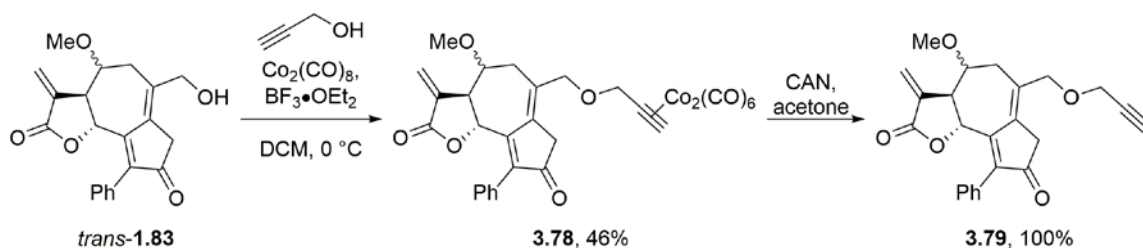
3.49b was reacted with **3.74** to determine its relative reactivity compared to the use of complex **3.30a** and $\text{BF}_3 \cdot \text{OEt}_2$. $\text{Co}_2(\text{CO})_6$ -alkyne **3.76** was obtained in 55% yield; a moderate yield compared to the 71% yield of **3.50b** without the gem-dimethyl groups obtained when using $\text{Co}_2(\text{CO})_6$ -propargyl alcohol **3.30a** and $\text{BF}_3 \cdot \text{OEt}_2$ (Table 10, Entry 2). Cobalt decomplexation afforded **3.77** in 46% yield.



Scheme 72. Synthesis of **3.74** and its application to the formation of **3.75** and **3.77**.

3.2.4 The synthesis of sesquiterpene lactone alkyne probes

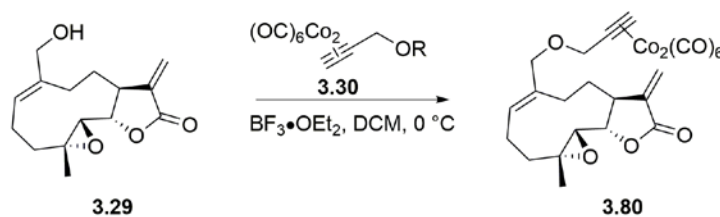
Finally, we used the optimized Nicholas reaction conditions for propargylation of high-value substrates to synthesize alkyne probes of sesquiterpene analogs. *trans*-Guaianolide analog **1.83**, which is unstable to basic conditions, was reacted with $\text{Co}_2(\text{CO})_6$ -propargyl alcohol **3.30a**, formed *in situ*, and $\text{BF}_3 \cdot \text{OEt}_2$, to afford $\text{Co}_2(\text{CO})_6$ -alkyne derivative **3.78** in 46% yield (Scheme 73). Employing complex **3.30a** isolated prior to the reaction gave a lower yield of 30% for **3.78**. Due to the limited quantities of **1.83** available, attempts to synthesize **3.78** using $\text{Co}_2(\text{CO})_6$ -methyl propargyl ether **3.30c** were not carried out, however, this protocol may improve yields. **3.78** was decomplexed using CAN to afford the guaianolide analog alkyne probe **3.79** in quantitative yield.



Scheme 73. Synthesis of guaianolide analog alkyne probe **3.79**.

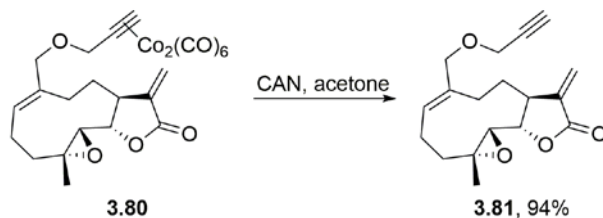
Next, the synthesis of MelB alkyne probe derivative **3.81** was pursued (Table 13). First, MelB **3.29** was reacted $\text{Co}_2(\text{CO})_6$ -propargyl alcohol **3.30a**, formed *in situ*, and $\text{BF}_3 \cdot \text{OEt}_2$. **3.80** formed immediately, as determined by TLC. However, Mel B **3.29** was not fully consumed so the reaction stirred for 45 min. Over this time, decomposition of $\text{Co}_2(\text{CO})_6$ -alkyne **3.80** was observed and isolated in only 20 % yield (Entry 1). Due to the observed product degradation, the reaction was repeated but only allowed to stir for 10 min, which doubled the isolated yield of **3.80** to 41% (Entry 2). Methyl propargyl ether complex **3.30c** was next employed in place of propargyl alcohol complex **3.30a**. When this reaction was allowed to stir for 1.5 h, **3.80** was obtained in 21% yield (Entry 3). Significant degradation had been observed (by TLC) after 40 minutes during this reaction; therefore, the reaction was repeated but stirred for only 40 min which afforded **3.80** in 39% yield. For this example, use of propargyl alcohol and methyl propargyl ether gave comparable results.

Table 13. Synthesis of MelB cobalt complexed alkyne probe **3.80**.



Entry	R (3.30)	Time	Yield (%)
1	H (3.30a)	45 min	20
2	H	10 min	41
3	Me (3.30c)	1.5 h	21
4	Me	40 min	39

Oxidative decomplexation of $\text{Co}_2(\text{CO})_6$ -alkyne **3.80** was the final step towards synthesis of a MelB alkyne probe. Reaction of **3.80** with ceric ammonium nitrate in acetone cleanly afforded **3.81** in 94% yield (Scheme 74).



Scheme 74. Oxidative decomplexation of **3.80** to afford propargylated Mel B **3.81**.

3.3 CONCLUSIONS

In conclusion, the Nicholas reaction offers an acid-mediated propargylation strategy for the preparation of biologically relevant alkyne probes. Conditions were optimized to allow high-value small molecules to be employed as the limiting reagent compared to the cobalt complexed propargyl synthons and Lewis acid. A variety of heteroatom nucleophiles can be propargylated using this method, including hydroxyl, sulfhydryl, amino, and carboxyl groups. The corresponding alkynyl derivatives were obtained after oxidative decomplexation using ceric ammonium nitrate.

Multiple cobalt complexed propargylium ion precursors were compared for various nucleophilic species. Dicobalt hexacarbonyl complexed propargyl alcohol is the preferred precursor for highly reactive nucleophilic species due to its low cost and volatility compared to methyl propargyl ether. However, for less nucleophilic heteroatoms, use of dicobalt hexacarbonyl complexed methyl propargyl ether avoids the competing homodimerization of the propargyl synthon, allowing the desired nucleophilic species to react selectively. Finally,

propargylium tetrafluoroborate salts allow propargylation of amino groups. Primary amino groups can be selectively mono- or di-propargylated depending on the steric nature of the propargylium salt.

This alternative, non-basic, propargylation protocol was compatible with a wide range of functionality. Both ethyl and methyl carboxyl protecting groups were tolerated but not directly compared. Carboxybenzyl, fluorenylmethoxycarbonyl, acetyl, and benzyloxy amino protecting groups were well tolerated with some variability in yields observed when various protecting groups were used on the same parent amino acid. *tert*-Butoxycarbonyl protecting group was tolerated when employed on a serine derivative, however, when used on a tyrosine derivative, evidence of protecting group instability was observed, resulting in low yields of the Nicholas reaction product. The Lewis acid being used, borontrifluoride diethyl etherate has been shown to be an effective deprotecting agent for Boc groups.¹⁰⁷ Functionally dense natural product analogs containing reactive covalent modifiers such as α -methylene- γ -butyrolactones and epoxides were also tolerated, allowing the synthesis of potential biological probes.

3.4 EXPERIMENTALS

3.4.1 General Methods

All commercially available compounds were used as received unless otherwise noted. Dichloromethane (DCM), diethyl ether (Et₂O), and tetrahydrofuran (THF) were purified by passing through alumina using a solvent purification system. Deuterated chloroform (CDCl₃) was stored over 4 Å molecular sieves. Boron trifluoride diethyl etherate (BF₃•OEt₂) was or

redistilled under a nitrogen atmosphere. Dicobalt octacarbonyl ($\text{Co}_2(\text{CO})_8$) was used as purchased and was stored at $-20\text{ }^\circ\text{C}$ and opened only in a nitrogen filled glove box. Purification of compounds by manual flash column chromatography was performed using silica gel (40-63 μm particle size, 60 \AA pore size) purchased from Sorbent Technologies. TLC analyses were performed on Silicycle SiliaPlate G silica gel glass plates (250 μm thickness) and visualized by UV irradiation (at 254 nm) and KMnO_4 stain. ^1H NMR and ^{13}C NMR spectra were recorded on Bruker Avance 300 MHz, 400 MHz, 500 MHz, or 600 MHz. Spectra were referenced to residual chloroform with or without 0.05% v/v TMS (7.26 ppm, ^1H ; 77.16 ppm, ^{13}C). Chemical shifts are reported in ppm, multiplicities are indicated by s (singlet), bs (broad singlet), d (doublet), t (triplet), q (quartet), p (pentet), and m (multiplet). Coupling constants, J , are reported in hertz (Hz). All NMR spectra were obtained at room temperature. IR spectra were obtained using a Nicolet Avatar E.S.P. 360 (NaCl plate) FT-IR. ESI mass spectrometry was performed on a Waters Q-TOF Ultima API, Micromass UK Limited.

The synthesis of the following compounds were completed by John Widen, from the Harki group at the University of Minnesota (Figure 23). Characterization for these compounds are included in the manuscript “Alkyne Ligation Handles: Propargylation of Hydroxyl, Sulfhydryl, Amino, and Carboxyl Groups via the Nicholas Reaction,” by Sarah M. Wells, John C. Widen, Daniel A. Harki, and Kay M. Brummond, submitted for publication 7/16/2016.

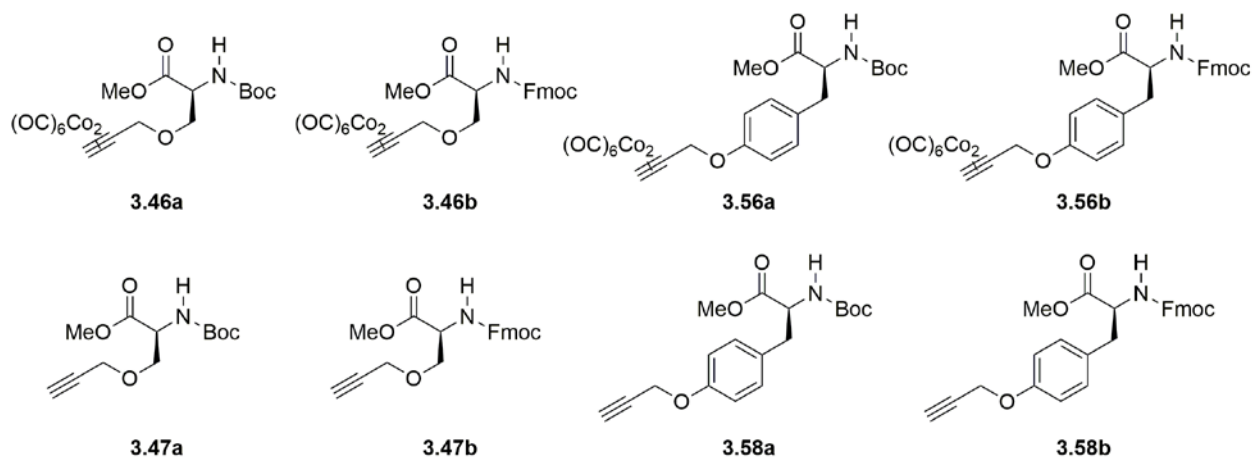
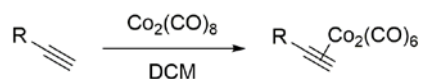
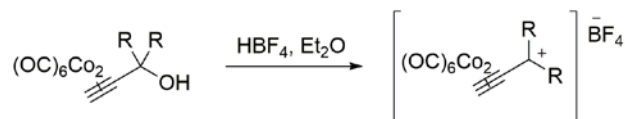


Figure 23. Compounds synthesized and characterized by collaborator John Widen.

3.4.2 General Procedures



General Procedure 3A: Coordination of alkyne to cobalt carbonyl complex. A single-necked, round-bottomed flask, equipped with a stir bar and a septum, was charged with $\text{Co}_2(\text{CO})_8$ (1 equiv) in a N_2 filled glove box. The flask was transferred out of the glove box and the septum was pierced with a nitrogen inlet needle. The flask was charged with DCM, followed by the alkyne (1 equiv), dissolved in DCM. The reaction stirred for 2 h, until evolution of CO gas, visible by small bubbles, was no longer observed. The contents were loaded directly onto a silica gel column for purification by flash column chromatography to afford the dicobalt hexacarbonyl complexed alkyne ($\text{Co}_2(\text{CO})_6$ -alkyne).



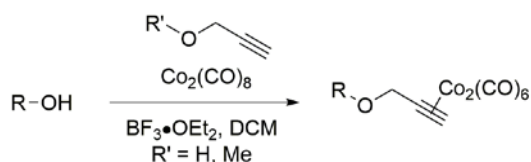
General Procedure 3B: Formation of tetra fluoroborate salts. A flame-dried 100 mL Schlenk flask equipped with a stir bar and septum was charged with either $\text{Co}_2(\text{CO})_6$ -propargyl alcohol **3.30a** or $\text{Co}_2(\text{CO})_6$ -2-methyl-3-butyn-2-ol (**3.S1**), dissolved in Et_2O . The flask was cooled to $-10\text{ }^\circ\text{C}$ on an ice/acetone bath. Tetrafluoroboric acid (54% by weight soln in Et_2O , 1.5 equiv) was added dropwise and the solution stirred for 2 h. Formation of a dark red precipitate was observed. The reaction was diluted with Et_2O . The septum was replaced with a Schlenk filtration apparatus. The apparatus was inverted and partial vacuum was applied to separate the solid from the Et_2O solution within the apparatus. The ether filtrate was removed via syringe and the crystals were dried under vacuum. The apparatus was transferred to the nitrogen filled glove box, where the crystals were isolated and stored.

General Procedure 3C: Nicholas Reaction Procedures

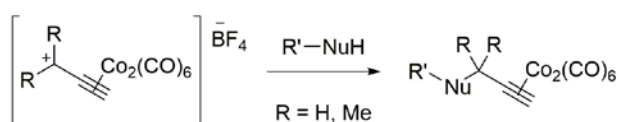


General Procedure 3C.1: Use of pre-made $\text{Co}_2(\text{CO})_6$ -alkyne. A single-necked, round-bottomed flask equipped with a stir bar and a septum pierced with a needle was charged with DCM (0.05 M), $\text{Co}_2(\text{CO})_6$ -propargyl alcohol **3.30a** or $\text{Co}_2(\text{CO})_6$ -methyl propargyl ether **3.30c** (2 equiv), and the nucleophilic species (1 equiv). The solution was cooled in an ice bath to $0\text{ }^\circ\text{C}$. $\text{BF}_3 \cdot \text{OEt}_2$ (2.5 equiv) was added dropwise and the reaction stirred until the nucleophile was fully consumed, or the reaction was no longer progressing, as determined by TLC. The reaction was quenched by the addition of saturated NaHCO_3 . The mixture was transferred to a separatory funnel, the layers were separated and the aqueous layer was extracted with DCM (3x). The combined organics were dried over MgSO_4 , filtered, and concentrated under reduced pressure.

The crude residue was purified by silica gel flash column chromatography to afford the $\text{Co}_2(\text{CO})_6$ -alkyne.

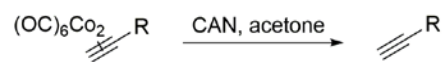


General Procedure 3C.2: *In situ* formation of dicobalt hexacarbonyl complexed alkyne. A single necked, round-bottomed flask, equipped with a stir bar and a septum was charged with $\text{Co}_2(\text{CO})_8$ (2 equiv) in a N_2 filled glove box. The flask was transferred out of the glovebox and the septum was pierced with a nitrogen inlet needle. Either propargyl alcohol or methyl propargyl ether (2 equiv), dissolved in DCM, was added and the reaction stirred for 1.5 h until evolution of CO gas was no longer observed. The solution was cooled to 0 °C in an ice bath. The nucleophilic species (1 equiv) was dissolved in DCM (0.05 M overall) and added to the flask via syringe, followed by the dropwise addition of $\text{BF}_3 \cdot \text{OEt}_2$ (2.5 equiv). The reaction stirred until the nucleophilic species was fully consumed, or the reaction was no longer progressing, as determined by TLC. The reaction was quenched by addition of saturated NaHCO_3 . The mixture was transferred to a separatory funnel, the layers were separated, and the aqueous layer was extracted with DCM (3x). The combined organic layers were dried over MgSO_4 , filtered, and concentrated under reduced pressure rotary evaporation. The crude residue was purified by silica gel flash column chromatography to afford the $\text{Co}_2(\text{CO})_6$ -alkyne.



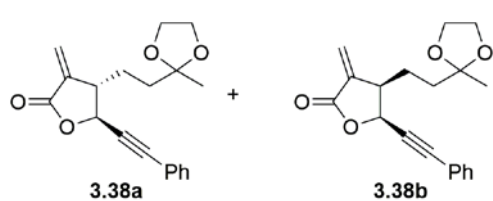
General Procedure 3C.3: Reaction of Tetrafluoroborate salts with nucleophiles. A single-necked, round-bottomed flask, equipped with a stir bar and a septum was charged with the propargylium tetrafluoroborate salt (1.3 equiv) in a N_2 filled glove box. The flask was transferred

out of the glove box and the septa was pierced with a N₂ inlet needle. The flask was cooled to 0 °C in an ice and water bath. DCM was added followed by the amino nucleophile (1 equiv) dissolved in DCM (0.05 M overall). The reaction stirred for 2 h or until complete as determined by TLC. The reaction was quenched by the addition of saturated NaHCO₃. The mixture was transferred to a separatory funnel; the layers were separated and the aqueous layer was extracted with DCM (3x). The combined organics were dried over MgSO₄, filtered, and concentrated under reduced pressure rotary evaporation. The crude residue was purified by silica gel flash column chromatography to afford the Co₂(CO)₆-alkyne.



General Procedure 3D: Oxidative Decomplexation of Co₂(CO)₆-alkynes. A single-necked, round-bottomed flask, equipped with a stir bar and a septum pierced with a N₂ inlet needle was charged with the Co₂(CO)₆-alkyne (1 equiv), dissolved in acetone (0.01 M). The solution was cooled in an ice bath to 0° C. Ceric ammonium nitrate (CAN, 5 equiv) was added to the flask in a single portion. The reaction stirred until complete as evidenced by TLC. The reaction was diluted with distilled water and Et₂O. The mixture was transferred to a separatory funnel. The layers were separated and the aqueous layer was extracted with Et₂O (3x). The combined organics were dried over MgSO₄, filtered, and concentrated under reduced pressure rotary evaporation. If necessary, the residue was purified by silica gel flash column chromatography to afford the alkyne.

3.4.3 Experimental procedures with compound characterization data



Trans and *cis*-4-(2-(2-methyl-1,3-dioxolan-2-yl)ethyl)-3-methylene-5-(phenylethynyl) dihydrofuran-2(3H)-one (**3.38a,b**). A 2 mL vial equipped with a stir bar and

cap pierced with a nitrogen inlet needle was charged with a solution of *Z/E* (2.8: 1) allylboronate **3.37** (43 mg, 0.13 mmol, 1 equiv) in toluene (0.7 mL) followed by a solution of 3-phenylpropionaldehyde (33 mg, 0.25 mmol, 2 equiv) in toluene (0.3 mL). The vial was lowered into a preheated oil bath (70 °C) and stirred for 6 d. The solution was cooled to RT and quenched by a 9:1 by volume solution of saturated ammonium chloride and ammonium hydroxide (7 mL). The contents were transferred to a separatory funnel and extracted with EtOAc (3 x 8 mL). The combined organics were dried over MgSO₄, gravity filtered, and concentrated using reduced pressure rotary evaporation. The crude material was purified by silica gel flash column chromatography (gradient of 10-20% ethyl acetate in hexanes) to afford 18 mg of *trans*-lactone **3.38a**, 9 mg of a mixture of *trans*- and *cis*-lactones **3.38a,b** (1 : 1.3), and 6 mg of a mixture of *trans*- and *cis*-lactones **3.38a,b** (1 : 3.0) in an overall 85% yield, as clear oils. *Cis*- and *trans*-configurations were determined by comparison to previous literature, where an X-ray was obtained for a *trans*-lactone compound.⁴²

Data for 3.38a,b

¹H NMR *Trans*-**3.38a** (400 MHz, CDCl₃): 7.45-7.36 (m, 2H), 7.35-7.31 (m, 3H), 6.35 (d, *J* = 2.4 Hz, 1H), 5.69 (d, *J* = 2.4 Hz, 1H), 4.98 (d, *J* = 5.2 Hz, 1H), 4.00-3.91 (m, 4H), 3.20-3.19 (m, 1H), 1.90-1.79 (m, 4H), 1.34 (s, 3H) ppm;
Cis-**3.38b** (500 MHz, CDCl₃): 7.46-7.44 (m, 2H), 7.35-7.32 (m, 3H), 6.33 (d, *J* = 3.0 Hz, 1H), 5.65 (d, *J* = 3.0 Hz, 1H), 5.48 (d, *J* = 8.0 Hz, 1H), 3.96-3.90 (m, 4H),

3.24-3.17 (m, 1H), 2.01-1.94 (m, 2H), 1.92-1.83 (m, 1H), 1.81-1.76 (m, 1H), 1.34 (s, 3H) ppm;

Impurities seen at 1.55, 1.25, 0.88 ppm.

¹³C NMR *Trans*-**3.38a** (100 MHz, CDCl₃): 169.4, 137.7, 132.0 (2C), 129.3, 128.5 (2C), 123.3, 121.7, 109.5, 88.0, 85.2, 72.5, 65.0, 64.9, 47.0, 35.8, 27.5, 24.1 ppm;

Cis-**3.38b** (125 MHz, CDCl₃): 169.7, 137.7, 132.0 (2C), 129.3, 128.5 (2C), 122.5, 121.7, 109.7, 89.9, 82.3, 71.6, 64.9, 64.8, 43.3, 36.1, 24.5, 23.9 ppm;

Impurities seen at 104.5, 22.8, 14.3 ppm.

IR (thin film)

2981, 2930, 2884, 2233, 1771, 1491, 1444, 1264, 1132, 1064, 759, 692 cm⁻¹;

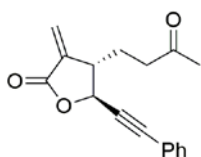
HRMS (FTMS + p ESI Full ms)

[M+H]⁺ calcd for C₁₉H₂₁O₄, 313.1434; found, 313.1433;

TLC *Trans*-**3.38a**: R_f = 0.25 (30% ethyl acetate in hexanes)

Cis-**3.38b**: R_f = 0.18 (30% ethyl acetate in hexanes)

Silica gel, UV



***Trans*-3-methylene-4-(3-oxobutyl)-5-(phenylethynyl)dihydrofuran-2(3H)-one (3.39)**. A 2 mL vial equipped with stir bar and cap pierced with a nitrogen

inlet needle was charged with pyridinium *p*-toluenesulfonate (7 mg, 0.029 mmol, 0.5 equiv), followed by dioxolane *trans*-**S2a** (18 mg, 0.058 mmol, 1 equiv) dissolved in acetone (1 mL). The vial was lowered into a preheated oil bath (60 °C) and stirred for 15 h. When the reaction was complete, as evidenced by TLC, the oil bath was removed and the vial cooled to RT. The reaction was diluted with EtOAc (4 mL). The contents were transferred to a separatory funnel, and washed with water (2 x 6 mL) followed by brine (6 mL). The organics

were dried over MgSO₄, gravity filtered, and concentrated under reduced pressure rotary evaporation. The crude residue was purified by silica gel flash column chromatography (20% EtOAc in hexanes) to afford 12 mg of **3.39** in 77% yield as a colorless oil.

Data for 3.39

¹H NMR (400 MHz, CDCl₃)

7.45-7.42 (m, 2H), 7.40-7.31 (m, 3H), 6.36 (d, *J* = 2.8 Hz, 1H), 5.69 (d, *J* = 2.4 Hz, 1H), 4.94 (d, *J* = 5.6 Hz, 1H), 3.24-3.19 (m, 1H), 2.74-2.64 (m, 2H), 2.17 (s, 3H), 2.16-2.07 (m, 1H), 1.94-1.84 (m, 1H) ppm;

¹³C NMR (100 MHz, CDCl₃)

207.0, 169.1, 137.4, 132.0 (2C), 129.4, 128.6 (2C), 123.3, 121.5, 88.3, 85.0, 72.4, 46.2, 39.7, 30.3, 26.3 ppm;

IR (thin film)

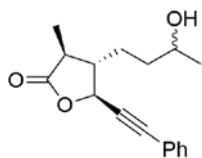
2921, 2852, 2233, 1769, 1714, 1491, 1444, 1408, 1364, 1268, 1130, 985, 759, 691 cm⁻¹;

HRMS (FTMS + p ESI Full ms)

[M+H]⁺ calcd for C₁₇H₁₇O₃, 269.1172; found, 296.1168;

TLC R_f = 0.22 (30% EtOAc in hexanes)

Silica gel, UV



4-(3-Hydroxybutyl)-3-methyl-5-(phenylethynyl)dihydrofuran-2(3H)-one

(3.40). A 10 mL, single-necked, round-bottomed flask equipped with a stir bar and a septum pierced with a needle was charged with ketone **3.39** (52 mg, 0.19

mmol, 1 equiv), dissolved in methanol (2.5 mL). The solution was cooled in an ice bath to 0 °C. Sodium borohydride (11 mg, 0.29 mmol, 1.5 equiv) was added in a single portion and the

reaction was stirred at 0 °C for 2 h, until complete as evidenced by TLC. The ice bath was removed and the reaction was quenched by adding 5% AcOH in water solution (6 mL). The reaction contents were transferred to a separatory funnel; the aqueous layer was separated and extracted with Et₂O (3 x 8 mL). The combined organic layers were washed with saturated NaHCO₃ (10 mL) and brine (10 mL), dried over MgSO₄, gravity filtered, and concentrated using reduced pressure rotary evaporation. The crude material was purified by silica gel flash column chromatography (gradient of 30-40% EtOAc in hexanes) to afford 41 mg of alcohol **3.40** (76% yield) as a colorless oil. The product was obtained as a 1:1 mixture of diastereomers that were inseparable by column chromatography.

Data for **3.40**

¹H NMR (600 MHz, CDCl₃)

7.47-7.42 (m, 2H), 7.38-7.30 (m, 3H), 4.82 (d, *J* = 9.0 Hz, 1H), 3.90-3.83 (m, 1H), 2.34 (dq, *J* = 10.8, 6.6 Hz, 1 H), 2.33-2.24 (m, 1H), 1.92-1.85 (m, 0.5H)*, 1.81-1.58 (m, 3.5 H), 1.35 (d, *J* = 6.6 Hz, 1.5H), 1.34 (d, *J* = 6.6 Hz, 1.5H)*, 1.24 (d, *J* = 7.2 Hz, 1.5H), 1.23 (d, *J* = 7.2 Hz, 1.5H)* ppm

Trace impurities are observed at 6.4, 5.7, 5.0, 4.7, 3.0, 2.1 ppm.

¹³C NMR (100 MHz, CDCl₃)

177.8, 131.9 (2C), 129.2, 128.6 (2C), 121.8, 88.0, 85.00, 84.97*, 73.02, 73.01*, 68.1, 67.8*, 51.0, 50.8*, 41.3, 36.6, 36.4*, 28.3, 28.1*, 24.0, 23.9*, 14.6, 14.5* ppm;

* Discernable signal for 1 of 2 diastereomers

IR (thin film)

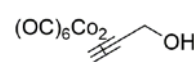
3430, 3059, 2969, 2934, 2360, 2232, 1780, 1491, 1456, 1331, 1166, 992, 759, 692
cm⁻¹;

HRMS (FTMS + p ESI Full ms)

[M+H]⁺ calcd for C₁₇H₂₁O₃, 273.1485; found, 273.1468;

TLC R_f = 0.24 (40% EtOAc in hexanes)

Silica gel, UV, potassium permanganate

 **Dicobalt hexacarbonyl complexed propargyl alcohol 3.30a.**⁹⁴ Followed general procedure 3A: Co₂(CO)₈ (793 mg, 2.3 mmol, 1.3 equiv), DCM (1.5 mL), propargyl alcohol (0.10 mL, 1.8 mmol, 1 equiv), dissolved in DCM (2.5 mL). The reaction was stirred for 2 h. The silica gel flash column chromatography was run with a gradient of 10-20% EtOAc in hexanes to afford 615 mg of Co₂(CO)₆-propargyl alcohol **3.30a** in quantitative yield, as a dark red solid.

Data for 3.30a

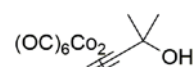
MP 48-52 °C

¹H NMR (300 MHz, CDCl₃)

6.08 (s, 1H), 4.81 (d, *J* = 6.0 Hz, 2H), 1.79 (t, *J* = 6.0 Hz, 1H) ppm;

TLC R_f = 0.28 (10% EtOAc in hexanes)

Silica gel, visible (red)

 **Dicobalt hexacarbonyl complexed 2-methyl-3-butyn-2-ol (3.S1).**⁹⁴ Followed general procedure 3A: Co₂(CO)₈ (1.37 g, 4.0 mmol, 1.0 equiv), DCM (15 mL), 2-methyl-3-butyn-2-ol (344 mg, 4.0 mmol, 1 equiv), dissolved in DCM (5 mL). The reaction was stirred for 2 h. The silica gel flash column chromatography was run with a gradient of 10-30% EtOAc in hexanes to afford 1.36 g of Co₂(CO)₆-2-methyl-3-butyn-2-ol **3.S1** in 92% yield, as a red solid.

Data for 3.S1

MP 37.9-40.1 °C

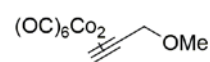
¹H NMR (300 MHz, CDCl₃)

6.03 (s, 1H), 1.71 (s, 1H), 1.59 (s, 6H) ppm;

Impurities observed at 1.54, 1.27, 0.88 ppm

TLC R_f = 0.26 (20% diethyl ether in hexanes)

Silica gel, visible (red)

 **Dicobalt hexacarbonyl complexed methyl propargyl ether 3.30c.** Followed general procedure 3A: Co₂(CO)₈ (195 mg, 0.57 mmol, 1 equiv), DCM (1.5 mL), methyl propargyl (40 mg, 0.57 mmol, 1 equiv), dissolved in DCM (3.0 mL). The reaction was stirred for 1.5 h. The silica gel flash column chromatography was run with a gradient of 0-2.5% Et₂O in hexanes to afford 94 mg of **3.30c** in 45% yield, as a dark red oil. Drying under high vacuum was not performed due to volatility.

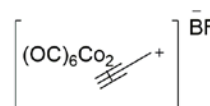
Data for 3.30c

¹H NMR (300 MHz, CDCl₃)

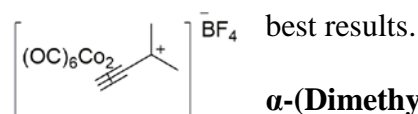
6.06 (s, 1H), 4.60 (s, 2H), 3.49 (s, 3H) ppm;

TLC R_f = 0.59 (10% Et₂O in hexanes)

Silica gel, visible (red)

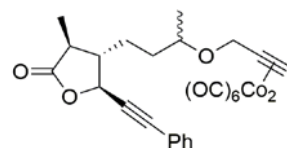
 **α-(Ethynyl)dicobalt hexacarbonyl carbonium tetrafluoroborate salt 3.30d.**⁹⁴ Follows General procedure 3B: Co₂(CO)₆-propargyl alcohol (500 mg, 1.46 mmol, 1 equiv), Et₂O (5 mL), HBF₄ (356 mg of a 54% by weight soln in Et₂O, 2.19 mmol, 1.5 equiv). The reaction was diluted with Et₂O (20 mL) prior to filtration and drying

which afforded 601 mg of salt **3.30d** in 60% yield as a red solid. Due to sensitivity to water and air, the salt was stored in the glove box and used within 24 h of isolation for



α -(Dimethylethynyl)dicobalt hexacarbonyl carbonium tetrafluoroborate

salt 3.74.⁹⁴ Follows General procedure 3B: $\text{Co}_2(\text{CO})_6$ -2-methyl-3-butyn-2-ol **3.S1** (774 mg, 2.09 mmol, 1 equiv), Et_2O (10 mL), HBF_4 (509 mg of a 54% by weight in Et_2O , 3.14 mmol, 1.5 equiv). The reaction was diluted with Et_2O (10 mL) prior to filtration and drying which afforded 558 mg of salt **3.74** in 61% yield as a red solid. Due to sensitivity to water and air, the salt was stored in the glove box and used within 24 h of isolation for best results.



Dicobalt hexacarbonyl complexed 3-methyl-5-(phenylethynyl)-4-(3-(prop-2-yn-1-yloxy)butyl)dihydrofuran-2(3H)-one (3.42). Method A:

Follows general procedure 3C.1: $\text{Co}_2(\text{CO})_6$ -propargyl alcohol complex **3.30a** (25 mg, 0.073 mmol, 2 equiv), alcohol **3.40** (10 mg, 0.037 mmol, 1 equiv), DCM (0.75 mL), and $\text{BF}_3 \cdot \text{OEt}_2$ (11.6 μL , 0.93 mmol, 2.5 equiv) The reaction stirred for 4 h. The crude residue was purified by silica gel flash column chromatography (gradient of 5-10% EtOAc in hexanes) to afford 12 mg of **3.42** in 55% yield as a dark red/brown oil. **Method B:** Follows general procedure 3C.2: propargyl alcohol (3.7 μL , 0.064 mmol, 2.2 equiv), DCM (0.36 mL), $\text{Co}_2(\text{CO})_8$ (20 mg, 0.058 mmol, 2 equiv), alcohol **3.40** (8 mg, 0.029 mmol, 1 equiv), dissolved in DCM (0.25 mL), and $\text{BF}_3 \cdot \text{OEt}_2$ (9.1 μL , 0.073 mmol, 2.5 equiv). The reaction stirred for 3.5 h. The crude residue was purified by silica gel flash column chromatography (gradient of 5-10% EtOAc in hexanes) to afford 10 mg of **3.42** in 60% yield as a dark red/brown oil. The product was a 1:1 mixture of diastereomers that were inseparable by column chromatography.

Data for **3.42**

¹H NMR (500 MHz, CDCl₃)

7.46-7.44 (m, 2H), 7.37-7.33 (m, 3H), 6.01 (d, *J* = 4.5 Hz, 1H), 4.79 (d, *J* = 9.0 Hz, 1H), 4.69 (dd, *J* = 13.0, 4.5 Hz, 1 H), 4.51 (d, *J* = 13.0, 1H), 3.71-3.64 (m, 1H), 2.34-2.19 (m, 2H), 1.95-1.87 (m, 0.5H)*, 1.80-1.61 (m, 3.5H), 1.33 (d, *J* = 6.8 Hz, 1.5H), 1.32 (d, *J* = 6.8 Hz, 1.5H)*, 1.24 (d, *J* = 6.3 Hz, 1.5H), 1.23 (d, *J* = 6.3 Hz, 1.5H)* ppm;

* Discernable signal for one of two diastereomers

¹³C NMR (125 MHz, CDCl₃)

199.8 (6C), 177.9, 131.9 (2C), 129.2, 128.5 (2C), 121.9, 92.7, 87.9, 85.1, 75.2, 75.0*, 73.1, 71.3, 68.6, 51.2, 51.0*, 41.3, 34.5, 34.3*, 27.8, 27.5*, 19.3, 14.6, 14.4* ppm;

IR (thin film)

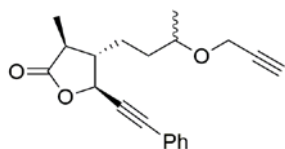
2971, 2934, 2094, 2052, 2022, 1784, 1491, 1456, 1377, 1327, 1164, 1086, 992, 758, 691 cm⁻¹;

HRMS (FTMS + p ESI Full ms)

[M+Na]⁺ calcd for C₂₆H₂₂O₉Co₂Na, 618.9820; found, 618.9807;

TLC R_f = 0.47 (20% ethyl acetate in hexanes)

Silica gel, visible, UV



3-Methyl-5-(phenylethynyl)-4-(3-(prop-2-yn-1-

yloxy)butyl)dihydrofuran-2(3H)-one (3.44).

Follows general

procedure 3D: cobalt complex **3.42** (15 mg, 0.025 mmol, 1 equiv),

acetone (3.0 mL), and CAN (69 mg, 0.13 mmol, 5 equiv) The reaction stirred for 30 min. The crude residue was purified by silica gel flash column chromatography (15% EtOAc in hexanes)

to afford 8 mg of alkyne **9** in 97% yield as a clear oil. The product was a 1:1 mixture of diastereomers that were inseparable by column chromatography.

Data for **9**

¹H NMR (400 MHz, CDCl₃)

7.46-7.43 (m, 2H), 7.36-7.33 (m, 3H), 4.83 (d, *J* = 8.8 Hz, 1H), 4.22 (dd, *J* = 15.6, 2.4 Hz, 0.5 H), 4.21 (dd, *J* = 15.6, 2.4 Hz, 0.5 H)*, 4.122 (dd, *J* = 15.6, 2.4 Hz, 0.5H), 4.115 (dd, *J* = 15.6, 2.4 Hz, 0.5H)*, 3.74-3.66 (m, 1H), 2.394 (t, *J* = 2.4 Hz, 0.5H), 2.387 (t, *J* = 2.4 Hz, 0.5H)*, 2.33-2.31 (m, 2H), 1.92-1.83 (m, 0.5H)*, 1.77-1.67 (m 3.5H), 1.35 (d, *J* = 6.8 Hz, 1.5H), 1.34 (d, *J* = 6.8 Hz, 1.5H)*, 1.19 (d, *J* = 6.0 Hz, 1.5H), 1.17 (d, *J* = 6.0 Hz, 1.5H)* ppm;

¹³C NMR (100 MHz, CDCl₃)

177.9, 131.93 (2C), 131.91 (2C)*, 129.2, 128.6 (2C), 121.8, 87.9, 85.0, 80.4, 74.1, 73.7, 73.1, 55.8, 55.7*, 51.0, 50.6*, 41.3, 34.2, 19.2, 14.7, 14.5* ppm;

* Discernable signal for one of two diastereomers

IR (thin film)

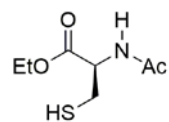
3291, 2924, 2853, 2232, 1780, 1491, 1457, 1166, 1076, 992, 759, 692 cm⁻¹;

HRMS (FTMS + p ESI Full ms)

[M+H]⁺ calcd for C₂₀H₂₃O₃, 311.1642; found, 311.1631;

TLC R_f = 0.50 (30% ethyl acetate in hexanes)

Silica gel, UV active



N-acetyl-L-cysteine ethyl ester (3.49a). Prepared in an analogous manner to that reported for synthesis of N-acetyl-L-cysteine methyl ester.¹⁰⁵ To a flame-dried,

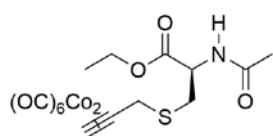
single-necked, 50 mL, round-bottomed flask, equipped with a stir bar and septum pierced with a

N₂ inlet needle was added acetonitrile (25 mL) and L-cysteine ethyl ester hydrochloride (**3.48**, 500 mg, 2.70 mmol, 1.1 equiv). The flask was cooled to 0 °C on an ice/water bath. DIEA (0.43 mL, 2.45 mmol, 1 equiv) was added, followed by acetyl chloride (0.17 mL, 2.45 mmol, 1 equiv) and the reaction was stirred for 30 min. The reaction was quenched by addition of saturated NH₄Cl (20 mL). The mixture was transferred to a separatory funnel and the aqueous was extracted with EtOAc (3 x 20 mL). The combined organics were washed with saturated NaHCO₃ (15 mL) and brine (15 mL), dried over sodium sulfate, filtered, and concentrated using reduced pressure rotary evaporation. The crude NMR showed a small amount of disulfide byproduct. The crude residue was purified by silica gel flash column chromatography (60% EtOAc in hexanes) to afford the title compound (153 mg, 33%). Characterization data matches that previously reported.¹¹⁴

Data for 3.49a.

¹H NMR (400 MHz, CDCl₃)

6.35 (bs, 1H), 4.87 (ddd, *J* = 7.6, 4.0, 4.0 Hz, 1H), 4.32-4.19 (m, 2H), 3.03, (dd, *J* = 8.8, 4.0 Hz, 2H), 2.09-2.04 (m, 1H), 2.07 (s, 3H), 1.30 (t, *J* = 7.2 Hz, 3H) ppm;



Dicobalt octacarbonyl complexed N-acetyl-S-(prop-2-yn-1-yl)cysteine ethyl ester (3.50a). Followed general procedure 3C.2: Co₂(CO)₈ (107 mg,

0.31 mmol), propargyl alcohol (18 mg, 0.314 mmol) dissolved in DCM (1.5 mL), N-acetyl-L-cysteine ethyl ester (**3.49a**)^{105, 114} (30 mg, 0.16 mmol) in DCM (1.5 mL), and BF₃•OEt₂ (49 μL, 0.39 mmol). The reaction was stirred for 2 h. The crude residue was purified by silica gel flash column chromatography (gradient of 10-30% EtOAc in hexanes) to yield 70 mg of **13c** in 86% yield, as a red oil.

Data for 3.50a

¹H NMR (300 MHz, CDCl₃)
6.31 (d, *J* = 4.5 Hz, 1H), 6.14 (s, 1H), 4.87-4.85 (m, 1H), 4.25-4.23 (m, 2H), 4.02-3.91 (m, 2H), 3.19 (dd, *J* = 13.5, 4.4 Hz, 1H), 3.06 (dd, *J* = 13.8, 4.7 Hz, 1H), 2.03 (s, 3H), 1.30 (t, *J* = 6.9 Hz, 3H) ppm;

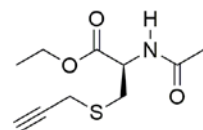
¹³C NMR (100 MHz, CDCl₃)
199.5 (6 C), 170.8, 170.0, 92.0, 73.4, 62.2, 52.2, 36.8, 34.7, 23.3, 14.3 ppm;

IR (thin film)
3295, 2984, 2093, 2052, 2020, 1742, 1655, 1543, 1374, 1208, 1032 cm⁻¹;

HRMS (FTMS + p ESI Full ms)
[M+Na]⁺ calcd for C₁₆H₁₅O₉NC₂NaS, 537.9024; found, 537.9035;

TLC R_f = 0.55 (50% ethyl acetate in hexanes)

Silica gel, visible, UV



***N*-acetyl-*S*-(prop-2-yn-1-yl)cysteine ethyl ester (3.51a)**. Followed general procedure 3D: Co₂(CO)₆-alkyne **3.50a** (23 mg, 0.045 mmol), acetone (4.0 mL), and CAN (99 mg, 0.18 mmol). The reaction was complete after 10 min of stirring. The work-up afforded 9 mg of alkyne **3.51a** in 83% yield as a colorless oil. Further purification was not performed.

Data for 3.51a

¹H NMR (500 MHz, CDCl₃)
6.42 (bs, 1H), 4.86 (dt, *J* = 7.5, 5.0 Hz, 1H), 4.25 (q, *J* = 7.0 Hz, 2H), 3.31 (dd, *J* = 17.0, 2.5 Hz, 1H), 3.25-3.21 (m, 2H), 3.14 (dd, *J* = 14.3, 5.3 Hz, 1H), 2.30 (t, *J* = 2.5 Hz, 1H), 2.08 (s, 3H), 1.31 (t, *J* = 7.0 Hz, 3H) ppm;

¹³C NMR (125 MHz, CDCl₃)

170.9, 170.3, 79.4, 72.1, 62.2, 51.9, 33.9, 23.3, 20.0, 14.3 ppm;

Impurity present at 29.8 ppm

IR (thin film)

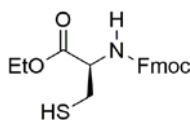
3287, 2919, 2850, 2361, 1739, 1660, 1539, 1374, 1213, 1028 cm⁻¹;

HRMS (FTMS + p ESI Full ms)

[M+H]⁺ calcd for C₁₀H₁₆O₃NS, 230.0845; found, 230.0846;

TLC R_f = 0.23 (50% ethyl acetate in hexanes)

Silica gel, potassium permanganate



***N*-Fluorenylmoethyloxycarbonyl-L-cysteine ethyl ester (3.49b)**. A flame-

dried, 15 mL, single-necked, round-bottomed flask equipped with a stir bar and a septum, pierced with an inlet needle was charged with L-cysteine ethyl ester hydrochloride salt (100 mg, 0.54 mmol, 1.1 equiv) and acetonitrile (2 mL). The solution was cooled in an ice bath to 0 °C. *N,N*-Diisopropylethylamine (35 μL, 0.49 mmol, 1 equiv) was added to the solution followed by *N*-(9-Fluorenyl-methoxycarbonyloxy) succinimide (FMoc-OSu) (165 mg, 0.49 mmol, 1 equiv). The reaction was slowly warmed to rt and stirred overnight (14 h). The solution was quenched by addition of saturated NH₄Cl. The flask contents were transferred to a separatory funnel; the aqueous layer was separated and extracted with ethyl acetate (3 x 10 mL). The combined organics were washed with saturated NaHCO₃ (15 mL) and brine (15 mL), dried over MgSO₄, gravity filtered, and concentrated under reduced pressure rotary evaporation. The crude material was purified by silica gel flash column chromatography (gradient of 10-20% EtOAc in hexanes) to afford 120 mg of **3.49b** in 66% yield as a white solid.

Data for 3.49b

MP 119-121 °C

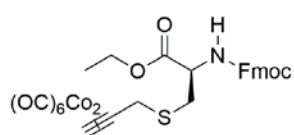
¹H NMR (400 MHz, CDCl₃)
7.77 (d, *J* = 7.6 Hz, 2H), 7.61 (d, *J* = 7.2 Hz, 2H), 7.41 (t, *J* = 7.4 Hz, 2H), 7.34 (app tt, *J* = 7.4, 1.4 Hz, 2H), 5.69 (d, *J* = 7.2 Hz, 1H), 4.66-4.63 (m, 1H), 4.47-4.40 (m, 2H), 4.30-4.23 (m, 3H), 3.03-3.00 (m, 2H), 1.36 (t, *J* = 8.8 Hz, 1H), 1.31 (t, *J* = 7.2 Hz, 3H) ppm;

¹³C NMR (100 MHz, CDCl₃)
170.1, 155.8, 144.0, 143.8, 141.49, 141.46, 127.9 (2 C), 127.2 (2 C), 125.24, 125.19, 120.18, 120.16, 67.2, 62.2, 55.3, 47.3, 27.3, 14.4 ppm;

IR (thin film)
3337, 3065, 2981, 1723, 1513, 1450, 1339, 1204, 1035, 759, 741 cm⁻¹.

HRMS (FTMS + p ESI Full ms)
[M+H]⁺ calcd for C₂₀H₂₂O₄NS, 372.1264; found, 372.1267;

TLC R_f = 0.28 (20% ethyl acetate in hexanes)
Silica gel, UV



Dicobalt hexacarbonyl complexed N-(((9H-fluoren-9-yl)methoxy)carbonyl)-S-(prop-2-yn-1-yl)-L-cysteine ethyl ester

(3.50b). Method A: Followed general procedure 3C.2: (55 mg, 0.16 mmol), propargyl alcohol (9 mg, 0.16 mmol), DCM (1.1 mL), *N*-Fmoc-L-cysteine ethyl ester (**3.49b**) (30.0 mg, 0.081 mmol) dissolved in DCM (0.6 mL), and BF₃•OEt₂ (25 Co₂(CO)₈ μL, 0.20 mmol). The reaction was stirred for 45 min. The crude residue was purified by silica gel flash column chromatography (gradient of 5-20% EtOAc in hexanes) to afford 40 mg of **3.50b** in 71% yield, as a red oil.
Method B: Followed general procedure 3C.1: Co₂(CO)₆-methyl propargyl ether **3.30c** (45 mg, 0.13 mmol), DCM (0.6 mL), *N*-Fmoc-L-cysteine ethyl ester (**3.49b**) (24 mg, 0.063 mmol)

dissolved in dichloromethane (0.6 mL), and boron trifluoride diethyl etherate (20 μ L, 0.156 mmol). The reaction was stirred for 2 h. The crude residue was purified by silica gel flash column chromatography (gradient of 10-20% diethyl ether in hexanes) to afford 29 mg of **3.50b** in 67% yield.

Data for 3.50b

$^1\text{H NMR}$ (400 MHz, CDCl_3)

7.77 (d, $J = 7.6$ Hz, 2H), 7.60 (d, $J = 7.6$ Hz, 2H), 7.41 (t, $J = 7.6$ Hz, 2H), 7.32 (t, $J = 7.6$ Hz, 2H), 6.13 (s, 1H), 5.66 (d, $J = 7.6$ Hz, 1H), 4.66 (dt, $J = 7.6, 5.0$ Hz, 1H), 4.44-4.35 (m, 2H), 4.28-4.22 (m, 3H), 3.99 (s, 2H), 3.19 (dd, $J = 14.0, 4.8$ Hz, 1H), 3.09 (dd, $J = 14.0, 5.2$ Hz, 1H), 1.32 (t, $J = 7.2$ Hz, 3H) ppm;

$^{13}\text{C NMR}$ (125 MHz, CDCl_3)

199.5 (6 C), 170.7, 155.9, 143.93, 143.86, 141.5 (2 C), 127.9 (2 C), 127.2 (2 C), 125.2 (2 C), 120.2 (2 C), 92.1, 73.4, 67.5, 62.3, 53.9, 47.3, 36.9, 35.1, 14.3 ppm;

IR (thin film)

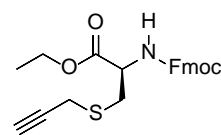
3345, 3070, 2923, 2094, 2053, 2023, 1726, 1507, 1450, 1339, 1204, 1052, 759, 741 cm^{-1} .

HRMS (FTMS + p ESI Full ms)

$[\text{M}+\text{H}]^+$ calcd for $\text{C}_{29}\text{H}_{24}\text{O}_{10}\text{NCO}_2\text{S}$, 695.9779; found, 695.9745;

TLC $R_f = 0.36$ (20% ethyl acetate in hexanes)

Silica gel, visible, UV



Ethyl N-(((9H-fluoren-9-yl)methoxy)carbonyl)-S-(prop-2-yn-1-yl)-L-cysteinate (3.51b). Followed general procedure D: $\text{Co}_2(\text{CO})_6$ -alkyne **3.50b**

(22 mg, 0.032 mmol), acetone (3.5 mL), and CAN (69 mg, 0.13 mmol). The reaction was

complete after 10 min of stirring. The work-up afforded 12 mg of alkyne **3.51b** in 92% yield as an off white oil. Further purification was not performed.

Data for 3.51b

¹H NMR (400 MHz, CDCl₃)

7.77 (d, *J* = 7.4 Hz, 2H), 7.61 (d, *J* = 7.4 Hz, 2H), 7.41 (t, *J* = 7.4 Hz, 2H), 7.32 (app tt, *J* = 7.4, 1.2 Hz, 2H), 5.64 (d, *J* = 7.6 Hz, 1H), 4.65 (dt, *J* = 8.0, 5.2 Hz, 1H), 4.46-4.38 (m, 2H), 4.28-4.23 (m, 3H), 3.32-3.22 (m, 2H), 3.22 (dd, *J* = 14.4, 4.8 Hz, 1H), 3.14 (dd, *J* = 14.0, 5.6 Hz, 1H), 2.26 (t, *J* = 2.6 Hz, 1H), 1.31 (t, *J* = 7.2 Hz, 3H) ppm;

Impurities observed at 1.2, 0.9 ppm.

¹³C NMR (125 MHz, CDCl₃)

170.8, 155.9, 144.0, 143.9, 141.5 (2 C), 127.9 (2 C), 127.2 (2 C), 125.2 (2 C), 120.2 (2 C), 79.4, 72.1, 67.3, 62.2, 53.7, 47.3, 34.0, 20.1, 14.3 ppm;

Impurity observed at 29.8 ppm.

IR (thin film)

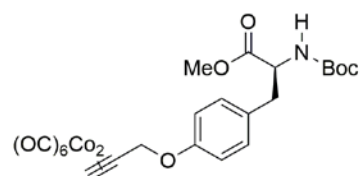
3291, 2924, 1723, 1517, 1450, 1339, 1210, 1051, 760, 741 cm⁻¹;

HRMS (FTMS + p ESI Full ms)

[M+H]⁺ calcd for C₂₃H₂₄O₄NS, 410.1421; found, 410.1424;

TLC R_f = 0.26 (20% ethyl acetate in hexanes)

Silica gel, UV



Co₂(CO)₆-N-[(1,1-dimethylethoxy)carbonyl]-O-(prop-2-yn-1-yl)-L-tyrosine methyl ester (3.56a). Method A: Follows general procedure 3C.2: propargyl alcohol (11 mg, 0.20 mmol), DCM (1.1

mL), $\text{Co}_2(\text{CO})_8$ (69 mg, 0.20 mmol), *N*-Boc-L-tyrosine methyl ester **3.55a** (30 mg, 0.10 mmol)¹⁰⁶ and $\text{BF}_3 \cdot \text{OEt}_2$ (32 μL , 0.26 mmol). The reaction stirred for 2 h. Both **3.56a** and **3.57** were observed by TLC. The crude residue was purified by silica gel flash column chromatography (gradient of 5-20% EtOAc in hexanes) to afford 20 mg of **3.56a** in 32% yield as a dark red/brown oil. Byproduct **3.57** was only isolated in trace amounts. The ^1H NMR of this sample of **S6** is included in the spectra section. Further characterization was not obtained due to small amounts.

This experiment was also performed by John Widen who consistently obtained **3.56a** in 45% yield.

Method B: Follows general procedure 3C.2: methyl propargyl ether (19 mg, 0.27 mmol), dichloromethane (2.0 mL), $\text{Co}_2(\text{CO})_8$ (93 mg, 0.27 mmol), *N*-Boc-L-tyrosine methyl ester **3.55a** (40 mg, 0.14 mmol) and $\text{BF}_3 \cdot \text{OEt}_2$ (42 μL , 0.34 mmol). The reaction stirred for 3 h. Both **3.56a** and **3.57** were observed by TLC. The crude residue was purified by silica gel flash column chromatography (gradient of 15-30% ethyl acetate in hexanes) to afford 19 mg of **3.56a** in 23% yield as a dark red/brown oil. Large amounts of baseline material was observed.

Data for **3.56a** (obtained by John Widen)

^1H NMR (500 MHz, CDCl_3):
7.05 (d, $J = 7.0$ Hz, 2H), 6.88 (d, $J = 8.0$ Hz, 2H), 6.05 (s, 1H), 5.15 (s, 2H), 4.95 (bs, 1H), 4.55 (bs, 1H), 3.72 (s, 3H), 3.03 (m, 2H), 1.42 (s, 9H) ppm

^{13}C NMR (125 MHz, CDCl_3):
199.3 (6 C), 172.4, 157.3, 155.1, 130.4 (2C), 128.6, 114.7 (2C), 89.5, 79.9, 71.7, 68.2, 54.5, 52.2, 37.5, 28.3 (3 C) ppm
Impurities seen at 129.7, 124.2, 28.8, 26.7

IR (thin film)
3445, 3368, 2979, 2956, 2929, 2097, 2056, 1746, 1716, 1612, 1585, 1510, 1445,
1392, 1367, 1244, 1216, 1172, 1111, 1059, 1018, 839, 779, 519, 497 cm^{-1} ;

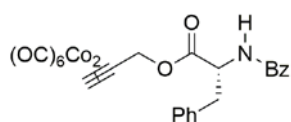
HRMS (FTMS + p ESI Full ms)
[M+Na]⁺ calc'd for C₂₄H₂₃Co₂NO₁₀Na 625.9878 m/z; found 625.9877 m/z;

TLC R_f = 0.44 (20% ethyl acetate in hexanes)
Silica gel, visible, UV

Data for 3.57 (obtained by Sarah Wells)

¹H NMR (400 MHz, CDCl₃)
6.95 (s, 1H), 6.88 (d, *J* = 8.0 Hz, 1H), 6.70-6.62 (m, 1H), 6.07 (s, 1H), 4.91-4.87
(m, 1 H), 4.79-4.71 (m, 1H), 4.58-4.49 (m, 1H), 4.10 (s, 1H), 3.72 (s, 3H), 3.08-
2.92 (m, 2H), 1.43 (s, 9H) ppm;

TLC R_f = 0.26 (20% ethyl acetate in hexanes)
Silica gel, visible, UV



Dicobalt hexacarbonyl prop-2-yn-1-yl benzoylphenylalaninate complex (3.60). Follows general procedure 3C.2: propargyl alcohol (11 mg, 0.20 mmol), DCM (1.1 mL), Co₂(CO)₈ (69 mg, 0.20 mmol), *N*-benzoyl-D-phenylalanine (**3.59**) (27 mg, 0.10 mmol, 1 equiv), dissolved in DCM (1.0 mL), and BF₃•OEt₂ (32 μ L, 0.26 mmol). The reaction stirred for 2 h. The crude residue was purified by silica gel flash column chromatography (10% EtOAc in hexanes) to afford 35 mg of **3.60** in 60% yield as a dark red oil.

Data for 3.60

¹H NMR (400 MHz, CDCl₃)

7.72-7.70 (m, 1H), 7.51 (t, $J = 7.6$ Hz, 1H), 7.42 (t, $J = 7.6$ Hz, 2H), 7.31-7.28 (m, 3H), 7.17-7.15 (m, 2H), 6.55 (d, $J = 7.2$ Hz, 1H), 6.08 (s, 2H), 5.44 (d, $J = 14.4$ Hz, 1H), 5.24 (d, $J = 14.0$ Hz, 1H), 5.18 (dt, $J = 7.6, 5.6$ Hz, 1H), 3.36 (dd, $J = 14.0, 5.6$ Hz, 1H), 3.27 (dd, $J = 14.0, 6.0$ Hz, 1H) ppm;

^{13}C NMR (125 MHz, CDCl_3)

199.1 (6C), 171.5, 166.9, 135.9, 134.0, 131.9, 129.5 (2C), 128.9 (2C), 128.8 (2C), 127.5, 127.2 (2C), 87.2, 72.4, 66.8, 53.8, 38.0 ppm;

IR (thin film)

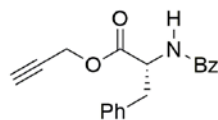
3031, 2925, 2097, 2056, 2025, 1746, 1647, 1531, 1487, 1178, 700 cm^{-1} .

HRMS (FTMS + p ESI Full ms)

$[\text{M}+\text{Na}]^+$ calcd for $\text{C}_{25}\text{H}_{17}\text{O}_9\text{NC}_2$, 615.9460; found, 615.9453;

TLC $R_f = 0.34$ (20% ethyl acetate in hexanes)

Silica gel, visible, UV



Prop-2-yn-1-yl benzoylphenylalaninate (3.61). Followed general procedure

3D: $\text{Co}_2(\text{CO})_6$ -alkyne **3.60** (20 mg, 0.034 mmol), acetone (2.5 mL), and CAN (75 mg, 0.138 mmol). The reaction was complete after 10 min of stirring. Reaction work up afforded 10 mg of pure alkyne **3.61** as a white sticky solid in 90% yield. Purification by silica gel column was not performed.

Data for 3.61

^1H NMR (400 MHz, CDCl_3)

7.72-7.70 (m, 2H), 7.53-7.47 (m, 1H), 7.45-7.41 (m, 2H), 7.32-7.26 (m, 3H), 7.19-7.17 (m, 2H), 6.53 (d, $J = 7.6$ Hz, 1H), 5.14 (dt, $J = 7.6, 5.6$ Hz, 1H), 4.82

(dd, $J = 15.6, 2.6$ Hz, 1H), 4.73 (dd, $J = 15.6, 2.6$ Hz, 1H), 3.33 (dd, $J = 13.8, 5.8$ Hz, 1H), 3.27 (dd, $J = 13.8, 5.4$ Hz, 1H), 2.54 (t, $J = 2.4$ Hz, 1H) ppm;

Impurities seen at 1.43, 1.25, 0.88 ppm.

^{13}C NMR (125 MHz, CDCl_3)

171.0, 167.0, 135.7, 134.0, 132.0, 129.6 (2C), 128.83 (2C), 128.80 (2C), 127.5, 127.2 (2C), 77.1, 75.8, 53.5, 53.0, 37.9 ppm;

IR (thin film)

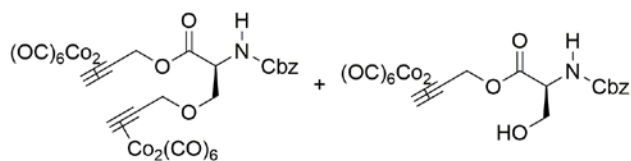
3396, 3277, 3070, 2920, 2851, 2131, 1762, 1647, 1521, 1488, 1205, 1171 cm^{-1} .

HRMS (FTMS + p ESI Full ms)

$[\text{M}+\text{H}]^+$ calcd for $\text{C}_{19}\text{H}_{17}\text{O}_3\text{N}$, 308.1281; found, 308.1282;

TLC $R_f = 0.21$ (20% ethyl acetate in hexanes)

Silica gel, UV



Dicobalt hexacarbonyl complexed prop-2-yn-1-yl N-((benzyloxy)carbonyl)-O-(prop-2-yn-1-yl)-L-serinate (3.63) and Dicobalt hexacarbonyl complexed prop-2-yn-1-yl ((benzyloxy)carbonyl)-L-serinate (3.64).

Follows general procedure C2: propargyl alcohol (23 mg, 0.42 mmol), DCM (3.5 mL), $\text{Co}_2(\text{CO})_8$ (143 mg, 0.42 mmol), *N*-benzyloxycarbonyl-L-serine **3.62** (50 mg, 0.21 mmol), additional DCM (0.7 mL), and $\text{BF}_3 \cdot \text{OEt}_2$ (65 μL , 0.52 mmol). The reaction stirred for 1.5 h. The crude residue was purified by silica gel flash column chromatography (gradient of 5-30% EtOAc in hexanes) to afford 78 mg of **3.63** in 42% yield as a dark red oil and 11 mg of **3.64** (9% yield) as a dark red oil.

Data for 3.63

^1H NMR (400 MHz, CDCl_3)

7.35 (s, 5H), 6.07 (s, 1H), 6.00 (s, 1H), 5.65 (d, $J = 8.4$ Hz, 1H), 5.37 (d, $J = 14.4$ Hz, 1H), 5.24 (d, $J = 14.4$ Hz, 1H), 5.14 (d, $J = 12.4$ Hz, 1H), 5.09 (d, $J = 12.4$ Hz, 1H), 4.68-4.65 (m, 1H), 4.63 (s, 2H), 4.16 (d, $J = 8.4$ Hz, 1H), 3.91 (d, $J = 7.2$ Hz, 1H), ppm;

^{13}C NMR (100 MHz, CDCl_3)

199.5 (6C), 199.1 (6C), 169.8, 156.1, 136.4, 128.7 (2C), 128.3 (2C), 128.1, 90.2, 87.5, 72.3, 72.1, 71.4, 70.8, 67.2, 67.0, 54.6 ppm;

IR (thin film)

3452, 3093, 2934, 2097, 2055, 1024, 1729, 1507, 1332, 1195, 1112, 1065 cm^{-1} ;

HRMS (FTMS + p ESI Full ms)

$[\text{M}+\text{Na}]^+$ calcd for $\text{C}_{29}\text{H}_{17}\text{O}_{17}\text{NCo}_4\text{Na}$, 909.7717; found, 909.7753;

TLC $R_f = 0.27$ (10% ethyl acetate in hexanes)

Silica gel, visible, UV

Data for 3.64

^1H NMR (400 MHz, CDCl_3)

7.37-7.33 (m, 5H), 6.08 (s, 1H), 5.70 (d, $J = 6.4$ Hz, 1H), 5.43 (d, $J = 14.2$ Hz, 1H), 5.33 (d, $J = 14.2$ Hz, 1H), 5.15 (d, $J = 12.0$ Hz, 1H), 5.11 (d, $J = 12.0$ Hz, 1H), 4.54 (br s, 1H), 4.11-3.92 (m, 2H), 2.05 (br s, 1H) ppm;

^{13}C NMR (125 MHz, CDCl_3)

199.1 (6C), 170.3, 156.3, 136.2, 128.7 (2C), 128.4 (2C), 128.3, 87.4, 72.4, 67.4, 66.9, 63.4, 56.2 ppm;

IR (thin film)

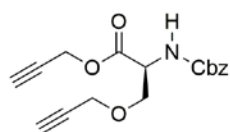
3439, 3091, 2933, 2360, 2098, 2057, 2026, 1725, 1521, 1456, 1333, 1191, 1063,
971, 698 cm⁻¹;

HRMS (FTMS + p ESI Full ms)

[M+Na]⁺ calcd for C₂₀H₁₅O₁₁NCO₂Na, 585.9201; found, 585.9205;

TLC R_f = 0.30 (30% ethyl acetate in hexanes)

Silica gel, visible, UV



Prop-2-yn-1-yl N-((benzyloxy)carbonyl)-O-(prop-2-yn-1-yl)-L-serinate

(3.66). A single-necked, 10 mL, round-bottomed flask, equipped with a stir

bar and a septum pierced with a needle was charged with the Co₂(CO)₆-dialkyne **3.63** (35 mg, 0.04 mmol, 1 equiv), dissolved in acetone (4 mL). The solution was cooled to 0° C in an ice bath. CAN (87 mg, 0.16 mmol, 4 equiv) was added to the flask in a single portion. After stirring for 10 min, the reaction was not complete as determined by TLC, and additional CAN (87 mg, 0.16 mmol, 4 equiv) was added. The reaction was stirred for 15 min. Upon completion, the reaction was diluted with distilled water (4 mL). The mixture was transferred to a separatory funnel. The aqueous layer was extracted with Et₂O (3 x 6 mL). The combined organics were dried over MgSO₄, filtered, and concentrated under reduced pressure rotary evaporation to afford 12 mg of **3.66** in 94% yield as a colorless oil. Purification of the crude material was not performed.

Data for 3.66

¹H NMR (400 MHz, CDCl₃)

7.37-7.31 (m, 5H), 5.62 (d, *J* = 8.4 Hz, 1H), 5.17-5.10 (m, 2H), 4.81-4.72 (m, 2H), 4.58 (dt, *J* = 8.4, 2.8 Hz, 1H), 4.15-4.10 (m, 2H), 4.01 (dd, *J* = 9.2, 2.8 Hz,

1H), 3.81 (dd, $J = 9.2, 2.8$ Hz, 1H), 2.50, (t, $J = 2.4$ Hz, 1H), 2.43 (t, $J = 2.4$ Hz, 1H) ppm;

Impurities present at 1.43, 1.25, 0.88 ppm

^{13}C NMR (100 MHz, CDCl_3)

169.6, 156.1, 136.3, 128.7, 128.4, 128.3, 78.8, 77.2, 75.6, 75.4, 69.5, 67.3, 58.8, 54.3, 53.3 ppm;

IR (thin film)

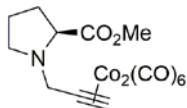
3288, 2915, 2850, 2129, 1750, 1715, 1515, 1456, 1342, 1260, 1027 cm^{-1} .

HRMS (FTMS + p ESI Full ms)

$[\text{M}+\text{H}]^+$ calcd for $\text{C}_{17}\text{H}_{18}\text{O}_5\text{N}$, 316.1180; found, 316.1181;

TLC $R_f = 0.27$ (30% ethyl acetate in hexanes)

Silica gel, UV, potassium permanganate



$\text{Co}_2(\text{CO})_6$ -*N*-propargyl-*L*-proline methyl ester (3.68). Follows general

procedure 3C.3: Tetrafluoroborate salt **3.30d** (140 mg, 0.340 mmol), DCM (5 mL), *L*-proline methyl ester **3.67** (57 mg, 0.44 mmol) dissolved in DCM (1.8 mL). The reaction stirred for 1.5 h. The crude residue was purified by silica gel flash column chromatography (gradient of 5-10% Et_2O in hexanes) to afford 75 mg of cobalt complexed alkyne **3.68** in 46% yield as a red oil.

Data for 3.68

^1H NMR (300 MHz, CDCl_3)

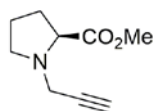
6.05 (s, 1H), 4.23 (d, $J = 15.6$ Hz, 1H), 3.97 (d, $J = 15.3$ Hz, 1H), 3.71 (s, 3H), 3.53 (dd, $J = 8.1, 5.1$ Hz, 1H), 3.23-3.14 (m, 1H), 2.71 (q, $J = 8.1$ Hz, 1H), 2.13, 1.78 (m, 4H) ppm;

¹³C NMR (100 MHz, CDCl₃)
199.9 (6C), 174.3, 91.8, 73.4, 64.2, 56.1, 52.8, 51.9, 29.4, 23.5 ppm;

IR (thin film)
2955, 2798, 2093, 2020, 1736, 1551, 1437, 1356, 1278, 1199, 1173 cm⁻¹;

HRMS (FTMS + p ESI Full ms)
[M+H]⁺ calcd for C₁₅H₁₄O₈NC₂, 453.9378; found, 453.9361;

TLC R_f = 0.37 (20% diethyl ether in hexanes)
Silica gel, UV, potassium permanganate



***N*-propargyl-L-proline methyl ester (3.69)**. Followed general procedure 3D: Co₂(CO)₆-alkyne **3.68** (20 mg, 0.044 mmol), acetone (5.0 mL), and CAN (97 mg, 0.18 mmol). After 1 h of stirring, **3.69** remained, as evidenced by proton NMR. An additional amount of ceric ammonium nitrate (10 mg, 0.018 mmol) was added and stirred for 20 min. The work-up afforded 5 mg of alkyne **3.69** in 68% yield as a colorless oil. Further purification was not performed. Characterization via ¹H NMR, ¹³C NMR, and HRMS was obtained, however, **3.69** appears to be unstable leading to decomposition and poor reproducibility of these data.

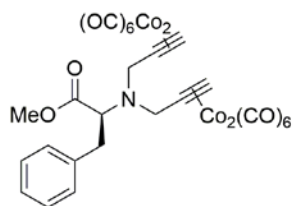
Data for 3.69

¹H NMR (400 MHz, CDCl₃)
3.74 (s, 3H), 3.61 (app t, *J* = 2.4 Hz, 2H), 3.45 (dd, *J* = 8.8, 6.8 Hz, 1H), 3.09-3.04 (m, 1H), 2.73 (td, *J* = 8.8, 7.6 Hz, 1H), 2.21 (t, *J* = 2.4 Hz, 1H), 2.19-2.11 (m, 1H), 2.03-1.76 (m, 3H) ppm;

¹³C NMR (100 MHz, CDCl₃)
174.3, 78.5, 73.3, 62.7, 52.3, 52.2, 41.3, 29.8, 23.4 ppm;
Impurity present at 30.5 ppm

HRMS (FTMS + p ESI Full ms)

$[M+H]^+$ calcd for $C_9H_{14}O_2N$, 168.1019; found, 168.1013;



Bis(dicobalthexacarbonyl) complexed *N,N*-di(prop-2-ynyl)-*L*-phenylalanine methyl ester (3.71). Follows general procedure 3C.3:

Tetrafluoroborate salt **3.30d** (46 mg, 0.11 mmol, 1 equiv), DCM (2 mL), *L*-phenyl alanine methyl ester **3.70** (20 mg, 0.11 mmol, 1 equiv) dissolved in DCM (0.3 mL). The reaction stirred for 1.5 h. The crude residue was purified by silica gel flash column chromatography (gradient of 2-20% Et₂O in hexanes) to afford 46 mg of cobalt complexed dialkyne **3.71** in 59% yield as a red oil.

Data for 3.71

¹H NMR (300 MHz, CDCl₃)

7.31-7.22 (m, 3H), 7.17 (d, $J = 7.2$ Hz, 2H), 6.10 (s, 2H), 4.41 (d, $J = 15.9$ Hz, 2H), 4.04-3.99 (m, 3H), 3.56 (s, 3H), 3.24-3.17 (m, 1H), 2.93 (dd, $J = 13.0, 4.2$ Hz, 1H) ppm;

¹³C NMR (100 MHz, CDCl₃)

199.7 (12C), 172.0, 137.3, 129.3 (2C), 128.7 (2C), 126.9, 91.1 (2C), 73.8 (2C), 64.4, 55.1 (2C), 51.3, 36.5 ppm;

IR (thin film)

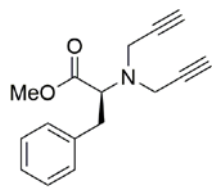
2093, 3052, 2017, 1735, 1425, 1200, 1165 cm⁻¹;

HRMS (FTMS + p ESI Full ms)

$[M+H]^+$ calcd for $C_{28}H_{18}O_{14}NC_4$, 827.8050; found, 827.8084;

TLC $R_f = 0.48$ (10% diethyl ether in hexanes)

Silica gel, UV, visible



***N,N*-di(prop-2-ynyl)-L-phenylalanine methyl ester (3.72)**. Followed general procedure 3D: $\text{Co}_2(\text{CO})_6$ -dialkyne **3.71** (21 mg, 0.025 mmol, 1 equiv), acetone (4.0 mL), and CAN (111 mg, 0.203 mmol, 8 equiv). The reaction was complete after 20 min of stirring. The crude residue was purified using silica gel flash column chromatography (gradient of 15-30% Et_2O in hexanes), which afforded 4 mg of alkyne **3.72** in 56% yield as an oil.

Data for 3.72

^1H NMR (400 MHz, CDCl_3)

7.30-7.26 (m, 2H), 7.23-7.7.18 (m, 3H), 3.75 (t, $J = 7.6$ Hz, 1H), 3.68 (d, $J = 2.4$ Hz, 4H), 3.57 (s, 3H), 3.05 (d, $J = 7.6$ Hz, 2H), 2.25 (t, $J = 2.4$ Hz, 2H) ppm;

^{13}C NMR (100 MHz, CDCl_3)

172.1, 137.5, 129.3 (2 C), 128.6 (2 C), 126.8, 79.3 (2 C), 73.1 (2 C), 65.9, 51.5, 40.1 (2 C), 36.5 ppm;

IR (thin film)

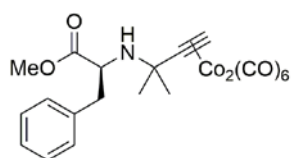
3250, 2991, 2914, 2813, 2344, 1714, 1478, 1421, 1347, 1199, 1153, 1112, 740, 692, 623 cm^{-1} ;

HRMS (FTMS + p ESI Full ms)

$[\text{M}+\text{H}]^+$ calcd for $\text{C}_{16}\text{H}_{18}\text{O}_2\text{N}$, 256.1332; found, 256.1335;

TLC $R_f = 0.37$ (20% diethyl ether in hexanes)

Silica gel, UV, potassium permanganate



$\text{Co}_2(\text{CO})_6$ -*N*-(1,1-dimethyl-3-propynyl)-L-phenylalanine methyl ester (3.S2). Follows general procedure 3C.3: Tetrafluoroborate salt **3.74** (77 mg, 0.18 mmol, 1.3 equiv), DCM (2.5 mL), L-phenylalanine methyl

ester **3.70** (24 mg, 0.14 mmol, 1 equiv) dissolved in DCM (0.5 mL). The reaction stirred for 40 min. The crude residue was purified by silica gel flash column chromatography (gradient of 5-20% Et₂O in hexanes) to afford 16 mg of cobalt complexed alkyne **3.S2** in 23% yield as a red oil.

Data for **3.S2**

¹H NMR (400 MHz, CDCl₃)

7.29-7.17 (m, 5H), 5.99 (s, 1H), 3.72 (dt, *J* = 7.6, 3.2 Hz, 1H), 3.62 (s, 3H), 2.92-2.81 (m, 2H), 1.90 (d, *J* = 8.4 Hz, 1H), 1.29 (s, 3H), 1.20 (s, 3H) ppm;

¹³C NMR (100 MHz, CDCl₃)

200.1 (6C), 176.6, 137.6, 129.6 (2C), 128.4 (2C), 126.8, 107.3, 72.2, 58.0, 56.7, 52.0, 41.9, 32.1, 30.9 ppm;

IR (thin film)

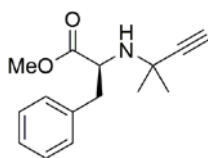
2973, 2927, 2092, 2050, 2019, 1739, 1455, 1194, 1172, 700 cm⁻¹;

HRMS (FTMS + p ESI Full ms)

[M+H]⁺ calcd for C₂₁H₂₀O₈NC₂, 531.9847; found, 531.9848;

TLC R_f = 0.35 (10% diethyl ether in hexanes)

Silica gel, Visible, UV



***N*-(1,1-dimethyl-3-propynyl)-L-phenylalanine methyl ester (**3.75**).**

Followed general procedure 3D: Co₂(CO)₆-alkyne **3.S2** (12 mg, 0.023 mmol), acetone (4.0 mL), and CAN (50 mg, 0.090 mmol). The reaction was complete after 20 min of stirring as indicated by consumption of **3.S2**, as evidenced by TLC. However, **3.75** was not visible by TLC until after the reaction work up. The crude residue was purified by silica gel flash column chromatography (10% Et₂O in hexanes) which afforded 4 mg of alkyne **3.75** in 64% yield as an colorless oil.

Data for 3.75

¹H NMR (400 MHz, CDCl₃)

7.30-7.26 (m, 2H), 7.23-7.19 (m, 3H), 3.73 (dd, *J* = 7.8, 6.4 Hz, 1H), 3.63 (s, 3H), 2.93 (dd, *J* = 13.4, 6.4 Hz, 1H), 2.84 (dd, *J* = 13.4, 7.8 Hz, 1H), 2.18 (s, 1H), 1.92 (bs, 1H), 1.31 (s, 3H), 1.19 (s, 3H) ppm;

¹³C NMR (100 MHz, CDCl₃)

176.3, 137.5, 129.6 (2C), 128.4 (2C), 126.8, 88.5, 70.1, 58.9, 51.7, 49.6, 41.4, 30.3, 29.6 ppm;

IR (thin film)

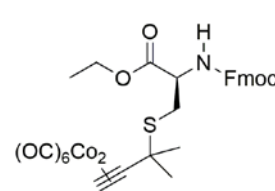
3286, 3027, 2977, 2929, 2368, 1736, 1458, 1438, 1196, 1171, 700 cm⁻¹;

HRMS (FTMS + p ESI Full ms)

[M+H]⁺ calcd for C₁₅H₂₀O₂N, 246.1489; found, 246.1478;

TLC R_f = 0.33 (20% diethyl ether in hexanes)

Silica gel, UV, potassium permanganate

 **Co₂(CO)₆-Ethyl N-(((9H-fluoren-9-yl)methoxy)carbonyl)-S-(1,1-dimethyl-3-propynyl)-L-cysteinate (3.76).** Follows general procedure 3C.3: Tetrafluoroborate salt **3.74** (62 mg, 0.14 mmol, 1.25 equiv), DCM (1.5 mL), *N*-(((9H-fluoren-9-yl)methoxy)carbonyl)-L-cysteine ethyl ester **3.49b** (42 mg, 0.11 mmol, 1 equiv) dissolved in DCM (0.8 mL). The reaction stirred for 2 h. The crude residue was purified by silica gel flash column chromatography (gradient of 15-30% Et₂O in hexanes) to afford 42 mg of **3.76** in 55% yield as a red oil.

Data for 3.76

¹H NMR (400 MHz, CDCl₃)

7.77 (d, $J = 7.6$ Hz, 2H), 7.60 (d, $J = 7.2$ Hz, 2H), 7.41 (app t, $J = 7.4$ Hz, 2H), 7.32 (app t, $J = 7.4$ Hz, 2H), 6.23 (s, 1H), 5.59 (d, $J = 7.6$ Hz, 1H), 4.71-4.66 (m, 1H), 4.39 (d, $J = 7.2$ Hz, 2H), 4.27-4.21 (m, 3H), 3.19-3.10 (m, 2H), 1.621 (s, 3H), 1.616 (s, 3H), 1.30 (t, $J = 7.2$ Hz, 3H) ppm;

^{13}C NMR (125 MHz, CDCl_3)

199.8 (6C), 170.5, 155.8, 144.0, 143.9, 141.5 (2C), 127.9 (2C), 127.2 (2C), 125.3 (2C), 120.2 (2C), 105.0, 73.1, 67.4, 62.2, 53.6, 48.9, 47.3, 32.7 (2C), 32.4, 14.3 ppm;

IR (thin film)

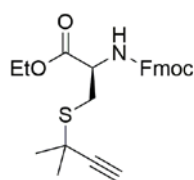
3338, 3070, 2979, 2092, 2053, 2022, 1725, 1510, 1451, 1200, 1052, 759, 740 cm^{-1} ;

HRMS (FTMS + p ESI Full ms)

$[\text{M}+\text{NH}_4]^+$ calcd for $\text{C}_{31}\text{H}_{31}\text{O}_{10}\text{N}_2\text{SCo}_2$, 741.0358; found, 741.0379;

TLC $R_f = 0.18$ (20% diethyl ether in hexanes)

Silica gel, visible, UV



***N*-(((9H-fluoren-9-yl)methoxy)carbonyl)-*S*-(1,1-dimethyl-3-propynyl)-*L*-cysteine ethyl ester (**3.77**). Followed general procedure 3D: $\text{Co}_2(\text{CO})_6$ -alkyne**

3.76 (47 mg, 0.069 mmol), acetone (6.9 mL), and CAN (152 mg, 0.28 mmol).

The reaction was complete after 15 min of stirring. The crude residue was purified by silica gel flash column chromatography (20% Et_2O in hexanes) which afforded 14 mg of alkyne **3.77** in 46% yield as a colorless oil.

Data for **3.77**

^1H NMR (400 MHz, CDCl_3)

7.77 (d, $J = 7.6$ Hz, 2H), 7.63-7.58 (m, 2H), 7.40 (t, $J = 7.4$ Hz, 2H), 7.30 (t, $J = 7.4$ Hz, 2H), 5.65 (d, $J = 8.0$ Hz, 1H), 4.69 (dt, $J = 8.0, 5.2$ Hz, 1H), 4.44-4.37 (m, 2H), 4.27-4.21 (m, 3H), 3.28-3.19 (m, 2H), 2.37 (s, 1H), 1.57 (s, 6H), 1.30 (t, $J = 7.0$ Hz, 3H) ppm;

^{13}C NMR (100 MHz, CDCl_3)

170.7, 155.9, 144.0, 143.9, 141.5, 141.4, 127.9 (2C), 127.2 (2C), 125.3 (2C), 120.1 (2C), 87.8, 70.9, 67.3, 62.1, 53.6, 47.3, 38.7, 33.2, 30.79, 30.75, 14.3 ppm;

IR (thin film)

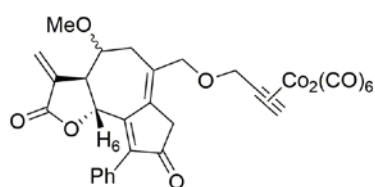
3292, 2976, 2925, 2365, 1719, 1509, 1449, 1339, 1208, 1051, 759, 740 cm^{-1} ;

HRMS (FTMS + p ESI Full ms)

$[\text{M}+\text{H}]^+$ calcd for $\text{C}_{25}\text{H}_{28}\text{O}_4\text{NS}$, 438.1734; found, 438.1725;

TLC $R_f = 0.23$ (30% diethyl ether in hexanes)

Silica gel, UV, potassium permanganate



Dicobalthexacarbonyl complexed guaianolide alkyne probe

(3.78). Follows general procedure 3C.2: propargyl alcohol (5 mg, 0.091 mmol), DCM (0.60 mL), $\text{Co}_2(\text{CO})_8$ (31 mg, 0.091 mmol), alcohol **1.83** (16 mg, 0.045 mmol), dissolved in DCM (0.40 mL), and $\text{BF}_3 \cdot \text{OEt}_2$ (15 μL , 0.11 mmol). The reaction was monitored by TLC and stirred for 2 h. The crude residue was purified by silica gel flash column chromatography (gradient of 10-30% EtOAc in hexanes) to afford 14 mg of **3.78** as a mixture of two diastereomers (2.1:1), determined by the integrations for H_6 at 5.78 and 5.38 ppm, in 46% yield as a dark red/brown oil.

Data for 3.78

^1H NMR (400 MHz, CDCl_3)

7.40-7.35 (m, 3 H), 7.31-7.26 (m, 2 H), 6.34 (d, $J = 3.6$ Hz, 1 H)**, 6.24 (d, $J = 3.2$ Hz, 1 H)*, 6.09 (s, 1 H), 5.86 (d, $J = 3.2$ Hz, 1 H)*, 5.78 (d, $J = 9.6$ Hz, 1 H)**, 5.47 (d, $J = 3.2$ Hz, 1 H)**, 5.38 (d, $J = 10.4$ Hz, 1 H)*, 4.71-4.61 (m, 2H), 4.33 (d, $J = 12.4$ Hz, 1 H)*, 4.25 (d, $J = 12.8$ Hz, 1 H)*, 4.26 (app s, 2 H)**, 4.10-4.05 (m, 1 H)**, 3.88-3.86 (m, 1 H)*, 3.51 (s, 3 H)*, 3.39 (s, 3H)**, 3.32-3.14 (m, 4 H), 2.52-2.41 (m, 1 H) ppm;

^{13}C NMR (100 MHz, CDCl_3)

201.4*, 201.1**, 199.6 (6C), 168.3**, 167.9*, 162.2**, 161.5*, 144.0**, 143.0*, 137.2*, 135.0**, 134.4*, 133.6**, 131.6*, 130.72**, 130.65*, 130.3**, 130.0*, 129.9**, 128.84**, 128.77*, 127.8**, 127.7*, 122.8**, 122.2*, 90.7**, 90.6*, 81.8*, 75.7*, 74.7**, 73.6**, 73.4*, 73.3**, 71.9*, 71.6**, 71.4**, 71.1*, 57.2**, 56.5*, 49.8, 40.0**, 39.7*, 33.8**, 29.5* ppm;

IR (thin film)

2927, 2829, 2372, 2093, 2051, 2022, 1773, 1702, 12.68, 1096, 1018, 697 cm^{-1} .

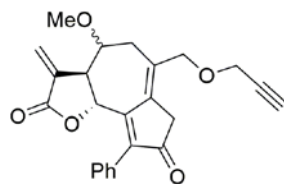
HRMS (FTMS + p ESI Full ms)

$[\text{M}+\text{H}]^+$ calcd for $\text{C}_{30}\text{H}_{23}\text{O}_{11}\text{Co}_2$, 676.9899; found, 676.9903;

TLC $R_f = 0.26^*$, 0.22^{**} (30% ethyl acetate/hexanes)

Silica gel, Visible, UV

*Major diastereomer, **minor diastereomer



Guaianolide analog alkyne probe (3.79). Follows general procedure

3D: cobalt complex **3.78** (14 mg, 0.021 mmol, 1 equiv), acetone (1.5 mL), and CAN (68 mg, 0.12 mmol, 6 equiv). The reaction stirred for 15 min. The reaction afforded 9 mg of alkyne **3.79** as a mixture of two diastereomers (2.1:1),

determined by the integrations for H₆ at 5.78 and 5.38 ppm, in quantitative yield as a colorless oil. The crude material was not purified further.

Data for 3.79

¹H NMR (400 MHz, CDCl₃)

7.38-7.35 (m, 3 H), 7.30-7.24 (m, 2 H), 6.36 (d, *J* = 3.2 Hz, 1 H)**, 6.24 (d, *J* = 3.2 Hz, 1 H)*, 5.88 (d, *J* = 2.8 Hz, 1 H)*, 5.78 (d, *J* = 9.6 Hz, 1 H)**, 5.52 (d, *J* = 3.2 Hz, 1 H)**, 5.38 (d, *J* = 10.4 Hz, 1 H)*, 4.23-4.16 (m, 4 H), 4.09-4.06 (m, 1 H)**, 3.87-3.84 (m, 1 H)*, 3.51 (s, 3 H)*, 3.43 (s, 3 H)**, 3.38-3.12 (m, 4 H), 2.52-2.46 (m, 2 H) ppm;

Impurities observed at 2.27, 1.43, 1.25, 0.87 ppm.

¹³C NMR (150 MHz, CDCl₃)

201.5*, 201.3**, 168.3**, 167.9*, 161.9**, 161.4*, 144.2**, 143.2*, 137.2*, 135.8**, 135.4*, 133.6**, 130.9*, 130.73**, 130.65*, 129.93 (2C)*, 129.89 (2C)**, 129.7**, 128.9**, 128.8*, 127.80 (2C)**, 127.75 (2C)*, 122.9**, 122.2*, 81.8*, 79.5*, 79.3**, 75.7*, 75.6**, 75.4*, 74.8**, 73.8**, 71.9**, 71.5*, 57.8**, 57.4**, 57.2*, 56.5*, 49.8*, 49.7**, 40.0**, 39.7*, 34.2*, 30.0* ppm;

Impurities observed at 67.6, 34.2, 29.9, 24.0, 22.9, 14.3 ppm

*Major diastereomer, **minor diastereomer

IR (thin film)

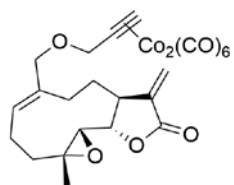
3279, 2933, 2852, 2115, 1769, 1703, 1492, 1445, 1269, 1134, 1095, 699 cm⁻¹.

HRMS (FTMS + p ESI Full ms)

[M+H]⁺ calcd for C₂₄H₂₃O₅, 391.1540; found, 391.1525;

TLC R_f = 0.18 (40% ethyl acetate/hexanes)

Silica gel, UV, potassium permanganate



Co₂(CO)₆-O-(prop-2-ynyl)-MelB (3.80). **Method A:** Follows general procedure 3C.2: Propargyl alcohol (4 mg, 0.076 mmol), DCM (0.5 mL), Co₂(CO)₈ (26 mg, 0.076 mmol), MelB (**3.29**)¹¹⁵ (10 mg, 0.038 mmol),

dissolved in DCM (0.3 mL), and BF₃•OEt₂ (12 μL, 0.095 mmol). The reaction was quenched after 10 min of stirring despite a small amount of Mel B remaining in the reaction. The crude residue was purified by silica gel flash column chromatography (gradient of 10-20% EtOAc in hexanes) to afford 9 mg of **3.80** in 41% yield as a dark red oil. **Method B:** Follows general procedure 3C.2: Methyl propargyl ether (8.0 mg, 0.11 mmol), DCM (0.8 mL), Co₂(CO)₈ (39 mg, 0.11 mmol), Mel B (**3.29**) (15 mg, 0.057 mmol), dissolved in DCM (0.4 mL), and BF₃•OEt₂ (18 μL, 0.14 mmol). The reaction was quenched after 40 min of stirring despite a small amount of Mel B remaining in the reaction. The crude residue was purified by silica gel flash column chromatography (gradient of 10-20% EtOAc in hexanes) to afford 13 mg of **3.80** in 39% yield.

Data for 3.80

¹H NMR (400 MHz, CDCl₃)

6.25 (s, 1H), 6.04 (s, 1H), 5.67 (bs, 1H), 5.51 (s, 1H), 4.62 (d, *J* = 13.2 Hz, 1H), 4.53 (d, *J* = 12.8 Hz, 1H), 4.25 (d, *J* = 11.2 Hz, 1H), 3.98 (d, *J* = 12.0 Hz, 1H), 3.86 (t, *J* = 9.6 Hz, 1H), 2.87-2.85 (m, 2H), 2.43-2.31 (m, 4H), 2.22-2.15 (m, 2H), 1.67-1.64 (m, 1H), 1.55 (s, 3H), 1.12-1.06 (m, 1H) ppm;

¹³C NMR (100 MHz, CDCl₃)

199.6 (6C), 169.6, 139.1, 136.8, 129.4, 120.2, 91.1, 81.2, 73.8, 71.8, 70.3, 63.6, 60.2, 43.2, 36.9, 25.7, 24.3, 23.8, 18.1 ppm;

IR (thin film)

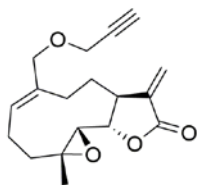
2931, 2360, 2095, 2053, 2023, 1770, 1262, 1138, 1075, 995 cm^{-1} ;

HRMS (FTMS + p ESI Full ms)

$[\text{M}+\text{H}]^+$ calcd for $\text{C}_{24}\text{H}_{23}\text{O}_{10}\text{Co}_2$, 588.9950; found, 588.9946;

TLC $R_f = 0.19$ (20% ethyl acetate in hexanes)

Silica gel, visible, UV



***O*-(prop-2-ynyl)-Mel B 3.81.** Followed general procedure 3D: $\text{Co}_2(\text{CO})_6$ -alkyne **3.80** (9 mg, 0.015 mmol), acetone (1.5 mL), and CAN (34 mg, 0.061 mmol). The reaction was complete after 10 min of stirring. Reaction work up

afforded 4 mg of alkyne **3.81** as a colorless oil in 94% yield. Further purification was not performed.

Data for 3.81

^1H NMR (400 MHz, CDCl_3)

6.24 (d, $J = 3.6$ Hz, 1H), 5.70-5.66 (m, 1H), 5.55 (d, $J = 3.2$ Hz, 1H), 4.18 (dd, $J = 16.0, 2.4$ Hz, 1H), 4.16 (d, $J = 10.8$ Hz, 1H), 4.08 (dd, $J = 16.0, 2.4$ Hz, 1H), 3.90 (d, $J = 11.6$ Hz, 1H), 3.86 (t, $J = 9.2$ Hz, 1H), 2.96-2.82 (m, 1H), 2.86 (d, $J = 9.6$ Hz, 1H), 2.53-2.45 (m, 1H), 2.44 (t, $J = 2.4$ Hz, 1H), 2.40-2.27 (m, 3H), 2.22-2.14 (m, 2H), 1.68-1.62 (m, 1H), 1.55 (s, 3H), 1.14-1.07 (m, 1H) ppm;

Impurity observed at 29.8 ppm.

^{13}C NMR (125 MHz, CDCl_3)

169.6, 139.2, 136.6, 130.4, 120.1, 81.3, 79.7, 74.8, 72.9, 63.6, 60.1, 57.4, 43.1, 36.9, 25.9, 24.6, 23.9, 18.2 ppm;

IR (thin film)

3274, 2921, 2850, 2112, 1764, 1261, 1138, 1073, 993, 815 cm^{-1} ;

HRMS (FTMS + p ESI Full ms)

$[M+H]^+$ calcd for $C_{18}H_{23}O_4$, 303.1591; found, 303.1595;

TLC $R_f = 0.20$ (30% ethyl acetate in hexanes)

Silica gel, UV, potassium permanganate

4.0 STUDIES ON THE GUAIANOLIDE NF- κ B MECHANISM OF INHIBITION

4.1 INTRODUCTION

Drug candidates containing electrophiles that undergo covalent bond-forming reactions with proteins *in vivo* have traditionally been avoided by pharmaceutical researchers.^{8c} However, a resurgence of these covalent drugs can partially be attributed to increased efforts toward understanding their molecular mechanisms of biological activity. Sesquiterpene lactones (SLs) are known to affect their anti-inflammatory and antiproliferative properties through inhibition of the inflammation central transcription factor, nuclear factor kappa B (NF- κ B).⁷ However, understanding the structural features that are responsible for the potent inhibitory properties as well as uncovering the exact mode of inhibition these compounds undergo within the NF- κ B pathway has been more difficult.

Defined quantitative structure-activity relationships (QSAR) between SL skeletal and topological structures with inhibition of NF- κ B are limited. The most comprehensive QSAR study to date evaluated 103 SLs from 6 different skeletal families; among these compounds, 22 guaianolides and 9 pseudoguaianolides were tested.¹¹⁶ The NF- κ B inhibition ability of all the sesquiterpene families had a strong correlation to the presence of alkylating centers in the form of unsaturated carbonyls. However, guaianolides had more specific correlations also related to structure coding parameters, attributed to the rigid nature of the guaianolide skeleton. The QSAR

analysis revealed that an increased number of hydroxyl groups in guaianolides can lead to diminished NF- κ B inhibition.¹¹⁶⁻¹¹⁷ While this study provides a good starting point for QSAR data, the conclusions are somewhat limited. Continuing to evaluate the NF- κ B inhibition of guaianolide-related compounds will add to the knowledge about the structure-activity relationship. This process is necessary to understanding the mechanism of inhibition for the development of potent analogs.

As mentioned, the biological activity, as well as cytotoxicity of SLs is linked to the presence of unsaturated carbonyls, seen in the form of α -methylene- γ -butyrolactones, α,β -unsaturated cyclopentenones, and other, acyclic α,β -unsaturated esters, ketones, and aldehydes. These electrophilic groups have been shown to react with biological nucleophiles, particularly cysteine sulfhydryl groups, through a hetero-Michael-type addition reaction. For example, when helenalin (**1.7**), which has two possible alkylating centers, is reacted with 1 equiv of cysteine in D₂O, hetero-Michael addition occurs selectively with the α -methylene- γ -butyrolactone moiety (adduct **4.1**, Figure 24A). Interestingly, when 1 equiv of glutathione, the most abundant non-protein thiol in eukaryotic cells, is reacted with helenalin (**1.7**), it selectively adds to the α,β -unsaturated cyclopentenone (adduct **4.2**). Both of these additions also occurred stereoselectively, resulting in the isomers shown in Figure 24A. When excess amounts of either cysteine or glutathione are employed, the thiols add to both alkylating centers of helenalin (**1.7**).^{9, 118} Cysteamine (**4.4**) has also been utilized as a model for biological thiols that can be used to quickly ascertain thiol reactivity of unsaturated carbonyls;¹¹⁹ stirring of costunolide (**4.3**) and cysteamine in DMSO formed the corresponding adduct **4.5**, determined by the disappearance of the alkenyl protons, H_a and H_b, in the crude NMR (Figure 24B).^{119a} These studies lend themselves to predict reactivity of SLs that contain unsaturated carbonyl alkylating centers *in*

in vivo. However, this does not replace the value that comes from understanding the exact NF- κ B protein targets responsible for biological activity, as well as non-specific targets that could lead to cytotoxicity.

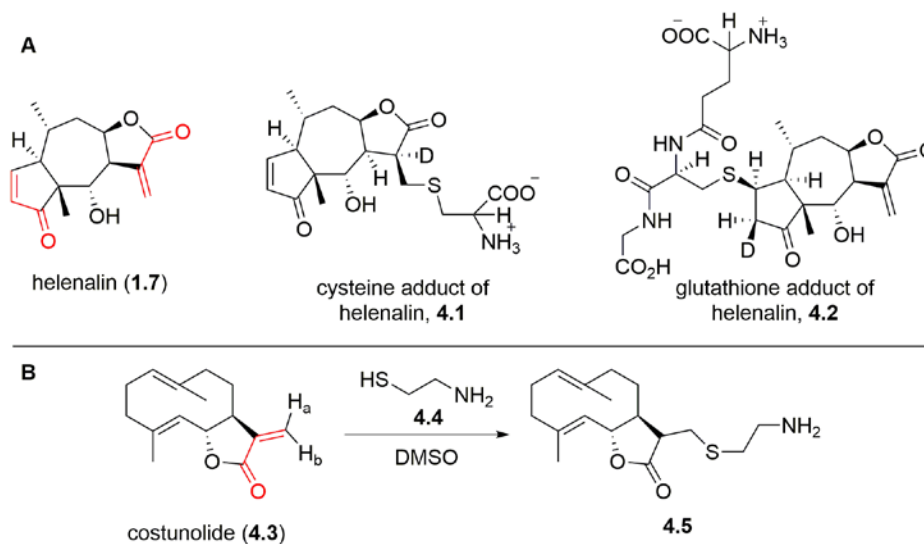


Figure 24. Examples of SL reactivity with biological thiols; A) Helenalin (**1.7**) adducts with cysteine and glutathione, B) Costunolide (**4.3**) adduct with cysteamine (**4.4**).

In cells, NF- κ B is comprised, most frequently, of the p50 and p65 (RelA) subunits, and is retained in the cytoplasm through binding with its inhibitor protein, I κ B. In response to stimuli (over 200 stimuli options), the IKK complex, made up of IKK α , IKK β , IKK γ , activates I κ B, with IKK β being the primary kinase. This activation results in phosphorylation of two serine residues of I κ B (Ser-177, Ser-181), leading to ubiquitination and degradation of the inhibitor protein. In turn, the NF- κ B dimer is now activated and freely translocates to the nucleus, where it binds with DNA and initiates transcription (Figure 25).^{10-11, 59} This cascading pathway has many potential sites of inhibition, usually falling into one of three categories: 1) blockage of incoming stimuli that activates the IKK complex, or early stage inhibition, 2) interference with one of the cytoplasmic events (phosphorylation of I κ B), 3) blockage of NF- κ B nuclear activity (either by

preventing its translocation from the cytoplasm to the nucleus, or by inhibiting NF- κ B/DNA binding.

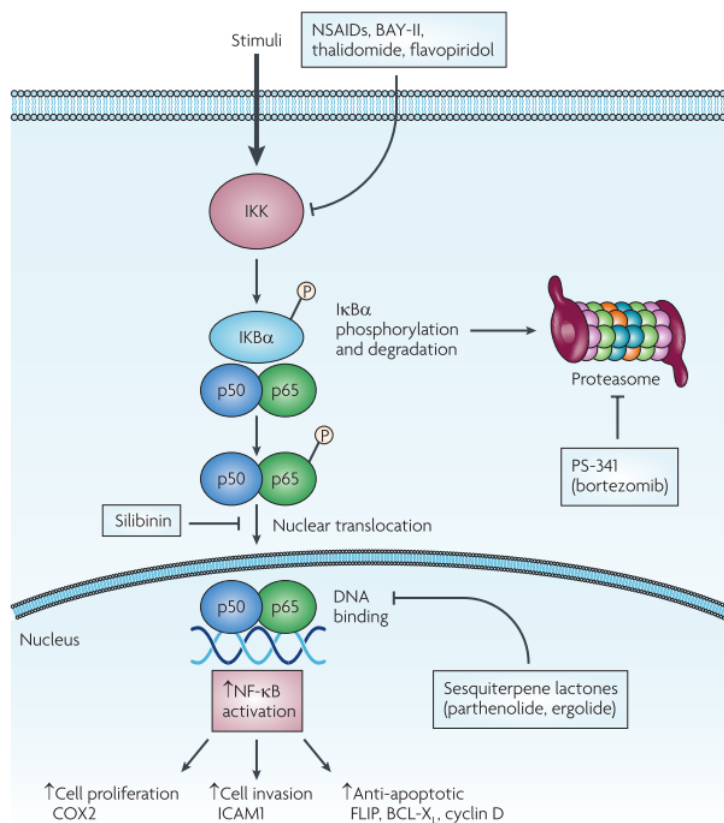


Figure 25. The NF- κ B pathway leading to gene transcription.¹¹ [Reprinted by permission from Macmillan Publishers Ltd: Nature Reviews Drug Discovery, 2008, 7, 1031-1040, copyright 2008.](#)

Thiol reactive compounds, including SLs, have been characterized to inhibit NF- κ B signaling by either blocking I κ B-degradation or by interfering with the NF- κ B/DNA binding event.⁵⁹ A case has been made that parthenolide (PTL, **1.3**) inhibits the I κ B degradation event by binding a cysteine (Cys-179) in the IKK β activation loop.¹²⁰ Gel shift assays performed by the Hehner group did not show that PTL blocked NF- κ B/oligonucleotide interactions.^{120a, 120b} Kwok and coworkers also studied the mechanism of inhibition for parthenolide; coming to a similar conclusion that it prevents I κ B degradation. Reduced PTL **4.6** was not effective for inhibition of NF- κ B signaling, supporting the importance of the α -methylene lactone moiety (Figure 26). A

biotinylated PTL derivative (**4.7**) confirmed IKK- β as a molecular target of PTL using protein profiling experiments. Finally, a mutant protein of IKK- β where Cys-179 was replaced with a serine was no longer sensitive to the inhibitory properties of PTL. This cysteine residue is positioned between the two serine residues (Ser-177,181) that undergo phosphorylation leading to IKK β degradation.^{120c}

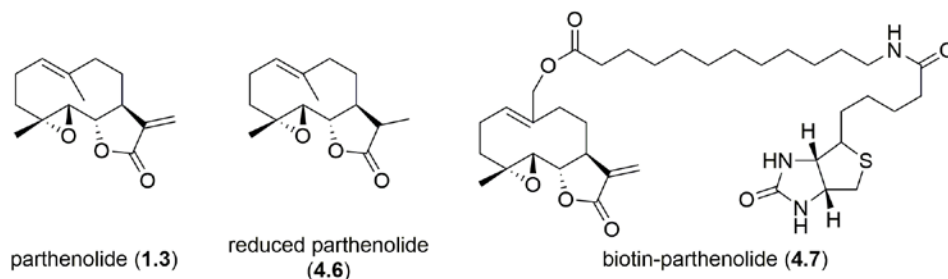


Figure 26. Structures of parthenolide derivatives used by Kwok to investigate the SL mechanism of inhibition.

On the other hand, a series of reports by the Merfort group have shown that PTL, as well as helenalin (**1.7**) and a few other SLs, inhibit NF- κ B by preventing the DNA/NF- κ B binding event. The Merfort group claims that their results, detailed within, contradict reports that parthenolide inhibits NF- κ B activation solely by preventing I κ B degradation.⁷ First, confocal laser scanning microscopy was used to examine cells that were activated using tumor necrosis factor- α (TNF- α) followed by treatment with helenalin (**1.7**). The results confirmed the presence of NF- κ B in the nucleus of the cells, showing that I κ B degradation was not inhibited, nor was the translocation of NF- κ B from the cytoplasm to the nucleus.¹²¹

Molecular docking studies were utilized to propose that helenalin covalently binds to NF- κ B with a cysteine residue (Cys-38) of the p65 unit.¹¹⁷ Experimental evidence for this proposal was achieved by the construction of NF- κ B/p65 mutants, where the proposed reactive cysteine residues were interchanged for serine residues. The inhibition of the NF- κ B mutants was evaluated by various SLs, including helenalin, PTL, and two other SLs (Figure 27); gel shift

assays (EMSA) were used to visualize the presence of the p65-oligonucleotide complex. For all SLs tested (at varying concentrations), the binding of the wild type NF- κ B to oligonucleotides was completely inhibited (contrary to reports by Hehner)^{120a, 120b}, however, when Cys-38 was replaced with a serine residue, no inhibition was observed, supporting evidence for a covalent binding event that occurs between Cys-38 and the SL inhibitor, and that this interaction is essential to the prevention of NF- κ B/DNA binding.¹²² Slight inhibition of I κ B degradation was also observed for all SLs tested, however, this mechanism of action was secondary to the prevention of NF- κ B/DNA binding; the amount of un-degraded I κ B was not sufficient to account for complete inhibition of NF- κ B/DNA binding. Finally, surface plasmon resonance confirmed interactions between helenalin and NF- κ B/p65 unit, but not between helenalin and the IKK complex.¹²³

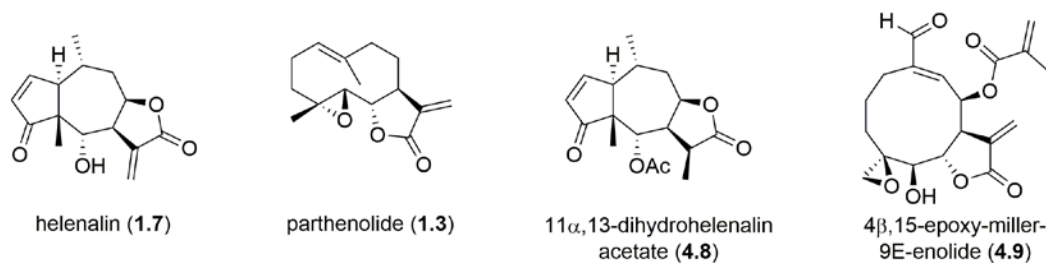


Figure 27. Sesquiterpene lactones evaluated in NF- κ B mutant (Cys \rightarrow Ser) experiments.

Merfort concludes that SLs inhibit NF- κ B primarily through the prevention of NF- κ B/DNA binding by alkylating Cys-38 in the binding domain of NF- κ B through a Michael-type addition; this mechanism of action can also be assumed as a general mechanism of action for all SLs containing α,β -unsaturated carbonyls.⁷ Merfort also hypothesized that the contradictory results for SLs acting by two different mechanisms of action could be contributed to the fact inhibition of I κ B degradation is observed when higher concentrations of the SL are used. This might hide the effect the SL has on p65, which is more visible at lower concentrations.⁷

In light of these studies, it is clear that understanding molecular mechanism of inhibition is of crucial importance when in the process of developing potential NF- κ B inhibitors. While these studies have focused on SLs and lend themselves to make conclusions about a wide range of α -methylene- γ -butyrolactone containing NPs, mechanism of NF- κ B inhibition studies pertaining specifically to 6,12-guaianolides are limited. Due to the potent NF- κ B inhibition that was demonstrated by *trans*-guaianolide analog **1.83** (Section 2.1), synthesized in our lab, we sought to further examine the structure-activity relationship of **1.83** analogs and the mechanism of action. Our goals included the following; 1) determine if the relative stereochemistry of the C8 methoxy group had an impact on the NF- κ B inhibition ability, 2) show whether or not the α -methylene lactone moiety was necessary for activity and if the group was thiol reactive, 3) identify protein targets of **1.83** through ABPP experiments.

4.2 EFFECT OF C8 STEREOCHEMISTRY ON NF- κ B INHIBITION

Trans-guaianolide **1.83** was previously established as a potent NF- κ B inhibitor, with comparable activity to parthenolide. However, *trans*-**1.83** was evaluated as a mixture of diastereomers in relation to the C8 methoxy group. To evaluate if the two diastereomers had differing or consistent NF- κ B inhibitory properties, they were separated via HPLC and characterized using NMR and computational techniques (Section 2.2.5). The major diastereomer was assigned as the 8 β H-isomer **1.83a**, while the minor diastereomer was assigned as the 8 α H-isomer **1.83b** (Figure 28). These compounds are still racemic mixtures of the designated relative stereochemistry.

Our collaborators in the Harki group at the University of Minnesota evaluated the separated diastereomers of **1.83** for inhibition of induced NF- κ B activity using a luciferase luminescence assay. A549 cells are treated with the potential inhibitors at varying concentrations, and then induced using TNF- α . This activation increases the luminescence which is then diminished in the presence of an NF- κ B inhibitor. Non-induced cells and cells induced without the presence of a potential inhibitor were used as control standards for the determination of relative NF- κ B activity of cells treated with 8 β H-**1.83a** and 8 α H-**1.83b**.^{119b}

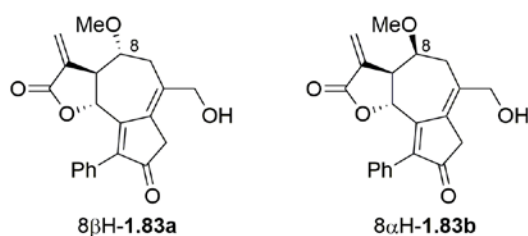


Figure 28. Structures of the two *trans*-**1.83** diastereomers.

The cells were treated with 1, 5, 10, and 20 μ M of both diastereomers (Table 14). At 20 μ M, 8 β H-**1.83a** lowered the induced NF- κ B levels to 31% while 8 α H-**1.83b** lowered NF- κ B levels to 41.5%. Inhibition was also observed at 10 μ M, with reduced NF- κ B levels at 66% and 75% for 8 β H-**1.83a** and 8 α H-**1.83b** respectively. While it was evident that the 8 β H-**1.83a** may be slightly more potent than 8 α H-**1.83b**, these two compounds were considered to be effectively equal inhibitors of NF- κ B. Interestingly, the values reported for the separated diastereomers of *trans*-**1.83** are slightly less potent than the previously reported data obtained from analysis of the mixture; which lowered induced NF- κ B activity to 57% when dosed at 10 μ M. The data from Table 14 is represented pictorially in Figure 29, with comparisons to the induced and non-induced controls.

Table 14. Relative NF- κ B activity of cells treated with 8 β H-**1.83a** and 8 α H-**1.83b**.

8 β H- 1.83a	1 μ M	5 μ M	10 μ M	20 μ M	8 α H- 1.83b	1 μ M	5 μ M	10 μ M	20 μ M
Trial 1	102.8	84.4	60.5	29.1	Trial 1	75.4	80.3	75.7	30.8
Trial 2	106.9	92.9	70.3	28.9	Trial 2	88.1	88.9	71.0	47.9
Trial 3	101.6	86.2	67.3	34.7	Trial 3	99.1	90.1	79.3	45.8
Average	103.8	87.8	66.0	30.9	Average	87.5	86.4	75.3	41.5

Values shown are the relative NF- κ B activity (%) of A549 cells induced with TNF- α 30 min after treatment with **1.83a** and **1.83b** compared to induced A549 cells induced with no inhibitor treatment.

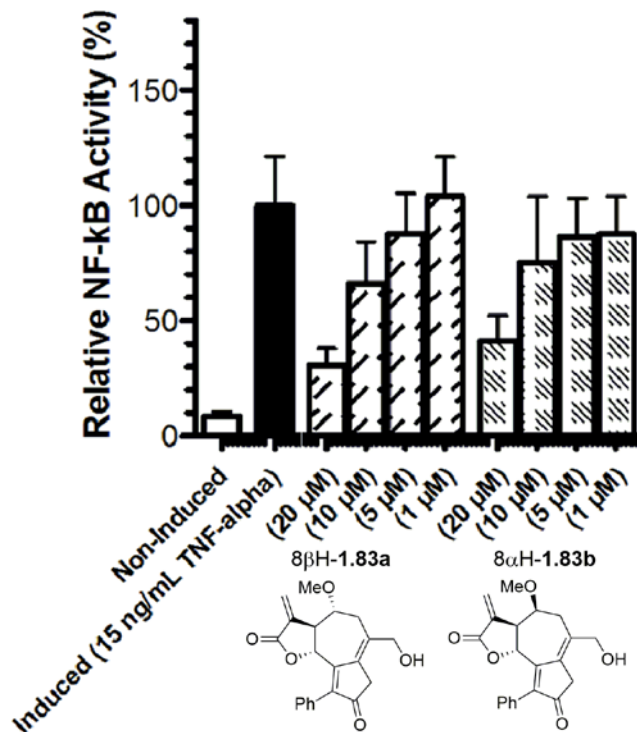
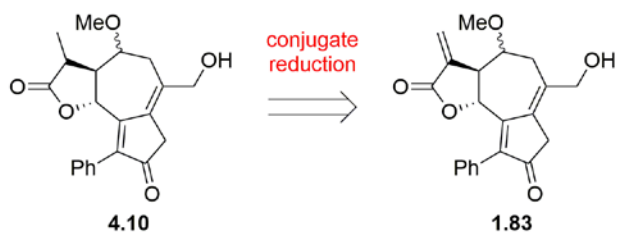


Figure 29. Pictorial representation of relative NF- κ B activity for cells treated with 8 β H-**1.83a** and 8 α H-**1.83b**.

4.3 THE IMPORTANCE OF THE α -METHYLENE- γ -BUTYROLACTONE FOR NF- κ B INHIBITION

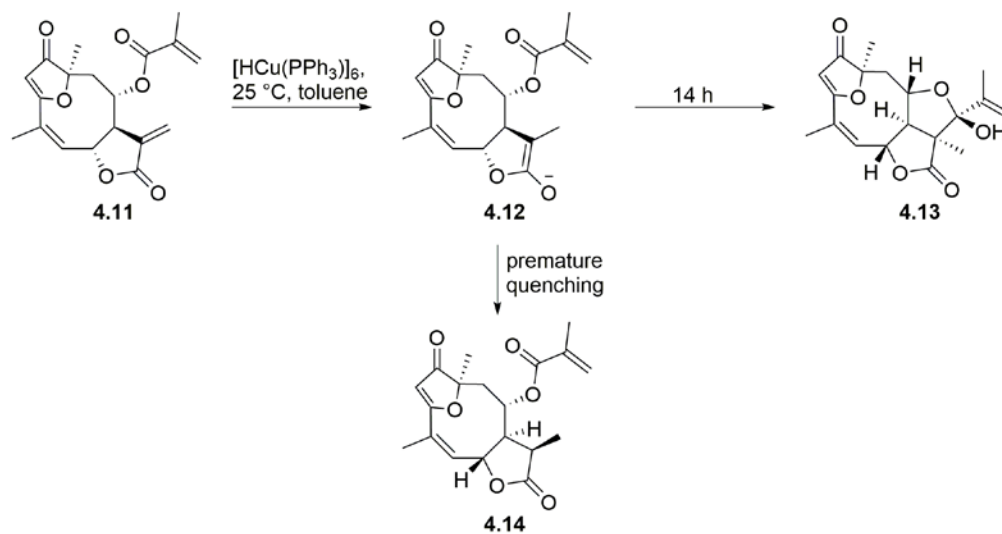
To confirm that the biological activity of guaianolide analog *trans*-**1.83** is dependent on the presence of the α -methylene- γ -butyrolactone moiety, we set out to synthesize the reduced α -methyl- γ -butyrolactone analog **4.10**. If obtained, **1.83** and **4.10** could be directly compared for

NF- κ B inhibition. We envisioned that **4.10** could be obtained in a single step from **1.83** via conjugate reduction (Scheme 75).



Scheme 75. Retrosynthetic analysis of **4.10**.

Conjugate reductions of α -methylene- γ -butyrolactones have most commonly been achieved using a reducing agent, such as sodium borohydride, or via a metal catalyzed hydrogenation, such as $H_2/Pd/C$ or $H_2/Wilkinson's$ catalyst.^{99, 124} However, we had concerns that these methods would not be compatible with our functionally dense system, which contains multiple carbonyls and unsaturated C-C bonds. Metal hydride reagents, such as Stryker's reagent ($[CuH(PPh_3)]_6$) have also been employed as a reducing agent, and have been shown selectivity for α -methylene- γ -butyrolactones within highly complex molecules. For example, eremantholide **4.13** was synthesized in one bio-mimetic synthetic step from furanoheliangolide **1.11** using Stryker's reagent; selective reaction with the α -methylene- γ -butyrolactone affords an enolate intermediate **4.12**, which then undergoes cyclization with the available unsaturated ester to give **4.12** (Scheme 76).¹²⁵ The conjugate hydride addition was determined to be the fast step while the enolate cyclization was the slow step. Premature quenching of **4.12** afforded **4.14**, therefore, without an available electrophilic group to react with the enolate intermediate, Stryker's reagent is also a viable reagent for the chemoselective reduction of α -methylene lactones to α -methyl lactones.



Scheme 76. Synthesis of α -methyl lactone **4.14** and eremantholide **4.13** from furanoheliangolide **4.11**.

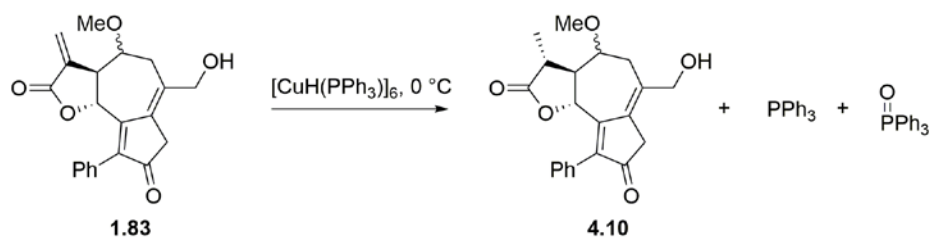
4.3.1 Synthesis of reduced methylene guaianolide analog **4.10**

In light of the reported selectivity of Stryker's reagent for α -methylene- γ -butyrolactones, this methodology was applied to *trans*-**1.83**. Synthetic investigations began by determining the appropriate solvent system (Table 15). Toluene is a traditional solvent for conjugate reductions using Stryker's reagent, however, THF has been reported to increase reaction rates presumably by coordination with the copper reagent.^{125c} Reacting *trans*-**1.83** with the 1 equiv of Stryker's reagent in 100% THF resulted in decomposition of **1.83** (Entry 1). Changing the solvent to a 5:1 mixture of toluene and THF gave a 31% yield of **4.10** while use of 100% toluene afforded **4.10** in 55% yield (Entries 2 and 3). Unfortunately, for both entries, the products were contaminated with triphenylphosphine (Ph_3P) and triphenylphosphine oxide (Ph_3PO), even after multiple attempts to purify via flash column chromatography. The conversion of *trans*-**1.83** to **4.10** occurred diastereoselectively; this was evidenced by the presence of only 2 diastereomers, as

seen in the starting material, pertaining to the stereochemistry of the C8 methoxy group (See Section 4.3.2 for further discussion).

Additional purification methods other than silica gel flash column chromatography were tried in an effort to remove the Ph₃P and Ph₃PO impurities. HPLC purification was effective for removing Ph₃P, but **4.10** was still contaminated with Ph₃PO, as both compounds are quite polar. Crystallization of the Ph₃P and Ph₃PO was attempted by dissolving **4.10** in a minimal amount of cold diethyl ether, and filtering off the observed crystals. This method was not effective for removing impurities in their entirety.

Table 15. Initial attempts to reduce methylene of *trans*-**1.83**: Solvent effects.

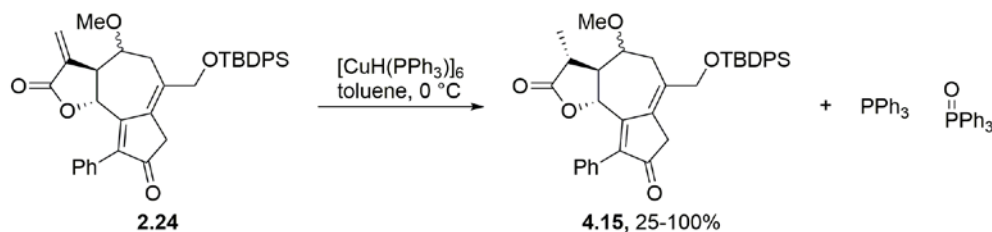


Entry	Solvent (0.0095 M)	Approx. yield 4.10
1	THF	0% (decomposition)
2	Toluene/THF (5:1)	31% ^a
3	Toluene	55% ^a

^a**4.10** contaminated with Ph₃P and Ph₃PO.

Next, we applied the hydride conjugate addition reaction to silyl-protected *trans*-guaianolide **2.24** (Scheme 77). **2.24** is significantly less polar ($R_f = 0.18$, 20% EtOAc in hexanes) than the silyl-deprotected **1.83** ($R_f = 0.41$, 100% EtOAc), so we predicted it would be more easily separated from Ph₃PO via chromatography methods. The methylene group was successfully reduced diastereoselectively in the presence of Stryker's reagent to afford **4.15**. The crude NMR spectra of these experiments again showed significant impurities related to the Ph₃P. For one experiment, column chromatography afforded both C8 diastereomers of **4.15**, with some separation, in quantitative yield with only trace impurities. However, this result was not

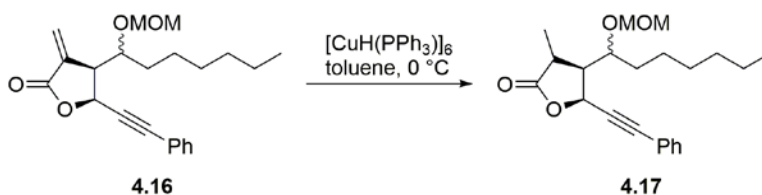
reproducible; while using the same reaction conditions, other experiments required more extensive purifications, resulting in diminished yield of **4.15** (Scheme 77). It was clear that removal of Ph_3P and Ph_3PO still required tedious chromatography strategies despite the less-polar nature of **4.15** compared to **4.10**.



Scheme 77. Reduction of **2.24** with $[\text{CuH}(\text{PPh}_3)]_6$ gave impure **4.15**.

Stryker's reagent is a copper hydride hexamer complex, so by using 1 equivalent of the reagent, 6 equiv of copper hydride are actually employed. Therefore, in attempts to limit the presence of impurities, the amount of Stryker's reagent required to fully consume the α -methylene- γ -butyrolactone starting material was optimized. Due to limited availability of our guaianolide analogs, we optimized the required amount of Stryker's reagent using *cis*-lactone **4.16** (Table 16).⁴³ To begin, **4.16** was stirred with 1 equiv of Stryker's reagent in toluene at 0 °C; 100% conversion to **4.17** was observed via crude ^1H NMR spectroscopy after 1 h (Entry 1). Both 0.8 and 0.4 equivalents also gave 100% conversion, but required 2 h of stirring (Entries 2 and 3). However, by employing 0.25 equiv of Stryker's reagent and stirring for 14 h, **4.16** was converted to **4.17** in only 70% (Entry 4). We concluded that at least 0.4 equiv Stryker's reagent should be employed to efficiently reduce α -methylene- γ -butyrolactones.

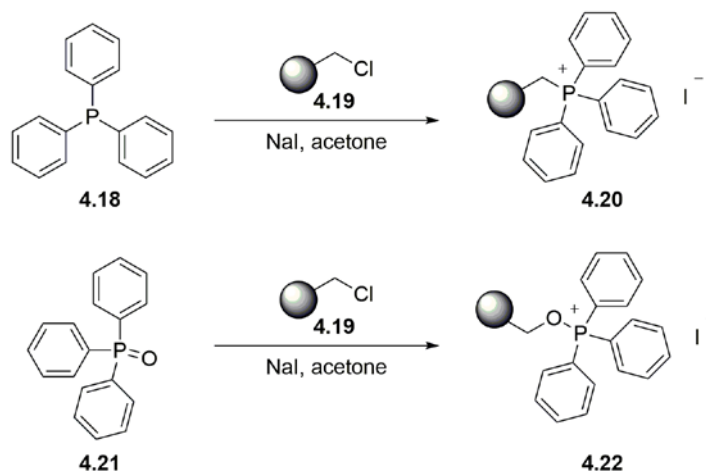
Table 16. Optimization of Stryker's reagent equiv using model system **4.16**.



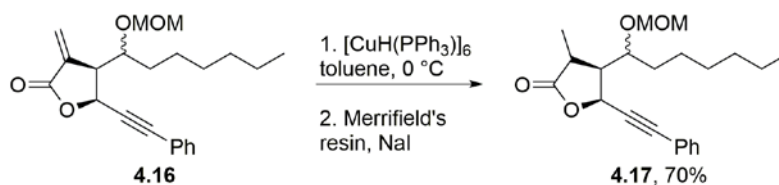
Entry	Equiv Stryker's reagent	Time	% conversion ^a
1	1 equiv	1 h	100
2	0.8 equiv	2 h	100
3	0.4 equiv	2 h	100
4	0.25 equiv	14 h	70

^aPercent conversion determined by crude ¹H NMR spectroscopy.

A solid supported scavenger was also tested for the removal of Ph_3P and Ph_3PO . In 2001, Lipshutz described a simple, expedient procedure for scavenging both Ph_3P (**4.18**) and Ph_3PO (**4.21**) using commercially available Merrifield's resin (**4.19**) along with sodium iodide.¹²⁶ Merrifield's resin is a polystyrene based resin made as a copolymer with styrene and chloromethylstyrene. When the benzylchloride groups are modified with sodium iodide, they can efficiently undergo substitution reactions with the Ph_3P derivatives, displacing the iodide (Scheme 78).



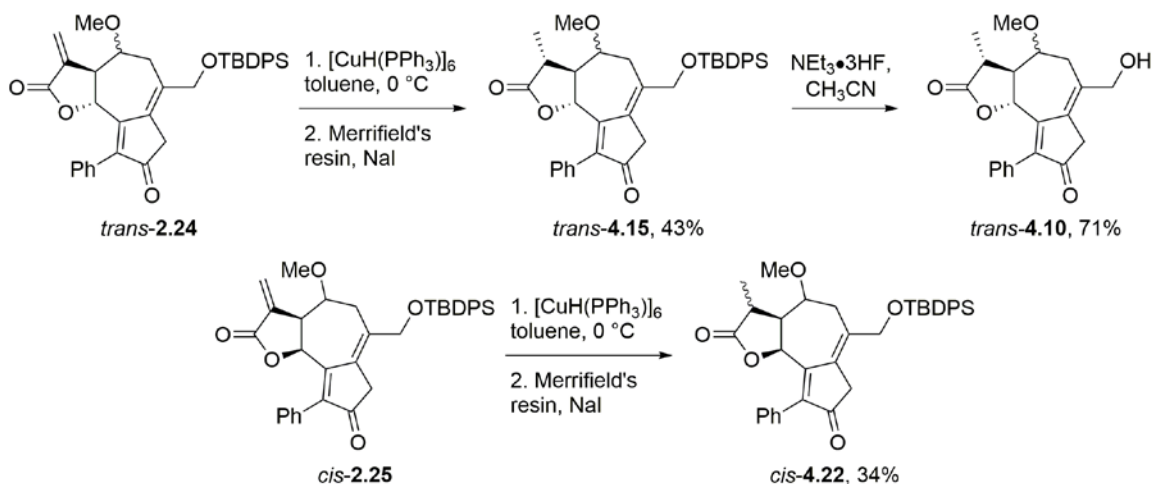
Scheme 78. Reactions of Merrifield's resin/ NaI scavenging system with Ph_3P **4.18** and Ph_3PO **4.21**.



Scheme 79. Reduction of **4.16** to afford **4.17** after triphenylphosphine scavenging.

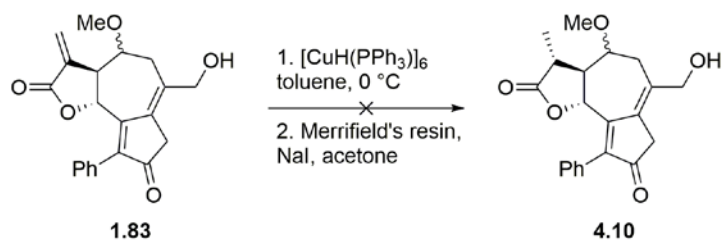
The iodine-modified Merrifield's resin purification method was first tested on model system *cis*- α -methylene- γ -butyrolactone **4.16**. The resulting crude mixture of **4.17** and the Ph_3P related impurities obtained from reacting **4.16** and Stryker's reagent was taken up in acetone, followed by the addition of Merrifield's resin and sodium iodide. A self-stirring incubator was used to swirl the mixture; a magnetic stir bar was not used because this would break down the resin, resulting in a more difficult separation. The process was monitored by TLC and after 16 h, Ph_3P and Ph_3PO were no longer observed. After filtration and washing of the resin, **4.17** was purified via column chromatography and afforded in 70% yield over the two steps (Scheme 79).

Next, iodine-modified Merrifield's resin was applied to the purification of reduced methylene guaianolide analog *trans*-**4.15** (Scheme 80). *Trans*-methylene lactone **2.24** was reduced using 0.5 equiv of the copper hydride hexamer to give **4.15** with 100% conversion. The crude residue was swirled with Merrifield's resin and sodium iodide to remove the Ph_3P impurities and *trans*-**4.15** was afforded in 43% yield over the two steps. In turn, *trans*-**4.15** was desilylated using trimethylamine trihydrofluoride to afford the reduced methylene guaianolide analog **4.10** in 71% yield. *Cis*-**2.25** (single diastereomer) was also tested during the process of optimizing this reaction sequence; *cis*-**4.22** was afforded in 34% yield (as a 9.6:1 mixture of diastereomers) after the two step process of 1,4-reduction and purification (Scheme 80).



Scheme 80. Synthesis and purification of *trans*-4.15, 4.10 and *cis*-4.22.

We originally proposed that reduced analog **4.10** could be obtained from a single synthetic step from *trans*-**1.83** with the unprotected allylic alcohol. While we showed previously that Stryker's reagent was efficient for converting *trans*-**1.83** to **4.10**, but the impurities had rendered the process ineffective. With the ability to remove the Ph_3P and Ph_3PO impurities using a scavenger system, we revisited the direct conversion of *trans*-**1.83** to reduced analog **4.10**. Guaianolide **1.83** was efficiently reduced using 0.5 equiv of Stryker's reagent (100% conversion by crude ^1H NMR), however, purification via with iodine-modified Merrifield's resin did not afford **4.10**, which was presumably unstable to the purification conditions (Scheme 81). Another possibility is that **4.10** was scavenged by the resin, however, iodine-modified Merrifield's resin has been shown to not scavenge free amines which are more nucleophilic than alcohols.¹²⁶ In the future, IR or MS analysis of the resin could confirm this hypothesis.



Scheme 81. Guaianolide analog **4.10** is not compatible with iodine-modified Merrifield's resin.

4.3.2 Assignment of relative C11 stereochemistry for α -methyl lactones **4.15** and **4.10**.

As mentioned, the transformation of the *trans*- α -methylene lactones to the α -methyl lactones occurred diastereoselectively for our substrates. For example, the reduction of the two C8 diastereomers of *trans*-lactone **2.24** ($8\beta\text{H}$ -**2.24a** and $8\alpha\text{H}$ -**2.24b**) resulted in two diastereomers *trans*-lactone **4.15** ($11\beta\text{H},8\beta\text{H}$ -**4.15a** and $11\beta\text{H},8\alpha\text{H}$ -**4.15b**) where C11 was reduced diastereoselectively to have a *trans*-relationship with C7 for both diastereomers. The relative stereochemistry of the methyl group at C11 was determined by comparing calculated and experimental ^1H NMR spectral data.

The two diastereomers of the reduced, silyl protected guaianolide analog **4.15a** and **4.15b** were isolated via chromatography. The major isomer of the silyl deprotected analog **4.10a** was also isolated (Figure 30). ^1H NMR data was obtained for these single isomers which allowed for resolution of additional coupling constants that could not be observed for the corresponding mixtures.

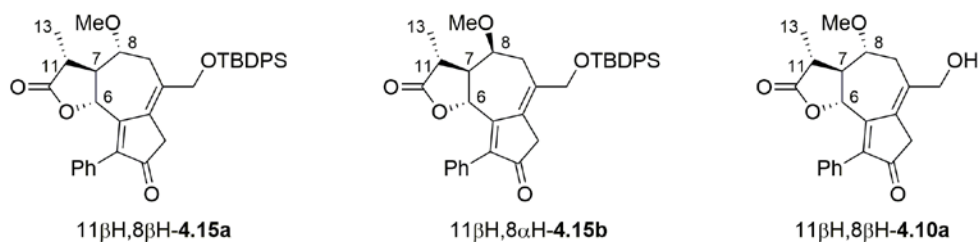


Figure 30. Isolated diastereomers of **4.15** and **4.10** for which experimental ^1H NMR spectra were obtained.

Calculations were performed for the possible isomers for the reduction of *trans*- α -methylene lactone **4.10** without the silyl protecting group; $8\beta\text{H}$ -**4.10a** could possibly result in $11\beta\text{H},8\beta\text{H}$ -**4.10a** or $11\alpha\text{H},8\beta\text{H}$ -**4.10c** while $8\alpha\text{H}$ -**4.10b** could result in $11\beta\text{H},8\alpha\text{H}$ -**4.10b** or $11\alpha\text{H},8\alpha\text{H}$ -**4.10d** (Figure 31). The structures were drawn in Spartan and the lowest energy conformers of each were determined using MMFF calculations. Then, ^1H NMR data was

calculated for the lowest energy conformer using B3LYP/6-31G* functionals. The chemical shifts shown in Table 17 and Table 18 are corrected chemical shifts.

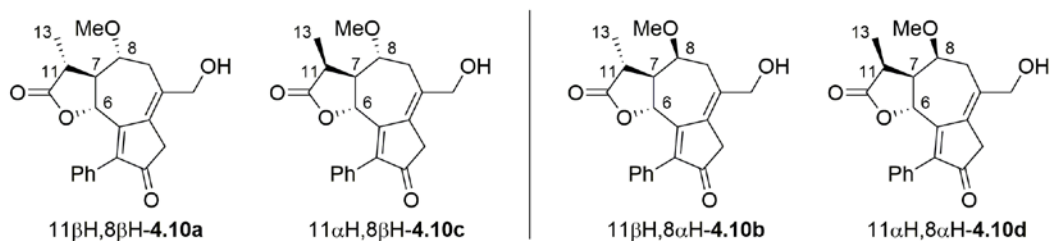


Figure 31. Diastereomers of **4.10** evaluated computationally.

Comparison of the calculated and experimental ^1H NMR data led to the stereochemical assignments of 11 β H,8 β H-**4.15a**, 11 β H,8 α H-**4.15b** and 11 β H,8 β H-**4.10a**. For all examples the methylene was reduced to afford a 7,11-*trans* relative stereochemistry. Experimentally, **4.15a** (with the silyl protecting group) and **4.10a** both had $J_{7,11}$ values of 11.6 Hz. This matched the computationally calculated coupling constant for **4.10a** ($J_{7,11} = 11.6$ Hz), whereas isomer **4.10c** with a 7,11-*cis* relationship, has a smaller calculated $J_{7,11}$ of 9.2 Hz (Table 17). Similarly, **4.15b** (with silyl protecting group) has an experimentally observed $J_{7,11}$ of 12.0 Hz, which corresponds favorably to the calculated $J_{7,11}$ of 11.5 Hz for **4.10b**. **4.10d** had a smaller $J_{7,11}$ value of 8.0 Hz (Table 18). In addition, the chemical shift for the H₆ proton of **4.15b** (5.61 ppm) was much closer to the calculated chemical shift for **4.10b** (5.67 ppm) than for isomer **4.10d** (6.14 ppm). Complete NMR assignments for experimental spectra of guaianolide analogs **4.15** and **4.10** can be found in Appendix A.

Table 17. ¹H NMR calculations compared to experimental data for **4.15a** and **4.10a**.

Position	11βH,8βH- 4.10a Calc ppm	11αH,8βH- 4.10c Calc ppm	11βH,8βH- 4.15a Exp ppm	11βH,8βH- 4.10a Exp ppm
6	5.28 (<i>J</i> = 10.3 Hz)	5.39 (<i>J</i> = 10.2 Hz)	5.29 (d, <i>J</i> = 11.6 Hz)	5.36 (d, <i>J</i> = 11.2 Hz)
7	2.10 (<i>J</i> = 8.4, 10.3, 11.6 Hz)	2.48 (<i>J</i> = 8.8, 9.2, 10.2 Hz)	2.21 (ddd, <i>J</i> = 7.2, 11.6, 11.6 Hz)	2.27 (ddd, <i>J</i> = 7.4, 11.6, 11.6 Hz)
8	3.35 (<i>J</i> = 2.6, 3.5, 8.4 Hz)	3.56 (<i>J</i> = 2.7, 3.5, 8.8 Hz)	3.73-3.68 (m)	3.73-3.69 (m)
11	2.21 (<i>J</i> = 6.6, 11.6 Hz)	2.47 (<i>J</i> = 6.7, 9.2 Hz)	2.50 (qd, <i>J</i> = 6.8, 11.6 Hz)	2.59-2.48 (m)

Table 18. ¹H NMR calculations compared to experimental data for **4.15b**.

Position	11βH,8αH- 4.10b Calc ppm	11αH,8αH- 4.10d Calc ppm	11βH,8αH- 4.15b Exp ppm (consistent with 4.10b)
6	5.67 (<i>J</i> = 10.1 Hz)	6.14 (<i>J</i> = 11.1 Hz)	5.61 (d, <i>J</i> = 10.8 Hz)
7	2.28 (<i>J</i> = 4.6, 10.1, 11.5 Hz)	2.42 (<i>J</i> = 0.6, 8.0, 11.1 Hz)	~2.3 (m)
8	3.74 (<i>J</i> = 4.6, 5.8, 9.8 Hz)	3.69 (<i>J</i> = 0.6, 3.0, 3.4 Hz)	3.69 (td, <i>J</i> = 6.0, 9.2 Hz)
11	2.95 (<i>J</i> = 6.6, 11.5 Hz)	2.24 (<i>J</i> = 6.7, 8.0 Hz)	3.00 (qd, <i>J</i> = 6.8, 12.0 Hz)

4.3.3 NF-κB inhibition of α-methyl-γ-butyrolactone analog **4.10a**

The reduced methylene analog 11βH,8βH-**4.10a** was evaluated using the same luminescence reporter assays used to evaluate the diastereomers of *trans*-**1.83** for inhibition of induced NF-κB activity. A549 cells were treated with 11βH,8βH-**4.10a** (racemic) at 1, 5, 10, and 20 μM concentrations and induced with TNF-α. For all concentrations, no reduction of the induced activity was observed. Triplicate data is shown in Table 19, while pictorial representations with a comparison to the controls (induced and non-induced cells) are shown in Figure 32. It was concluded that α-methyl lactone analog 11βH,8βH-**4.10a** is unable to inhibit induced NF-κB activity. Given that 8βH-**1.83a** showed potent NF-κB inhibition at similar concentrations, and the only structural difference between 8βH-**1.83a** and 11βH,8βH-**4.10a** is the

presence of the α -methylene- γ -butyrolactone moiety, it is clear this functional group is required and essential to the mechanism of inhibition.

Table 19. Relative NF- κ B activity of cells treated with 11 β H,8 β H-**4.10a**.

11 β H,8 β H- 4.10a	1 μ M	5 μ M	10 μ M	20 μ M
Trial 1	101.2	90.9	79.8	94.7
Trial 2	147.9	116.4	123.0	122.5
Trial 3	103.2	95.7	109.2	101.4
Average	117.4	101.0	104.0	106.2

Values shown are the relative NF- κ B activity (%) of A549 cells induced with TNF- α a 30 min after treatment with **4.10a** (at varying concentrations) compared to induced A549 cells induced with no inhibitor treatment.

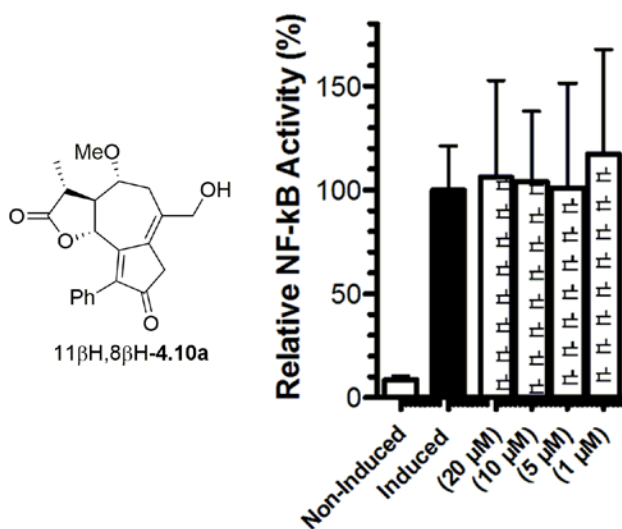
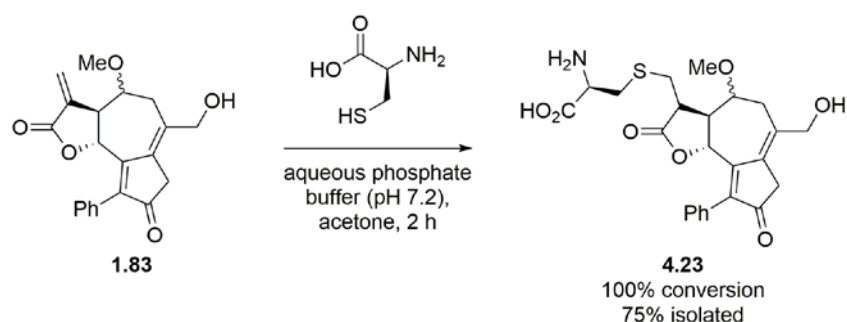


Figure 32. Pictorial representation of relative NF- κ B activity for cells treated with **4.10a**. Induced cells were treated with TNF- α (15 ng/mL).

4.4 REACTIVITY OF GUAIANOLIDE ANALOG **1.83** WITH CYSTEINE

Merfort proposed that SLs inhibit NF- κ B by selectively alkylating a cysteine residue (Cys-38) in the DNA binding domain of NF- κ B.⁷ To show this is a possible mechanism of inhibition for our the guaianolide analogs, *trans*-**1.83** was reacted with L-cysteine in an aqueous phosphate buffer (pH 7.2). A small amount of acetone was also used to solubilize **1.83**. The

reaction was monitored by both TLC and ^1H NMR spectroscopy. Complete consumption of *trans*-**1.83** was observed after 2 h. In the NMR, this was confirmed by the complete disappearance of the signals corresponding to the methylene protons at 6.25 and 5.85 ppm. Purification of the crude material afforded adduct **4.23** in 75% yield (Scheme 82). The reaction occurred diastereoselectivity, as was seen for the previously reported reaction of helenalin with cysteine.¹¹⁸ Also, analysis of the adduct **4.23** by NMR spectroscopy confirmed that the cysteine selectively reacted with the α -methylene- γ -butyrolactone; the dienone moiety was still intact.



Scheme 82. Reaction of *trans*-**1.83** with L-cysteine to afford adduct **4.23**.

4.5 ABPP TARGET IDENTIFICATION STUDIES

Our goal of determining the molecular targets of *trans*-guaianolide **1.83** required the synthesis of an activity based probe (ABP). An ABP must contain either an analytical reporter group or ligation handle, such as an alkyne, that can later be modified through a bioorthogonal reaction. Alkynes have become the preferred modification group due to their small size, compatibility with biological systems, and success in bioorthogonal reactions (for more information on ABPs, see Section 3.1). To this end, we envisioned that an alkynyl group could be installed onto *trans*-guaianolide **1.83** through propargylation of the allylic alcohol, to afford

alkyne probe **3.79** (Figure 33). To account for non-specific binding interactions in the protein pull-down experiments, we also set out to synthesize the analogous inactive probe **4.24**, which has an α -methyl lactone rather than an α -methylene lactone. By performing the same protein pull-down experiments with both **3.79** and **4.24**, a comparison can be made between the two probes to understand what proteins interact specifically with the α -methylene- γ -butyrolactone of the active probe **3.79**.

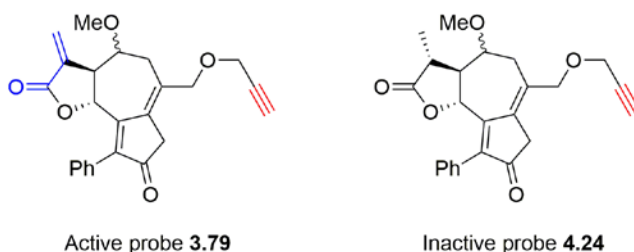
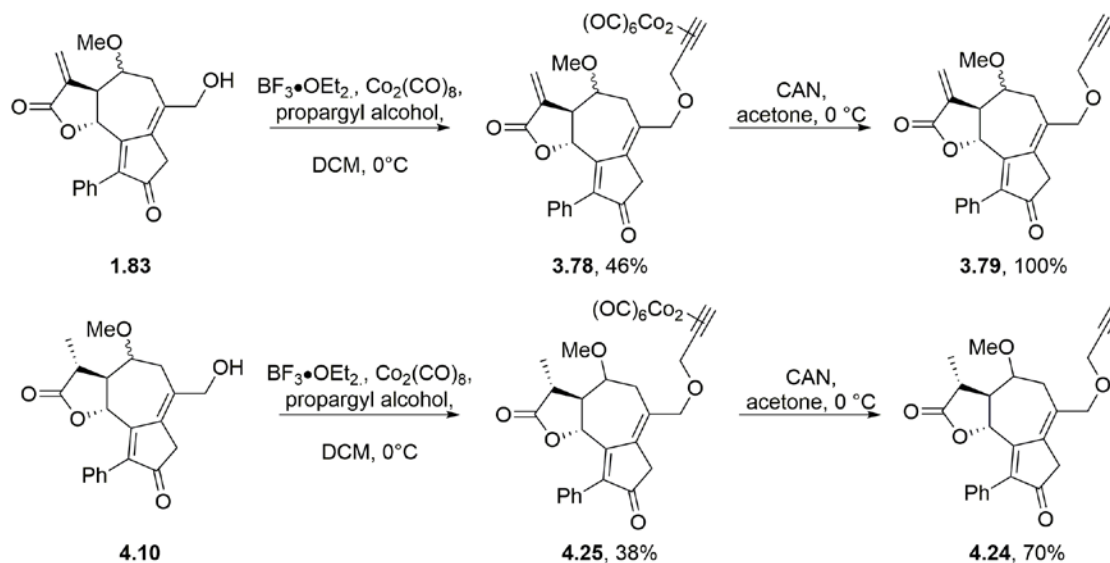


Figure 33. Proposed structures for an active and inactive activity based probe related to guaianolide analog **1.83**.

4.5.1 Synthesis of active and non-active guaianolide alkyne probes

Propargylation of hydroxyl groups is commonly achieved using the Williamson ether synthesis, where a hydroxyl group is deprotonated to form the corresponding alkoxide and then reacted with propargyl bromide to afford the corresponding propargyl ether. When **1.83** was stirred with sodium hydride for 1 h, decomposition was observed. As a result, we turned to the Nicholas reaction as an acid-mediated alternative for propargylation of hydroxyl groups. As previously discussed in Section 3.2.4, alkyne probe **3.79** was available from **1.83** in 46% yield over the 2 step process (Scheme 83). The Nicholas reaction was also utilized to synthesize the inactive probe via propargylation of the allylic alcohol of **4.10**. α -Methyl lactone **4.10** was reacted with $\text{Co}_2(\text{CO})_8$, propargyl alcohol, and $\text{BF}_3 \cdot \text{OEt}_2$ at 0 °C to afford **4.25** in 38% yield. In turn, **4.24** was achieved in 70% yield after decomplexation of **4.25**.



Scheme 83. Synthesis of active alkyne probe **3.79** and inactive probe **4.24**.

4.5.2 NF- κ B inhibition of guaianolide alkyne probe **3.79**.

One concern when designing ABPs for protein target identification is that the biological activity of the probe should be similar to that of the original parent bioactive molecule for which the probe was made.⁷⁷ The reporter group or ligation handle that is installed should not interfere with the covalent binding events *in vivo*, which could result in diminished bioactivity. For this reason, alkyne probe **3.79** was evaluated for inhibition of induced NF- κ B activity and compared to *trans*-**1.83**, the parent biomolecule of interest.

Table 20. Relative NF- κ B activity averages for cells treated with alkyne probe **3.79**.

Alkyne probe				
3.79	1 μ M	5 μ M	10 μ M	20 μ M
Trial 1	101.9	71.3	41.1	5.9
Trial 2	102.1	66.9	48.7	8.7
Trial 3	97.8	72.9	47.3	10.6
Average	100.6	70.4	45.7	8.4

Values shown are the relative NF- κ B activity (%) of A549 cells induced with TNF- α 30 min after treatment with **3.79** compared to induced A549 cells induced with no inhibitor treatment.

Interestingly, alkyne probe **3.79**, evaluated as a 2.2:1 mixture of diastereomers, showed increased inhibition ability compared to the alcohol containing *trans*-**1.83** (Table 20, Figure 34). At 20 μ M, **3.79** lowered NF- κ B activity to 8%, comparative to non-induced levels. The relative NF- κ B inhibition of 8 β H-**1.83a** and 8 α H-**1.83b** reduced NF- κ B to 31% and 42% respectively at this concentration, also shown in Figure 34 for comparison. When cells were treated with **3.79** at 10 μ M, the relative NF- κ B activity was reduced to 46% compared to non-treated cells. Given the potency of alkyne probe **3.79**, it is clear the alkyne ligation handle does not prevent the activity of the compound, and therefore can be used as a chemical tool for understanding the molecular targets of guaianolide analogs with an α -methylene- γ -butyrolactone.

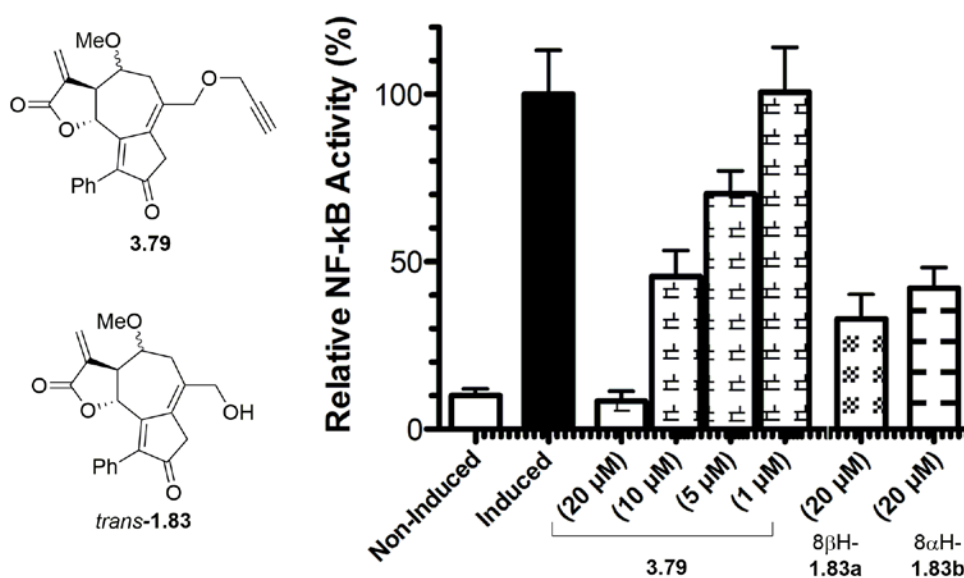


Figure 34. Pictorial representation of relative NF- κ B activity for cells treated with alkyne probe **3.79**. Data obtained for cells treated with both diastereomers of *trans*-**1.83** are also included for comparison. Cells were induced with TNF- α (15ng/mL).

4.6 CONCLUSIONS

In conclusion, progress has been made towards understanding the means by which *trans*-guaianolide **1.83** asserts its inhibitory properties toward NF- κ B. The separated diastereomers **8 β H-1.83a** and **8 α H-1.83b** were evaluated using relative NF- κ B inhibition assays which revealed that the two diastereomers had similar biological properties. Due to this assessment, other analogs could continue to be evaluated as mixture of diastereomers, with relation to the C8 methoxy group.

Previous reports have discussed the importance of the α -methylene- γ -butyrolactone for the inhibitory properties of sesquiterpene lactones. In efforts to show this was also the case for guaianolide analog **1.83**, a reduced methylene derivative **4.10** was prepared. This was achieved by reacting **2.24** with Stryker's reagent, a copper hydride complex that selectively reduced the α -methylene- γ -butyrolactone diastereoselectively to afford **11 β H,8 β H-4.15a** and **11 β H,8 α H-4.15b**. Due to triphenylphosphine and triphenylphosphine oxide impurities that resulted from using Stryker's reagent, a solid supported scavenger, iodine-modified Merrifield's resin, was used in the purification process of **4.15**, which was then desilylated to afford **4.10**. The reduced analog **4.10a** has no ability to inhibit induced NF- κ B activity, thereby revealing the necessity of the α -methylene- γ -butyrolactone for this bioactivity. Selective covalent modification of the α -methylene- γ -butyrolactone upon stirring of *trans*-**1.83** and L-cysteine also supports this conclusion.

Determining the molecular targets of *trans*-**1.83** *in vivo* would add to the knowledge about this compounds mechanism of inhibition. Toward this end, an alkyne probe derivatives **3.79** and **4.24** were designed for use in ABPP experiments. Due to the base-sensitive nature of *trans*-**1.83**, the Nicholas reaction was employed to successfully synthesize these probes.

Effective ABP probes must have similar biological properties compared to their parent biomolecule to indicate that the installed alkynyl group does not interfere with the binding events responsible for the NF- κ B inhibition. Alkyne probe **3.79** actually displayed increased potency toward NF- κ B compared to its parent molecule **1.83**. Therefore, the alkynyl group does not interfere with the potency of these guaianolide analogs for NF- κ B inhibition. In fact, an ether group at this position may be superior to the allylic alcohol present in **1.83**. Both alkyne probes will be used for ABPP to determine their molecular targets in the NF- κ B pathway.

4.7 EXPERIMENTALS

4.7.1 General Methods

All commercially available compounds were used as received unless otherwise noted. Dichloromethane (DCM), diethyl ether (Et₂O), and tetrahydrofuran (THF) were purified by passing through alumina using a solvent purification system. Deuterated chloroform (CDCl₃) was stored over 4 Å molecular sieves. Stryker's reagent ([HCu(PPh₃)]₆) was purchased from Acros organics and was stored and handled in a nitrogen filled glove box. Boron trifluoride diethyl etherate (BF₃•OEt₂) was redistilled under a nitrogen atmosphere. Dicobalt octacarbonyl (Co₂(CO)₈) was used as purchased and was stored at -20 °C and opened only in a nitrogen filled glove box. Purification of the compounds via manual flash column chromatography was performed using silica gel (40-63 μm particle size, 60 Å pore size) purchased from Sorbent Technologies. TLC analyses were performed on Silicycle SiliaPlate G silica gel glass plates (250 μm thickness) and visualized by UV irradiation (at 254 nm), KMnO₄ stain, and/or Ninhydrin

stain. ^1H NMR and ^{13}C NMR spectra were recorded on Bruker Avance 300 MHz, 400 MHz, 500 MHz, or 600 MHz. Spectra were referenced to residual chloroform (7.26 ppm, ^1H ; 77.16 ppm, ^{13}C). Chemical shifts are reported in ppm, multiplicities are indicated by s (singlet), bs (broad singlet), d (doublet), t (triplet), q (quartet), p (pentet), and m (multiplet). Coupling constants, J , are reported in hertz (Hz). All NMR spectra were obtained at room temperature. IR spectra were obtained using a Nicolet Avatar E.S.P. 360 (NaCl plate) FT-IR. ESI mass spectrometry was performed on a Waters Q-TOF Ultima API, Micromass UK Limited.

4.7.2 General Procedures

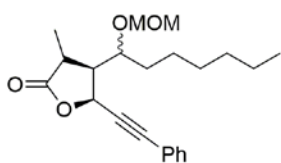
General procedure 4A: Reduction of α -methylene lactone with Stryker's reagent followed by scavenging of triphenylphosphine and triphenylphosphine oxide with Merrifield's resin. A flame-dried, single-necked, round-bottomed flask equipped with a stir bar was charged with Stryker's reagent ($[\text{CuH}(\text{PPh}_3)]_6$, 0.5 equiv) in a N_2 filled glove box. The flask was fitted with a rubber septum, transferred to a fume hood, and the septum was pierced with a N_2 inlet needle. The flask was charged with toluene and cooled to $0\text{ }^\circ\text{C}$ on an ice/water bath. The α -methylene- γ -butyrolactone (1 equiv) was dissolved in toluene (0.01 M overall) and added to the reaction flask via syringe. The reaction stirred until the methylene lactone was consumed, as evidenced by TLC or crude ^1H NMR spectroscopy. The reaction was quenched by the addition of saturated aqueous solution of NH_4Cl . The mixture was transferred to a separatory funnel and the aqueous layer was extracted with diethyl ether (3x). The combined organics were dried over MgSO_4 , filtered, and concentrated using reduced pressure rotary evaporation. The crude material was taken up in acetone (0.02 M) and transferred to a microwave vial. Sodium iodide (6 equiv) was added followed by Merrifield's resin (4.4 mmol/g loaded resin, 6.6 equiv). The vial was

sealed and swirled (no stir bar) in an incubator at rt for 18 h. The slurry was filtered through a fritted filter and the resin was rinsed successively with THF, water, acetone, and methanol (2x each solvent). The filtrate was reduced to half volume using reduced pressure rotary evaporation and then extracted with Et₂O (3x). The combined organics were dried over MgSO₄, filtered, and concentrated. The crude residue was purified using silica gel flash column chromatography to afford the α -methyl lactone.

4.7.3 General Calculations Procedure for 4.10 isomers.

The calculations performed for the compounds in Section 4.3.2 were performed using MacSpartan '14 Mechanics Program. The lowest energy conformation was defined using MMFF calculations. The lowest energy conformers were then used to calculate ¹H NMR spectral data using B3LYP/631G* functionals with NMR options. These calculations generated chemical shifts (both corrected and uncorrected) for all atoms, as well as coupling constants for proton-proton coupling.

4.7.4 Experimental procedures with compound characterization data



4-(1-(methoxymethoxy)heptyl)-3-methyl-5-

(phenylethynyl)dihydrofuran-2(3H)-one 4.17.

Follows general procedure 4A: Stryker's reagent (110 mg of a 1.3:1 ratio of diastereomers, 0.056 mmol, 1.0 equiv), toluene (2.0 mL), *cis*-guaianolide **4.16** (20 mg, 0.056 mmol) dissolved in toluene (3.6 mL). The reactions stirred for 1 h before the first work up. The crude ¹H NMR spectrum revealed formation of **4.17** with contamination of Ph₃P and Ph₃PO. The

second step was performed in acetone (2.0 mL), with sodium iodide (101 mg, 0.672 mmol, 12 equiv), and Merrifield's resin (168 mg, 0.224 mmol, 13.2 equiv). The crude residue from the second work up was purified using silica gel flash column chromatography (15% EtOAc in hexanes) to afford the title compound (14 mg, 70%) as a colorless oil and as a 1.3:1 ratio of diastereomers.

Data for 4.17.

¹H NMR (300 MHz, CDCl₃)

7.46-7.39 (m, 2H), 7.37-7.28 (m, 3H), 5.46 (d, *J* = 7.2 Hz, 1H), 5.43 (d, *J* = 6.6 Hz, 1H)*, 4.82-4.04 (m, 2H), 4.12-4.04 (m, 1H)*, 4.03-3.97 (m, 1H), 3.40 (s, 3H), 3.39 (s, 3H)*, 2.99-2.89 (m, 1H)*, 2.61-2.56 (m, 2H), 1.96-1.80 (m, 1H), 1.62-1.22 (m, 11H), 0.92-0.83 (m, 3H) ppm;

¹³C NMR (100 MHz, CDCl₃)

179.2, 178.8*, 131.8, 131.7*, 129.3*, 129.2*, 128.64*, 128.59, 121.8, 97.1, 97.0*, 89.5*, 89.3, 84.6*, 83.3, 78.7, 76.4*, 71.6*, 70.6, 56.2, 50.2, 46.0, 36.7*, 35.9, 32.3, 32.2*, 31.9, 29.8*, 29.6, 24.2, 23.8*, 22.7, 15.2, 14.2, 12.4 ppm;

*Discernable signal for the minor diastereomer

HRMS (FTMS + p ESI Full ms)

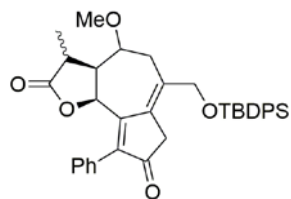
[M+H]⁺ calculated for C₂₂H₃₁O₄, 359.2217; found, 359.2203;

IR (thin film)

2929, 2854, 2238, 1784, 1491, 1463, 1156, 1037, 987, 758, 692 cm⁻¹;

TLC R_f = 0.43 (20% EtOAc in hexanes)

Silica gel, UV visible



α -Methyl *cis*-lactone 4.22. Follows general procedure 4A: Stryker's reagent (33 mg, 0.017 mmol), toluene (2.0 mL), *cis*-guaianolide analog **2.25** (20 mg of a single diastereomer, 0.034 mmol) dissolved in toluene (1.4 mL). The reaction stirred for 20 min before the first work up. The crude NMR revealed formation of **4.22** with contamination of Ph_3P and Ph_3PO . The second step was performed in acetone (1.5 mL), with sodium iodide (36 mg, 0.204 mmol), Merrifield's resin (51 mg, 0.224 mmol). The crude residue from the second work up was purified using silica gel flash column chromatography (gradient of 15-20% EtOAc in hexanes) to afford the title compound (7 mg, 34%) as a colorless oil and as a 9.6:1 ratio of diastereomers, determined by the integrations for H_6 at 5.63 and 5.44 ppm.

Data for 4.22.

^1H NMR (400 MHz, CDCl_3)

7.70-7.62 (m, 4H), 7.49-7.37 (m, 9H), 7.26-7.22 (m, 2H), 5.63 (d, $J = 7.2$ Hz, 1H)*, 5.44 (d, $J = 6.0$ Hz, 1H), 4.27 (d, $J = 13.0$ Hz, 1H), 4.20 (d, $J = 13.0$ Hz, 1H), 3.64 (dd, $J = 9.4, 4.2$ Hz, 1H), 3.38 (s, 3H)*, 3.37 (s, 3H), 3.27-3.18 (m, 1H), 3.03-2.88 (m, 3H), 2.78 (d, $J = 20.8$ Hz, 1H), 2.61-2.48 (m, 1H), 1.44 (d, $J = 7.2$ Hz, 3H), 1.38 (d, $J = 7.2$ Hz 3H)*, 1.07 (s, 9H) ppm;

* Discernable signal for minor diastereomer

^{13}C NMR (125 MHz, CDCl_3)

201.7, 178.6, 158.0, 135.8, 135.7, 133.2, 132.9, 130.4, 130.2, 130.1, 129.70, 129.65, 129.3, 128.83, 128.77, 128.1, 128.0, 74.4, 65.7, 57.1, 45.1, 40.5, 38.5, 31.7, 30.5, 27.0, 19.4, 11.9 ppm;

HRMS (FTMS + p ESI Full ms)

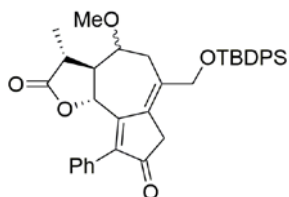
[M+H]⁺ calcd for C₃₇H₄₁O₅Si, 593.2718; found, 593.2719;

IR (thin film)

3035, 2898, 2824, 1756, 1686, 1454, 1412, 1150, 1093, 983, 726, 693 cm⁻¹;

TLC R_f = 0.15 (20% EtOAc in hexanes)

Silica gel, UV visible



α -Methyl *trans*-lactone 4.15. Follows general procedure 4A: Stryker's reagent (50 mg, 0.025 mmol, 0.5 equiv), toluene (3.8 mL), *trans*-guaianolide analog **2.24** (30 mg of a 1.6:1 mixture of diastereomers,

0.051 mmol) dissolved in toluene (1.2 mL). The reaction stirred for 1 h before the first work up.

The crude NMR revealed formation of **4.15** with contamination of Ph₃P and Ph₃PO. The second step was performed in acetone (1.8 mL), with sodium iodide (46 mg, 0.31 mmol), Merrifield's resin (76 mg of a 4.4 mmol/g loaded resin, 0.33 mmol). The crude residue from the second work up was purified using silica gel flash column chromatography (gradient of 15-30% EtOAc in hexanes) to afford the title compound (13 mg, 43%) as a 1.4:1 mixture of diastereomers.

- When the iodine-modified Merrifield's resin was not used, extensive purification via silica gel column chromatography was required. This allowed slight separation of the two diastereomers 11 β H,8 β H-**4.15a** and 11 β H,8 α H-**4.15b**, which were used for NMR characterization.

Data for 11 β H,8 β H-4.15a.

¹H NMR (400 MHz, CDCl₃)

7.72-7.64 (m, 4 H), 7.50-7.33 (m, 9 H), 7.24-7.20 (m, 2 H), 5.29 (d, *J* = 11.2 Hz, 1 H), 4.33 (d, *J* = 13.0 Hz, 1 H), 4.21 (d, *J* = 13.0 Hz, 1 H), 3.73-3.68 (m, 1 H), 3.36 (s, 3 H), 3.31 (dd, *J* = 16.0, 2.4 Hz, 1 H), 2.88 (d, *J* = 20.8 Hz, 1 H), 2.72 (d,

$J = 20.8$ Hz, 1 H), 2.50 (dq, $J = 11.6, 6.8$ Hz, 1 H), 2.41-2.34 (m, 1 H), 2.21 (ddd, $J = 11.6, 11.6, 7.2$ Hz, 1 H), 1.29 (d, $J = 6.8$ Hz, 3 H), 1.09 (s, 9 H) ppm;

Impurity seen at 1.25 ppm.

^{13}C NMR (100 MHz, CDCl_3)

201.8, 176.5, 162.2, 142.6, 135.7, 133.6, 133.1, 132.3, 131.3, 130.3, 130.2, 129.8, 128.5, 128.03, 127.97, 127.7, 82.9, 75.9, 66.5, 56.6, 53.4, 41.9, 39.4, 29.6, 27.0, 19.5, 14.6 ppm;

TLC $R_f = 0.13$ (20% EtOAc in hexanes)

Silica gel, UV visible

Data for 11 β H,8 α H-4.15b.

^1H NMR (400 MHz, CDCl_3)

7.70-7.65 (m, 4H), 7.51-7.32 (m, 9H), 7.26-7.24 (m, 2H), 5.61 (d, $J = 10.8$ Hz, 1H), 4.27 (app s, 2H), 3.69 (dt, $J = 9.2, 6.0$ Hz, 1H), 3.45 (s, 3H), 3.27 (dd, $J = 14.0, 6.4$ Hz, 1H), 3.00 (dq, $J = 12.0, 6.8$ Hz, 1H), 2.81 (d, $J = 20.8$ Hz, 1H), 2.74 (d, $J = 20.8$ Hz, 1H), 2.39-2.26 (m, 2H), 1.18 (d, $J = 6.8$ Hz, 3H), 1.10 (s, 9H) ppm;

Impurities seen at 4.12, 2.05, and 1.26 ppm due to the presence of EtOAc.

^{13}C NMR (100 MHz, CDCl_3)

201.4, 177.2, 162.6, 143.7, 135.69, 135.65, 133.13, 133.09, 133.0, 132.0, 131.3, 130.3, 129.7, 128.6, 128.09, 128.06, 127.8, 74.8, 72.8, 66.0, 57.5, 53.1, 39.5, 35.0, 32.9, 27.0, 19.5, 13.5 ppm;

Impurities seen at 60.6, 29.9, 21.2, 14.4 ppm

TLC $R_f = 0.16$ (20% EtOAc in hexanes)

Silica gel, UV visible

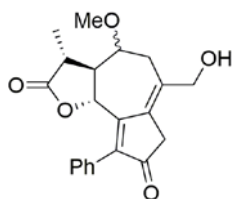
HRMS, IR data obtained using from the 1.4:1 mixture of diastereomers:

HRMS (FTMS + p ESI Full ms)

$[M+H]^+$ calcd for $C_{37}H_{41}O_5Si$, 593.2718; found, 593.2721;

IR (thin film)

2930, 2856, 1783, 1703, 1460, 1428, 1164, 1105, 701 cm^{-1} ;



11 α H-trans-guaianolide analog 4.10. A flame-dried, 5 mL, single-necked

flask with a stir bar and septum was charged with silyl ether **4.15** (16 mg of a

1.4:1 mixture of diastereomers, 0.027 mmol, 1 equiv), dissolved in

acetonitrile (0.9 mL). $NEt_3 \cdot 3HF$ was added dropwise (11 mg, 0.068 mmol, 2.5 equiv). The

reaction flask was lowered into a pre-heated oil bath (50 °C) and stirred for 17 h. The reaction

was cooled to rt and diluted with water (2 mL) and Et_2O (2 mL). The reaction mixture was

transferred to a separatory funnel and the flask was rinsed with additional water and Et_2O . The

organic layer was separated and the aqueous layer was extracted with Et_2O (2 x 5 mL). The

combined organics were dried over $MgSO_4$, filtered, and concentrated using reduced pressure

rotary evaporation. The crude reaction mixture was purified by silica gel flash column

chromatography (50 mL of 50% $EtOAc$ in hexanes followed by 100 mL 100% $EtOAc$) to afford

the title compound (6.5 mg, 71%) as a colorless oil and as a 1.2:1 mixture of diastereomers.

- When 11 β H,8 β H-**4.15a** (15 mg, 0.0253 mmol, 1 equiv) as a single diastereomer was stirred with $NEt_3 \cdot 3HF$ using the same procedure, 6 mg of 11 β H,8 β H-**4.10a** was afforded in 63% yield.

Data for **4.10** as a 1.2:1 mixture of diastereomers (**4.10a** : **4.10b**).

1H NMR (500 MHz, $CDCl_3$)

7.41-7.31 (m, 3H), 7.29-7.24 (m, 2H), 5.66 (d, $J = 10.5$ Hz, 1H)*, 5.36 (d, $J = 11.0$ Hz, 1H), 4.29 (d, $J = 12.0$ Hz, 1H), 4.28 (app s, 2H)*, 4.18 (d, $J = 12.0$ Hz, 1H), 3.77-3.69 (m, 1H), 3.48 (s, 3H), 3.46 (s, 3H)*, 3.32-3.13 (m, 2H), 3.08 (dd, $J = 15.5, 2.5$ Hz, 1H), 3.05-2.98 (m, 1H)*, 2.58-2.49 (m, 2H), 2.47-2.36 (m, 2H)*, 2.27 (ddd, $J = 11.5, 11.5, 4.5$ Hz, 1H), 1.30 (d, $J = 7.0$ Hz, 3H), 1.18 (d, $J = 7.0$ Hz, 3H)* ppm;

Impurities seen at 9.20, 6.25, 5.30, 5.11, 2.13, 2.04, 1.43, 1.26, 0.88 ppm.

^{13}C NMR (125 MHz, CDCl_3)

201.5, 201.3*, 177.1*, 176.3, 162.6*, 162.0, 144.4*, 143.7, 134.2*, 133.9, 132.8, 131.7*, 131.2*, 131.1, 129.8, 129.7*, 128.73*, 128.69, 127.84*, 127.78, 82.9, 75.8, 74.7*, 72.8*, 65.3*, 65.2, 57.6*, 57.1, 53.6, 53.1*, 41.9, 39.8*, 39.6, 35.1*, 33.5*, 31.2, 14.6, 13.4* ppm;

Impurities seen at 171.3, 60.5, 14.4 ppm.

* Minor **4.10b** diastereomer

HRMS (FTMS + p ESI Full ms)

$[\text{M}+\text{H}]^+$ calcd for $\text{C}_{21}\text{H}_{23}\text{O}_5$, 355.15400; found, 355.15417;

IR (thin film)

3433, 2923, 2853, 1778, 1696, 1457, 1392, 1227, 1166, 1095, 1032 cm^{-1} ;

TLC $R_f = 0.21$ (100% EtOAc)

Silica gel, UV visible

Data for **4.10a** as a single diastereomer

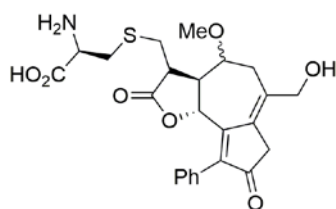
^1H NMR (400 MHz, CDCl_3)

7.40-7.33 (m, 3 H), 7.27-7.22 (m, 2 H), 5.36 (d, $J = 11.2$ Hz, 1 H), 4.30 (d, $J = 12.4$ Hz, 1 H), 4.18 (d, $J = 12.4$ Hz, 1 H), 3.73-3.69 (m, 1 H), 3.48 (s, 3 H), 3.29 (d, $J = 20.4$ Hz, 1 H), 3.16 (d, $J = 20.4$ Hz, 1 H), 3.08 (dd, $J = 15.6, 2.4$ Hz, 1 H), 2.59-2.48 (m, 2 H), 2.27 (ddd, $J = 11.6, 11.6, 7.4$ Hz, 1 H), 1.31 (d, $J = 7.4$ Hz, 3 H) ppm;

Impurities seen at 7.69, 7.52, 7.49, 4.14, 2.04, 1.25, 0.88 ppm;

^{13}C NMR (125 MHz, CDCl_3)

201.4, 176.3, 162.0, 143.6, 133.9, 132.8, 131.1, 129.8, 128.7, 127.8, 82.9, 75.8, 65.2, 57.1, 53.5, 41.9, 39.5, 31.2, 14.6 ppm;



Cysteine adduct 4.23. In a vial, **1.83** (12 mg of a 4:1 ratio of $8\beta\text{H}$ -

1.83a: $8\alpha\text{H}$ -**1.83b**, 0.034 mmol, 1 equiv) was dissolved in 1 mL

DCM. This solution was transferred to a 5 mL flask, the DCM was

evaporated off using reduced pressure rotary evaporation, and the **1.83** was dried under high vacuum. The flask was equipped with a stir bar and charged with acetone (0.069 mL) followed by aqueous phosphate buffer with a pH of 7.2 (1 mL). L-Cysteine (4 mg, 0.034 mmol, 1 equiv) was added and stirred for 2 h while the reaction was monitored by TLC (solvent system was the bottom layer of CHCl_3 /methanol/water, 7:3:1, product visible using ninhydrin stain). Upon completion of the reaction, the solvent was evaporated under reduced pressure giving a yellow orange crude material (22 mg). The crude material was purified using silica gel flash chromatography (bottom layer of CHCl_3 , methanol, water solution; 7:3:1) to give 12 mg of adduct **4.23** in 75% yield. ^1H NMR of the crude material had shown the presence of both diastereomers, however only the $8\beta\text{H}$ -adduct was obtained after purification. The purified material of **4.23** became contaminated with DMF through unknown means.

Data for 4.23

¹H NMR (600MHz, D₂O)

7.43-7.41 (m, 3 H), 7.24-7.22 (m, 2 H), 5.74 (d, *J* = 11.0 Hz, 1 H), 4.29 (d, *J* = 13.2 Hz, 1 H), 4.15 (dd, *J* = 13.2, 2.4 Hz, 1 H), 4.06-4.02 (m, 1 H), 3.89-3.86 (m, 1H), 3.46 (s, 3 H), 3.40 (d, *J* = 21.0 Hz, 1 H), 3.39-3.30 (m, 1 H), 3.32 (d, *J* = 21.0 Hz, 1 H), 3.19-2.91 (m, 5 H) 2.67-2.60 (m, 2 H) ppm;

Impurities seen at 7.91, 2.99, and 2.83 ppm due to the presence of DMF.

¹³C NMR (150 MHz, D₂O)

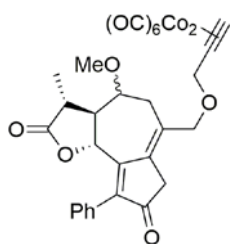
208.2, 178.8, 173.3, 165.9, 142.04, 136.2, 133.8, 132.3, 130.3, 129.1, 128.7, 82.5, 78.0, 65.1, 56.8, 54.6, 49.6, 47.6, 39.7, 35.0, 31.0, 30.5 ppm;

Impurities seen at 165.7, 129.3, 37.7, and 32.2 ppm.

TLC

R_f = 0.14 (bottom layer of a chloroform, methanol, and water solution; 7:3:1)

Silica gel, UV, Ninhydrin stain.



Co₂(CO)₆-reduced methylene alkyne probe 4.25. Follows general procedure 3C.2 (Section 3.4.2): Propargyl alcohol (2 mg, 0.037 mmol), DCM (0.3 mL), Co₂(CO)₈ (13 mg, 0.037 mmol), guaianolide analog **4.10** (7 mg of a 1.2:1 mixture of diastereomers, 0.018 mmol), dissolved in DCM (0.2

mL), and BF₃•OEt₂ (7 mg, 0.046 mmol). The reaction was stirred for 45 min. The crude residue was purified by silica gel flash column chromatography (gradient of 20-50% ethyl acetate in hexanes) to afford 5 mg of **4.25** in 38% yield as a dark red oil and as a ~1 :1 mixture of diastereomers. ¹H NMR showed that **4.25** was 85% pure, due to contamination with an unknown, but structurally related by-product.

- When 11 β H,8 β H-**4.10a** (4 mg of a single diastereomer, 0.013 mmol) was subjected to the same procedure, 1 mg of the corresponding 11 β H,8 β H-**4.25a** was afforded in 16% yield.

Data for **4.25** as mixture of diastereomers.

¹H NMR (500 MHz, CDCl₃)

7.49-7.32 (m, 3 H), 7.30-7.25 (m, 2 H), 6.08 (s, 1 H), 5.66 (d, *J* = 11.0 Hz, 1 H)*, 5.35 (d, *J* = 11.0 Hz, 1 H), 4.72-4.62 (m, 2 H), 4.35-4.21 (m, 2 H), 3.80-3.65 (m, 1 H), 3.45 (s, 3 H), 3.42 (s, 3 H)*, 3.31-2.96 (m, 3 H), 2.58-2.48 (m, 1 H), 2.46-2.34 (m, 1 H), 2.33-2.23 (m, 1 H), 1.30 (d, *J* = 7.0 Hz, 3 H), 1.15 (d, *J* = 7.0 Hz, 3 H)* ppm;

Impurities seen at 10.0, 5.78, 5.59, 5.26, 4.12, 3.50, 3.43, 2.80-2.68, 2.04, 1.43, 1.26, 0.88 ppm.

*Discernable signal for the 11 β H,8 α H-**4.25b** diastereomer.

¹³C NMR (125 MHz, CDCl₃)

201.7, 201.2*, 199.8, 177.2, 176.4*, 162.7, 162.1*, 144.5*, 143.4, 135.2, 134.3*, 133.1, 131.4*, 131.2, 131.1*, 129.8*, 129.7, 128.8*, 128.7, 127.9, 127.8*, 91.7, 91.4*, 83.0, 75.9, 74.6*, 73.3*, 73.2, 72.4*, 71.5, 71.1*, 57.4, 56.7*, 53.5*, 53.1, 42.0, 40.0, 39.8*, 35.0*, 33.7*, 29.9, 14.6*, 13.3 ppm;

Impurities seen at 130.1, 128.0, 60.5, 21.2 14.4 ppm;

*Discernable signal for one of the diastereomers.

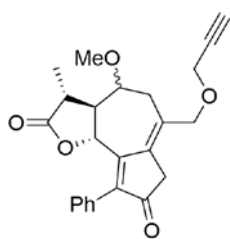
TLC R_f = 0.38 (40% EtOAc in hexanes)

Silica gel, UV visible

Data for 11 β H,8 β H-**4.25a** as a single diastereomer.

¹H NMR (400 MHz, CDCl₃)

7.40-7.32 (m, 3 H), 7.28-7.24 (m, 2 H), 6.08 (s, 1 H), 5.35 (d, $J = 10.8$ Hz, 1 H), 4.68 (d, $J = 12.0$ Hz, 1 H), 4.63 (d, $J = 13.6$ Hz, 1 H), 4.33 (d, $J = 12.4$ Hz, 1 H), 4.22 (d, $J = 12.8$ Hz, 1 H), 3.76-3.69 (m, 1 H), 3.45 (s, 3 H), 3.25 (app s, 2 H), 3.23-3.16 (m, 1 H), 2.58-2.47 (m, 1 H), 2.44-2.38 (m, 1 H), 2.27 (ddd, $J = 11.6, 11.6, 7.0$ Hz, 1 H), 1.30 (d, $J = 7.0$ Hz, 3 H) ppm;



Reduced methylene alkyne probe 4.24. Follows general procedure 3D (Section 3.4.2): cobalt complex **4.25** (5 mg of a 1:1 mixture of diastereomers, 0.0066 mmol, 1 equiv), acetone (0.5 mL), and ceric ammonium nitrate (15 mg, 0.027 mmol, 4 equiv). The reaction stirred for 15 min. The crude residue

was purified by silica gel flash column chromatography (gradient of 30-50% Et₂O in hexanes to afford 2 mg of propargyl ether **4.24** as a mixture of two diastereomers (1.2:1) in 70% yield as a colorless oil. ¹H NMR revealed the material was 78% pure with an inseparable, unidentified impurity. The mixture was sent to collaborators Dan Harki and John Widen for further purification, characterization, and biological evaluation.

Data for 4.24.

¹H NMR (500 MHz, CDCl₃)

7.49 -7.31 (m, 3 H), 7.29-7.25 (m, 2 H), 5.66 (d, $J = 11.0$ Hz, 1 H)*, 5.34 (d, $J = 11.0$ Hz, 1 H), 4.28-4.15 (m, 4 H), 3.84-3.62 (m, 1 H), 3.46 (s, 3 H)*, 3.45 (s, 3 H), 3.36-2.97 (m, 3 H), 2.59-2.44 (m, 3 H), 2.43-2.09 (m, 1 H), 1.30 (d, $J = 6.3$ Hz, 3 H). 1.19 (d, $J = 6.3$ Hz, 3 H)* ppm;

* Discernable signal for one of the diastereomers.

Impurities seen at 10.0, 5.77, 5.46, 4.12, 3.49, 3.43, 2.70, 2.04, 1.54, 1.38, 1.25, 0.87 ppm.

TLC

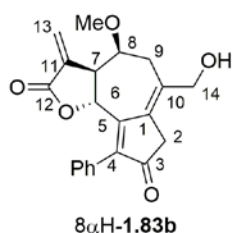
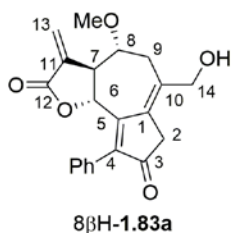
$R_f = 0.34$ (50% Et₂O in hexanes)

Silica gel, UV visible

APPENDIX A

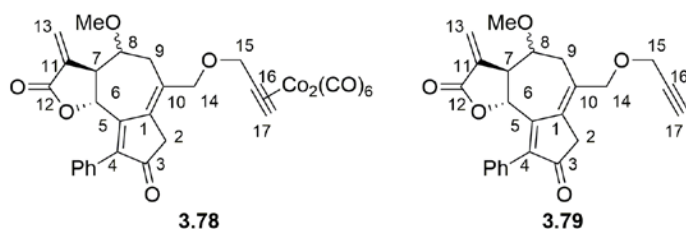
TABLES OF NMR DATA FOR GUAIANOLIDE ANALOGS

Table 21. ^1H and ^{13}C NMR data for **1.83a** and **1.83b**.



Compound	8βH-1.83a		8αH-1.83b	
Position	^1H signal(s) ppm	^{13}C signal(s) ppm	^1H signal(s) ppm	^{13}C signal(s) ppm
1	---	133.9	---	133.7
2	3.29 (d, $J = 21.0$ Hz, 1 H), 3.17 (d, $J = 21.0$ Hz, 1 H)	39.5	3.28-3.15 (m, 2 H)	39.9
3	---	201.4	---	201.3
4	---	143.3	---	144.1
5	---	161.6	---	162.2
6	5.39 (d, $J = 10.5$ Hz, 1 H)	75.8	5.78 (d, $J = 9.2$ Hz, 1 H)	74.9
7	3.18-3.13 (m, 1 H)	50.0	3.37-3.31 (m, 1H)	49.8
8	3.86 (ddd, $J = 8.0, 4.0, 2.5$ Hz, 1 H)	81.7	4.14-4.07 (m, 1 H)	74.0
9	3.16-3.12 (m, 1 H) 2.56 (dd, $J = 15.8, 2.5$ Hz, 1 H)	30.6	3.27 (dd, $J = 15.2, 6.8$ Hz, 1 H) 2.53 (dd, $J = 15.2, 8.4$ Hz, 1 H)	33.9
10	---	133.0	---	132.2
11	---	137.2	---	134.2
12	---	167.8	---	168.4
13	6.25 (d, $J = 3.5$ Hz, 1 H) 5.85 (d, $J = 3.0$ Hz, 1 H)	122.1	6.36 (d, $J = 3.6$ Hz, 1 H) 5.52 (d, $J = 3.2$ Hz, 1 H)	123.0
14	4.31 (d, $J = 12.5$ Hz, 1H), 4.19 (d, $J = 12.5$ Hz, 1 H)	65.3	4.34-4.26 (m, 2 H)	65.6
-OMe	3.54 (s, 3 H)	56.9	3.45 (s, 3 H)	57.5
Phenyl ring	7.40-7.32 (m, 3 H) 7.27-7.24 (m, 2 H)	130.7, 130.0, 128.8, 127.8,	7.45-7.32 (m, 3 H), 7.30-7.26 (m, 2 H)	130.8, 130.0, 128.9, 127.9

Table 22. ¹H and ¹³C NMR data for **3.78** and **3.79**.

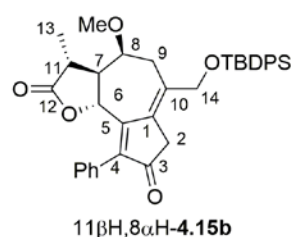
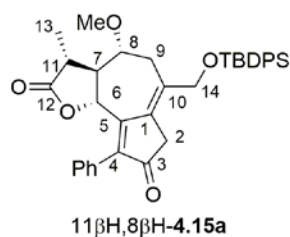


Compound	3.78		3.79	
Position	¹ H signal(s) ppm	¹³ C signal(s) ppm	¹ H signal(s) ppm	¹³ C signal(s) ppm
1	---	134.0, 133.6*	---	135.4, 133.6*
2	3.32-3.14 (m, 2 H)	40.0*, 39.7	3.39-3.24 (m, 2 H)	40.0*, 39.7
3	---	201.4, 201.0*	---	201.5, 201.3*
4	---	144.0*, 143.0	---	144.2*, 143.2
5	---	162.2*, 161.5	---	161.9*, 161.4
6	5.78 (d, <i>J</i> = 9.6 Hz, 1 H) 5.38 (d, <i>J</i> = 10.4 Hz, 1 H)	75.7, 74.7*	5.78 (d, <i>J</i> = 9.6 Hz, 1 H)* 5.38 (d, <i>J</i> = 10.4 Hz, 1 H)	75.7, 74.8*
7	3.32-3.14 (m, 1 H)	49.8	3.22-3.11 (m, 1 H)	49.8, 49.7*
8	4.10-4.05 (m, 1 H)* 3.88-3.86 (m, 1 H)	81.8, 73.6*	4.09-4.06 (m, 1 H)* 3.87-3.84 (m, 1 H)	81.8, 73.8*
9	3.32-3.14 (m, 1 H) 2.52-2.41 (m, 1 H)	33.8*, 29.5	3.22-3.11 (m, 1 H) 2.52-2.46 (m, 1 H)	34.2*, 30.0
10	---	131.6, 130.3*	---	130.9, 129.7*
11	---	137.2, 135.0*	---	137.2, 135.8*
12	---	168.3*, 167.9	---	168.3*, 167.9
13	6.34 (d, <i>J</i> = 3.6 Hz, 1 H)* 6.24 (d, <i>J</i> = 3.2 Hz, 1 H) 5.86 (d, <i>J</i> = 3.2 Hz, 1 H) 5.47 (d, <i>J</i> = 3.2 Hz, 1 H)*	122.8*, 122.2	6.36 (d, <i>J</i> = 3.2 Hz, 1 H)* 6.24 (d, <i>J</i> = 3.2 Hz, 1 H) 5.88 (d, <i>J</i> = 2.8 Hz, 1 H) 5.52 (d, <i>J</i> = 3.2 Hz, 1 H)*	122.9*, 122.2
14	4.33 (d, <i>J</i> = 12.4 Hz, 1H), 4.25 (d, <i>J</i> = 12.8 Hz, 1 H) 4.26 (app s, 2 H)*	73.4, 73.3*	4.23-4.16 (m, 2 H)	75.6, 75.4*
15	4.71-4.61 (m, 2 H)	71.4*, 71.1	4.23-4.16 (m, 2 H)	71.9*, 71.5
16	---	90.7*, 90.6	---	79.5, 79.3*
17	6.09 (s, 1 H)	71.9, 71.6*	2.52-2.46 (m, 1 H)	57.8*, 57.2
Co ₂ (CO) ₆	---	199.6	---	---
-OMe	3.51 (s, 3 H) 3.39 (s, 3 H)*	57.2*, 56.5	3.51 (s, 3 H) 3.43 (s, 3 H)*	57.4*, 56.5
Phenyl ring	7.40-7.35 (m, 3 H) 7.31-7.26 (m, 2 H)	130.72*, 130.65, 130.0, 129.9*, 128.84*, 128.77, 127.8*, 127.7	7.38-7.35 (m, 3 H) 7.30-7.24 (m, 2 H)	130.73*, 130.65, 129.93, 129.89*, 128.9*, 128.8, 127.80*, 127.75

*Discernable signal for minor diastereomer.

*Discernable signal for minor diastereomer.

Table 23. ^1H and ^{13}C NMR data for **4.15a** and **4.15b**.

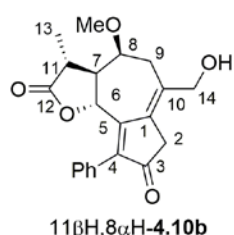
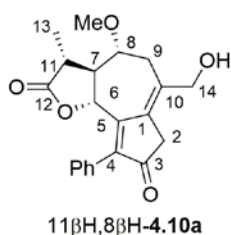


Compound	4.15a		4.15b	
Position	^1H signal(s) ppm	^{13}C signal(s) ppm	^1H signal(s) ppm	^{13}C signal(s) ppm
1	---	133.6	---	b
2	2.88 (d, $J = 20.8$ Hz, 1 H), 2.72 (d, $J = 20.8$ Hz, 1 H)	39.4	2.81 (d, $J = 20.8$ Hz, 1 H) 2.74 (d, $J = 20.8$ Hz, 1 H)	39.5
3	---	201.8	---	201.4
4	---	142.6	---	143.7
5	---	162.2	---	162.6
6	5.29 (d, $J = 11.6$ Hz, 1 H)	75.9	5.61 (d, $J = 10.8$ Hz, 1 H)	74.8
7	2.21 (ddd, $J = 11.6, 11.6, 7.2$ Hz, 1 H)	53.4	2.39-2.26 (m, 1 H)	53.1
8	3.73-3.68 (m, 1 H)	82.9	3.69 (dt, $J = 9.2, 6.0$ Hz, 1 H)	72.8
9	3.31 (dd, $J = 16.0, 2.4$ Hz, 1 H) 2.41-2.34 (m, 1 H)	29.6	3.27 (dd, $J = 14.0, 6.4$ Hz, 1 H) 2.39-2.26 (m, 1 H)	32.9
10	---	a	---	b
11	2.50 (dq, $J = 11.6, 6.8$ Hz, 1 H)	41.9	3.00 (dq, $J = 12.0, 6.8$ Hz, 1 H)	35.0
12	---	176.5	---	177.2
13	1.29 (d, $J = 6.8$ Hz, 3 H),	14.6	1.18 (d, $J = 6.8$ Hz, 3 H)	13.5
14	4.33 (d, $J = 13.0$ Hz, 1 H), 4.21 (d, $J = 13.0$ Hz, 1 H)	66.5	4.27 (app s, 2 H)	66.0
-OMe	3.36 (s, 3 H)	56.6	3.45 (s, 3 H)	57.1
Phenyl ring	7.72-7.64 (m, 4 H) 7.50-7.33 (m, 9 H) 7.24-7.20 (m, 2 H)	a, 129.8, 128.5, 127.7	7.70-7.65 (m, 4 H) 7.51-7.32 (m, 9 H) 7.26-7.24 (m, 2 H)	b, 129.7, 128.6, 127.8
TBDPS phenyl		135.7, 133.1, 130.3, 130.2 128.03, 127.97		135.69, 135.65, 133.13, 133.09, 130.03, 130.00, 128.09, 128.06
TBDPS tert-butyl	1.09 (s, 9 H)	27.0, 19.5	1.10 (s, 9 H)	27.0, 19.5

^aC10, and the substituted aromatic carbon are the signals at 132.3, and 131.3, but could not be assigned.

^bC1, C10, and the substituted aromatic carbon are the signals at 133.0, 132.0, and 131.3 but could not be assigned.

Table 24. ^1H and ^{13}C NMR data for **4.10a** and **4.10b**.



Compound	4.10a		4.10b^b	
Position	^1H signal(s) ppm	^{13}C signal(s) ppm	^1H signal(s) ppm	^{13}C signal(s) ppm
1	---	133.9	---	134.2
2	3.29 (d, $J = 20.4$ Hz, 1 H), 3.16 (d, $J = 20.4$ Hz, 1 H)	39.5	(3.31-3.14 m, 2H)	39.8
3	---	201.4	---	201.3
4	---	143.6	---	144.4
5	---	162.0	---	162.6
6	5.36 (d, $J = 11.2$ Hz, 1 H)	75.8	5.66 (d, $J = 10.5$ Hz, 1 H)	74.7
7	2.27 (ddd, $J = 11.6, 11.6, 7.4$ Hz, 1 H)	53.5	2.47-2.36 (m, 1 H)	53.1
8	3.73-3.69 (m, 1 H)	82.9	3.78-3.70 (m 1 H)	72.8
9	3.08 (dd, $J = 15.6, 2.4$ Hz, 1 H) 2.59-2.48 (m, 1 H)	31.2	c 2.47-2.36 (m, 1 H)	33.5
10	---	a	---	d
11	2.59-2.48 (m, 1 H)	41.9	3.05-2.98 (m, 1 H)	35.1
12	---	177.1	---	177.1
13	1.31 (d, $J = 7.4$ Hz, 3 H)	14.6	1.18 (d, $J = 7.0$ Hz, 3 H)	13.4
14	4.30 (d, $J = 12.4$ Hz, 1 H), 4.18 (d, $J = 12.4$ Hz, 1 H)	65.2	4.28 (app s, 2 H)	65.3
-OMe	3.48 (s, 3 H)	57.1	3.46 (s, 3 H)	57.6
Phenyl ring	7.40-7.33 (m, 3 H), 7.27-7.22 (m, 2 H)	a, 129.8, 128.7, 127.8	7.40-7.33 (m, 3 H), 7.27-7.22 (m, 2 H)	129.7, 128.7, 127.8, d

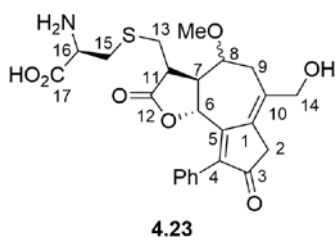
^aC10, and the substituted aromatic carbon are the signals at 132.8 and 131.1, but could not be assigned.

^b**4.10b** was not isolated. Assignments based upon spectrum obtained for a mixture of **4.10a** and **b**

^c ^1H of position 9 buried in multiplet from 3.31-3.12 ppm

^dC10, and the substituted aromatic carbon are the signals at 131.7, and 131.2 but could not be assigned.

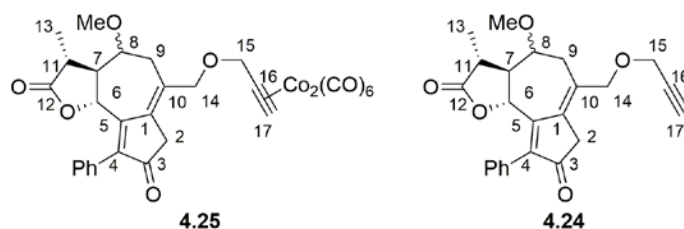
Table 25. ^1H and ^{13}C NMR data for cysteine adduct **4.23**.



Position	^1H Signal(s)	^{13}C signal(s)
1	---	136.2
2	3.40 (d, $J = 21.0$ Hz, 1 H) 3.32 (d, $J = 21.0$ Hz, 1 H)	39.7
3	---	208.2
4	---	142.0
5	---	165.9
6	5.74 (d, $J = 11.0$ Hz, 1 H)	78.0
7	2.67-2.60 (m, 1 H)	49.6
8	4.06-4.02 (m, 1 H)	82.5
9	3.39-3.30 (m, 1 H) 2.67-2.60 (m, 1 H)	35.0
10	---	133.8
11	3.19-2.91 (m, 1 H)	47.6
12	---	178.8
13	3.19-2.91 (m, 2 H)	a
14	4.29 (d, $J = 13.2$ Hz, 1 H), 4.15 (dd, $J = 13.2, 2.4$ Hz, 1 H)	65.1
15	3.19-2.91 (m, 2 H)	a
16	3.89-3.86 (m, 1H)	54.6
17	---	173.3
OMe	3.46 (s, 3 H)	56.8
Phenyl	7.43-7.41 (m, 2 H), 7.24-7.22 (m, 3 H)	132.3, 130.3, 129.1, 128.7

^aC13 and C15 are represented by the signals at 31.0 and 30.5 ppm

Table 26. ^1H NMR data for **4.25** and **4.24**.



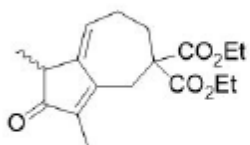
Compound	11βH,8βH-4.25a	4.25^a	4.24^a
Position	^1H signal(s)	^1H signal(s)	^{13}C signal(s)
1	---	---	135.2, 134.3*
2	3.25 (app s, 2 H)	3.31-2.96 (m, 2H)	40.0, 39.8*
3	---	---	201.7, 201.2*
4	---	---	144.5, 143.4*
5	---	---	162.7, 162.1*
6	5.35 (d, $J = 10.8$ Hz, 1 H)	5.66, (d, $J = 11.0$ Hz, 1 H)* 5.35 (d, $J = 11.0$ Hz, 1 H)	75.9, 74.6*
7	2.27 (ddd, $J = 11.6, 11.6, 7.0$ Hz, 1H)	2.33-2.23 (m, 1H)	53.5*, 53.1
8	3.76-3.69 (m, 1H)	3.80-3.65 (m, 1H)	83.0, 73.3*
9	3.23-3.16 (m, 1 H) 2.44-2.38 (m, 1 H)	3.31-2.96 (m, 2H) 2.46-2.34 (m, 1H)	33.7*, 29.9
10	---	---	133.1, 131.4*
11	2.58-2.47 (m, 1H)	2.58-2.48 (m, 1H)	42.0, 35.0*
12	---	---	177.2, 176.4*
13	1.30 (d, $J = 7.0$ Hz, 3H)	1.30 (d, $J = 7.0$ Hz, 3H) 1.15 (d, $J = 7.0$ Hz, 3H)*	14.6*, 13.3
14	4.33 (d, $J = 12.4$ Hz, 1H), 4.22 (d, $J = 12.8$ Hz, 1 H)	4.35-4.21 (m, 2H)	73.2, 72.4*
15	4.68 (d, $J = 12.0$ Hz, 1 H) 4.63 (d, $J = 13.6$ Hz, 1 H)	4.72-4.62 (m, 2H)	71.5, 71.1*
16	---	---	91.7, 91.4*
17	6.08 (s, 1H)	6.08 (s, 1H)	71.9, 71.6*
$\text{Co}_2(\text{CO})_6$	---	---	199.8
-OMe	3.45 (s, 3H)	3.45 (s, 3H) 3.42 (s, 3H)*	57.4, 56.7*
Phenyl ring	7.40-7.32 (m, 3 H) 7.28-7.24 (m, 2 H)	7.49-7.32 (m, 3H) 7.30-7.25 (m, 2H)	131.2, 131.1*, 129.8*, 129.7, 128.8*, 128.7, 127.9, 127.8*

*Discernable signal for one diastereomer. ^aSpectrum obtained of an impure mixture of diastereomers.
^bH₇, H₉, H₁₁ are represented by 3.36 (m, 1H), 2.59-2.44 (m, 2H), and 2.43-2.09 (m, 1H) but could not be assigned due to the impure nature of the spectrum and possible overlap of signals for the 2 diastereomers.

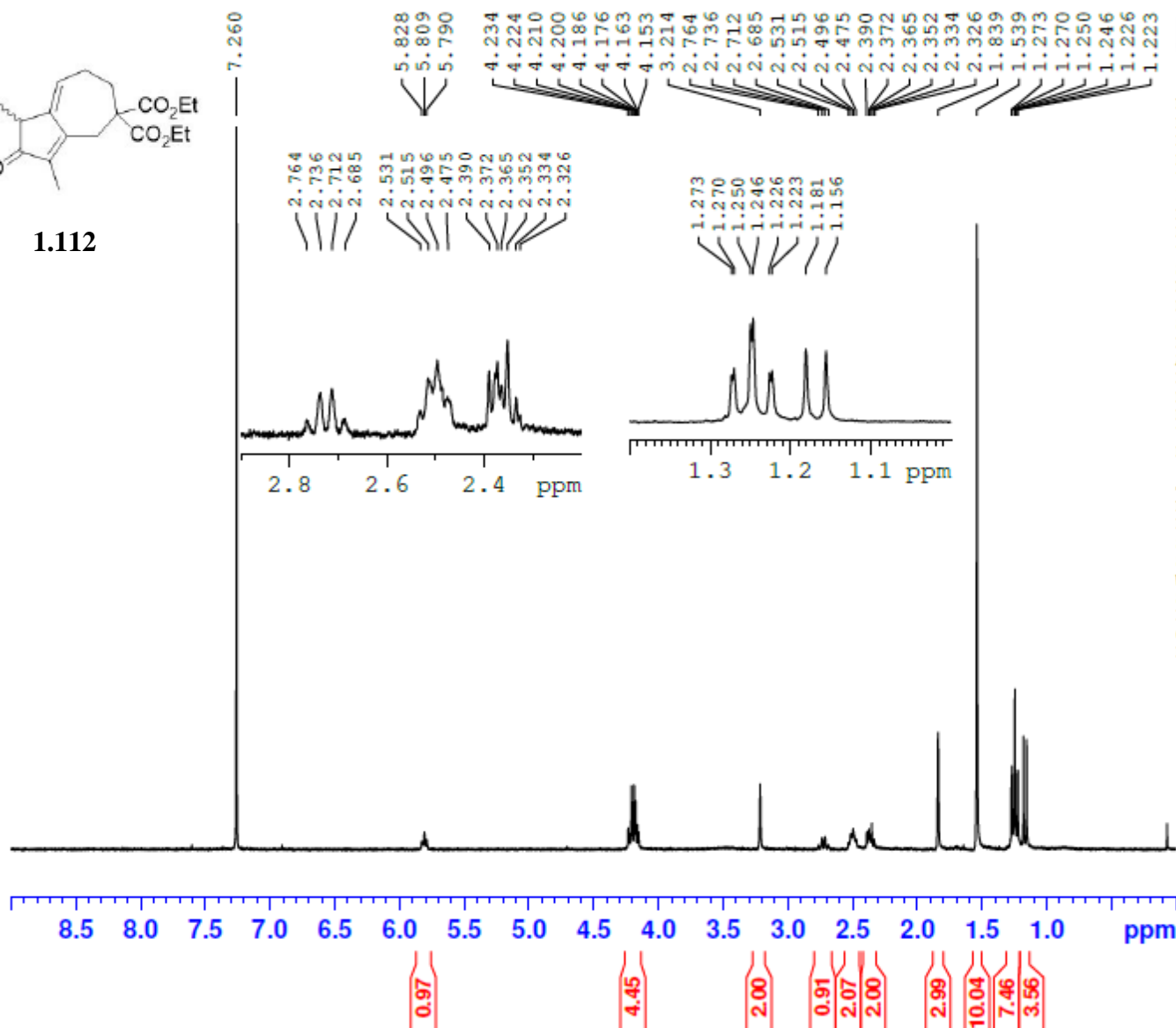
APPENDIX B

^1H AND ^{13}C NMR SPECTRA

SW04-083-A



1.112



NAME SW04-083-A
 EXPNO 10
 PROCNO 1
 Date_ 20131023
 Time 9.47
 INSTRUM spect
 PROBHD 5 mm QNP 1H/1
 PULPROG zg30
 ID 32768
 SOLVENT CDCl3
 NS 16
 DS 2
 SWH 6188.119 Hz
 FIDRES 0.188846 Hz
 AQ 2.6477044 sec
 RG 322
 DW 80.800 usec
 DE 6.50 usec
 TE -923.0 K
 D1 1.00000000 sec

----- CHANNEL f1 -----
 NUC1 1H
 P1 12.71 usec
 SI 32768
 SF 300.2300089 MHz
 WDW EM
 SSB 0
 LB 0.10 Hz
 GB 0
 PC 1.00

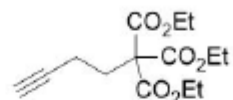
SW04-175-Aco12 1H 400



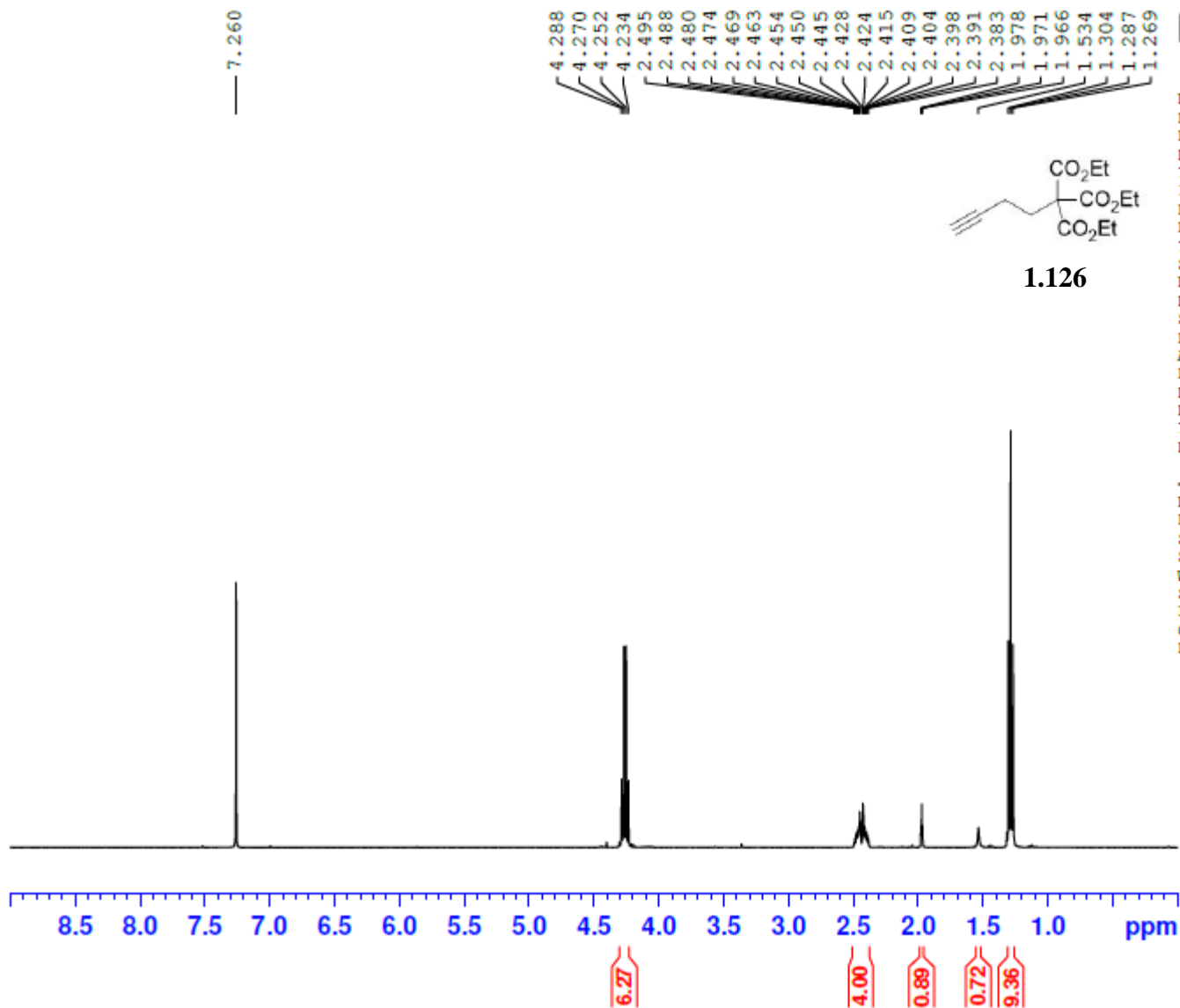
NAME SW04-175-Aco12
EXPNO 10
PROCNO 1
Date_ 20140310
Time_ 14.03
INSTRUM spect
PROBHD 5 mm PABBO BB-
PULPROG zg30
ID 65536
SOLVENT CDC13
NS 16
DS 2
SWH 8223.685 Hz
FIDRES 0.125483 Hz
AQ 3.9846387 sec
RG 161
DW 60.800 usec
DE 6.50 usec
TE 305.1 K
D1 1.00000000 sec

----- CHANNEL f1 -----
NUC1 1H
P1 13.75 usec
SI 65536
SF 400.1300100 MHz
WDW EM
SSB 0
LB 0.30 Hz
GB 0
PC 1.00

4.288
4.270
4.252
4.234
2.495
2.488
2.480
2.474
2.469
2.463
2.454
2.450
2.445
2.428
2.424
2.415
2.409
2.404
2.398
2.391
2.383
1.978
1.971
1.966
1.534
1.304
1.287
1.269



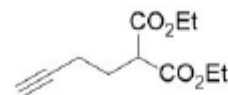
1.126



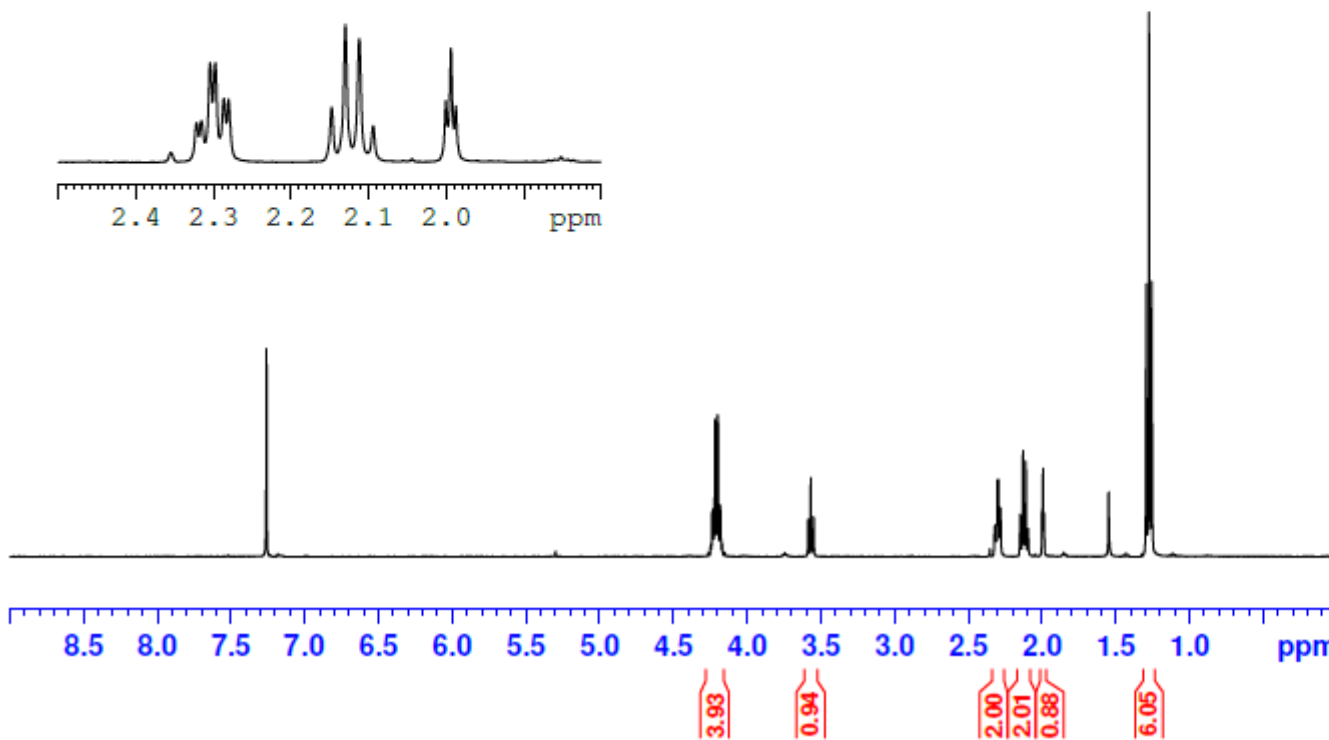
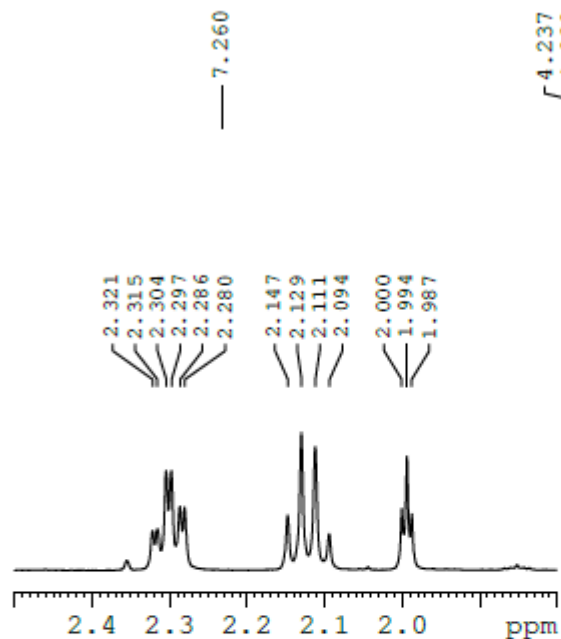
SW04-139-A 1H 400



NAME SW04-139-A
EXPNO 10
PROCNO 1
Date_ 20140204
Time 12.25
INSIRUM spect
PROBHD 5 mm PABBO BB-
PULPROG zg30
ID 65536
SOLVENT CDCl3
NS 16
DS 2
SWH 8223.685 Hz
FIDRES 0.125483 Hz
AQ 3.9846387 sec
RG 144
DW 60.800 usec
DE 6.50 usec
TE 263.1 K
D1 1.00000000 sec



1.127

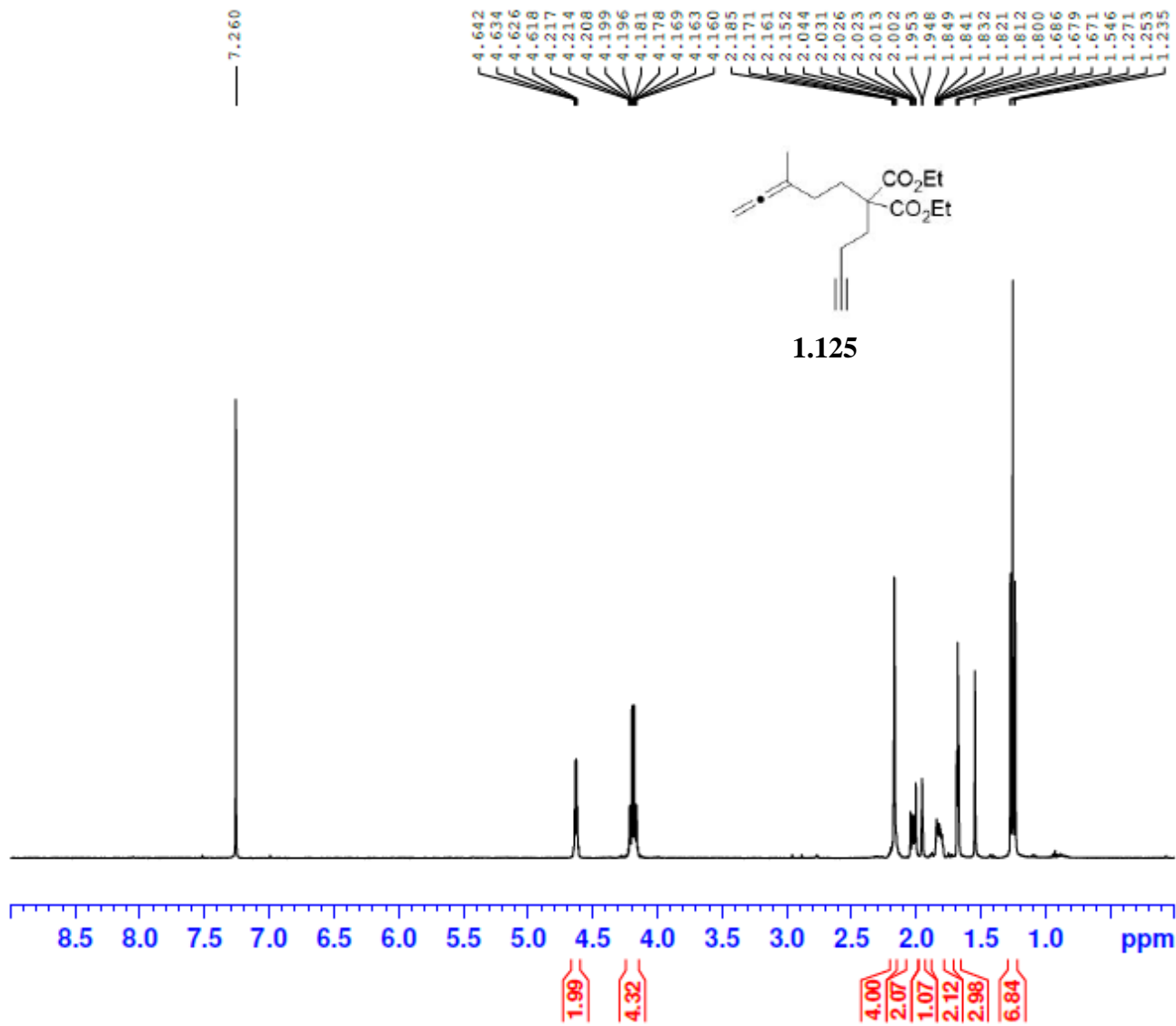


SW04-206-A 1H 400



NAME SW04-206-A
EXPNO 10
PROCNO 1
Date_ 20140407
Time 9.23
INSTRUM spect
PROBHD 5 mm PABBO BB-
PULPROG zg30
ID 65536
SOLVENT CDCl3
NS 16
DS 2
SWH 8223.685 Hz
FIDRES 0.125483 Hz
AQ 3.9846387 sec
RG 144
DW 60.800 usec
DE 6.50 usec
TE -2612.1 K
D1 1.00000000 sec

----- CHANNEL f1 -----
NUC1 1H
P1 13.75 usec
SI 65536
SF 400.1300100 MHz
WDW EM
SSB 0
LB 0.30 Hz
GB 0
PC 1.00



SW04-206-A 13C 400

— 205.99

— 171.17

— 97.78

83.46

77.48

77.16

76.84

75.20

68.84

61.46

56.86

31.75

30.64

28.11

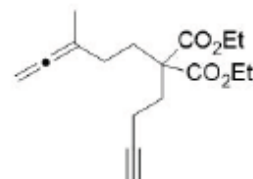
18.97

14.20

14.11

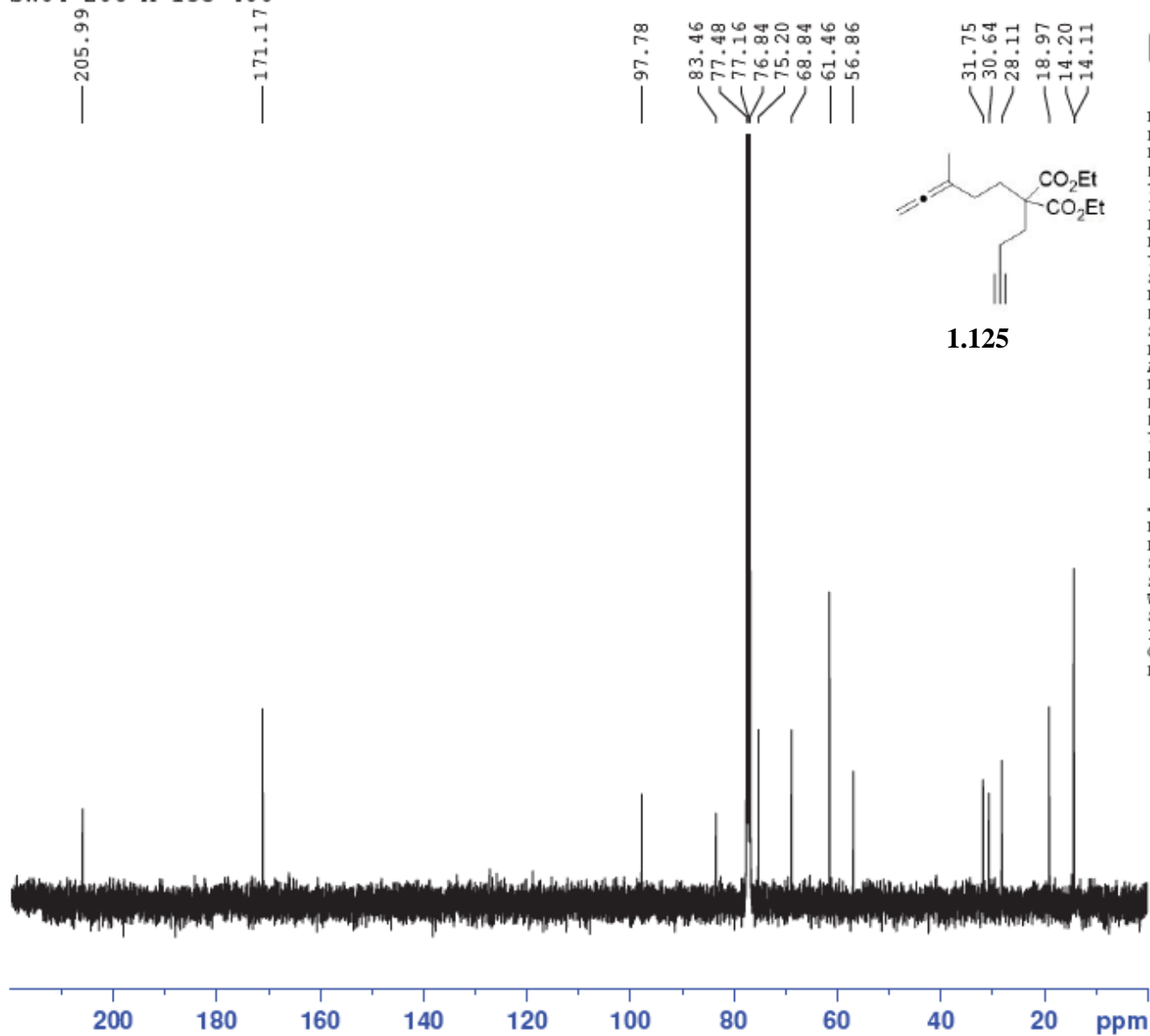


NAME SW04-206-A
EXPNO 11
PROCNO 1
Date_ 20140407
Time 22.03
INSTRUM spect
PROBHD 5 mm PABBO BB-
PULPROG zgpg30
ID 65536
SOLVENT CDCl3
NS 2048
DS 4
SWH 24038.461 Hz
FIDRES 0.366798 Hz
AQ 1.3631988 sec
RG 203
DW 20.800 usec
DE 6.50 usec
TE 2577.1 K
D1 2.0000000 sec
D11 0.0300000 sec



1.125

----- CHANNEL f1 -----
NUC1 13C
P1 10.00 usec
SI 32768
SF 100.6127538 MHz
WDW EM
SSB 0
LB 1.00 Hz
GB 0
PC 1.40



SW04-155-C 1H 400

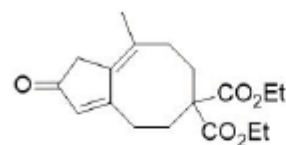
—7.260

—5.973

4.167
4.164
4.149
4.146
4.131
4.129
4.113
2.940
2.918
2.581
2.567
2.552
2.369
2.353
2.339
2.305
2.287
2.275
1.865
1.250
1.232
1.214
0.885
0.877
0.870

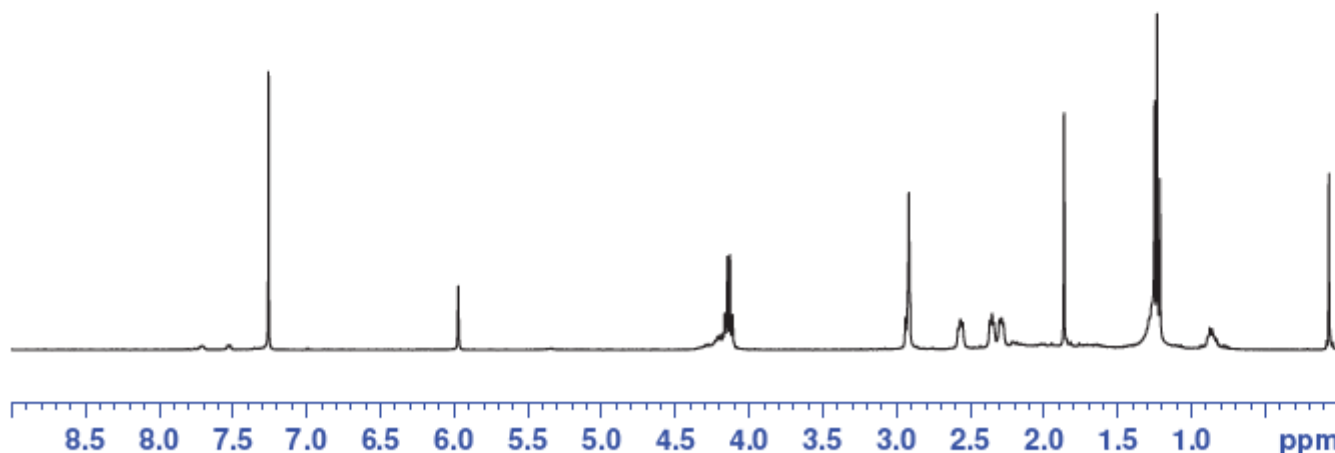


NAME SW04-155-C
EXPNO 10
PROCNO 1
Date_ 20140215
Time_ 13.09
INSTRUM spect
PROBHD 5 mm PABBO BB-
PULPROG zg30
TD 65536
SOLVENT CDCl3
NS 16
DS 2
SWH 8223.685 Hz
FIDRES 0.125483 Hz
AQ 3.9846387 sec
RG 144
DW 60.800 usec
DE 6.50 usec
TE -365.2 K
D1 1.00000000 sec



1.128

----- CHANNEL f1 -----
NUC1 1H
P1 13.75 usec
SI 65536
SF 400.1300102 MHz
WDW EM
SSB 0
LB 0.30 Hz
GB 0
PC 1.00



1.00

4.52

4.36

2.19

2.40

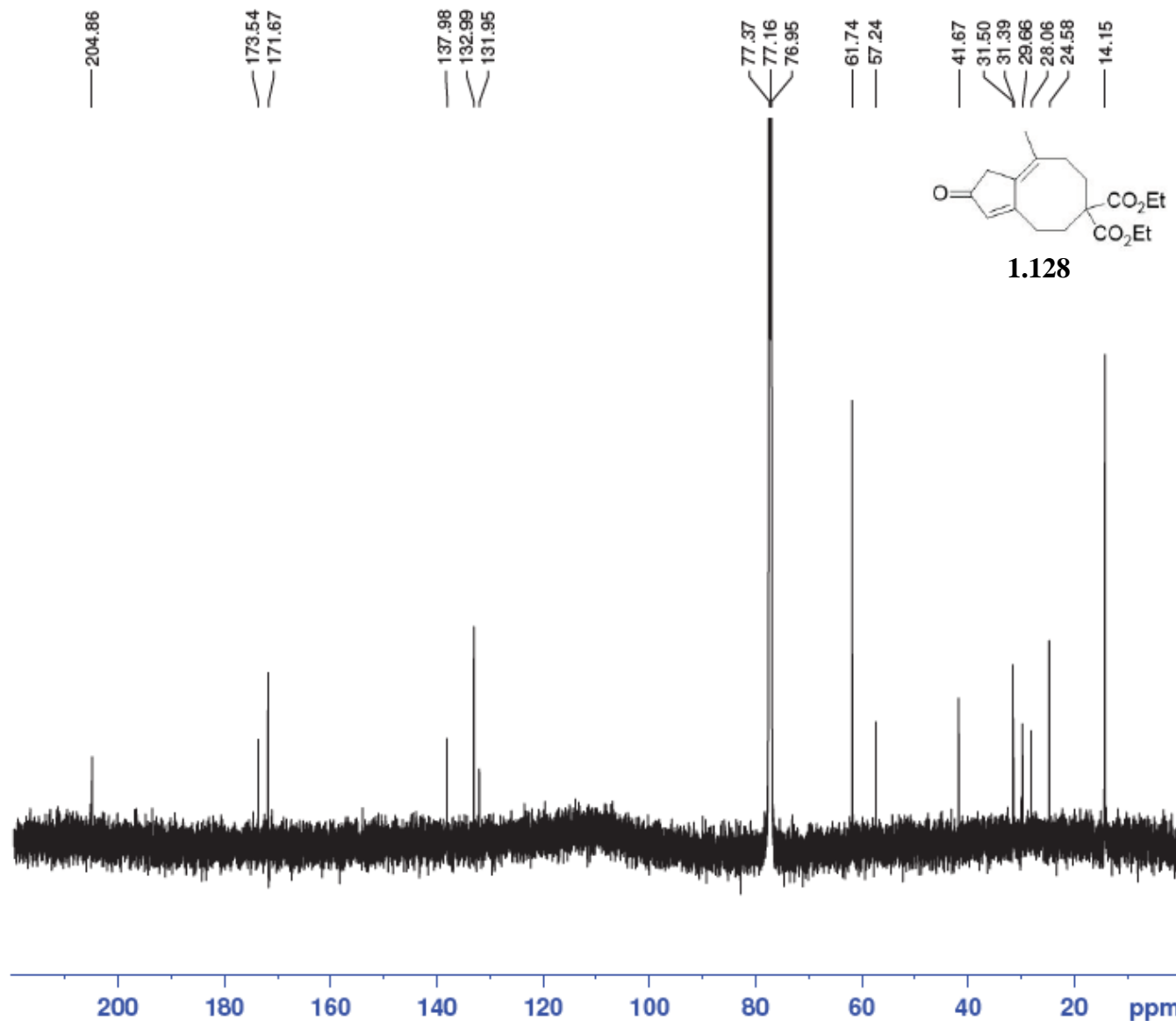
2.54

3.42

9.73

2.34

SW08-024-A 13C 600



NAME SW08-024-A
 EXPNO 1
 PROCNO 1
 Date_ 20160518
 Time 7.18
 INSTRUM spect
 PROBHD 5 mm PABBO BB-
 PULPROG zgpg30
 TD 65536
 SOLVENT CDC13
 NS 21000
 DS 4
 SWH 36057.691 Hz
 FIDRES 0.550197 Hz
 AQ 0.9088159 sec
 RG 203
 DW 13.867 usec
 DE 6.50 usec
 TE 297.9 K
 D1 2.00000000 sec
 D11 0.03000000 sec
 TDO 1

----- CHANNEL f1 -----
 NUC1 13C
 P1 11.50 usec
 PL1 0.00 dB
 PL1W 97.46119690 W
 SFO1 151.0637542 MHz

----- CHANNEL f2 -----
 CPDPRG2 waltz16
 NUC2 1H
 PCPD2 70.00 usec
 PL2 -2.00 dB
 PL12 14.19 dB
 PL13 120.00 dB
 PL2W 19.70630455 W
 PL12W 0.47381112 W
 PL13W 0.00000000 W
 SFO2 600.7124028 MHz
 SI 32768
 SF 151.0486270 MHz
 WDW EM
 SSB 0
 LB 1.00 Hz
 GB 0
 PC 1.40

SW06-069-C 1H 300

7.719
7.710
7.703
7.697
7.446
7.444
7.434
7.429
7.423
7.417
7.412
7.402
7.398
7.393
7.373
7.260

5.299
4.373
4.367
4.361
4.213
4.207
4.201
4.192
4.186
4.180

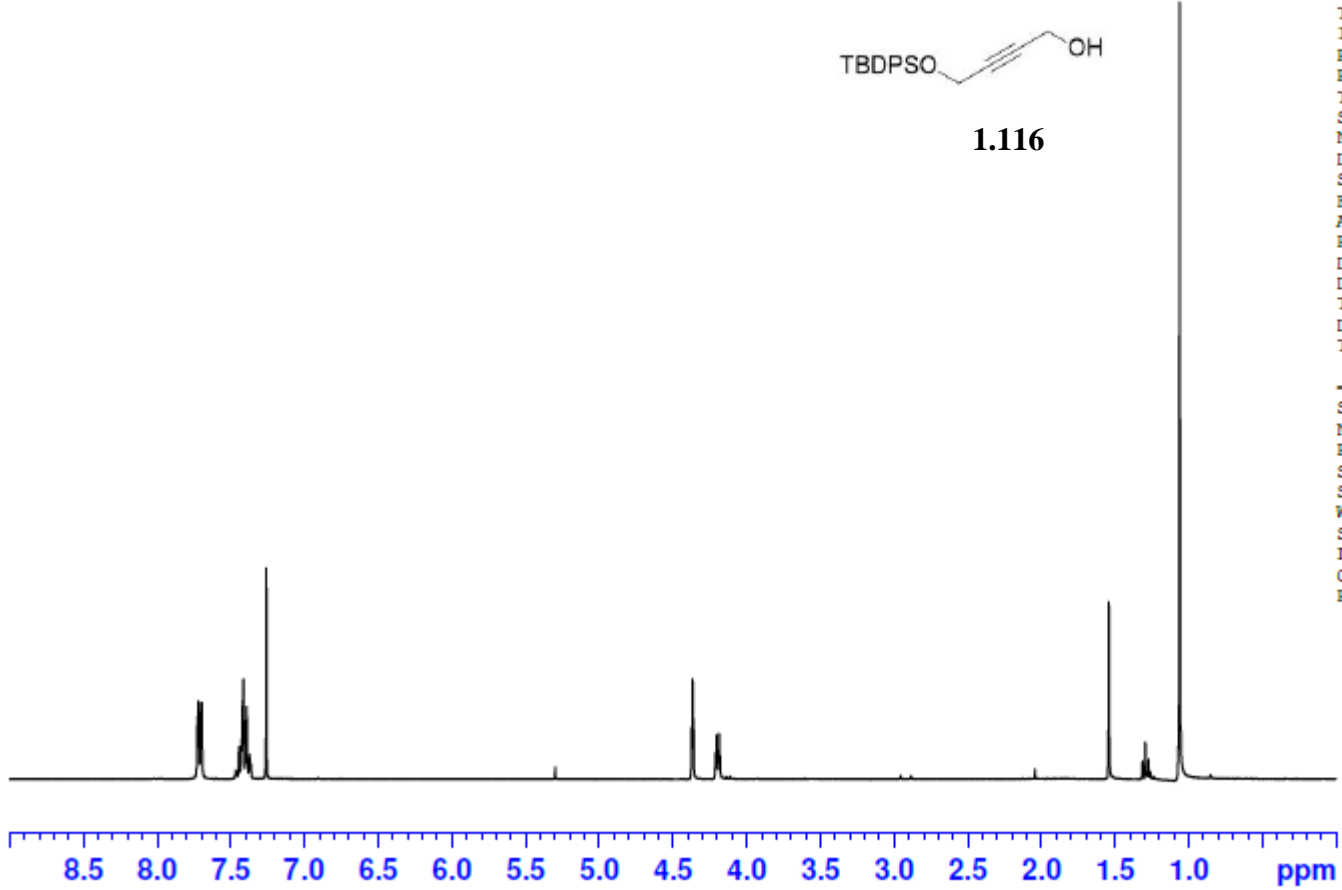
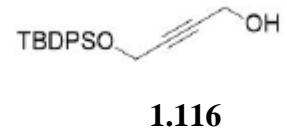
2.955
2.885

2.045
1.542
1.315
1.294
1.273
1.063



NAME SW06-069-C
EXPNO 10
PROCNO 1
Date_ 20150113
Time_ 8.23
INSTRUM spect
PROBHD 5 mm QNP 1H/1
PULPROG zg30
TD 32768
SOLVENT CDCl3
NS 16
DS 2
SWH 6188.119 Hz
FIDRES 0.188846 Hz
AQ 2.6477044 sec
RG 322
DW 80.800 usec
DE 6.50 usec
TE -926.9 K
D1 1.00000000 sec
TD0 1

----- CHANNEL f1 -----
SFO1 300.2318540 MHz
NUC1 1H
P1 12.71 usec
SI 32768
SF 300.2300088 MHz
WDW EM
SSB 0
LB 0.10 Hz
GB 0
PC 1.00



4.01
6.02

2.00
1.95
0.08

0.03
0.04

0.10

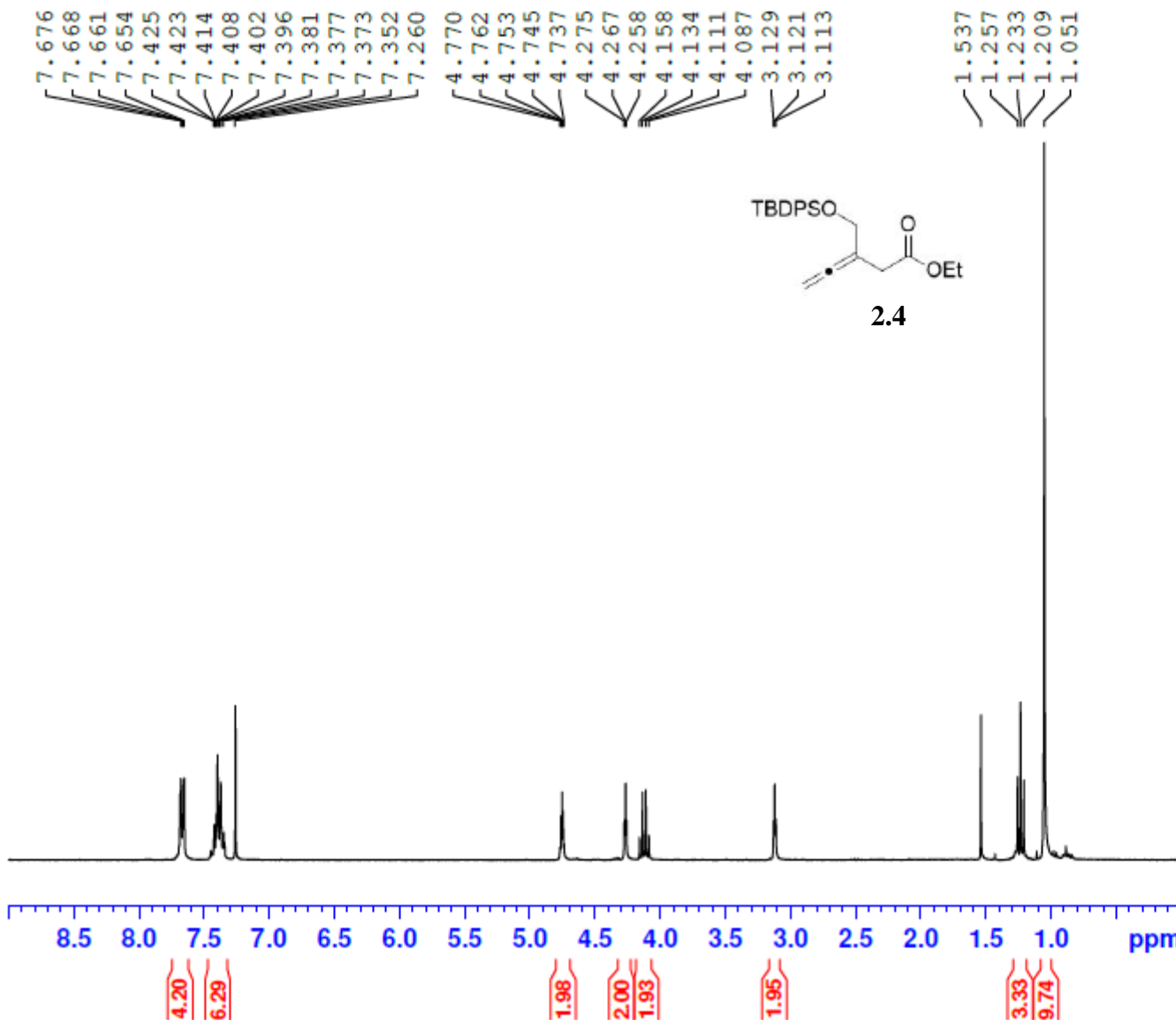
0.95
9.51

SW06-080-A 1H 300



NAME SW06-080-A
EXPNO 10
PROCNO 1
Date_ 20150127
Time 11.19
INSTRUM spect
PROBHD 5 mm QNP 1H/1
PULPROG zg30
ID 32768
SOLVENT CDCl3
NS 16
DS 2
SWH 6188.119 Hz
FIDRES 0.188846 Hz
AQ 2.6477044 sec
RG 322
DW 80.800 usec
DE 6.50 usec
TE -927.3 K
D1 1.00000000 sec
TD0 1

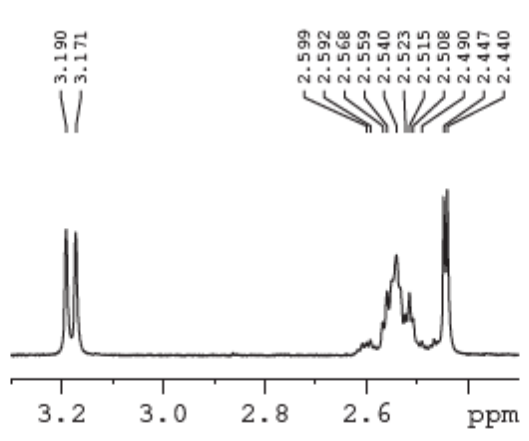
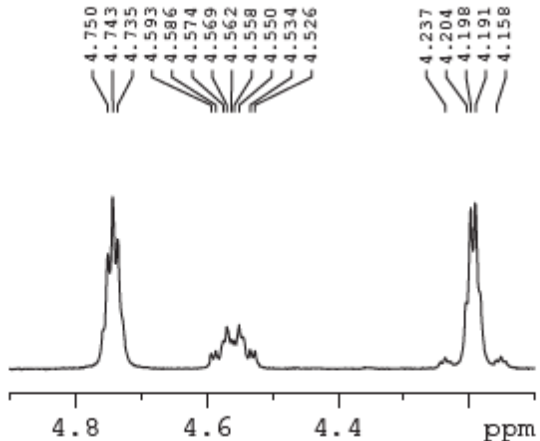
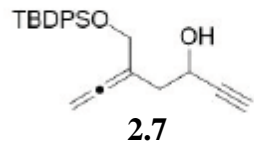
----- CHANNEL f1 -----
SFO1 300.2318540 MHz
NUC1 1H
P1 12.71 usec
SI 32768
SF 300.2300085 MHz
WDW EM
SSB 0
LB 0.10 Hz
GB 0
PC 1.00



SW07-190-A 1H 300

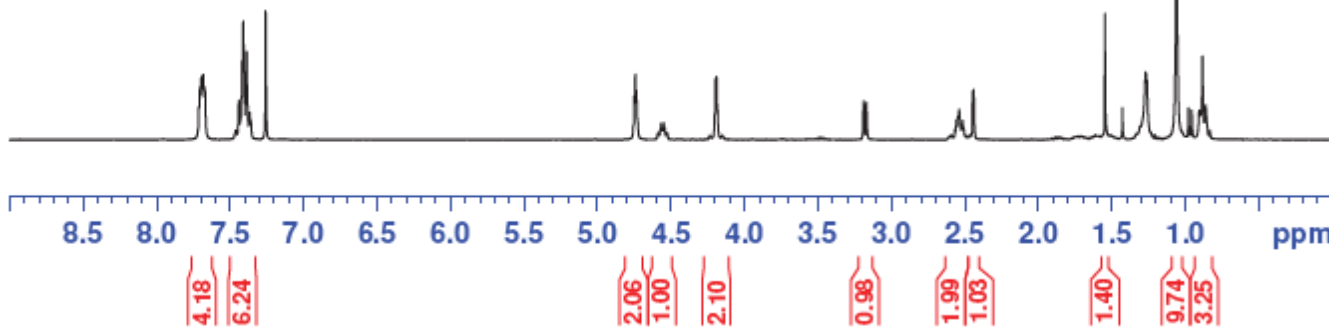


7.715
7.710
7.704
7.698
7.691
7.684
7.678
7.672
7.442
7.432
7.426
7.420
7.413
7.389
7.369
7.360
7.259
4.750
4.743
4.735
4.593
4.586
4.574
4.569
4.562
4.558
4.550
4.534
4.526
4.237
4.204
4.198
4.191
4.151
3.190
3.171
2.592
2.568
2.559
2.540
2.523
2.515
2.508
2.490
2.447
2.440
2.440
1.547
1.428
1.270
1.061
0.979
0.957
0.885



NAME sw07-190-A
EXPNO 10
PROCNO 1
Date_ 20160328
Time 13.32
INSTRUM spect
PROBHD 5 mm QNP 1H/1
PULPROG zg30
TD 32768
SOLVENT CDCl3
NS 16
DS 2
SWH 6188.119 Hz
FIDRES 0.188846 Hz
AQ 2.6477044 sec
RG 228
DW 80.800 usec
DE 6.50 usec
TE -926.8 K
D1 1.00000000 sec
TD0 1

----- CHANNEL f1 -----
SFO1 300.2318540 MHz
NUC1 1H
P1 12.71 usec
SI 32768
SF 300.2300088 MHz
WDW EM
SSB 0
LB 0.10 Hz
GB 0
PC 1.00

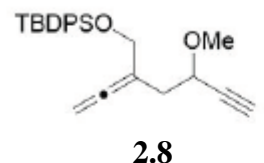


SW07-007-A 1H 400

7.692
7.689
7.673
7.423
7.410
7.406
7.395
7.377
7.360
7.263
7.260

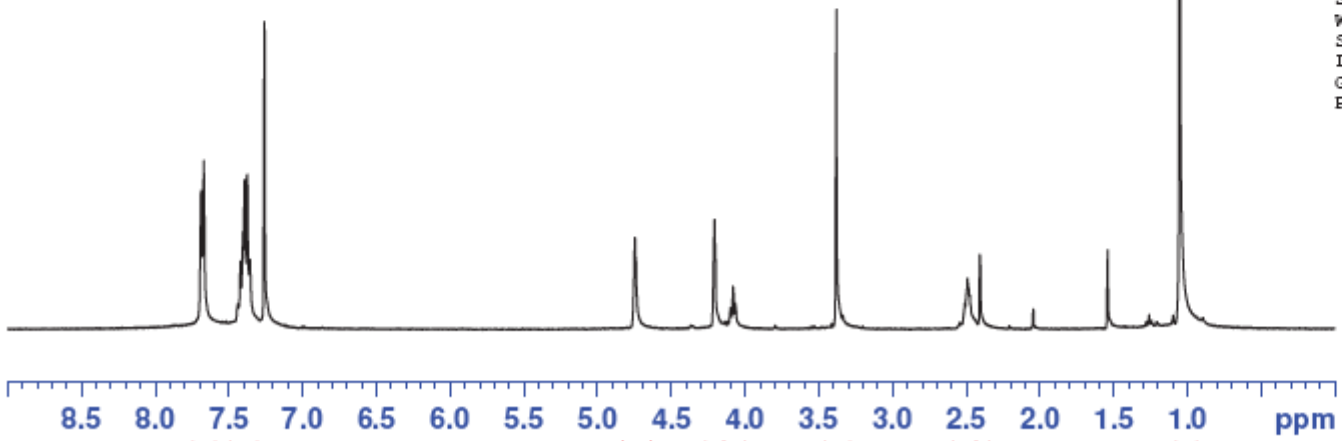
4.747
4.740
4.208
4.101
4.097
4.084
4.080
4.066
3.381
2.509
2.492
2.486
2.476
2.408
2.404
1.540

1.053



NAME SW07-007-A
EXPNO 10
PROCNO 1
Date_ 20150603
Time 11.34
INSTRUM spect
PROBHD 5 mm PABBO BB-
PULPROG zg30
TD 65536
SOLVENT CDCl3
NS 16
DS 2
SWH 8223.685 Hz
FIDRES 0.125483 Hz
AQ 3.9846387 sec
RG 161
DW 60.800 usec
DE 6.50 usec
TE 297.9 K
D1 1.00000000 sec

----- CHANNEL f1 -----
NUC1 1H
P1 13.75 usec
SI 65536
SF 400.1300101 MHz
WDW EM
SSB 0
LB 0.30 Hz
GB 0
PC 1.00



4.41
6.53

2.00

1.97
1.26

3.01

1.88
1.02

9.56

SW07-195-B 1H 300

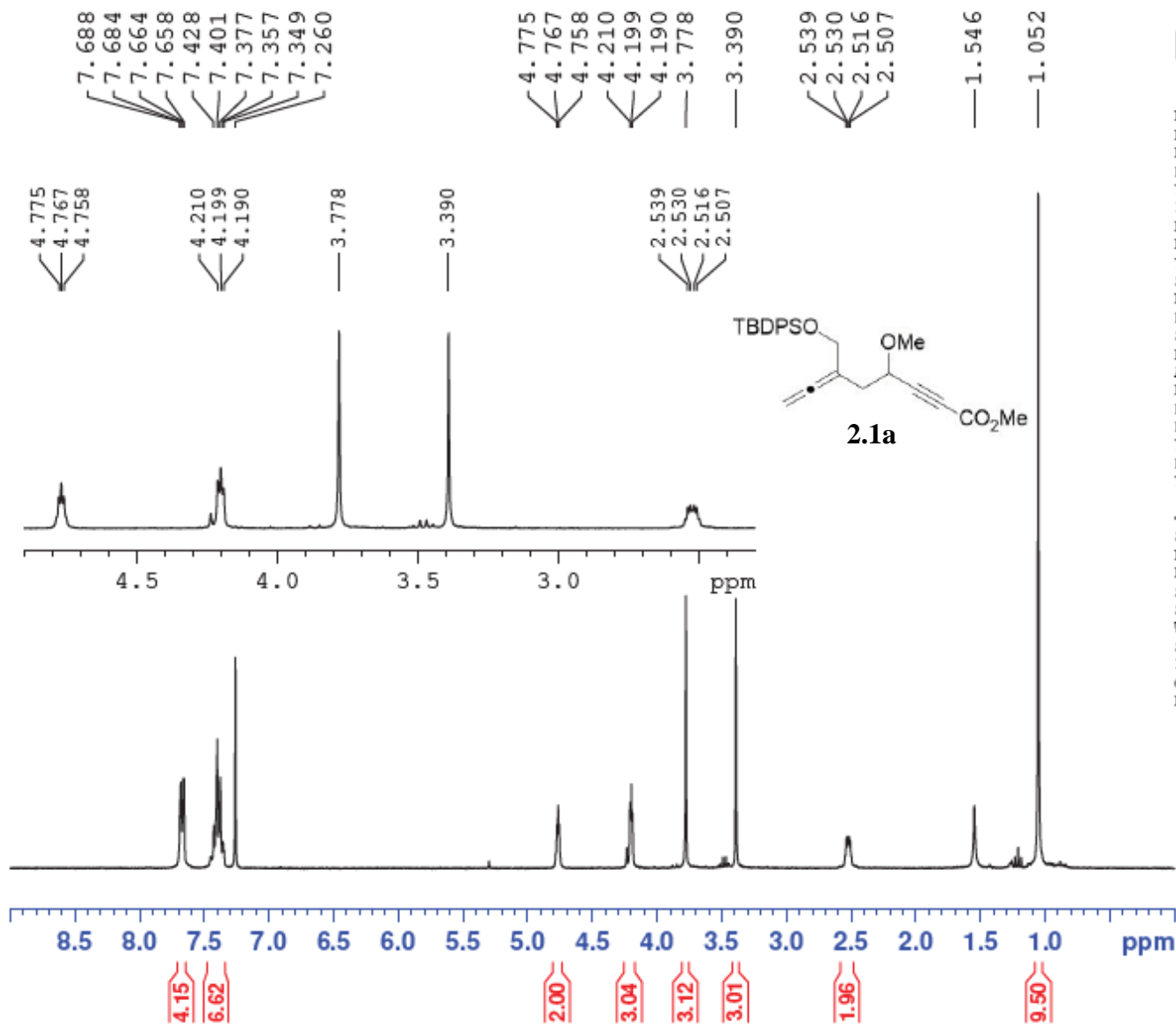


```

NAME      SW07-195-B
EXPNO     10
PROCNO    1
Date_     20160404
Time      14.20
INSTRUM   spect
PROBHD    5 mm QNP 1H/1
PULPROG   zg30
TD         32768
SOLVENT   CDCl3
NS         16
DS         2
SWH        6188.119 Hz
FIDRES    0.188846 Hz
AQ         2.6477044 sec
RG         322
DW         80.800 usec
DE         6.50 usec
TE         -926.8 K
D1         1.00000000 sec
TD0        1
  
```

```

----- CHANNEL f1 -----
SFO1     300.2318540 MHz
NUC1      1H
P1        12.71 usec
SI        32768
SF        300.2300087 MHz
WDW       EM
SSB       0
LB        0.10 Hz
GB        0
PC        1.00
  
```

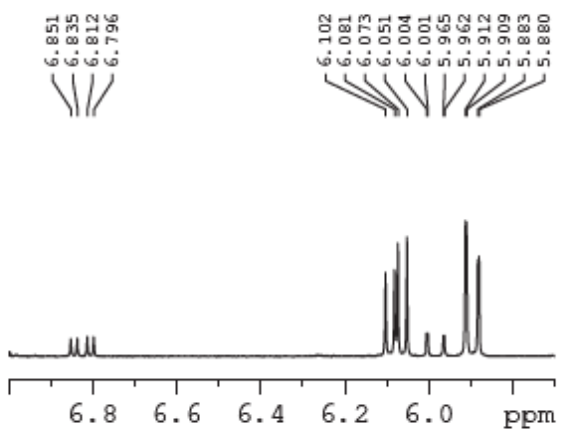
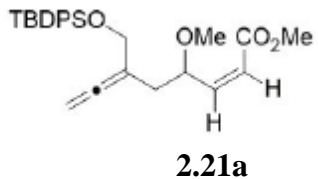


SW08-030-alkene 1H 400

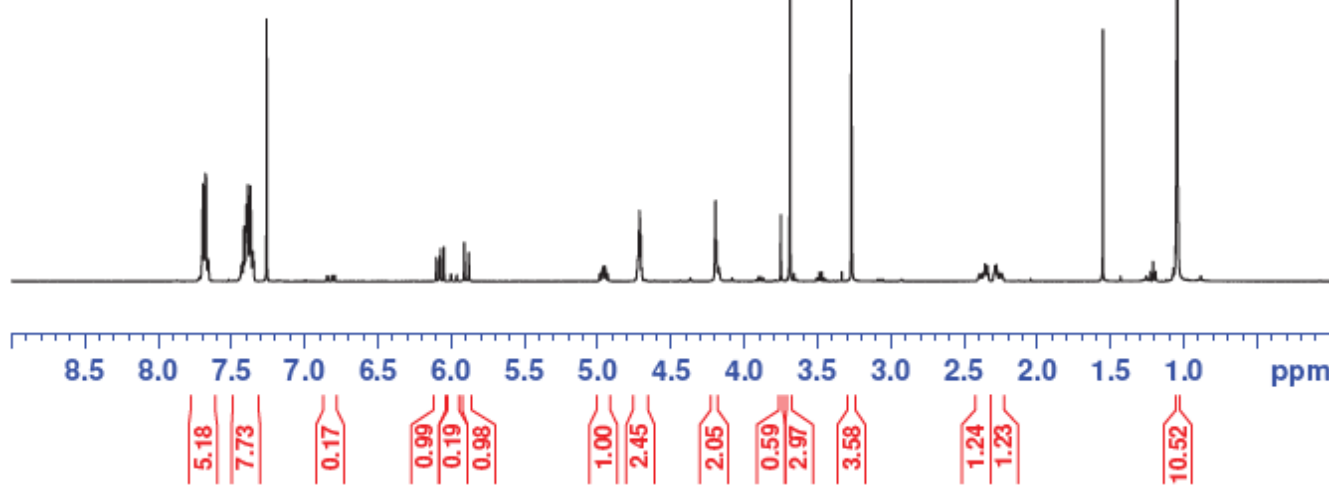
7.698
7.694
7.684
7.679
7.675
7.661
7.657
7.426
7.416
7.409
7.403
7.399
7.394
7.389
7.370
7.354
7.349
7.260
6.102
6.081
6.073
6.051
5.912
5.909
5.883
5.880
4.969
4.966
4.952
4.949
4.726
4.721
4.715
4.708
4.701
4.203
4.196
4.189
3.751
3.688
3.268
2.365
2.358
2.351
2.346
2.340
2.292
2.286
2.279
2.272
1.554
1.049
1.044



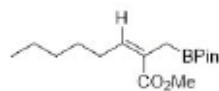
NAME SW08-030-alkene
EXPNO 10
PROCNO 1
Date_ 20160526
Time_ 16.24
INSTRUM spect
PROBHD 5 mm PABBO BB-
PULPROG zg30
ID 65536
SOLVENT CDC13
NS 16
DS 2
SWH 8012.820 Hz
FIDRES 0.122266 Hz
AQ 4.0894966 sec
RG 128
DW 62.400 usec
DE 6.50 usec
TE 96.3 K
D1 1.0000000 sec
ID0 1



----- CHANNEL f1 -----
SFO1 400.1324710 MHz
NUC1 1H
P1 13.75 usec
SI 65536
SF 400.1300105 MHz
WDW EM
SSB 0
LB 0.30 Hz
GB 0
PC 1.00



SW08-027-0735B 1H 600



Z-2.2d

7.260

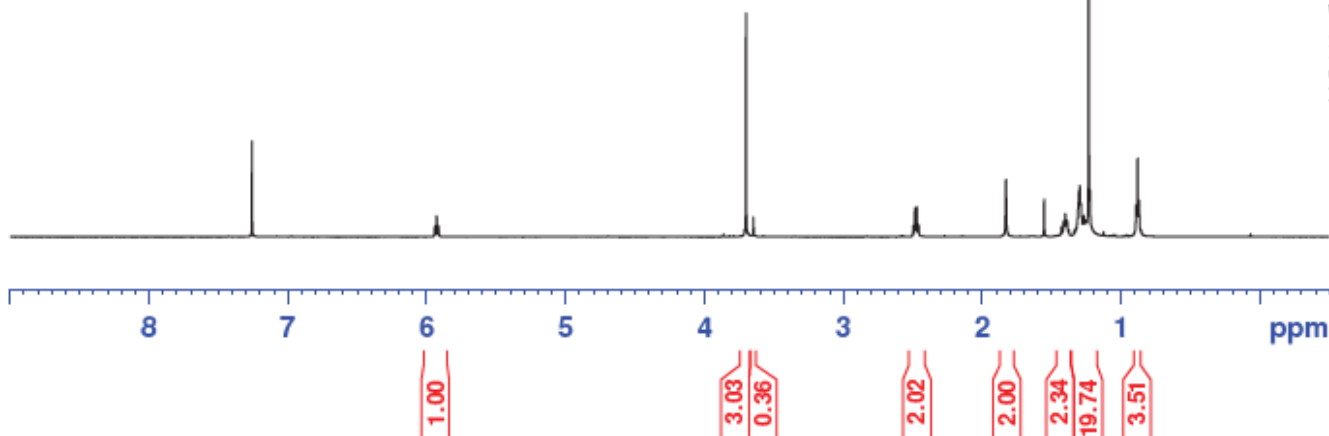
5.942
5.930
5.918

3.701
3.649
2.496
2.484
2.471
2.459
1.829
1.554
1.431
1.427
1.414
1.402
1.390
1.378
1.309
1.303
1.297
1.291
1.234
1.222
0.894
0.882
0.871



NAME SW08-027-0735B
EXPNO 1
PROCNO 1
Date_ 20160517
Time 9.03
INSTRUM spect
PROBHD 5 mm PABBO BB-
PULPROG zg30
TD 65536
SOLVENT CDCl3
NS 16
DS 2
SWH 12335.526 Hz
FIDRES 0.188225 Hz
AQ 2.6564426 sec
RG 144
DW 40.533 usec
DE 6.50 usec
TE 298.1 K
D1 1.00000000 sec
TDO 1

----- CHANNEL f1 -----
NUC1 1H
P1 10.86 usec
PL1 -2.00 dB
PL1W 19.70630455 W
SFO1 600.7137096 MHz
SI 32768
SF 600.7100140 MHz
WDW EM
SSB 0
LB 0.30 Hz
GB 0
PC 1.00

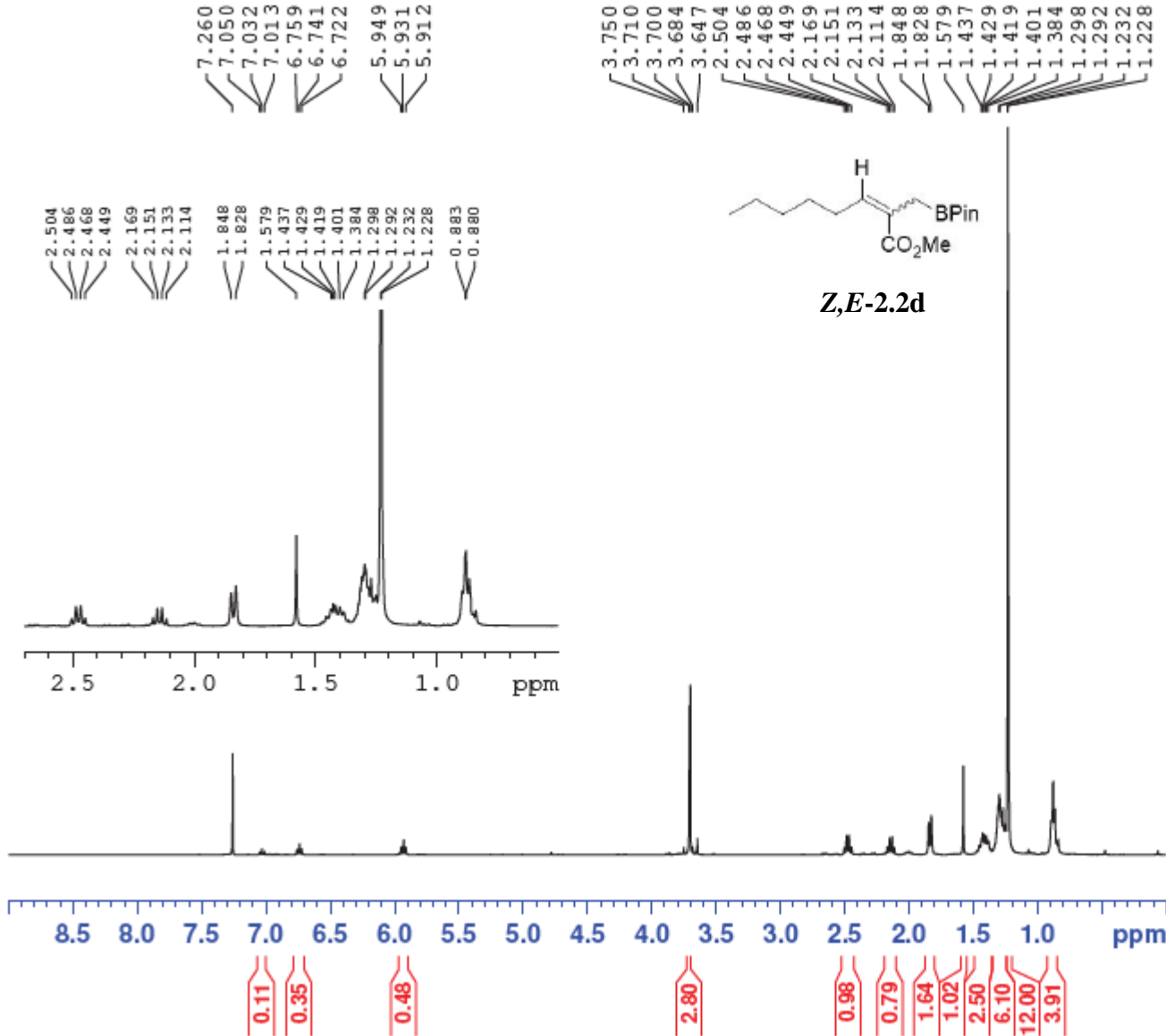


SW07-035-C 1H 400

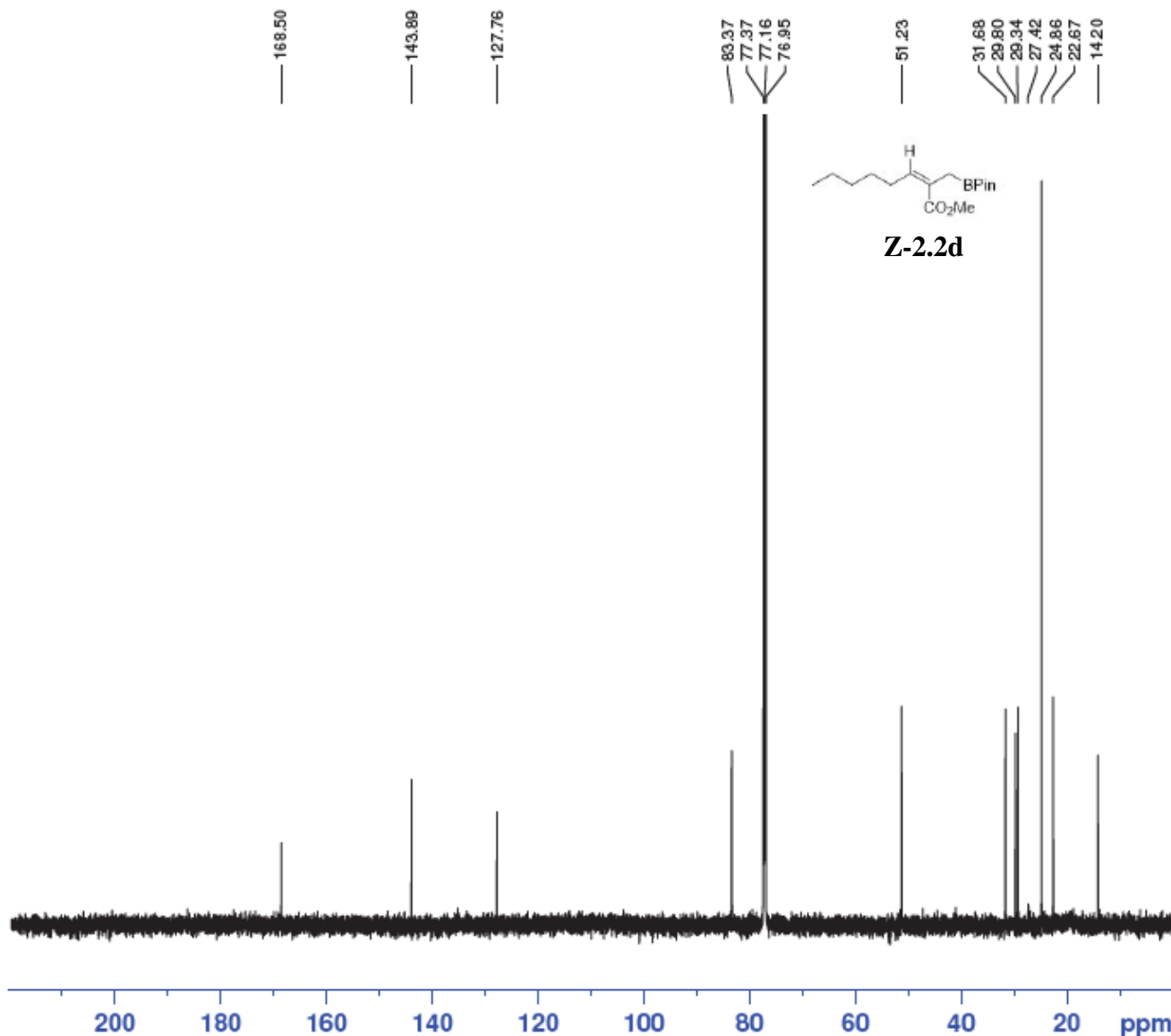


NAME SW07-035-C
EXPNO 10
PROCNO 1
Date_ 20150709
Time_ 10.33
INSTRUM spect
PROBHD 5 mm PABBO BB-
PULPROG zg30
ID 65536
SOLVENT CDCl3
NS 16
DS 2
SWH 8223.685 Hz
FIDRES 0.125483 Hz
AQ 3.9846387 sec
RG 114
DW 60.800 use
DE 6.50 use
TE 95.4 K
D1 1.00000000 sec

----- CHANNEL f1 -----
NUC1 1H
P1 13.75 use
SI 65536
SF 400.1300099 MHz
WDW EM
SSB 0
LB 0.30 Hz
GB 0
PC 1.00



SW08-027-0735B 13C 600



NAME SW08-027-0735B
EXPNO 2
PROCNO 1
Date_ 20160517
Time 10.29
INSTRUM spect
PROBHD 5 mm PABBO BB-
PULPROG zgpg30
TD 65536
SOLVENT CDC13
NS 1600
DS 4
SWH 36057.691 Hz
FIDRES 0.550197 Hz
AQ 0.9088159 sec
RG 203
DW 13.867 usec
DE 6.50 usec
TE 298.1 K
D1 2.00000000 sec
D11 0.03000000 sec
TDO 1

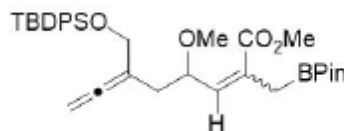
----- CHANNEL f1 -----
NUC1 13C
P1 11.50 usec
PL1 0.00 dB
PL1W 97.46119690 W
SFO1 151.0637542 MHz

----- CHANNEL f2 -----
CPDPRG2 waltz16
NUC2 1H
PCPD2 70.00 usec
PL2 -2.00 dB
PL12 14.19 dB
PL13 120.00 dB
PL2W 19.70630455 W
PL12W 0.47381112 W
PL13W 0.00000000 W
SFO2 600.7124028 MHz
SI 32768
SF 151.0486274 MHz
WDW EM
SSB 0
LB 1.00 Hz
GB 0
PC 1.40

SW07-203-B 1H 400



7.695
7.681
7.665
7.661
7.428
7.410
7.385
7.367
7.351
7.260
7.185
6.542
6.519
5.752
5.730
4.719
4.712
4.706
4.679
4.198
4.192
4.186
4.179
4.176
4.160
3.726
3.663
3.505
3.488
3.470
3.453
3.254
3.231
2.356
2.293
2.286
2.272
2.266
2.260
2.046
1.893
1.883
1.866
1.544
1.300
1.276
1.227
1.212
1.209
1.195
1.192
1.043
0.883

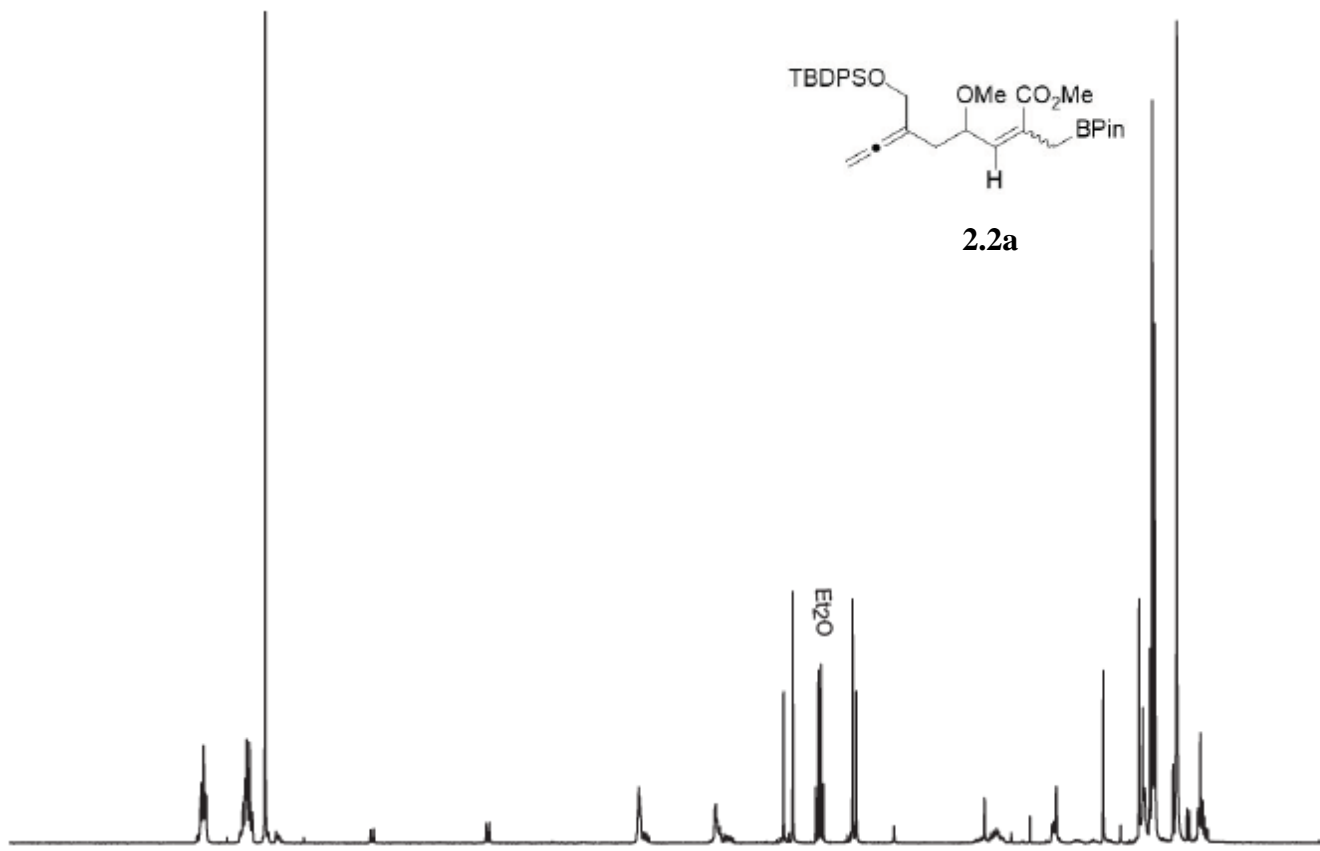


2.2a

```

NAME          SW07-203-B
EXPNO         10
PROCNO        1
Date_         20160416
Time_         11.25
INSTRUM       spect
PROBHD        5 mm PABBO BB-
PULPROG       zg30
ID            65536
SOLVENT       CDCl3
NS            16
DS            2
SWH           8012.820 Hz
FIDRES        0.122266 Hz
AQ            4.0894966 sec
RG            144
DW            62.400 usec
DE            6.50 usec
TE            92.6 K
D1            1.00000000 sec
TD0           1

----- CHANNEL f1 -----
SFO1          400.1324710 MHz
NUC1          1H
P1            13.75 usec
SI            65536
SF            400.1300098 MHz
WDW           EM
SSB           0
LB            0.30 Hz
GB            0
PC            1.00
    
```



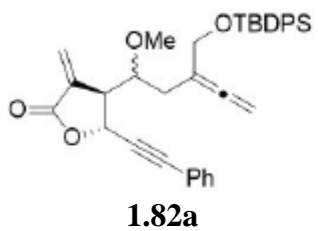
4.35
6.50
0.35
0.56
2.60
2.53
1.07
1.74
2.90
3.00
2.39
1.95
1.44
4.81
16.22
10.28
3.15

SW08-001-02B 1H 400

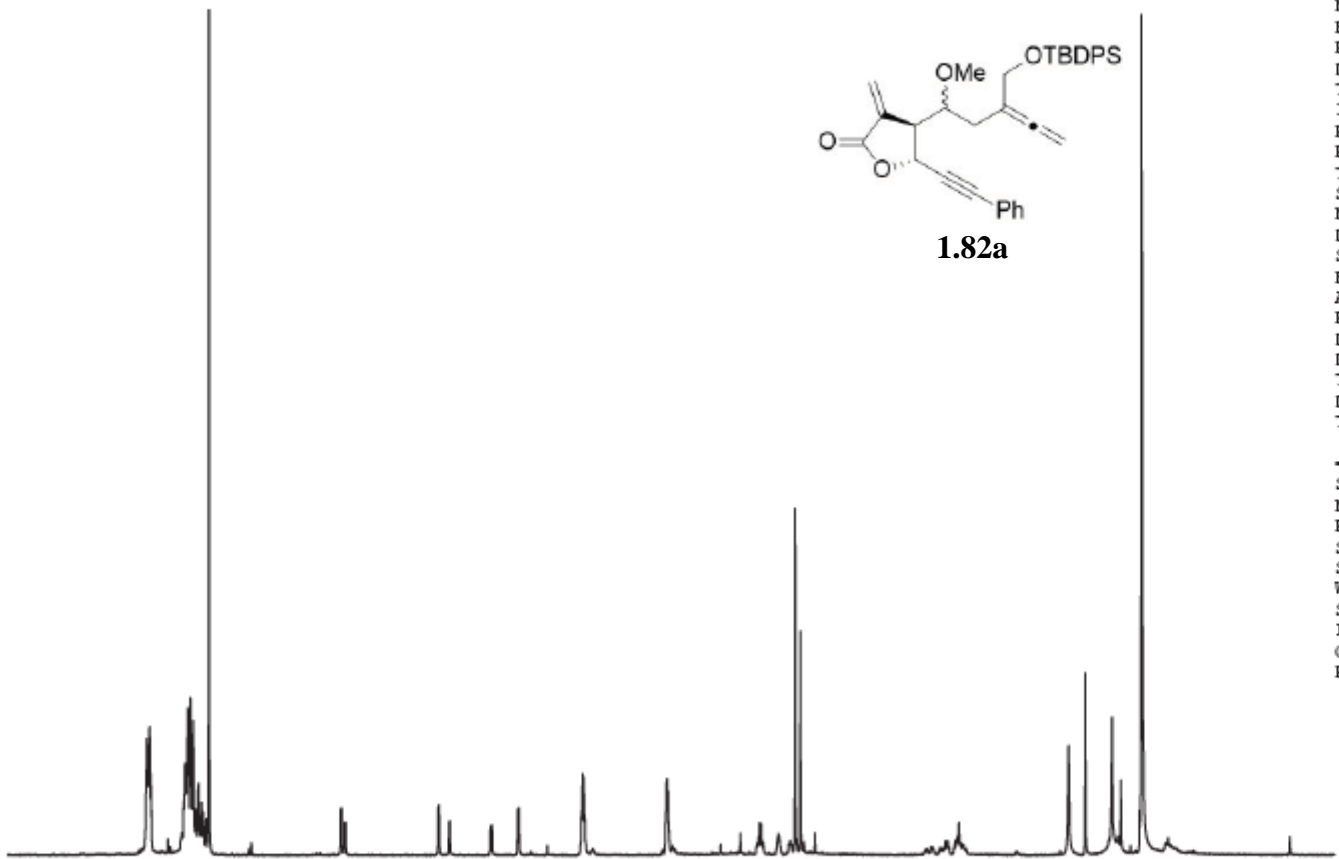
7.678
7.675
7.668
7.664
7.659
7.655
7.648
7.429
7.427
7.420
7.413
7.409
7.403
7.399
7.383
7.365
7.334
7.328
7.310
7.260
6.385
6.379
6.357
6.351
5.735
5.730
5.664
5.659
5.388
5.377
5.206
5.198
4.781
4.775
4.768
4.761
4.217
4.214
4.207
3.605
3.600
3.588
3.473
3.470
3.362
3.326
2.281
2.272
1.543
1.432
1.254
1.195
1.059



NAME SW08-001-c2B
 EXPNO 10
 PROCNO 1
 Date_ 20160505
 Time_ 11.09
 INSTRUM spect
 PROBHD 5 mm PABBO BB-
 PULPROG zg30
 ID 65536
 SOLVENT CDC13
 NS 16
 DS 2
 SWH 8012.820 Hz
 FIDRES 0.122266 Hz
 AQ 4.0894966 sec
 RG 144
 DW 62.400 usec
 DE 6.50 usec
 TE 98.1 K
 D1 1.0000000 sec
 TD0 1



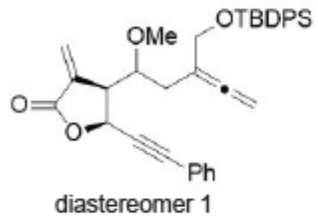
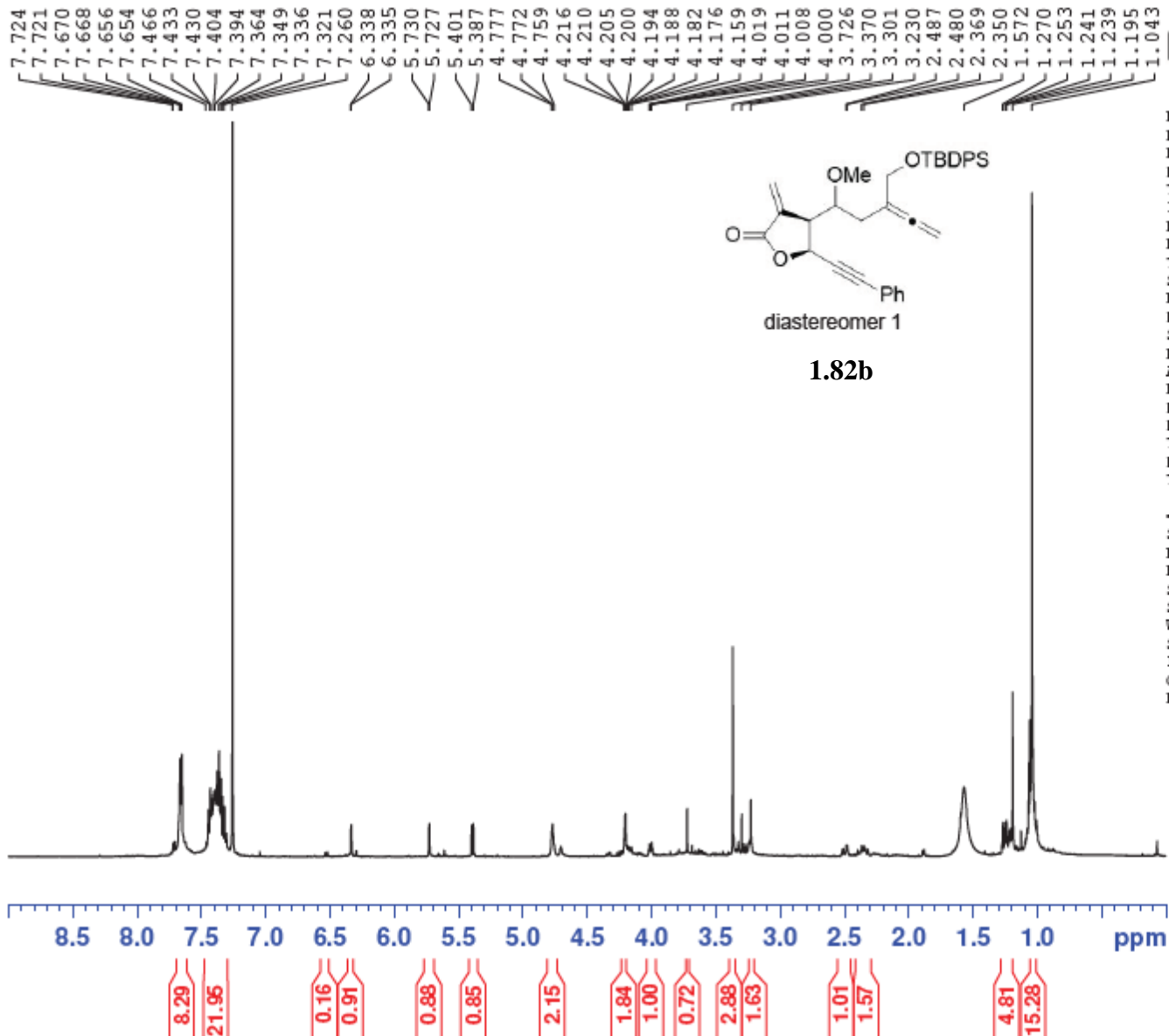
----- CHANNEL f1 -----
 SFO1 400.1324710 MHz
 NUC1 1H
 P1 13.75 usec
 SI 65536
 SF 400.1300105 MHz
 WDW EM
 SSB 0
 LB 0.30 Hz
 GB 0
 PC 1.00



8.0 7.5 7.0 6.5 6.0 5.5 5.0 4.5 4.0 3.5 3.0 2.5 2.0 1.5 1.0 0.5 ppm

5.06
12.86
1.00
0.60
0.39
0.38
0.61
2.02
2.07
1.09
0.66
0.45
1.96
1.25
2.50
2.02
0.98
10.59

SW06-094-C 1H 500



1.82b

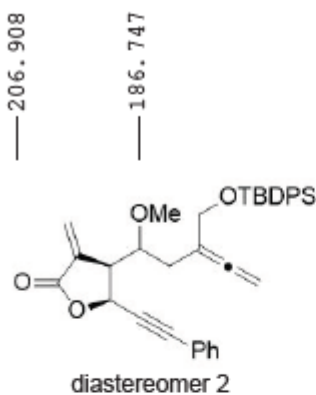


```

NAME          SW06-094-C
EXPNO         10
PROCNO        1
Date_         20160526
Time          12.36
INSTRUM       spect
PROBHD        5 mm PABBO BB/
PULPROG       zg30
ID            65536
SOLVENT       CDCl3
NS            16
DS            2
SWH           10000.000 Hz
FIDRES        0.152588 Hz
AQ            3.2768500 sec
RG            203
DW            50.000 usec
DE            6.50 usec
TE            508.2 K
D1            1.00000000 sec
ID0           1

----- CHANNEL f1 -----
SFO1          500.1630887 MHz
NUC1           1H
P1            11.45 usec
SI            65536
SF            500.1600127 MHz
WDW           EM
SSB           0
LB            0.30 Hz
GB            0
PC            1.00
  
```

SW06-094-C 1H 500



1.82b

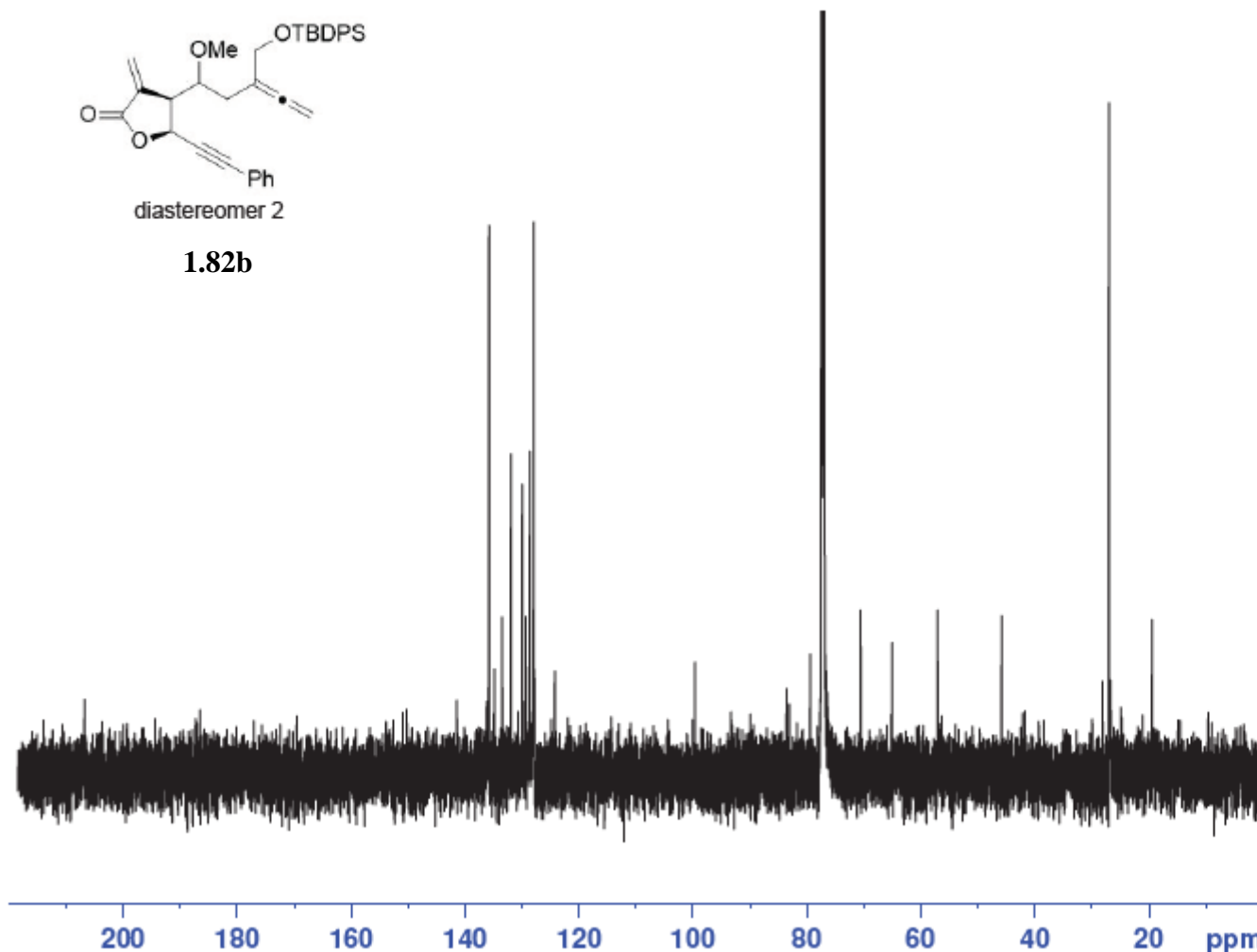
141.635
135.734
134.829
133.448
131.932
129.940
129.270
128.602
127.860
127.763
124.219

— 99.548 —

83.570
83.095
79.345
77.416
77.162
76.908
70.501
64.933
57.004

— 45.853 —

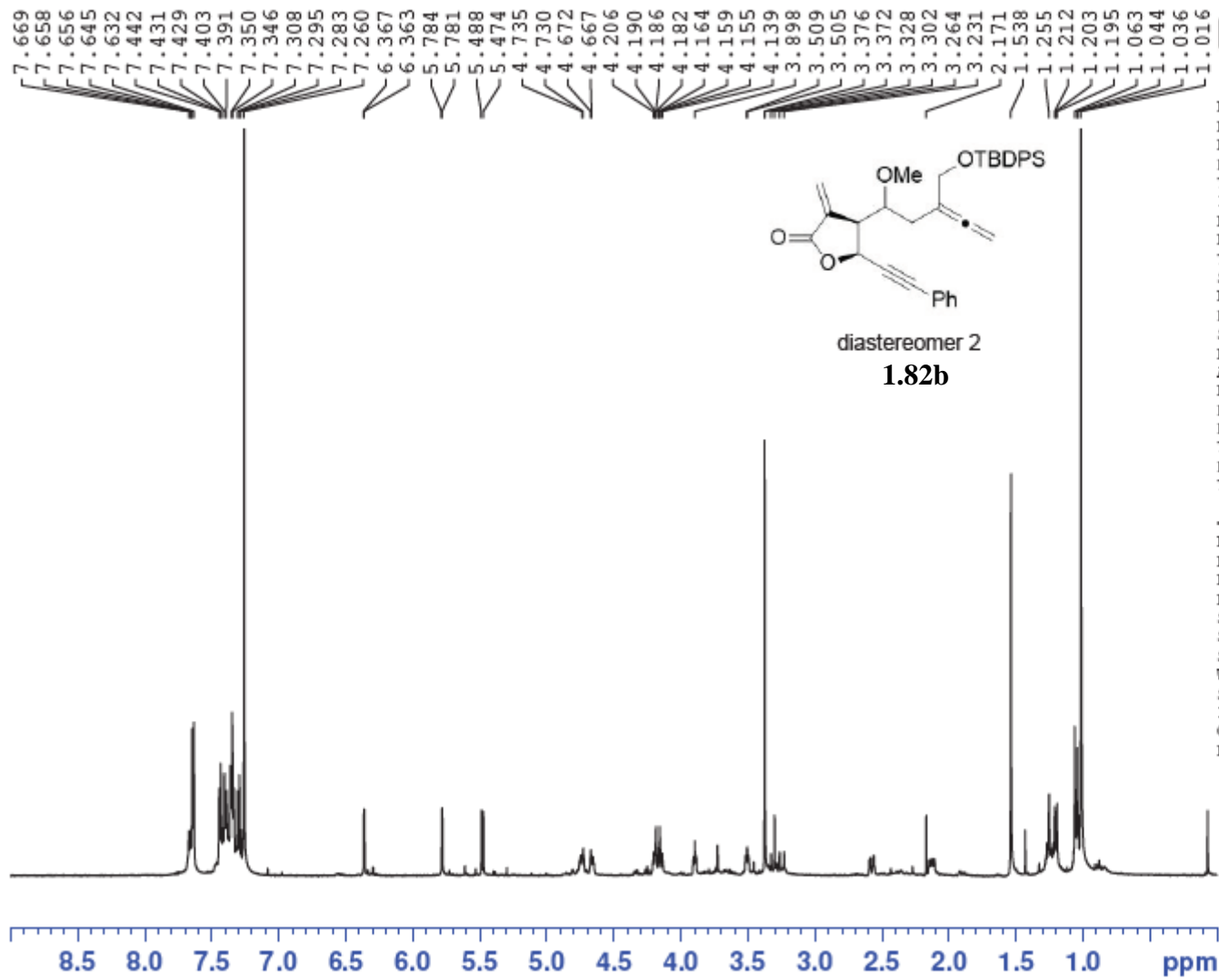
28.126
26.982
— 19.428 —



NAME SW06-094-C
EXPNO 11
PROCNO 1
Date_ 20160526
Time 23.47
INSTRUM spect
PROBHD 5 mm PABBO BB/
PULPROG zgpg30
TD 65536
SOLVENT CDCl3
NS 3072
DS 2
SWH 29761.904 Hz
FIDRES 0.454131 Hz
AQ 1.1010548 sec
RG 203
DW 16.800 usec
DE 6.50 usec
TE 517.2 K
D1 2.00000000 sec
D11 0.03000000 sec
TD0 1

----- CHANNEL f1 -----
SFO1 125.7779086 MHz
NUC1 13C
P1 10.50 usec
SI 32768
SF 125.7653130 MHz
WDW EM
SSB 0
LB 1.00 Hz
GB 0
PC 1.40

SW08-028-07136D 1H 600

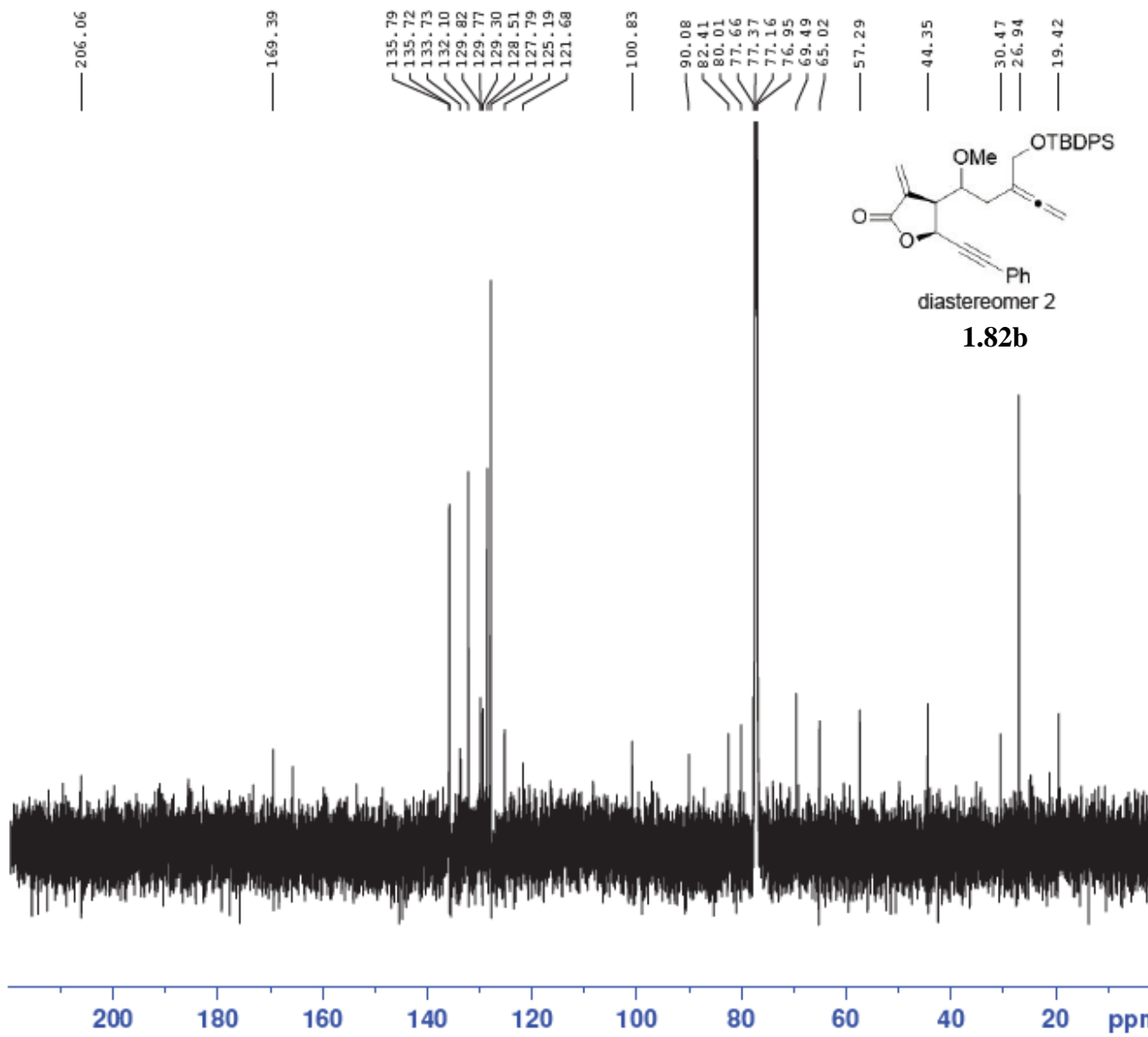


```

NAME SW08-028-07136D
EXPNO 1
PROCNO 1
Date_ 20160517
Time 10.52
INSTRUM spect
PROBHD 5 mm PABBO BB-
PULPROG zg30
TD 65536
SOLVENT CDCl3
NS 16
DS 2
SWH 12335.526 Hz
FIDRES 0.188225 Hz
AQ 2.6564426 sec
RG 203
DW 40.533 usec
DE 6.50 usec
TE 298.2 K
D1 1.00000000 sec
TD0 1

----- CHANNEL f1 -----
NUC1 1H
P1 10.86 usec
PL1 -2.00 dB
PL1W 19.70630455 W
SFO1 600.7137096 MHz
SI 32768
SF 600.7100142 MHz
WDW EM
SSB 0
LB 0.30 Hz
GB 0
PC 1.00
    
```

SW08-028-07136D 13C 600

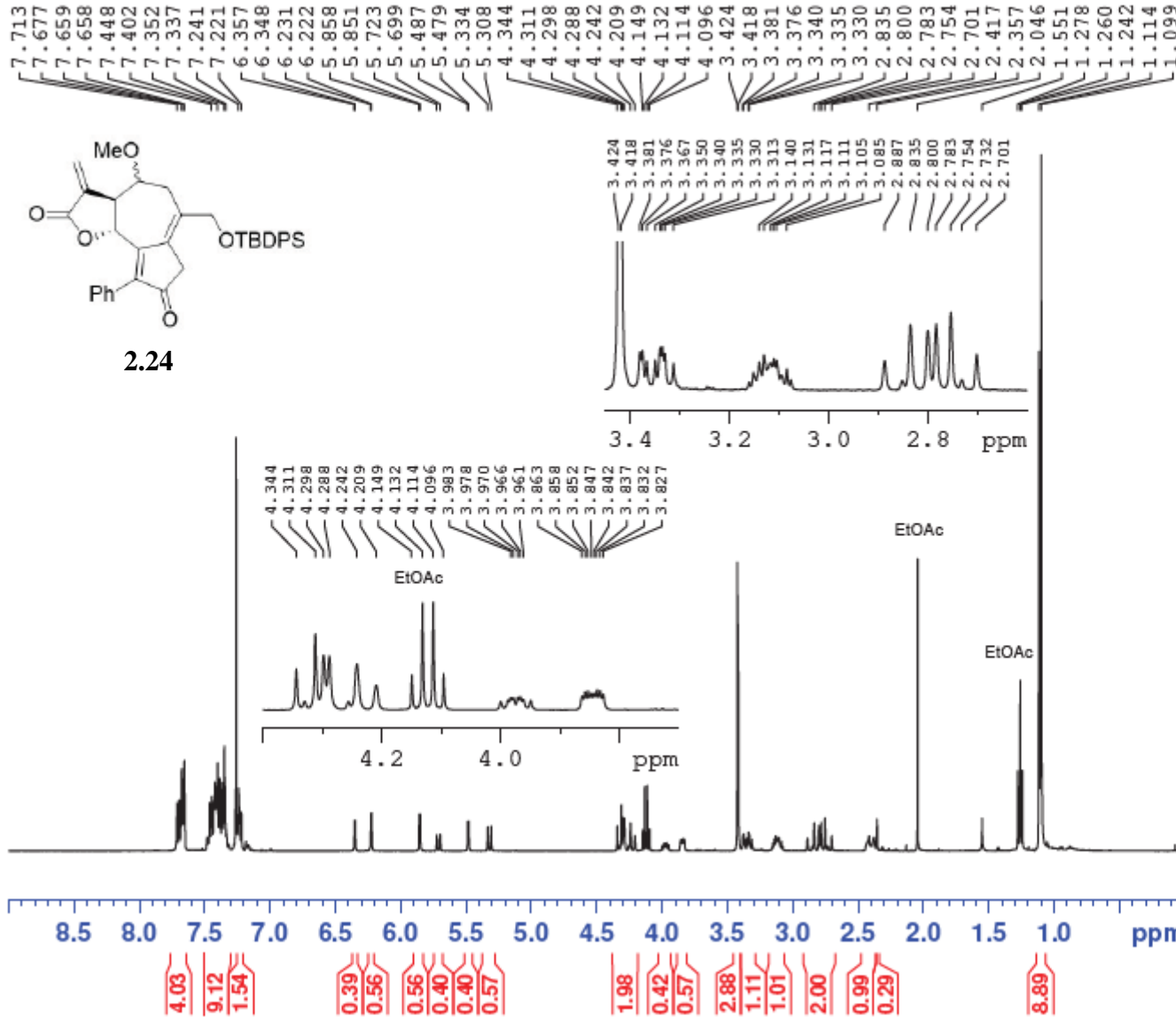


NAME SW08-028-07136D
EXPNO 2
PROCNO 1
Date_ 20160517
Time 13.46
INSTRUM spect
PROBHD 5 mm PABBO BB-
PULPROG zgpg30
TD 65536
SOLVENT CDCl3
NS 3400
DS 4
SWH 36057.691 Hz
FIDRES 0.550197 Hz
AQ 0.9088159 sec
RG 203
DW 13.867 usec
DE 6.50 usec
TE 298.1 K
D1 2.0000000 sec
D11 0.0300000 sec
TD0 1

----- CHANNEL f1 -----
NUC1 13C
P1 11.50 usec
PL1 0.00 dB
PL1W 97.46119690 W
SFO1 151.0637542 MHz

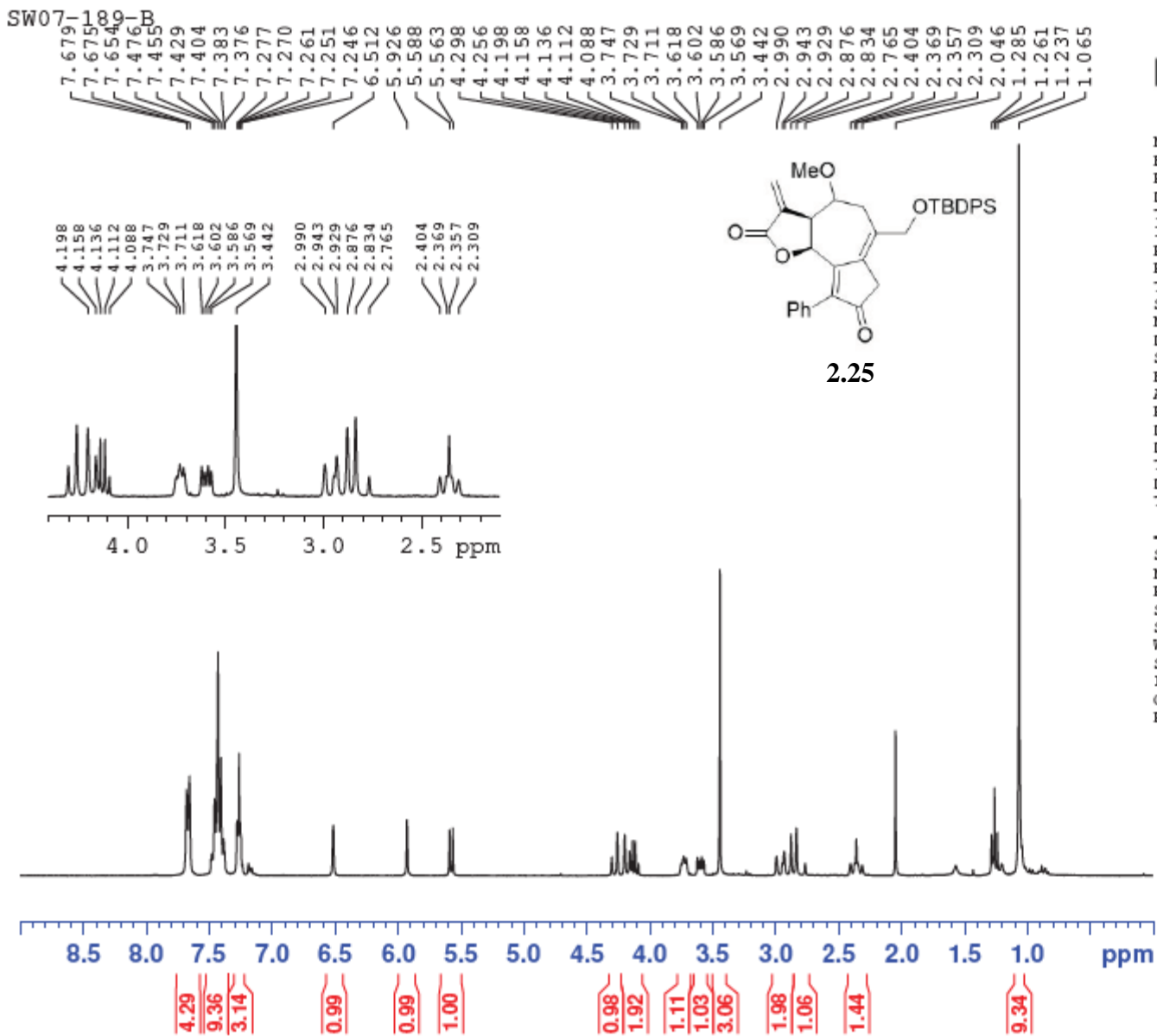
----- CHANNEL f2 -----
CPDPRG2 waltz16
NUC2 1H
PCPD2 70.00 usec
PL2 -2.00 dB
PL12 14.19 dB
PL13 120.00 dB
PL2W 19.70630455 W
PL12W 0.47381112 W
PL13W 0.00000000 W
SFO2 600.7124028 MHz
SI 32768
SF 151.0486270 MHz
WDW EM
SSB 0
LB 1.00 Hz
GB 0
PC 1.40

SW07-150-A



NAME SW07-150-A
 EXPNO 10
 PROCNO 1
 Date_ 20151219
 Time 11.21
 INSTRUM spect
 PROBHD 5 mm PABBO BB-
 PULPROG zg30
 ID 65536
 SOLVENT CDCl3
 NS 16
 DS 2
 SWH 8012.820 Hz
 FIDRES 0.122266 Hz
 AQ 4.0894966 sec
 RG 114
 DW 62.400 usec
 DE 6.50 usec
 TE 94.5 K
 D1 1.00000000 sec
 ID0 1

----- CHANNEL f1 -----
 SFO1 400.1324710 MHz
 NUC1 1H
 P1 13.75 usec
 SI 65536
 SF 400.1300103 MHz
 WDW EM
 SSB 0
 LB 0.30 Hz
 GB 0
 PC 1.00



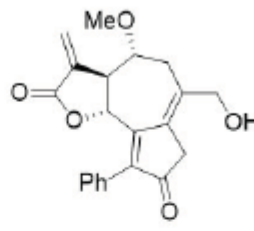
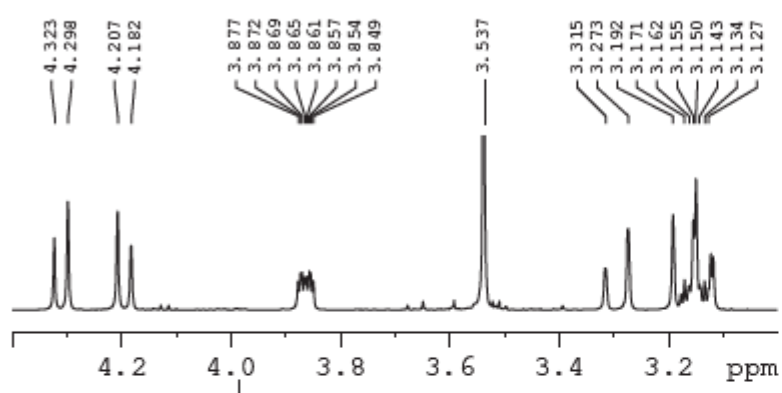
NAME SW07-189-B
 EXPNO 10
 PROCNO 1
 Date_ 20160324
 Time 14.49
 INSTRUM spect
 PROBHD 5 mm QNP 1H/1
 PULPROG zg30
 TD 32768
 SOLVENT CDCl3
 NS 16
 DS 2
 SWH 6188.119 Hz
 FIDRES 0.188846 Hz
 AQ 2.6477044 sec
 RG 128
 DW 80.800 usec
 DE 6.50 usec
 TE -928.5 K
 D1 1.00000000 sec
 TD0 1

----- CHANNEL f1 -----
 SFO1 300.2318540 MHz
 NUC1 1H
 P1 12.71 usec
 SI 32768
 SF 300.2300088 MHz
 WDW EM
 SSB 0
 LB 0.10 Hz
 GB 0
 PC 1.00

SW04-191-A 1H 500



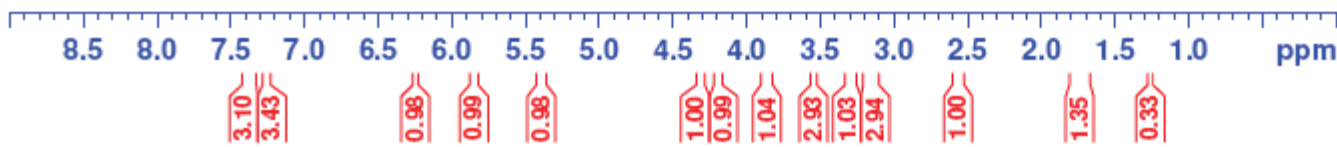
7.392
7.380
7.377
7.374
7.365
7.360
7.358
7.352
7.350
7.266
7.260
7.251
7.248
6.249
5.852
5.846
5.399
5.378
4.323
4.298
4.207
4.182
3.877
3.869
3.865
3.861
3.857
3.854
3.849
3.537
3.315
3.273
3.192
3.171
3.162
3.155
3.150
3.143
3.134
3.127
3.123
3.118
2.579
2.574
2.548
2.542
1.733
1.720
1.258
1.254



1.83a

NAME SW04-191-A
EXPNO 2
PROCNO 1
Date_ 20140322
Time 12.05
INSTRUM spect
PROBHD 5 mm PABBO BB-
PULPROG zg30
TD 65536
SOLVENT CDCl3
NS 16
DS 2
SWH 10330.578 Hz
FIDRES 0.157632 Hz
AQ 3.1719923 sec
RG 203
DW 48.400 usec
DE 6.50 usec
TE 297.7 K
D1 1.00000000 sec

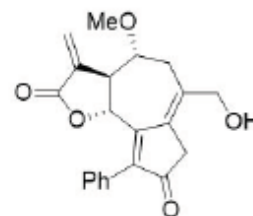
----- CHANNEL f1 -----
NUC1 1H
P1 10.20 usec
SI 65536
SF 500.1600126 MHz
WDW EM
SSB 0
LB 0.30 Hz
GB 0
PC 1.00



SW04-191-A 13C 500

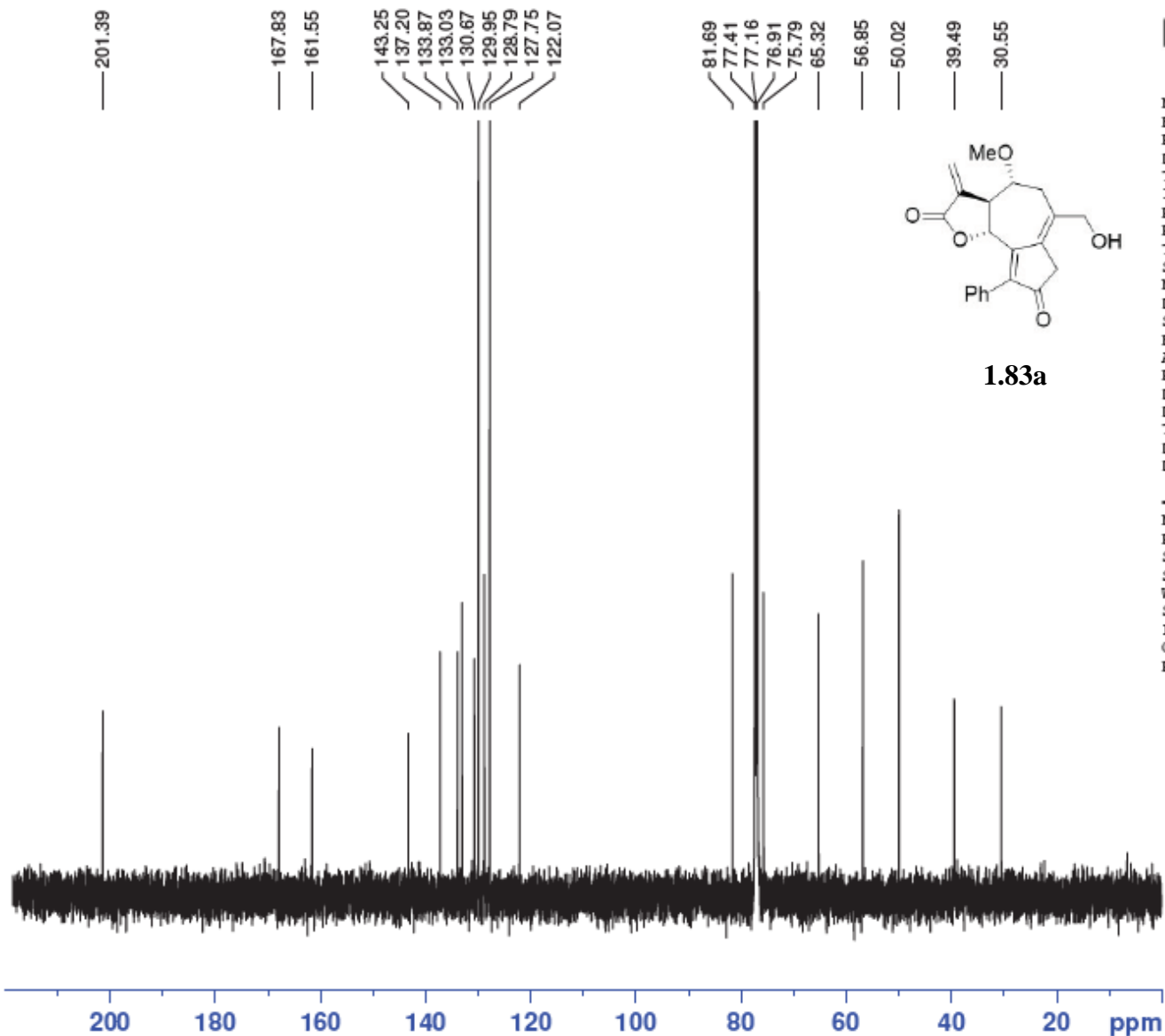


NAME SW04-191-A
EXPNO 3
PROCNO 1
Date_ 20140322
Time 13.42
INSTRUM spect
PROBHD 5 mm PABBO BB-
PULPROG zgpg30
TD 65536
SOLVENT CDCl3
NS 1684
DS 4
SWH 29761.904 Hz
FIDRES 0.454131 Hz
AQ 1.1010548 sec
RG 203
DW 16.800 usec
DE 6.50 usec
TE 298.1 K
D1 2.00000000 sec
D11 0.03000000 sec

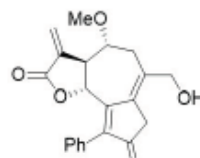


1.83a

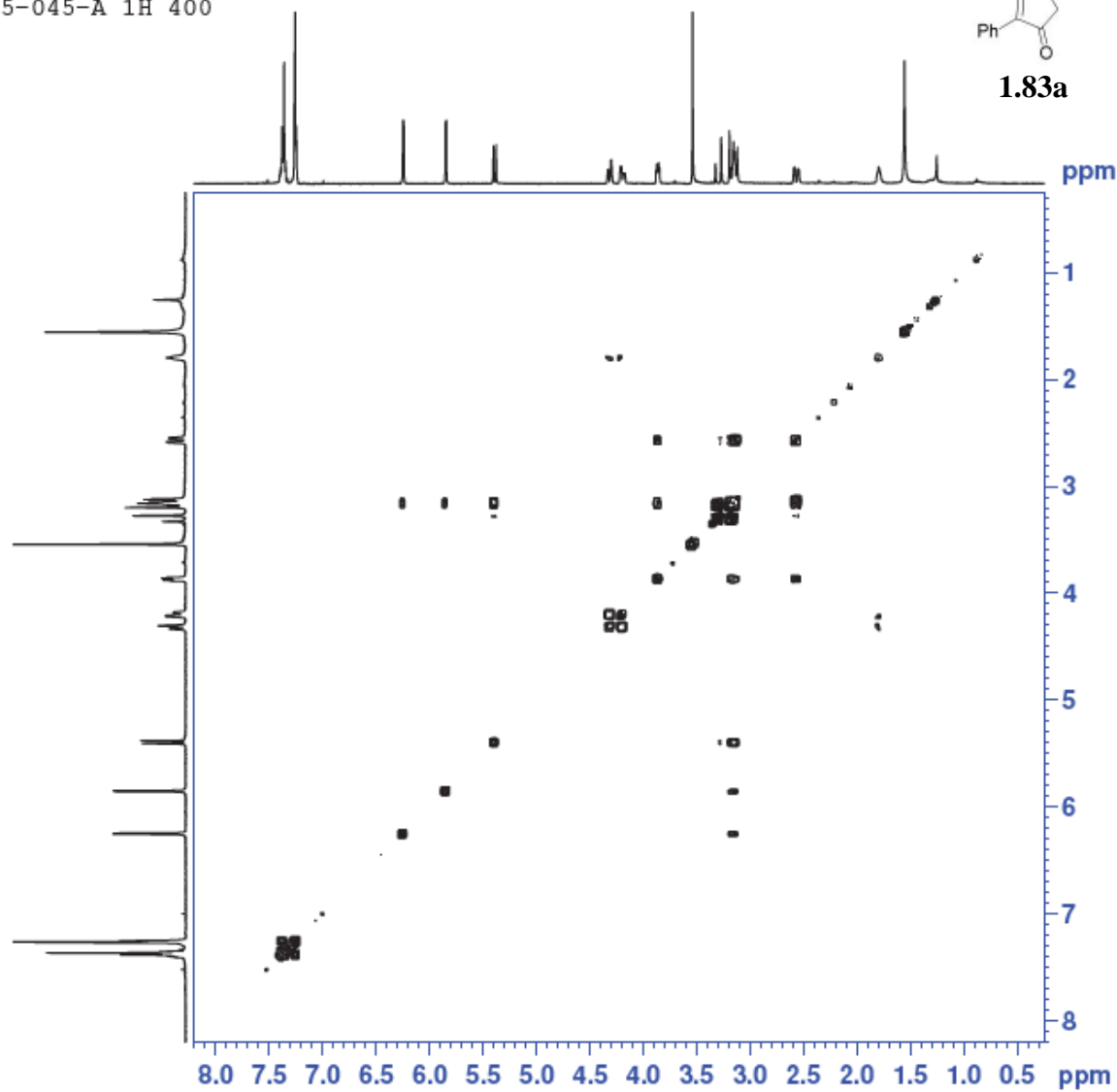
----- CHANNEL f1 -----
NUC1 13C
P1 8.80 usec
SI 32768
SF 125.7653142 MHz
WDW EM
SSB 0
LB 1.00 Hz
GB 0
PC 1.40



SW05-045-A 1H 400



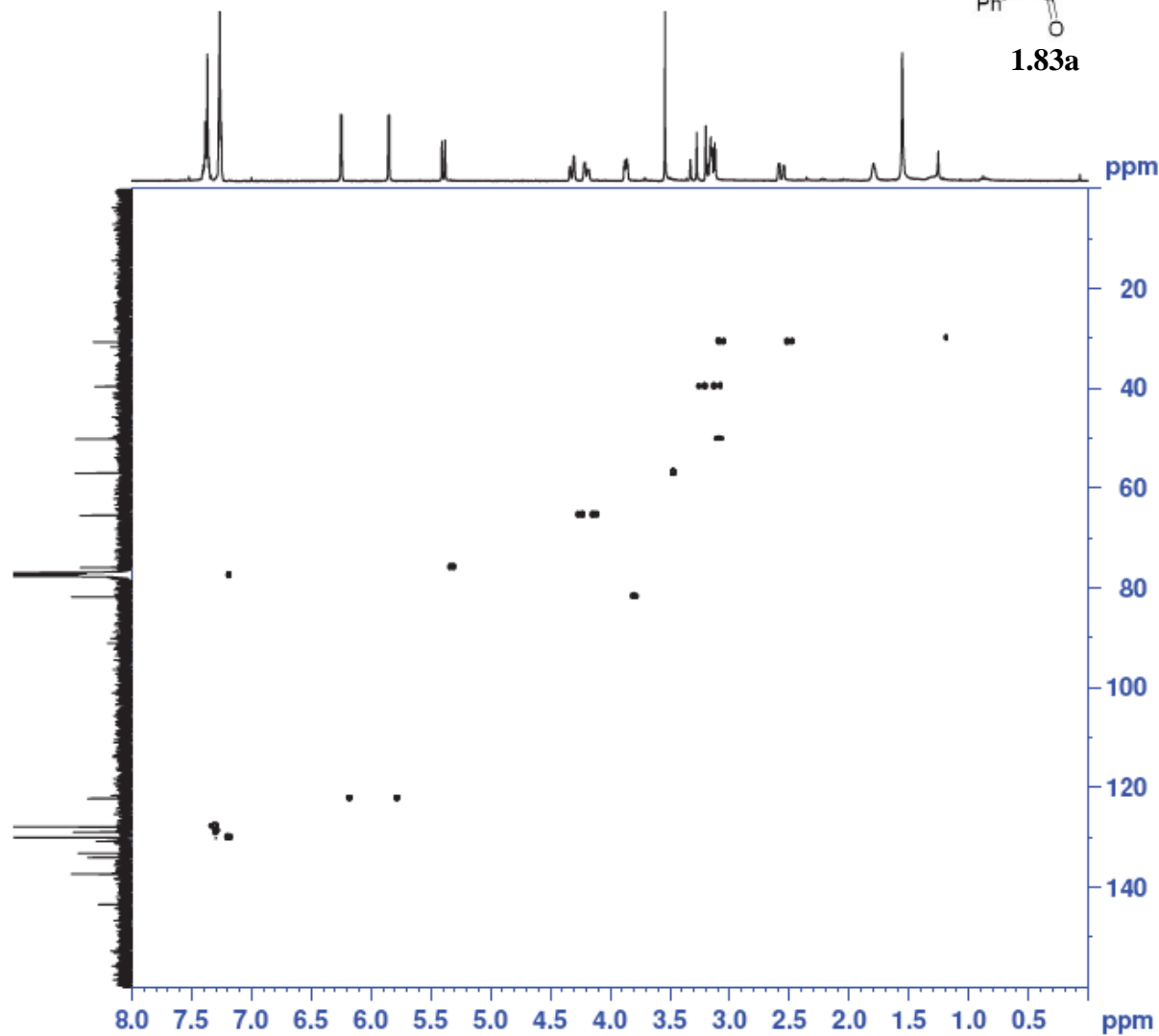
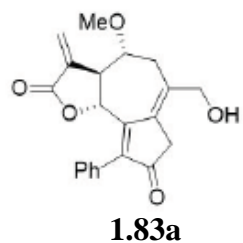
1.83a



NAME SW05-045-A
EXPNO 12
PROCNO 1
Date_ 20160520
Time 3.05
INSTRUM spect
PROBHD 5 mm PABBO BB-
PULPROG cosygpppqf
TD 2048
SOLVENT CDCl3
NS 1
DS 8
SWH 3184.713 Hz
FIDRES 1.555036 Hz
AQ 0.3215860 sec
RG 64
DW 157.000 usec
DE 6.50 usec
TE 98.0 K
D0 0.00000300 sec
D1 1.87015700 sec
D11 0.03000000 sec
D12 0.00002000 sec
D13 0.00000400 sec
D16 0.00020000 sec
IN0 0.00031400 sec

----- CHANNEL f1 -----
SF01 400.1317011 MHz
NUC1 1H
P0 13.75 usec
P1 13.75 usec
P17 2500.00 usec
ND0 1
TD 128
SF01 400.1317 MHz
FIDRES 24.880573 Hz
SW 7.959 ppm
FnMODE QF
SI 1024
SF 400.1300104 MHz
WDW QSINE
SSB 0
LB 0.00 Hz
GB 0
PC 1.40
SI 1024
MC2 QF
SF 400.1300104 MHz
WDW QSINE
SSB 0
LB 0.00 Hz
GB 0

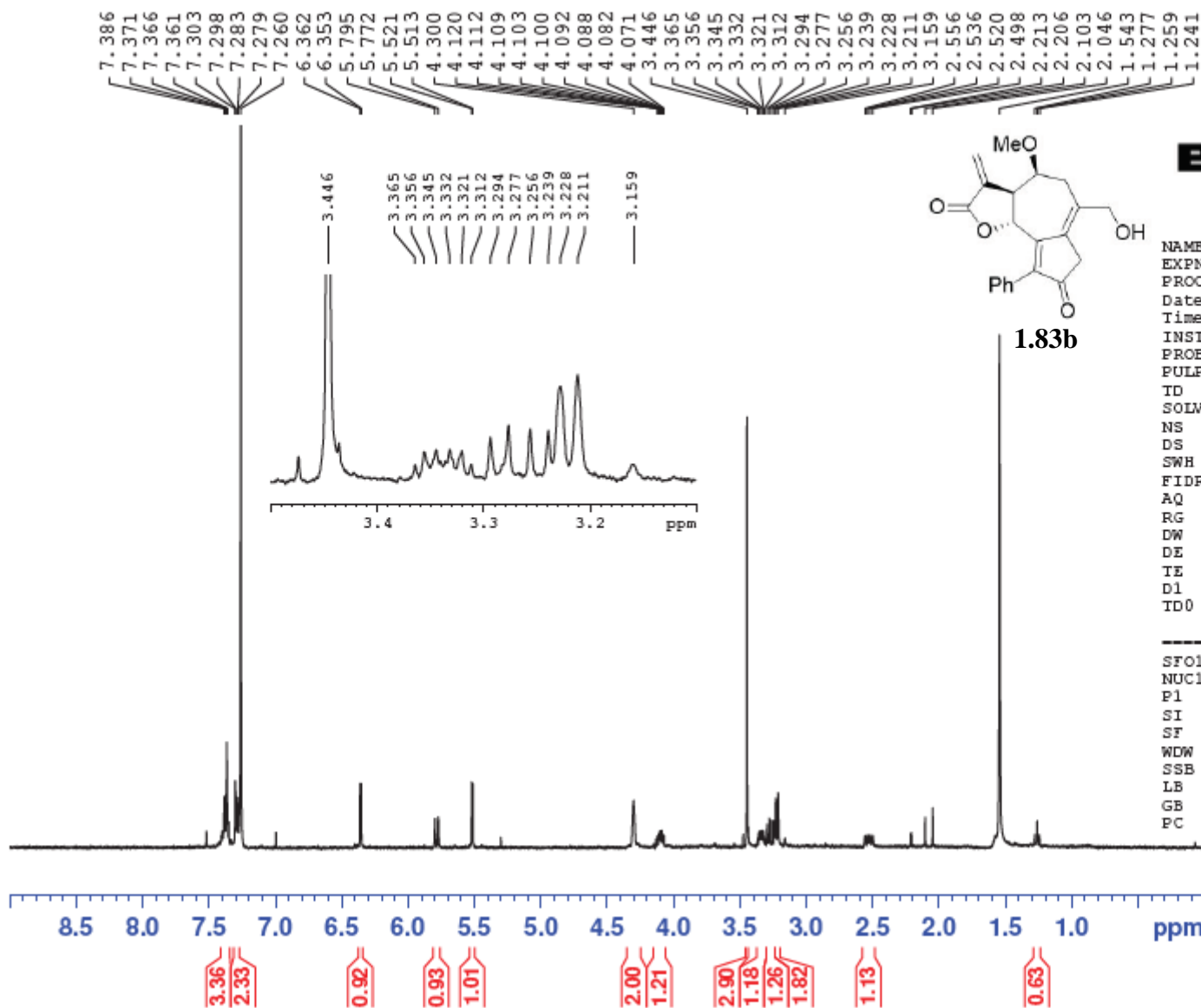
SW05-045-A



NAME SW05-045-A
EXPNO 21
PROCNO 1
Date_ 20160520
Time 20.16
INSTRUM spect
PROBHD 5 mm PABBO BB-
PULPROG hsqcetgp
TD 1024
SOLVENT CDCl3
NS 8
DS 16
SWH 3086.420 Hz
FIDRES 3.014082 Hz
AQ 0.1659380 sec
RG 203
DW 162.000 usec
DE 6.50 usec
TE 96.0 K
CNST2 145.0000000
D0 0.00000300 sec
D1 1.43262100 sec
D4 0.00172414 sec
D11 0.03000000 sec
D16 0.00020000 sec
INO 0.00003000 sec
ZGPTNS

----- CHANNEL f1 -----
SFO1 400.1316771 MHz
NUC1 1H
P1 13.75 usec
P2 27.50 usec
P28 1000.00 usec
ND0 2
TD 256
SFO1 100.6203 MHz
FIDRES 65.104164 Hz
SW 165.639 ppm
FnMODE Echo-Antiecho
SI 1024
SF 400.1300383 MHz
WDW QSINE
SSB 2
LB 0.00 Hz
GB 0
PC 1.40
SI 1024
MC2 echo-antiecho
SF 100.6127685 MHz
WDW QSINE
SSB 2
LB 0.00 Hz
GB 0

SW08-012-05086



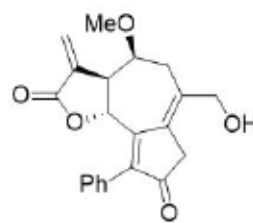
NAME SW08-012-05086
 EXPNO 10
 PROCNO 1
 Date_ 20160503
 Time_ 16.50
 INSTRUM spect
 PROBHD 5 mm PABBO BB-
 PULPROG zg30
 ID 65536
 SOLVENT CDCl3
 NS 16
 DS 2
 SWH 8012.820 Hz
 FIDRES 0.122266 Hz
 AQ 4.0894966 sec
 RG 181
 DW 62.400 usec
 DE 6.50 usec
 TE 95.9 K
 D1 1.00000000 sec
 TD0 1

----- CHANNEL f1 -----
 SF01 400.1324710 MHz
 NUC1 1H
 P1 13.75 usec
 SI 65536
 SF 400.1300098 MHz
 WDW EM
 SSB 0
 LB 0.30 Hz
 GB 0
 PC 1.00

SW08-012-05086B 1H 400



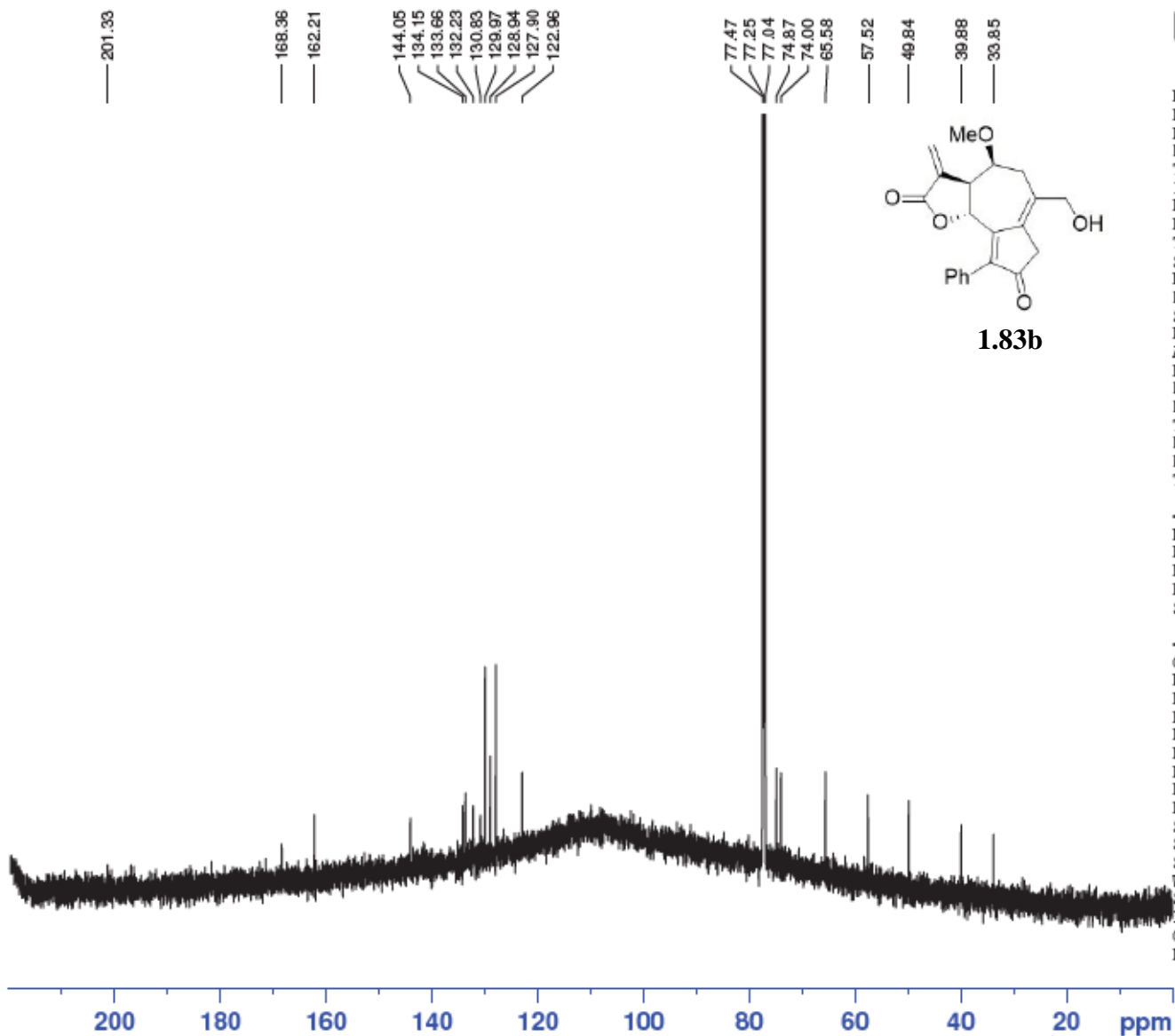
NAME SW08-012-05086B
 EXPNO 100
 PROCNO 1
 Date_ 20160505
 Time 15.29
 INSTRUM spect
 PROBHD 5 mm PABBO BB-
 PULPROG zgpg30
 TD 65536
 SOLVENT CDC13
 NS 19084
 DS 4
 SWH 36057.691 Hz
 FIDRES 0.550197 Hz
 AQ 0.9088159 sec
 RG 203
 DW 13.867 usec
 DE 6.50 usec
 TE 296.5 K
 D1 2.00000000 sec
 D11 0.03000000 sec
 TDO 1



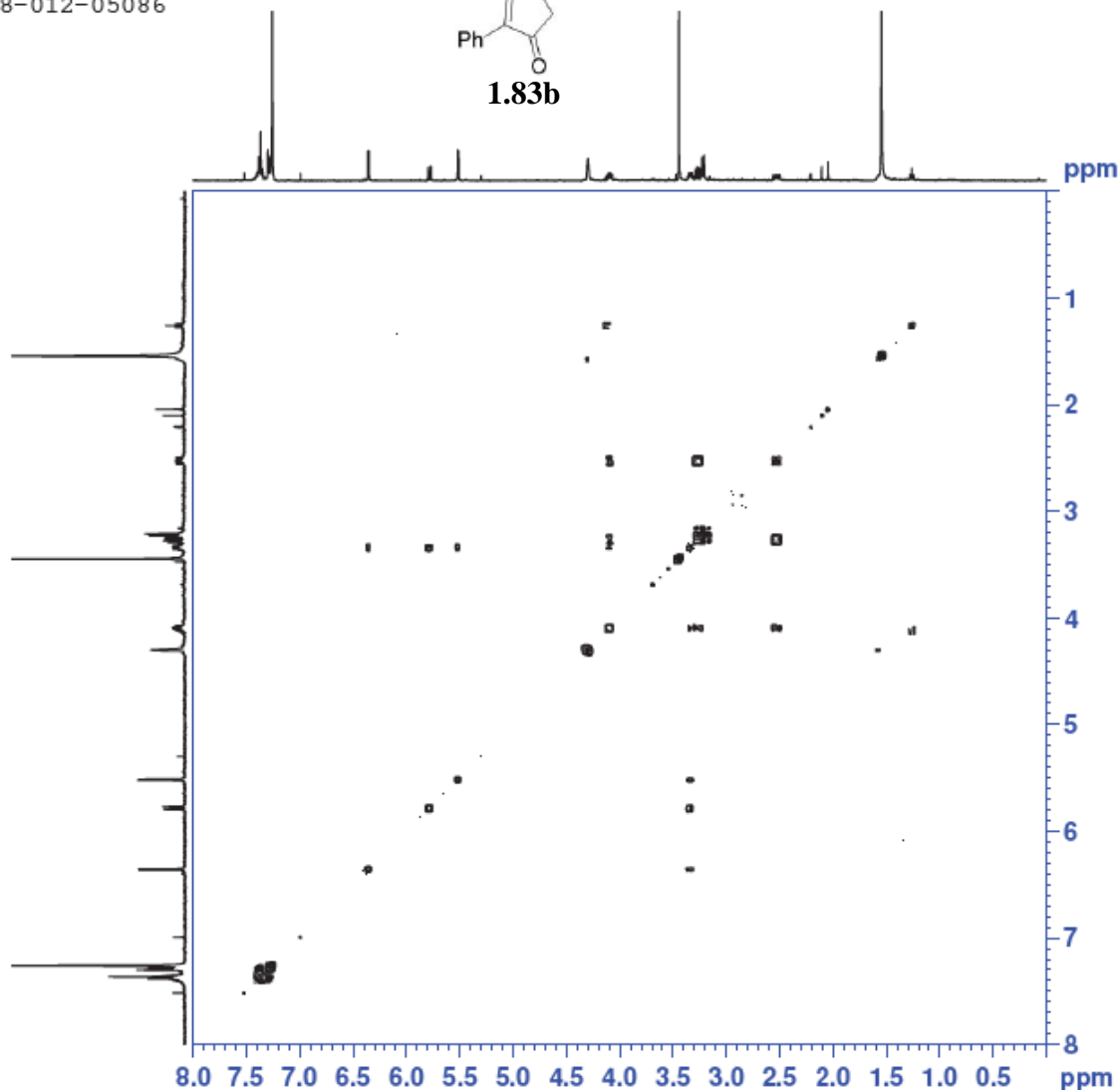
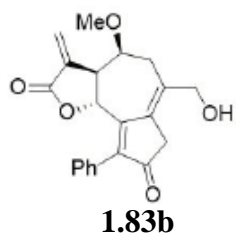
1.83b

----- CHANNEL f1 -----
 NUC1 13C
 P1 11.50 usec
 PL1 0.00 dB
 PL1W 97.46119690 W
 SFO1 151.0637542 MHz

----- CHANNEL f2 -----
 CPDPRG2 waltz16
 NUC2 1H
 PCPD2 70.00 usec
 PL2 -2.00 dB
 PL12 14.19 dB
 PL13 120.00 dB
 PL2W 19.70630455 W
 PL12W 0.47381112 W
 PL13W 0.00000000 W
 SFO2 600.7124028 MHz
 SI 65536
 SF 151.0486149 MHz
 WDW GM
 SSB 0
 LB -1.00 Hz
 GB 0.035
 PC 1.40



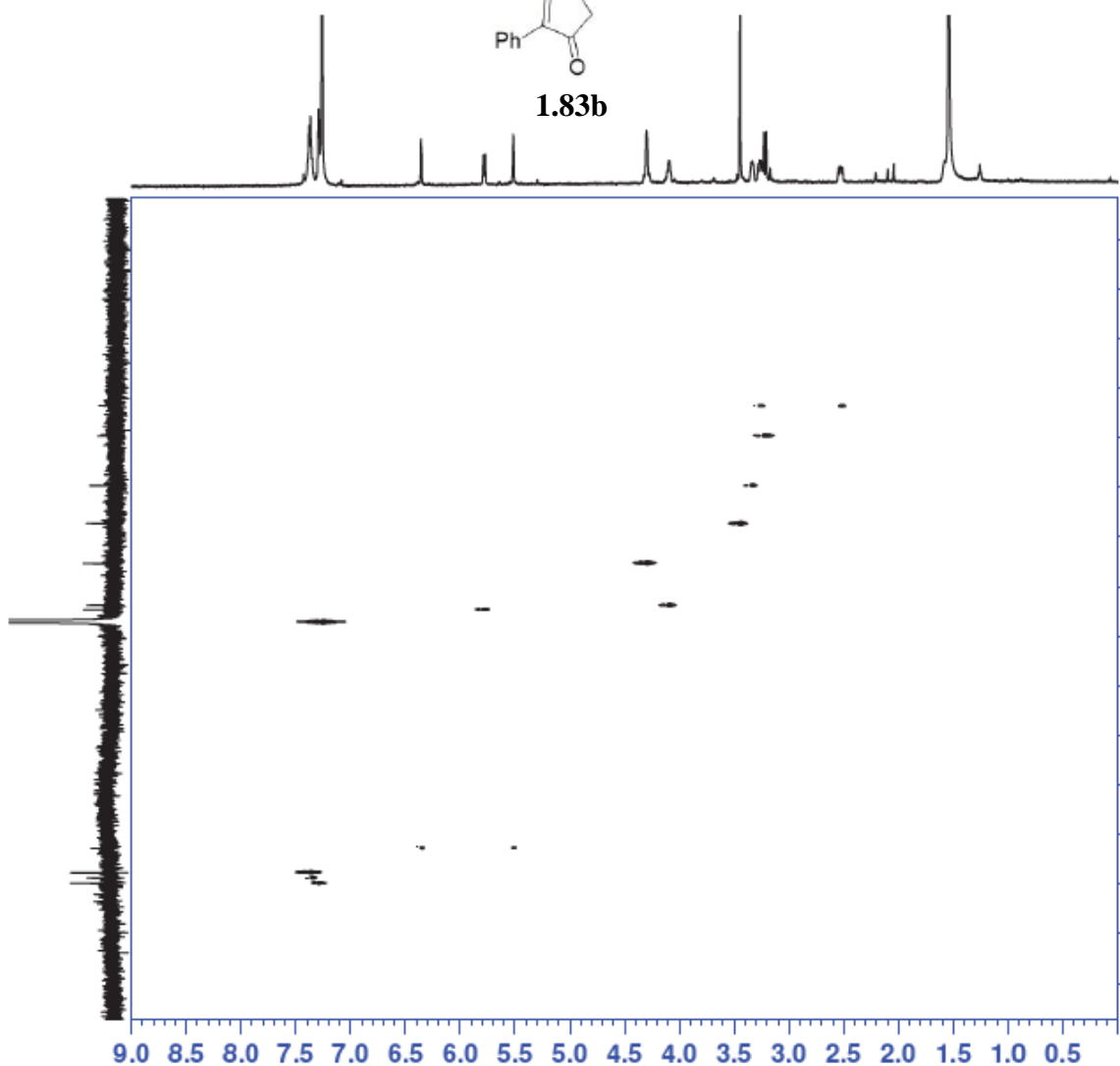
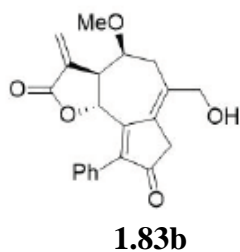
SW08-012-05086



NAME SW08-012-05086
EXPNO 12
PROCNO 1
Date_ 20160504
Time_ 2.56
INSTRUM spect
PROBHD 5 mm PABBO BB-
PULPROG cosygpppqf
ID 2048
SOLVENT CDCl3
NS 1
DS 8
SWH 3012.048 Hz
FIDRES 1.470727 Hz
AQ 0.3400180 sec
RG 114
DW 166.000 usec
DE 6.50 usec
TE 96.7 K
D0 0.00000300 sec
D1 1.85172498 sec
D11 0.03000000 sec
D12 0.00002000 sec
D13 0.00000400 sec
D16 0.00020000 sec
IN0 0.00033200 sec

----- CHANNEL f1 -----
SFO1 400.1316666 MHz
NUC1 1H
P0 13.75 usec
P1 13.75 usec
P17 2500.00 usec
ND0 1
ID 128
SFO1 400.1317 MHz
FIDRES 23.531626 Hz
SW 7.528 ppm
FnMODE QF
SI 1024
SF 400.1300098 MHz
WDW QSINE
SSB 0
LB 0.00 Hz
GB 0
PC 1.40
SI 1024
MC2 QF
SF 400.1300098 MHz
WDW QSINE
SSB 0
LB 0.00 Hz
GB 0

SW08-012-05086B 1H 400



NAME SW08-012-05086B
 EXPNO 10
 PROCNO 1
 Date_ 20160506
 Time 5.18
 INSTRUM spect
 PROBRD 5 mm PABBO EB-
 PULPROG hsqc01
 TD 1024
 SOLVENT CDCl3
 NS 32
 DS 16
 SWH 8012.820 Hz
 FIDRES 7.825020 Hz
 AQ 0.0639476 sec
 RG 203
 DM 62.400 usec
 DE 6.50 usec
 TE 295.9 K
 CNST2 145.0000000
 D0 0.0000000 usec
 D1 1.5000000 usec
 D4 0.09172414 usec
 D11 0.03000000 usec
 D13 0.00000400 usec
 D16 0.00020000 usec
 D24 0.00110000 usec
 IN0 0.00002000 usec
 RGPRMS

----- CHANNEL f1 -----
 NUCL1 1H
 P1 12.35 usec
 P2 24.70 usec
 P28 0.00 usec
 PL1 -2.00 dB
 PL1W 19.70630455 W
 SFO1 600.7130500 MHz

----- CHANNEL f2 -----
 CPDPRG2 garp
 NUCL2 13C
 P3 11.90 usec
 P4 23.80 usec
 PCPD2 60.00 usec
 PL2 0.00 dB
 PL12 14.05 dB
 PL2W 97.46119690 W
 PL12W 3.83558583 W
 SFO2 151.0599153 MHz

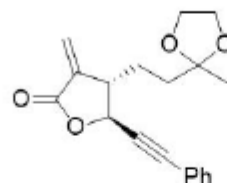
----- GRADIENT CHANNEL -----
 GPNAM1 SINE.100
 GPNAM2 SINE.100
 CPZ1 00.00 A
 CPZ2 20.19 A
 P16 1000.00 usec
 NDO 2
 ID 512
 SFO1 151.0599 MHz
 FIDRES 48.970822 Hz
 SW 165.639 ppm
 FRMDE Echo-AntiEcho
 SI 1024
 SF 600.7100134 MHz
 MDM QSINE
 SSB 2
 LB 0.00 Hz
 GB 0
 PC 1.40
 SI 1024
 MC2 echo-antiEcho
 SF 151.0486500 MHz
 MDM QSINE
 SSB 2
 LB 0.00 Hz
 GB 0

SW07-024-B 1H 400

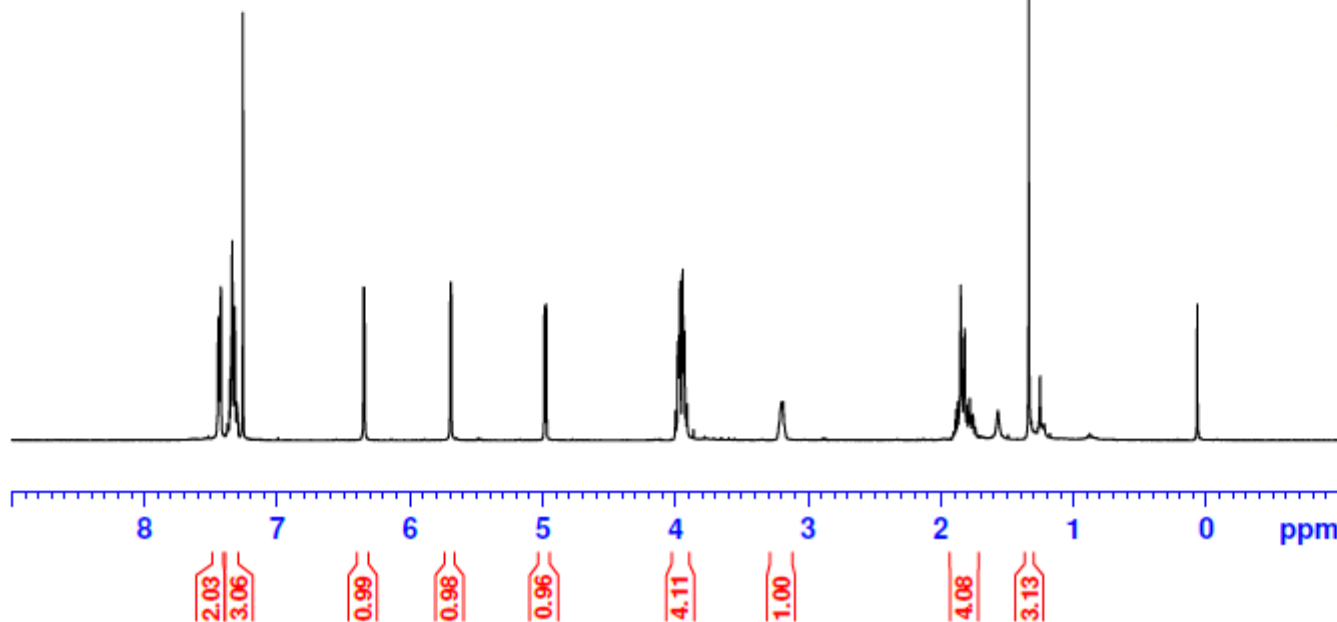
7.448
7.444
7.429
7.425
7.359
7.351
7.348
7.340
7.329
7.321
7.306
7.260
6.351
6.345
5.696
5.690
4.988
4.975
4.000
3.983
3.979
3.974
3.969
3.966
3.962
3.950
3.947
3.943
3.938
3.933
3.929
3.912
3.203
3.196
3.190
1.882
1.851
1.842
1.822
1.782
1.571
1.337
1.252
0.068



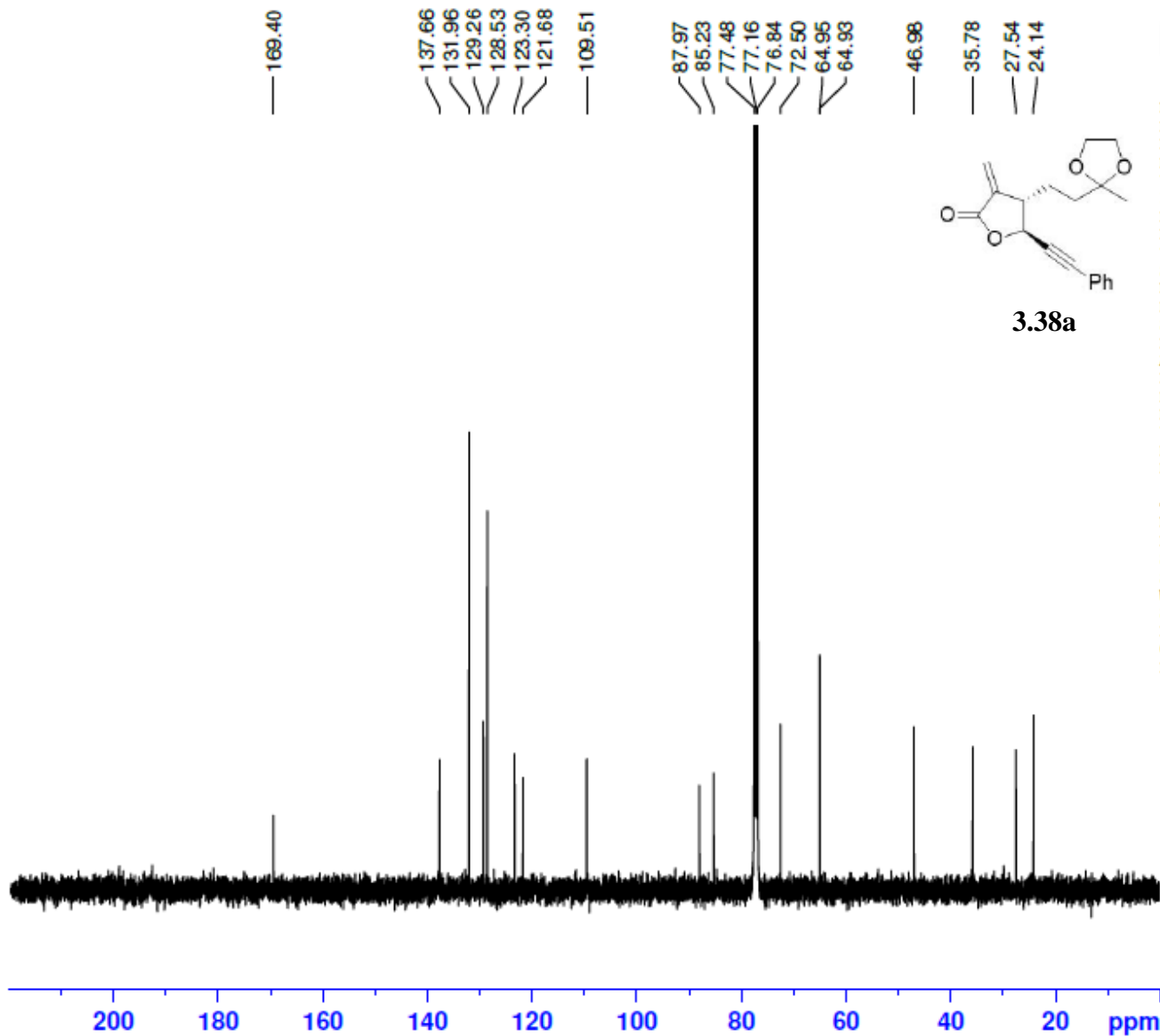
NAME SW07-024-B
EXPNO 10
PROCNO 1
Date_ 20150625
Time 8.39
INSTRUM spect
PROBHD 5 mm PABBO BB-
PULPROG zg30
ID 65536
SOLVENT CDC13
NS 16
DS 2
SWH 8223.685 Hz
FIDRES 0.125483 Hz
AQ 3.9846387 sec
RG 128
DW 60.800 usec
DE 6.50 usec
TE 94.7 K
D1 1.00000000 sec



----- CHANNEL f1 -----
NUC1 1H
P1 13.75 usec
SI 65536
SF 400.1300101 MHz
WDW EM
SSB 0
LB 0.30 Hz
GB 0
PC 1.00



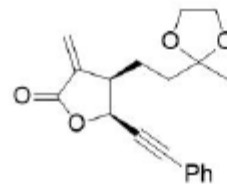
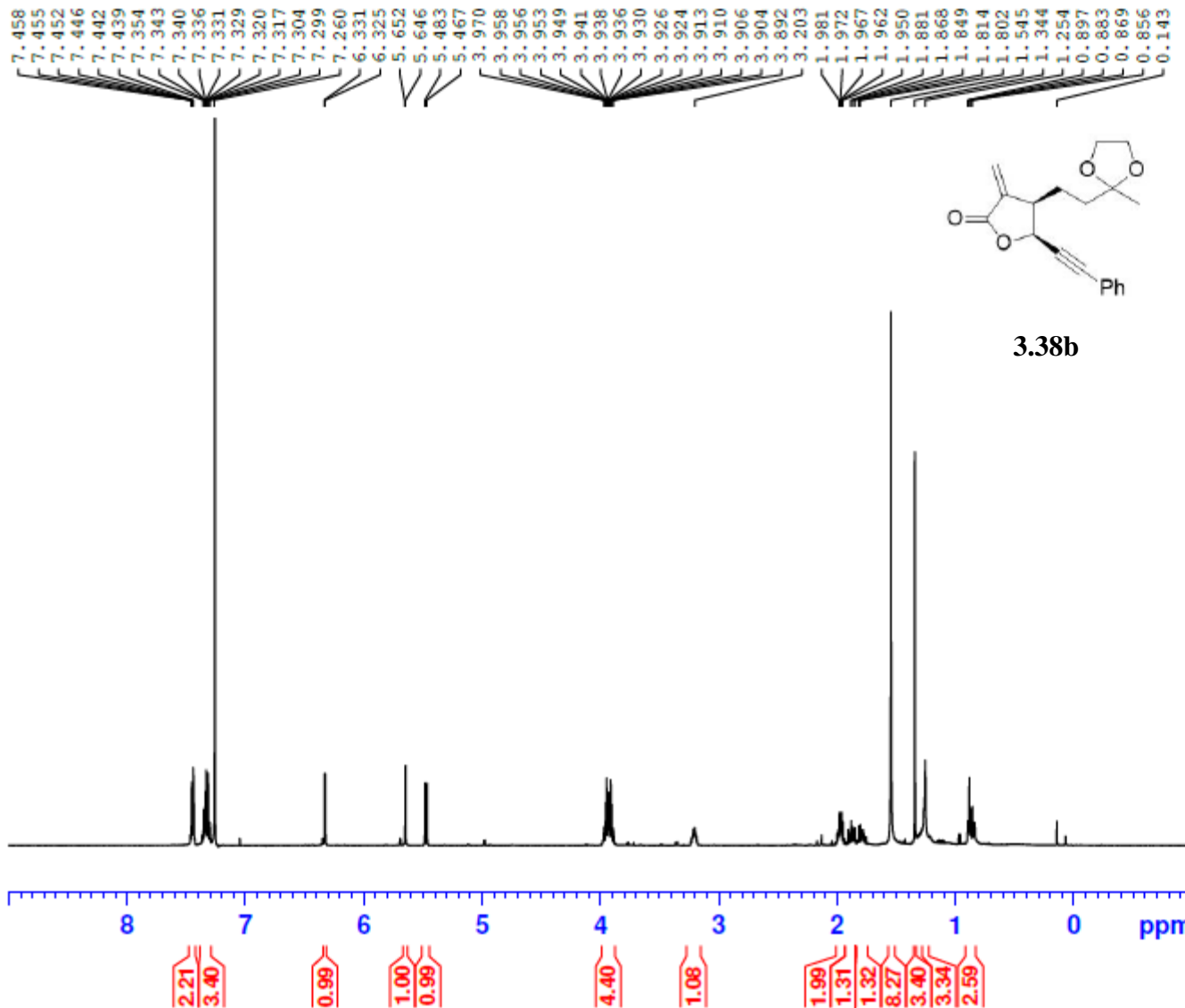
SW07-009-B 13C 400



NAME SW07-009-B
EXPNO 11
PROCNO 1
Date_ 20150617
Time 1.51
INSTRUM spect
PROBHD 5 mm PABBO BB-
PULPROG zgpg30
ID 65536
SOLVENT CDCl3
NS 3072
DS 4
SWH 24038.461 Hz
FIDRES 0.366798 Hz
AQ 1.3631988 sec
RG 144
DW 20.800 usec
DE 6.50 usec
TE 70.7 K
D1 2.00000000 sec
D11 0.03000000 sec

----- CHANNEL f1 -----
NUC1 13C
P1 10.00 usec
SI 32768
SF 100.6127562 MHz
WDW EM
SSB 0
LB 1.00 Hz
GB 0
PC 1.40

SW07-024-C 1H 500



3.38b

NAME SW07-024-C
EXPNO 10
PROCNO 1
Date_ 20150707
Time 18.30
INSIRUM spect
PROBHD 5 mm PABBO BB/
PULPROG zg30
ID 65536
SOLVENT CDCl3
NS 16
DS 2
SWH 10000.000 Hz
FIDRES 0.152588 Hz
AQ 3.2768500 sec
RG 203
DW 50.000 usec
DE 6.50 usec
TE 298.2 K
D1 1.00000000 sec
TD0 1

----- CHANNEL f1 -----
SFO1 500.1630887 MHz
NUC1 1H
P1 11.45 usec
SI 65536
SF 500.1600125 MHz
WDW EM
SSB 0
LB 0.30 Hz
GB 0
PC 1.00

SW07-024-C 13C 500

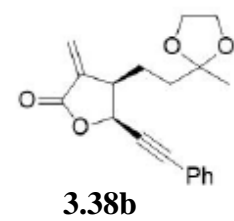


— 169.724

137.694
132.025
129.266
128.528
122.543
121.726
— 109.731

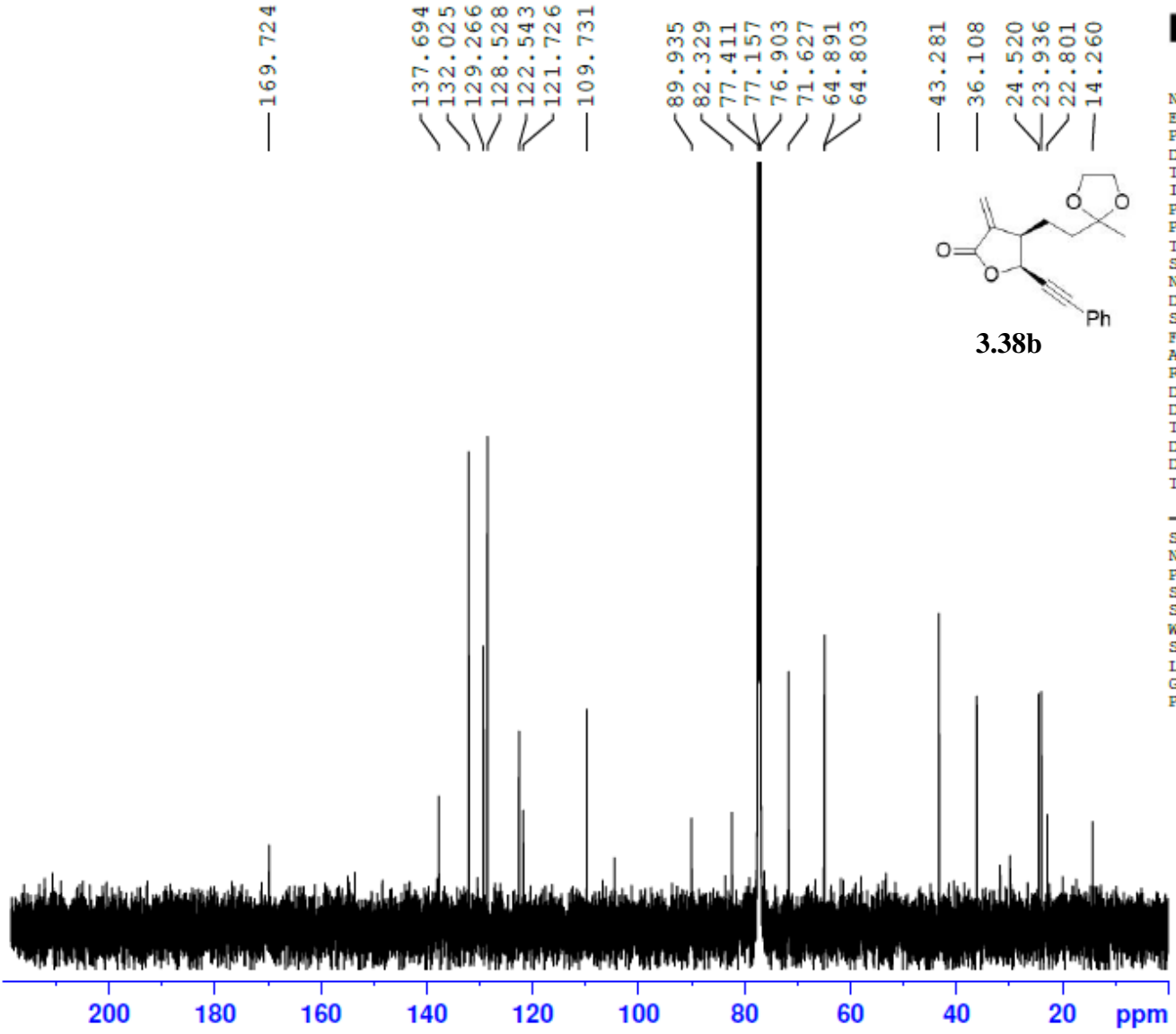
89.935
82.329
77.411
77.157
76.903
71.627
64.891
64.803

— 43.281
— 36.108
24.520
23.936
22.801
— 14.260



NAME SW07-024-C
EXPNO 11
PROCNO 1
Date_ 20150707
Time 23.48
INSTRUM spect
PROBHD 5 mm PABBO BB/
PULPROG zgpg30
ID 65536
SOLVENT CDCl3
NS 3072
DS 2
SWH 29761.904 Hz
FIDRES 0.454131 Hz
AQ 1.1010548 sec
RG 203
DW 16.800 usec
DE 6.50 usec
TE 298.3 K
D1 2.00000000 sec
D11 0.03000000 sec
ID0 1

----- CHANNEL f1 -----
SFO1 125.7779086 MHz
NUC1 13C
P1 10.50 usec
SI 32768
SF 125.7653131 MHz
WDW EM
SSB 0
LB 1.00 Hz
GB 0
PC 1.40

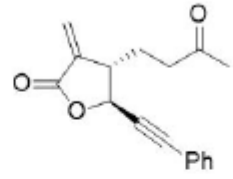


SW07-033-A

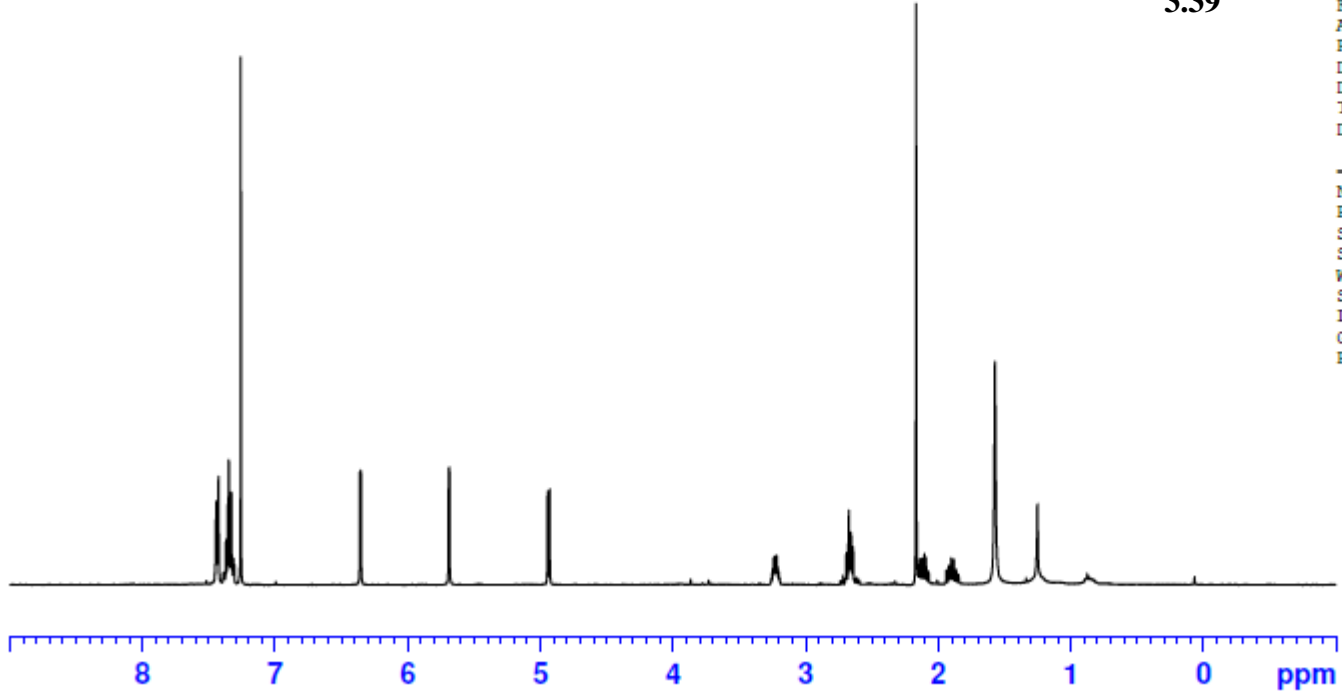
7.449
7.446
7.435
7.430
7.425
7.371
7.364
7.360
7.355
7.349
7.345
7.337
7.334
7.330
7.315
7.309
7.260
6.361
6.354
5.692
5.686
4.945
4.931
3.240
3.232
3.225
3.218
2.692
2.674
2.662
2.659
2.656
2.644
2.168
2.145
2.141
2.126
2.124
2.105
2.091
1.903
1.883
1.573
1.251



NAME SW07-033-A
EXPNO 10
PROCNO 1
Date_ 20150707
Time_ 14.43
INSTRUM spect
PROBHD 5 mm PABBO BB-
PULPROG zg30
TD 65536
SOLVENT CDCl3
NS 16
DS 2
SWH 8223.685 Hz
FIDRES 0.125483 Hz
AQ 3.9846387 sec
RG 161
DW 60.800 usec
DE 6.50 usec
TE 96.3 K
D1 1.00000000 sec



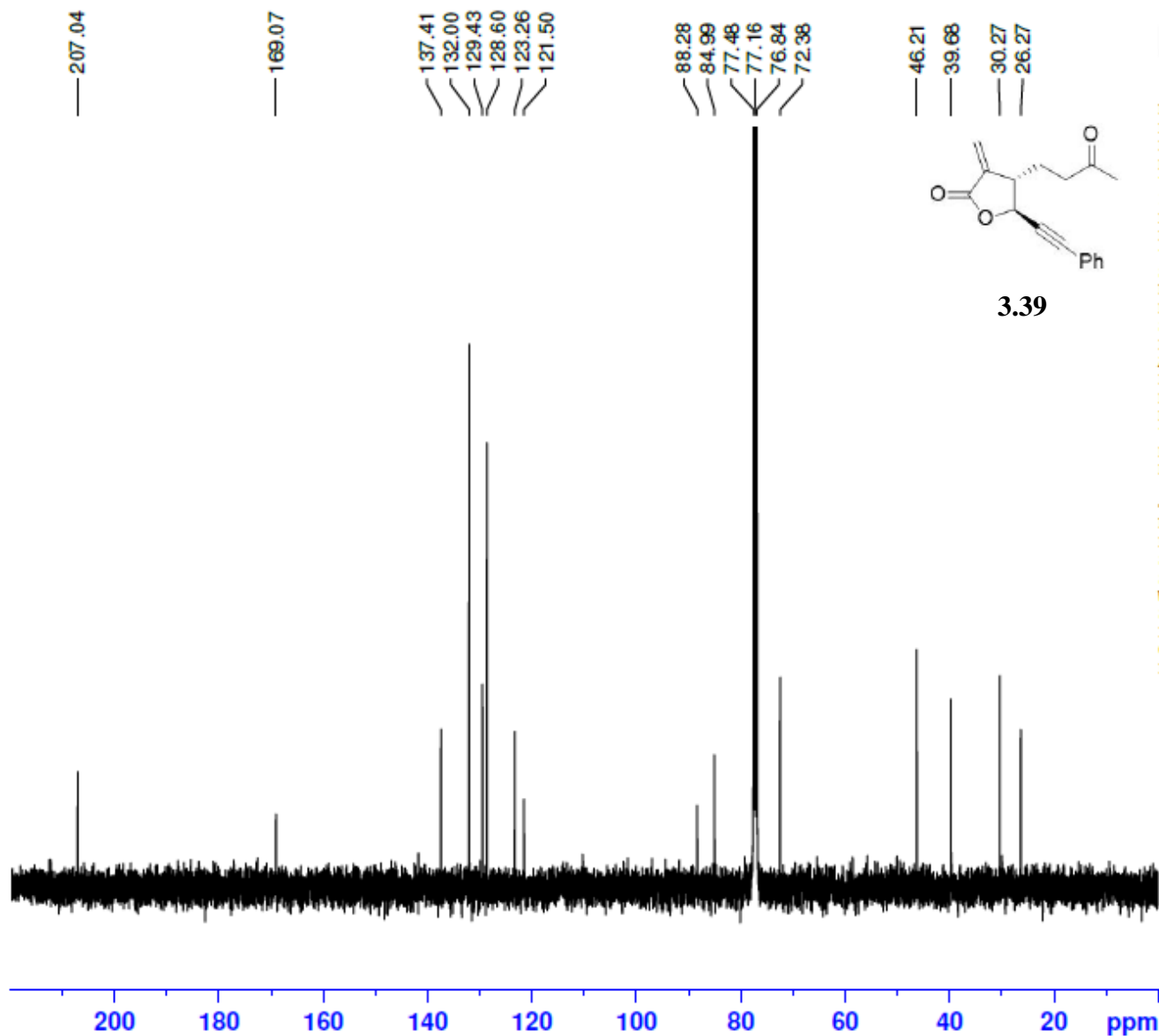
3.39



----- CHANNEL f1 -----
NUC1 1H
P1 13.75 usec
SI 65536
SF 400.1300104 MHz
WDW EM
SSB 0
LB 0.30 Hz
GB 0
PC 1.00

1.97
3.02
1.00
1.00
0.97
0.98
2.04
2.95
1.19
1.11
4.21
1.46
0.39

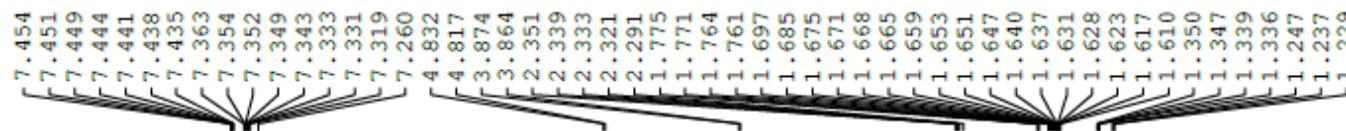
SW07-033-A 13C



NAME SW07-033-A
EXPNO 11
PROCNO 1
Date_ 20150708
Time 4.34
INSTRUM spect
PROBHD 5 mm PABBO BB-
PULPROG zgpg30
ID 65536
SOLVENT CDCl3
NS 2048
DS 4
SWH 24038.461 Hz
FIDRES 0.366798 Hz
AQ 1.3631988 sec
RG 181
DW 20.800 usec
DE 6.50 usec
TE 95.5 K
D1 2.00000000 sec
D11 0.03000000 sec

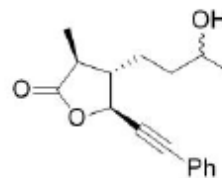
----- CHANNEL f1 -----
NUC1 13C
P1 10.00 usec
SI 32768
SF 100.6127552 MHz
WDW EM
SSB 0
LB 1.00 Hz
GB 0
PC 1.40

SW06-003-1H CDC13 600MHz

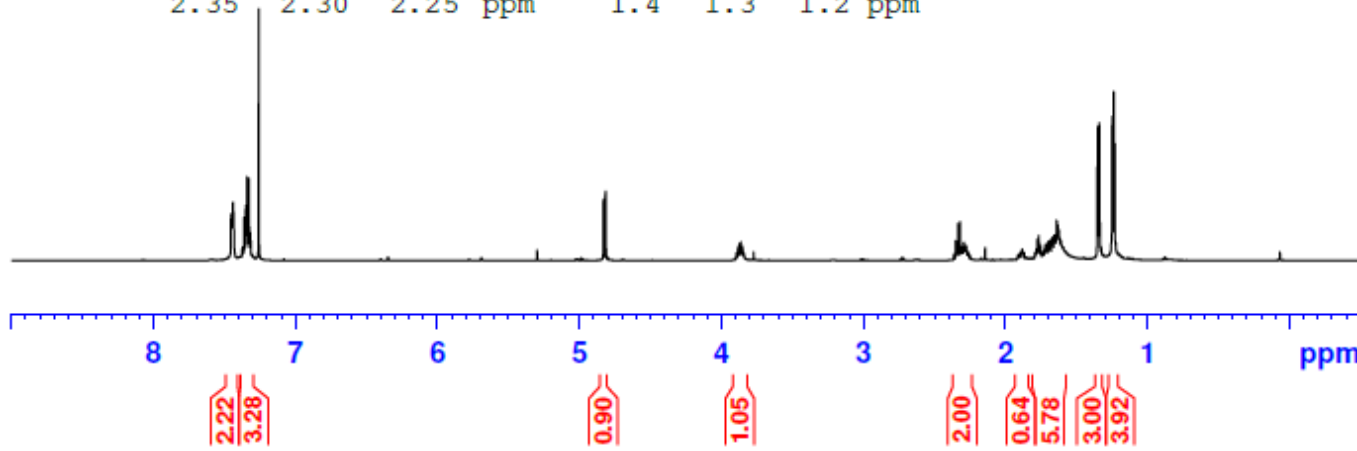
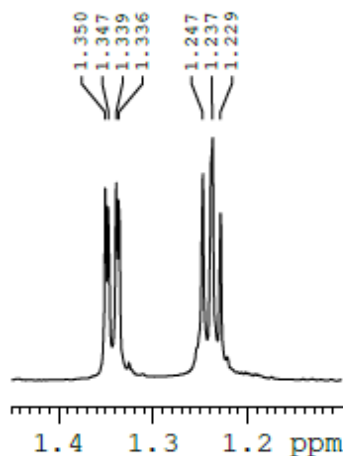
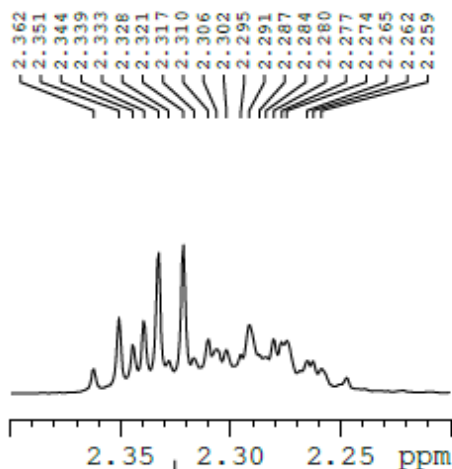


```

NAME          SW06-003-1H
EXPNO         1
PROCNO        1
Date_         20160627
Time          14.14
INSTRUM       spect
PROBHD        5 mm PABBO BB-
PULPROG       zg30
TD            65536
SOLVENT       CDC13
NS            32
DS            2
SWH           12335.526 Hz
FIDRES        0.188225 Hz
AQ            2.6564426 sec
RG            161
DW            40.533 usec
DE            6.50 usec
TE            294.4 K
D1            1.00000000 sec
TD0           1
    
```



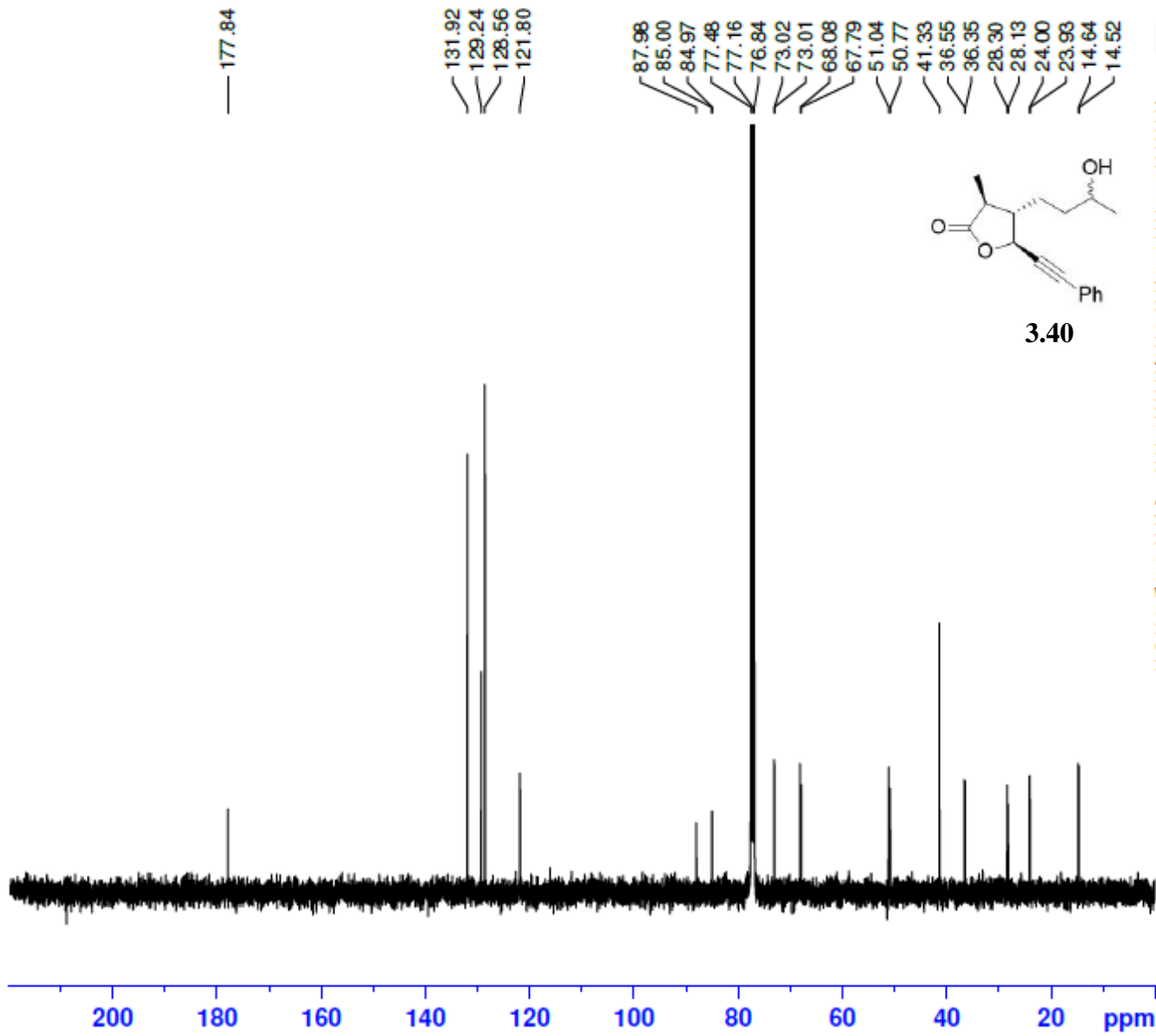
3.40



```

----- CHANNEL f1 -----
NUC1          1H
P1            10.86 usec
PL1           -2.00 dB
PL1W         19.70630455 W
SFO1         600.7137096 MHz
SI            32768
SF            600.7100142 MHz
WDW           EM
SSB           0
LB            0.30 Hz
GB            0
PC            1.00
    
```

SW06-117-B 13C 400



NAME SW06-117-B
 EXPNO 21
 PROCNO 1
 Date_ 20150305
 Time 0.33
 INSTRUM spect
 PROBHD 5 mm PABBO BB-
 PULPROG zgpg30
 ID 65536
 SOLVENT CDC13
 NS 2048
 DS 4
 SWH 24038.461 Hz
 FIDRES 0.366798 Hz
 AQ 1.3631988 sec
 RG 203
 DW 20.800 usec
 DE 6.50 usec
 IE 94.8 K
 D1 2.00000000 sec
 D11 0.03000000 sec

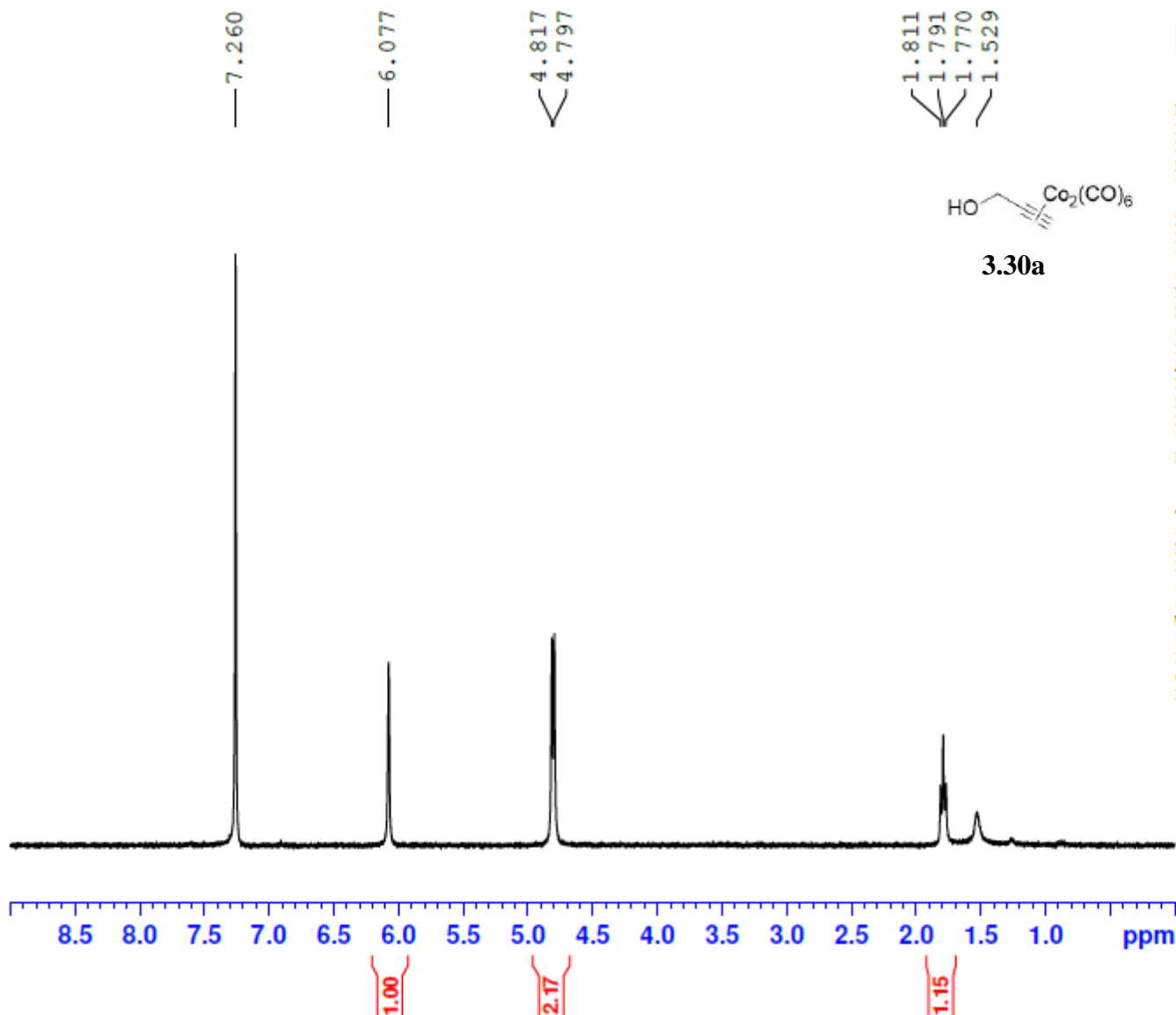
----- CHANNEL f1 -----
 NUC1 13C
 P1 10.00 usec
 SI 32768
 SF 100.6127550 MHz
 WDW EM
 SSB 0
 LB 1.00 Hz
 GB 0
 PC 1.40

SW07-164-SM



NAME SW07-164-SM
EXPNO 10
PROCNO 1
Date_ 20160119
Time 9.54
INSTRUM spect
PROBHD 5 mm QNP 1H/1
PULPROG zg30
TD 32768
SOLVENT CDCl3
NS 16
DS 2
SWH 6188.119 Hz
FIDRES 0.188846 Hz
AQ 2.6477044 sec
RG 322
DW 80.800 usec
DE 6.50 usec
TE -925.8 K
D1 1.00000000 sec
ID0 1

----- CHANNEL f1 -----
SFO1 300.2318540 MHz
NUC1 1H
P1 12.71 usec
SI 32768
SF 300.2300091 MHz
WDW EM
SSB 0
LB 0.10 Hz
GB 0
PC 1.00

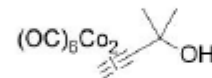


SW07-115-B 1H 300

— 7.260

— 6.034

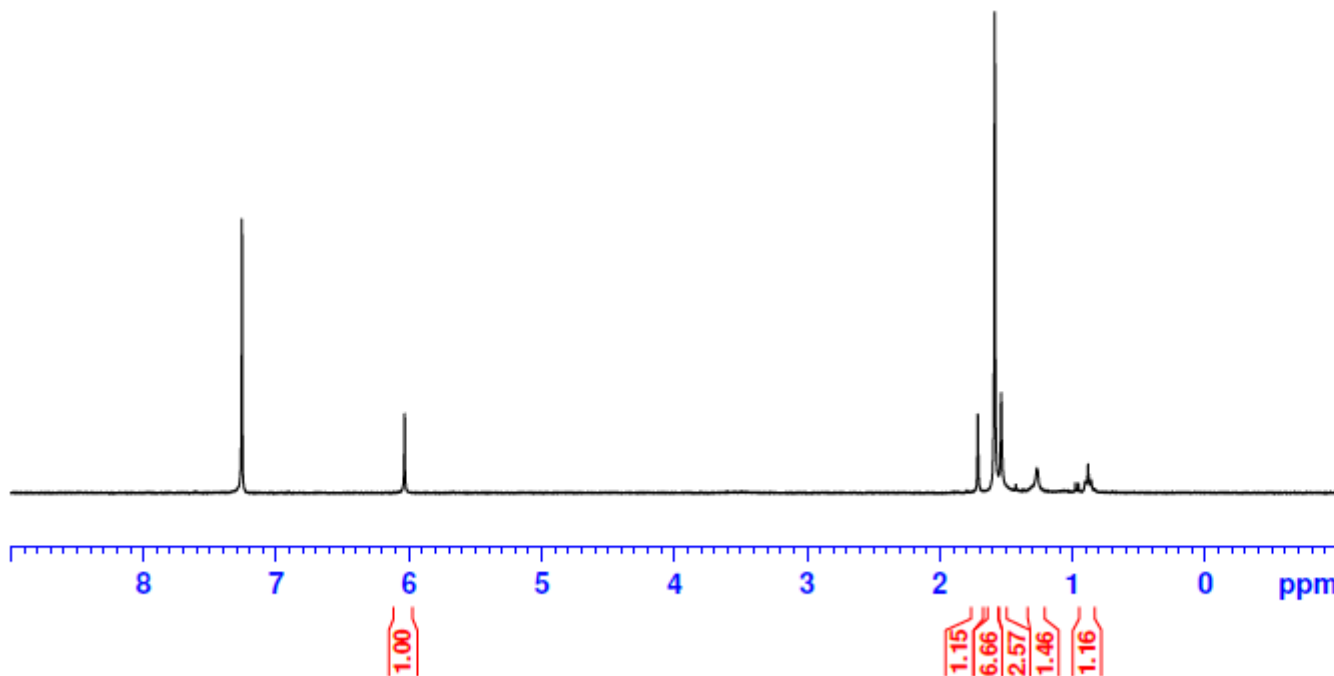
1.714
1.587
1.537
1.271
— 0.884



3.S1

NAME SW07-115-B
EXPNO 10
PROCNO 1
Date_ 20151008
Time 14.36
INSTRUM spect
PROBHD 5 mm QNP 1H/1
PULPROG zg30
ID 32768
SOLVENT CDCl3
NS 16
DS 2
SWH 6188.119 Hz
FIDRES 0.188846 Hz
AQ 2.6477044 sec
RG 322
DW 80.800 usec
DE 6.50 usec
TE -922.4 K
D1 1.00000000 sec
TD0 1

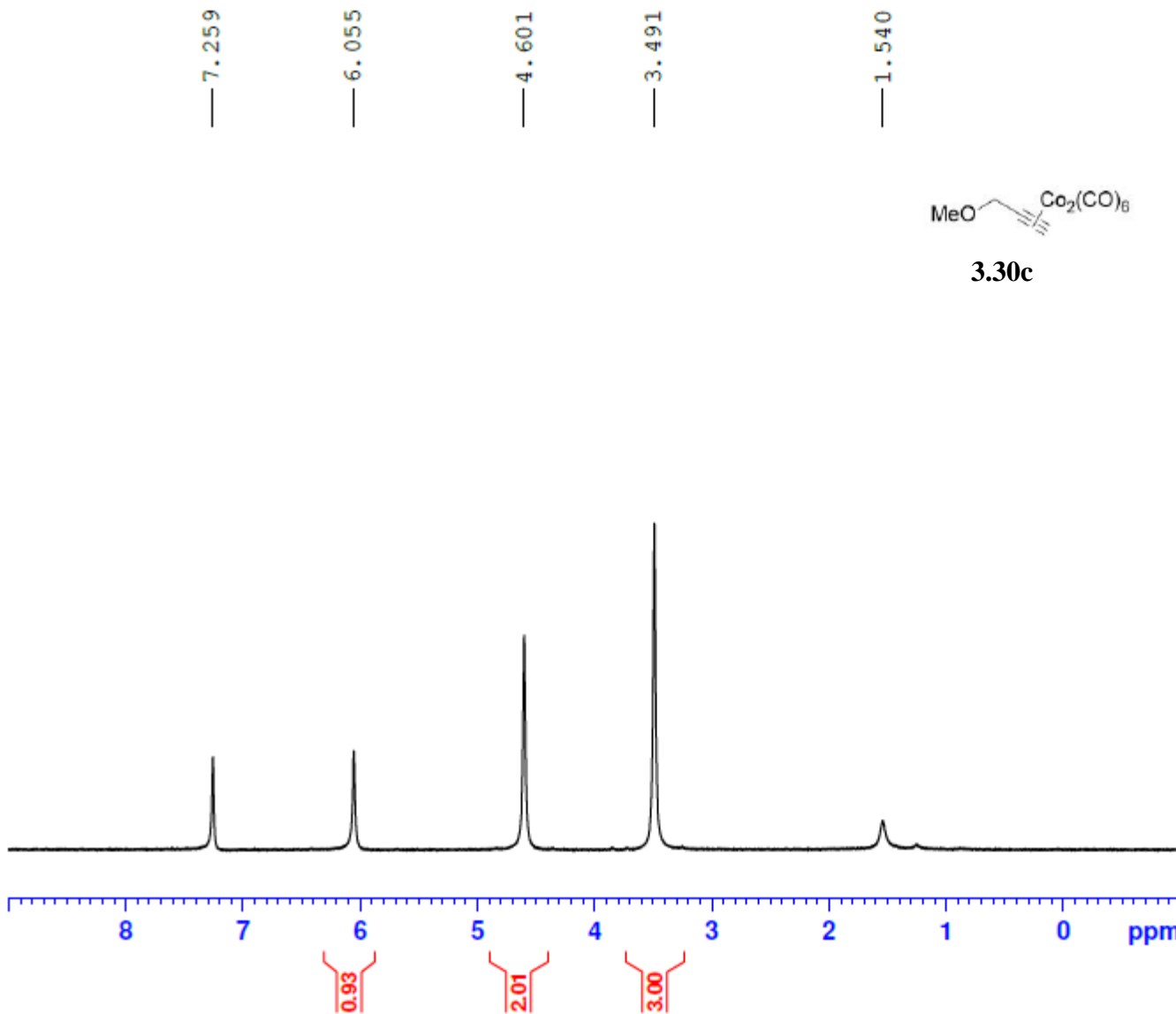
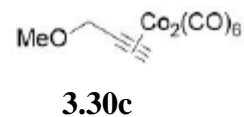
----- CHANNEL f1 -----
SFO1 300.2318540 MHz
NUC1 1H
P1 12.71 usec
SI 32768
SF 300.2300888 MHz
WDW EM
SSB 0
LB 0.10 Hz
GB 0
PC 1.00



SW07-052-cr 1H 300

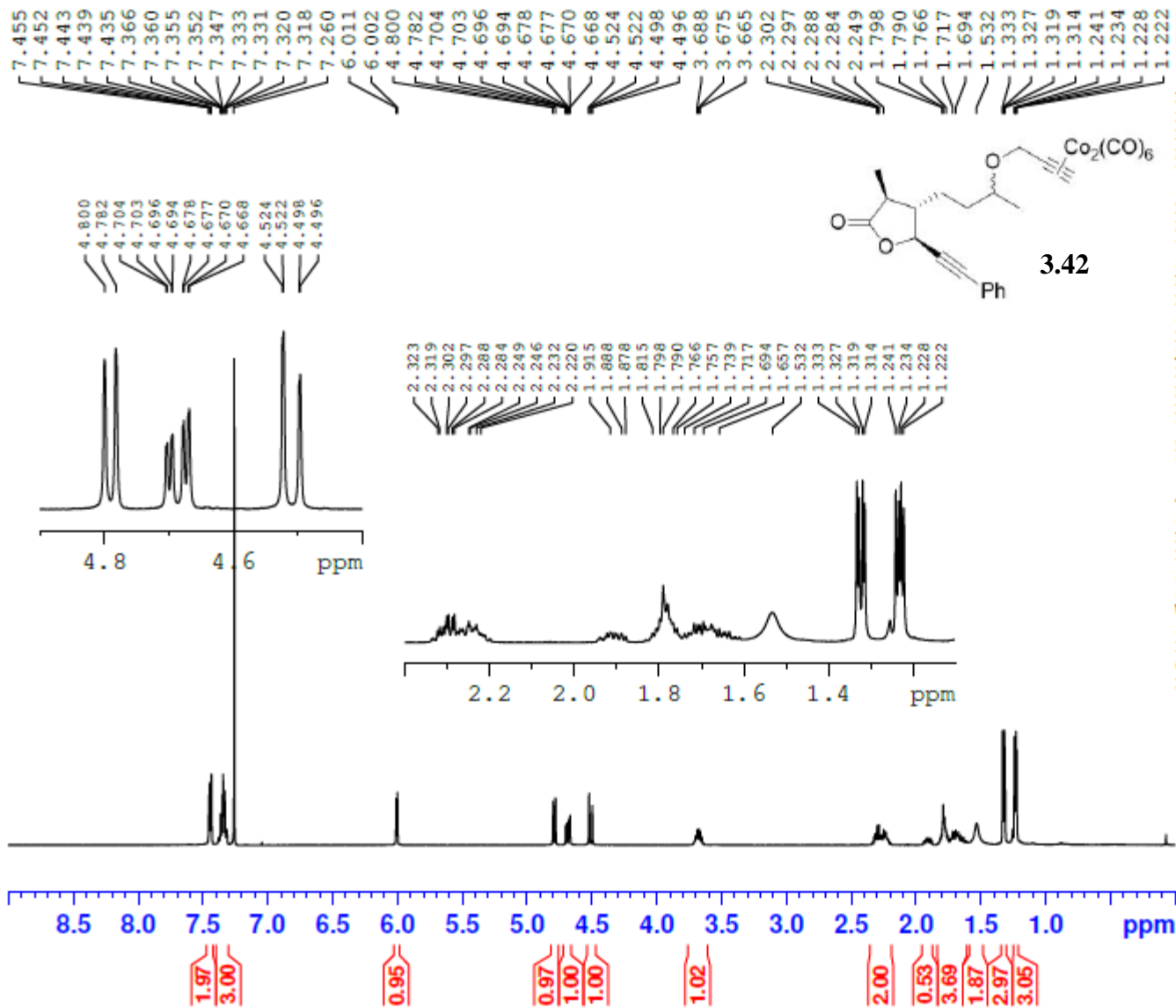


NAME SW07-052-cr
EXPNO 10
PROCNO 1
Date_ 20150728
Time 15.47
INSTRUM spect
PROBHD 5 mm QNP 1H/1
PULPROG zg30
ID 32768
SOLVENT CDCl3
NS 16
DS 2
SWH 6188.119 Hz
FIDRES 0.188846 Hz
AQ 2.6477044 sec
RG 322
DW 80.800 usec
DE 6.50 usec
TE -930.4 K
D1 1.00000000 sec
TD0 1



----- CHANNEL f1 -----
SFO1 300.2318540 MHz
NUC1 1H
P1 12.71 usec
SI 32768
SF 300.2300091 MHz
WDW EM
SSB 0
LB 0.10 Hz
GB 0
PC 1.00

SW06-199-A 1H 500



```

NAME SW06-199-A
EXPNO 10
PROCNO 1
Date_ 20150518
Time 12.47
INSTRUM spect
PROBHD 5 mm PABBO BB/
PULPROG zg30
ID 65536
SOLVENT CDCl3
NS 16
DS 2
SWH 10000.000 Hz
FIDRES 0.152588 Hz
AQ 3.2768500 sec
RG 203
DW 50.000 usec
DE 6.50 usec
TE 298.2 K
D1 1.00000000 sec
ID0 1
  
```

```

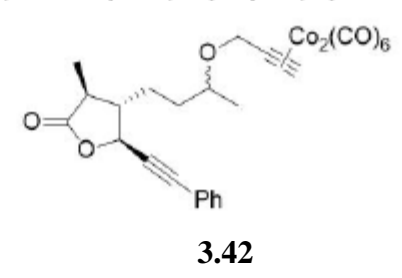
----- CHANNEL f1 -----
SFO1 500.1630887 MHz
NUC1 1H
P1 11.45 usec
SI 65536
SF 500.1600119 MHz
WDW EM
SSB 0
LB 0.30 Hz
GB 0
PC 1.00
  
```

SW06-199-A 13C 500



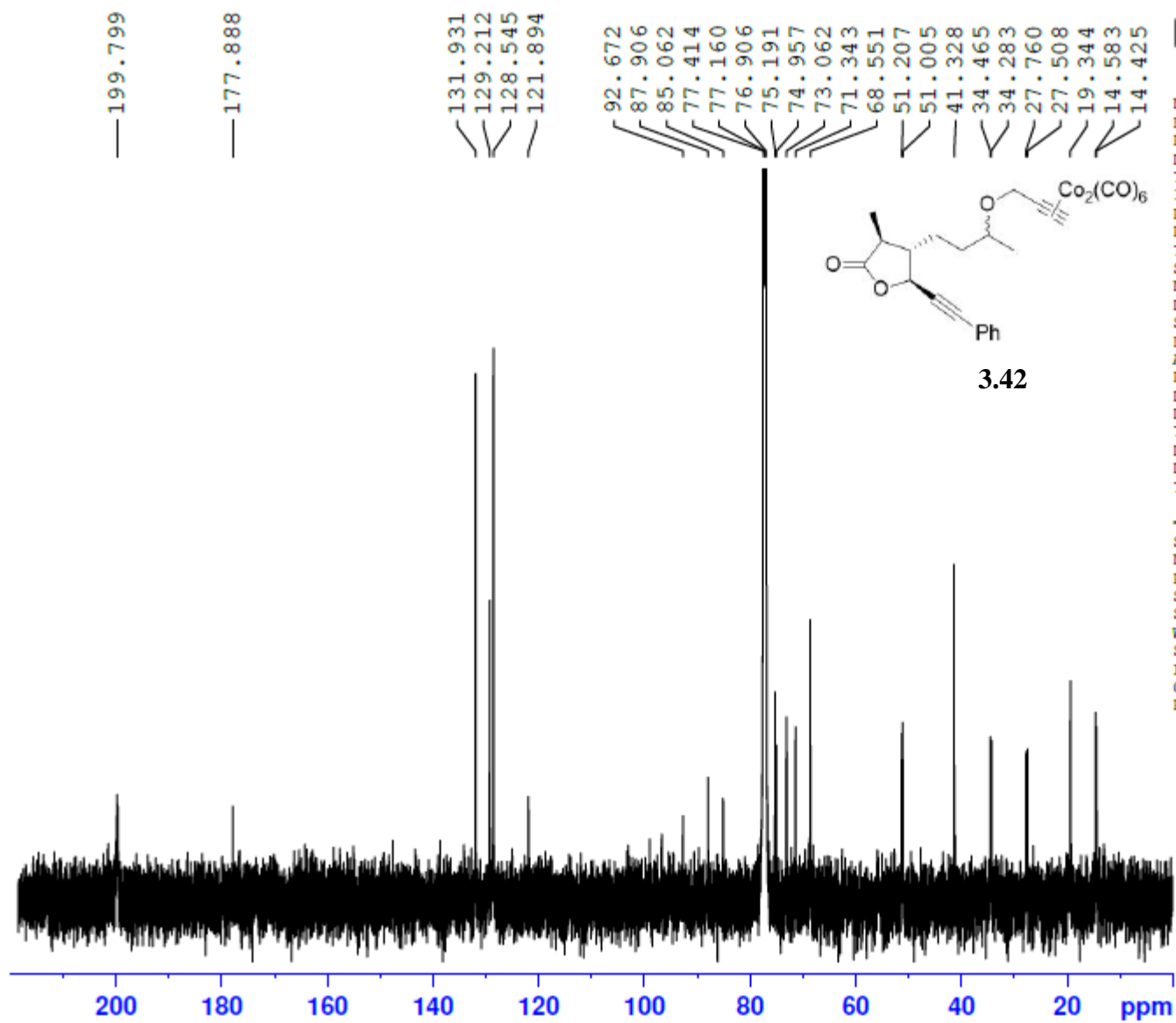
—199.799
—177.888

131.931
129.212
128.545
121.894
92.672
87.906
85.062
77.414
77.160
76.906
75.191
74.957
73.062
71.343
68.551
51.207
51.005
41.328
34.465
34.283
27.760
27.508
19.344
14.583
14.425

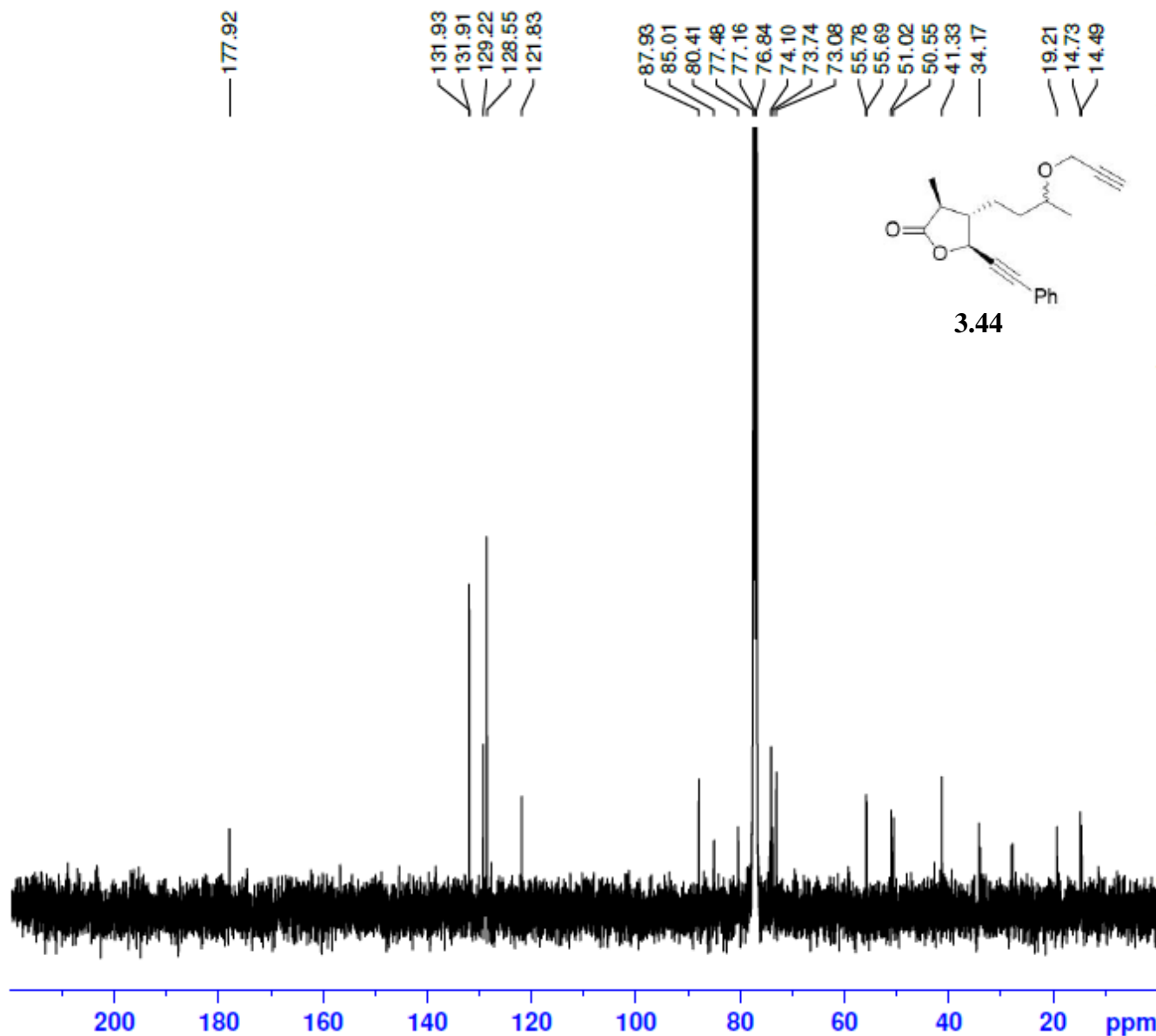


NAME SW06-199-A
EXPNO 20
PROCNO 1
Date_ 20150520
Time 0.43
INSTRUM spect
PROBHD 5 mm PABBO BB/
PULPROG zgpg30
ID 65536
SOLVENT CDCl3
NS 4096
DS 2
SWH 29761.904 Hz
FIDRES 0.454131 Hz
AQ 1.1010548 sec
RG 203
DW 16.800 usec
DE 6.50 usec
TE 298.5 K
D1 2.00000000 sec
D11 0.03000000 sec
TD0 1

----- CHANNEL f1 -----
SFO1 125.7779086 MHz
NUC1 13C
P1 10.50 usec
SI 32768
SF 125.7653126 MHz
WDW EM
SSB 0
LB 1.00 Hz
GB 0
PC 1.40



SW06-123-A 13C 400B



NAME SW06-123-A
EXPNO 2
PROCNO 1
Date_ 20150307
Time 14.50
INSTRUM spect
PROBHD 5 mm PADUL 13C
PULPROG zgpg30
ID 65536
SOLVENT CDCl3
NS 4394
DS 4
SWH 24038.461 Hz
FIDRES 0.366798 Hz
AQ 1.3631988 sec
RG 45.2
DW 20.800 usec
DE 6.50 usec
TE 295.4 K
D1 3.0000000 sec
D11 0.0300000 sec
TD0 1

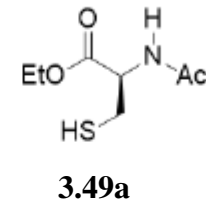
----- CHANNEL f1 -----
NUC1 13C
P1 10.00 usec
PL1 -0.44 dB
PL1W 39.19395828 W
SFO1 100.6479773 MHz

----- CHANNEL f2 -----
CPDPRG2 waltz16
NUC2 1H
PCPD2 90.00 usec
PL2 -3.90 dB
PL12 15.81 dB
PL13 120.00 dB
PL2W 21.64248466 W
PL12W 0.23137002 W
PL13W 0.00000000 W
SFO2 400.2316009 MHz
SI 32768
SF 100.6379009 MHz
WDW EM
SSB 0
LB 1.00 Hz
GB 0
PC 1.40

SW06-088-cr 1H 400

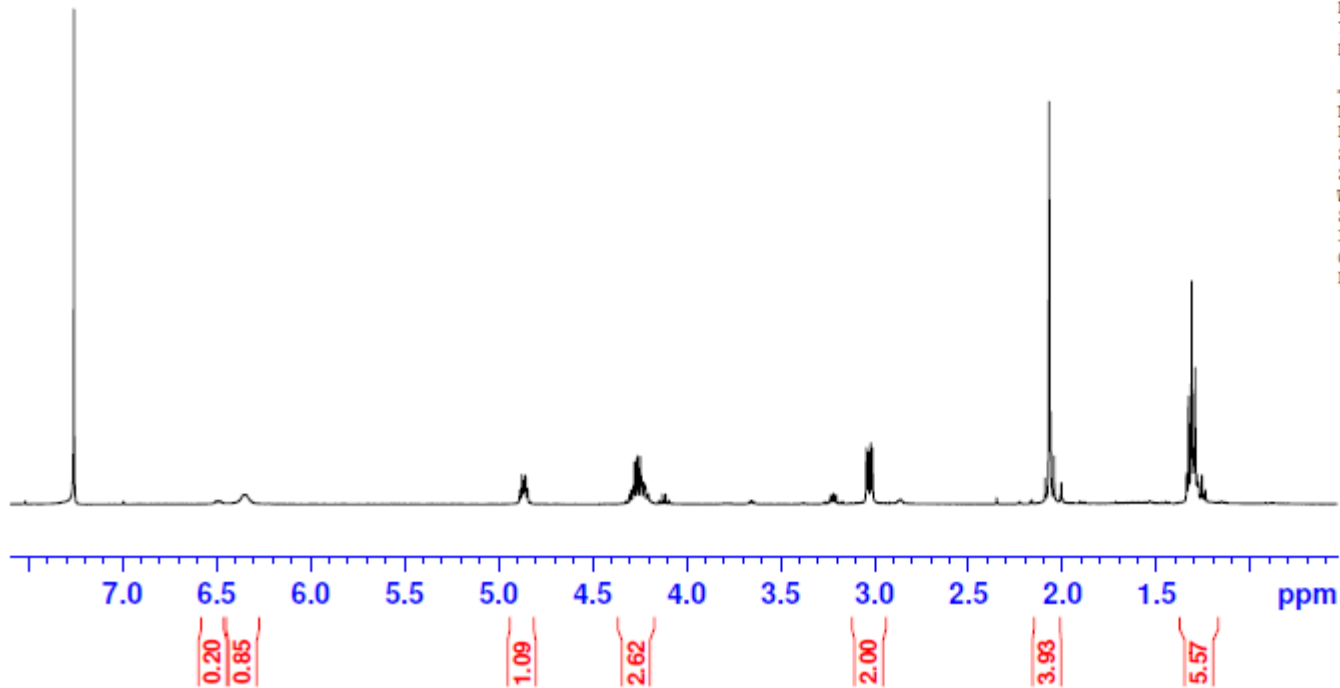


7.260
6.501
6.483
6.354
4.886
4.876
4.867
4.857
4.848
4.295
4.286
4.281
4.277
4.263
4.259
4.246
4.241
4.228
4.225
4.221
4.129
4.111
3.233
3.221
3.216
3.204
3.042
3.032
3.020
3.010
2.093
2.071
2.064
2.044
2.007
1.340
1.329
1.317
1.312
1.302
1.294
1.284
1.278



NAME SW06-088-cr
EXPNO 10
PROCNO 1
Date_ 20150129
Time 14.37
INSTRUM spect
PROBHD 5 mm PABBO BB-
PULPROG zg30
TD 65536
SOLVENT CDCl3
NS 16
DS 2
SWH 8223.685 Hz
FIDRES 0.125483 Hz
AQ 3.9846387 sec
RG 161
DW 60.800 usec
DE 6.50 usec
TE 96.5 K
D1 1.00000000 sec

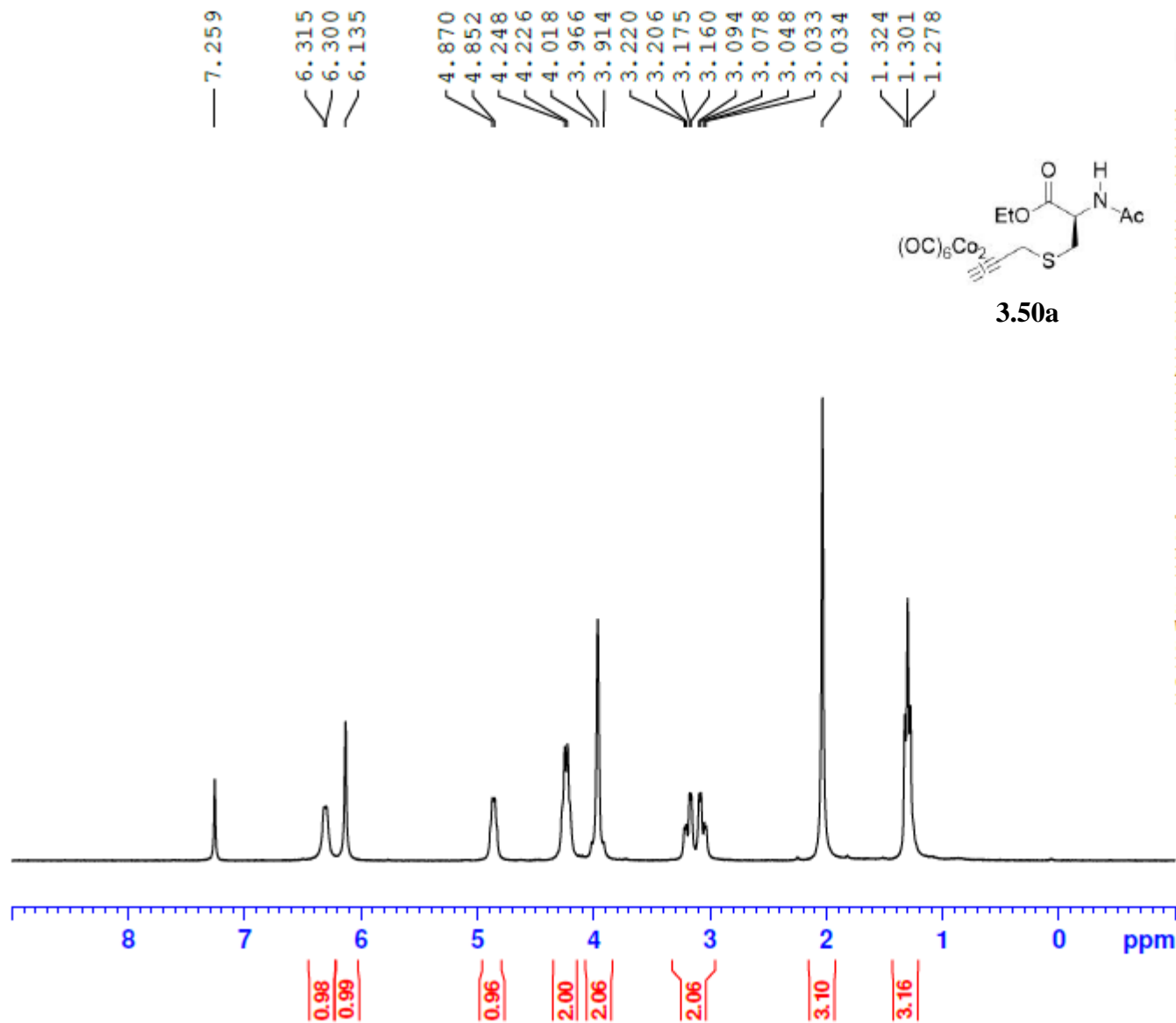
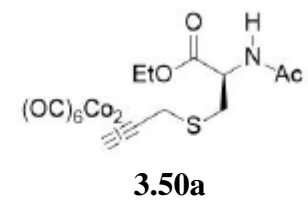
----- CHANNEL f1 -----
NUC1 1H
P1 13.75 usec
SI 65536
SF 400.1300112 MHz
WDW EM
SSB 0
LB 0.30 Hz
GB 0
PC 1.00



SW06-102-C 1H 300



NAME SW06-102-C
EXPNO 10
PROCNO 1
Date_ 20150213
Time_ 16.20
INSTRUM spect
PROBHD 5 mm QNP 1H/1
PULPROG zg30
ID 32768
SOLVENT CDCl3
NS 16
DS 2
SWH 6188.119 Hz
FIDRES 0.188846 Hz
AQ 2.6477044 sec
RG 128
DW 80.800 usec
DE 6.50 usec
TE -929.4 K
D1 1.00000000 sec
ID0 1



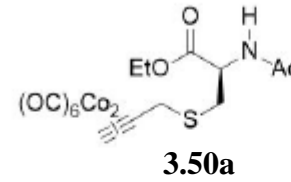
----- CHANNEL f1 -----
SFO1 300.2318540 MHz
NUC1 1H
P1 12.71 usec
SI 32768
SF 300.2300093 MHz
WDW EM
SSB 0
LB 0.10 Hz
GB 0
PC 1.00

SW06-102-C 13C 400



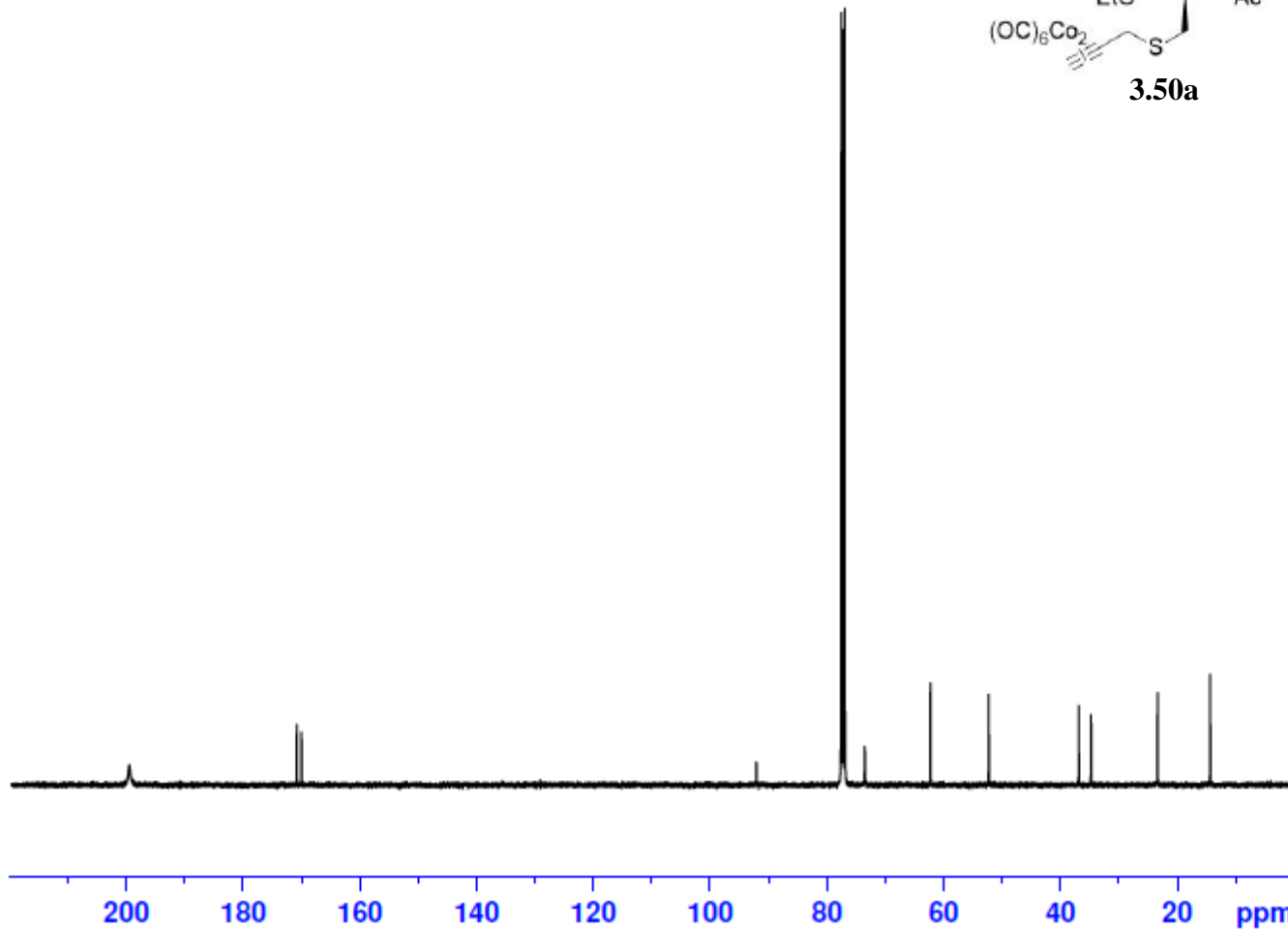
199.51
170.80
169.95

92.00
77.48
77.16
76.84
73.43
62.22
52.20
36.76
34.65
23.26
14.25



NAME SW06-102-C
EXPNO 10
PROCNO 1
Date_ 20150214
Time_ 5.45
INSTRUM spect
PROBHD 5 mm PABBO BB-
PULPROG zgpg30
ID 65536
SOLVENT CDCl3
NS 3072
DS 4
SWH 24038.461 Hz
FIDRES 0.366798 Hz
AQ 1.3631988 sec
RG 203
DW 20.800 usec
DE 6.50 usec
TE 97.6 K
D1 2.00000000 sec
D11 0.03000000 sec

----- CHANNEL f1 -----
NUC1 13C
P1 10.00 usec
SI 32768
SF 100.6127552 MHz
WDW EM
SSB 0
LB 1.00 Hz
GB 0
PC 1.40

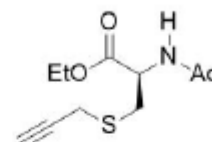


SW06-195-cr 1H 500

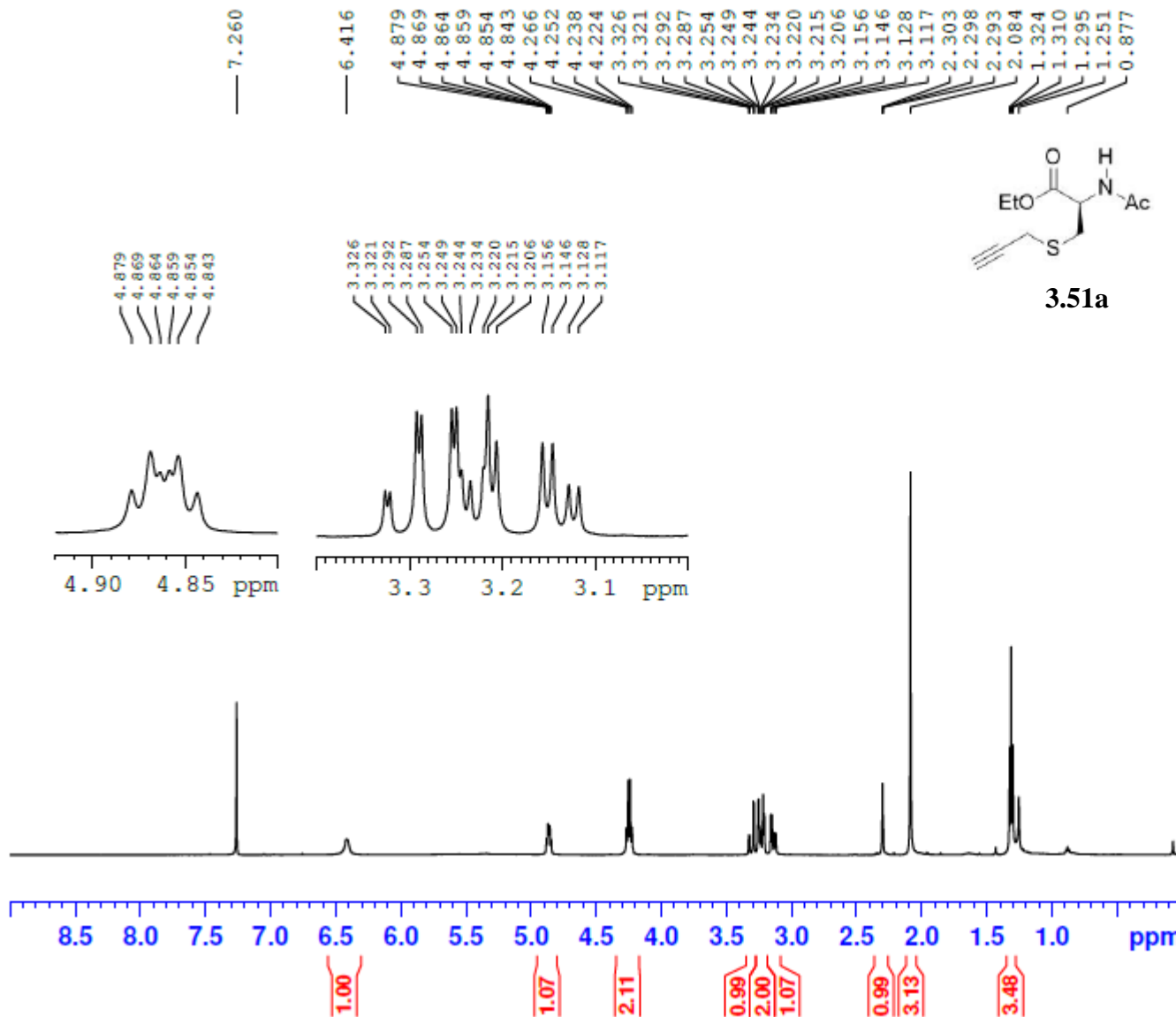


```

NAME      SW06-195-cr
EXPNO     10
PROCNO    1
Date_     20150513
Time      17.30
INSTRUM   spect
PROBHD    5 mm PABBO BB/
PULPROG   zg30
ID         65536
SOLVENT   CDCl3
NS         16
DS         2
SWH        10000.000 Hz
FIDRES     0.152588 Hz
AQ         3.2768500 sec
RG         203
DW         50.000 usec
DE         6.50 usec
TE         298.2 K
D1         1.00000000 sec
TD0        1
    
```



3.51a



```

----- CHANNEL f1 -----
SFO1      500.1630887 MHz
NUC1       1H
P1         11.45 usec
SI         65536
SF         500.1600124 MHz
WDW        EM
SSB        0
LB         0.30 Hz
GB         0
PC         1.00
    
```

SW06-195-cr 1H 500

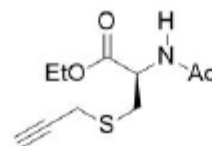
170.868
170.253

79.398
77.413
77.159
76.905
72.094
62.194
51.916

33.863
29.849
23.277
20.066
14.265

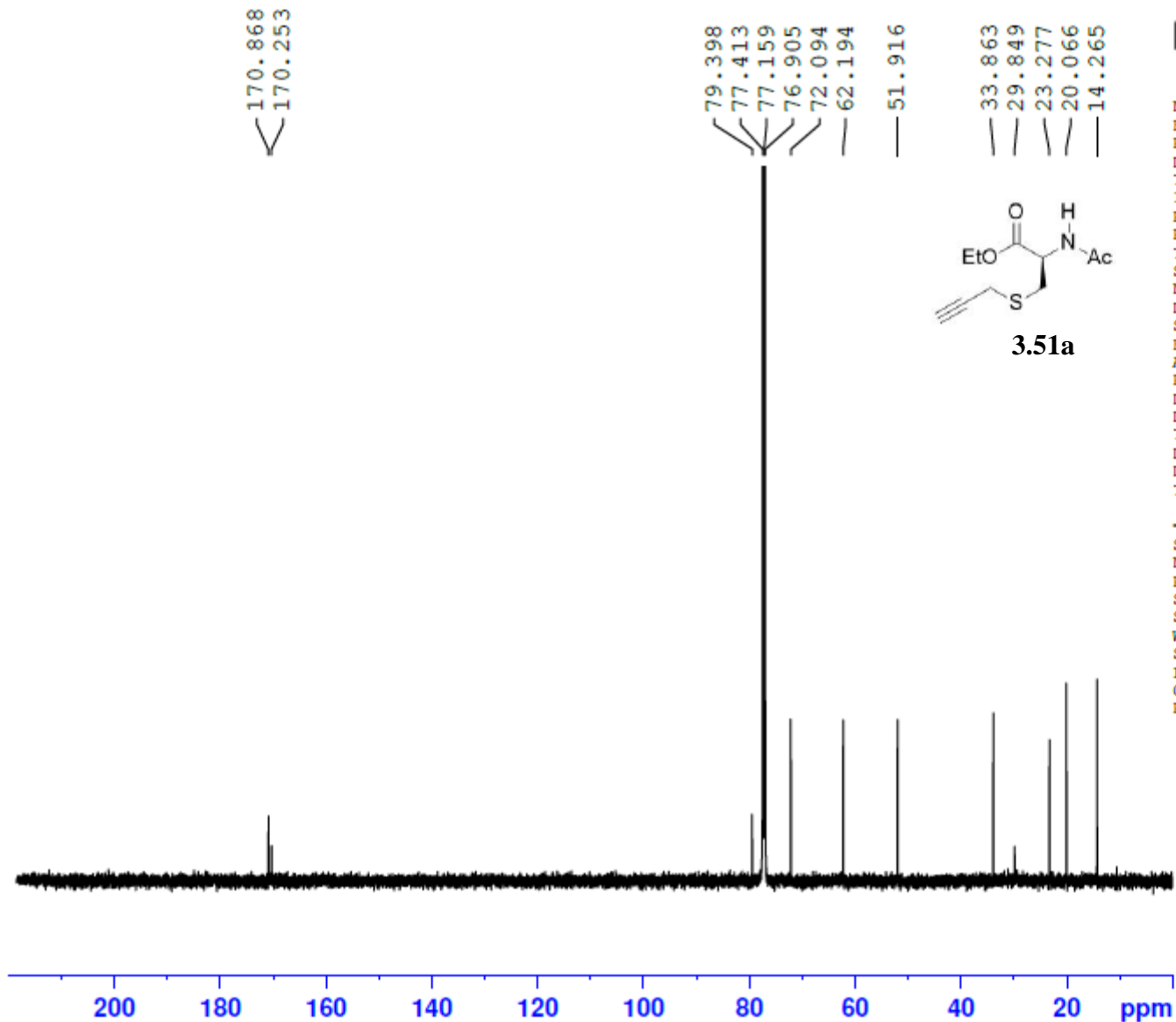


NAME SW06-195-cr
EXPNO 11
PROCNO 1
Date_ 20150515
Time_ 0.46
INSTRUM spect
PROBHD 5 mm PABBO BB/
PULPROG zgpg30
ID 65536
SOLVENT CDC13
NS 2048
DS 2
SWH 29761.904 Hz
FIDRES 0.454131 Hz
AQ 1.1010548 sec
RG 203
DW 16.800 usec
DE 6.50 usec
TE 298.6 K
D1 2.00000000 sec
D11 0.03000000 sec
TD0 1



3.51a

----- CHANNEL f1 -----
SFO1 125.7779086 MHz
NUC1 13C
P1 10.50 usec
SI 32768
SF 125.7653129 MHz
WDW EM
SSB 0
LB 1.00 Hz
GB 0
PC 1.40

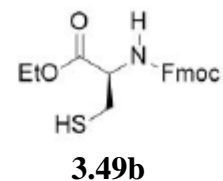


SW06-206-B

7.784
7.765
7.622
7.604
7.431
7.412
7.394
7.350
7.347
7.343
7.332
7.328
7.325
7.313
7.309
7.306
7.260

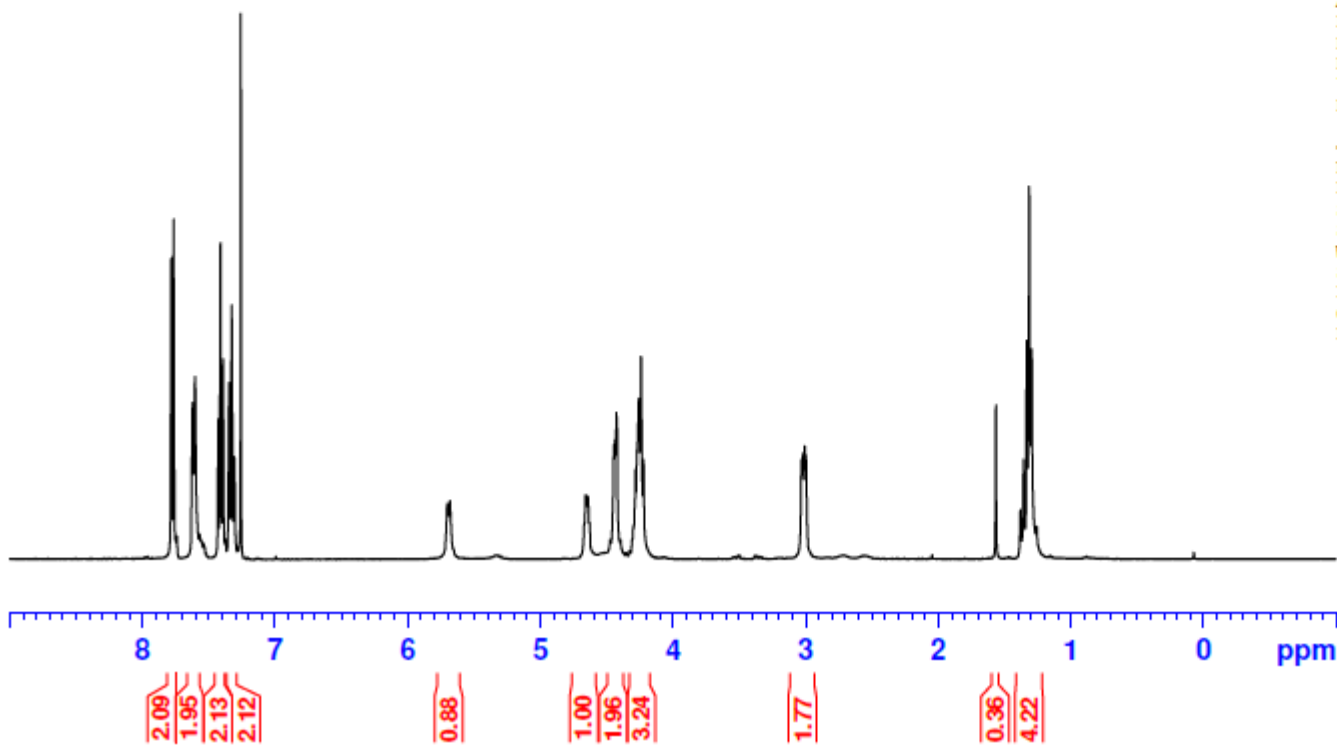
5.701
5.683
4.659
4.650
4.641
4.631
4.473
4.447
4.438
4.428
4.396
4.300
4.283
4.271
4.256
4.242
4.225
3.030
3.020
3.008
2.996

1.566
1.380
1.358
1.332
1.314
1.296



NAME SW06-206-B
EXPNO 20
PROCNO 1
Date_ 20150606
Time 14.33
INSTRUM spect
PROBHD 5 mm PABBO BB-
PULPROG zg30
TD 65536
SOLVENT CDC13
NS 16
DS 2
SWH 8223.685 Hz
FIDRES 0.125483 Hz
AQ 3.9846387 sec
RG 114
DW 60.800 usec
DE 6.50 usec
TE 97.1 K
D1 1.00000000 sec

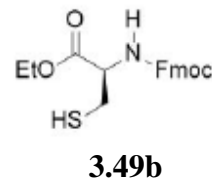
----- CHANNEL f1 -----
NUC1 1H
P1 13.75 usec
SI 65536
SF 400.1300102 MHz
WDW EM
SSB 0
LB 0.30 Hz
GB 0
PC 1.00



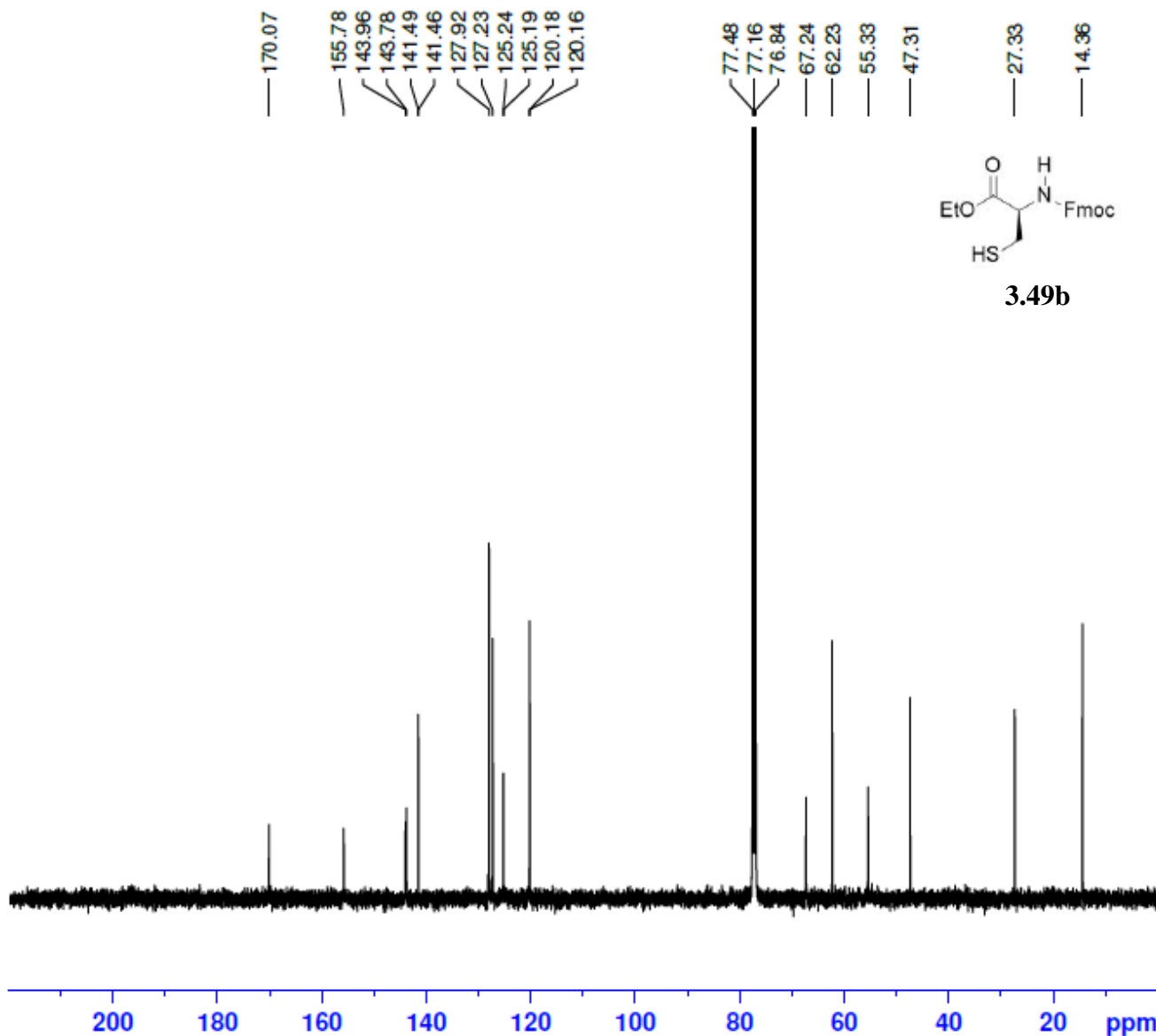
SW06-206-B 13C 400



```
NAME SW06-206-B
EXPNO 21
PROCNO 1
Date_ 20150607
Time 23.17
INSTRUM spect
PROBHD 5 mm PABBO BB-
PULPROG zgpg30
TD 65536
SOLVENT CDC13
NS 3072
DS 4
SWH 24038.461 Hz
FIDRES 0.366798 Hz
AQ 1.3631988 sec
RG 161
DW 20.800 usec
DE 6.50 usec
TE 93.6 K
D1 2.0000000 sec
D11 0.0300000 sec
```



```
----- CHANNEL f1 -----
NUC1 13C
P1 10.00 usec
SI 32768
SF 100.6127562 MHz
WDW EM
SSB 0
LB 1.00 Hz
GB 0
PC 1.40
```

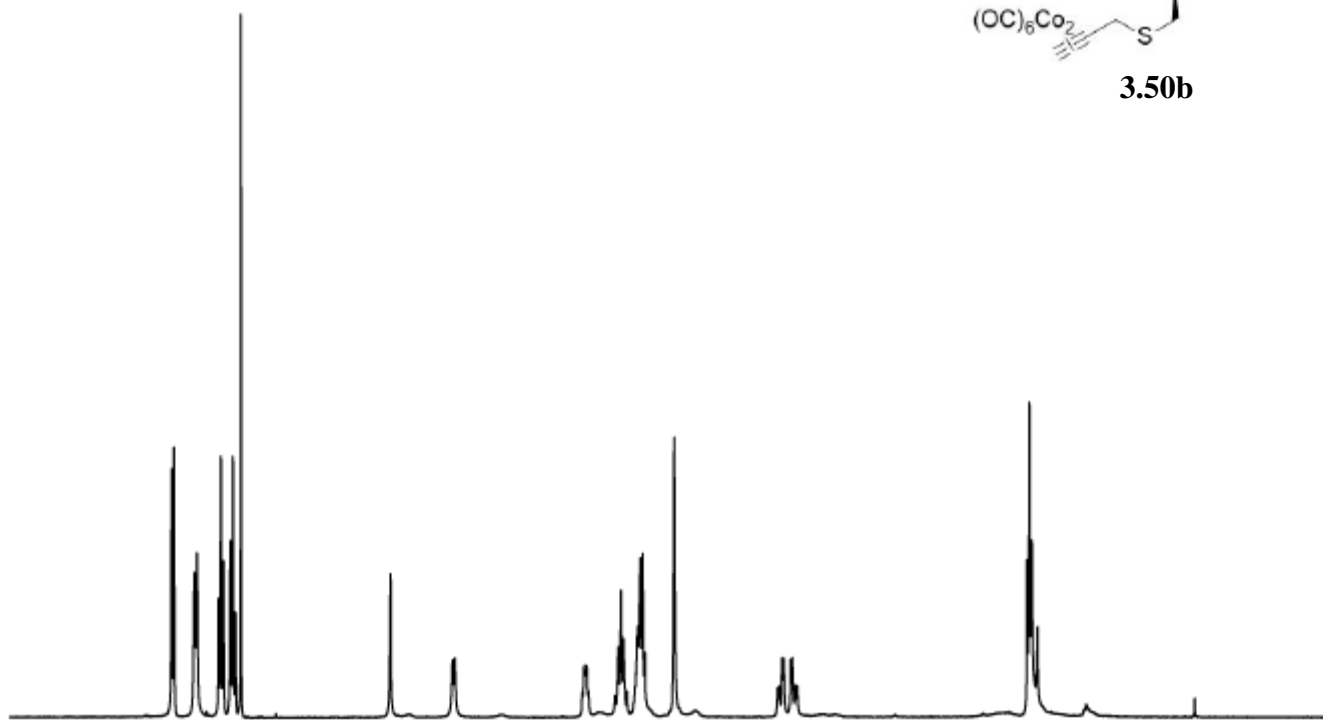
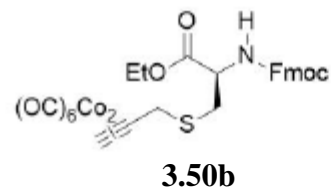


SW06-138-C 1H 400

7.782
7.763
7.610
7.591
7.428
7.410
7.391
7.339
7.321
7.302
7.260
6.134
5.666
5.647
4.685
4.673
4.654
4.641
4.441
4.415
4.395
4.376
4.350
4.283
4.274
4.266
4.250
4.233
4.216
3.993
3.215
3.203
3.180
3.168
3.116
3.103
3.081
3.068
1.335
1.317
1.299
1.256
0.888
0.072



NAME SW06-138-C
EXPNO 10
PROCNO 1
Date_ 20150331
Time_ 18.10
INSTRUM spect
PROBHD 5 mm PABBO BB-
PULPROG zg30
ID 65536
SOLVENT CDCl3
NS 16
DS 2
SWH 8223.685 Hz
FIDRES 0.125483 Hz
AQ 3.9846387 sec
RG 128
DW 60.800 usec
DE 6.50 usec
TE 91.6 K
D1 1.00000000 sec



----- CHANNEL f1 -----
NUC1 1H
P1 13.75 usec
SI 65536
SF 400.1300104 MHz
WDW EM
SSB 0
LB 0.30 Hz
GB 0
PC 1.00

2.23
2.18
2.18
2.14
0.93
0.89
0.93
1.96
3.22
1.83
0.94
1.00
3.33
0.75

SW06-138-C 13C 400

— 199.46
— 170.666

— 155.85

143.91
143.86
141.46

127.91
127.23
125.24
120.17

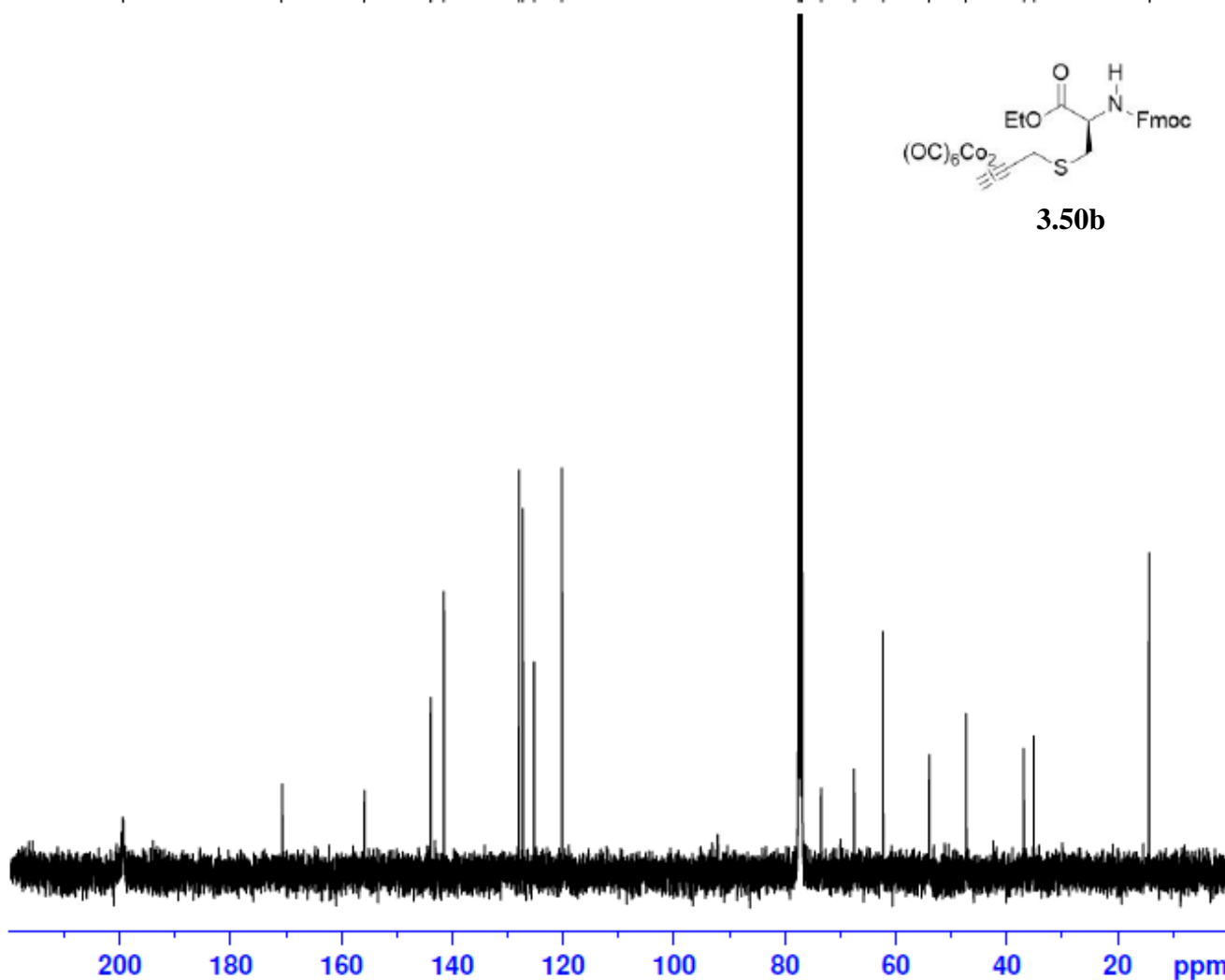
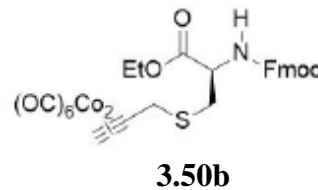
77.48
77.16
76.84
73.39
67.45
62.26
53.88
47.24
36.83
35.04

— 14.29

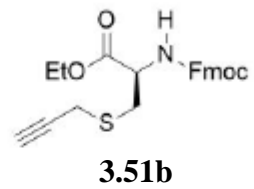
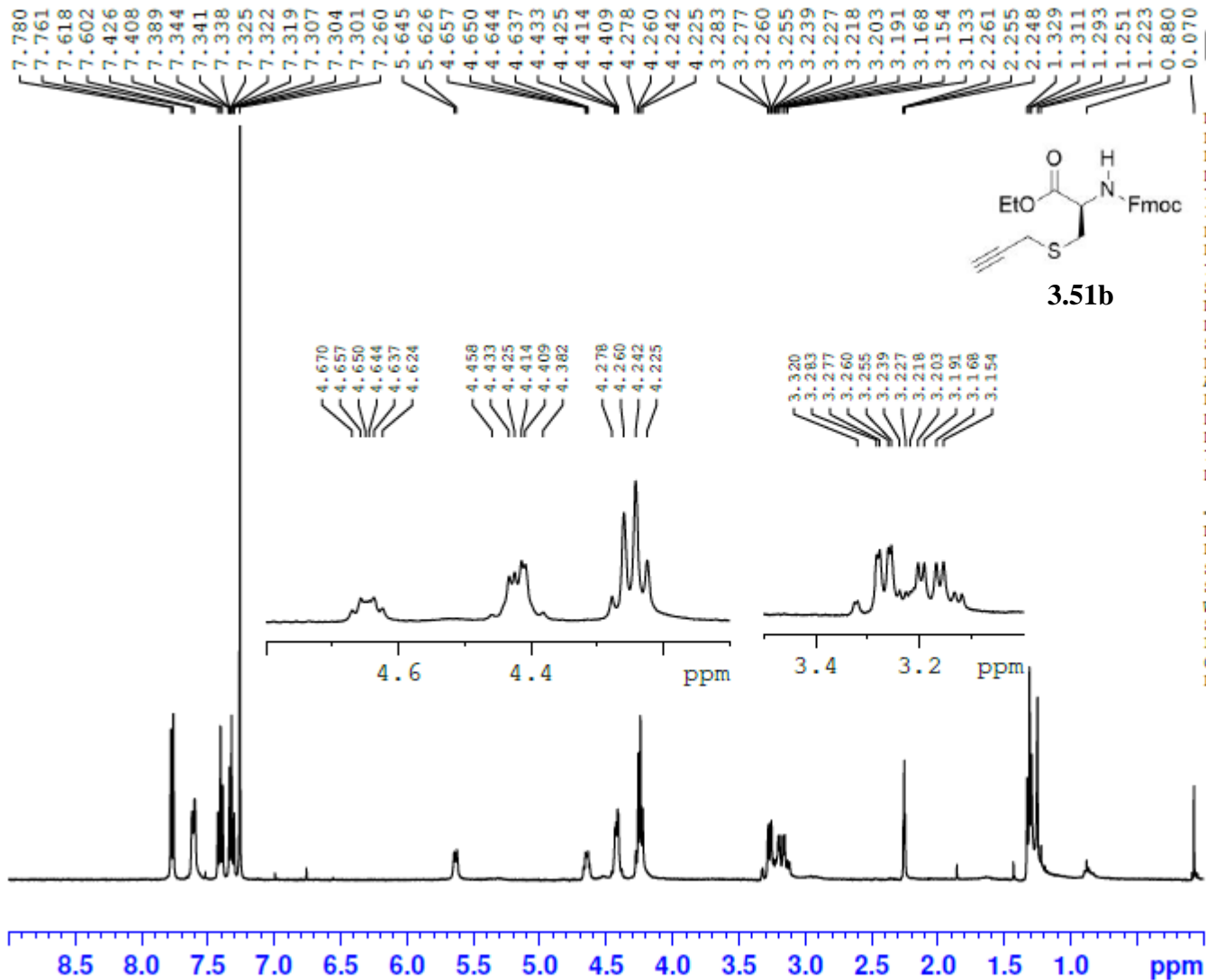


NAME SW06-138-C
EXPNO 11
PROCNO 1
Date_ 20150401
Time_ 1.15
INSTRUM spect
PROBHD 5 mm PABBO BB-
PULPROG zgpg30
ID 65536
SOLVENT CDCl3
NS 2048
DS 4
SWH 24038.461 Hz
FIDRES 0.366798 Hz
AQ 1.3631988 sec
RG 203
DW 20.800 usec
DE 6.50 usec
TE 96.9 K
D1 2.0000000 sec
D11 0.0300000 sec

----- CHANNEL f1 -----
NUC1 13C
P1 10.00 usec
SI 32768
SF 100.6127549 MHz
WDW EM
SSB 0
LB 1.00 Hz
GB 0
PC 1.40



SW06-164-cr 1H 400



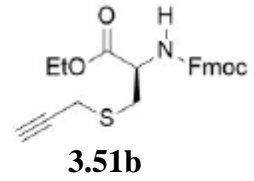
NAME SW06-164-cr
 EXPNO 10
 PROCNO 1
 Date_ 20150415
 Time 16.06
 INSTRUM spect
 PROBHD 5 mm PABBO BB-
 PULPROG zg30
 ID 65536
 SOLVENT CDC13
 NS 16
 DS 2
 SWH 8223.685 Hz
 FIDRES 0.125483 Hz
 AQ 3.9846387 sec
 RG 161
 DW 60.800 usec
 DE 6.50 usec
 TE 90.5 K
 D1 1.0000000 sec

----- CHANNEL f1 -----
 NUC1 1H
 P1 13.75 usec
 SI 65536
 SF 400.1300100 MHz
 WDW EM
 SSB 0
 LB 0.30 Hz
 GB 0
 PC 1.00

SW06-164 cr 13 C 500

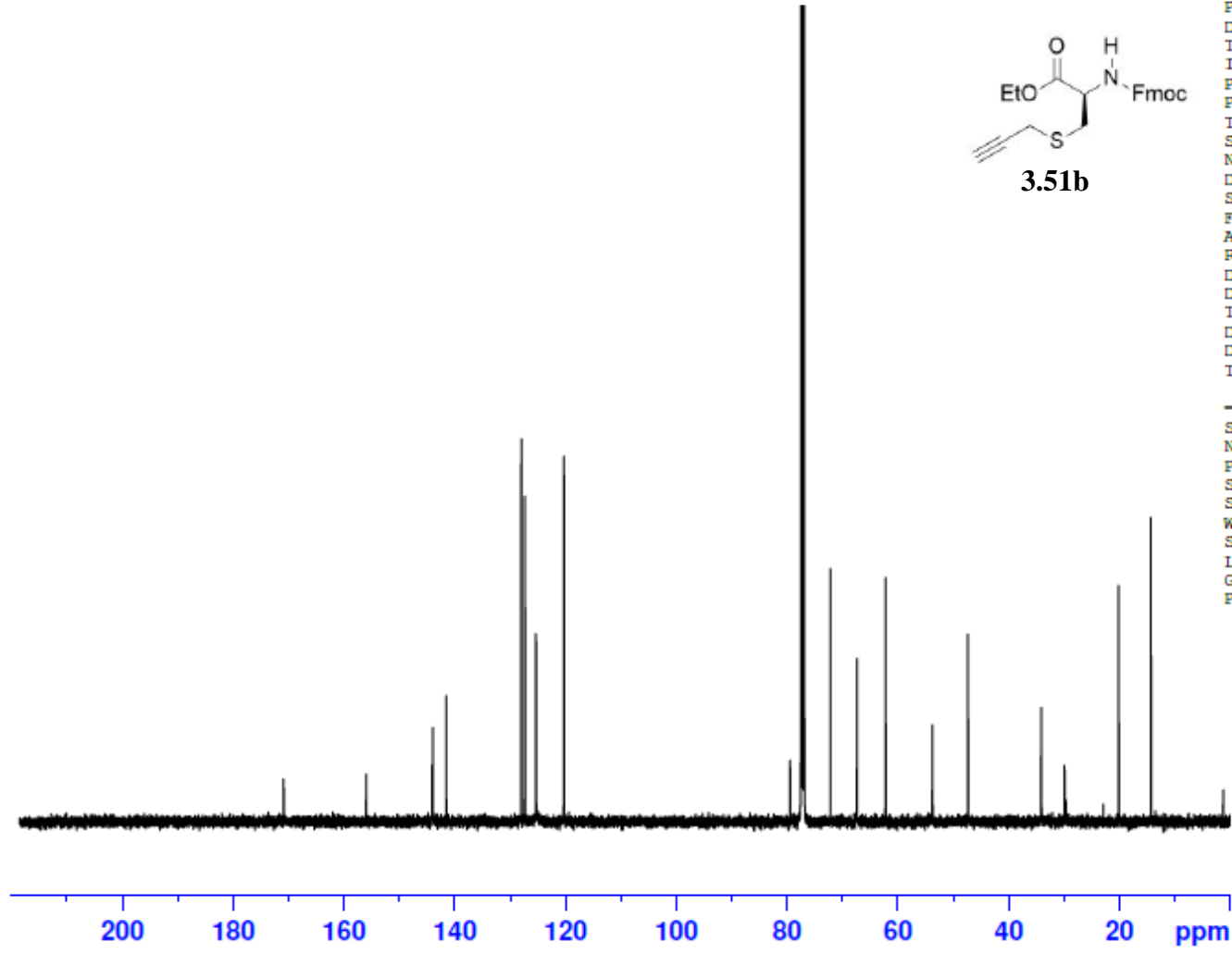


170.807
155.901
143.982
143.876
141.485
127.891
127.241
125.240
120.157
79.382
77.414
77.160
76.906
72.146
67.320
62.164
53.686
47.301
34.044
29.846
20.090
14.284



NAME SW06-164 cr
EXPNO 11
PROCNO 1
Date_ 20150512
Time_ 6.40
INSTRUM spect
PROBHD 5 mm PABBO BB/
PULPROG zgpg30
TD 65536
SOLVENT CDCl3
NS 2048
DS 2
SWH 29761.904 Hz
FIDRES 0.454131 Hz
AQ 1.1010548 sec
RG 203
DW 16.800 usec
DE 6.50 usec
TE 298.6 K
D1 2.0000000 sec
D11 0.0300000 sec
TD0 1

----- CHANNEL f1 -----
SFO1 125.7779086 MHz
NUC1 13C
P1 10.50 usec
SI 32768
SF 125.7653142 MHz
WDW EM
SSB 0
LB 1.00 Hz
GB 0
PC 1.40

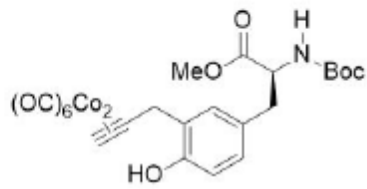


SW06-166-D 1H 400

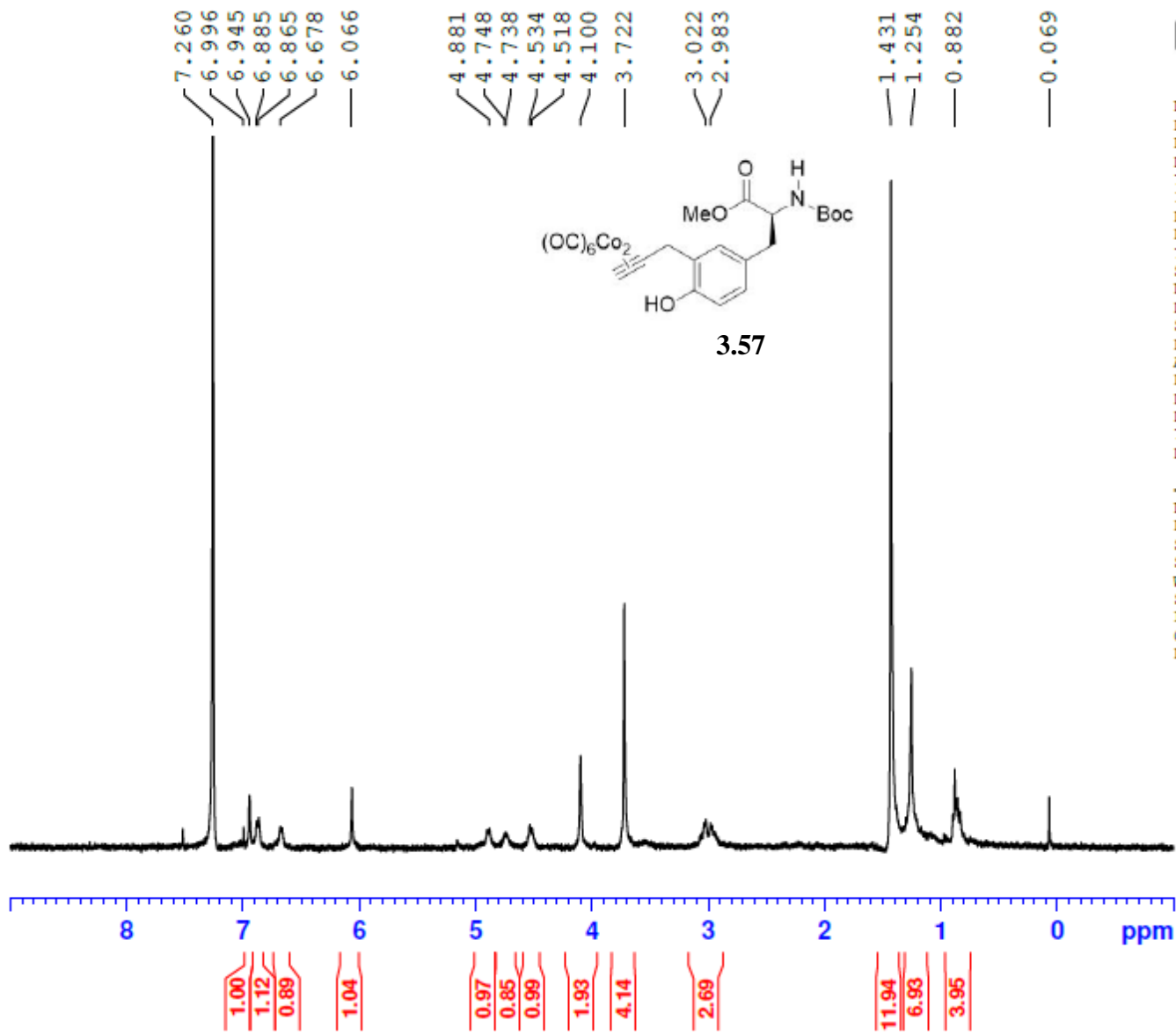


NAME SW06-166-D
EXPNO 10
PROCNO 1
Date_ 20150421
Time 17.09
INSTRUM spect
PROBHD 5 mm PABBO BB-
PULPROG zg30
ID 65536
SOLVENT CDCl3
NS 16
DS 2
SWH 8223.685 Hz
FIDRES 0.125483 Hz
AQ 3.9846387 sec
RG 181
DW 60.800 usec
DE 6.50 usec
TE 94.1 K
D1 1.0000000 sec

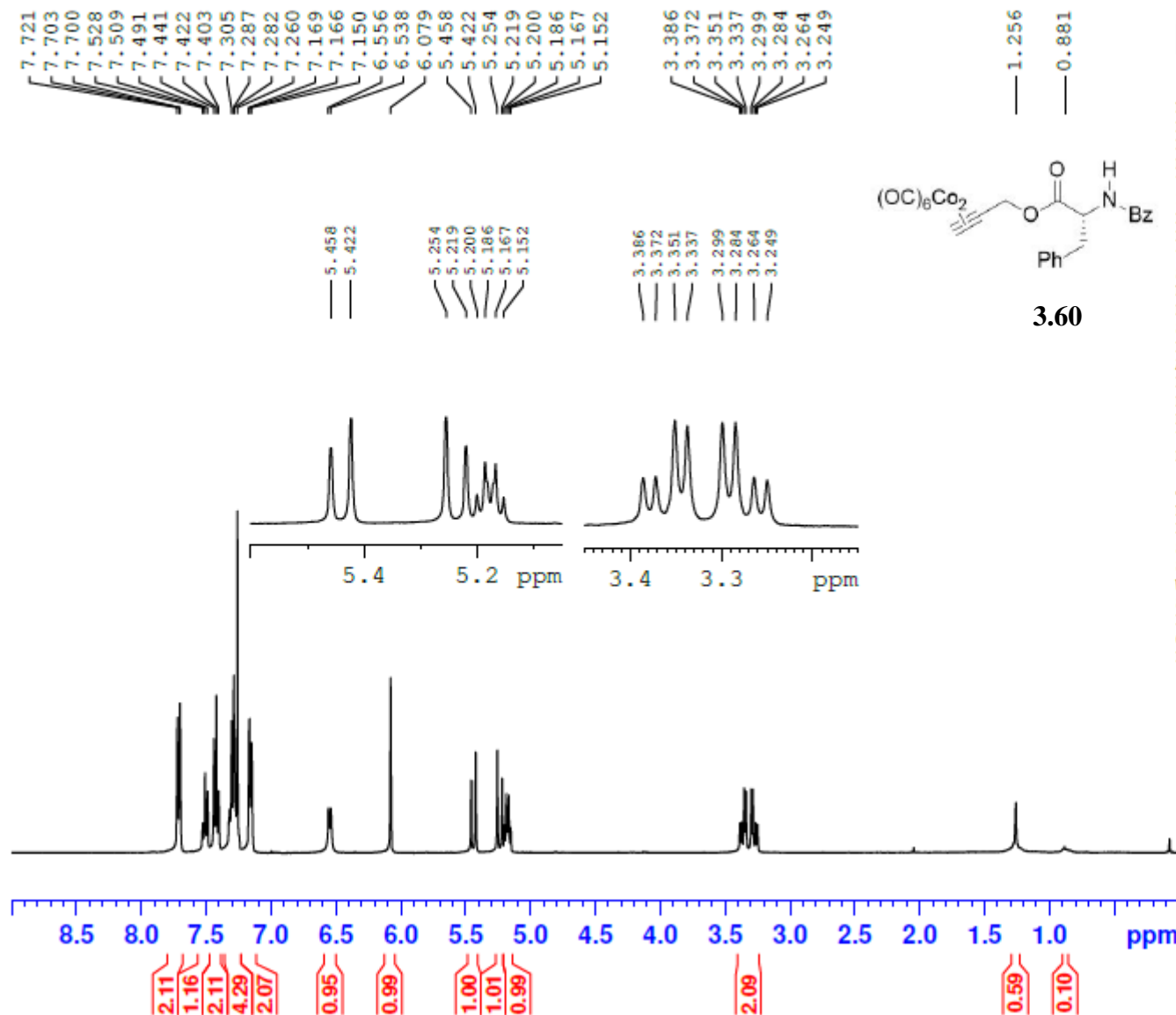
----- CHANNEL f1 -----
NUC1 1H
P1 13.75 usec
SI 65536
SF 400.1300096 MHz
WDW EM
SSB 0
LB 0.30 Hz
GB 0
PC 1.00



3.57



SW06-065-C 1H 400



```

NAME          SW06-065-C
EXPNO         10
PROCNO        1
Date_         20150108
Time_         18.42
INSTRUM       spect
PROBHD        5 mm PABBO BB-
PULPROG       zg30
ID            65536
SOLVENT       CDC13
NS            16
DS            2
SWH           8223.685 Hz
FIDRES        0.125483 Hz
AQ            3.9846387 sec
RG            128
DW            60.800 usec
DE            6.50 usec
IE            96.1 K
D1            1.00000000 sec

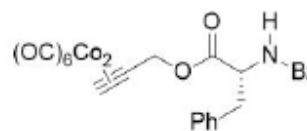
----- CHANNEL f1 -----
NUC1          1H
P1            13.75 usec
SI            65536
SF            400.1300108 MHz
WDW           EM
SSB           0
LB            0.30 Hz
GB            0
PC            1.00
    
```

SW06-169-C 13C 500

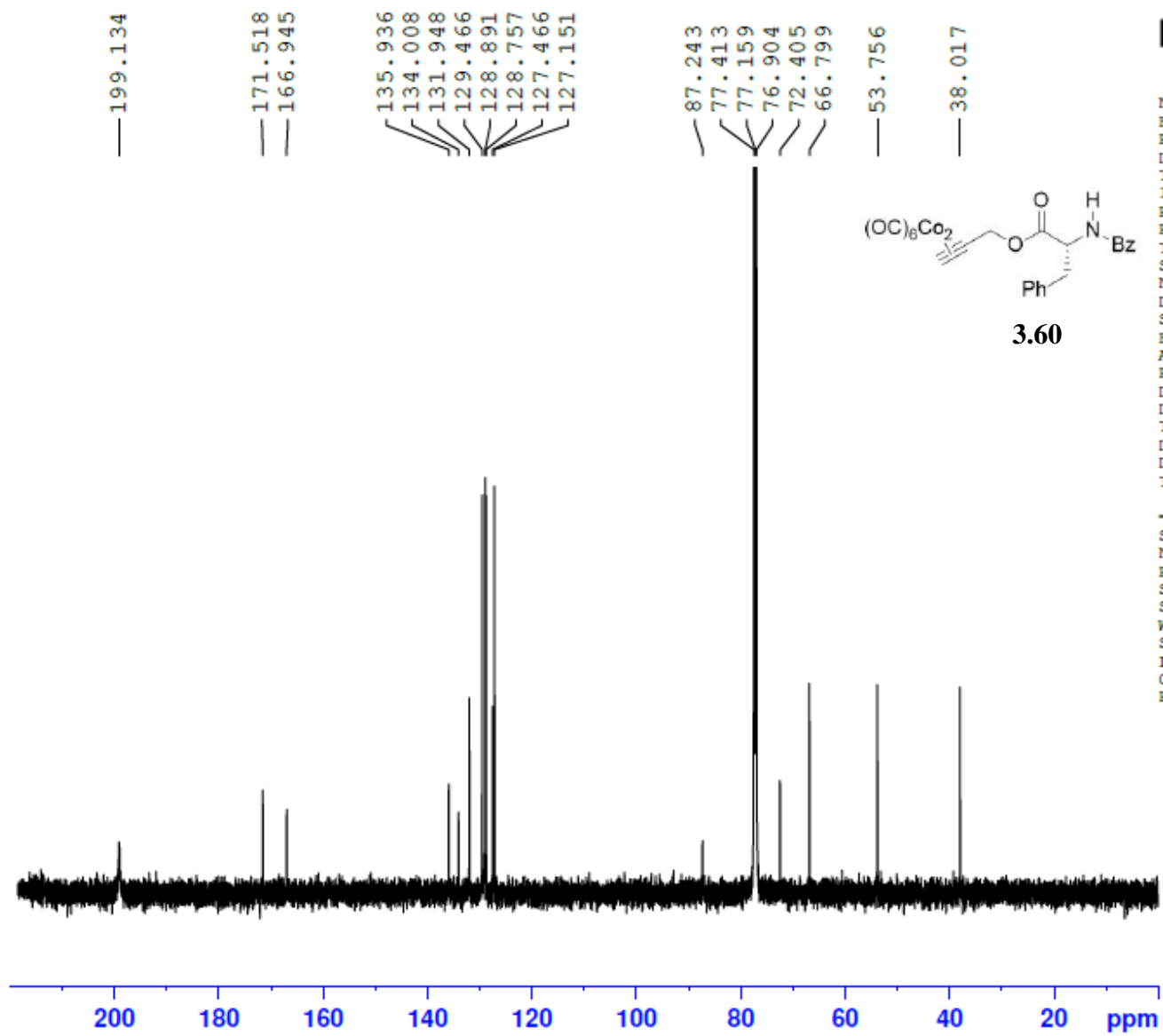


NAME SW06-169-C
EXPNO 10
PROCNO 1
Date_ 20150425
Time 2.37
INSTRUM spect
PROBHD 5 mm PABBO BB/
PULPROG zgpg30
ID 65536
SOLVENT CDCl3
NS 2048
DS 2
SWH 29761.904 Hz
FIDRES 0.454131 Hz
AQ 1.1010548 sec
RG 203
DW 16.800 usec
DE 6.50 usec
TE 299.2 K
D1 2.00000000 sec
D11 0.03000000 sec
TD0 1

----- CHANNEL f1 -----
SFO1 125.7779086 MHz
NUC1 13C
P1 10.50 usec
SI 32768
SF 125.7653129 MHz
WDW EM
SSB 0
LB 1.00 Hz
GB 0
PC 1.40

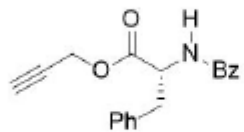


3.60



SW06-165- 1H 400

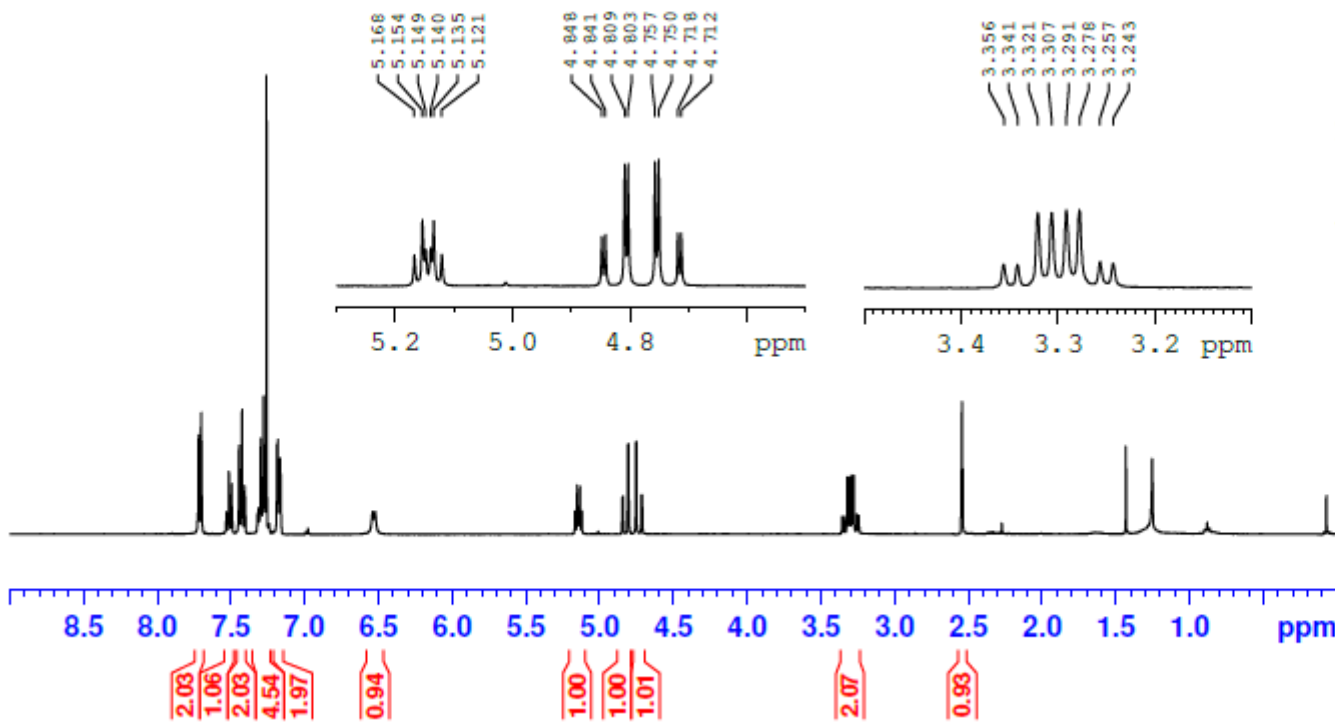
7.721 7.708 7.703 7.699 7.515 7.499 7.496 7.493 7.446 7.442 7.429 7.426 7.408 7.406 7.316 7.300 7.296 7.286 7.282 7.277 7.272 7.268 7.260 7.189 7.184 7.169 7.166 6.542 6.523 5.168 5.154 5.149 5.140 5.135 5.121 4.848 4.841 4.809 4.803 4.757 4.750 4.718 4.712 4.841 4.809 4.803 4.757 4.718 4.712 3.321 3.307 3.291 3.278 3.257 3.243 3.307 3.291 3.278 2.550 2.544 2.538 1.432 1.254 0.070



3.61

NAME SW06-165-cr
 EXPNO 10
 PROCNO 1
 Date_ 20150415
 Time 16.11
 INSTRUM spect
 PROBHD 5 mm PABBO BB-
 PULPROG zg30
 ID 65536
 SOLVENT CDCl3
 NS 16
 DS 2
 SWH 8223.685 Hz
 FIDRES 0.125483 Hz
 AQ 3.9846387 sec
 RG 144
 DW 60.800 usec
 DE 6.50 usec
 TE 90.6 K
 D1 1.00000000 sec

----- CHANNEL f1 -----
 NUC1 1H
 P1 13.75 usec
 SI 65536
 SF 400.1300098 MHz
 WDW EM
 SSB 0
 LB 0.30 Hz
 GB 0
 PC 1.00

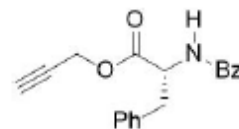


SW06-165-cr 1H 500

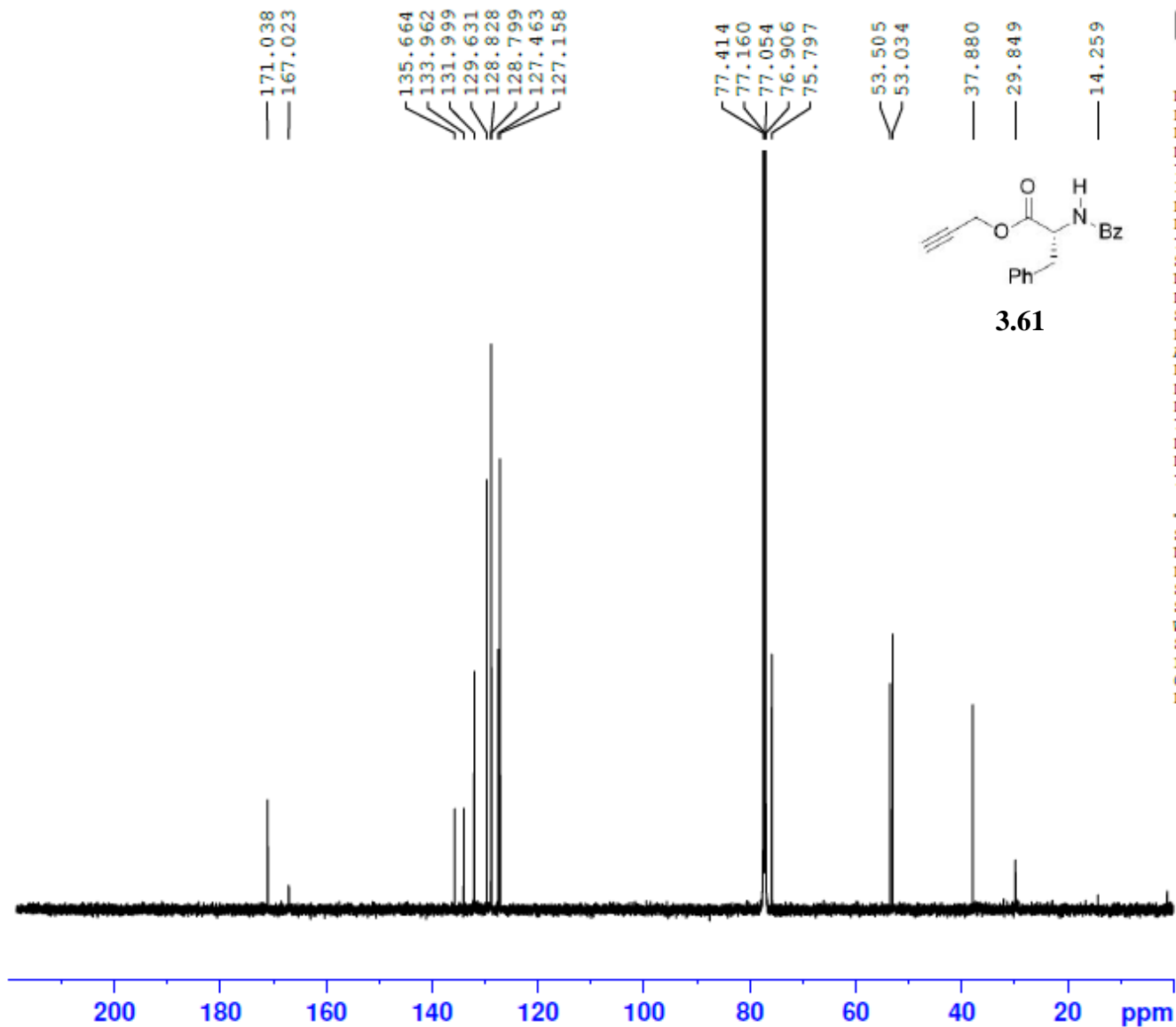


NAME SW06-165-cr
EXPNO 11
PROCNO 1
Date_ 20150502
Time 0.44
INSTURM spect
PROBHD 5 mm PABBO BB/
PULPROG zgpg30
ID 65536
SOLVENT CDCl3
NS 2048
DS 2
SWH 29761.904 Hz
FIDRES 0.454131 Hz
AQ 1.1010548 sec
RG 203
DW 16.800 usec
DE 6.50 usec
TE 298.2 K
D1 2.00000000 sec
D11 0.03000000 sec
TD0 1

----- CHANNEL f1 -----
SFO1 125.7779086 MHz
NUC1 13C
P1 10.50 usec
SI 32768
SF 125.7653137 MHz
WDW EM
SSB 0
LB 1.00 Hz
GB 0
PC 1.40



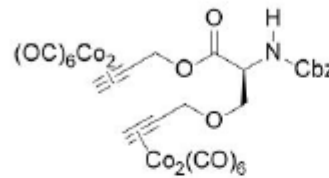
3.61



SW06-158-B 1H 400

7.354
7.260
6.066
5.999
5.660
5.639
5.388
5.352
5.258
5.222
5.157
5.126
5.107
5.076
4.680
4.658
4.632
4.173
4.152
3.923
3.905

1.254

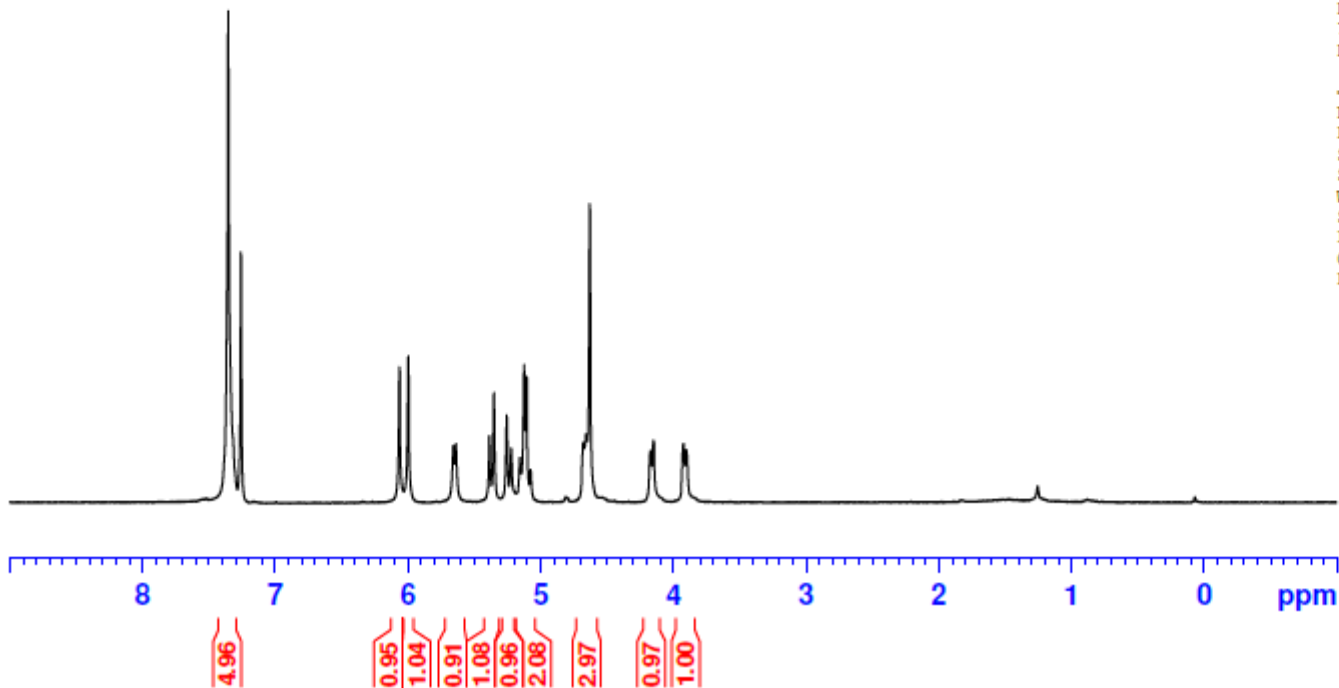


3.63



NAME SW06-158-B
EXPNO 10
PROCNO 1
Date_ 20150414
Time 17.59
INSTRUM spect
PROBHD 5 mm PABBO BB-
PULPROG zg30
TD 65536
SOLVENT CDCl3
NS 16
DS 2
SWH 8223.685 Hz
FIDRES 0.125483 Hz
AQ 3.9846387 sec
RG 144
DW 60.800 usec
DE 6.50 usec
TE 94.7 K
D1 1.00000000 sec

----- CHANNEL f1 -----
NUC1 1H
P1 13.75 usec
SI 65536
SF 400.1300100 MHz
WDW EM
SSB 0
LB 0.30 Hz
GB 0
PC 1.00



SW06-158-B 13C 400

199.50
199.08

169.78

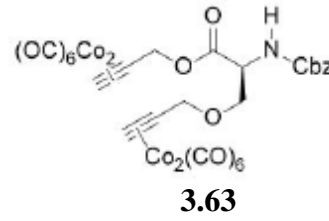
156.05

136.39
128.65
128.28
128.12

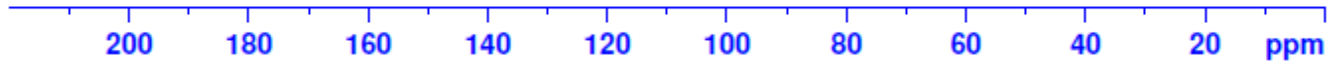
90.21
87.52
77.48
77.16
76.84
72.31
72.12
71.38
70.78
67.18
66.96
54.63



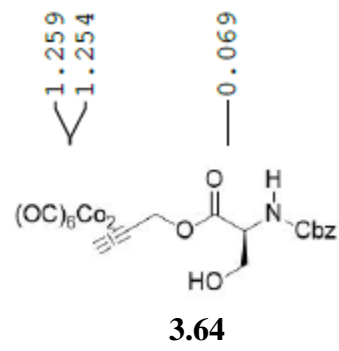
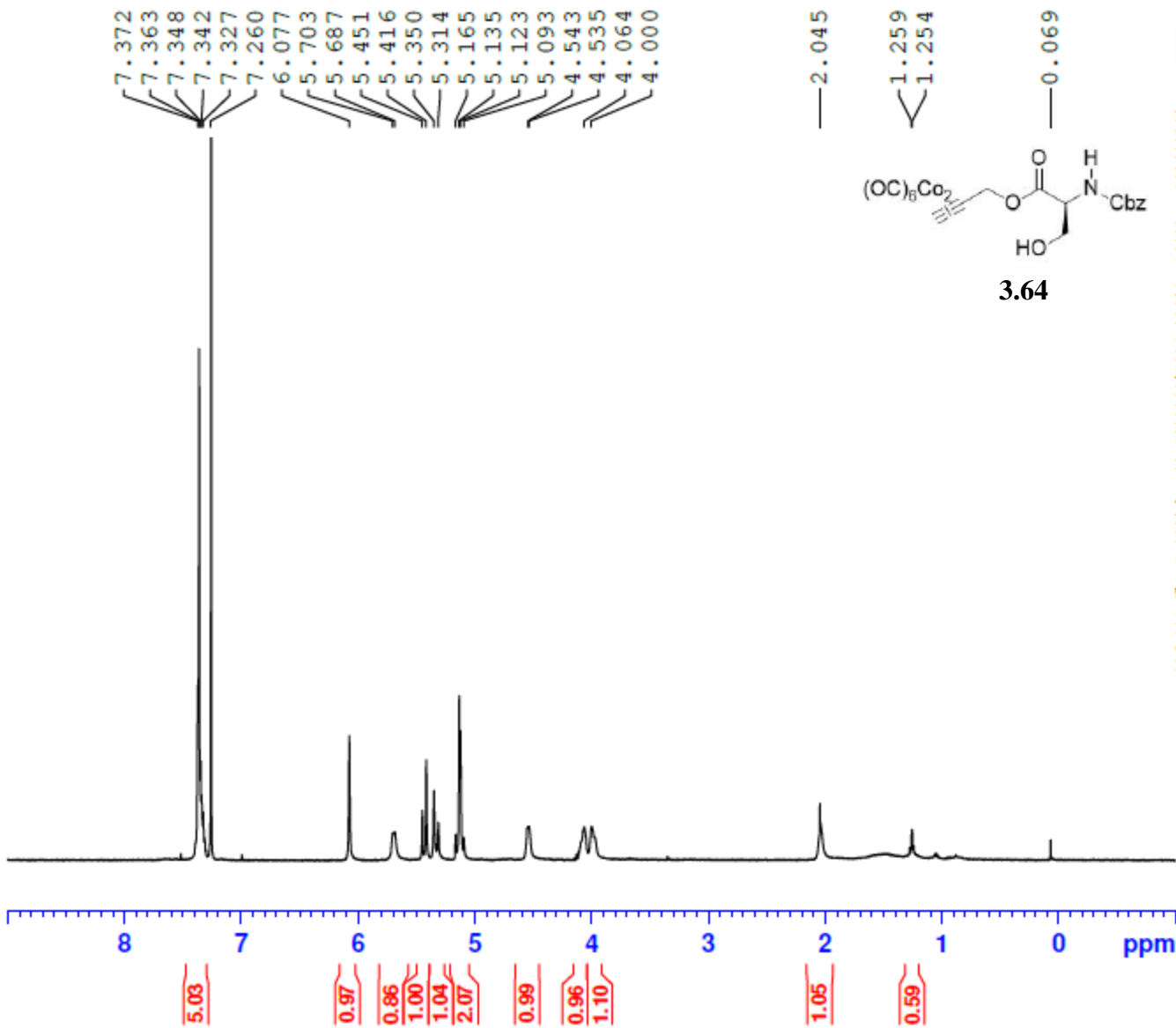
NAME SW06-158-B
EXPNO 20
PROCNO 1
Date_ 20150415
Time_ 23.28
INSTRUM spect
PROBHD 5 mm PABBO BB-
PULPROG zgpg30
ID 65536
SOLVENT CDC13
NS 2048
DS 4
SWH 24038.461 Hz
FIDRES 0.366798 Hz
AQ 1.3631988 sec
RG 203
DW 20.800 usec
DE 6.50 usec
IE 92.7 K
D1 2.00000000 sec
D11 0.03000000 sec



----- CHANNEL f1 -----
NUC1 13C
P1 10.00 usec
SI 32768
SF 100.6127549 MHz
WDW EM
SSB 0
LB 1.00 Hz
GB 0
PC 1.40



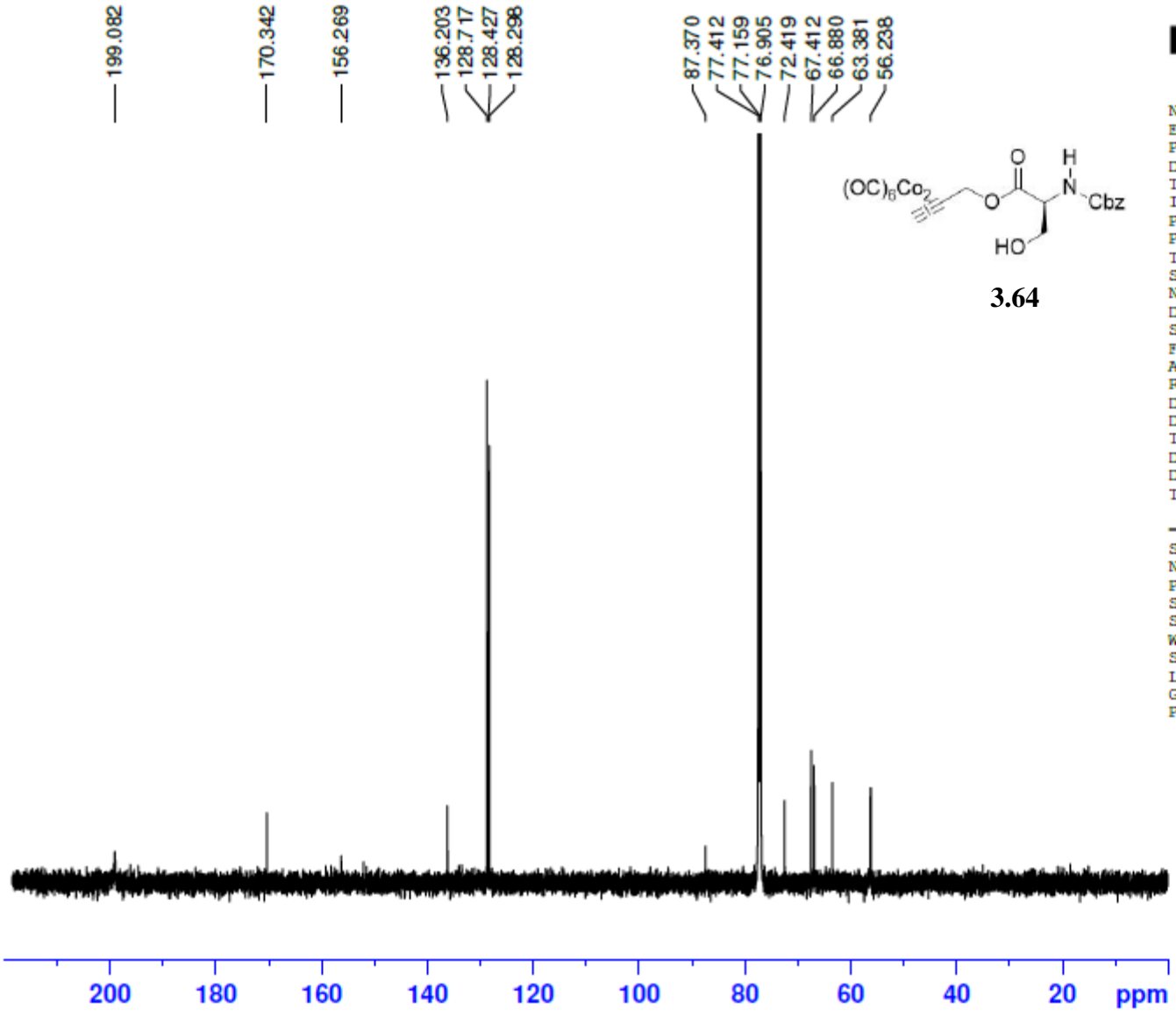
SW06-202-C 1H 400



NAME SW06-202-C
EXPNO 10
PROCNO 1
Date_ 20150522
Time 13.34
INSTRUM spect
PROBHD 5 mm PABBO BB-
PULPROG zg30
ID 65536
SOLVENT CDCl3
NS 16
DS 2
SWH 8223.685 Hz
FIDRES 0.125483 Hz
AQ 3.9846387 sec
RG 161
DW 60.800 usec
DE 6.50 usec
TE 94.3 K
D1 1.00000000 sec

----- CHANNEL f1 -----
NUC1 1H
P1 13.75 usec
SI 65536
SF 400.130099 MHz
WDW EM
SSB 0
LB 0.30 Hz
GB 0
PC 1.00

SW06-202-C 13C 500

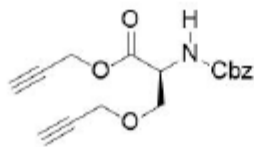


```
NAME SW06-202-C
EXPNO 10
PROCNO 1
Date_ 20150526
Time 0.37
INSTRUM spect
PROBHD 5 mm PABBO BB/
PULPROG zgpg30
TD 65536
SOLVENT CDCl3
NS 3072
DS 2
SWH 29761.904 Hz
FIDRES 0.454131 Hz
AQ 1.1010548 sec
RG 203
DW 16.800 usec
DE 6.50 usec
TE 298.2 K
D1 2.00000000 sec
D11 0.03000000 sec
TD0 1

----- CHANNEL f1 -----
SFO1 125.7779086 MHz
NUC1 13C
P1 10.50 usec
SI 32768
SF 125.7653131 MHz
WDW EM
SSB 0
LB 1.00 Hz
GB 0
PC 1.40
```

SW06-196-cr 1H 400

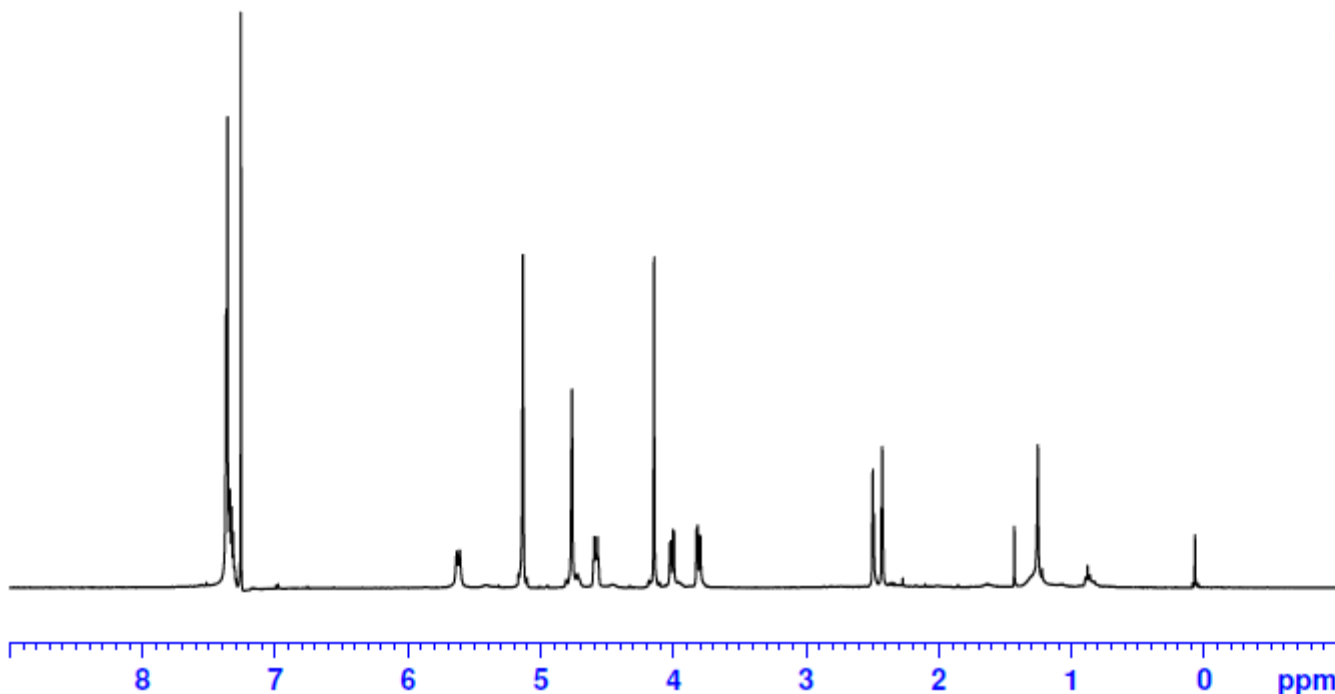
7.372
7.361
7.349
7.339
7.330
7.318
7.260
5.632
5.611
5.166
5.135
5.103
4.811
4.804
4.766
4.728
4.722
4.602
4.595
4.587
4.581
4.573
4.566
4.149
4.144
4.027
4.020
4.004
3.996
3.826
3.819
3.803
3.795
2.502
2.496
2.490
2.432
2.426
2.421
1.432
1.253
1.222
0.880
0.070



3.66

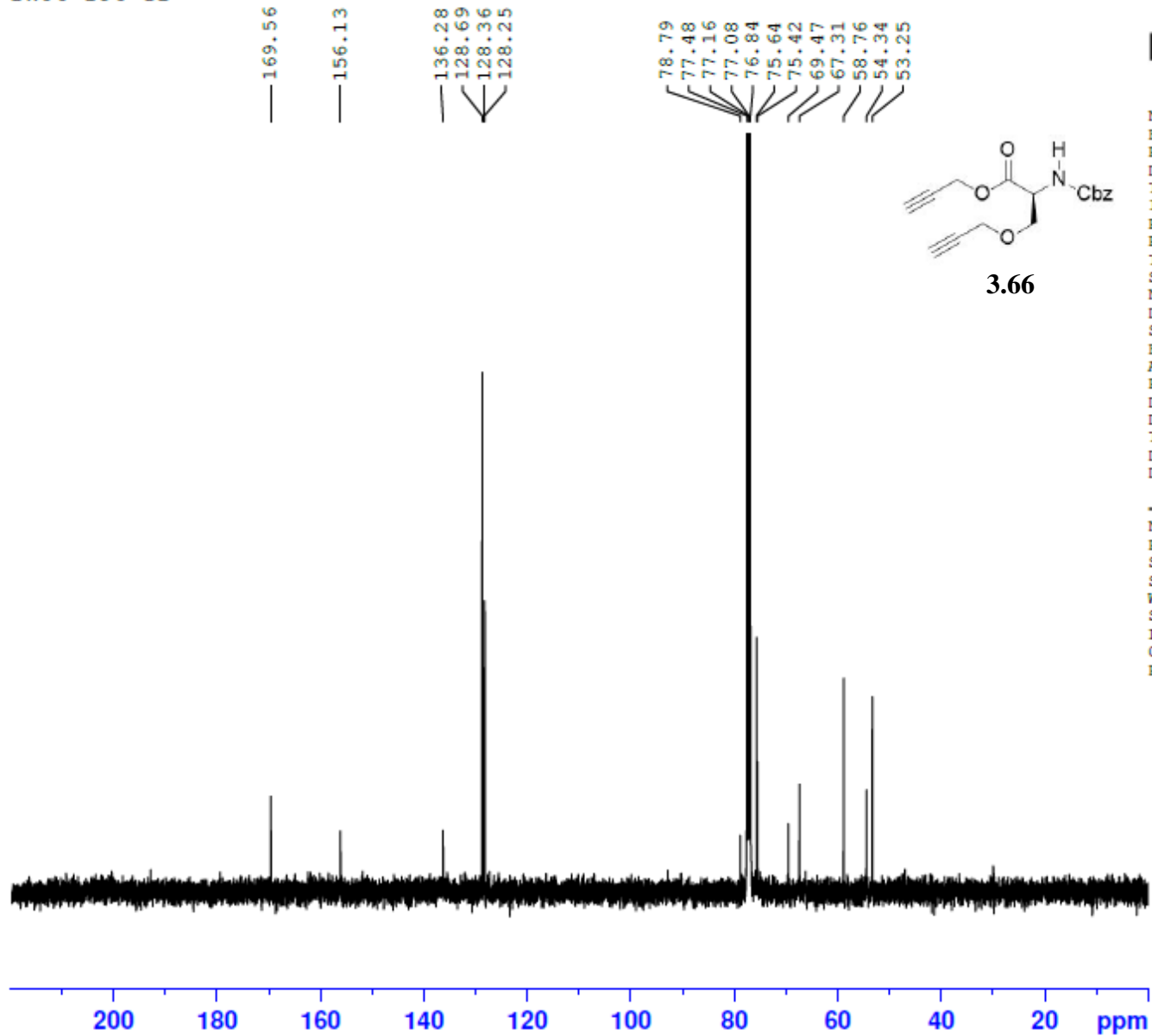
NAME SW06-196-cr
EXPNO 20
PROCNO 1
Date_ 20150515
Time_ 9.03
INSTRUM spect
PROBHD 5 mm PABBO BB-
PULPROG zg30
ID 65536
SOLVENT CDCl3
NS 16
DS 2
SWH 8223.685 Hz
FIDRES 0.125483 Hz
AQ 3.9846387 sec
RG 144
DW 60.800 usec
DE 6.50 usec
TE 296.8 K
D1 1.00000000 sec

----- CHANNEL f1 -----
NUC1 1H
P1 13.75 usec
SI 65536
SF 400.1300103 MHz
WDW EM
SSB 0
LB 0.30 Hz
GB 0
PC 1.00



5.17
0.87
2.08
2.00
0.92
2.03
1.03
1.04
0.94
1.06
1.89
0.52

SW06-196-cr



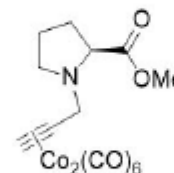
NAME SW06-196-cr
EXPNO 11
PROCNO 1
Date_ 20150515
Time 6.32
INSIRUM spect
PROBHD 5 mm PABBO BB-
PULPROG zgpg30
ID 65536
SOLVENT CDCl3
NS 2048
DS 4
SWH 24038.461 Hz
FIDRES 0.366798 Hz
AQ 1.3631988 sec
RG 128
DW 20.800 usec
DE 6.50 usec
TE 297.2 K
D1 2.00000000 sec
D11 0.03000000 sec

----- CHANNEL f1 -----
NUC1 13C
P1 10.00 usec
SI 32768
SF 100.6127550 MHz
WDW EM
SSB 0
LB 1.00 Hz
GB 0
PC 1.40

SW07-060-C



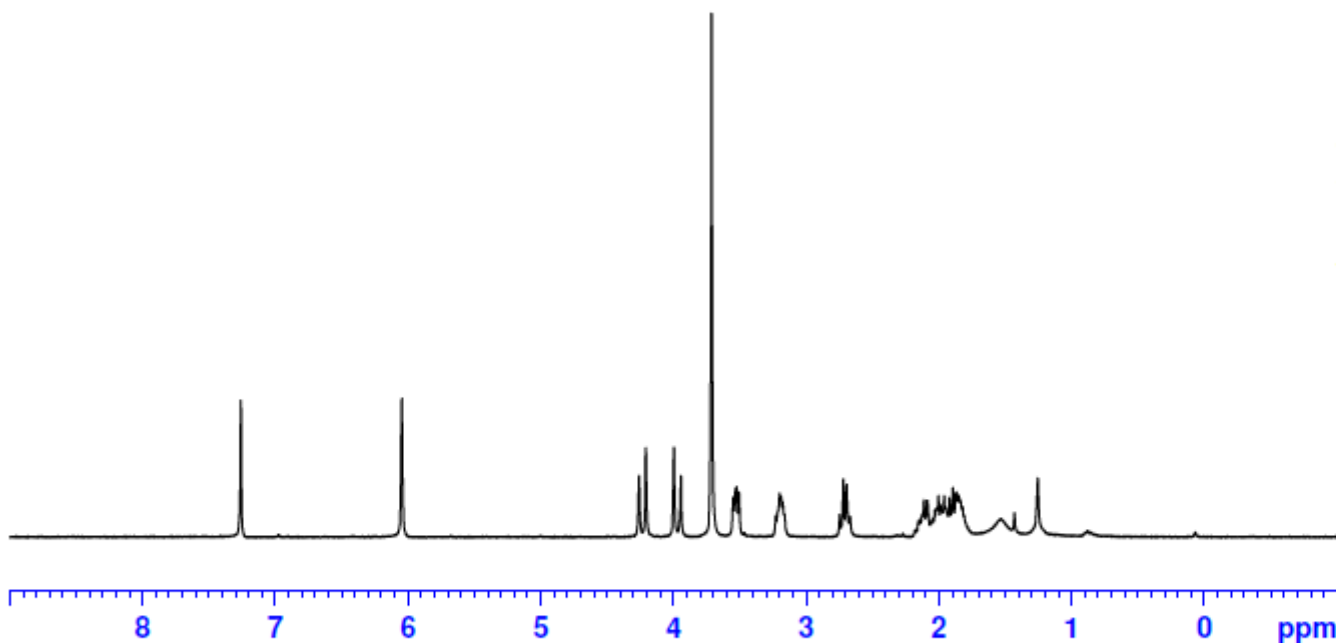
7.260
6.046
4.259
4.207
3.996
3.945
3.712
3.551
3.534
3.524
3.506
3.228
3.201
3.190
3.175
2.747
2.720
2.694
2.668
2.126
2.111
2.086
2.030
2.017
2.002
1.985
1.960
1.936
1.920
1.895
1.868
1.850
1.837
1.822
1.807



3.68

NAME SW07-060-C
EXPNO 10
PROCNO 1
Date_ 20150804
Time 18.03
INSTRUM spect
PROBHD 5 mm QNP 1H/1
PULPROG zg30
ID 32768
SOLVENT CDCl3
NS 16
DS 2
SWH 6188.119 Hz
FIDRES 0.188846 Hz
AQ 2.6477044 sec
RG 322
DW 80.800 usec
DE 6.50 usec
TE -922.2 K
D1 1.00000000 sec
TD0 1

----- CHANNEL f1 -----
SFO1 300.2318540 MHz
NUC1 1H
P1 12.71 usec
SI 32768
SF 300.2300085 MHz
WDW EM
SSB 0
LB 0.10 Hz
GB 0
PC 1.00

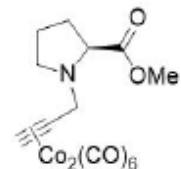


0.98
1.03
1.03
2.97
1.00
1.03
1.03
4.32
1.16
0.81

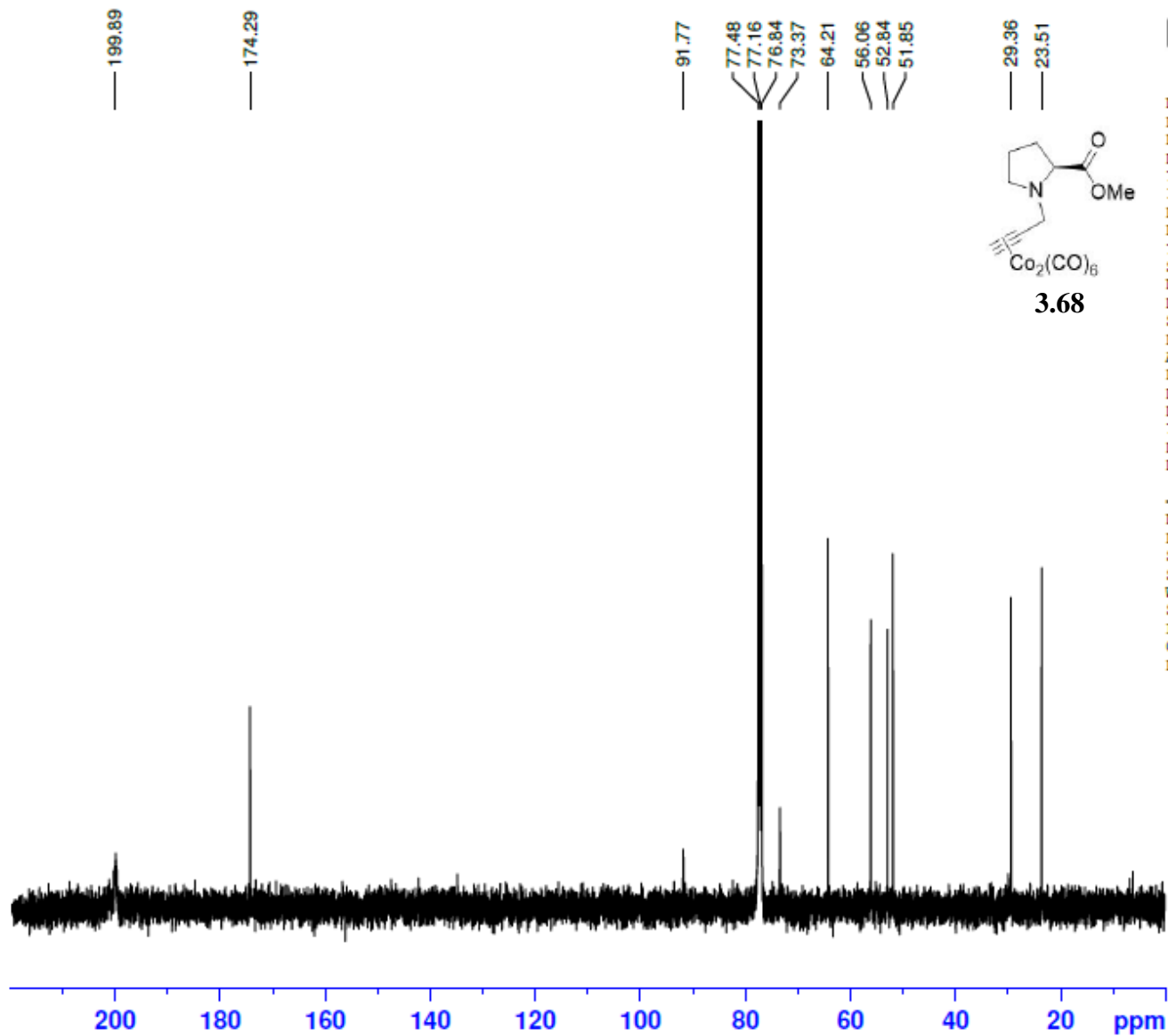
SW07-060-C 13C 400



NAME SW07-060-C
EXPNO 10
PROCNO 1
Date_ 20150805
Time 4.43
INSTRUM spect
PROBHD 5 mm PABBO BB-
PULPROG zgpg30
TD 65536
SOLVENT CDCl3
NS 2048
DS 4
SWH 24038.461 Hz
FIDRES 0.366798 Hz
AQ 1.3631988 sec
RG 181
DW 20.800 usec
DE 6.50 usec
TE 95.5 K
D1 2.00000000 sec
D11 0.03000000 sec



3.68



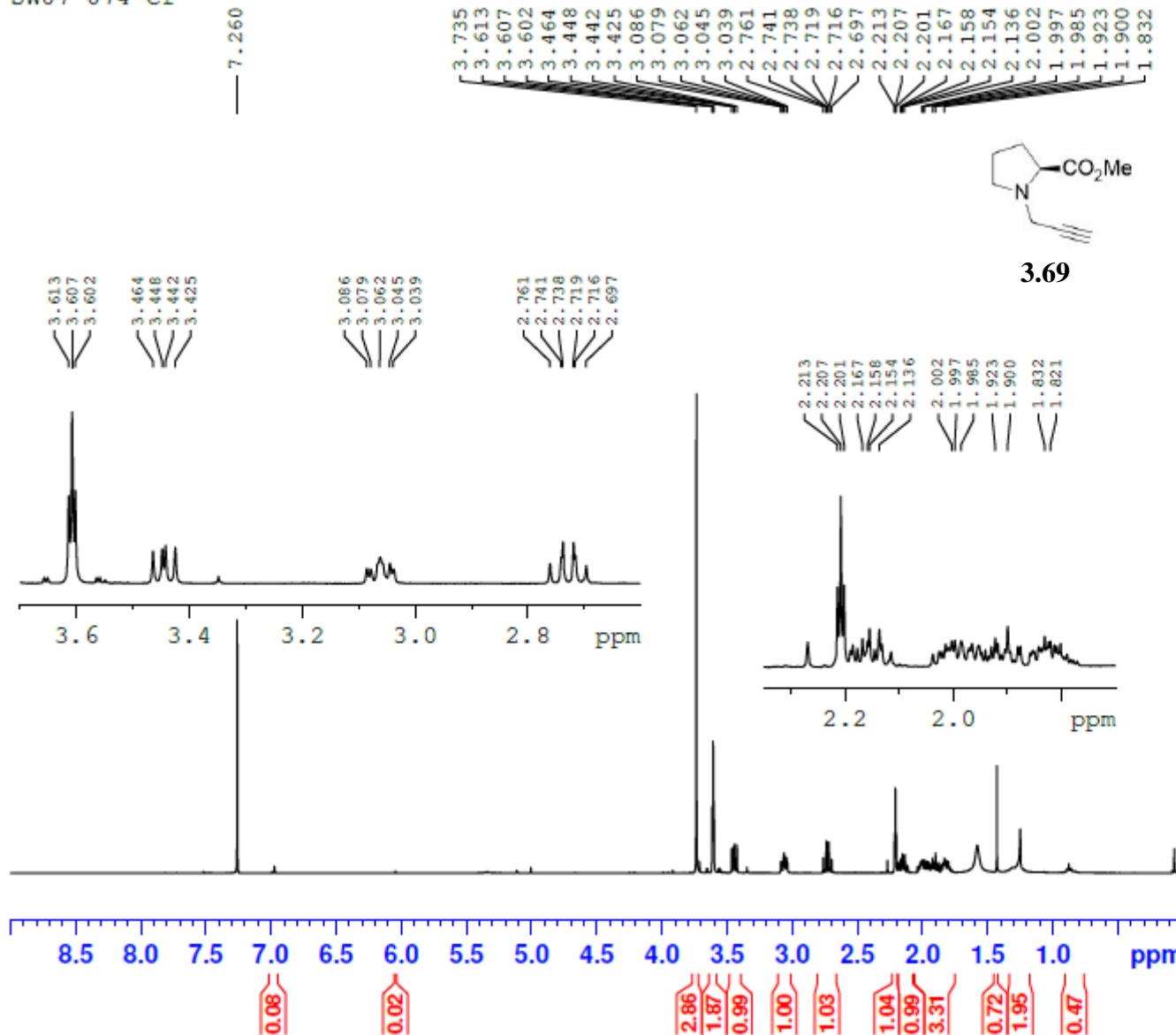
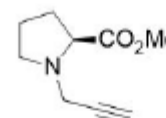
----- CHANNEL f1 -----
NUC1 13C
P1 10.00 usec
SI 32768
SF 100.6127546 MHz
WDW EM
SSB 0
LB 1.00 Hz
GB 0
PC 1.40

SW07-074-cr

7.260



NAME SW07-074-cr
 EXPNO 10
 PROCNO 1
 Date_ 20150814
 Time 17.03
 INSTRUM spect
 PROBHD 5 mm PABBO BB-
 PULPROG zg30
 ID 65536
 SOLVENT CDC13
 NS 16
 DS 2
 SWH 8223.685 Hz
 FIDRES 0.125483 Hz
 AQ 3.9846387 sec
 RG 144
 DW 60.800 usec
 DE 6.50 usec
 TE 93.5 K
 D1 1.00000000 sec

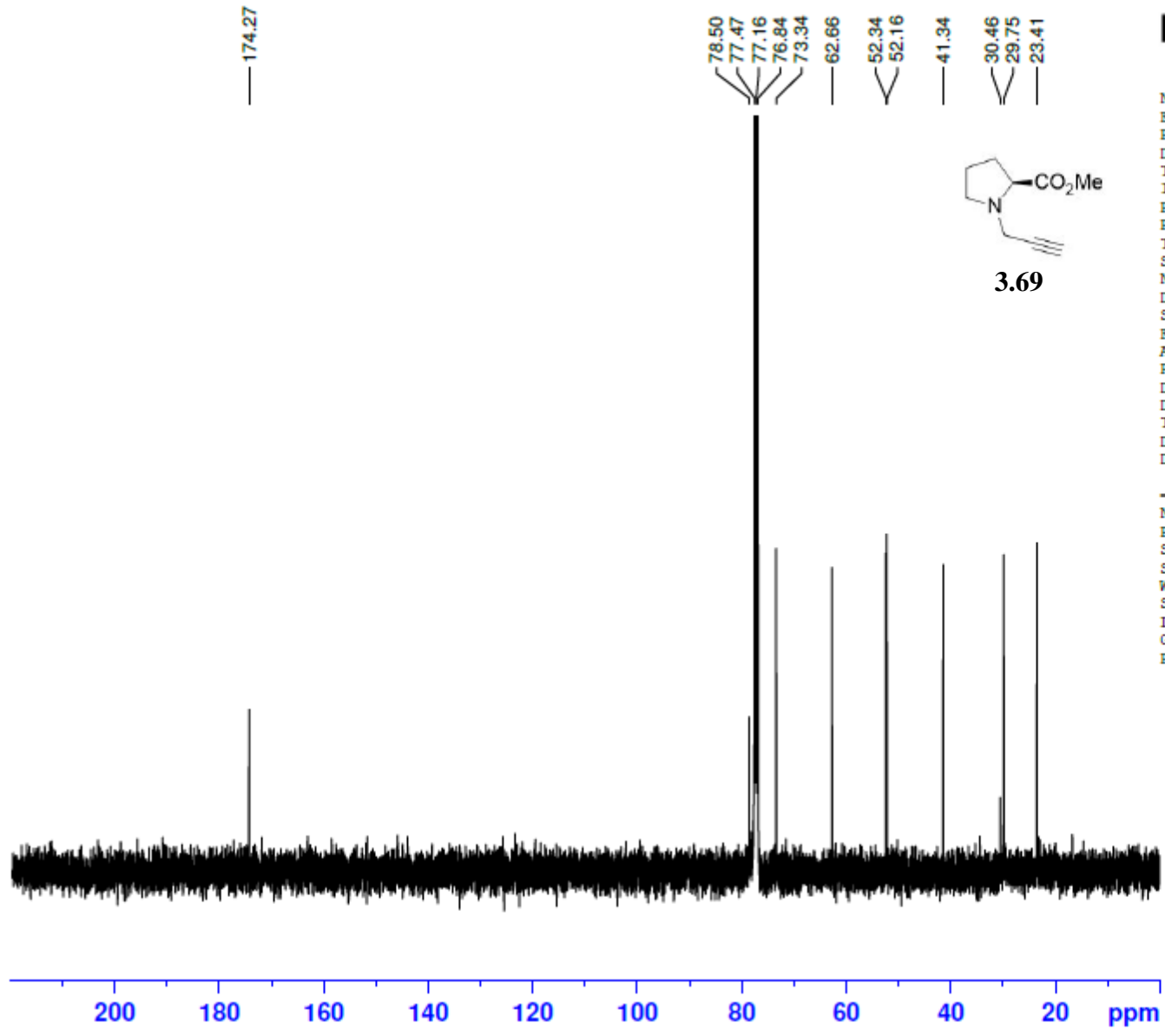
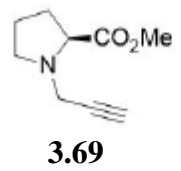


----- CHANNEL f1 -----
 NUC1 1H
 P1 13.75 usec
 SI 65536
 SF 400.1300099 MHz
 WDW EM
 SSB 0
 LB 0.30 Hz
 GB 0
 PC 1.00

SW07-074-cr 13C 400



NAME SW07-074-cr
EXPNO 11
PROCNO 1
Date_ 20150816
Time 1.33
INSTRUM spect
PROBHD 5 mm PABBO BB-
PULPROG zgpg30
ID 65536
SOLVENT CDCl3
NS 2048
DS 4
SWH 24038.461 Hz
FIDRES 0.366798 Hz
AQ 1.3631988 sec
RG 144
DW 20.800 usec
DE 6.50 usec
TE 95.0 K
D1 2.0000000 sec
D11 0.0300000 sec



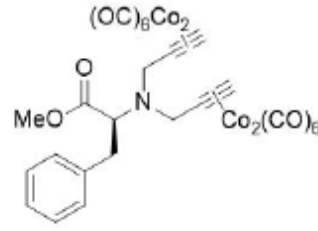
----- CHANNEL f1 -----
NUC1 13C
P1 10.00 usec
SI 32768
SF 100.6127555 MHz
WDW EM
SSB 0
LB 1.00 Hz
GB 0
PC 1.40

SW07-111-B 1H 400

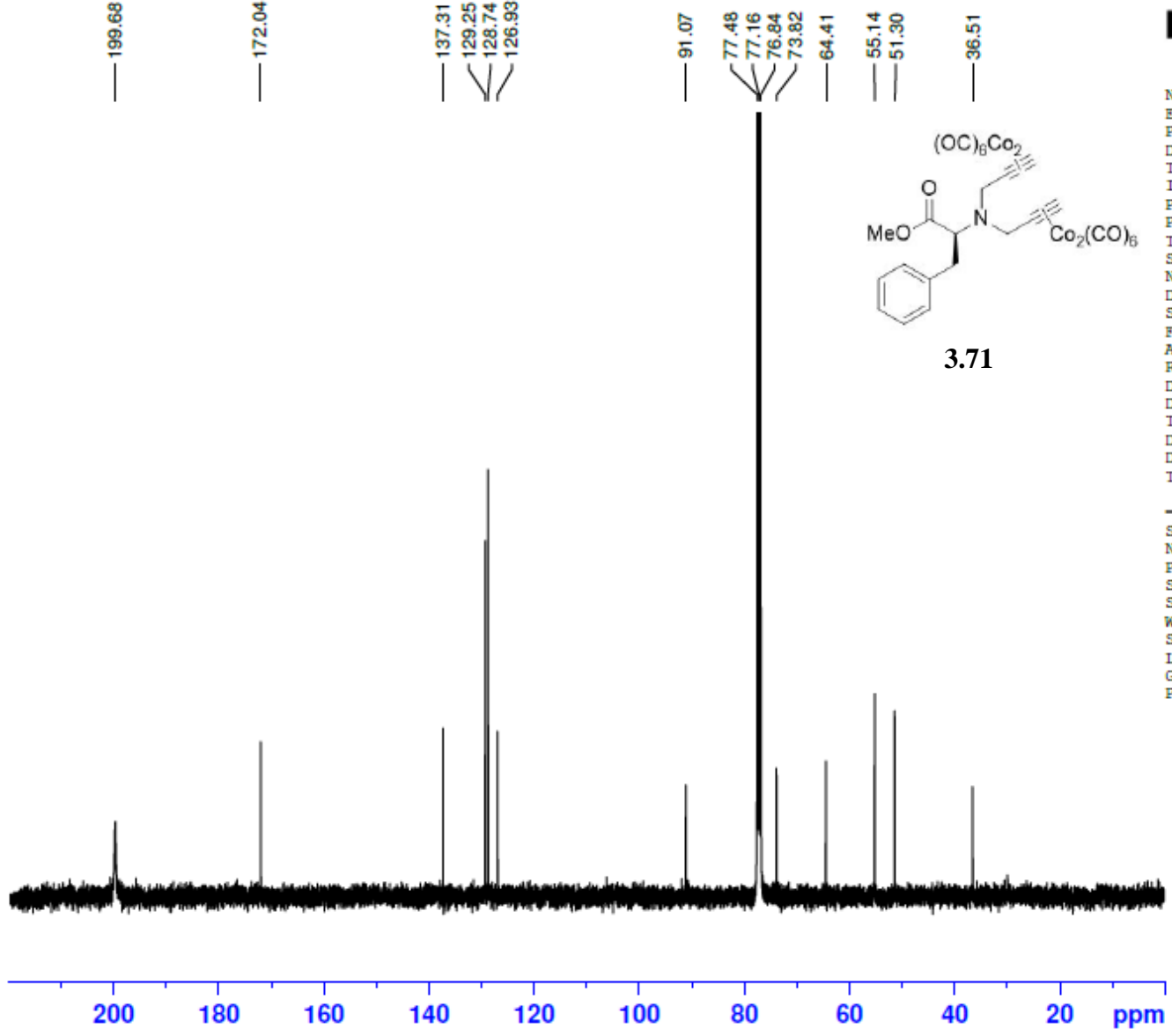


NAME SW07-111-B
EXPNO 11
PROCNO 1
Date_ 20151014
Time 3.34
INSTRUM spect
PROBHD 5 mm PABBO BB-
PULPROG zgpg30
ID 65536
SOLVENT CDCl3
NS 3072
DS 4
SWH 24038.461 Hz
FIDRES 0.366798 Hz
AQ 1.3631988 sec
RG 203
DW 20.800 usec
DE 6.50 usec
TE 97.8 K
D1 2.00000000 sec
D11 0.03000000 sec
TD0 1

----- CHANNEL f1 -----
SFO1 100.6228293 MHz
NUC1 13C
P1 10.00 usec
SI 32768
SF 100.6127541 MHz
WDW EM
SSB 0
LB 1.00 Hz
GB 0
PC 1.40



3.71



SW07-118-A

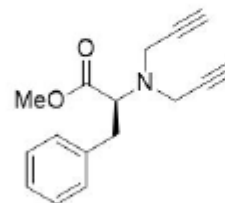
7.295
7.292
7.275
7.260
7.225
7.222
7.205
7.201
7.184

3.766
3.747
3.728
3.680
3.674
3.568
3.061
3.042
2.257
2.251
2.245

1.554
1.432
1.253

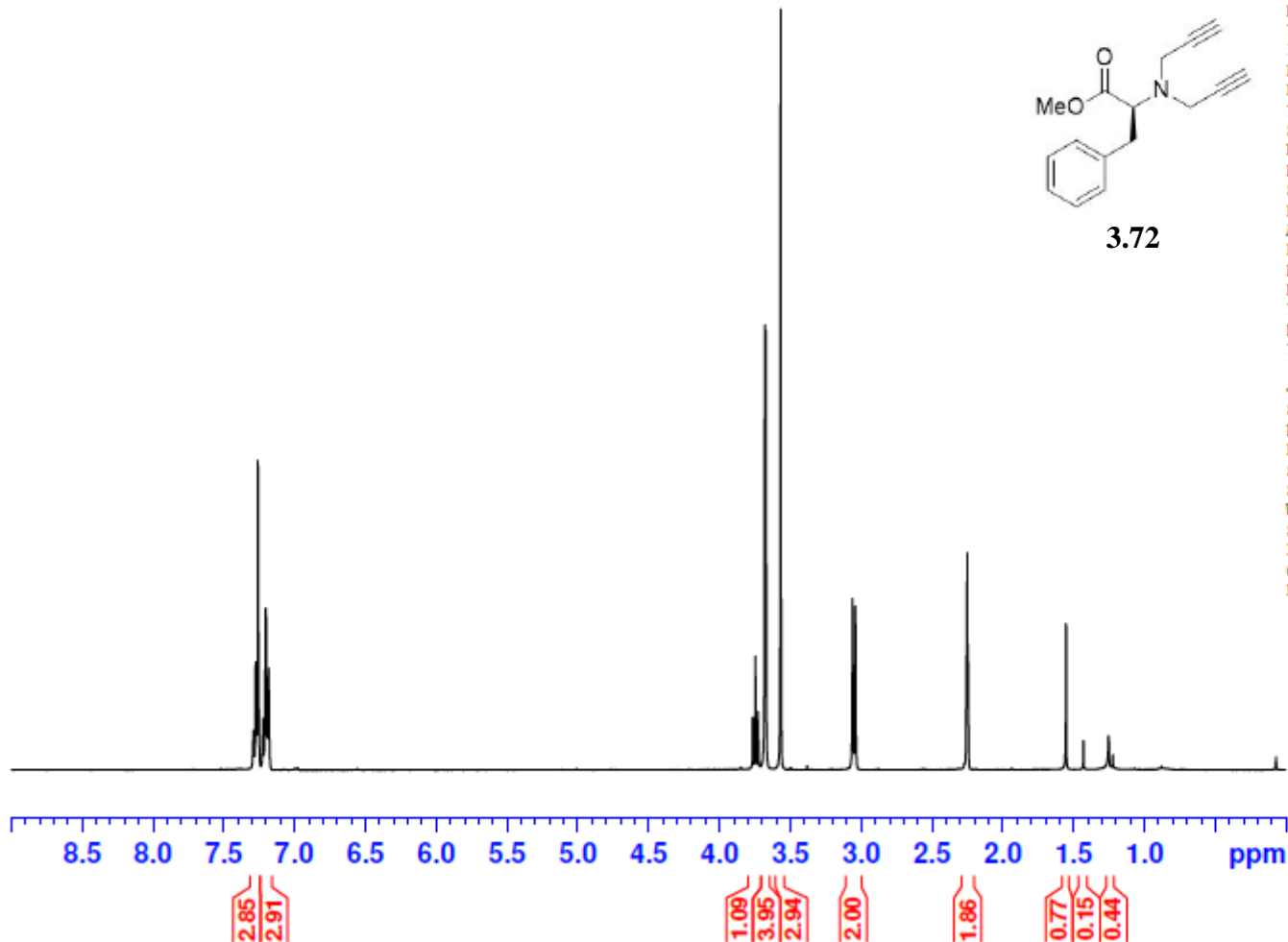


NAME SW07-118-A
EXPNO 10
PROCNO 1
Date_ 20151014
Time 18.07
INSTRUM spect
PROBHD 5 mm PABBO BB-
PULPROG zg30
ID 65536
SOLVENT CDCl3
NS 16
DS 2
SWH 8012.820 Hz
FIDRES 0.122266 Hz
AQ 4.0894966 sec
RG 128
DW 62.400 usec
DE 6.50 usec
TE 96.8 K
D1 1.0000000 sec
ID0 1



3.72

----- CHANNEL f1 -----
SFO1 400.1324710 MHz
NUC1 1H
P1 13.75 usec
SI 65536
SF 400.1300106 MHz
WDW EM
SSB 0
LB 0.30 Hz
GB 0
PC 1.00

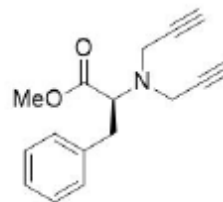


SW07-118-A 13C 400

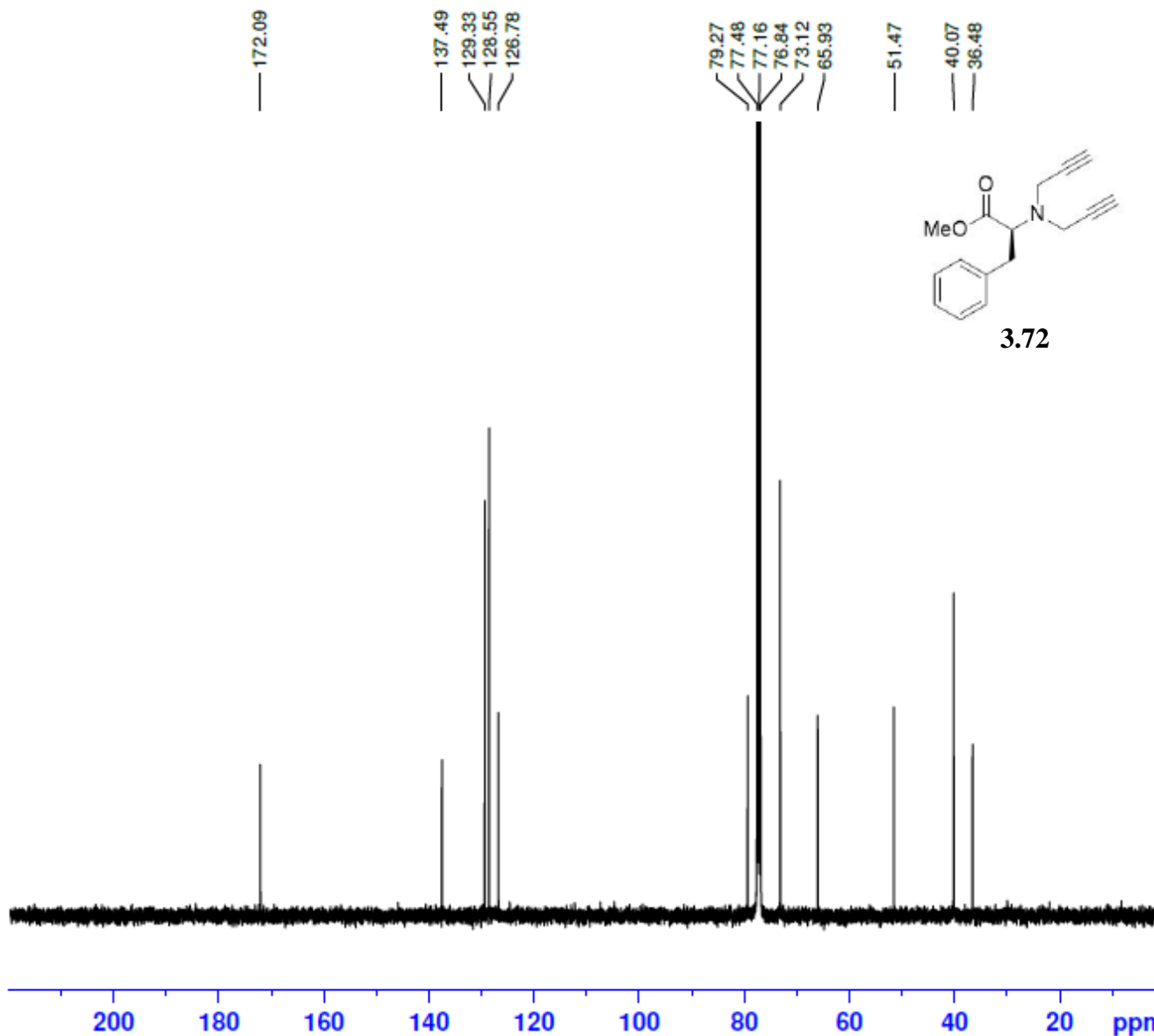


NAME SW07-118-A
EXPNO 11
PROCNO 1
Date_ 20151014
Time 23.00
INSTRUM spect
PROBHD 5 mm PABBO BB-
PULPROG zgpg30
ID 65536
SOLVENT CDCl3
NS 3072
DS 4
SWH 24038.461 Hz
FIDRES 0.366798 Hz
AQ 1.3631988 sec
RG 181
DW 20.800 usec
DE 6.50 usec
TE 97.9 K
D1 2.00000000 sec
D11 0.03000000 sec
TD0 1

----- CHANNEL f1 -----
SFO1 100.6228293 MHz
NUC1 13C
P1 10.00 usec
SI 32768
SF 100.6127546 MHz
WDW EM
SSB 0
LB 1.00 Hz
GB 0
PC 1.40



3.72

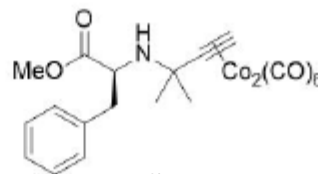


SW07-123-C 1H 400

7.292
7.275
7.260
7.231
7.214
7.190
7.172

— 5.994

3.745
3.727
3.708
3.690
3.624
2.919
2.902
2.886
2.870
2.859
2.841
2.808
1.907
1.886
1.358
1.343
1.292
1.256
1.200

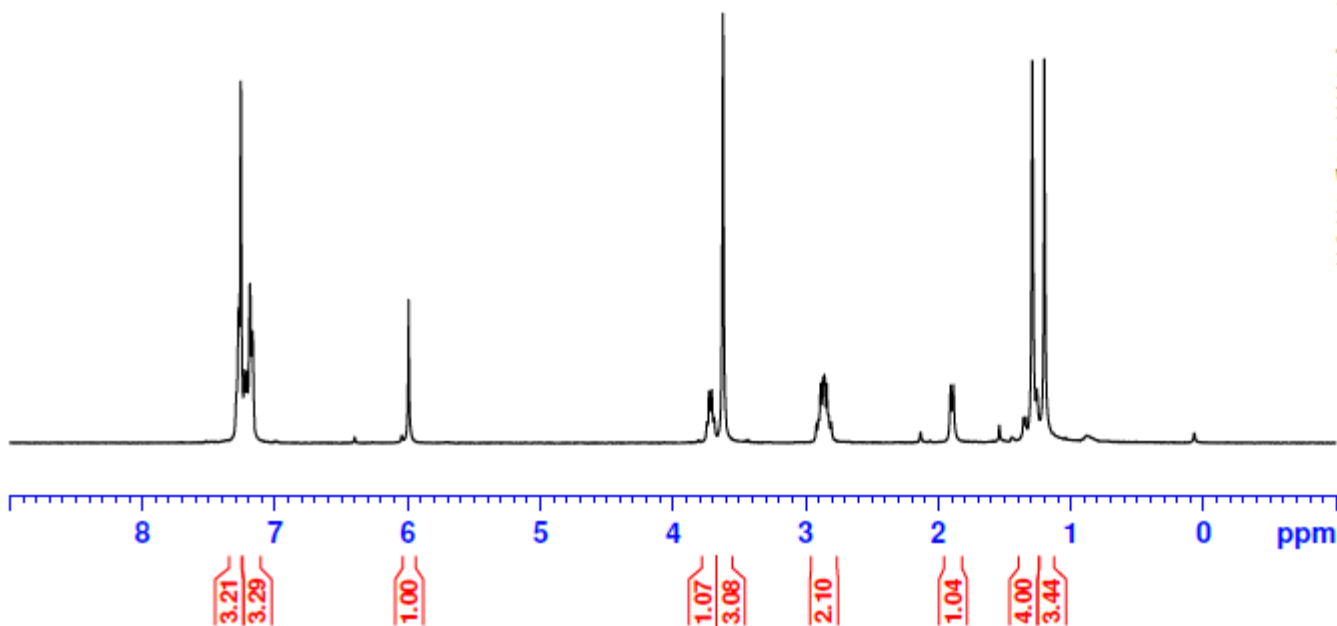


3.S2



NAME SW07-123-c
EXPNO 10
PROCNO 1
Date_ 20151021
Time 16.09
INSIRUM spect
PROBHD 5 mm PABBO BB-
PULPROG zg30
TD 65536
SOLVENT CDC13
NS 16
DS 2
SWH 8012.820 Hz
FIDRES 0.122266 Hz
AQ 4.0894966 sec
RG 144
DW 62.400 usec
DE 6.50 usec
TE 93.4 K
D1 1.00000000 sec
ID0 1

----- CHANNEL f1 -----
SFO1 400.1324710 MHz
NUC1 1H
P1 13.75 usec
SI 65536
SF 400.1300091 MHz
WDW EM
SSB 0
LB 0.30 Hz
GB 0
PC 1.00

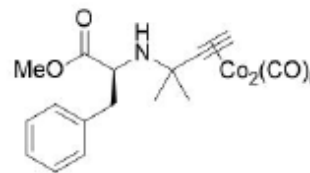


SW07-123-C 13C 400

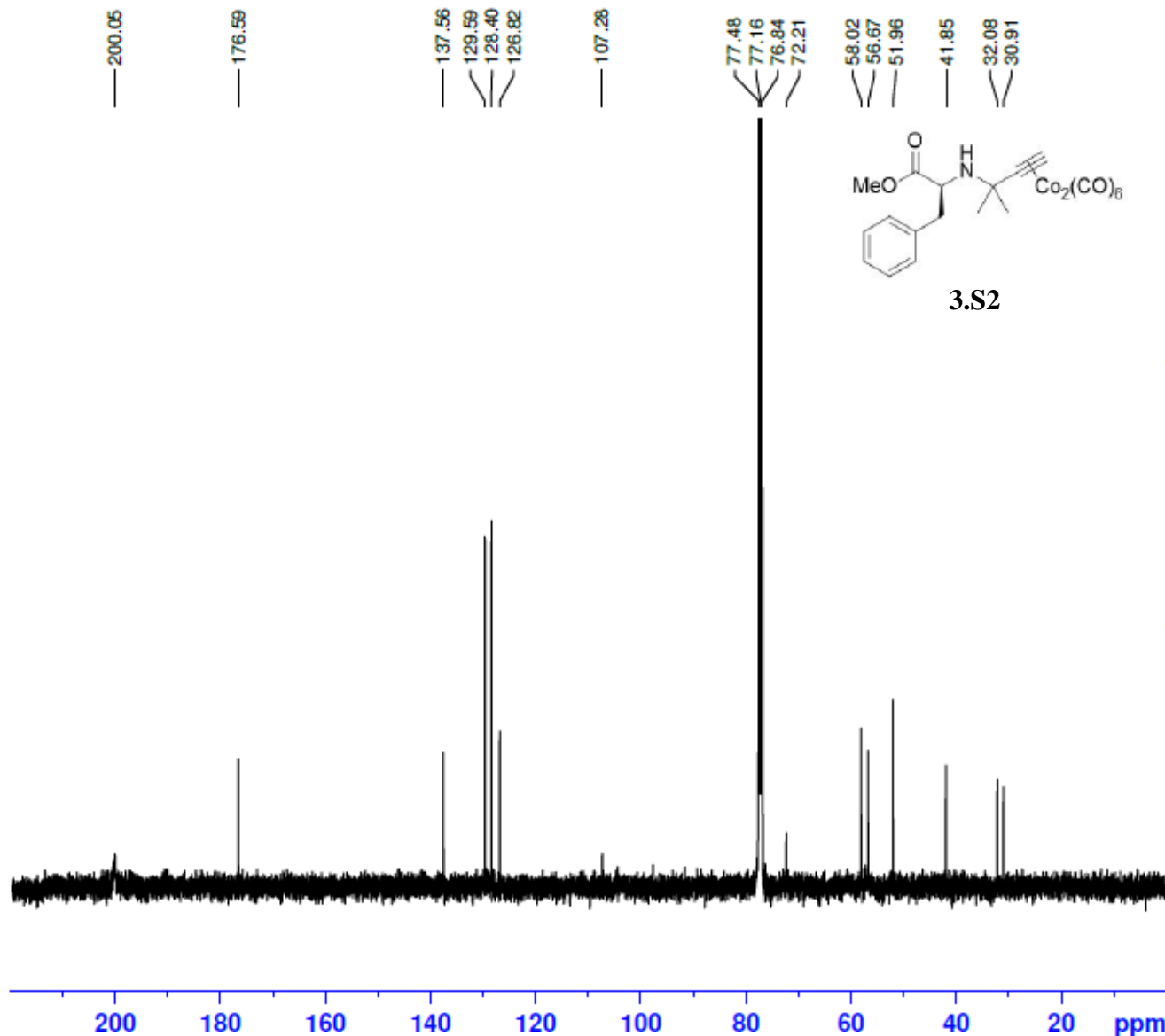


NAME SW07-123-C
EXPNO 11
PROCNO 1
Date_ 20151021
Time_ 23.01
INSTRUM spect
PROBHD 5 mm PABBO BB-
PULPROG zgpg30
ID 65536
SOLVENT CDCl3
NS 3072
DS 4
SWH 24038.461 Hz
FIDRES 0.366798 Hz
AQ 1.3631988 sec
RG 181
DW 20.800 usec
DE 6.50 usec
TE 95.9 K
D1 2.0000000 sec
D11 0.0300000 sec
ID0 1

----- CHANNEL f1 -----
SFO1 100.6228293 MHz
NUC1 13C
P1 10.00 usec
SI 32768
SF 100.6127540 MHz
WDW EM
SSB 0
LB 1.00 Hz
GB 0
PC 1.40



3.S2

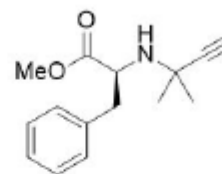


SW07-131-A 1H 400
 7.296
 7.277
 7.260
 7.231
 7.229
 7.215
 7.195

3.751
 3.734
 3.731
 3.715
 3.630
 2.951
 2.936
 2.918
 2.902
 2.863
 2.844
 2.830
 2.810
 2.180
 1.916
 1.549
 1.311
 1.252
 1.188

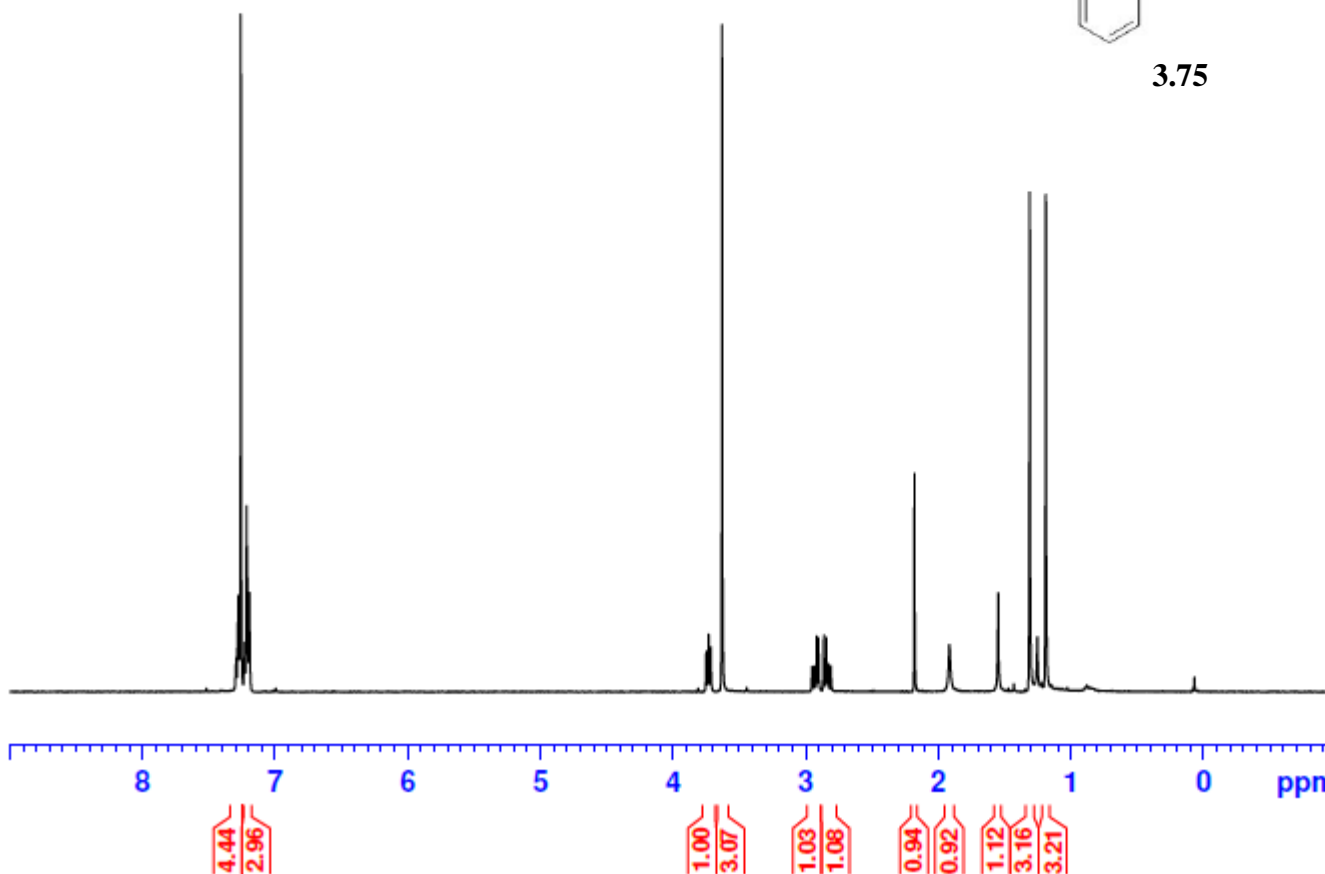


NAME SW07-131-A
 EXPNO 10
 PROCNO 1
 Date_ 20151103
 Time_ 17.21
 INSTRUM spect
 PROBHD 5 mm PABBO BB-
 PULPROG zg30
 ID 65536
 SOLVENT CDCl3
 NS 16
 DS 2
 SWH 8012.820 Hz
 FIDRES 0.122266 Hz
 AQ 4.0894966 sec
 RG 144
 DW 62.400 usec
 DE 6.50 usec
 TE 91.8 K
 D1 1.00000000 sec
 ID0 1



3.75

----- CHANNEL f1 -----
 SFO1 400.1324710 MHz
 NUC1 1H
 P1 13.75 usec
 SI 65536
 SF 400.1300105 MHz
 WDW EM
 SSB 0
 LB 0.30 Hz
 GB 0
 PC 1.00

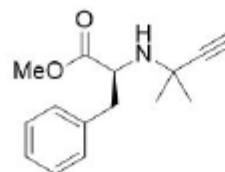


SW07-131-A 13C 400

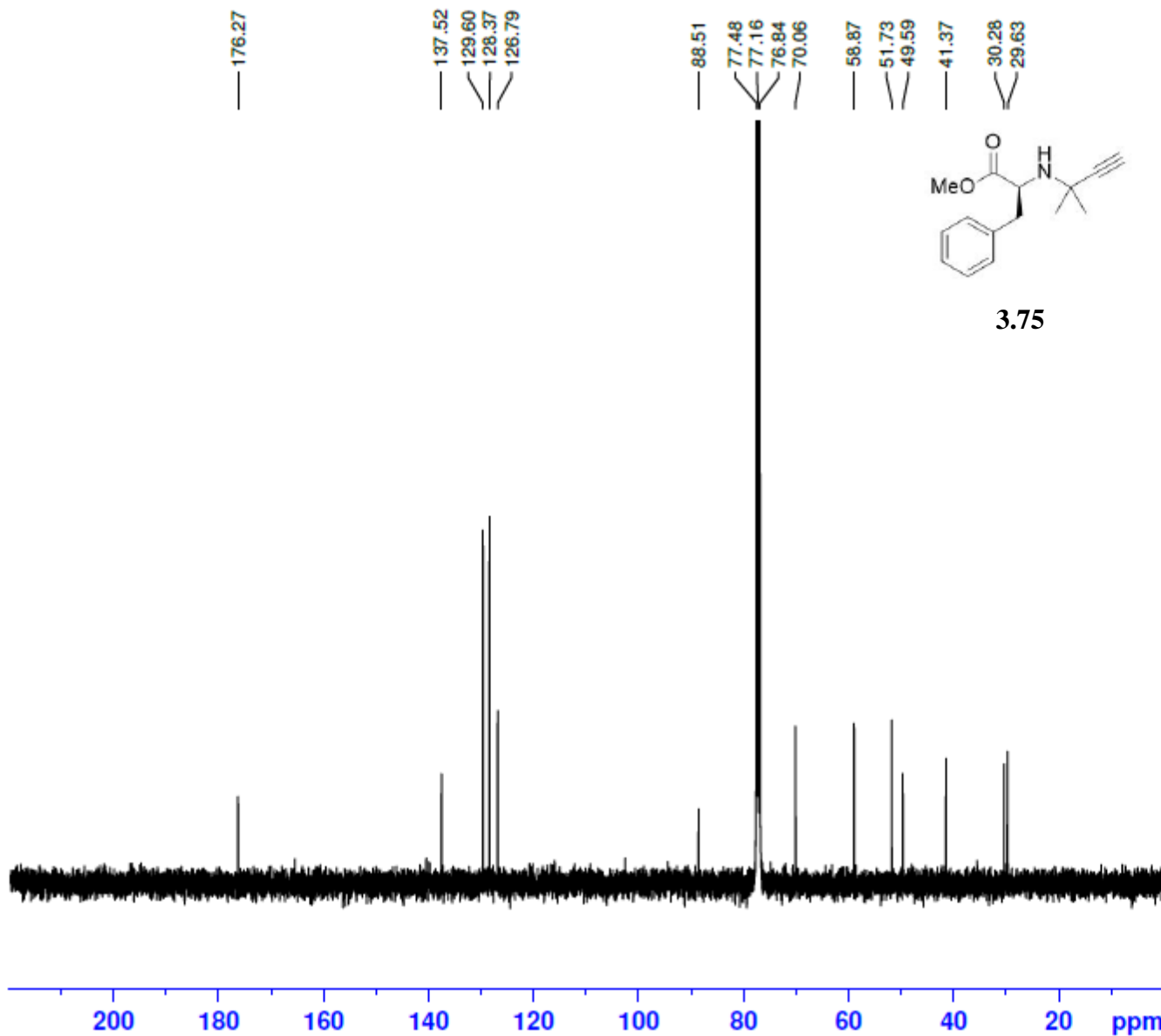


NAME SW07-131-A
EXPNO 11
PROCNO 1
Date_ 20151103
Time_ 23.00
INSTRUM spect
PROBHD 5 mm PABBO BB-
PULPROG zgpg30
ID 65536
SOLVENT CDCl3
NS 3072
DS 4
SWH 24038.461 Hz
FIDRES 0.366798 Hz
AQ 1.3631988 sec
RG 203
DW 20.800 usec
DE 6.50 usec
TE 97.2 K
D1 2.00000000 sec
D11 0.03000000 sec
TD0 1

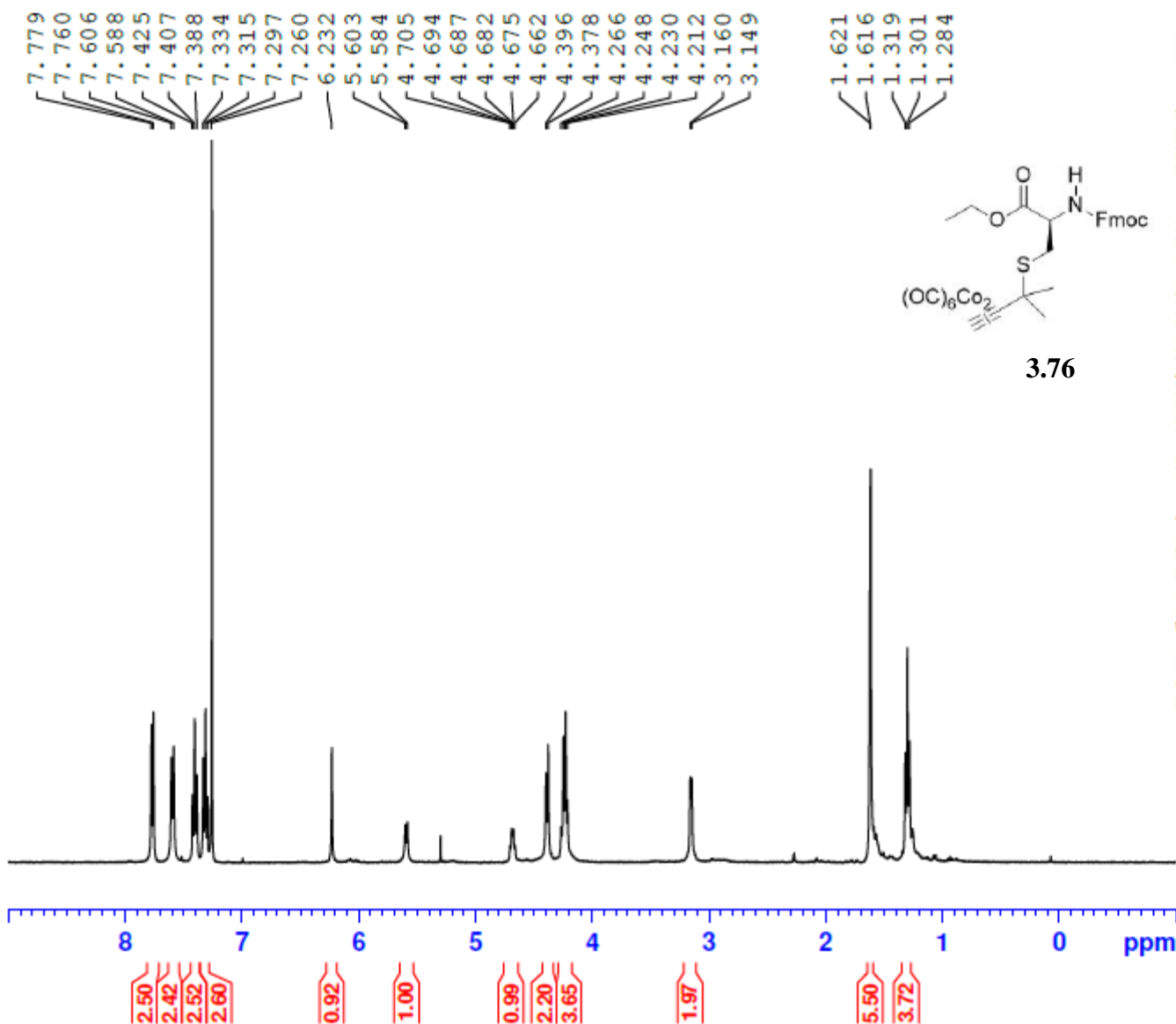
----- CHANNEL f1 -----
SFO1 100.6228293 MHz
NUC1 13C
P1 10.00 usec
SI 32768
SF 100.6127542 MHz
WDW EM
SSB 0
LB 1.00 Hz
GB 0
PC 1.40



3.75



SW07-141-B



NAME SW07-141-B
 EXPNO 20
 PROCNO 1
 Date_ 20151210
 Time_ 14.12
 INSTRUM spect
 PROBHD 5 mm PABBO BB-
 PULPROG zg30
 ID 65536
 SOLVENT CDC13
 NS 16
 DS 2
 SWH 8012.820 Hz
 FIDRES 0.122266 Hz
 AQ 4.0894966 sec
 RG 144
 DW 62.400 usec
 DE 6.50 usec
 IE 96.4 K
 D1 1.0000000 sec
 ID0 1

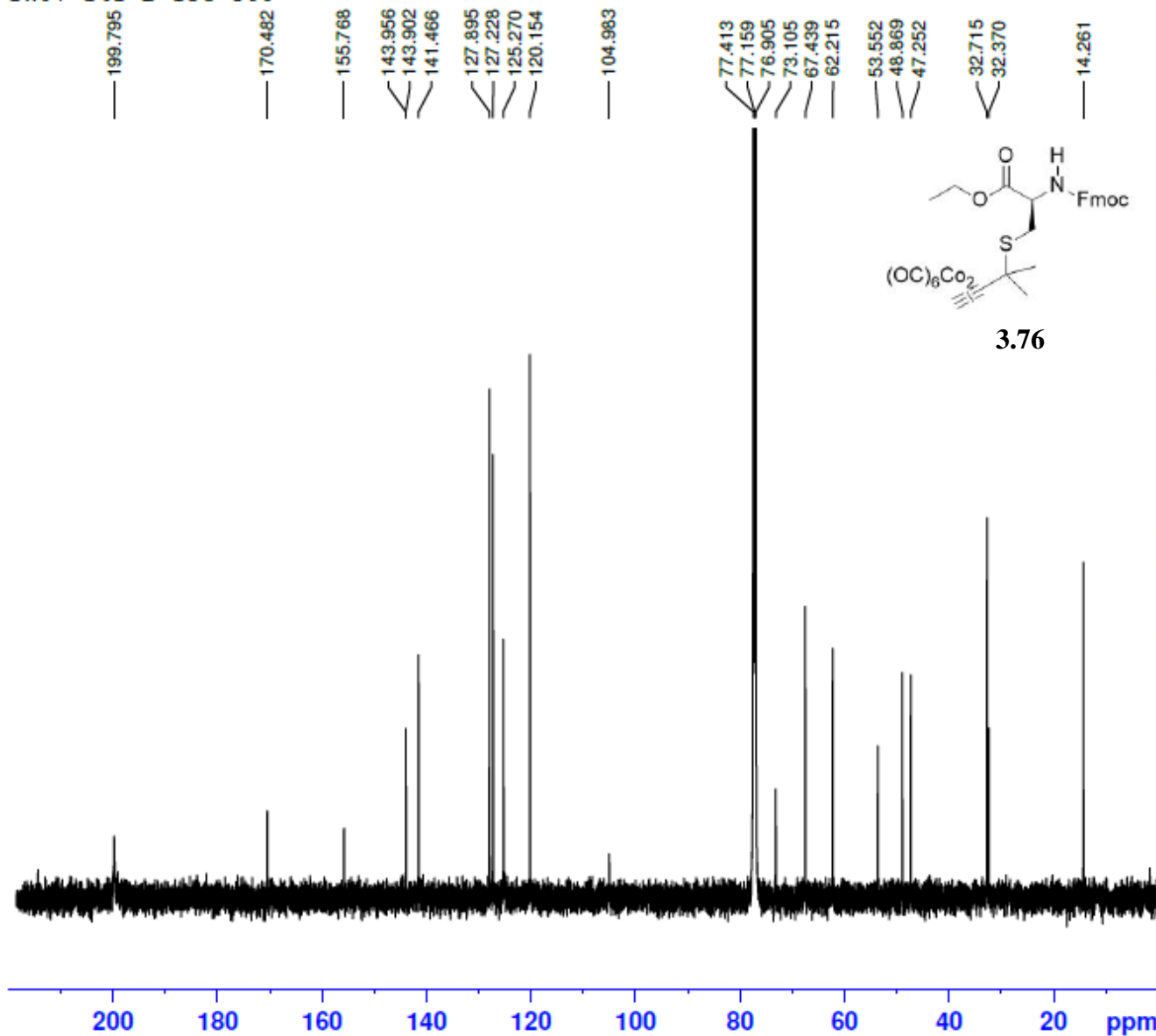
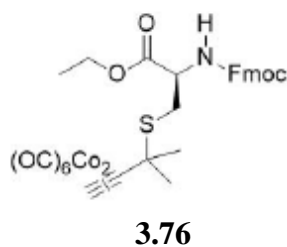
----- CHANNEL f1 -----
 SFO1 400.1324710 MHz
 NUC1 1H
 P1 13.75 usec
 SI 65536
 SF 400.1300096 MHz
 WDW EM
 SSB 0
 LB 0.30 Hz
 GB 0
 PC 1.00

SW07-141-B 13C 500



NAME SW07-141-B
EXPNO 10
PROCNO 1
Date_ 20151212
Time 1.36
INSTRUM spect
PROBHD 5 mm PABBO BB/
PULPROG zgpg30
ID 65536
SOLVENT CDCl3
NS 5120
DS 2
SWH 29761.904 Hz
FIDRES 0.454131 Hz
AQ 1.1010548 sec
RG 203
DW 16.800 usec
DE 6.50 usec
TE 298.7 K
D1 2.00000000 sec
D11 0.03000000 sec
ID0 1

----- CHANNEL f1 -----
SFO1 125.7779086 MHz
NUC1 13C
P1 10.50 usec
SI 32768
SF 125.7653128 MHz
WDW EM
SSB 0
LB 1.00 Hz
GB 0
PC 1.40

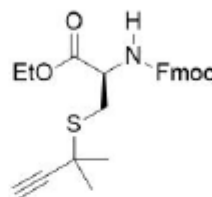


SW07-147-A 1H 400

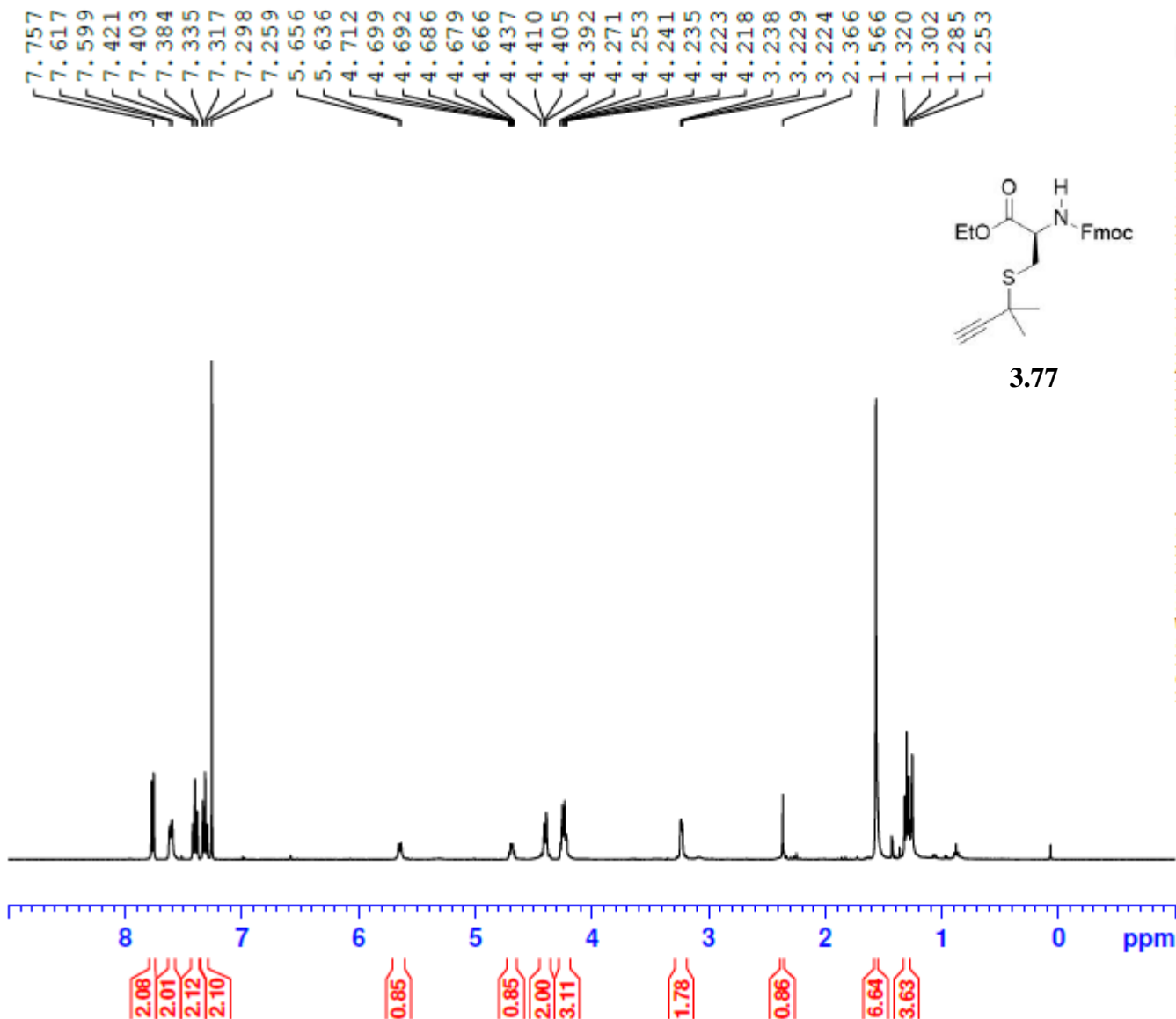


NAME SW07-147-A
EXPNO 10
PROCNO 1
Date_ 20151214
Time_ 13.46
INSIRUM spect
PROBHD 5 mm PABBO BB-
PULPROG zg30
ID 65536
SOLVENT CDCl3
NS 16
DS 2
SWH 8012.820 Hz
FIDRES 0.122266 Hz
AQ 4.0894966 sec
RG 144
DW 62.400 usec
DE 6.50 usec
TE 96.5 K
D1 1.00000000 sec
ID0 1

----- CHANNEL f1 -----
SFO1 400.1324710 MHz
NUC1 1H
P1 13.75 usec
SI 65536
SF 400.1300108 MHz
WDW EM
SSB 0
LB 0.30 Hz
GB 0
PC 1.00



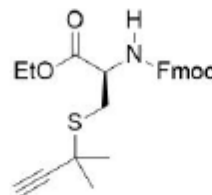
3.77



SW07-147-A 13C 400



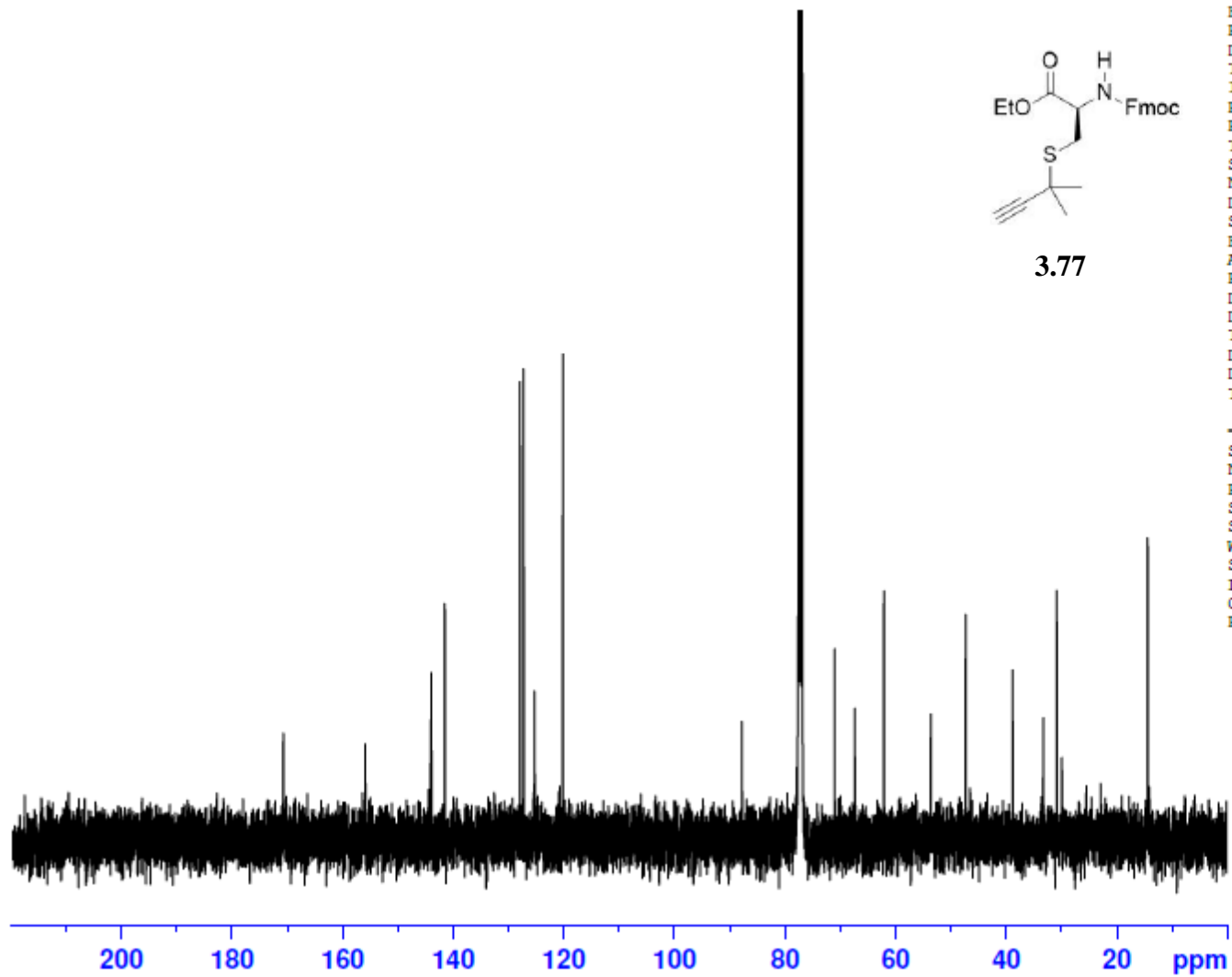
170.73 155.90 144.03 143.92 141.47 141.44 127.87 127.23 125.32 120.14 87.76 77.48 77.16 76.84 70.93 67.31 62.06 53.57 47.26 38.72 33.19 30.79 30.75 29.85 14.32



3.77

NAME SW07-147-A
EXPNO 11
PROCNO 1
Date_ 20151214
Time 22.59
INSTRUM spect
PROBHD 5 mm PABBO BB-
PULPROG zgpg30
ID 65536
SOLVENT CDCl3
NS 3072
DS 4
SWH 24038.461 Hz
FIDRES 0.366798 Hz
AQ 1.3631988 sec
RG 161
DW 20.800 usec
DE 6.50 usec
TE 96.4 K
D1 2.0000000 sec
D11 0.0300000 sec
TD0 1

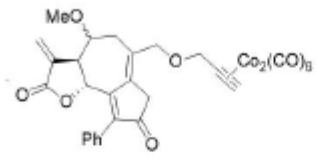
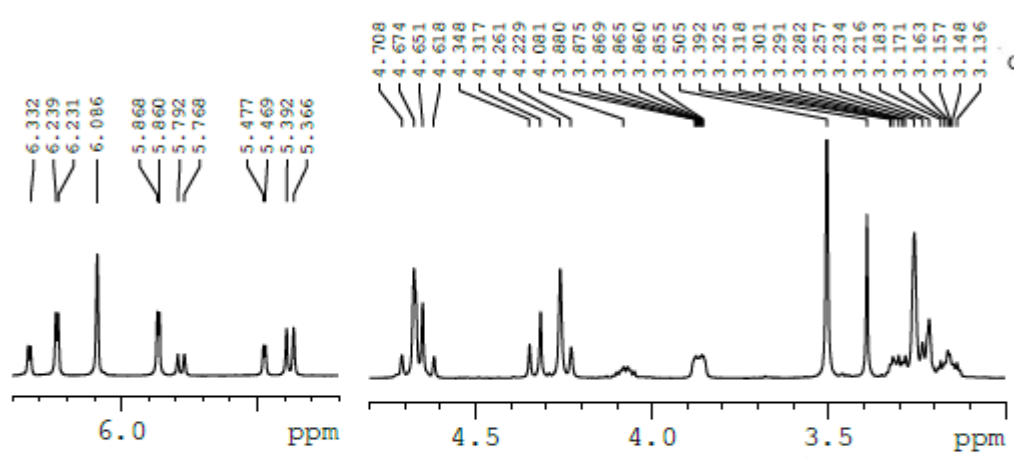
----- CHANNEL f1 -----
SFO1 100.6228293 MHz
NUC1 13C
P1 10.00 usec
SI 32768
SF 100.6127543 MHz
WDW EM
SSB 0
LB 1.00 Hz
GB 0
PC 1.40



SW06-030-C 1H 400



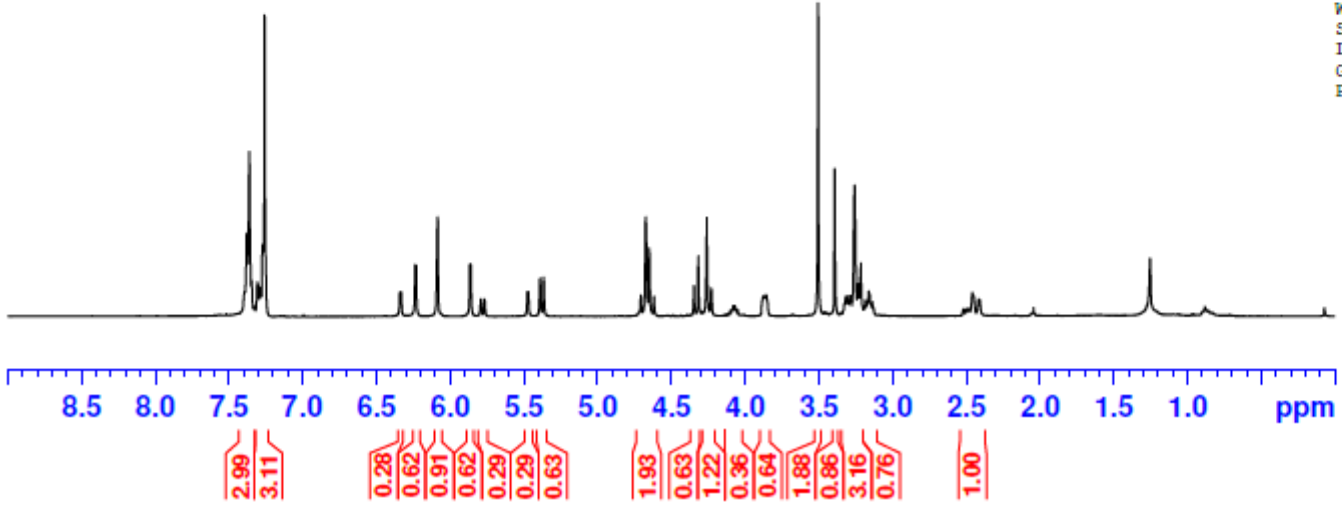
7.395
7.381
7.364
7.349
7.309
7.305
7.290
7.274
7.269
7.260
6.341
6.332
6.239
6.231
6.086
5.868
5.860
5.792
5.768
5.477
5.469
5.392
5.366
4.708
4.674
4.651
4.618
5.768
5.477
5.469
5.392
5.366
4.708
4.674
4.651
4.618
4.348
4.317
4.261
4.229
4.081
3.880
3.875
3.869
3.865
3.860
3.855
3.850
3.845
3.840
3.835
3.830
3.825
3.820
3.815
3.810
3.805
3.800
3.795
3.790
3.785
3.780
3.775
3.770
3.765
3.760
3.755
3.750
3.745
3.740
3.735
3.730
3.725
3.720
3.715
3.710
3.705
3.700
3.695
3.690
3.685
3.680
3.675
3.670
3.665
3.660
3.655
3.650
3.645
3.640
3.635
3.630
3.625
3.620
3.615
3.610
3.605
3.600
3.595
3.590
3.585
3.580
3.575
3.570
3.565
3.560
3.555
3.550
3.545
3.540
3.535
3.530
3.525
3.520
3.515
3.510
3.505
3.500
3.495
3.490
3.485
3.480
3.475
3.470
3.465
3.460
3.455
3.450
3.445
3.440
3.435
3.430
3.425
3.420
3.415
3.410
3.405
3.400
3.395
3.390
3.385
3.380
3.375
3.370
3.365
3.360
3.355
3.350
3.345
3.340
3.335
3.330
3.325
3.320
3.315
3.310
3.305
3.300
3.295
3.290
3.285
3.280
3.275
3.270
3.265
3.260
3.255
3.250
3.245
3.240
3.235
3.230
3.225
3.220
3.215
3.210
3.205
3.200
3.195
3.190
3.185
3.180
3.175
3.170
3.165
3.160
3.155
3.150
3.145
3.140
3.135
3.130
3.125
3.120
3.115
3.110
3.105
3.100
3.095
3.090
3.085
3.080
3.075
3.070
3.065
3.060
3.055
3.050
3.045
3.040
3.035
3.030
3.025
3.020
3.015
3.010
3.005
3.000
2.995
2.990
2.985
2.980
2.975
2.970
2.965
2.960
2.955
2.950
2.945
2.940
2.935
2.930
2.925
2.920
2.915
2.910
2.905
2.900
2.895
2.890
2.885
2.880
2.875
2.870
2.865
2.860
2.855
2.850
2.845
2.840
2.835
2.830
2.825
2.820
2.815
2.810
2.805
2.800
2.795
2.790
2.785
2.780
2.775
2.770
2.765
2.760
2.755
2.750
2.745
2.740
2.735
2.730
2.725
2.720
2.715
2.710
2.705
2.700
2.695
2.690
2.685
2.680
2.675
2.670
2.665
2.660
2.655
2.650
2.645
2.640
2.635
2.630
2.625
2.620
2.615
2.610
2.605
2.600
2.595
2.590
2.585
2.580
2.575
2.570
2.565
2.560
2.555
2.550
2.545
2.540
2.535
2.530
2.525
2.520
2.515
2.510
2.505
2.500
2.495
2.490
2.485
2.480
2.475
2.470
2.465
2.460
2.455
2.450
2.445
2.440
2.435
2.430
2.425
2.420
2.415
2.410
2.405
2.400
2.395
2.390
2.385
2.380
2.375
2.370
2.365
2.360
2.355
2.350
2.345
2.340
2.335
2.330
2.325
2.320
2.315
2.310
2.305
2.300
2.295
2.290
2.285
2.280
2.275
2.270
2.265
2.260
2.255



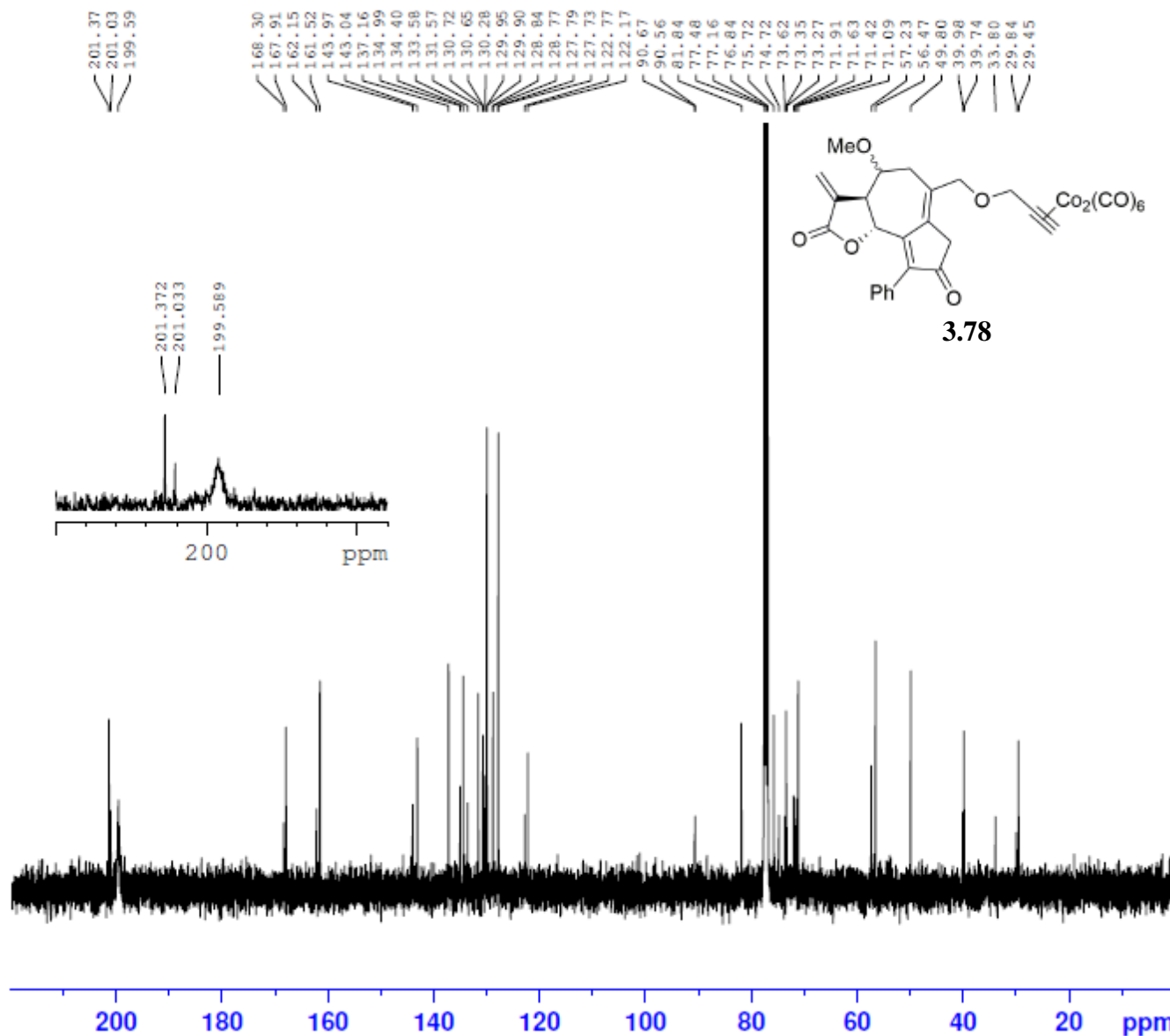
3.78

NAME SW06-030-C
 EXPNO 20
 PROCNO 1
 Date_ 20141114
 Time 17.01
 INSTRUM spect
 PROBHD 5 mm PABBO BB-
 PULPROG zg30
 TD 65536
 SOLVENT CDCl3
 NS 16
 DS 2
 SWH 8223.685 Hz
 FIDRES 0.125483 Hz
 AQ 3.9846387 sec
 RG 114
 DW 60.800 usec
 DE 6.50 usec
 TE 94.6 K
 D1 1.00000000 sec

----- CHANNEL f1 -----
 NUC1 1H
 P1 13.75 usec
 SI 65536
 SF 400.1300105 MHz
 WDW EM
 SSB 0
 LB 0.30 Hz
 GB 0
 PC 1.00



SW06-030-C 13C 400



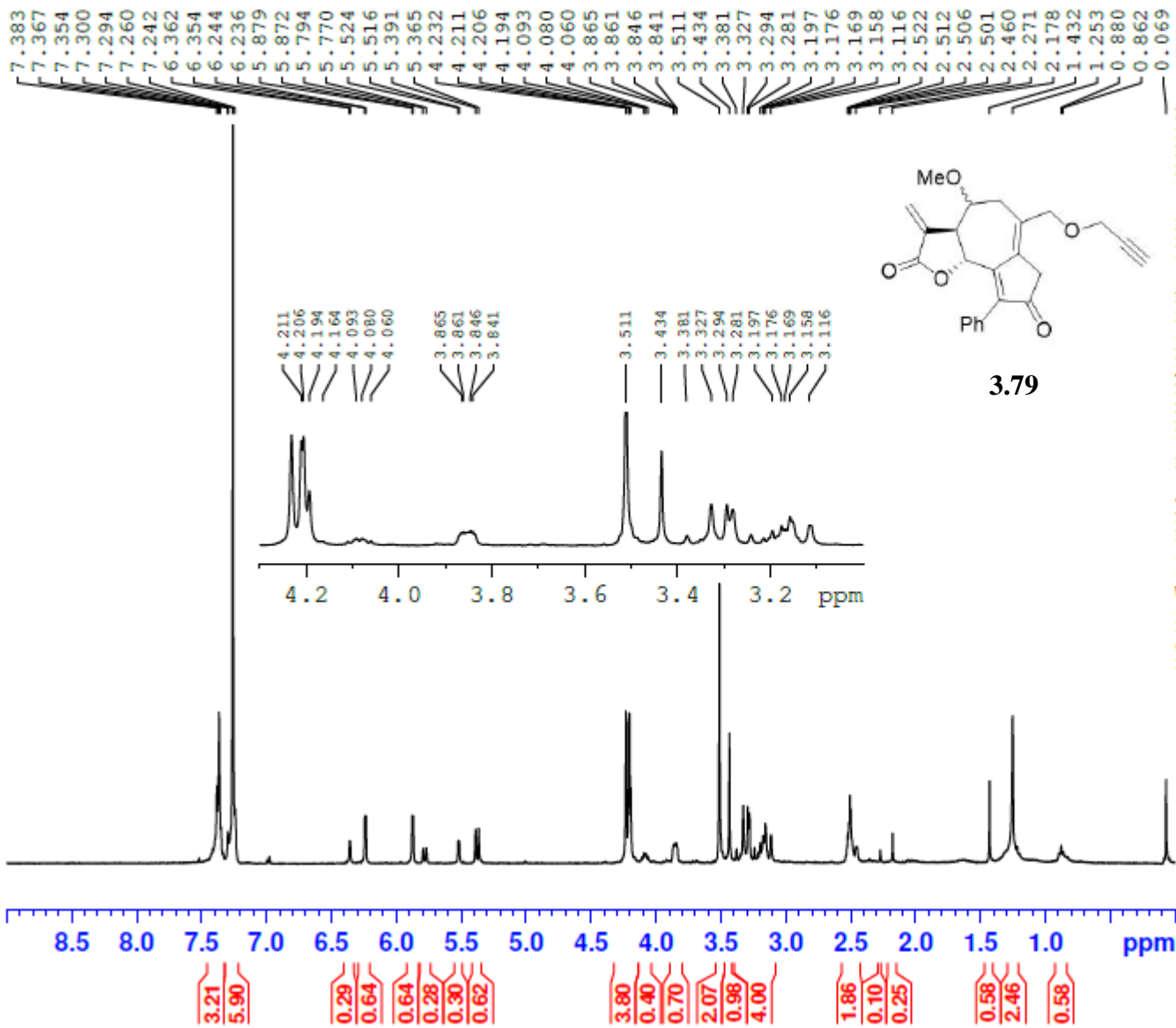
```

NAME          SW06-030-C
EXPNO         21
PROCNO        1
Date_         20141115
Time          6.09
INSTRUM       spect
PROBHD        5 mm PABBO BB-
PULPROG       zgpg30
TD            65536
SOLVENT       CDC13
NS            2200
DS            4
SWH           24038.461 Hz
FIDRES        0.366798 Hz
AQ            1.3631988 sec
RG            203
DW            20.800 usec
DE            6.50 usec
TE            93.3 K
D1            2.00000000 sec
D11           0.03000000 sec
  
```

```

----- CHANNEL f1 -----
NUC1          13C
P1            10.00 usec
SI            32768
SF            100.6127547 MHz
WDW           EM
SSB           0
LB            1.00 Hz
GB            0
PC            1.40
  
```

SW06-039-cr 1H 400



```

NAME          SW06-039-cr
EXPNO         10
PROCNO        1
Date_         20141117
Time          18.53
INSIRUM       spect
PROBHD        5 mm PABBO BB-
PULPROG       zg30
ID            65536
SOLVENT       CDCl3
NS            16
DS            2
SWH           8223.685 Hz
FIDRES        0.125483 Hz
AQ            3.9846387 sec
RG            161
DW            60.800 usec
DE            6.50 usec
IE            94.1 K
D1            1.00000000 sec

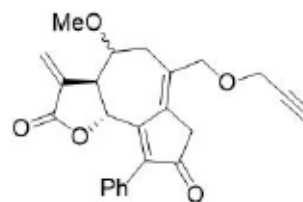
----- CHANNEL f1 -----
NUC1          1H
P1            13.75 usec
SI            65536
SF            400.1300101 MHz
WDW           EM
SSB           0
LB            0.30 Hz
GB            0
PC            1.00
    
```

SW06-039-cr 13C

600MHZ



201.512
201.25
168.29
167.93
161.87
161.38
144.15
143.22
137.17
135.83
135.43
133.60
130.91
130.73
130.65
129.93
129.89
129.68
128.86
128.78
127.80
127.75
122.85
122.23
81.79
79.48
79.34
77.37
77.16
76.95
75.70
75.55
75.41
74.75
73.75
71.93
71.50
67.59
67.83
57.42
57.19
56.46
49.83
49.72
40.02
39.65
34.21
29.97
29.85
29.70
29.67
23.99
22.85
14.27

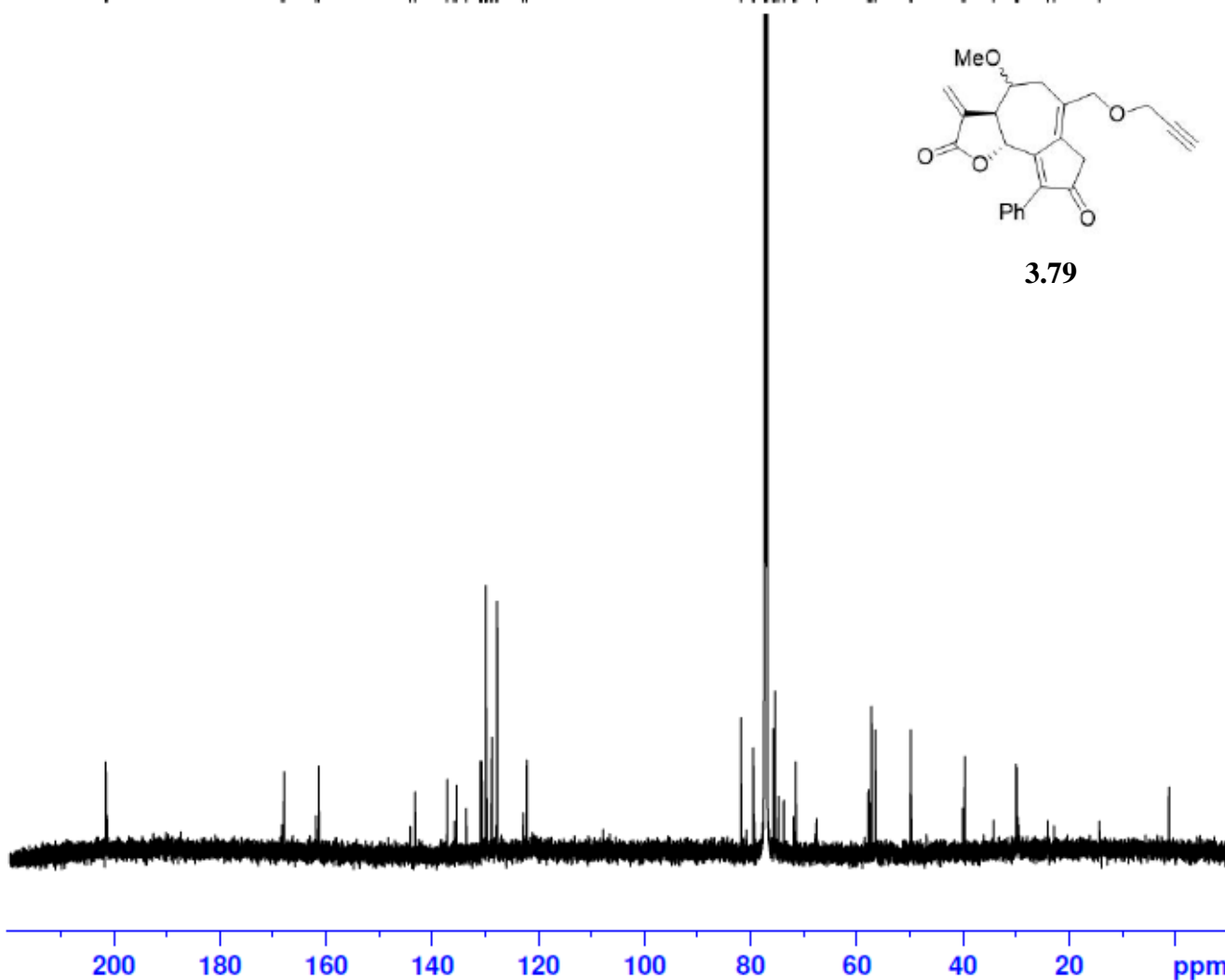


3.79

NAME SW06-039-cr dry
EXPNO 2
PROCNO 1
Date_ 20150623
Time 16.32
INSTRUM spect
PROBHD 5 mm PABBO BB-
PULPROG zgpg30
TD 65536
SOLVENT CDCl3
NS 27093
DS 4
SWH 36057.691 Hz
FIDRES 0.550197 Hz
AQ 0.9088159 sec
RG 203
DW 13.867 usec
DE 6.50 usec
TE 298.2 K
D1 2.00000000 sec
D11 0.03000000 sec
TD0 1

----- CHANNEL f1 -----
NUC1 13C
P1 11.50 usec
PL1 0.00 dB
PL1W 97.46119690 W
SFO1 151.0637542 MHz

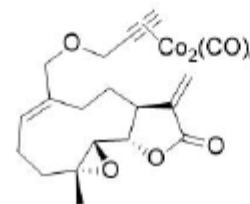
----- CHANNEL f2 -----
CPDPRG2 waltz16
NUC2 1H
PCPD2 70.00 usec
PL2 -2.00 dB
PL12 14.19 dB
PL13 120.00 dB
PL2W 19.70630455 W
PL12W 0.47381112 W
PL13W 0.00000000 W
SFO2 600.7124028 MHz
SI 32768
SF 151.0486269 MHz
WDW EM
SSB 0
LB 1.00 Hz
GB 0
PC 1.40



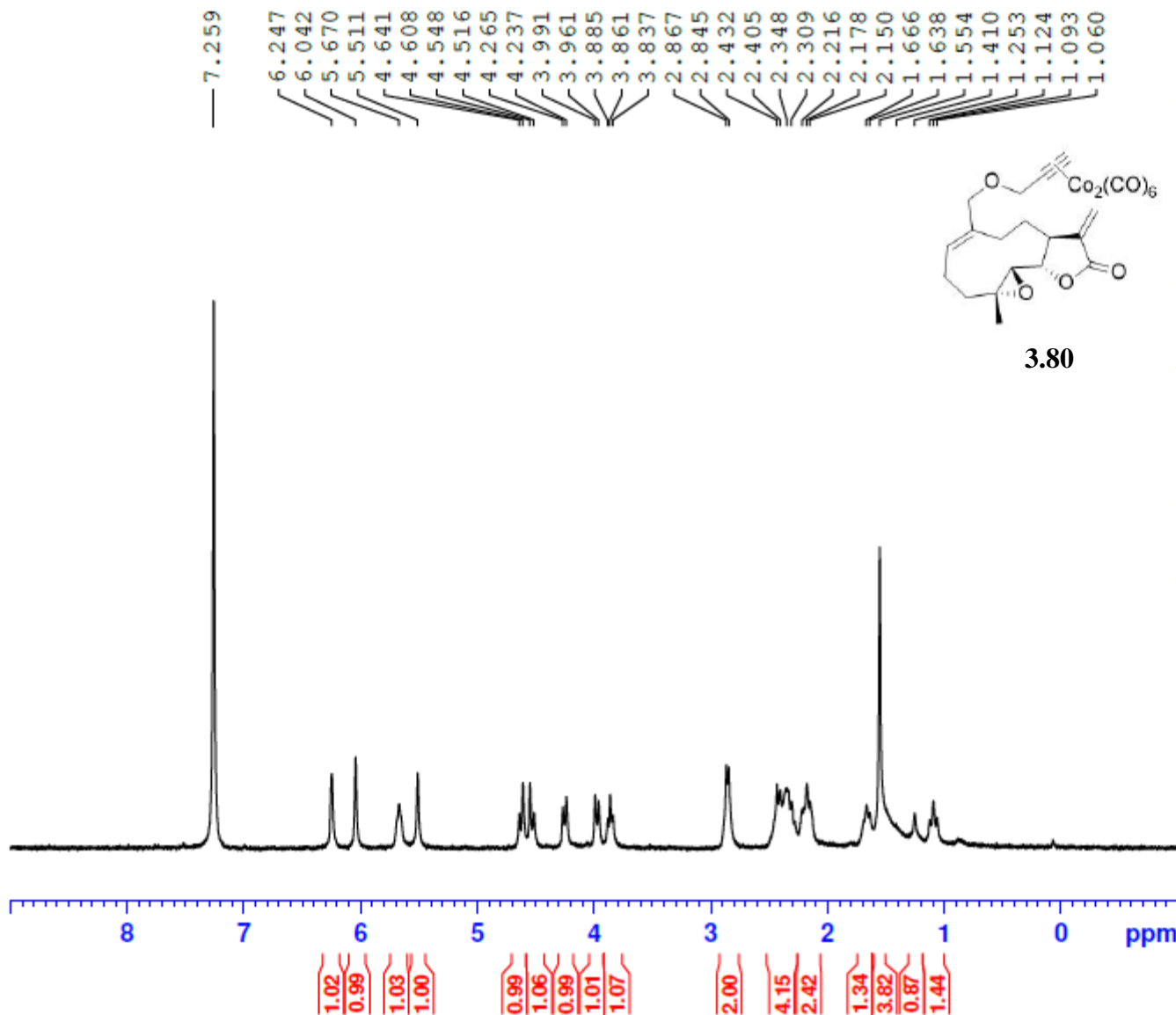
SW06-183-C 1H 400



NAME SW06-183-C
EXPNO 20
PROCNO 1
Date_ 20150507
Time 12.52
INSIRUM spect
PROBHD 5 mm PABBO BB-
PULPROG zg30
ID 65536
SOLVENT CDCl3
NS 16
DS 2
SWH 8223.685 Hz
FIDRES 0.125483 Hz
AQ 3.9846387 sec
RG 181
DW 60.800 usec
DE 6.50 usec
TE 90.6 K
D1 1.00000000 sec



3.80



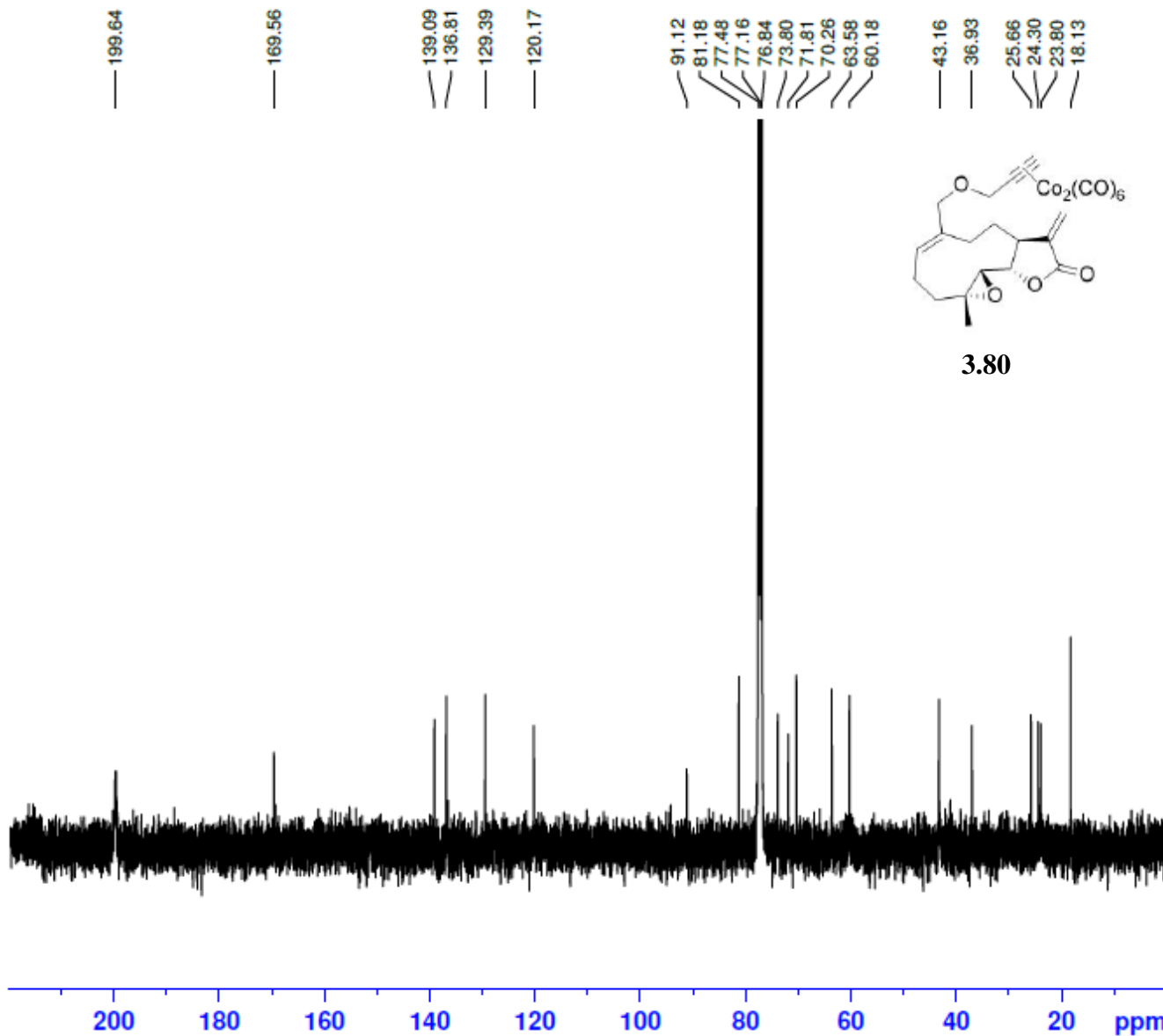
----- CHANNEL f1 -----
NUC1 1H
P1 13.75 usec
SI 65536
SF 400.1300102 MHz
WDW EM
SSB 0
LB 0.30 Hz
GB 0
PC 1.00

SW06-183-C 1H 400

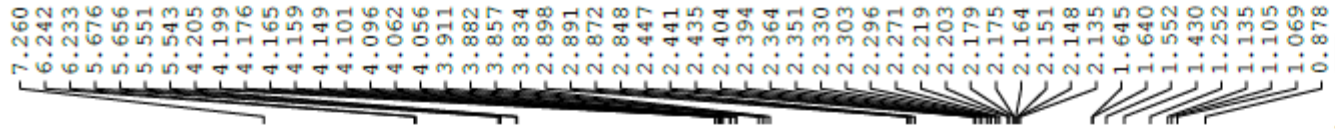


NAME SW06-183-C
EXPNO 11
PROCNO 1
Date_ 20150505
Time 7.27
INSTRUM spect
PROBHD 5 mm PABBO BB-
PULPROG zgpg30
ID 65536
SOLVENT CDCl3
NS 2048
DS 4
SWH 24038.461 Hz
FIDRES 0.366798 Hz
AQ 1.3631988 sec
RG 203
DW 20.800 usec
DE 6.50 usec
TE 95.3 K
D1 2.00000000 sec
D11 0.03000000 sec

----- CHANNEL f1 -----
NUC1 13C
P1 10.00 usec
SI 32768
SF 100.6127547 MHz
WDW EM
SSB 0
LB 1.00 Hz
GB 0
PC 1.40

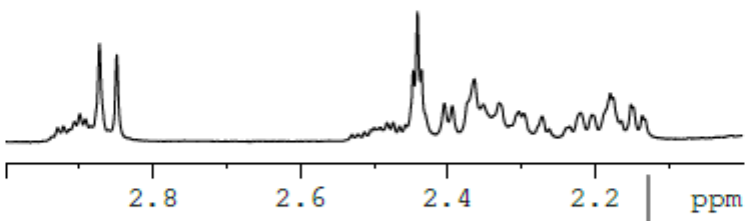
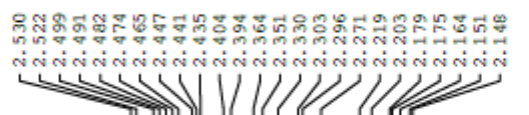
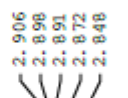
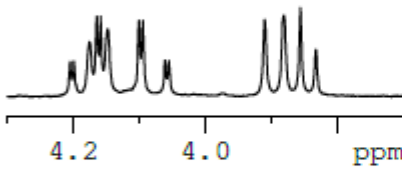
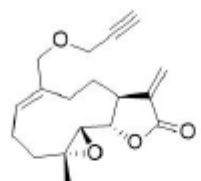


SW06-191- 1H 400



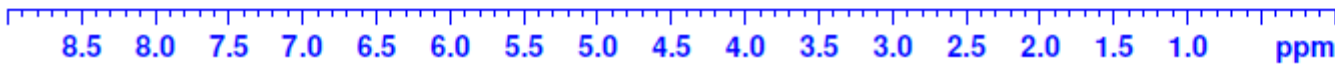
```

NAME          SW06-191-cr
EXPNO         10
PROCNO        1
Date_         20150512
Time          17.34
INSIRUM       spect
PROBHD        5 mm PABBO BB-
PULPROG       zg30
ID            65536
SOLVENT       CDC13
NS            16
DS            2
SWH           8223.685 Hz
FIDRES        0.125483 Hz
AQ            3.9846387 sec
RG            161
DW            60.800 usec
DE            6.50 usec
TE            3049.3 K
D1            1.00000000 sec
  
```

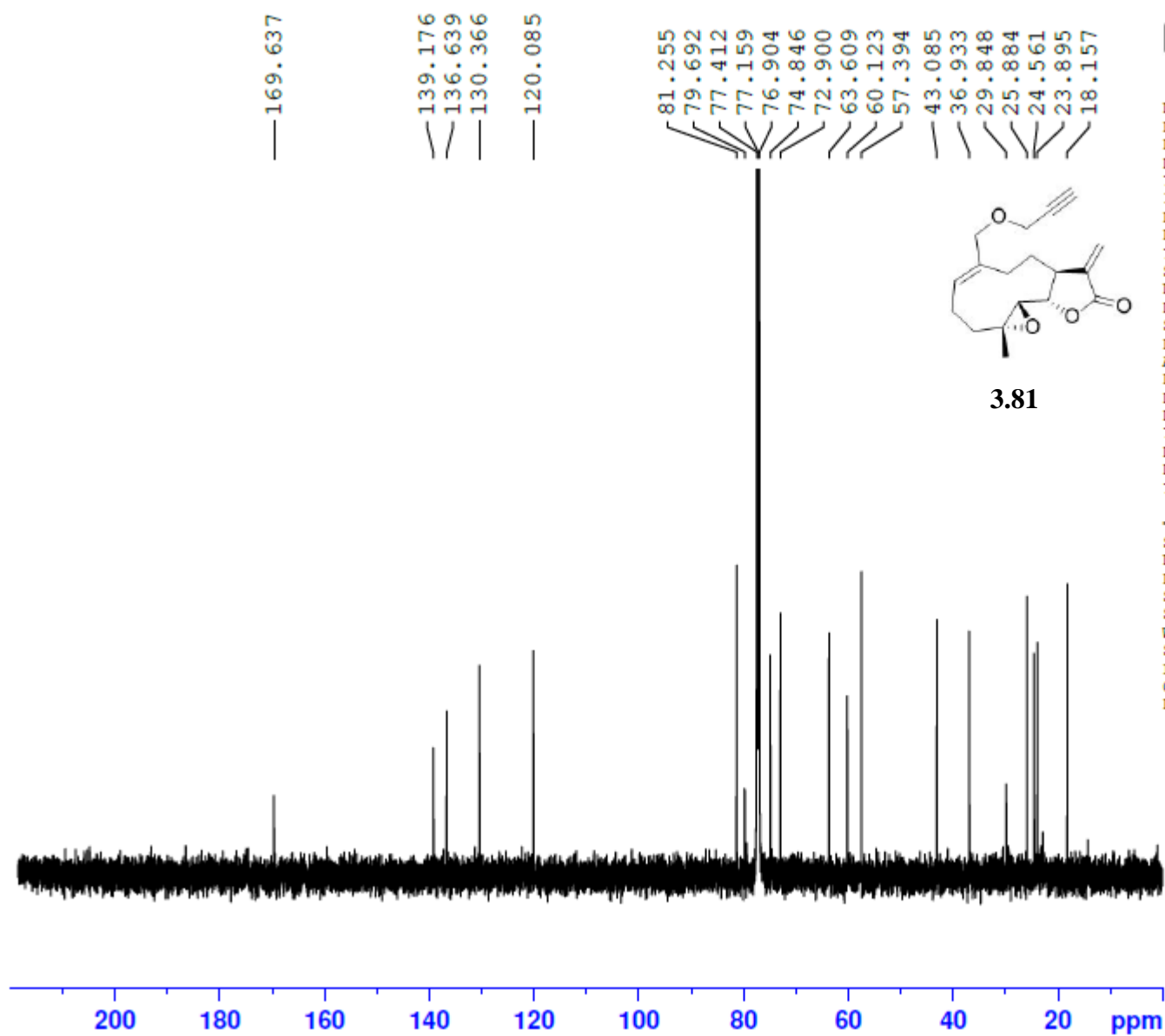


```

----- CHANNEL f1 -----
NUC1          1H
P1            13.75 usec
SI            65536
SF            400.1300100 MHz
WDW           EM
SSB           0
LB            0.30 Hz
GB            0
PC            1.00
  
```

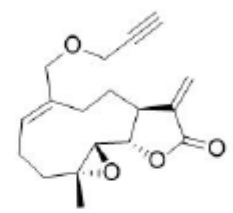


SW06-191-cr 13C 500



NAME SW06-191-cr
EXPNO 10
PROCNO 1
Date_ 20150513
Time 6.46
INSTRUM spect
PROBHD 5 mm PABBO BB/
PULPROG zgpg30
ID 65536
SOLVENT CDCl3
NS 2048
DS 2
SWH 29761.904 Hz
FIDRES 0.454131 Hz
AQ 1.1010548 sec
RG 203
DW 16.800 usec
DE 6.50 usec
TE 298.5 K
D1 2.00000000 sec
D11 0.03000000 sec
TD0 1

----- CHANNEL f1 -----
SFO1 125.7779086 MHz
NUC1 13C
P1 10.50 usec
SI 32768
SF 125.7653131 MHz
WDW EM
SSB 0
LB 1.00 Hz
GB 0
PC 1.40

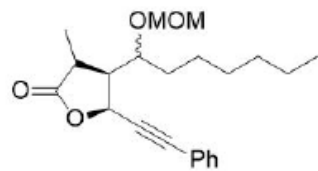


SW07-175-A 1H 300

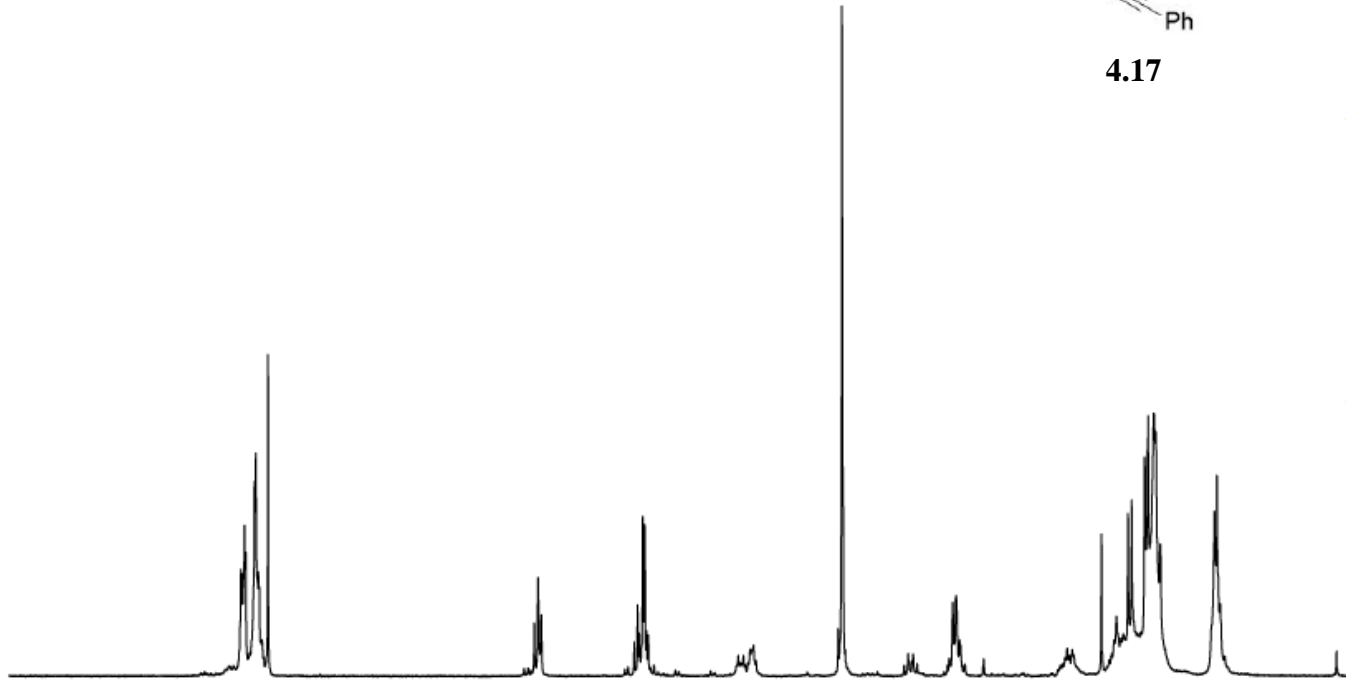
7.448
7.442
7.437
7.431
7.425
7.417
7.411
7.349
7.342
7.324
7.318
7.300
7.260
5.467
5.443
5.421
4.796
4.773
4.763
4.739
4.725
4.713
4.702
4.096
4.062
4.016
4.001
3.993
3.398
3.394
3.394
2.953
2.919
2.653
2.643
2.631
2.607
2.600
1.883
1.869
1.850
1.838
1.652
1.551
1.474
1.448
1.361
1.339
1.300
1.286
1.256
0.891
0.875
0.853



NAME SW07-175-A
EXPNO 10
PROCNO 1
Date_ 20160211
Time 14.10
INSTRUM spect
PROBHD 5 mm QNP 1H/1
PULPROG zg30
TD 32768
SOLVENT CDC13
NS 16
DS 2
SWH 6188.119 Hz
FIDRES 0.188846 Hz
AQ 2.6477044 sec
RG 203
DW 80.800 usec
DE 6.50 usec
TE -927.9 K
D1 1.00000000 sec
TD0 1



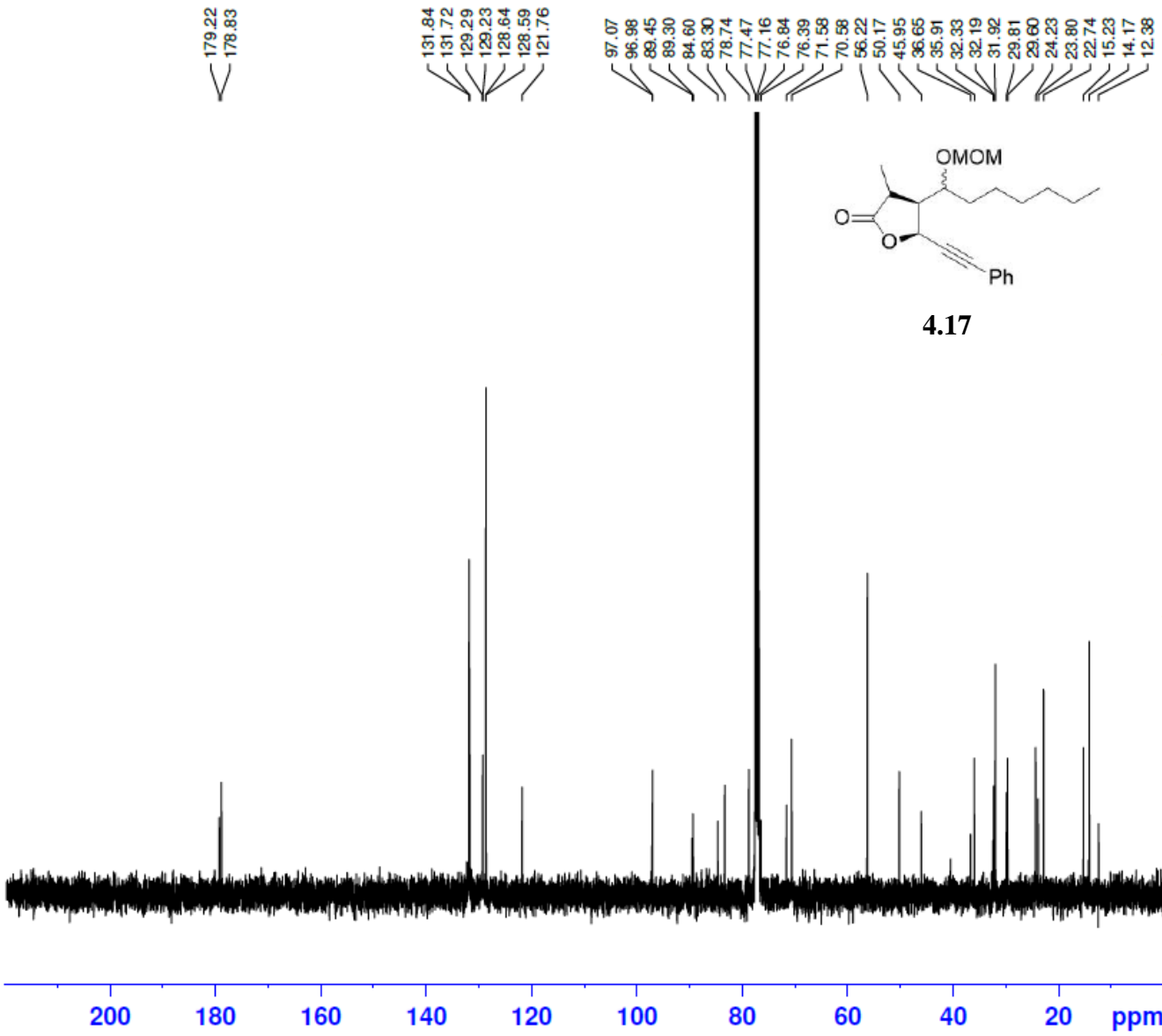
4.17



===== CHANNEL f1 =====
SFO1 300.2318540 MHz
NUC1 1H
P1 12.71 usec
SI 32768
SF 300.2300090 MHz
WDW EM
SSB 0
LB 0.10 Hz
GB 0
PC 1.00

2.02
3.23
0.93
1.89
1.00
3.10
0.40
1.47
0.97
13.97
3.49

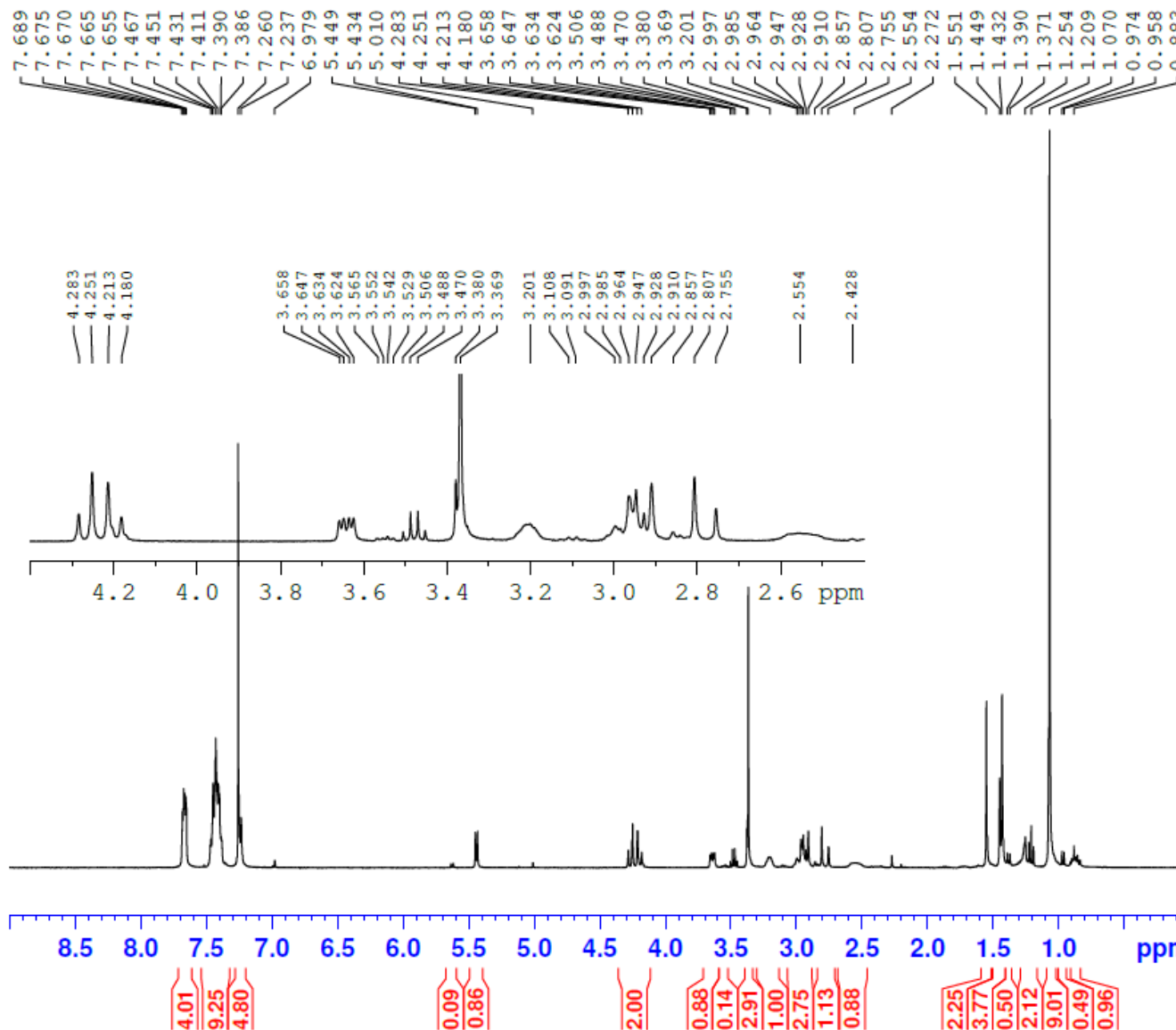
SW07-175-A 13C 400



NAME SW07-175-A
EXPNO 10
PROCNO 1
Date_ 20160601
Time_ 0.40
INSTRUM spect
PROBHD 5 mm PABBO BB-
PULPROG zgpg30
TD 65536
SOLVENT CDC13
NS 2048
DS 4
SWH 24038.461 Hz
FIDRES 0.366798 Hz
AQ 1.3631988 sec
RG 203
DW 20.800 usec
DE 6.50 usec
TE 96.8 K
D1 2.0000000 sec
D11 0.0300000 sec
TDO 1

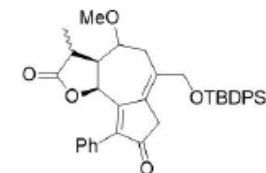
==== CHANNEL f1 =====
SFO1 100.6228293 MHz
NUC1 13C
P1 10.00 usec
SI 32768
SF 100.6127555 MHz
WDW EM
SSB 0
LB 1.00 Hz
GB 0
PC 1.40

SW07-192-B



NAME SW07-192-B
 EXPNO 10
 PROCNO 1
 Date_ 20160329
 Time 16.37
 INSTRUM spect
 PROBHD 5 mm PABBO BB-
 PULPROG zg30
 TD 65536
 SOLVENT CDCl3
 NS 16
 DS 2
 SWH 8012.820 Hz
 FIDRES 0.122266 Hz
 AQ 4.0894966 sec
 RG 144
 DW 62.400 usec
 DE 6.50 usec
 TE 91.3 K
 D1 1.00000000 sec
 TDO 1

==== CHANNEL f1 =====
 SFO1 400.1324710 MHz
 NUC1 1H
 P1 13.75 usec
 SI 65536
 SF 400.1300099 MHz
 WDW EM
 SSB 0
 LB 0.30 Hz
 GB 0
 PC 1.00



4.22

SW07-192-B

— 201.721

— 178.605

158.003
137.033
135.779
135.672
133.206
132.910
130.414
130.202
130.130
129.704
129.654
129.284
128.825
128.774
128.064
128.036
125.669

— 74.369

— 65.718

57.145

56.755

45.131

40.528

38.501

31.727

30.482

26.988

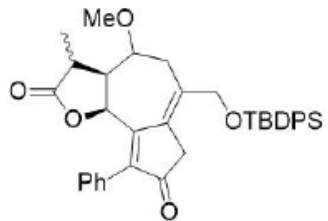
— 19.404

— 11.879



```

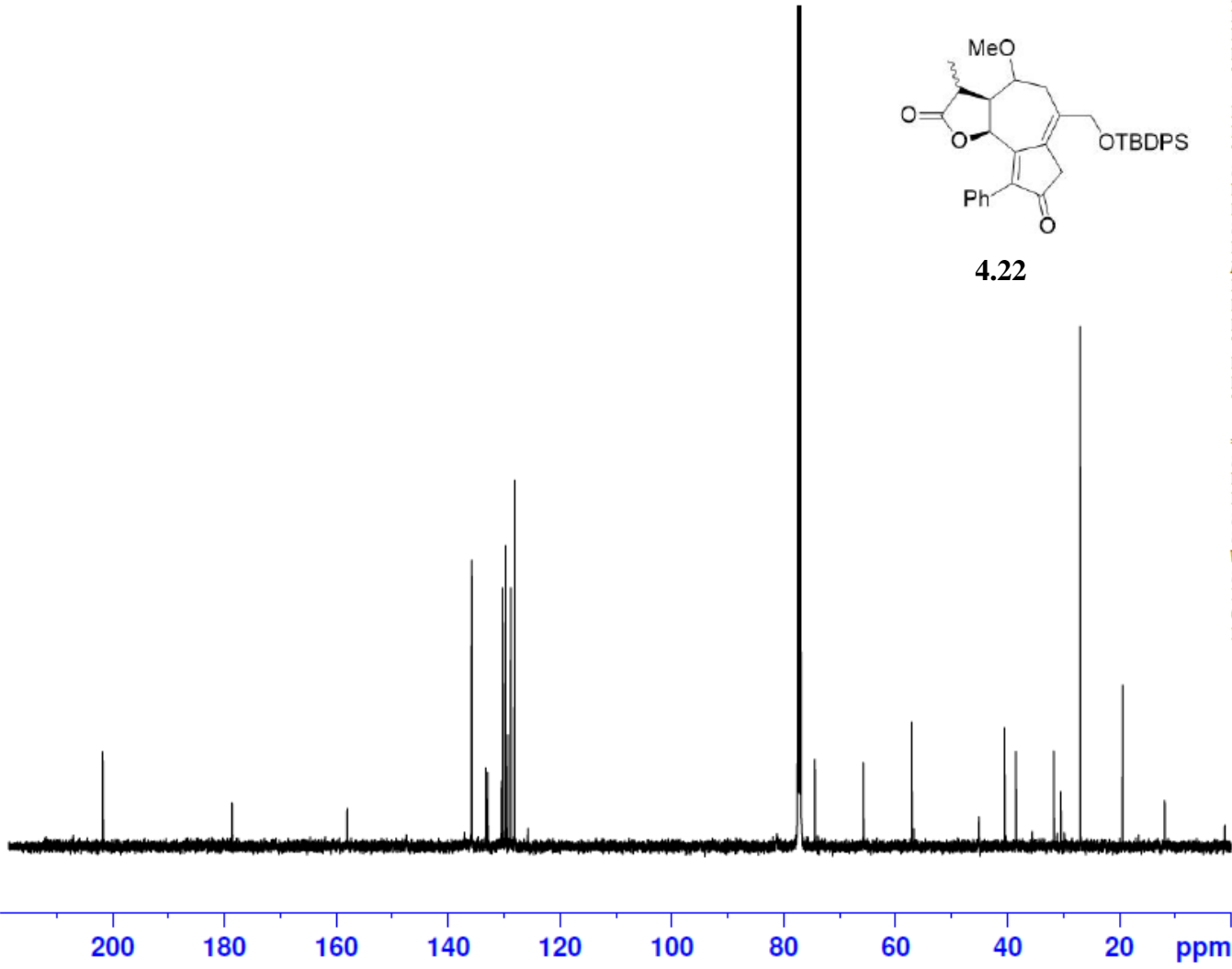
NAME          SW07-192-B
EXPNO         10
PROCNO        1
Date_         20160401
Time          3.26
INSTRUM       spect
PROBHD        5 mm PABBO BB/
PULPROG       zgpg30
TD            65536
SOLVENT       CDC13
NS            5000
DS            2
SWH           29761.904 Hz
FIDRES        0.454131 Hz
AQ            1.1010548 sec
RG            203
DW            16.800 usec
DE            6.50 usec
TE            298.2 K
D1            2.00000000 sec
D11           0.03000000 sec
TD0           1
    
```



4.22

```

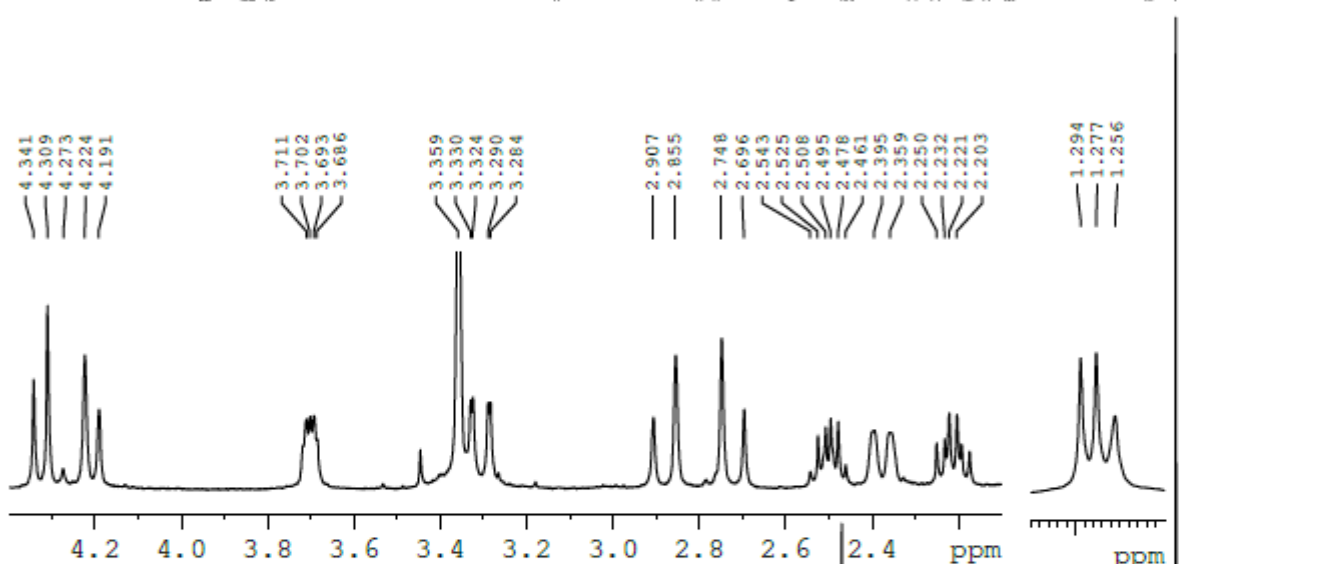
===== CHANNEL f1 =====
SFO1         125.7779086 MHz
NUC1          13C
P1            10.50 usec
SI            32768
SF           125.7653134 MHz
WDW           EM
SSB           0
LB            1.00 Hz
GB            0
PC            1.40
    
```



SW06-050-Ddry 1H 400



7.709
7.706
7.690
7.686
7.666
7.663
7.647
7.643
7.427
7.409
7.393
7.375
7.362
7.359
7.343
7.260
7.231
7.226
7.211
7.211
5.306
5.278
4.341
4.309
4.224
4.191
3.711
3.702
3.693
3.686
3.359
3.330
3.324
3.290
3.284
3.284
2.907
2.855
2.748
2.696
2.543
2.525
2.508
2.495
2.478
2.461
2.395
2.359
2.250
2.232
2.221
2.203
2.203
2.193
1.294
1.277
1.256
1.093

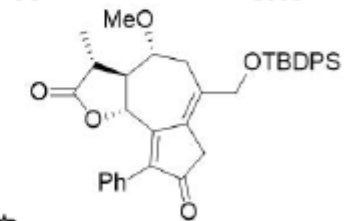


```

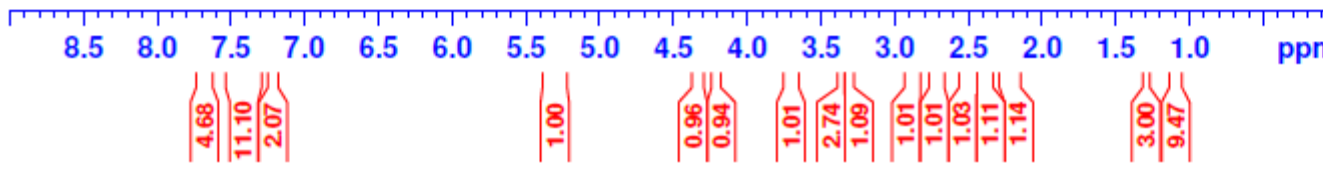
NAME SW06-050-Ddry
EXPNO 10
PROCNO 1
Date_ 20141211
Time 17.04
INSIRUM spect
PROBHD 5 mm PABBO BB-
PULPROG zg30
ID 65536
SOLVENT CDCl3
NS 16
DS 2
SWH 8223.685 Hz
FIDRES 0.125483 Hz
AQ 3.9846387 sec
RG 114
DW 60.800 usec
DE 6.50 usec
TE -495.0 K
D1 1.00000000 sec
  
```

```

----- CHANNEL f1 -----
NUC1 1H
P1 13.75 usec
SI 65536
SF 400.130093 MHz
WDW EM
SSB 0
LB 0.30 Hz
GB 0
PC 1.00
  
```



4.15a

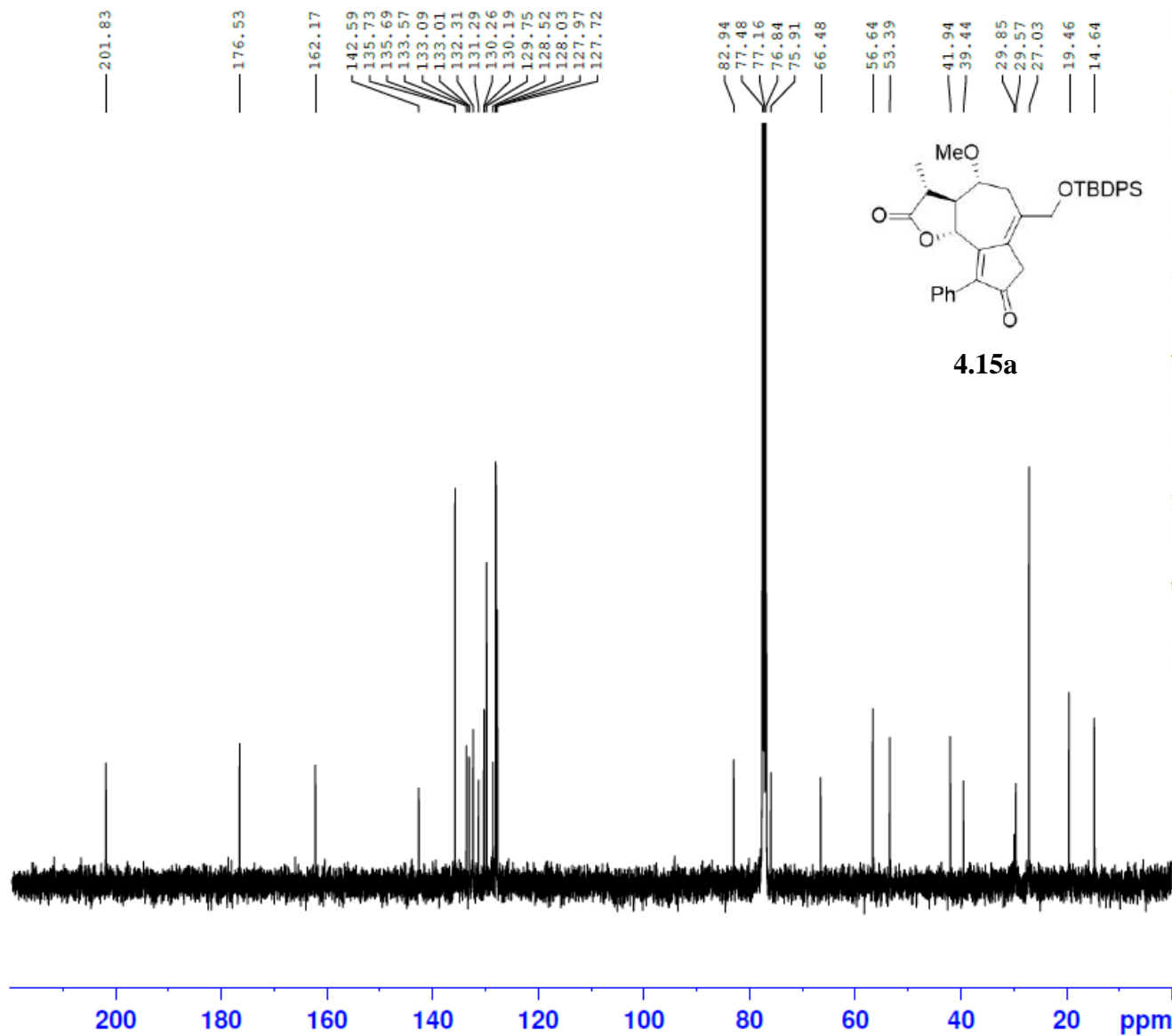


SW06-050-Ddry 13C 400

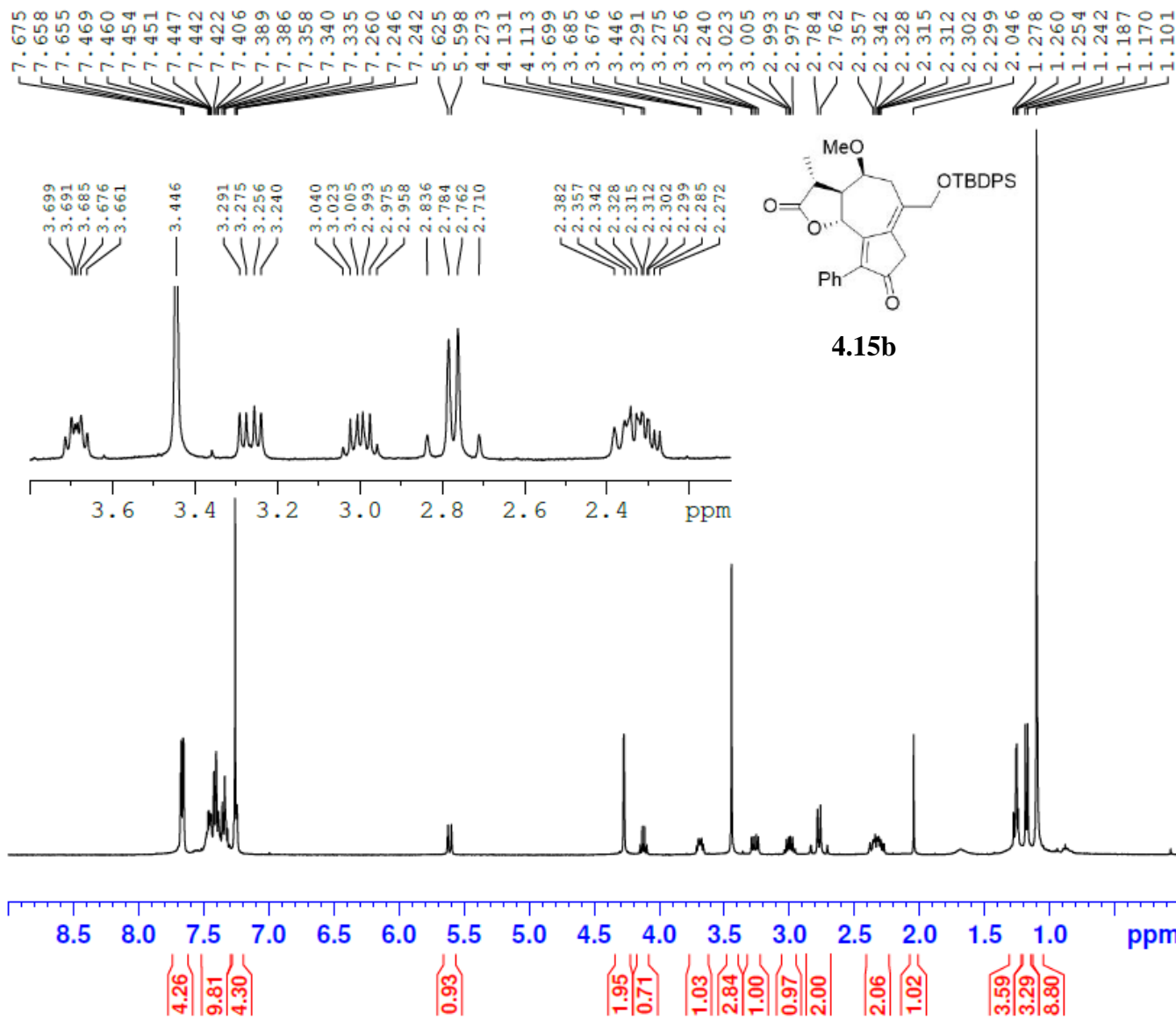


NAME SW06-050-Ddry
EXPNO 11
PROCNO 1
Date_ 20141212
Time 7.35
INSTRUM spect
PROBHD 5 mm PABBO BB-
PULPROG zgpg30
TD 65536
SOLVENT CDC13
NS 3072
DS 4
SWH 24038.461 Hz
FIDRES 0.366798 Hz
AQ 1.3631988 sec
RG 203
DW 20.800 usec
DE 6.50 usec
TE 1292.5 K
D1 2.0000000 sec
D11 0.0300000 sec

==== CHANNEL f1 =====
NUC1 13C
P1 10.00 usec
SI 32768
SF 100.6127548 MHz
WDW EM
SSB 0
LB 1.00 Hz
GB 0
PC 1.40



SW06-050-C 1H 400



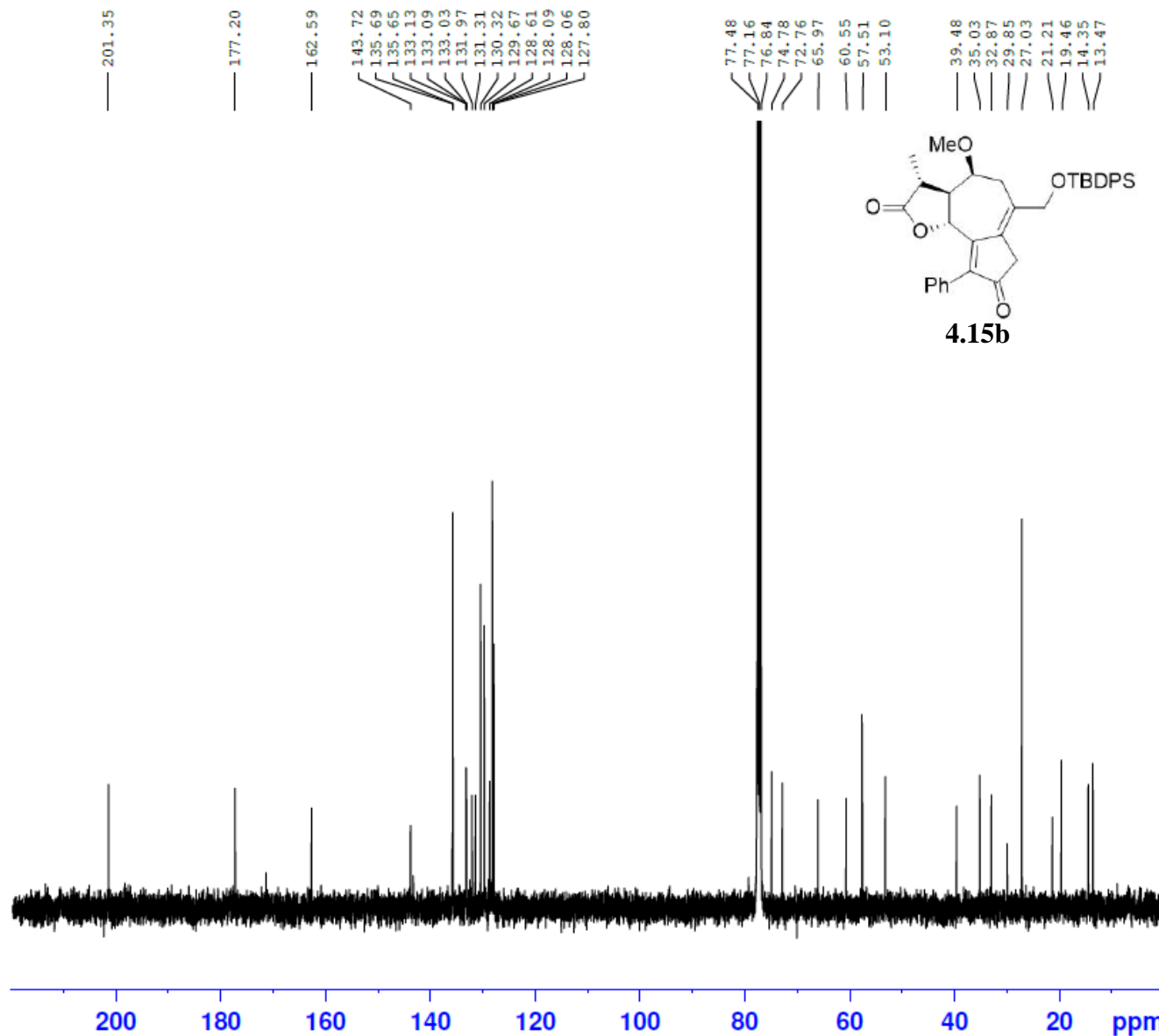
```

NAME          SW06-050-C
EXPNO         10
PROCNO        1
Date_         20141211
Time          16.58
INSTRUM       spect
PROBHD        5 mm PABBO BB-
PULPROG       zg30
TD            65536
SOLVENT       CDC13
NS            16
DS            2
SWH           8223.685 Hz
FIDRES        0.125483 Hz
AQ            3.9846387 sec
RG            128
DW            60.800 usec
DE            6.50 usec
TE            -304.4 K
D1            1.00000000 sec
    
```

```

===== CHANNEL f1 =====
NUC1          1H
P1            13.75 usec
SI            65536
SF            400.1300105 MHz
WDW           EM
SSB           0
LB            0.30 Hz
GB            0
PC            1.00
    
```

SW06-050-C 1H 400



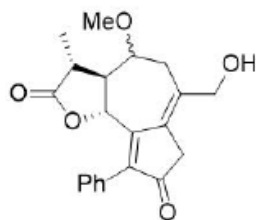
NAME SW06-050-C
EXPNO 11
PROCNO 1
Date_ 20141212
Time 4.34
INSTRUM spect
PROBHD 5 mm PABBO BB-
PULPROG zgpg30
TD 65536
SOLVENT CDCl3
NS 3072
DS 4
SWH 24038.461 Hz
FIDRES 0.366798 Hz
AQ 1.3631988 sec
RG 203
DW 20.800 usec
DE 6.50 usec
TE -290.6 K
D1 2.0000000 sec
D11 0.0300000 sec

==== CHANNEL f1 =====
NUC1 13C
P1 10.00 usec
SI 32768
SF 100.6127547 MHz
WDW EM
SSB 0
LB 1.00 Hz
GB 0
PC 1.40

SW07-200-B 1H 500



7.371
7.356
7.352
7.348
7.294
7.291
7.278
7.260
7.255
7.252
7.239
7.236
5.670
5.649
5.366
5.344
5.298
5.116
4.302
4.278
4.142
4.128
4.113
4.099
3.479
3.464
3.350
3.289
3.265
3.213
3.182
3.169
3.140
3.065
3.060
2.529
2.519
2.506
2.417
2.258
2.131
2.044
1.434
1.422
1.310
1.296
1.273
1.258
1.253
1.244
1.189
1.175
0.879

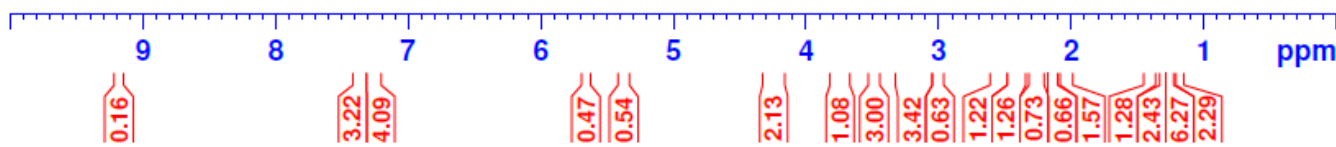
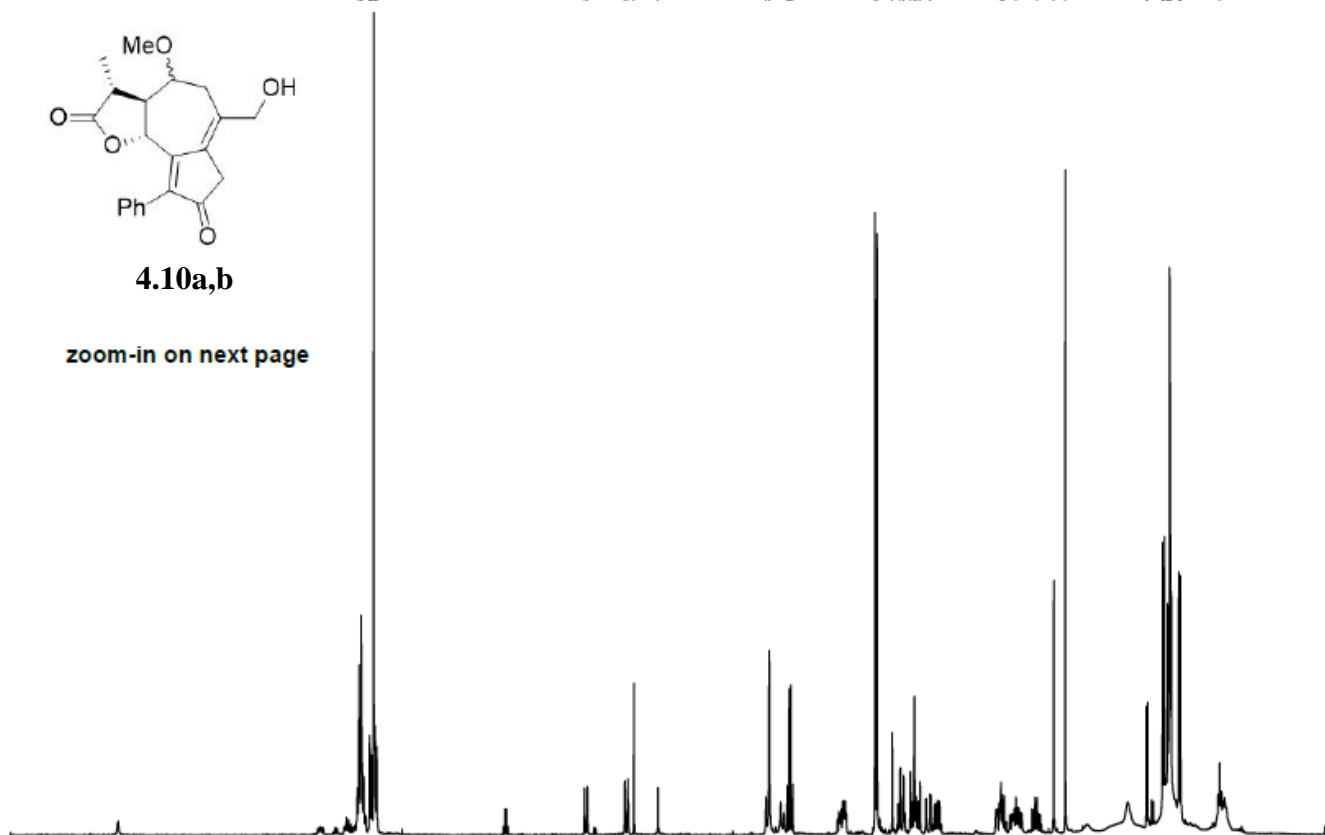


4.10a,b

zoom-in on next page

NAME SW07-200-B
EXPNO 10
PROCNO 1
Date_ 20160409
Time 12.10
INSTRUM spect
PROBHD 5 mm PABBO BB/
PULPROG zg30
TD 65536
SOLVENT CDCl3
NS 16
DS 2
SWH 10000.000 Hz
FIDRES 0.152588 Hz
AQ 3.2768500 sec
RG 114
DW 50.000 usec
DE 6.50 usec
TE 298.0 K
D1 1.00000000 sec
TD0 1

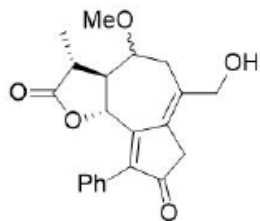
==== CHANNEL f1 =====
SFO1 500.1630887 MHz
NUC1 1H
P1 11.45 usec
SI 65536
SF 500.1600115 MHz
WDW EM
SSB 0
LB 0.30 Hz
GB 0
PC 1.00



SW07-200-B 1H 500



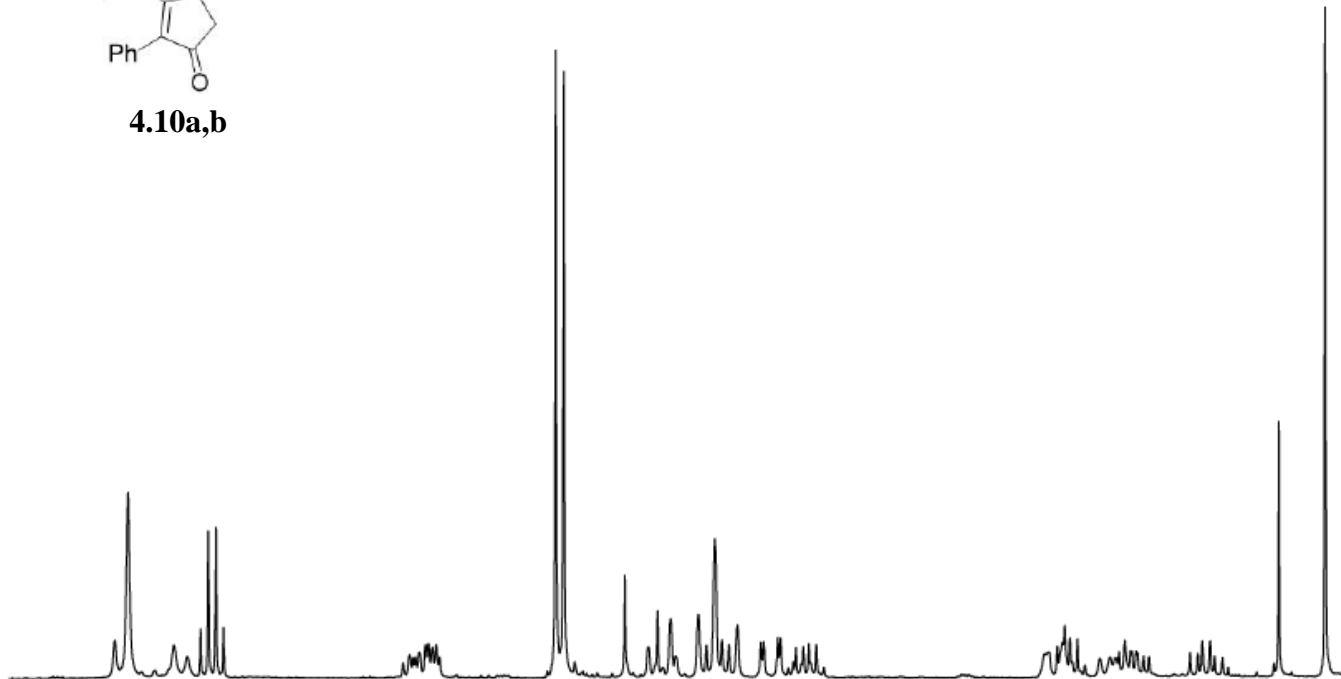
4.302
4.278
4.192
4.142
4.128
4.113
4.099
3.752
3.734
3.722
3.717
3.709
3.702
3.479
3.464
3.350
3.306
3.289
3.265
3.213
3.198
3.182
3.169
3.156
3.140
3.096
3.091
3.065
3.060
3.031
3.017
3.007
2.993
2.566
2.558
2.543
2.534
2.529
2.519
2.506
2.428
2.417
2.406
2.404
2.396
2.393
2.295
2.281
2.272
2.258
2.249
2.131
2.044



4.10a,b

NAME SW07-200-B
EXPNO 10
PROCNO 1
Date_ 20160409
Time 12.10
INSTRUM spect
PROBHD 5 mm PABBO BB/
PULPROG zg30
TD 65536
SOLVENT CDCl3
NS 16
DS 2
SWH 10000.000 Hz
FIDRES 0.152588 Hz
AQ 3.2768500 sec
RG 114
DW 50.000 usec
DE 6.50 usec
TE 298.0 K
D1 1.0000000 sec
TD0 1

==== CHANNEL f1 =====
SFO1 500.1630887 MHz
NUC1 1H
P1 11.45 usec
SI 65536
SF 500.1600115 MHz
WDW EM
SSB 0
LB 0.30 Hz
GB 0
PC 1.00



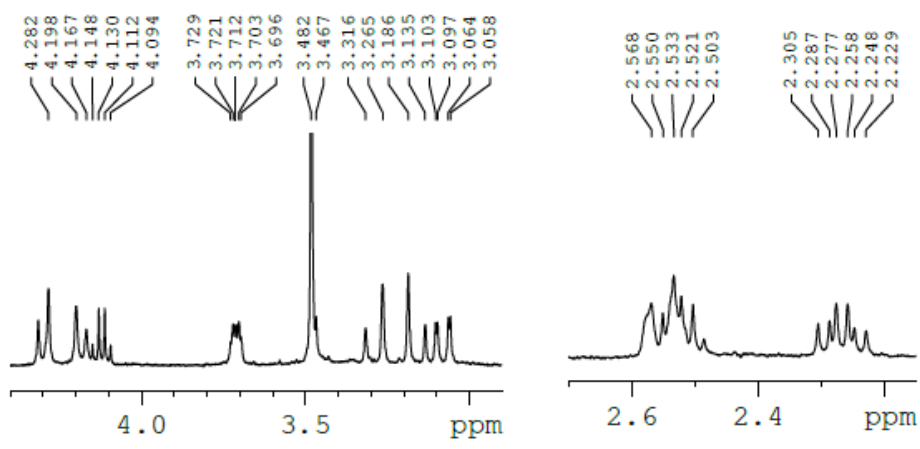
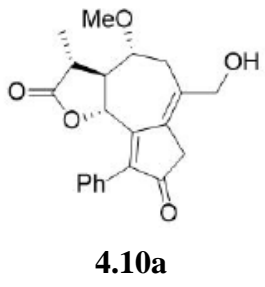
4.4 4.2 4.0 3.8 3.6 3.4 3.2 3.0 2.8 2.6 2.4 2.2 ppm

2.13 1.08 3.00 3.42 0.63 1.22 1.26 0.73 0.66 1.57

SW06-054-C 1H 400

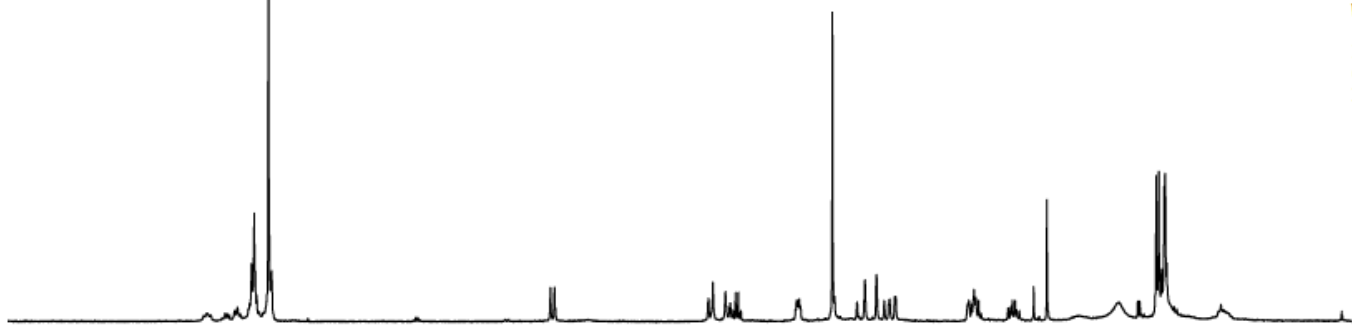


7.468
7.373
7.354
7.340
7.260
7.239
5.371
5.343
4.313
4.282
4.198
4.167
4.148
4.130
4.112
3.729
3.721
3.712
3.703
3.696
3.482
3.467
3.316
3.265
3.186
3.135
3.103
3.097
3.064
3.058
2.568
2.550
2.533
2.521
2.503
2.305
2.287
2.277
2.258
2.248
2.229
2.134
2.045
1.566
1.437
1.423
1.314
1.296
1.277
1.259
1.254
1.241
0.880



NAME SW06-054-C
EXPNO 10
PROCNO 1
Date_ 20141217
Time 14.29
INSTRUM spect
PROBHD 5 mm PABBO BB-
PULPROG zg30
TD 65536
SOLVENT CDC13
NS 16
DS 2
SWH 8223.685 Hz
FIDRES 0.125483 Hz
AQ 3.9846387 sec
RG 181
DW 60.800 usec
DE 6.50 usec
TE 2678.8 K
D1 1.00000000 sec

===== CHANNEL f1 =====
NUC1 1H
P1 13.75 usec
SI 65536
SF 400.1300106 MHz
WDW EM
SSB 0
LB 0.30 Hz
GB 0
PC 1.00



8.5 8.0 7.5 7.0 6.5 6.0 5.5 5.0 4.5 4.0 3.5 3.0 2.5 2.0 1.5 1.0 ppm

0.56
0.40
0.68
3.31
1.01
0.96
2.09
1.02
3.04
1.12
1.10
1.10
2.00
1.08
0.29
0.99
2.45
0.48
3.25
4.42
1.45

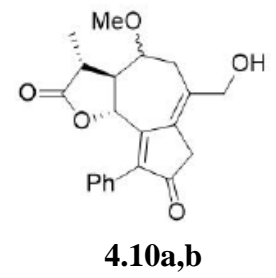
SW07-200-B 13C 500



201.456
201.318

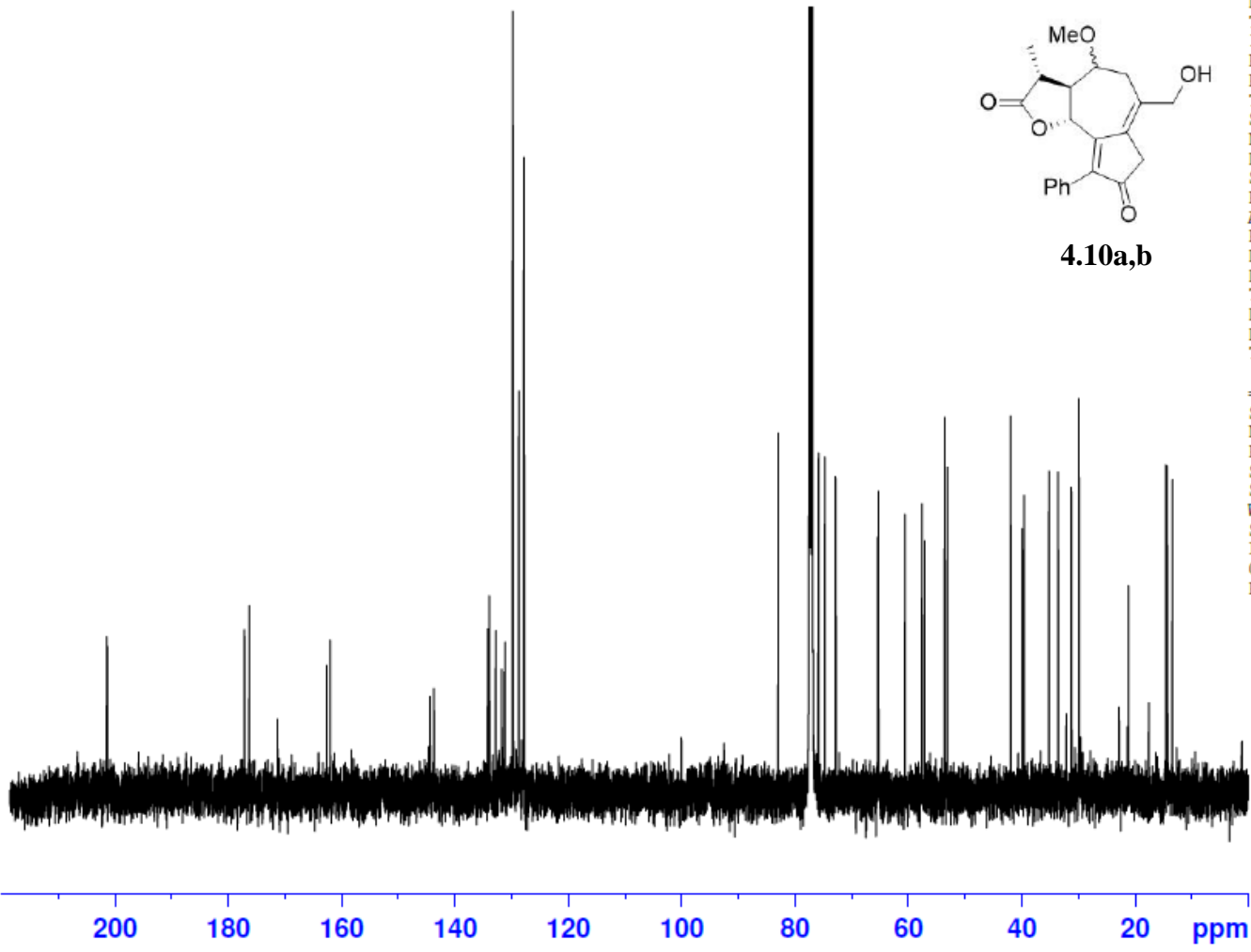
177.120
176.289
171.302
162.579
162.017
144.393
143.669
134.200
133.910
132.796
131.738
131.235
131.130
129.793
129.692
128.727
128.690
127.848
127.777

82.902
75.838
74.719
72.777
65.337
65.238
60.544
57.582
57.102
53.560
53.097
41.904
39.808
39.550
35.135
33.518
31.172
29.852
21.191
14.559
14.351
13.439



NAME SW07-200-B
EXPNO 11
PROCNO 1
Date_ 20160409
Time 16.35
INSTRUM spect
PROBHD 5 mm PABBO BB/
PULPROG zgpg30
TD 65536
SOLVENT CDC13
NS 5000
DS 2
SWH 29761.904 Hz
FIDRES 0.454131 Hz
AQ 1.1010548 sec
RG 203
DW 16.800 usec
DE 6.50 usec
TE 299.0 K
D1 2.00000000 sec
D11 0.03000000 sec
TD0 1

==== CHANNEL f1 =====
SFO1 125.7779086 MHz
NUC1 13C
P1 10.50 usec
SI 32768
SF 125.7653121 MHz
WDW EM
SSB 0
LB 1.00 Hz
GB 0
PC 1.40

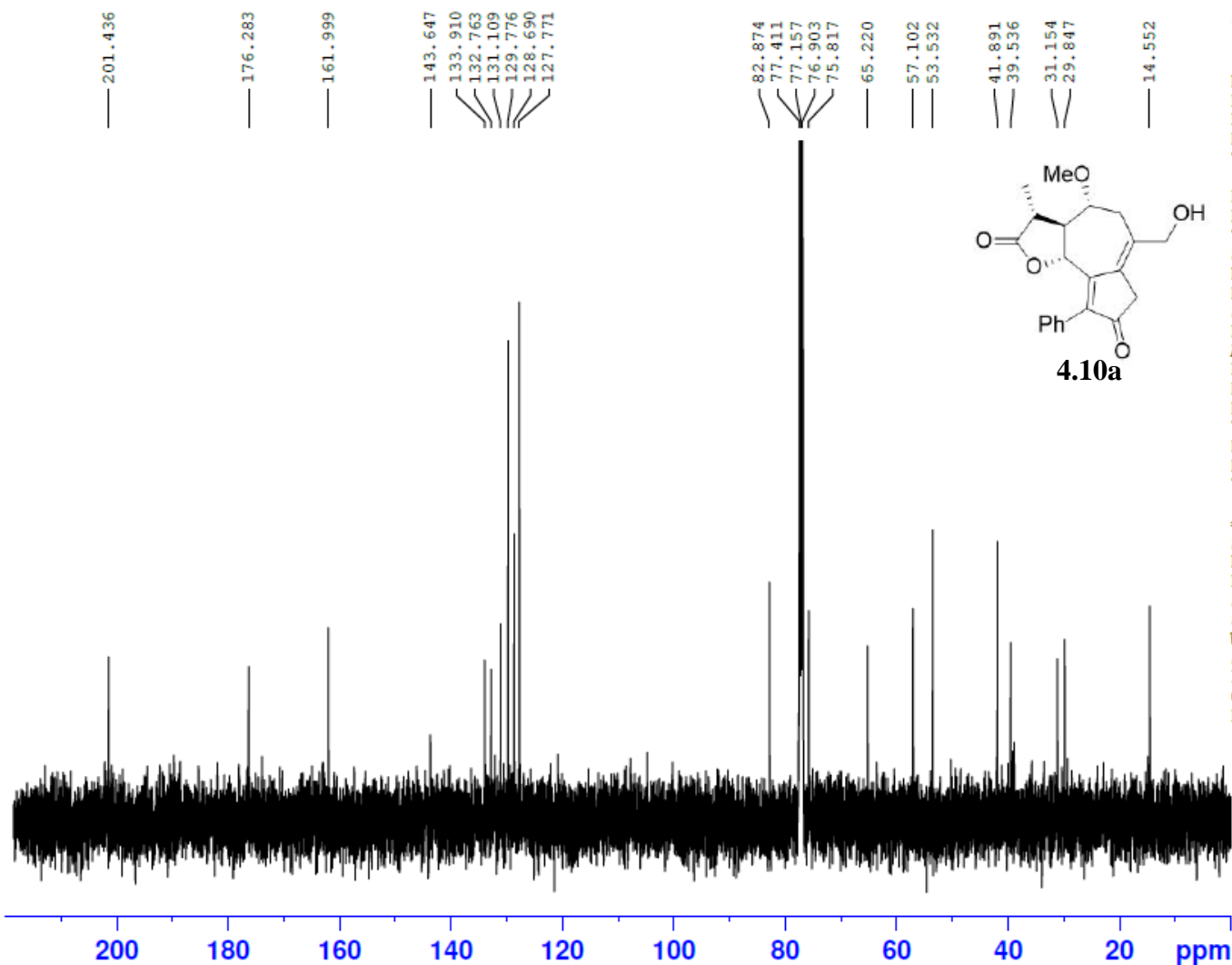


SW06-054-C 13C, 500



NAME SW06-054-C
EXPNO 1
PROCNO 1
Date_ 20141223
Time 11.26
INSTRUM spect
PROBHD 5 mm PABBO BB/
PULPROG zgpg30
TD 65536
SOLVENT CDC13
NS 998
DS 2
SWH 29761.904 Hz
FIDRES 0.454131 Hz
AQ 1.1010548 sec
RG 203
DW 16.800 usec
DE 6.50 usec
TE 298.2 K
D1 2.00000000 sec
D11 0.03000000 sec
TD0 1

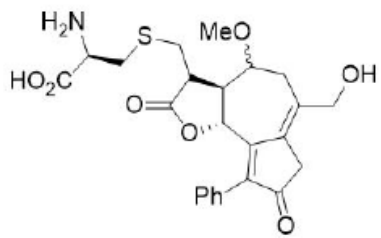
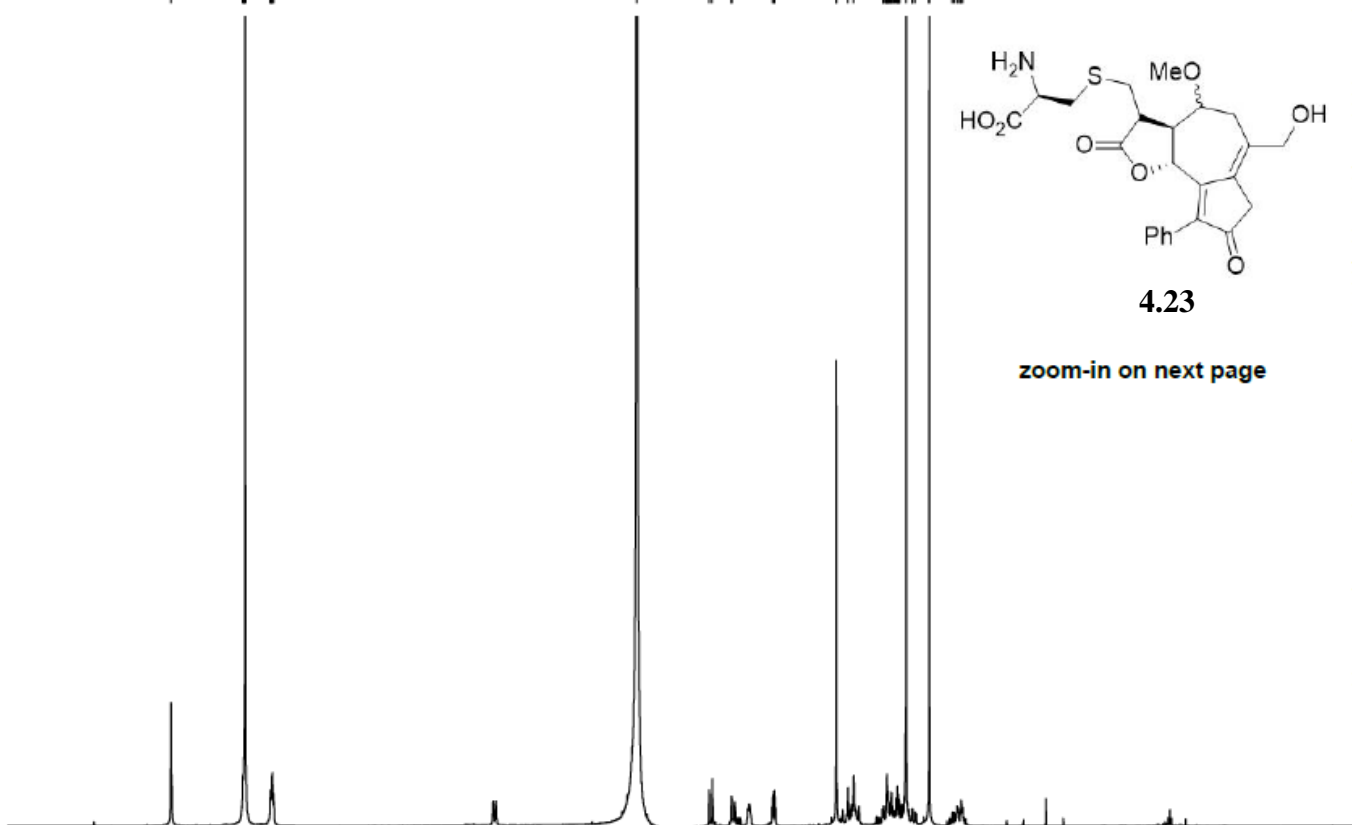
==== CHANNEL f1 =====
SFO1 125.7779080 MHz
NUC1 13C
P1 10.50 usec
SI 32768
SF 125.7653149 MHz
WDW EM
SSB 0
LB 1.00 Hz
GB 0
PC 1.40



SW04-007-impure
600MHz



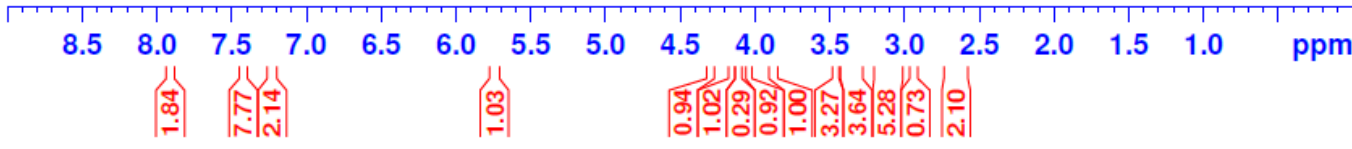
7.906
7.426
7.421
7.416
7.411
7.405
7.242
7.238
7.234
7.229
7.226
7.221
4.790
4.307
4.285
4.159
4.155
3.881
3.875
3.868
3.456
3.451
3.379
3.339
3.143
3.141
3.136
3.123
3.118
3.116
3.111
3.109
3.102
3.098
3.091
3.086
3.079
3.072
3.065
3.057
3.047
3.045
3.042
3.035
3.033
2.990
2.947
2.945
2.929
2.835
2.834
2.680
2.668
2.648
2.640
2.627
2.620
2.609



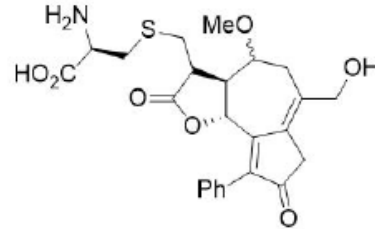
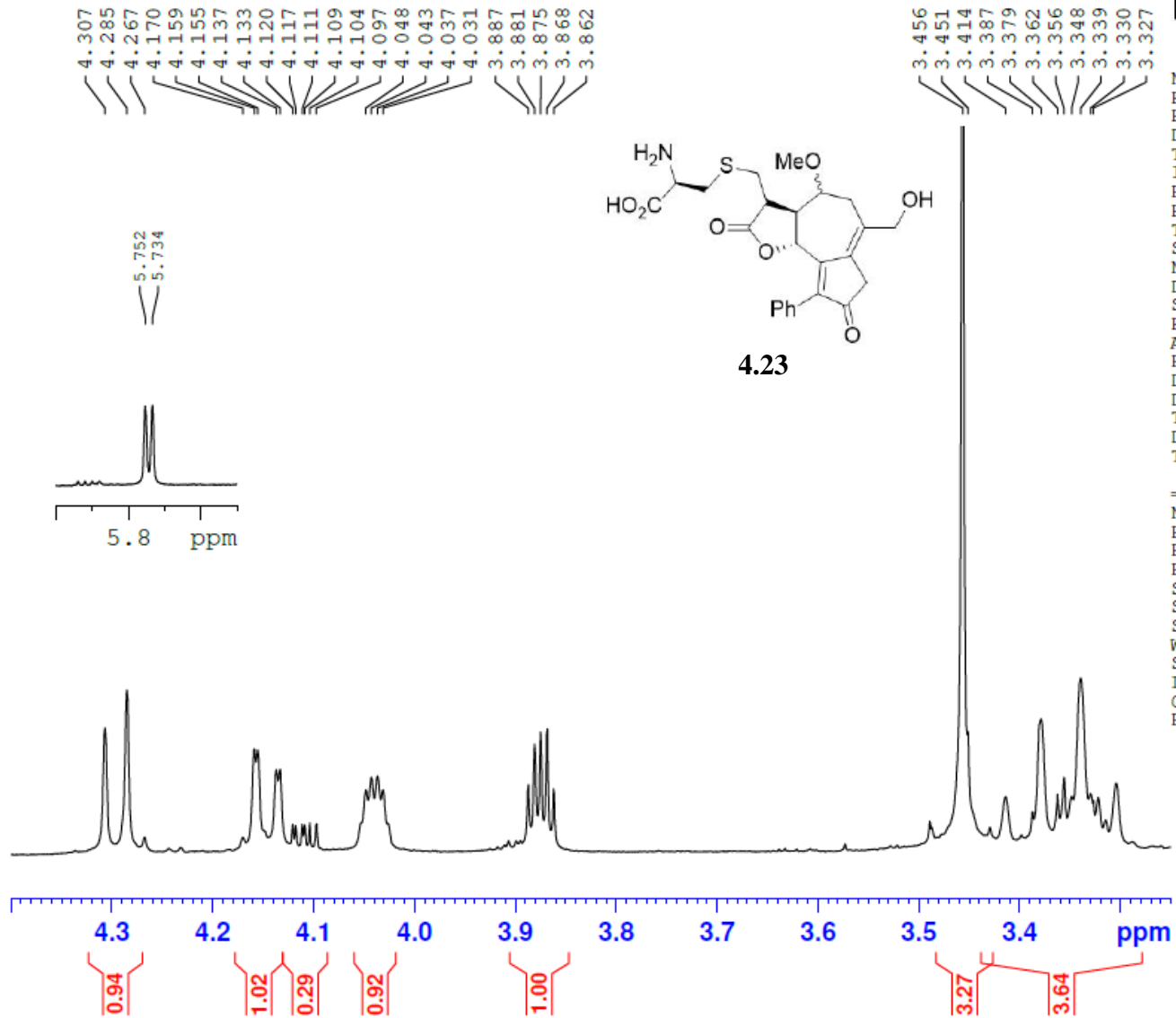
4.23
zoom-in on next page

NAME SW04-007-impure
EXPNO 1
PROCNO 1
Date_ 20130810
Time 10.19
INSTRUM spect
PROBHD 5 mm PABBO BB-
PULPROG zg30
TD 65536
SOLVENT D2O
NS 16
DS 2
SWH 12335.526 Hz
FIDRES 0.188225 Hz
AQ 2.6564426 sec
RG 64
DW 40.533 usec
DE 6.50 usec
TE 294.8 K
D1 1.00000000 sec
TD0 1

===== CHANNEL f1 =====
NUC1 1H
P1 10.86 usec
PL1 -2.00 dB
PL1W 19.70630455 W
SFO1 600.7137096 MHz
SI 32768
SF 600.7099452 MHz
WDW EM
SSB 0
LB 0.30 Hz
GB 0
PC 1.00



SW04-007-impure
600MHz

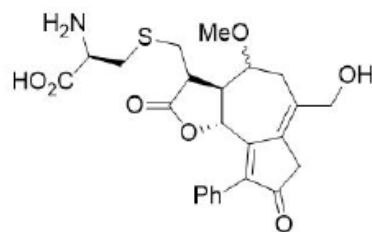


```

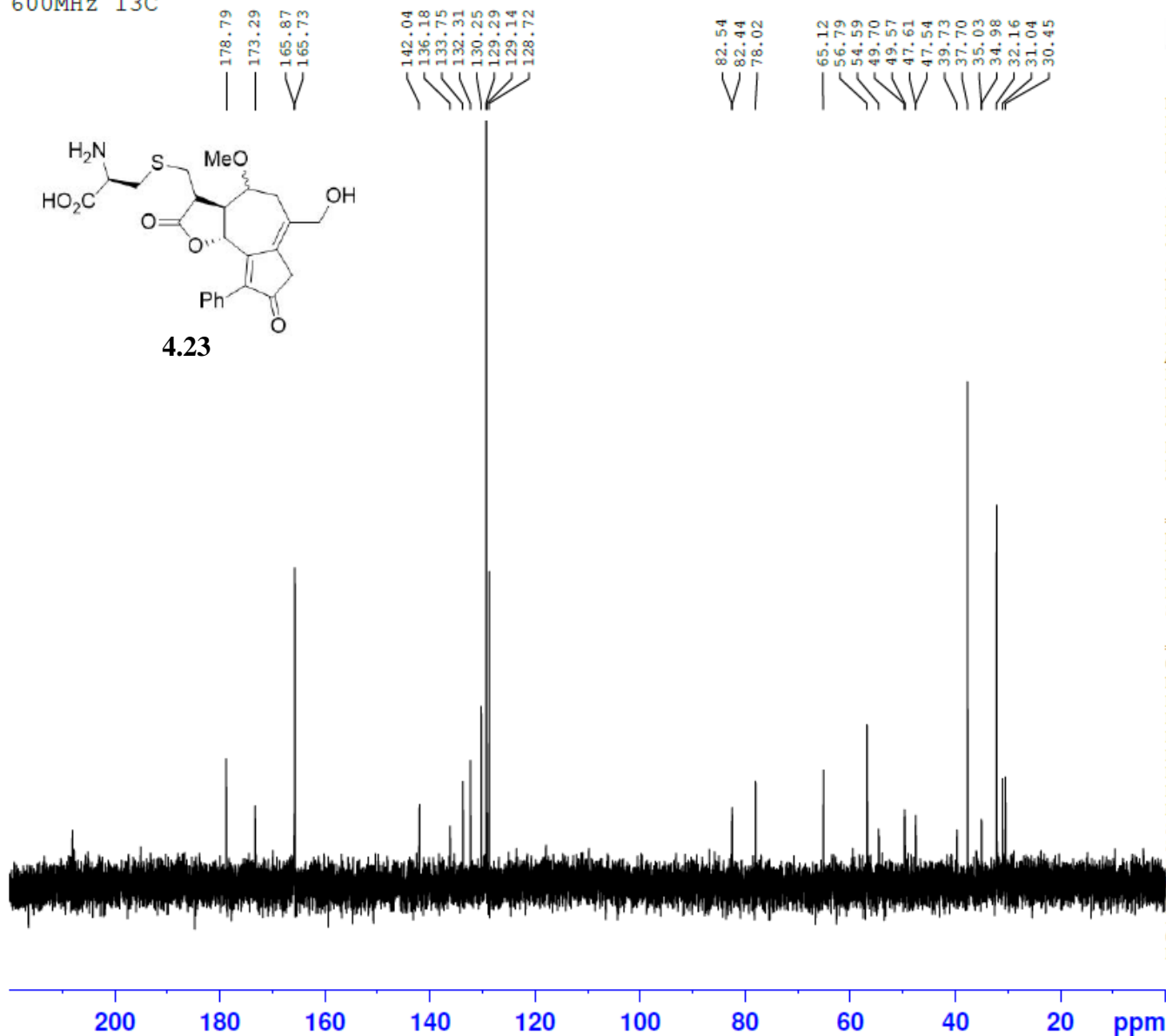
NAME SW04-007-impure
EXPNO 1
PROCNO 1
Date_ 20130810
Time 10.19
INSTRUM spect
PROBHD 5 mm PABBO BB-
PULPROG zg30
TD 65536
SOLVENT D2O
NS 16
DS 2
SWH 12335.526 Hz
FIDRES 0.188225 Hz
AQ 2.6564426 sec
RG 64
DW 40.533 usec
DE 6.50 usec
TE 294.8 K
D1 1.00000000 sec
TD0 1

===== CHANNEL f1 =====
NUC1 1H
P1 10.86 usec
PL1 -2.00 dB
PL1W 19.70630455 W
SFO1 600.7137096 MHz
SI 32768
SF 600.7099452 MHz
WDW EM
SSB 0
LB 0.30 Hz
GB 0
PC 1.00
  
```

SW04-007-impure
600MHz 13C



4.23



```

NAME SW04-007-impure
EXPNO 2
PROCNO 1
Date_ 20130810
Time 12.27
INSTRUM spect
PROBHD 5 mm PABBO BB-
PULPROG zgpg30
TD 65536
SOLVENT D2O
NS 2400
DS 4
SWH 36057.691 Hz
FIDRES 0.550197 Hz
AQ 0.9088159 sec
RG 203
DW 13.867 usec
DE 6.50 usec
TE 295.1 K
D1 2.00000000 sec
D11 0.03000000 sec
TD0 1
  
```

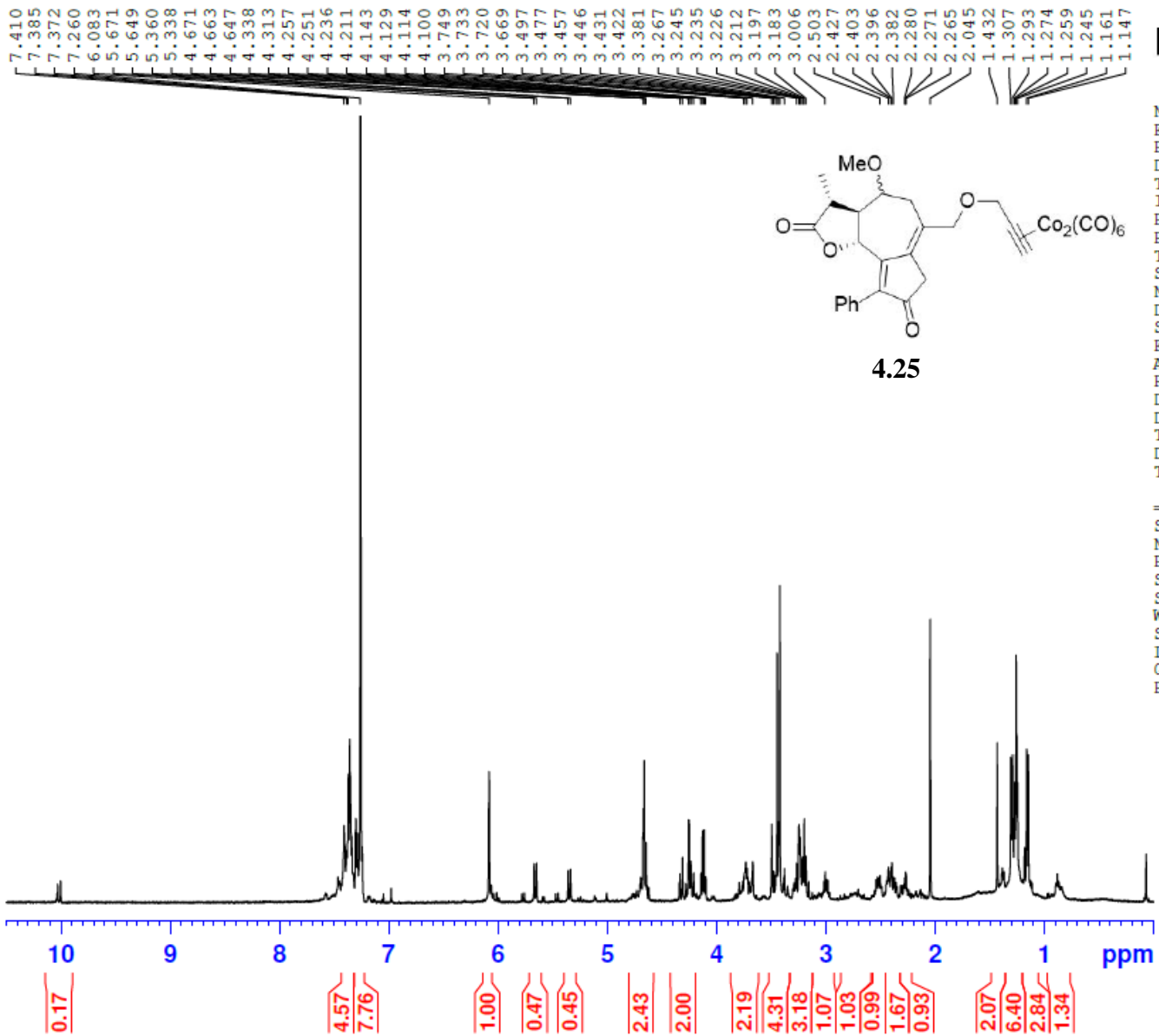
```

===== CHANNEL f1 =====
NUC1 13C
P1 11.50 usec
PL1 0.00 dB
PL1W 97.46119690 W
SFO1 151.0637542 MHz
  
```

```

===== CHANNEL f2 =====
CPDPRG2 waltz16
NUC2 1H
PCPD2 70.00 usec
PL2 -2.00 dB
PL12 14.19 dB
PL13 120.00 dB
PL2W 19.70630455 W
PL12W 0.47381112 W
PL13W 0.00000000 W
SFO2 600.7124028 MHz
SI 32768
SF 151.0485235 MHz
WDW EM
SSB 0
LB 1.00 Hz
GB 0
PC 1.40
  
```

SW07-201-D 1H 500



```

NAME          SW07-201-D
EXPNO         10
PROCNO        1
Date_         20160412
Time          18.58
INSTRUM       spect
PROBHD        5 mm PABBO BB/
PULPROG       zg30
TD            65536
SOLVENT       CDC13
NS            16
DS            2
SWH           10000.000 Hz
FIDRES        0.152588 Hz
AQ            3.2768500 sec
RG            203
DW            50.000 usec
DE            6.50 usec
TE            297.9 K
D1            1.00000000 sec
TD0           1
    
```

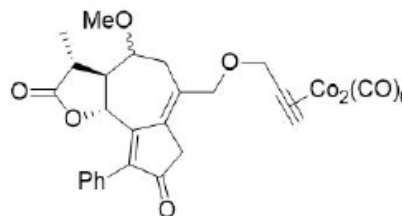
```

===== CHANNEL f1 =====
SFO1          500.1630887 MHz
NUC1           1H
P1             11.45 usec
SI            65536
SF            500.1600119 MHz
WDW            EM
SSB            0
LB            0.30 Hz
GB            0
PC            1.00
    
```


SW07-201-D 13C 500

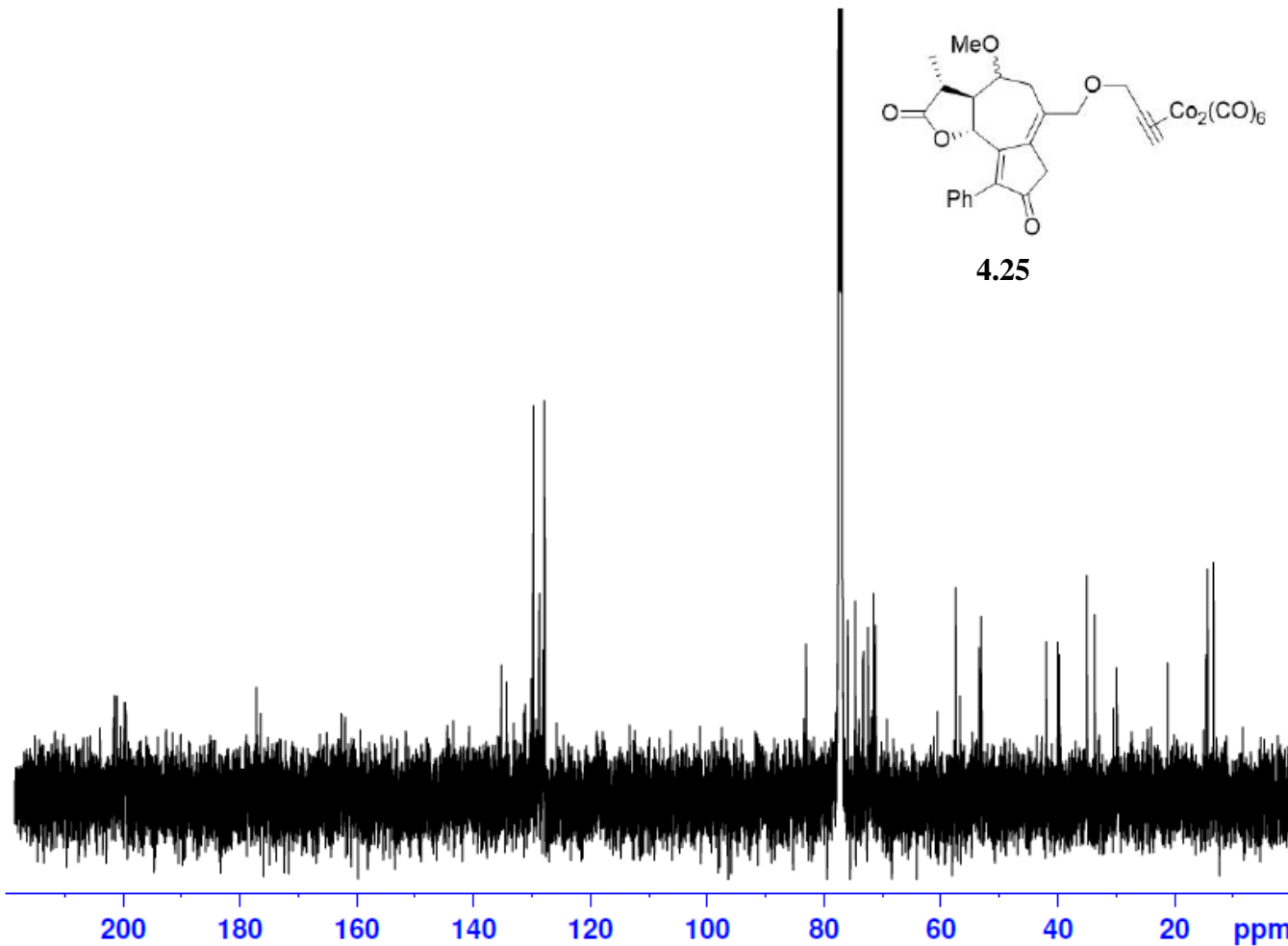


201.709
201.209
199.834
177.199
176.449
162.693
162.068
144.513
143.445
135.222
133.075
131.411
131.201
131.123
129.795
129.701
128.763
128.676
128.051
128.049
127.851
127.762
91.736
91.439
83.003
77.411
77.157
76.903
75.857
74.623
73.315
73.220
72.398
71.455
71.136
57.395
53.450
53.105
41.951
40.017
39.802
35.034
33.712
29.928
21.189
14.628
14.351
13.310

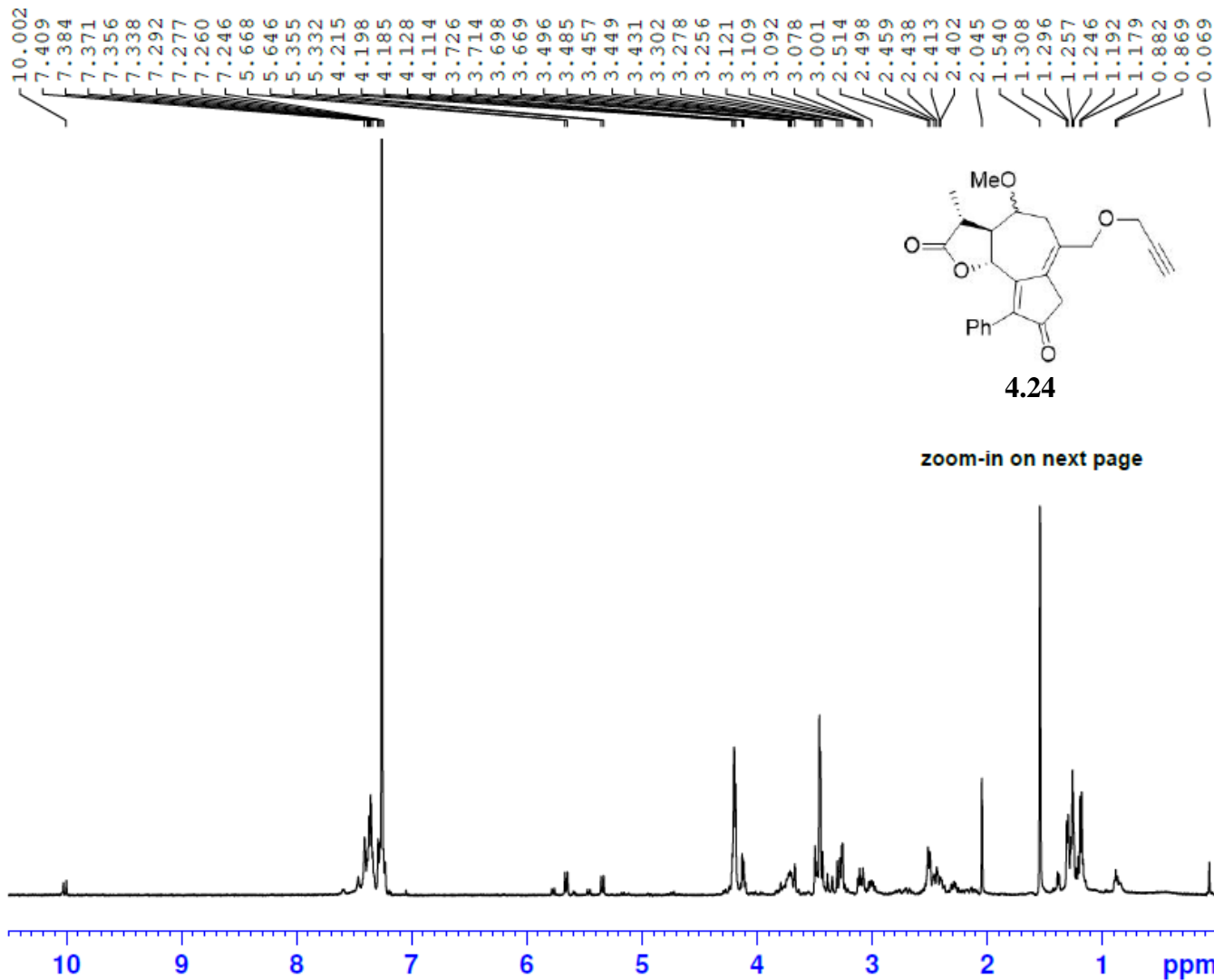


NAME SW07-201-D
EXPNO 11
PROCNO 1
Date_ 20160414
Time 1.30
INSTRUM spect
PROBHD 5 mm PABBO BB/
PULPROG zgpg30
TD 65536
SOLVENT CDCl3
NS 5000
DS 2
SWH 29761.904 Hz
FIDRES 0.454131 Hz
AQ 1.1010548 sec
RG 203
DW 16.800 usec
DE 6.50 usec
TE 298.7 K
D1 2.00000000 sec
D11 0.03000000 sec
TD0 1

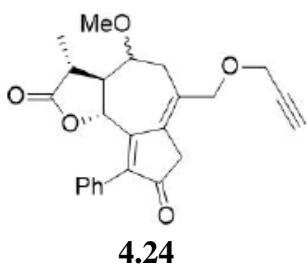
==== CHANNEL f1 =====
SFO1 125.7779086 MHz
NUC1 13C
P1 10.50 usec
SI 32768
SF 125.7653131 MHz
WDW EM
SSB 0
LB 1.00 Hz
GB 0
PC 1.40



SW07-205-AB 1H 500



NAME SW07-205-AB
EXPNO 10
PROCNO 1
Date_ 20160415
Time 15.43
INSTRUM spect
PROBHD 5 mm PABBO BB/
PULPROG zg30
TD 65536
SOLVENT CDCl3
NS 16
DS 2
SWH 10000.000 Hz
FIDRES 0.152588 Hz
AQ 3.2768500 sec
RG 203
DW 50.000 usec
DE 6.50 usec
TE 297.4 K
D1 1.0000000 sec
TDO 1



zoom-in on next page

==== CHANNEL f1 =====
SFO1 500.1630887 MHz
NUC1 1H
P1 11.45 usec
SI 65536
SF 500.1600114 MHz
WDW EM
SSB 0
LB 0.30 Hz
GB 0
PC 1.00

Integration values: 0.25, 5.57, 10.64, 0.50, 0.41, 4.05, 1.09, 2.35, 4.44, 2.87, 2.00, 0.79, 3.75, 1.45, 1.17, 0.73, 1.93, 3.21, 3.31, 1.31

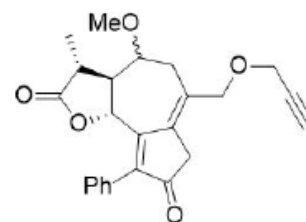
SW07-205-AB 1H 500

5.782
5.760
5.668
5.646
5.472
5.452
5.355
5.332

4.215
4.198
4.185
4.128
4.114
3.726
3.714
3.698
3.669
3.496
3.485
3.457
3.449
3.431
3.302
3.278
3.256
3.121
3.109
3.092
3.078
3.028
3.013
3.001
2.990
2.514
2.498
2.459
2.438
2.413
2.402
2.045

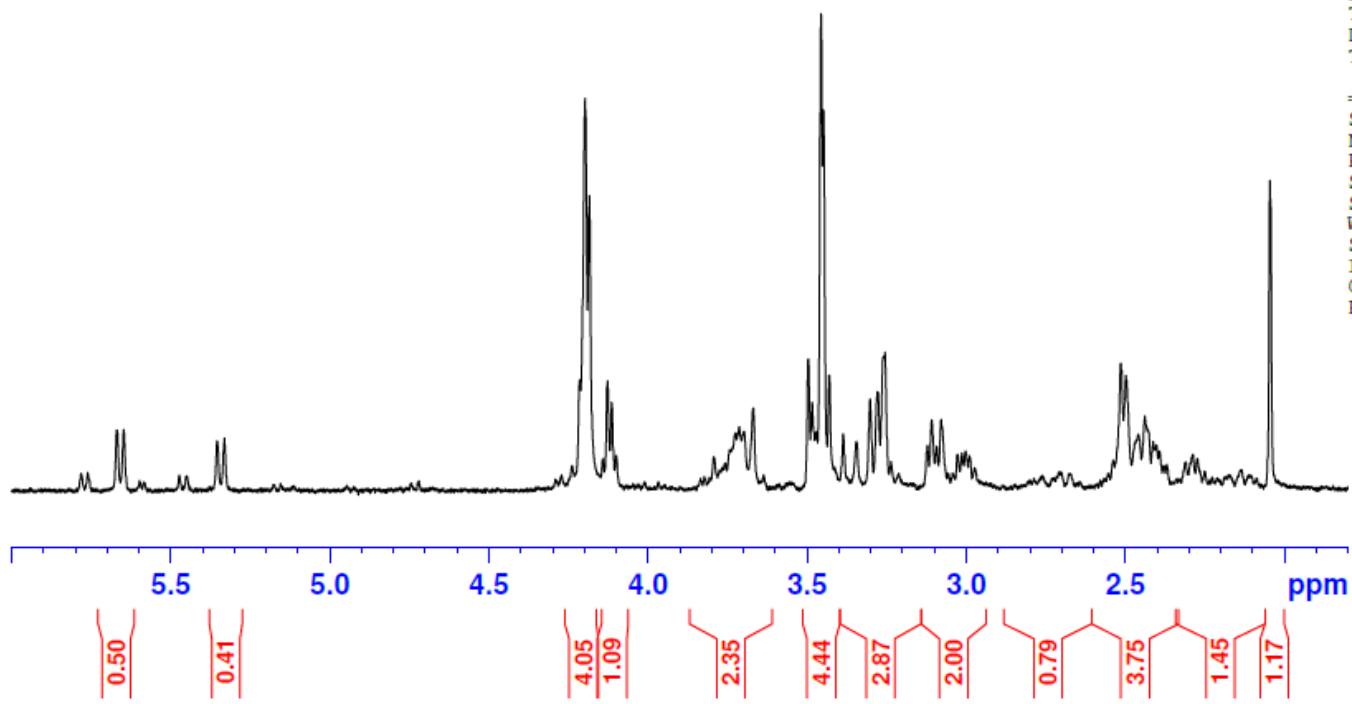


NAME SW07-205-AB
EXPNO 10
PROCNO 1
Date_ 20160415
Time_ 15.43
INSTRUM spect
PROBHD 5 mm PABBO BB/
PULPROG zg30
TD 65536
SOLVENT CDC13
NS 16
DS 2
SWH 10000.000 Hz
FIDRES 0.152588 Hz
AQ 3.2768500 sec
RG 203
DW 50.000 usec
DE 6.50 usec
TE 297.4 K
D1 1.00000000 sec
TD0 1



4.24

===== CHANNEL f1 =====
SFO1 500.1630887 MHz
NUC1 1H
P1 11.45 usec
SI 65536
SF 500.1600114 MHz
WDW EM
SSB 0
LB 0.30 Hz
GB 0
PC 1.00



BIBLIOGRAPHY

1. (a) Harvey, A. L., *Drug Discovery Today*, **2008**, *13*, 894-901; (b) Newman, D. J.; Cragg, G. M., *J. Nat. Prod.* **2016**, *79*, 629-661.
2. Ghantous, A.; Gali-Muhtasib, H.; Vuorela, H.; Saliba, N. A.; Darwiche, N., *Drug Discovery Today* **2010**, *15*, 668-678.
3. Thi Quynh Doan, N.; Brogger Christensen, S., *Curr. Pharm. Des.* **2015**, *21*, 5501-5517.
4. Tu, Y., *Nat. Med.* **2011**, *17*, 1217-1220.
5. Guzman, M. L.; Rossi, R. M.; Neelakantan, S.; Li, X.; Corbett, C. A.; Hassane, D. C.; Becker, M. W.; Bennett, J. M.; Sullivan, E.; Lachowicz, J. L.; Vaughan, A.; Sweeney, C. J.; Matthews, W.; Carroll, M.; Liesveld, J. L.; Crooks, P. A.; Jordan, C. T., *Blood* **2007**, *110*, 4427-4435.
6. Kitson, R. R. A.; Millemaggi, A.; Taylor, R. J. K., *Angew. Chem. Int. Ed.* **2009**, *48*, 9426-9451.
7. Merfort, I., *Curr. Drug Targets* **2011**, *12*, 1560-1573.
8. (a) Potashman, M. H.; Duggan, M. E., *J. Med. Chem.* **2009**, *52*, 1231-1246; (b) Singh, J.; Petter, R. C.; Baillie, T. A.; Whitty, A., *Nat. Rev. Drug Discov.* **2011**, *10*, 307-317; (c) Bauer, R. A., *Drug Discovery Today* **2015**, *20*, 1061-1073.
9. Schmidt, T. J.; Lyß, G.; Pahl, H. L.; Merfort, I., *Bioorg. Med. Chem.* **1999**, *7*, 2849-2855.
10. Baud, V.; Karin, M., *Nat. Rev. Drug Discov.* **2009**, *8*, 33-40.
11. Dey, A.; Tergaonkar, V.; Lane, D. P., *Nat. Rev. Drug Discov.* **2008**, *7*, 1031-1040.
12. Drew, D. P.; Krichau, N.; Reichwald, K.; Simonsen, H. T., *Phytochem. Rev.* **2009**, *8*, 581-599.
13. Rosén, J.; Gottfries, J.; Muresan, S.; Backlund, A.; Oprea, T. I., *J. Med. Chem.* **2009**, *52*, 1953-1962.

14. (a) Blanco, J. G.; Gil, R. R.; Alvarez, C. I.; Patrino, L. C.; Genti-Raimondi, S.; Flury, A., *FEBS Lett.* **1997**, *409*, 396-400; (b) Blanco, J. G.; Gil, R. R.; Bocco, J. L.; Meragelman, T. L.; Genti-Raimondi, S.; Flury, A., *J. Pharmacol. Exp. Ther.* **2001**, *297*, 1099-1105.
15. (a) Castañeda-Acosta, J.; Fischer, N. H.; Vargas, D., *J. Nat. Prod.* **1993**, *56*, 90-98; (b) Zhai, J.-D.; Li, D.; Long, J.; Zhang, H.-L.; Lin, J.-P.; Qiu, C.-J.; Zhang, Q.; Chen, Y., *J. Org. Chem.* **2012**, *77*, 7103-7107.
16. Barton, D. H. R.; De Mayo, P.; Shafiq, M., *J. Chem. Soc.* **1957**, 929-35.
17. (a) Marx, J. N.; White, E. H., *Tetrahedron* **1969**, *25*, 2117-2120; (b) Edgar, M. T.; Greene, A. E.; Crabbe, P., *J. Org. Chem.* **1979**, *44*, 159-160; (c) Zhang, W.; Luo, S.; Fang, Chen, Q.; Hu, H.; Jia, X.; Zhai, H., *J. Am. Chem. Soc.* **2005**, *127*, 18-19.
18. (a) Manzano, F. L.; Guerra, F. M.; Moreno-Dorado, F. J.; Jorge, Z. D.; Massanet, G. M., *Org. Lett.* **2006**, *8*, 2879-2882; (b) Marín-Barrios, R.; García-Cabeza, A. L.; Moreno-Dorado, F. J.; Guerra, F. M.; Massanet, G. M., *J. Org. Chem.* **2014**, *79*, 6501-6509.
19. Lee, E.; Yoon, C. H.; Sung, Y.-s.; Kim, Y. K.; Yun, M.; Kim, S., *J. Am. Chem. Soc.* **1997**, *119*, 8391-8392.
20. Lee, E.; Yoon, C. H., *J. Chem. Soc., Chem. Commun.* **1994**, 479-481.
21. Andrews, S. P.; Ball, M.; Wierschem, F.; Cleator, E.; Oliver, S.; Högenauer, K.; Simic, O.; Antonello, A.; Hüniger, U.; Smith, M. D.; Ley, S. V., *Chem. Eur. J.* **2007**, *13*, 5688-5712.
22. Kalidindi, S.; Jeong, W. B.; Schall, A.; Bandichhor, R.; Nosse, B.; Reiser, O., *Angew. Chem. Int. Ed.* **2007**, *46*, 6361-6363.
23. (a) Devreese, A. A.; Demuyne, M.; De Clercq, P. J.; Vandewalle, M., **1983**, *39*, 3039-3048; (b) Devreese, A. A.; Demuyne, M.; De Clercq, P. J.; Vandewalle, M., **1983**, *39*, 3049-3054.
24. Carret, S.; Deprés, J.-P., **2007**, *46*, 6870-6873.
25. Burke, M. D.; Schreiber, S. L., *Angew. Chem. Int. Ed.* **2004**, *43*, 46-58.
26. Wallock, N. J.; Donaldson, W. A., *Org. Lett.* **2005**, *7*, 2047-2049.
27. Gone, J. R.; Wallock, N. J.; Lindeman, S.; Donaldson, W. A., *Tetrahedron Lett.* **2009**, *50*, 1023-1025.
28. Coquerel, Y.; Filippini, M.-H.; Bensa, D.; Rodriguez, J., *Chem. Eur. J.* **2008**, *14*, 3078-3092.
29. Reboul, I.; Boddaert, T.; Coquerel, Y.; Rodriguez, J., *Eur. J. Org. Chem.* **2008**, *2008*, 5379-5382.

30. Khand, I. U.; Knox, G. R.; Pauson, P. L.; Watts, W. E.; Foreman, M. I., *J. Chem. Soc., Perkin Trans. 1* **1973**, 977-981.
31. (a) Brummond, K. M.; Kent, J. L., *Tetrahedron* **2000**, *56*, 3263-3283; (b) *The Pauson-Khand reaction: scope, variations and applications*. John Wiley & Sons: Chichester, 2012.
32. (a) Ahmar, M.; Locatelli, C.; Colombier, D.; Cazes, B., *Tetrahedron Lett.* **1997**, *38*, 5281-5284; (b) Pagenkopf, B. L.; Belanger, D. B.; O'Mahony, D. J. R.; Livinghouse, T., *Synthesis* **2000**, *2000*, 1009-1019.
33. (a) Brummond, K. M.; Wan, H., *Tetrahedron Lett.* **1998**, *39*, 931-934; (b) Brummond, K. M.; Wan, H.; Kent, J. L., *J. Org. Chem.* **1998**, *63*, 6535-6545.
34. (a) Kobayashi, T.; Koga, Y.; Narasaka, K., *J. Organomet. Chem.* **2001**, *624*, 73-87; (b) Brummond, K. M.; Chen, H.; Fisher, K. D.; Kerekes, A. D.; Rickards, B.; Sill, P. C.; Geib, S. J., *Org. Lett.* **2002**, *4*, 1931-1934.
35. Bayden, A. S.; Brummond, K. M.; Jordan, K. D., *Organometallics* **2006**, *25*, 5204-5206.
36. (a) Brummond, K. M.; Chen, D., *Org. Lett.* **2008**, *10*, 705-708; (b) Brummond, K. M.; Davis, M. M.; Huang, C., *J. Org. Chem.* **2009**, *74*, 8314-8320; (c) Grillet, F.; Brummond, K. M., *J. Org. Chem.* **2013**, *78*, 3737-3754.
37. (a) Mukai, C.; Nomura, I.; Yamanishi, K.; Hanaoka, M., *Org. Lett.* **2002**, *4*, 1755-1758; (b) Mukai, C.; Nomura, I.; Kitagaki, S., *J. Org. Chem.* **2003**, *68*, 1376-1385.
38. Brummond, K. M.; Chen, D.; Davis, M. M., *J. Org. Chem.* **2008**, *73*, 5064-5068.
39. Brummond, K. M.; Gao, D., *Org. Lett.* **2003**, *5*, 3491-3494.
40. Hirose, T.; Miyakoshi, N.; Mukai, C., *J. Org. Chem.* **2008**, *73*, 1061-1066.
41. (a) Jørgensen, L.; McKerrall, S. J.; Kuttruff, C. A.; Ungeheuer, F.; Felding, J.; Baran, P. S., *Science* **2013**, *341*, 878-882; (b) Kawamura, S.; Chu, H.; Felding, J.; Baran, P. S., *Nature* **2016**, *532*, 90-93.
42. Grillet, F.; Huang, C.; Brummond, K. M., *Org. Lett.* **2011**, *13*, 6304-6307.
43. Wen, B.; Hexum, J. K.; Widen, J. C.; Harki, D. A.; Brummond, K. M., *Org. Lett.* **2013**, *15*, 2644-2647.
44. Burns, N. Z.; Baran, P. S.; Hoffmann, R. W., *Angew. Chem. Int. Ed.* **2009**, *48*, 2854-2867.
45. Padgett, H. C.; Csendes, I. G.; Rapoport, H., *J. Org. Chem.* **1979**, *44*, 3492-3496.
46. (a) Johnson, W. S.; Werthemann, L.; Bartlett, W. R.; Brocksom, T. J.; Li, T.-T.; Faulkner, D. J.; Petersen, M. R., *J. Am. Chem. Soc.* **1970**, *92*, 741-743; (b) Zhang, Z.;

- Liu, C.; Kinder, R. E.; Han, X.; Qian, H.; Widenhoefer, R. A., *J. Am. Chem. Soc.* **2006**, *128*, 9066-9073; (c) Stoll, A. H.; Blakey, S. B., *J. Am. Chem. Soc.* **2010**, *132*, 2108-2109.
47. Wegner, H. A.; de Meijere, A.; Wender, P. A., *J. Am. Chem. Soc.* **2005**, *127*, 6530-6531.
48. Hong, X.; Stevens, M. C.; Liu, P.; Wender, P. A.; Houk, K. N., *J. Am. Chem. Soc.* **2014**, *136*, 17273-17283.
49. Murakami, M.; Ubukata, M.; Itami, K.; Ito, Y., *Angew. Chem. Int. Ed.* **1998**, *37*, 2248-2250.
50. Denmark, S. E.; Muhuhi, J. M., *J. Am. Chem. Soc.* **2010**, *132*, 11768-11778.
51. Hayashi, Y.; Ogawa, K.; Inagaki, F.; Mukai, C., *Org. Biomol. Chem.* **2012**, *10*, 4747-4751.
52. Sanger, A. R., *J. Chem. Soc., Dalton Trans.* **1977**, 120-129.
53. Mukai, C.; Inagaki, F.; Yoshida, T.; Yoshitani, K.; Hara, Y.; Kitagaki, S., *J. Org. Chem.* **2005**, *70*, 7159-7171.
54. Mukai, C.; Hirose, T.; Teramoto, S.; Kitagaki, S., *Tetrahedron* **2005**, *61*, 10983-10994.
55. Inagaki, F.; Narita, S.; Hasegawa, T.; Kitagaki, S.; Mukai, C., *Angew. Chem. Int. Ed.* **2009**, *48*, 2007-2011.
56. Chiou, W.-H.; Lin, Y.-H.; Chen, G.-T.; Gao, Y.-K.; Tseng, Y.-C.; Kao, C.-L.; Tsai, J.-C., *Chem. Commun.* **2011**, *47*, 3562-3564.
57. Alemán, J.; del Solar, V.; Martín-Santos, C.; Cubo, L.; Ranninger, C. N., *J. Org. Chem.* **2011**, *76*, 7287-7293.
58. (a) Hall, D. G., *Synlett* **2007**, *2007*, 1644-1655; (b) Elford, T. G.; Hall, D. G., *J. Am. Chem. Soc.* **2010**, *132*, 1488-1489.
59. Gilmore, T. D.; Herscovitch, M., *Oncogene* **2006**, *25*, 6887-6899.
60. Trost, B. M.; Livingston, R. C., *J. Am. Chem. Soc.* **2008**, *130*, 11970-11978.
61. Robinson, J. M.; Sakai, T.; Okano, K.; Kitawaki, T.; Danheiser, R. L., *J. Am. Chem. Soc.* **2010**, *132*, 11039-11041.
62. Tsuda, T.; Yoshida, T.; Kawamoto, T.; Saegusa, T., *J. Org. Chem.* **1987**, *52*, 1624-1627.
63. Tsuda, T.; Hayashi, T.; Satomi, H.; Kawamoto, T.; Saegusa, T., *J. Org. Chem.* **1986**, *51*, 537-540.
64. Kennedy, J. W. J.; Hall, D. G., *J. Org. Chem.* **2004**, *69*, 4412-4428.

65. Nyzam, V.; Belaud, C.; Villieras, J., *Tetrahedron Lett.* **1993**, *34*, 6899-6902.
66. Chataigner, I.; Zammattio, F.; Lebreton, J.; Villieras, J., *Tetrahedron* **2008**, *64*, 2441-2455.
67. Kennedy, J. W. J.; Hall, D. G., *J. Am. Chem. Soc.* **2002**, *124*, 898-899.
68. Yang, P.-Y.; Liu, K.; Ngai, M. H.; Lear, M. J.; Wenk, M. R.; Yao, S. Q., *J. Am. Chem. Soc.* **2010**, *132*, 656-666.
69. (a) Hoye, T. R.; Eklov, B. M.; Voloshin, M., *Org. Lett.* **2004**, *6*, 2567-2570; (b) Hoye, T. R.; Aspaas, A. W.; Eklov, B. M.; Ryba, T. D., *Org. Lett.* **2005**, *7*, 2205-2208.
70. (a) Smith, S. G.; Goodman, J. M., *J. Am. Chem. Soc.* **2010**, *132*, 12946-12959; (b) Willoughby, P. H.; Jansma, M. J.; Hoye, T. R., *Nat. Protocols* **2014**, *9*, 643-660; (c) Kocsis, L. S.; Brummond, K. M., *Org. Lett.* **2014**, *16*, 4158-4161.
71. Yan, M.; Jin, T.; Ishikawa, Y.; Minato, T.; Fujita, T.; Chen, L.-Y.; Bao, M.; Asao, N.; Chen, M.-W.; Yamamoto, Y., *J. Am. Chem. Soc.* **2012**, *134*, 17536-17542.
72. Richmond, E.; Moran, J., *J. Org. Chem.* **2015**, *80*, 6922-6929.
73. (a) Krysiak, J.; Breinbauer, R., Activity-Based Protein Profiling for Natural Product Target Discovery. In *Activity-Based Protein Profiling*, Sieber, S. A., Ed. Springer Berlin Heidelberg: 2012; Vol. 324, pp 43-84; (b) Böttcher, T.; Pitscheider, M.; Sieber, S. A., *Angew. Chem. Int. Ed.* **2010**, *49*, 2680-2698.
74. (a) Nodwell, M.; Sieber, S., ABPP Methodology: Introduction and Overview. In *Activity-Based Protein Profiling*, Sieber, S. A., Ed. Springer Berlin Heidelberg: 2012; Vol. 324, pp 1-41; (b) Cravatt, B. F.; Wright, A. T.; Kozarich, J. W., *Annu. Rev. Biochem.* **2008**, *77*, 383-414.
75. Su, Y.; Ge, J.; Zhu, B.; Zheng, Y.-G.; Zhu, Q.; Yao, S. Q., *Curr. Opin. Chem. Biol.* **2013**, *17*, 768-775.
76. Martell, J.; Weerapana, E., *Molecules* **2014**, *19*, 1378.
77. Lehmann, J.; Wright, M. H.; Sieber, S. A., *Chem. Eur. J.* **2016**, *22*, 4666-4678.
78. (a) Kolb, H. C.; Finn, M. G.; Sharpless, K. B., *Angew. Chem. Int. Ed.* **2001**, *40*, 2004-2021; (b) Sletten, E. M.; Bertozzi, C. R., *Angew. Chem. Int. Ed.* **2009**, *48*, 6974-6998; (c) Ramil, C. P.; Lin, Q., *Chem. Commun.* **2013**, *49*, 11007-11022.
79. Gololobov, Y. G.; Kasukhin, L. F., *Tetrahedron* **1992**, *48*, 1353-1406.
80. Saxon, E.; Bertozzi, C. R., *Science* **2000**, *287*, 2007-2010.

81. (a) Blackman, M. L.; Royzen, M.; Fox, J. M., *J. Am. Chem. Soc.* **2008**, *130*, 13518-13519; (b) Yu, Z.; Pan, Y.; Wang, Z.; Wang, J.; Lin, Q., *Angew. Chem. Int. Ed.* **2012**, *51*, 10600-10604.
82. Rostovtsev, V. V.; Green, L. G.; Fokin, V. V.; Sharpless, K. B., *Angew. Chem. Int. Ed.* **2002**, *41*, 2596-2599.
83. Hong, V.; Steinmetz, N. F.; Manchester, M.; Finn, M. G., *Bioconjugate Chem.* **2010**, *21*, 1912-1916.
84. Agard, N. J.; Prescher, J. A.; Bertozzi, C. R., *J. Am. Chem. Soc.* **2004**, *126*, 15046-15047.
85. Speers, A. E.; Cravatt, B. F., *Chem. Biol.* **11**, 535-546.
86. Gushwa, N. N.; Kang, S.; Chen, J.; Taunton, J., *J. Am. Chem. Soc.* **2012**, *134*, 20214-20217.
87. Staub, I.; Sieber, S. A., *J. Am. Chem. Soc.* **2008**, *130*, 13400-13409.
88. Böttcher, T.; Sieber, S. A., *J. Am. Chem. Soc.* **2010**, *132*, 6964-6972.
89. Wirth, T.; Pestel, G. F.; Ganal, V.; Kirmeier, T.; Schuberth, I.; Rein, T.; Tietze, P. L. F.; Sieber, P. S. A., *Angew. Chem. Int. Ed.* **2013**, *52*, 6921-6925.
90. Kreuzer, J.; Bach, N. C.; Forler, D.; Sieber, S. A., *Chem. Sci.* **2015**, *6*, 237-245.
91. Fiori, K. W.; Du Bois, J., *J. Am. Chem. Soc.* **2007**, *129*, 562-568.
92. Li, J.; Cisar, J. S.; Zhou, C.-Y.; Vera, B.; Williams, H.; Rodríguez, A. D.; Cravatt, B. F.; Romo, D., *Nat. Chem.* **2013**, *5*, 510-517.
93. (a) Nicholas, K. M., *Acc. Chem. Res.* **1987**, *20*, 207-214; (b) Teobald, B. J., *Tetrahedron* **2002**, *58*, 4133-4170; (c) Diaz, D. D.; Betancort, J. M.; Martin, V. S., *Synlett* **2007**, 343-359.
94. Lockwood, R. F.; Nicholas, K. M., *Tetrahedron Lett.* **1977**, *18*, 4163-4165.
95. Gohain, M.; Marais, C.; Bezuidenhout, B. C. B., *Tetrahedron Lett.* **2012**, *53*, 1048-1050.
96. Ortega, N.; Martin, V. S.; Martin, T., *J. Org. Chem.* **2010**, *75*, 6660-6672.
97. Diaz, D. D.; Martin, V. S., *Tetrahedron Lett.* **2000**, *41*, 9993-9996.
98. Manuscript describing the synthesis of XX in preparation.
99. Pinel, B.; Dubois, J.; Séraphin, D.; Richomme, P., *J. Enzyme Inhib. Med. Chem.* **2010**, *25*, 172-179.

100. Jaime, C.; Ortuno, R. M.; Font, J., *J. Org. Chem.* **1986**, *51*, 3946-3951.
101. Chen, X.-N.; Zhang, J.; Yin, Y.-Q.; Huang, X.-Y.; Sun, J., *J. Organomet. Chem.* **1999**, *579*, 227-234.
102. Hayashi, Y.; Yamaguchi, H.; Toyoshima, M.; Okado, K.; Toyo, T.; Shoji, M., *Chem. Eur. J.* **2010**, *16*, 10150-10159.
103. Johansson, H.; Pedersen, D. S., *Eur. J. Org. Chem.* **2012**, *2012*, 4267-4281.
104. (a) Bennett, S. C.; Gelling, A.; Went, M. J., *J. Organomet. Chem.* **1992**, *439*, 189-199; (b) Gelling, A.; Mohmand, G. F.; Jeffery, J. C.; Went, M. J., *J. Chem. Soc., Dalton Trans.* **1993**, 1857-1862; (c) Hope-Weeks, L. J.; Mays, M. J.; Woods, A. D., *J. Chem. Soc., Dalton Trans.* **2002**, 1812-1819; (d) Golovko, V. B.; Mays, M. J.; Solan, G. A., *J. Organomet. Chem.* **2007**, *692*, 4985-4994; (e) Hagendorn, T.; Brase, S., *RSC Adv.* **2014**, *4*, 15493-15495.
105. Aroyan, C. E.; Dermenci, A.; Miller, S. J., *J. Org. Chem.* **2010**, *75*, 5784-5796.
106. Page, P. C. B.; Buckley, B. R.; Farah, M. M.; Blacker, A. J., *Eur. J. Org. Chem.* **2009**, *2009*, 3413-3426.
107. Evans, E. F.; Lewis, N. J.; Kapfer, I.; Macdonald, G.; Taylor, R. J. K., *Synth. Commun.* **1997**, *27*, 1819-1825.
108. Betancort, J. M.; Rodríguez, C. M.; Martín, V. S., *Tetrahedron Lett.* **1998**, *39*, 9773-9776.
109. Shea, K. M.; Closser, K. D.; Quintal, M. M., *J. Org. Chem.* **2005**, *70*, 9088-9091.
110. Amouri, H.; Bégué, J.-P.; Chennoufi, A.; Bonnet-Delpon, D.; Gruselle, M.; Malézieux, B., *Org. Lett.* **2000**, *2*, 807-809.
111. Varghese, V.; Saha, M.; Nicholas, K. M., *Org. Synth.* **1989**, *67*, 141.
112. Vizniowski, C. S.; Green, J. R.; Breen, T. L.; Dalacu, A. V., *J. Org. Chem.* **1995**, *60*, 7496-7502.
113. Tyrrell, E.; Heshmati, P.; Sarrazin, L., *Synlett* **1993**, *1993*, 769-771.
114. Hsu, J.-L.; Fang, J.-M., *J. Org. Chem.* **2001**, *66*, 8573-8584.
115. Nasim, S.; Pei, S.; Hagen, F. K.; Jordan, C. T.; Crooks, P. A., *Bioorg. Med. Chem.* **2011**, *19*, 1515-1519.
116. Siedle, B.; García-Piñeres, A. J.; Murillo, R.; Schulte-Mönting, J.; Castro, V.; Rüngeler, P.; Klaas, C. A.; Da Costa, F. B.; Kisiel, W.; Merfort, I., *J. Med. Chem.* **2004**, *47*, 6042-6054.

117. Rüngeler, P.; Castro, V.; Mora, G.; Gören, N.; Vichnewski, W.; Pahl, H. L.; Merfort, I.; Schmidt, T. J., *Bioorg. Med. Chem.* **1999**, *7*, 2343-2352.
118. Schmidt, T. J., *Bioorg. Med. Chem.* **1997**, *5*, 645-653.
119. (a) Avonto, C.; Tagliatalata-Scafati, O.; Pollastro, F.; Minassi, A.; Di Marzo, V.; De Petrocellis, L.; Appendino, G., *Angew. Chem. Int. Ed.* **2011**, *50*, 467-471; (b) Hexum, J. K.; Tello-Aburto, R.; Struntz, N. B.; Harned, A. M.; Harki, D. A., *ACS Med. Chem. Lett.* **2012**, *3*, 459-464.
120. (a) Hehner, S. P.; Hofmann, T. G.; Droge, W.; Schmitz, M. L., *J. Immunol.* **1999**, *163*, 5617-5623; (b) Hehner, S. P.; Heinrich, M.; Bork, P. M.; Vogt, M.; Ratter, F.; Lehmann, V.; Schulze-Osthoff, K.; Droge, W.; Schmitz, M. L., *J. Biol. Chem.* **1998**, *273*, 1288-1297; (c) Kwok, B. H. B.; Koh, B.; Ndubuisi, M. I.; Elofsson, M.; Crews, C. M., *Chem. Biol.* **2001**, *8*, 759-766.
121. Lyß, G.; Knorre, A.; Schmidt, T. J.; Pahl, H. L.; Merfort, I., *J. Biol. Chem.* **1998**, *273*, 33508-33516.
122. Garcia-Pineros, A. J.; Castro, V.; Mora, G.; Schmidt, T. J.; Strunck, E.; Pahl, H. L.; Merfort, I., *J. Biol. Chem.* **2001**, *276*, 39713-39720.
123. Büchele, B.; Zugmaier, W.; Lunov, O.; Syrovets, T.; Merfort, I.; Simmet, T., *Anal. Biochem.* **2010**, *401*, 30-37.
124. (a) Da Silva, G.; Heleno, V.; Constantino, M., *Molecules* **2000**, *5*, 908; (b) Zhang, Q.; Lu, Y.; Ding, Y.; Zhai, J.; Ji, Q.; Ma, W.; Yang, M.; Fan, H.; Long, J.; Tong, Z.; Shi, Y.; Jia, Y.; Han, B.; Zhang, W.; Qiu, C.; Ma, X.; Li, Q.; Shi, Q.; Zhang, H.; Li, D.; Zhang, J.; Lin, J.; Li, L.-Y.; Gao, Y.; Chen, Y., *J. Med. Chem.* **2012**, *55*, 8757-8769; (c) Yang, Z.-J.; Ge, W.-Z.; Li, Q.-Y.; Lu, Y.; Gong, J.-M.; Kuang, B.-J.; Xi, X.; Wu, H.; Zhang, Q.; Chen, Y., *J. Med. Chem.* **2015**, *58*, 7007-7020.
125. (a) Sass, D. C.; Gomes Heleno, V. C.; Callegari Lopes, J. L.; Constantino, M. G., *Tetrahedron Lett.* **2008**, *49*, 3877-3880; (b) Sass, D. C.; Heleno, V. C. G.; Morais, G. O.; Lopes, J. L. C.; Lopes, N. P.; Constantino, M. G., *Org. Biomol. Chem.* **2011**, *9*, 6148-6153; (c) Sass, D. C.; Heleno, V. C. G.; Cavalcante, S.; da Silva Barbosa, J.; Soares, A. C. F.; Constantino, M. G., *J. Org. Chem.* **2012**, *77*, 9374-9378.
126. Lipshutz, B. H.; Blomgren, P. A., *Org. Lett.* **2001**, *3*, 1869-1871.